EPIGENETIC MECHANISMS IN NEURAL PLASTICITY

EDITED BY: Daniel Ortuño-Sahagún, Reinhard Schliebs and Merce Pallàs
PUBLISHED IN: Frontiers in Cellular Neuroscience and
Frontiers in Molecular Neuroscience

frontiers Research Topics

frontiers

ISSN 1664-8714
ISBN 978-2-88963-000-4
DOI 10.3389/978-2-88963-000-4

About Frontiers

Frontiers is more than just an open-access publisher of scholarly articles: it is a pioneering approach to the world of academia, radically improving the way scholarly research is managed. The grand vision of Frontiers is a world where all people have an equal opportunity to seek, share and generate knowledge. Frontiers provides immediate and permanent online open access to all its publications, but this alone is not enough to realize our grand goals.

Frontiers Journal Series

The Frontiers Journal Series is a multi-tier and interdisciplinary set of open-access, online journals, promising a paradigm shift from the current review, selection and dissemination processes in academic publishing. All Frontiers journals are driven by researchers for researchers; therefore, they constitute a service to the scholarly community. At the same time, the Frontiers Journal Series operates on a revolutionary invention, the tiered publishing system, initially addressing specific communities of scholars, and gradually climbing up to broader public understanding, thus serving the interests of the lay society, too.

Dedication to Quality

Each Frontiers article is a landmark of the highest quality, thanks to genuinely collaborative interactions between authors and review editors, who include some of the world's best academicians. Research must be certified by peers before entering a stream of knowledge that may eventually reach the public - and shape society; therefore, Frontiers only applies the most rigorous and unbiased reviews.
Frontiers revolutionizes research publishing by freely delivering the most outstanding research, evaluated with no bias from both the academic and social point of view. By applying the most advanced information technologies, Frontiers is catapulting scholarly publishing into a new generation.

What are Frontiers Research Topics?

Frontiers Research Topics are very popular trademarks of the Frontiers Journals Series: they are collections of at least ten articles, all centered on a particular subject. With their unique mix of varied contributions from Original Research to Review Articles, Frontiers Research Topics unify the most influential researchers, the latest key findings and historical advances in a hot research area! Find out more on how to host your own Frontiers Research Topic or contribute to one as an author by contacting the Frontiers Editorial Office: researchtopics@frontiersin.org

EPIGENETIC MECHANISMS IN NEURAL PLASTICITY

Topic Editors:
Daniel Ortuño-Sahagún, Universidad de Guadalajara, Mexico
Reinhard Schliebs, University of Leipzig, Germany
Merce Pallàs, University of Barcelona, Spain

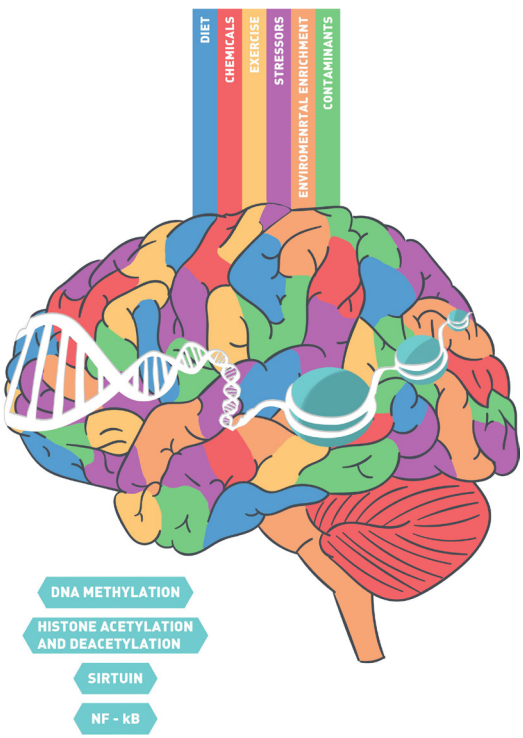

Image: Bernardo Magallanes and Daniel Ortuño.

Neural plasticity is a unique and adaptive feature of nervous system, which allows neurons to reorganize their interactions in response to a stimulation (intrinsic or extrinsic) to maintain their function. For these reasons, epigenetics emerges as a potential field for developing strategies to modulate changes in pathological situation because extrinsic factors and pharmacological tools can modify neural functioning in organisms during their life. Diet, exercise, environmental aspects, stressors or drugs are available to alter those mechanisms. Epigenetic involves certain molecular signaling pathways, as DNA methylation and histone acetylation and deacetylation, and the emerging non-coding small RNA, mainly microRNA, as a commanders of a number of translation processes. As most of molecular nervous cell alterations, epigenetic mechanisms play an important role in neural plasticity.

This eBook collects the burgeoning advances in epigenetic mechanisms, focusing on new insights into cellular and molecular neurobiological mechanisms that underlie brain functioning in health and pathological conditions. Contributions go from basic cellular mechanism to therapeutic opportunities to tackle the challenges on nervous central system development and neurodegeneration.

Citation: Ortuño-Sahagún, D., Schliebs, R., Pallàs, M., eds. (2019). Epigenetic Mechanisms in Neural Plasticity. Lausanne: Frontiers Media. doi: 10.3389/978-2-88963-000-4

Table of Contents

CHAPTER 3
PLASTICITY MODIFICATION BY ENVIROMENT THROUGH EPIGENETIC TAGS

frontiers in Cellular Neuroscience

EDITORIAL
published: 24 April 2019
doi: 10.3389/fncel.2019.00118

Editorial: Epigenetic Mechanisms Regulating Neural Plasticity

Daniel Ortuño-Sahagún[1]*, *Reinhard Schliebs*[2]* and *Merce Pallàs*[3]*

[1] *Laboratorio de Neuroinmunomodulación Molecular, Instituto de Investigación en Ciencias Biomédicas, Centro Universitario de Ciencias de las Salud, Universidad de Guadalajara, Guadalajara, Mexico,* [2] *Medical Faculty, Paul Flechsig Institute for Brain Research, University of Leipzig, Leipzig, Germany,* [3] *Department of Pharmacology and Therapeutic Chemistry, Institut de Neurociències, University of Barcelona, Barcelona, Spain*

Keywords: neural plasticity, epigenetics (MeSH), aging, epigenetic regulating mechanisms, central nervous system, epigenome, neurodegenerative disease, CNS disorders

Editorial on the Research Topic

Epigenetic Mechanisms Regulating Neural Plasticity

While larger parts of the genome have been deciphered and sequenced during the last decade, it is now possible to identify practically all the genes that a cell or tissue transcribes and translates at a given moment in time (Wheeler et al., 2008). Thus, the challenge we are now facing is to understand the epigenetic regulation of all this information, it will be the next great task in the near future. The central nervous system (CNS), and especially the brain, has evolved to make humans the way they are, and it is strongly influenced and affected by epigenetic factors (Stroud et al., 2017). Indeed, many extrinsic factors can alter neural activity during the lifetime of an organism (from the embryo to adult and during aging), including diet, exercise, environmental variations, stressors, etc. These stimuli exert their effect through processes commonly referred to as "Epigenetic mechanisms" (Sen et al., 2016), which mainly involve DNA methylation and demethylation, protein acetylation and deacetylation (mainly histones) and regulatory small non-coding RNAs, primarily microRNAs (miRNA) activity, all important events in the regulation of neuronal plasticity. Consequently, this special issue aims to shed light on the physiological and pathological processes affected by epigenetic mechanisms that are involved in the regulation of neural plasticity, highlighting the potential diagnostic and therapeutic strategies that may become commonplace in the future. Accordingly, this volume presents a collection of works, both reviews and original studies, that address the aforementioned issues, representing the ideas of 100 researchers from eight countries on three continents.

Epigenetic mechanisms have been proposed to strongly participate in the adaptive features of the CNS, both those of a physiological (from embryonic development through aging) and pathological (from cancer to neurodegenerative conditions) nature. Changes in the epigenome allow neurons to reorganize in response to intrinsic or extrinsic stimuli, and to develop or maintain specific activities. As such, the study of epigenetics is potentially interesting when attempting to develop strategies that modulate changes provoked in pathological conditions, particularly since extrinsic factors and pharmacological tools can modify neural function in an organism throughout its life. Therefore, diet, exercise, environmental conditions, stressors or drugs can alter pathological events to benefit the patient, driving epigenetic processes that co-ordinate a number of translational processes.

Post-translational modifications have been implicated in neurological pathologies like Parkinson's disease (PD), including protein acetylation. In fact, when acetylated proteins and peptides were characterized in primary fibroblasts from patients with inherited and idiopathic PD, differences were described in the hyperacetylated and hypoacetylated peptides between the two pathological entities (see Yakhine-Diop et al.). Additionally, acetyl-CoA metabolism is relevant in regulating multiple protein acetylation reactions in the brain, which in turn regulate the functional

OPEN ACCESS

Edited and reviewed by:
Christian Hansel,
University of Chicago, United States

Reviewed by:
Paola Tognini,
University of California, Irvine, United States

***Correspondence:**
Daniel Ortuño-Sahagún
dortuno@cucs.udg.mx
Reinhard Schliebs
reinhard.schliebs@googlemail.com
Merce Pallàs
mpallaslliberia@gmail.com

Received: *26 January 2019*
Accepted: *11 March 2019*
Published: *24 April 2019*

Citation:
Ortuño-Sahagún D, Schliebs R and Pallàs M (2019) Editorial: Epigenetic Mechanisms Regulating Neural Plasticity. Front. Cell. Neurosci. 13:118. doi: 10.3389/fncel.2019.00118

and adaptative properties of brain cells (both neuronal and non-neuronal). Ronowska et al. highlights the importance of the changes in intraneuronal acetyl-CoA and its compartmentalization, which contributes to the development of different neurodegenerative brain disorders.

Epigenetic elements or tags can be read (recognized), written (established), and erased (removed) in nucleosomes, mainly through DNA methylation and demethylation. The influence of demethylation in the adult brain and on neurological disorders, as well as its possible functional consequences for health and disease, has been reviewed by Bayraktar and Kreutz. Similarly, a key role for epigenetic DNA modifications has been identified by Andrés-Benito et al. demonstrating a decrease in the methylation of the Katanin Interactor Protein gene (KIAA0566) in association with age and the presence of neurofibrillary tangles, the main pathological characteristics of taupathies. Indeed, this particular alteration in DNA methylation has important implications for the regulation of microtubule homeostasis in locus coeruleus neurons. The review by Penas and Navarro focuses on the implication of a wider set of epigenetic changes that appear to trigger modifications in nociception after neural lesions, including histone modifications, DNA methylation, the expression of non-coding RNAs and altered chromatin modifier activity. As such, novel putative targets to manage neuropathic pain are proposed, which remains an unmet clinical need, such as histone deacetylases (HDAC1, Sirt1), histone demethylases (JMJD3), histone methyltransferases (G9a, EZH2), DNA methyltransferase (DNMT3b), transcriptional repressor complex (REST), Methyl CpG binding protein (MeCP2), and various non-coding RNAs. The correct delivery of microRNAs is a key factor for their possible therapeutic application and Reza-Zaldivar et al. explain why exosomes could constitute an adequate vehicle for the delivery of microRNAs in biological systems, for example, as an alternative treatment for Alzheimer's disease.

In addition to the aforementioned epigenetic mechanisms, stress, changes in diet and the environment, or even situations of extreme environments like outer space, can influence neuroplasticity and consequently, affect the activity of the CNS. In this respect, Herrera et al. demonstrate that controlling dietary long-chain polyunsaturated fatty acid (L-CPFA) content modulates the expression of synaptogenesis-related neuronal proteins, in conjunction with the influence of hormones. Indeed, estradiol and progesterone levels, as well as cyclic ovarian secretory activity, may modulate the effects of dietary L-CPFA in cerebral cortex physiology, which for example, may have clinical implications for postmenopausal women. In addition, Benoit et al. show how nutrient variations and hormonal changes early in development can reprogram metabolism in adulthood. Specifically, they demonstrate the changes in expression of eleven microRNAs induced by hyperinsulinemia and/or hyperleptinemia in the arcuate nucleus, a master regulator of energy homeostasis. This reveals how an altered perinatal environment can affect metabolism in adulthood.

With respect to the importance of the environment on genomic expression, Griñán-Ferré et al. demonstrate how significant improvements in brain function and cognitive abilities can be achieved in a model of aging through interventions that involve environmental enrichment. Importantly, these authors demonstrate that epigenetic mechanisms at least in part drive some of the beneficial effects of environmental enrichment, such as the decreased neuroinflammation and enhanced synaptic function. As described previously, environmental enrichment increases the cognitive reserve in humans, helping combat the deleterious effects of neurodegeneration (Redolat and Mesa-Gresa, 2012). Hence, the individual's physical and social surroundings are clearly important in providing the brain with some arms to resist neurodegenerative processes, increasing resilience of paramount importance in aging processes.

By contrast, the work by Muñoz-Llanos et al. focuses on the effect of chronic stress on synaptic plasticity in the hippocampus, giving importance to the effect of epigenetic mechanisms on learning and memory processes. They identified miRNA-92a and miR-485 as potential targets to produce changes in gene regulatory networks within the hippocampus of stressed rats, modifying the dynamics of neuroplasticity. As such, these non-coding regulatory RNAs could represent novel targets for the treatment of depression.

Finally, Cui et al. present a detailed genomic analysis of the differentiation of neuronal stem cells (NSCs) in outer space flights. During such spaceflight experimental conditions, NSCs maintain a greater capacity for stemness even though their growth rate slows down. This type of study will help us begin to understand the possible physiological changes in the CNS associated with future space travel.

In conjunction, in this volume breakthrough new information is collected regarding the cellular and molecular mechanisms underlying synaptic plasticity in neurodegenerative diseases like Parkinson's, or Alzheimer's, as well as in other CNS disorders like depression or neuropathic pain. In addition, further valuable information is provided regarding the physiology of the brain, all from the perspective of epigenetic regulation.

AUTHOR CONTRIBUTIONS

All authors listed have made a substantial, direct and intellectual contribution to the work, and approved it for publication.

FUNDING

This work was supported by the Ministerio de Economía, Industria y Competitividad and Fondo Europeo de Desarrollo Regional (MINECO-FEDER) (SAF2016-77703).

ACKNOWLEDGMENTS

We would like to thank the authors for having confidence in us with regard to this initiative and for their commitment to this proposal, by sending their manuscripts and sharing their leading-edge research data and stimulating ideas. We are also in debt and grateful to all of the reviewers for their generously devoted time and highly valuable insights.

REFERENCES

Redolat, R., and Mesa-Gresa, P. (2012). Potential benefits and limitations of enriched environments and cognitive activity on age-related behavioural decline. *Curr. Top. Behav. Neurosci.* 10, 293–316. doi: 10.1007/7854_2011_134

Sen, P., Shah, P. P., Nativio, R., and Berger, S. L. (2016). Epigenetic mechanisms of longevity and aging. *Cell* 166, 822–839. doi: 10.1016/j.cell.2016.07.050

Stroud, H., Su, S. C., Hrvatin, S., Greben, A. W., Renthal, W., Boxer, L. D., et al. (2017). Early-life gene expression in neurons modulates lasting epigenetic states. *Cell* 171, 1151–1164.e16. doi: 10.1016/j.cell.2017.09.047

Wheeler, D. A., Srinivasan, M., Egholm, M., Shen, Y., Chen, L., McGuire, A., et al. (2008). The complete genome of an individual by massively parallel DNA sequencing. *Nature* 452, 872–876. doi: 10.1038/nature06884

Conflict of Interest Statement: The authors declare that the research was conducted in the absence of any commercial or financial relationships that could be construed as a potential conflict of interest.

frontiers in Cellular Neuroscience

ORIGINAL RESEARCH
published: 17 April 2018
doi: 10.3389/fncel.2018.00097

Acetylome in Human Fibroblasts From Parkinson's Disease Patients

Sokhna M. S. Yakhine-Diop[1,2], Mario Rodríguez-Arribas[1,2], Guadalupe Martínez-Chacón[1,2], Elisabet Uribe-Carretero[1,2], Rubén Gómez-Sánchez[3], Ana Aiastui[1,4,5], Adolfo López de Munain[1,5,6,7,8], José M. Bravo-San Pedro[9,10,11,12,13], Mireia Niso-Santano[1,2], Rosa A. González-Polo[1,2] and José M. Fuentes[1,2*]*

[1] Centro de Investigación Biomédica en Red en Enfermedades Neurodegenerativas, Madrid, Spain, [2] Departamento de Bioquímica y Biología Molecular y Genética, Facultad de Enfermería y Terapia Ocupacional, Universidad de Extremadura, Cáceres, Spain, [3] Department of Cell Biology, University of Groningen, University Medical Center Groningen, Groningen, Netherlands, [4] Cell Culture Plataform, Donostia University Hospital, San Sebastián, Spain, [5] Neuroscience Area of Biodonostia Health Research Institute, Donostia University Hospital, San Sebastián, Spain, [6] Department of Neurology, Donostia University Hospital, San Sebastian, Spain, [7] Ilundain Fundazioa, San Sebastian, Spain, [8] Department of Neurosciences, University of the Basque Country UPV-EHU, San Sebastián, Spain, [9] Equipe 11 labellisèe Ligue Contre le Cancer, Centre de Recherche des Cordeliers, Paris, France, [10] INSERM U1138, Paris, France, [11] Université Paris Descartes/Paris V, Sorbonne Paris Cité, Paris, France, [12] Université Pierre et Marie Curie/Paris VI, Paris, France, [13] Gustave Roussy Comprehensive Cancer Institute, Villejuif, France

Parkinson's disease (PD) is a multifactorial neurodegenerative disorder. The pathogenesis of this disease is associated with gene and environmental factors. Mutations in leucine-rich repeat kinase 2 (LRRK2) are the most frequent genetic cause of familial and sporadic PD. Moreover, posttranslational modifications, including protein acetylation, are involved in the molecular mechanism of PD. Acetylation of lysine proteins is a dynamic process that is modulated in PD. In this descriptive study, we characterized the acetylated proteins and peptides in primary fibroblasts from idiopathic PD (IPD) and genetic PD harboring G2019S or R1441G *LRRK2* mutations. Identified acetylated peptides are modulated between individuals' groups. Although acetylated nuclear proteins are the most represented in cells, they are hypoacetylated in IPD. Results display that the level of hyperacetylated and hypoacetylated peptides are, respectively, enhanced in genetic PD and in IPD cells.

Keywords: acetylation, LRRK2, peptides, Parkinson, proteins

OPEN ACCESS

Edited by:
Merce Pallas,
Universitat de Barcelona, Spain

Reviewed by:
Joaquin Jordan,
Universidad de Castilla La Mancha Albacete, Spain
Carlos Guillén,
Complutense University of Madrid, Spain

***Correspondence:**
Rosa A. González-Polo
rosapolo@unex.es
José M. Fuentes
jfuentes@unex.es

***Received:** 30 January 2018*
***Accepted:** 22 March 2018*
***Published:** 17 April 2018*

Citation:
Yakhine-Diop SMS, Rodríguez-Arribas M, Martínez-Chacón G, Uribe-Carretero E, Gómez-Sánchez R, Aiastui A, López de Munain A, Bravo-San Pedro JM, Niso-Santano M, González-Polo RA and Fuentes JM (2018) Acetylome in Human Fibroblasts From Parkinson's Disease Patients. Front. Cell. Neurosci. 12:97. doi: 10.3389/fncel.2018.00097

INTRODUCTION

Parkinson's disease (PD) is a disabling neurological disorder that is in progressive evolution. This neurodegeneration mainly affects the dopaminergic neurons of the *susbtancia nigra pars compacta* that are in part responsible for clinical motor symptoms. The widespread of this neurodegeneration from the midbrain to other neurotransmitter (serotoninergic and noradrenergic) systems elicits the appearance of non-motor symptoms (Politis and Loane, 2011; Deusser et al., 2015). Although well not understood, the etiopathogenesis of PD has thought related to environmental factors and gene mutations. Almost 90% of PD cases are sporadic (Ammal Kaidery et al., 2013), and may due to the susceptibility of genetic predisposition to environmental factors (Yakhine-Diop et al., 2014). Mutations in leucine-rich repeat kinase 2 (LRRK2) have been associated with autosomal dominant PD and involved in familial and idiopathic cases. Among six pathogenic LRRK2 mutations

Abbreviations: CI, Confidence interval; FA, Trifluoroacetic acid; FDR, False decoy recovery; GAPDH, Glyceraldehyde-3-phosphate dehydrogenase; H2B, Histone 2B; HAT, Histone acetyltransferase; HDAC, Histone deacetylase; ID, Identification; IPD, Idiopathic Parkinson's disease; K, Lysine; LC-MS, Liquid chromatography-mass spectrometry; LRRK2, Leucine-rich repeat kinase 2; PD, Parkinson's disease; PDHA1, Pyruvate dehydrogenase; PSPEP, Proteomics System Performance Evaluation Pipeline Software; ROS, Reactive oxygen species.

(R1441G/C/H, Y1699C, G2019S, and I2020T), the most frequent is the G2019S that affect almost 5% of familial PD and 2% of sporadic PD (Li et al., 2014). G2019S and R1441G are located, respectively, in the kinase and GTP domains of LRRK2 protein. Both mutations participate in the pathogenicity of PD through the impairment of LRRK2 enzymatic activity (Martin et al., 2014).

Evidence has reported that PARK genes, among other *synuclein* (*SNCA*) and *LRRK2*, regulate epigenetic mechanisms, thereby modulate gene expression (Coppedè, 2012). Indeed, gene expression is altered through posttranslational modifications of histones (methylation, phosphorylation, ubiquitination, and acetylation) and affects individual phenotypes (Ammal Kaidery et al., 2013). Parkinsonism-related toxins modulate histone acetylation by either decreasing histone deacetylase (HDAC) activity (Song et al., 2011) or increasing histone acetyltransferase (HAT) activity (Song et al., 2010). Studies, in PD post mortem brains, have reported that histone acetylation is upregulated in midbrain neurons; however, in some patients, this acetylation level varies differentially according to the brain regions and cell types (Park et al., 2016).

Acetylation is the transfer of an acetyl group from acetyl coenzyme A to the ε-amino group of lysine residues in proteins (histone and non-histone proteins) or to the α-amino group of the N-terminus of proteins. N-terminal acetylation is an irreversible reaction that is catalyzed by N-terminal acetyltransferases, whereas lysine acetylation is regulated by the balance of two enzymes HAT and HDAC (Drazic et al., 2016). The combination of these both acetylation reactions constitutes the acetylome. Acetylome in PD models is poorly characterized, only the variation of histone acetylation has been widely reported. Given that it may have an important role in PD pathogenesis, we identified some of those proteins that are acetylated in PD-associated (G2019S and R1441G) *LRRK2* mutations and idiopathic PD. Importantly, there are more acetylated peptides in genetic PD models and acetylated proteins are mainly nuclear and cytosolic.

MATERIALS AND METHODS

Cell Culture

Fibroblasts from PD patients (with or without *LRRK2* mutations) and from control subjects were provided by Dr. Adolfo López de Munaín. Experiments were performed using four cell lines: Control (Co, patients who did not develop PD), IPD (IPD, PD patients without *LRRK2* mutations), GS (PD patients with G2019S *LRRK2* mutation), and RG (PD patients with R1441G *LRRK2* mutation). This study was carried out in accordance with the recommendations of Comité Ético de Investigación Clínica del Área Sanitaria de Gipuzkoa. All subjects gave written informed consent in accordance with the Declaration of Helsinki. Cells were grown in Dulbecco's modified Eagle's medium (DMEM, Sigma-Aldrich, D6546) supplemented with 10% of fetal bovine serum (FBS, Sigma-Aldrich, F7524), 1% L-glutamine (Sigma-Aldrich, G7513) and 2 mL streptomycin/penicillin (HyClone, Thermo Fisher Scientific, SV30010) at 37°C in 5% CO_2/95% air. To confirm the G2019S or R1441G *LRRK2* mutations in cells, DNA was extracted (Macherey-Nagel Kit, 740952.50) and sequenced at STAB VIDA (Caparica, Portugal). In this study, we worked with pooled cell lines ranging from three to four cell lines (**Table 1**). Human fibroblasts (HFs) were seeded at a density of 3.5×10^4 cells/mL and from lower passages.

Digestion and Desalting of Peptides

Samples (Co, IPD, GS, and RG) were resuspended in 400 μL of 50 mM ammoniun bicarbonate and quantified by Bradford protein assay (BioRad). For each sample, 2 mg protein were diluted in 8 M Urea in-solution trypsin digestion. Proteins were reduced, alkylated, and digested with a 1:20 (w /w) ratio of recombinant trypsin sequencing grade (Roche) overnight at 37°C. Peptides from digested proteins were desalted and concentrated with a C18 reversed phase chromatography (ZipTip C18, Millipore) and the peptides were eluted in 50% acetonitrile (ACN)/0.1% trifluoroacetic acid (FA). Finally, the samples were freeze-dried in SpeedVac and dissolved in 200 μL of NETN (100 mM NaCl, 1 mM EDTA, 50 mM Tris pH 8, and 0.5% Nonidet P40) buffer for affinity enrichment of lysine-acetylated peptides.

Enrichment of Lysine-Acetylated Peptides

Samples in NETN buffer were incubated with anti-acetyl lysine agarose beads (catalog no. PTM-104, PTM Biolabs) at 4°C overnight with gentle shaking. After incubation, the beads were carefully washed three times with NETN buffer, twice with ETN buffer (1 mM EDTA, 50 mM Tris pH 8, and 100 mM NaCl), and once with water. The immunoprecipitated peptides were eluted with 1% FA and dried in a SpeedVac. The resulting peptides were cleaned with C18 Zip Tips (Millipore) according to the manufacturer's instructions and were dissolved in 12 μL of 2% ACN/0.1% FA then subjected to LC–MS/MS analysis by Triple TOF 5600 (SCIEX).

TABLE 1 | Presentation of the four groups of pooled cell lines.

Groups	Names	Dates of Birth	Genotypes
Co	Co1	1956–1977	LRRK2 WT
	Co2		LRRK2 WT
	Co3		LRRK2 WT
	Co4		LRRK2 WT
IPD	IPD1	1928–1954	LRRK2 WT
	IPD2		LRRK2 WT
	IPD3		LRRK2 WT
GS	GS1	1945–1949	G2019S Heterozygous
	GS2		G2019S Heterozygous
	GS3		G2019S Heterozygous
RG	RG1	1931–1942	R1441G Heterozygous
	RG2		R1441G Heterozygous
	RG3		R1441G Heterozygous

The control group consists of four individuals, the IPD, GS and RG groups of three individuals each. We present in this table the range age of each group, and the genotype of each individual.

Protein Identification

MS/MS data sets were identified using Mascot licensed version 2.3.02 (Matrix Sciences) and ProteinPilot (revision 4895; AB SCIEX 5.0.1) using the Paragon algorithm (5.0.1.0, 4874). All data files were searched using the SwissProtHuman 2015_09_17 database with 42136 sequences. Search parameters in Mascot for acetylated peptides were as follows: trypsin digestion with five missed cleavages to account the inability of trypsin to cleave at acetylated lysine residues. Lysine acetylation, N-terminal acetylation and methionine oxidation were set as variable modifications, and carbamidomethyl cysteine as a fixed modification. Precursor ion and fragment ion mass tolerances were set to 30 ppm and 0.6 Da, respectively. Further, the decoy database search (Mascot integrated decoy approach) was used to false decoy recovery (FDR) calculation and the percolator algorithm applied to Mascot results. The acceptances criteria for proteins identification were a FDR < 1% and at least one peptide identified with a confidence interval (CI > 95%). In ProteinPilot, the following sample parameters were used: trypsin digestion, cysteine alkylation with iodoacetamide, and acetylation emphasis. A thorough identification (ID) search was done. Thus, a local FDR of 1% was chosen using the ProteinPilot FDR analysis tool (PSPEP) algorithm and a peptide CI value of 95%.

Protein Relative Quantification

For human proteins relative quantification in (Co, IPD, GS, and RG) samples, the Raw profile data files (.raw) were imported into Progenesis LC-MS for proteomics (64-bit version v 4.1; Nonlinear Dynamics/Waters). Imported runs were chromatographic aligned to the reference run identified by the software. All runs were selected for peak picking with the automatic sensitivity method (default settings) and filtered to include only peaks with a charge state between 2 and 5. All detected features were normalized against the reference run by Progenesis LC-MS. Between-subject comparison was used as experimental design (Co, IPD, GS, and RG). Spectral data from selected features (p-value < 0.05) were transformed to Mascot generic format (MGF) files with Progenesis LC-MS and exported for peptide/protein identification to Mascot search engine, using the searched parameters above described. Mascot search results, that exceed the acceptance criteria for identification (FDR < 1%, peptides with individual ion scores >13, p < 0.05), were imported into Progenesis LC-MS as XML files and analyzed according to the following criteria: only were used quantitation from non-conflicting peptides. For each protein, the number or reported peptides was determined by counting unique peptide sequence. Only proteins reported by one or more peptides with a p-value < 0.05 were quantified.

Protein abundance was calculated from the sum of all unique normalized peptide ion abundance. Protein reported abundance is the geometric mean of the biological replicates. Proteins with a likelihood of quantification smaller than 0.05 (Anova p-value) were considered to be significantly regulated. Normalized peptide intensities were used to calculate fold-changes between samples. Relative abundance of human proteins (fold change) in three conditions compared with corresponding proteins in control samples were quantified by the ratio of summed peptide ion normalized abundance in each group to evaluate the enrichment of the protein. Differentially expressed proteins (p < 0.05) were considered with a fold change ≥1.3 and at least 1 identified peptides in at least one of replicates.

Immunofluorescence

HFs were seeded on 96-well plate at a density of 3500 cells/well. Cells were successively fixed with 4% PFA and permeabilized with 0.1% Triton (Sigma-Aldrich, T9284) for 20 and 5 min, respectively, at room temperature (RT). Once permeabilized, plated cells were incubated with bovine serum albumin (BSA)/PBS solution (1 mg/mL) for 1 h at RT and then with the primary antibody acetyl-H4 (G-2) (Ser1K5K8K12) (1:50, Santa Cruz Biotechnology, sc-393472), while shaking overnight at 4°C. The following day, cells were reincubated with Alexa Fluor® 568 (1:100 Thermo Scientific, A11004)-conjugated secondary antibodies for 1 h at RT. Nuclei were stained with Hoechst 33342 (2 μM, Sigma Aldrich, B2261). Images were visualized using an Olympus IX51 inverted microscope.

Statistical Analyses

Statistical analyses were assessed by Student's t-test, Chi-Squared test or Anova test. The results were considered significant at p<0.05.

RESULTS

Detection of Acetylated Proteins

We determined the N-terminal acetylation and acetylated lysine (Ac-K) proteins in fibroblasts from PD patients and control subjects. In **Tables 2**, **3**, we have listed some of those acetylated proteins. Some of them (fructose bisphosphate aldolase C (ALDOC), Glyceraldehyde-3-phosphate dehydrogenase (GAPDH), Alpha-Enolase, pyruvate kinase) are enzymes that participate at different steps of glycolysis pathway (TeSlaa and Teitell, 2014). The rest of acetylated proteins are implicated in cell proliferation, acetylation, apoptosis and nucleosome wrap, as well in the link between glycolysis and citric acid cycle. Most of those proteins were located in the nucleus and the cytoplasm and represent, respectively, 52 and 36% of acetylated proteins in PD patients (**Figure 1A**). The less represented were found in plasma membrane (8%) and mitochondrion (4%).This distribution did not change in the control group but the proportion slightly differs. The number of Ac-K sites on proteins varied from one to ten (**Tables 2**, **3**) and can be found on distinct peptides. Furthermore, in PD models some acetylated proteins had more or less Ac-K sites than Control line (**Table 2**). Interestingly, we found that the ratio of acetylated peptides/non-acetylated peptides was enhanced in GS and RG cells while it was decreased in IPD cells (**Figure 1B**). We inferred that there were more acetylated peptides levels in familial PD than in sporadic PD. These variations were significant between genetic and idiopathic PD.

TABLE 2 | Acetylated proteins in fibroblasts from PD patients with or without LRRK2 mutation.

Protein ID	Protein Name	Subcellular Location	Ac-K Sites
P07355	Annexin A2	Extracellular space, Extracellular matrix	10
P04083	Annexin A1	Nucleus, Cytoplasm, Cell membrane	1
P08670	Vimentin	Cytoplasm	2
Q9BQE3	α-Tubulin 1C	Cytoplasm, Cytoskeleton	1
P68363	α-Tubulin 1B	Cytoplasm, Cytoskeleton	1
P14618	Pyruvate kinase	Cytoplasm, Nucleus	2
Q6PEY2	α-Tubulin 3E	Cytoplasm, Cytoskeleton.	1
P08758	Annexin A5	–	4
P21333	Filamin-A	Cytoplasm, Cell cortex, Cytoskeleton.	1
P62805	Histone H4	Nucleus, Chromosome	4
Q9GZZ1	NAA50	Cytoplasm	2
Q09472	HAT p300	Cytoplasm, Nucleus.	5
Q92793	CBP	Cytoplasm, Nucleus.	2
Q99880	H2B1L	Nucleus, Chromosome	4
P04406	GAPDH	Cytoplasm, Cytoskeleton	4
P68371	β-Tubulin 4B	Cytoplasm, Cytoskeleton, Nucleus	1
P07437	β-Tubulin	Cytoplasm, Cytoskeleton.	1
P06733	Alpha-enolase	Cytoplasm, Cell membrane	4
O43809	CPSF5	Nucleus	1
P62328	Thymosin β-4	Cytoplasm, Cytoskeleton.	3
P22392	NME2	Cytoplasm, Nucleus	2
Q15942	Zyxin	Cytoplasm, Cytoskeleton, Nucleus, Cell junction	2
P21796	VDAC1	Outer mitochondrial membrane	1
P20962	Parathymosin	Nucleus	4
P08559	PDHA1	Mitochondrial matrix	4
P06454	Prothymosin α	Nucleus	5
P68871	Hemoglobin β	–	1
P02042	Hemoglobin Δ	–	1
P09972	ALDOC	–	1
P04792	Heat shock protein beta-1	Cytoplasm, Nucleus	1
P06703	Protein S100-A6	Nucleus envelope, Cell membrane	1
P00338	LDHA A	Cytoplasm	4

We specified the subcellular location of proteins and the number of acetylation sites. Lines filled in blue represent the most relevant variations identified in PD models compared to control.

TABLE 3 | Acetylated proteins in human fibroblasts from control subjects.

Protein ID	Protein Name	Subecellular Location	Ac-K Sites
P07355	Annexin A2	Extracellular space, Extracellular matrix	10
P04083	Annexin A1	Nucleus, Cytoplasm, Cell membrane	2
P08670	Vimentin	Cytoplasm	4
Q9BQE3	Tubulin α-1C	Cytoplasm, Cytoskeleton	2
P08758	Annexin A5	–	3
P21333	Filamin-A	Cytoplasm, Cell cortex, Cytoskeleton.	1
P62805	Histone H4	Nucleus, Chromosome	3
Q9GZZ1	NAA50	Cytoplasm	2
Q09472	HAT p300	Cytoplasm, Nucleus.	1
Q92793	CBP	Cytoplasm, Nucleus.	2
Q99880	H2B1L	Nucleus, Chromosome	4–7
P04406	GAPDH	Cytoplasm, Cytoskeleton	2
P68371	Tubulin β-4B	Cytoplasm, Cytoskeleton, Nucleus	1
P07437	Tubulin β	Cytoplasm, Cytoskeleton.	1
P06733	Alpha-enolase	Cytoplasm, Cell membrane	4
O43809	CPSF5	Nucleus	1
P62328	Thymosin β-4	Cytoplasm, Cytoskeleton.	2
P22392	NME2	Cytoplasm, Nucleus	2
Q15942	Zyxin	Cytoplasm, Cytoskeleton, Nucleus, Cell junction	2
P21796	VDAC1	Outer mitochondrial membrane	1
P20962	Parathymosin	Nucleus	2
P06454	Prothymosin α	Nucleus	4
P68871	Hemoglobin β	–	1
P02042	Hemoglobin Δ	–	1
P09972	ALDOC	–	1
P06703	Protein S100-A6	Nucleus envelope, Cell membrane	1
P00338	LDHA A	Cytoplasm	4
P04075	ALDOA	–	1
P08133	ANXA6	Cytoplasm	4
P06748	NPM	Cytoplasm, Nucleus	1
Q8NCA9	ZN784	Nucleus	1
P33778	H2B1B	Nucleus	3
P16401	Histone1.5	Nucleus	2

The subcellular location of proteins and the number of Ac-k sites.

Identification of Acetylated Peptides and Proteins in PD Fibroblasts

To elucidate these differences, PD patients' data were compared to Co data. We observed that there were four acetylated proteins only belonged to Co (**Figures 1C–E**), however two of them (Nucleophosmin and Zinc finger protein 784) were constant. The pairs of thymosin β4 and H2B1B or H2B1B and H2B1M or Annexin A6 and Histone 1.5 were additionnally found in Co line when compared to IPD, GS, and RG lines, respectively. Moreover, Co and PD lines have acetylated proteins in common. From the detected acetylated proteins based on the comparison effectuated respect to Co line, distinct acetylated peptides were identified and were characteristic of each group. Thus, 2 out of 5 acetylated peptides [**S**TVHEILCK (Annexin A2 protein) and **K**GS**KK**AVT**K**AQKK (H2B1L protein)] are specific to IPD line, 2 to GS line [FLEQQN**K**ILLAELEQLK (Vimentin protein) and **K**GS**KK**AVTK (H2B1C protein)] and 1 out of 3 to RG line [GVTQFGN**K**YIQQTK (CPSF5 protein)]. Of note, proteins can be acetylated in one or more peptides, and following the group of healthy subjects or PD patients, the acetylation of

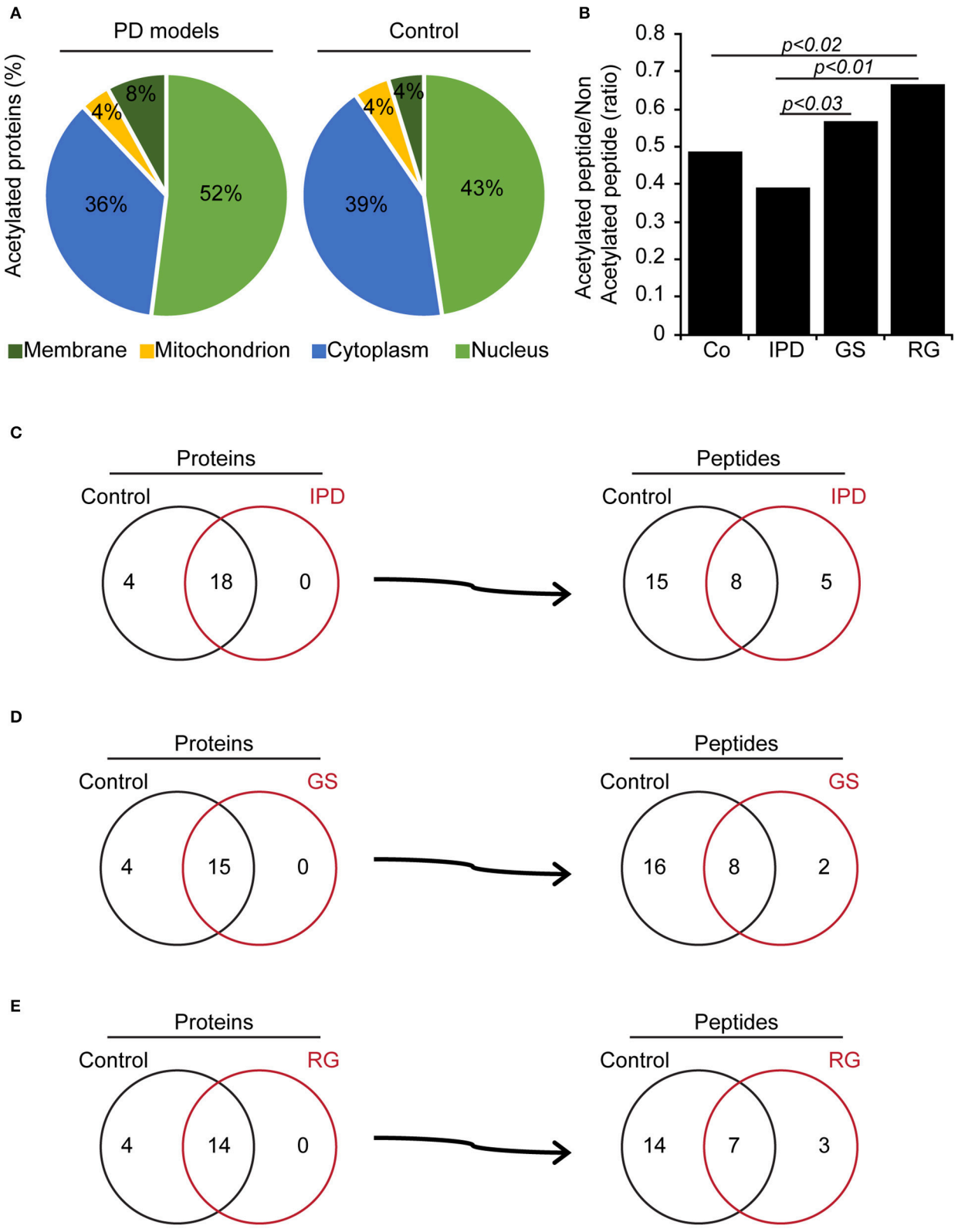

FIGURE 1 | Acetylated proteins in human fibroblasts. **(A)** Subcellular location of acetylated proteins (%) in human fibroblasts. **(B)** Ratio of identified acetylated peptides/non-acetylated peptides in human fibroblasts, $p < 0.03$, $p < 0.02$ and $p < 0.01$ compared to control (χ^2-test). **(C–E)** Comparison of acetylated proteins and identified acetylated peptides per proteins between Co line and PD models. **(C)** Co and IPD lines, **(D)** Co and GS lines **(E)** Co and RG lines represent the acetylome of each group and what they share in common.

one protein might change from one peptide to another and be monoactylated, polyacetylated or inexistent. Given that the fold change of acetylated peptides depend on the relative abundance of proteins, the level of acetylated peptides was classified in three categories (Normal, hypoacetylated, and hyperacetylated). Therefore, it exists more hypoacetylated peptides in IPD line than in Co line. Also, the percentage of hyperacetylated peptides was significantly increased in cells harboring LRRK2 mutations (**Figure 2A**). By immunofluorescence staining, we observed that the intensity of acetylated Histone 4 was significantly reduced in IPD line (**Figures 2B,C**).

DISCUSSION

Dysregulation of acetylation machinery can lead to neurodegenerative diseases. In fact, protein aggregation is a hallmark of neurodegeneration and it is regulated by protein acetylation including lysine acetylation (Lee and Finkel, 2009) and N-terminal acetylation. It has been reported that the N-terminal acetylation of SNCA prevents its aggregation by stabilizing protein formation (Bartels et al., 2014), besides that, N-terminal acetylation can also act as a recognition tag to mediate protein degradation (Zattas et al., 2013), thus N-acetylation deficiency could be associated with PD pathogenesis. Despite this protective effect, N-terminal acetylation can disturb further proteasome degradation interplaying the N-terminal ubiquitylation of α-amino group of proteins substrates (Tatham et al., 2013).

Even though 80% of human proteins are acetylated at their N-terminal, they are poorly considered (Aksnes et al., 2016). In this study, the proteins N-terminally acetylated in PD models are annexin A2, putative annexin A2-like protein, cytosolic (Thymosin β4, α-enolase), nuclear (parathymosin, protein S100-A6, prothymosin α), and participate in various cellular processes. These proteins are more represented in IPD line. In common to IPD and GS lines, prothymosin α (Qi et al., 2010) and

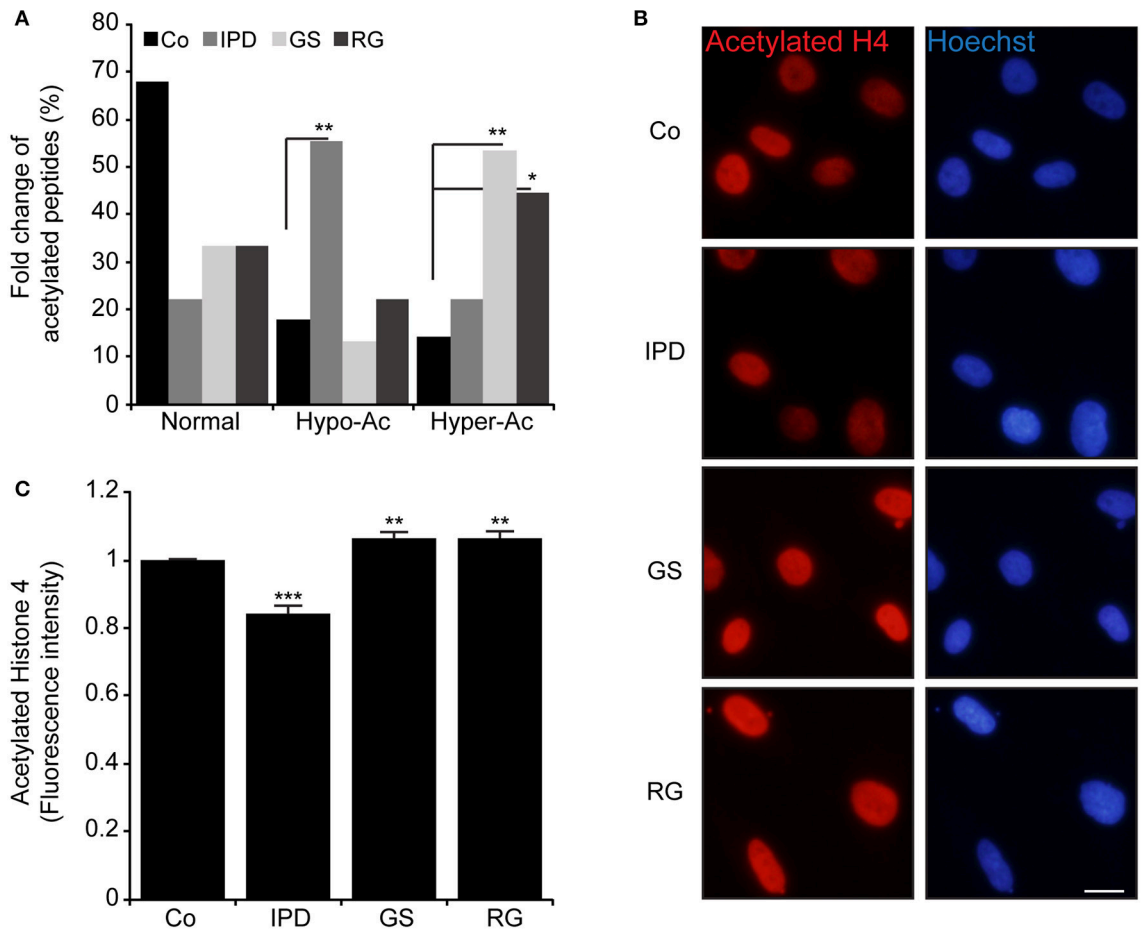

FIGURE 2 | Modulation of acetylated peptides in human fibroblast **(A)** Represents in % the fold change of hypoacetylated and hyperacetylated peptides in HFs compared to Co, $^{*}p < 0.05$ and $^{**}p < 0.01$ (χ^2-test). **(B,C)**. Acetylated histone 4 (Ac-H4K5K8K12) (red) was detected by immunofluorescence and the nuclei were stained with Hoechst 33342 (blue), Original magnification: 20X, scale bar corresponds to 10 μm. **(C)** Represents the quantification of fluorescence intensity of labeled Ac-H4K5K8K12 by imageJ ($n = 200$ cells). Data represent the mean ± SEM of at least three independent experiments, $^{**}p < 0.01$ and $^{***}p < 0.001$ respect to Co (Student's *t*-test).

protein S100-A6 (Bartkowska et al., 2017) are, respectively, anti-apoptotic and stress modulator. α-Enolase is found in RG line whereas annexin A2 is in all PD models. Annexins (A1, A2, and A5) are calcium sensors that translocate to plasma or nuclear membrane (Skrahina et al., 2008) and affect apoptosis pathways (Debret et al., 2003; Jiang et al., 2015). It remains to investigate whether the N-acetylated form of these proteins have a crucial role in the progression of PD. Acetylated thymosin β4 is common to both genetic PD lines, this protein has a critical role in actin polymerization (Mannherz et al., 2010). Moreover, *LRRK2* mutations influence cytoskeleton organization. In fact, GTP LRRK2 domain interacts with β-tubulin and increases the lysine acetylation of α-tubulin. However, this interaction is altered with G2019S and R1441G *LRRK2* mutations and affects the stability of microtubules (Law et al., 2014). Indeed, neither microtubule structure nor conformation has affected by α-tubulin acetylation but influences the tubulin-binding proteins therefore tubulin functions (Howes et al., 2014). Damaged mitochondria-induced reactive oxygen species (ROS) are responsible for α-tubulin hyperacetylation (Bonet-Ponce et al., 2016). Such modification is required for an adaptive cell response through autophagy induction, consequently, this hyperacetylation is negatively regulated by p300 upon stress (Mackeh et al., 2014). In G2019S *LRRK2* mutation, the reduction of mitochondrial membrane potential is accompanied by an increase of ROS production and an enhancement of the basal autophagy level (Yakhine-Diop et al., 2014). An impairment of autophagy induction was also observed in IPD and R1441G LRRK2 lines (Data not shown). The HATs p300 and CBP are acetylated in RG line, respectively, at five and 2 lysine positions, which means p300 basal activity is increased (Drazic et al., 2016). Even though, HAT and HDAC are involved in the modulation of protein acetylation, acetyl-CoA availability is critical. In mammals, acetyl CoA is in part generated from pyruvate by pyruvate dehydrogenase (PDHA1). Pyruvate is the final product of glycolysis pathway (Drazic et al., 2016). Some enzymes of this pathway are lysine acetylated in IPD, GS, and RG lines. This posttranslational modification can increase or decrease the enzymatic activity of certain proteins. In the case of acetylated PDHA1 in RG line, its activity is decreased (Drazic et al., 2016), therefore the level of acetyl-CoA formation from glycolysis may be reduced. The different pathways (glycolysis and fatty acid β-oxidation) generating acetyl CoA interplay in mitochondria. Generally, mitochondria are defective in PD, this dysfunction disturbs the acetylation machinery by reducing HDAC Class III (sirtuins) activity (Schwab et al., 2017). Additionally, an imbalance between HDAC and HAT activities lead to hyperacetylation (Park et al., 2016) or hypoacetylation of proteins. Taken together, proteins are acetylated in IPD and LRRK2 mutations-associated PD. However, it occurs more hyperacetylated proteins in cells harboring LRRK2 mutations than in IPD lines. This variation seems to be associated with the disease. Moreover, in healthy subjects harboring the R1441G *LRRK2* mutation, the intensity of acetylated proteins was enhanced (Data not shown). The molecular mechanism of protein acetylation in PD remains unclear. It will be interesting to elucidate how proteins can be hypoacetylated in IPD rather than in Genetic PD.

AUTHOR CONTRIBUTIONS

JF conceived the project. SY-D, JB-S, RG-S, MN-S, RG-P, and JF designed the experiments. SY-D, MR-A, GM-C, and EU-C performed experiments. MR-A performed the statistical analyses. Authors assisted in data analysis and interpretation. AA and AL performed the human fibroblast biopsies and culture. SY-D and JF wrote the manuscript. All authors revised and approved the content of the manuscript for publication.

ACKNOWLEDGMENTS

We are grateful to the patients and donors without which these work would not have been possible. The authors thank M. P. Delgado-Luceño. The proteomic analysis was performed in the Proteomics Facility of UCM that belongs to ProteoRed, PRB2-ISCIII, supported by grant PT13/0001. SY-D was supported by Isabel Gemio Foundation. EU-C was supported by a FPU predoctoral fellowship (FPU16/00684) from Ministerio de Educación, Cultura y Deporte, Spain. RG-S was supported by a Marie Sklodowska-Curie Individual Fellowship (IF-EF) (655027) from the European Commission. JB-S was funded by La Ligue Contre le Cancer. MN-S was supported by Contrato Ramon y Cajal (RYC-2016-20883) from Ministerio de Economia y Competitividad, Spain. MR-A was supported by a FPU predoctoral fellowship (FPU13/01237) from Ministerio de Educación, Cultura y Deporte, Spain. JF received research support from the Instituto de Salud Carlos III, CIBERNED (CB06/05/004) and Instituto de Salud Carlos III, FIS (PI15/00034). RG-P was supported by a Contrato destinado a la retención y atracción del talento investigador, TA13009 from Junta de Extremadura, as well as research support from the Instituto de Salud Carlos III, FIS (PI14/00170). This work was also supported by Fondo Europeo de Desarrollo Regional (FEDER) from the European Union. The authors also thank FUNDESALUD for helpful assistance.

REFERENCES

Aksnes, H., Drazic, A., Marie, M., and Arnesen, T. (2016). First things first: vital protein marks by N-terminal acetyltransferases. *Trends Biochem. Sci.* 41, 746–760. doi: 10.1016/j.tibs.2016.07.005

Ammal Kaidery, N., Tarannum, S., and Thomas, B. (2013). Epigenetic landscape of Parkinson's disease: emerging role in disease mechanisms and therapeutic modalities. *Neurotherapeutics* 10, 698–708. doi: 10.1007/s13311-013-0211-8

Bartels, T., Kim, N. C., Luth, E. S., and Selkoe, D. J. (2014). N-alpha-acetylation of alpha-synuclein increases its helical folding propensity, GM1 binding specificity and resistance to aggregation. *PLoS ONE* 9:e103727. doi: 10.1371/journal.pone.0103727

Bartkowska, K., Swiatek, I., Aniszewska, A., Jurewicz, E., Turlejski, K., Djavadian, A., et al. (2017). Stress-dependent changes in the CacyBP/SIP interacting protein S100A6 in the mouse brain. *PLoS ONE* 12:e0169760. doi: 10.1371/journal.pone.0169760

Bonet-Ponce, L., Saez-Atienzar, S., da Casa, C., Sancho-Pelluz, J., Barcia, J. M., Martinez-Gil, N., et al. (2016). Rotenone induces the formation of 4-hydroxynonenal aggresomes. role of ROS-mediated tubulin hyperacetylation and autophagic flux disruption. *Mol. Neurobiol.* 53, 6194–6208. doi: 10.1007/s12035-015-9509-3

Coppedè, F. (2012). Genetics and epigenetics of Parkinson's disease. *Sci. World J.* 2012:489830. doi: 10.1100/2012/489830

Debret, R., El Btaouri, H., Duca, L., Rahman, I., Radke, S., Antonicelli, B., et al. (2003). Annexin A1 processing is associated with caspase-dependent apoptosis in BZR cells. *FEBS Lett.* 546, 195–202. doi: 10.1016/S0014-5793(03)00570-2

Deusser, J., Schmidt, S., Ettle, B., Plotz, S., Huber, S., Kohl, C. P., et al. (2015). Serotonergic dysfunction in the A53T α-synuclein mouse model of Parkinson's disease. *J. Neurochem.* 135, 589–597. doi: 10.1111/jnc.13253

Drazic, A., Myklebust, L. M., Ree, R., and Arnesen, T. (2016). The world of protein acetylation. *Biochim. Biophys. Acta* 1864, 1372–1401. doi: 10.1016/j.bbapap.2016.06.007

Howes, S. C., Alushin, G. M., Shida, T., Nachury, M. V., and Nogales, E. (2014). Effects of tubulin acetylation and tubulin acetyltransferase binding on microtubule structure. *Mol. Biol. Cell* 25, 257–266. doi: 10.1091/mbc.E13-07-0387

Jiang, S. L., Pan, D. Y., Gu, C., Qin, H. F., and Zhao, S. H. (2015). Annexin A2 silencing enhances apoptosis of human umbilical vein endothelial cells *in vitro*. *Asian Pac. J. Trop. Med.* 8, 952–957. doi: 10.1016/j.apjtm.2015.10.006

Law, B. M., Spain, V. A., Leinster, V. H., Chia, R., Beilina, A., Harvey, H. J., et al. (2014). A direct interaction between leucine-rich repeat kinase 2 and specific β-tubulin isoforms regulates tubulin acetylation. *J. Biol. Chem.* 289, 895–908. doi: 10.1074/jbc.M113.507913

Lee, I. H., and Finkel, T. (2009). Regulation of autophagy by the p300 acetyltransferase. *J. Biol. Chem.* 284, 6322–6328. doi: 10.1074/jbc.M807135200

Li, J. Q., Tan, L., and Yu, J. T. (2014). The role of the LRRK2 gene in Parkinsonism. *Mol. Neurodegener.* 9:47. doi: 10.1186/1750-1326-9-47

Mackeh, R., Lorin, S., Ratier, A., Mejdoubi-Charef, N., Baillet, A., Perdiz, A., et al. (2014). Reactive oxygen species, AMP-activated protein kinase, and the transcription cofactor p300 regulate α-tubulin acetyltransferase-1 (α TAT-1/MEC-17)-dependent microtubule hyperacetylation during cell stress. *J. Biol. Chem.* 289, 11816–11828. doi: 10.1074/jbc.M113.507400

Mannherz, H. G., Mazur, A. J., and Jockusch, B. (2010). Repolymerization of actin from actin:thymosin β4 complex induced by diaphanous related formins and gelsolin. *Ann. N. Y. Acad. Sci.* 1194, 36–43. doi: 10.1111/j.1749-6632.2010.05467.x

Martin, I., Kim, J. W., Dawson, V. L., and Dawson, T. M. (2014). LRRK2 pathobiology in Parkinson's disease. *J. Neurochem.* 131, 554–565. doi: 10.1111/jnc.12949

Park, G., Tan, J., Garcia, G., Kang, Y., Salvesen, G., and Zhang, Z. (2016). Regulation of histone acetylation by autophagy in Parkinson Disease. *J. Biol. Chem.* 291, 3531–3540. doi: 10.1074/jbc.M115.675488

Politis, M., and Loane, C. (2011). Serotonergic dysfunction in Parkinson's disease and its relevance to disability. *Sci. World J.* 11, 1726–1734. doi: 10.1100/2011/172893

Qi, X., Wang, L., and Du, F. (2010). Novel small molecules relieve prothymosin α-mediated inhibition of apoptosome formation by blocking its interaction with Apaf-1. *Biochemistry* 49, 1923–1930. doi: 10.1021/bi9022329

Schwab, A. J., Sison, S. L., Meade, M. R., Broniowska, K. A., Corbett, J. A. and Ebert, A. D. (2017). Decreased sirtuin deacetylase activity in LRRK2 G2019S iPSC-derived dopaminergic neurons. *Stem Cell Reports* 9, 1839–1852. doi: 10.1016/j.stemcr.2017.10.010

Skrahina, T., Piljić, A., and Schultz, C. (2008). Heterogeneity and timing of translocation and membrane-mediated assembly of different annexins. *Exp. Cell Res.* 314, 1039–1047. doi: 10.1016/j.yexcr.2007.11.015

Song, C., Kanthasamy, A., Jin, H., Anantharam, V., and Kanthasamy, A. G. (2011). Paraquat induces epigenetic changes by promoting histone acetylation in cell culture models of dopaminergic degeneration. *Neurotoxicology* 32, 586–595. doi: 10.1016/j.neuro.2011.05.018

Song, C., Kanthasamy, A., Anantharam, V., Sun, F., and Kanthasamy, A. G. (2010). Environmental neurotoxic pesticide increases histone acetylation to promote apoptosis in dopaminergic neuronal cells: relevance to epigenetic mechanisms of neurodegeneration. *Mol. Pharmacol.* 77, 621–632. doi: 10.1124/mol.109.062174

Tatham, M. H., Plechanovova, A., Jaffray, E. G., Salmen, H., and Hay, R. T. (2013). Ube2W conjugates ubiquitin to α-amino groups of protein N-termini. *Biochem. J.* 453, 137–145. doi: 10.1042/BJ20130244

TeSlaa, T., and Teitell, M. A. (2014). Techniques to monitor glycolysis. *Methods Enzymol.* 542, l91–114. doi: 10.1016/B978-0-12-416618-9.00005-4

Yakhine-Diop, S. M., Bravo-San Pedro, J. M., Gómez-Sánchez, R., Rodríguez-Arribas, E., Rodriguez-Arribas, M., Gonzalez-Polo, V., et al. (2014). G2019S LRRK2 mutant fibroblasts from Parkinson's disease patients show increased sensitivity to neurotoxin 1-methyl-4-phenylpyridinium dependent of autophagy. *Toxicology* 324, 1–9. doi: 10.1016/j.tox.2014.07.001

Zattas, D., Adle, D. J., Rubenstein, E. M., and Hochstrasser, M. (2013). N-terminal acetylation of the yeast Derlin Der1 is essential for Hrd1 ubiquitin-ligase activity toward luminal ER substrates. *Mol. Biol. Cell* 24, 890–900. doi: 10.1091/mbc.E12-11-0838

Conflict of Interest Statement: The authors declare that the research was conducted in the absence of any commercial or financial relationships that could be construed as a potential conflict of interest.

frontiers in Cellular Neuroscience

REVIEW
published: 10 July 2018
doi: 10.3389/fncel.2018.00169

The Regulatory Effects of Acetyl-CoA Distribution in the Healthy and Diseased Brain

Anna Ronowska, Andrzej Szutowicz, Hanna Bielarczyk, Sylwia Gul-Hinc, Joanna Klimaszewska-Łata, Aleksandra Dyś, Marlena Zyśk and Agnieszka Jankowska-Kulawy*

Department of Laboratory Medicine, Faculty of Medicine, Medical University of Gdańsk, Gdańsk, Poland

Brain neurons, to support their neurotransmitter functions, require a several times higher supply of glucose than non-excitable cells. Pyruvate, the end product of glycolysis, through pyruvate dehydrogenase complex reaction, is a principal source of acetyl-CoA, which is a direct energy substrate in all brain cells. Several neurodegenerative conditions result in the inhibition of pyruvate dehydrogenase and decrease of acetyl-CoA synthesis in mitochondria. This attenuates metabolic flux through TCA in the mitochondria, yielding energy deficits and inhibition of diverse synthetic acetylation reactions in all neuronal sub-compartments. The acetyl-CoA concentrations in neuronal mitochondrial and cytoplasmic compartments are in the range of 10 and 7 μmol/L, respectively. They appear to be from 2 to 20 times lower than acetyl-CoA Km values for carnitine acetyltransferase, acetyl-CoA carboxylase, aspartate acetyltransferase, choline acetyltransferase, sphingosine kinase 1 acetyltransferase, acetyl-CoA hydrolase, and acetyl-CoA acetyltransferase, respectively. Therefore, alterations in acetyl-CoA levels alone may significantly change the rates of metabolic fluxes through multiple acetylation reactions in brain cells in different physiologic and pathologic conditions. Such substrate-dependent alterations in cytoplasmic, endoplasmic reticulum or nuclear acetylations may directly affect ACh synthesis, protein acetylations, and gene expression. Thereby, acetyl-CoA may regulate the functional and adaptative properties of neuronal and non-neuronal brain cells. The excitotoxicity-evoked intracellular zinc excess hits several intracellular targets, yielding the collapse of energy balance and impairment of the functional and structural integrity of postsynaptic cholinergic neurons. Acute disruption of brain energy homeostasis activates slow accumulation of amyloid-β_{1-42} (Aβ). Extra and intracellular oligomeric deposits of Aβ affect diverse transporting and signaling pathways in neuronal cells. It may combine with multiple neurotoxic signals, aggravating their detrimental effects on neuronal cells. This review presents evidences that changes of intraneuronal levels and compartmentation of acetyl-CoA may contribute significantly to neurotoxic pathomechanisms of different neurodegenerative brain disorders.

Keywords: acetyl-CoA, acetylcholine, *N*-acetyl-L-aspartate, nerve growth factor, protein acetylations, metabolic compartmentation, neuronal metabolism, neurodegeneration

OPEN ACCESS

Edited by:
Daniel Ortuño-Sahagún, Universidad de Guadalajara, Mexico

Reviewed by:
Thad A. Rosenberger, University of North Dakota, United States
Bilikere S. Dwarakanath, Shanghai Proton and Heavy Ion Center (SPHIC), China

****Correspondence:***
Andrzej Szutowicz
aszut@gumed.edu.pl

Received: *21 March 2018*
Accepted: *31 May 2018*
Published: *10 July 2018*

Citation:
Ronowska A, Szutowicz A, Bielarczyk H, Gul-Hinc S, Klimaszewska-Łata J, Dyś A, Zyśk M and Jankowska-Kulawy A (2018) The Regulatory Effects of Acetyl-CoA Distribution in the Healthy and Diseased Brain. Front. Cell. Neurosci. 12:169. doi: 10.3389/fncel.2018.00169

INTRODUCTION

Cellular diversity is a principal morphologic and functional property of the brain. It includes the existence of different classes of neuronal, astroglial, microglial, and oligodendroglial cells, and also several supporting vascular and meningeal membranes cells. The neurons constitute a relatively small but highly heterogenous, and not evenly distributed, fraction of the whole brain cell population (Herculano-Houzel, 2014). Their principal function neurotransmission includes synthesis, vesicular accumulation, and quantal release of diverse neurotransmitters and regulatory compounds. The former, when released in quantal mode from depolarized axonal terminals, may exert either activatory or inhibitory effects on postsynaptic parts of recipient neurons. Continuous generation of action potentials and restoration of resting membrane potentials with a 5–50 Hz frequency, requires high rates of energy production. These two neuronal parameters may be traced *in vivo* by electroencephalography and CT-PET-MRI functional imaging (Jagust et al., 2015). Three dimensional mapping and dynamic studies of regional ^{18}F-deoxyglucose uptake, or changes in phosphocreatine, ATP, *N*-acetyl-L-aspartate (NAA) or lactate levels may provide a precise picture of energy metabolism in each selected anatomical structure of the brain. They also provide an accurate localization and analysis of metabolic disturbances in diverse brain pathologies (Kochunov et al., 2010; Kato et al., 2016; Zhong et al., 2014). Several reports indicate that shifts in cellular compartmentation and rates of metabolism of direct energy precursors such as pyruvate/lactate and its conversion to acetyl-CoA by PDHC may take part in the adaptative processes during brain maturation, aging, and diverse neuropathophysiological conditions (Halim et al., 2010; Jha et al., 2016). Hence, acetyl-CoA as an immediate substrate for TCA and diverse key acetylation reactions should be considered as one of the key regulatory signals in these conditions (Szutowicz et al., 2013, 2017; Pietrocola et al., 2015; Peng et al., 2016).

ACETYL-CoA PRECURSORS IN THE BRAIN

Glucose and Derived Metabolites as a Principal Source of Acetyl-CoA and Energy in the Brain

Neurons contribute to 50–80% of overall energy balance of the whole brain using glucose oxidative metabolism as a principal energy source. Its adequate provision is assured by the presence of the high capacity medium affinity GLUT1 transporter (Km ∼ 8.0 mM) on the blood brain barrier and the high affinity GLUT3 transporter (Km ∼ 2.8 mM) on neuronal plasma membranes, respectively (Simpson et al., 2007). They may secure an adequate glucose supply even at serious hypoglycemic conditions of 2 mM range. In addition, the expression of GLUT1 transporter is inversely regulated by glycemia adapting the brain to chronic hyper or hypoglycemic conditions. Such homeostatic mechanisms stabilize glucose availability in brain extracellular compartments. The high energy demand in neurons results from their neurotransmitter functions linked with continuous depolarization/repolarization cycles of 5–50 Hz frequency. The maintenance of this basal neuronal function requires marked energy expenses for the restoration of membrane potential and preservation of the stable neurotransmitter pool in synaptic vesicles. Therefore, neurons are more susceptible than glial cells to diverse range pathologic inputs that limit the supply of oxygen and/or glucose and lactate as principal energy substrates (Szutowicz et al., 2013, 2017).

On the other hand, glial cells – that outnumber neurons depending on the region by 10 to 1 – produce only ca. 30–40% of the overall brain energy pool, utilizing a 50% fraction of supplied glucose (Jolivet et al., 2009; Herculano-Houzel, 2014). This divergence is caused by the fact that glial cells, mainly astrocytes, are net producers of lactate due to the relative prevalence of glycolysis over oxidative metabolism. The lactate released from the glial cells is taken up by neurons through MCT2 monocarboxylate transporters, of high affinity to lactate and pyruvate with Km values equal to 0.5 and 0.1 mM, respectively (Pérez-Escuredo et al., 2016). Reuptake of lactate by astroglia is prevented due to the presence of low affinity MCT4 transporters of Km about 25 mM. Thereby, lactate may be complementary to the glucose source of intraneuronal pyruvate, which in mitochondria is metabolized by PDHC, yielding acetyl-CoA. The latter is an energy precursor directly feeding the TCA cycle through citrate synthase step. In fact cultured neuronal cells grow and function well with pyruvate/lactate as the only energy substrates in the medium (Wohnsland et al., 2010). On the other hand, there are indications that *in vivo* both neurons and astroglia produce an excess of lactate, making the net contribution of extracellular lactate to the neuronal energy metabolism non-significant (Mangia et al., 2011). Astroglial cells also synthesize and release large amounts of L-glutamine, which is taken up by adjacent neurons. In glutamatergic and GABA-ergic neurons it is converted by phosphate activated glutaminase (EC 3.5.1.2) and glutamate decarboxylase (EC 4.1.1.15) to neurotransmitters: glutamate and γ-aminobutyrate (GABA), respectively.

In astrocytes, a fraction of glutamate, after conversion to α-ketoglutarate by glutamate dehydrogenase (EC 1.4.1.2)/aspartate aminotransferase (EC 2.6.1.1) reactions, may enter the TCA cycle at the KDHC step (Waagepetersen et al., 2007). In neurons, this pathway is much less active. Therefore, in neurons the metabolic flux of pyruvate through PDHC remains a key factor that determines the availability of acetyl-CoA for energy production in mitochondrial compartment and maintenance of their viability (Szutowicz et al., 1996, 2013).

Abbreviations: βHB, β-hydroxybutyrate; AAT, aspartate-*N*-acetyltransferase; AcAc, acetoacetate; ACh, acetylcholine; AD, Alzheimer's disease; ALS, amyotrophic lateral sclerosis; AT-1, acetyl-CoA transporter-1(endplasmic reticulum); ChAT, choline acetyltransferase; ER, endoplasmic reticulum; HACU, high affinity choline transporter; HAT, histone acetyltransferase; HBDH, β-hydroxybutyrate dehydrogenase; HC, (−)hydroxycitrate; KDHC, α-ketoglutarate dehydrogenase complex; NAA, *N*-acetyl-L-aspartate; NGF, nerve growth factor; NOS; nitrogen oxide reactive species; PDHC, pyruvate dehydrogenase complex; RA, retinoic acid ROS, reactive oxygen species; SphK1, sphingosine kinase 1; TCA, tricarboxylic acid cycle; VAChT, vesicular acetylcholine transporter.

In accordance with this, the activities of PDHC in the brain homogenates and isolated mitochondria were found to be 4 – 10 times higher than in respective fractions of non-excitable tissues (Szutowicz, 1979; Szutowicz and Łysiak, 1980; Tomaszewicz et al., 2003; Bielarczyk et al., 2015). Also, rates of glucose uptake, glycolysis and pyruvate utilization in brain neurons are significantly higher than in astroglial, microglial, or oligodendroglial cells (Herculano-Houzel, 2011; Mangia et al., 2011; Klimaszewska-Łata et al., 2015). These findings are compatible with lower rates of overall oxidative metabolism in the glial than in the neuronal compartment (Thevenet et al., 2016). Therefore, physiologic and pathologic alterations of overall brain energy metabolism, observed in CT-PET-MRI as images of phosphocreatine, or NAA, reflect those taking place mainly in the neuronal compartments (Kochunov et al., 2010).

Beta-Hydroxybutyrate/Acetoacetate and Brain Acetyl-CoA

Brain cells are also capable utilizing β-hydroxybutyrate/acetoacetate (β-HB, AcAc) as a complementary source of acetyl-CoA both for energy production in mitochondria and for cytoplasmic synthetic pathways. Under physiologic non-fasting conditions their plasma concentrations are below 0.05 mM, which precludes their effective transport by MCT2 transporter, as its Kms for these metabolites are about 1 mM (Pérez-Escuredo et al., 2016). Therefore, at similar concentrations the uptake and rate of β-HB metabolism are 5 times slower than those of pyruvate. However, in a starvation or diabetic ketoacidosis brain, the levels of β-HB may rise up to 5 and higher millimolar concentrations. In such conditions β-HB may enter the brain cell mitochondria, being effectively metabolized to acetyl-CoA through β-hydroxybutyrate dehydrogenase (HBDH, EC 1.1.1.30), 3-oxoacid CoA-transferase (EC 2.8.3.5.), and acetoacetyl-CoA thiolase (EC 2.3.1.9) pathways (Buckley and Williamson, 1973; Chechik et al., 1987). In brain nerve terminals, β-HB in concentrations of 2.5–20.0 mM could supply up to a 30% pool of acetyl-CoA required for energy production and diverse synthetic pathways, including ACh synthesis (Szutowicz et al., 1994b, 1998b). In such conditions, β-HB slightly reduced pyruvate utilization due to competition for MCT2 transporter (Szutowicz et al., 1994b; Pérez-Escuredo et al., 2016). However, it did not affect glucose oxidation (McKenna, 2012). Therefore, under ketonemic conditions β-HB may support glucose in the maintenance of the proper level of acetyl-CoA in the brain (Szutowicz et al., 1994b, 1998b; Simpson et al., 2007).

In fact β-HB markedly increased the level of acetyl-CoA in the mitochondrial compartment of brain nerve terminals (**Figure 1B**) (Szutowicz et al., 1998b). Synaptosomes from the brains of diabetic-ketonemic rats displayed higher levels of acetyl-CoA and rates of ACh synthesis (Szutowicz et al., 1994b, 1998b). β-HB may also prevent death of glucose deprived cultured primary cortical neurons, in energy independent mode through acetylation-induced degradation of LC3-II/p62 proteins in activated autophagosomes (Camberos-Luna et al., 2016). In high concentration β-HB also increased oxygen consumption, ATP levels, histone acetylation, and BDNF expression in cultured primary neurons from mice brain, yielding an increase of their resistance to oxidative stress (Marosi et al., 2016). Recent studies demonstrated that dietary feeding of 3xTg mice with β-HB increased the level of acetyl-CoA, accompanied by increases in NAA, citrate, and other TCA intermediates in hippocampus along with an improvement in behavioral tests (Pawlosky et al., 2017).

PET-MRI studies revealed that, in contrast to glucose, AcAc metabolism is not altered in the brains of AD patients (Cunnane et al., 2011; Castellano et al., 2015). Thus, the apparent neuroprotective effects of this ketoacid could result from the supply of acetyl-CoA by pathway bypassing glycolysis and PDHC, which are impaired in AD and other neurodegenerative diseases (Szutowicz et al., 1996, 1998b, 2013; Bubber et al., 2005; Yao et al., 2009; Jankowska-Kulawy et al., 2010; Camberos-Luna et al., 2016; Kato et al., 2016; Pawlosky et al., 2017). The ketone-evoked support of acetyl-CoA/energy metabolism may explain their protective effects against amyloid toxicity in brains of PDGFB-APPSwInd AD mice (Yin et al., 2016). These findings indicate that intermittent metabolic glucose to β-HB switching, linked with fasting-feeding cycles, may promote neuroplasticity and resistance to neurodegeneration (Mattson et al., 2018). This would be compatible with the thesis that caloric restriction – known to lengthen the lifespan of several species – may be mediated through β-HB increasing supplementation of NAPH, and expression of antioxidant enzymes (Veech et al., 2017). Clinical studies have revealed that caloric restriction, which induces ketonemia, was accompanied by slight improvements of cognitive functions in elderly people with mild cognitive impairment (Krikorian et al., 2012). Such mechanism may also contribute to the ability of β-HB to calm neuronal spiking in epileptic brains, and decrease the incidence of subclinical epileptiform activity in AD patients (Vossel et al., 2016).

In glial cells, activities of HBDH and acetoacetyl-CoA thiolase were found to be two–threefold higher than in neurons (Chechik et al., 1987). Therefore, in ketonemic conditions these ketoacids may became a significant precursor of intramitochondrial acetyl-CoA in non-neuronal cellular compartments of the brain. These data indicate that irrespective of origin, acetyl-CoA is a central point of energy metabolism in cell mitochondria and a primary precursor for multiple synthetic and signaling pathways in various extramitochondrial compartments (Szutowicz et al., 2013, 2017).

The level of acetyl-CoA in every cell type, including neurons and neuroglia, is resultant of rates of its synthesis and utilization within mitochondria and outward transport for consumption in a broad range of synthetic pathways taking place in extramitochondrial compartments (Szutowicz et al., 1996, 2013, 2017; Kouzarides, 2000; Pietrocola et al., 2015; Drazic et al., 2016).

Acetate and Brain Acetyl-CoA

Acetate has to be reactivated by acetyl-CoA synthase (ACS, EC 6.2.1.1.). Oligodendroglia expresses acetyl-CoA synthases 1 and 2 that are located in cytoplasmic and mitochondrial compartments. They may resynthesize acetyl-CoA, supplying it directly for myelin lipids synthesis/protein acetylations, and energy production, respectively (Reijnierse et al., 1975; Szutowicz et al., 1982; Moffett et al., 2013). Low activities of ACS in nerve

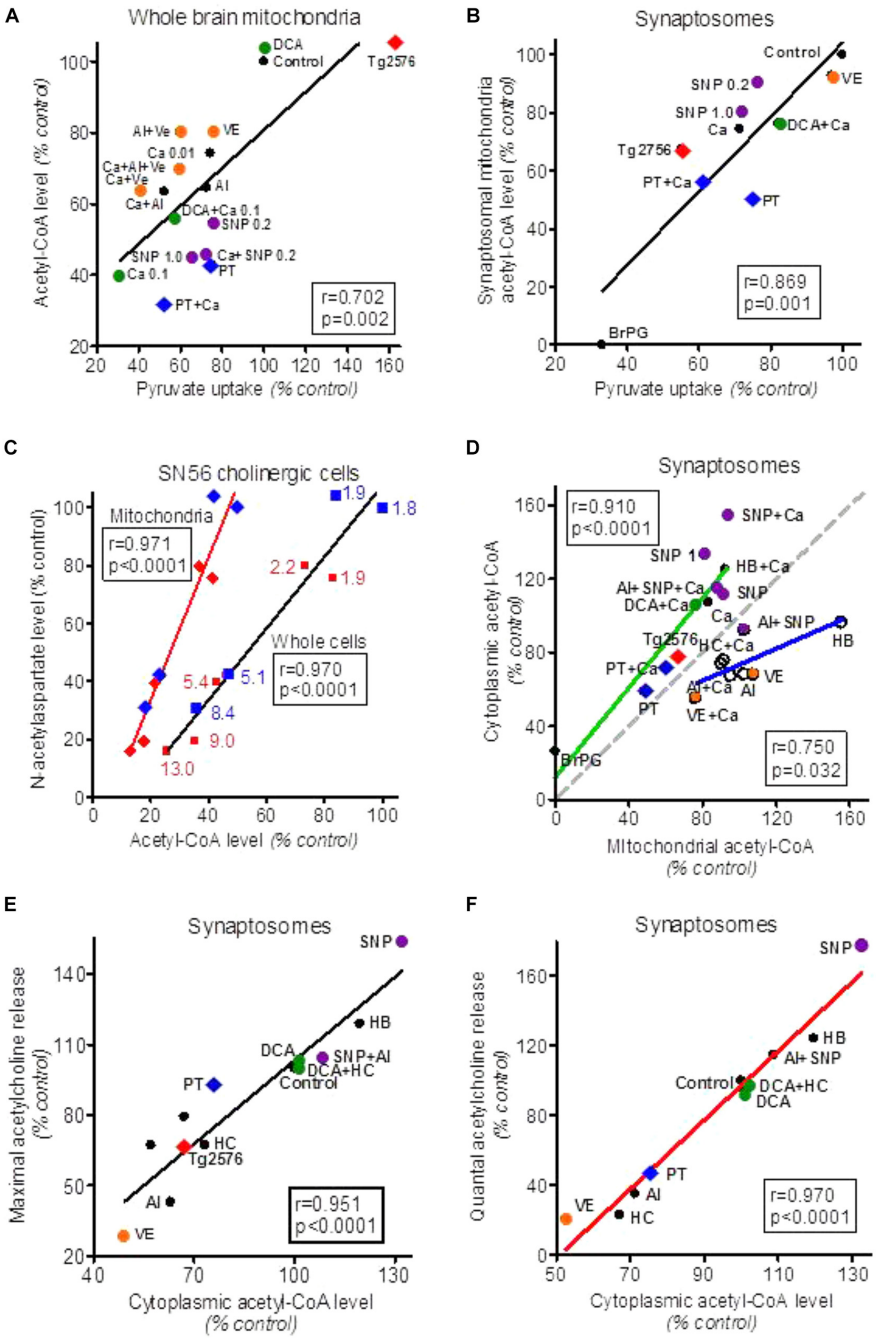

FIGURE 1 | Alterations of acetyl-CoA levels in forebrain cellular compartments in different experimental models of neurotoxicity and neurodegeneration. **(A)** Effects of variations in pyruvate uptake on acetyl-CoA level in whole brain (predominately glial) mitochondria treated with different cytotoxic and cytoprotective compounds. **(B)** Effects of alterations in pyruvate uptake by isolated brain synaptosomes on acetyl-CoA level in their mitochondria. **(C)** Effects of Zn overload of SN56 non-differentiated (blue) and differentiated (red) cholinergic neuroblastoma cells (blue and red numbers indicate intracellular Zn in nmol/mg protein) on acetyl-CoA level in whole cells and cell's mitochondria and their *N*-acetylaspartate content. **(D)** Correlations between cytoplasmic and mitochondrial acetyl-CoA levels in synaptosomes treated with cytotoxic/cytoprotective agents increasing (green plot) or decreasing/not affecting mitochondrial membrane permeability (blue plot). The gray dotted line corresponds to theoretical stoichiometric compartmentalization of acetyl-CoA. **(E)** Effect of alterations in synaptoplasmic acetyl-CoA level on maximal Ca^{++}/K^{+} depolarization-evoked acetylcholine release/synthesis in synaptosomes treated with different cytotoxic and cytoprotective compounds. **(F)** Effect of alterations in synaptoplasmic acetyl-CoA level on Ca-dependent (quantal) acetylcholine release by synaptosomes treated with different cytotoxic and cytoprotective compounds. Al, aluminum 0.25 mmol/L; BrP, 3-bromopyruvate 0.25 mmol/L; Ca, Calcium 0.01 and 0.1 with mitochondria, Ca 1.0 mmol/L with synaptosomes; DCA, dichoroacetate 0.05 mmol/L; HB, β-hydroxybutyrate 20 mmol/L; HC, (–) hydroxycitrate 1.0 mmol/L; PT, pyrythiamin-thiamin deficient synaptosomes; SNP, sodium nitroprusside 0.2 and 1.0 mmol/L; Tg2576, transgenic AD mice; VE, verapamil 0.1 mmol/L. Data were recalculated to relative values from original data: Bielarczyk and Szutowicz (1989), Szutowicz et al. (1994a, 1998a), Tomaszewicz et al. (1997), Bielarczyk et al. (1998, 2015), Jankowska-Kulawy et al. (2010), Zyśk et al. (2017).

terminals and relatively high ones in whole brain mitochondrial fractions point to neuroglia as a principal acetate utilizing compartment of the brain (Szutowicz, 1979; Szutowicz et al., 1982; Moffett et al., 2013). However, the rate of acetate uptake was found to be independent of astroglia activity. It would suggest no direct modulating contribution of acetate to the energy metabolism of astroglial cells (Rowlands et al., 2017). On the other hand, substantial amounts of endogenous acetate may be formed by hydrolysis of acetyl-CoA, which is generated by PDHC from pyruvate derived from glucose or lactate (Łysiak et al., 1976; Rae et al., 2012). Such a thesis is also supported by the fact that over 80% of brain acetyl-CoA hydrolase (EC 3.1.2.1) activity is located in whole brain mitochondria and synaptosomal mitochondria fractions (Szutowicz et al., 1980, 1982). In fact, whole brain mitochondria utilizing pyruvate without provision of oxaloacetate, released significant amounts of acetate (Łysiak et al., 1976). On the other hand, low V_{max} and high acetyl-CoA Km of cytoplasmic acetyl-CoA hydrolase may suggest very slow metabolic flux through this catabolic pathway (Prass et al., 1980; Hovik et al., 1991; Suematsu and Isohashi, 2006). Nevertheless, intramitochondrially generated acetate, after being transferred to the cytoplasm, could be used by chromatin-bound ACS2 for direct acetylations of nuclear histones, yielding alterations in gene expression in brain neurons. Through such a mechanism the acetate could regulate memory consolidation in the hippocampus (Mews et al., 2017). These findings also suggest that the regulatory effects of acetate on cell metabolism occur rather *via* altering levels of acetylation of regulatory proteins than by direct influx into energy generating pathways (Rowlands et al., 2017).

Citrate and Brain Acetyl-CoA

One should stress that in brain mitochondria the rate of acetyl-CoA utilization for citrate synthesis is about two orders of magnitude higher than the rate of its hydrolysis when comparing V_{max} values of citrate synthase and acetyl-CoA hydrolase, respectively (**Table 1**) (Wlassics et al., 1988; Suematsu and Isohashi, 2006). Also, isolated whole brain mitochondria or synaptosomes utilizing pyruvate with malate, accumulated several times greater amounts of citrate than those of acetate (Łysiak et al., 1976). Citrate is released from mitochondria to the cytoplasm by the citrate-malate antiporter mechanism, where it is converted back to acetyl-CoA through ATP-citrate lyase reaction (ACL, EC 2.3.3.8.) (Srere, 1965; Angielski and Szutowicz, 1967; Szutowicz et al., 1981, 1996; Gnoni et al., 2009). The (-)hydroxycitrate (HC) in 1 mmol/L concentration was found to be specific, competitive to citrate inhibitor of ACL (Szutowicz et al., 1976). At 0.5 mmol/L citrate concentration, comparable with its levels in the brain, being in range of 0.2–0.4 mmol/L, HC with Ki of 3.8 μmol/L, brought about complete inhibition of brain ACL activity, without affecting other enzymes involved in acetyl-CoA and energy metabolism (Szutowicz et al., 1976; Carlsson and Chapman, 1981; Pawlosky et al., 2017). Therefore, HC was used as a selective tool for investigating the significance of the ACL pathway in maintenance of the proper level of cytoplasmic acetyl-CoA and its contribution to different extramitochondrial synthetic pathways in the brain (Patel and Owen, 1976; Szutowicz et al., 1976, 1981, 1989, 1996, 2013; Rícný and Tucek, 1981, 1982; Constantini et al., 2007).

In depolarized nerve terminals isolated from the rat forebrain, utilizing pyruvate or glucose, 1 mmol/L HC caused a ca. 30% decrease of cytoplasmic and no alterations in intramitochondrial levels of acetyl-CoA, accompanied by respective increase of citrate accumulation and a decrease of ACh synthesis (Szutowicz et al., 1976, 1981, 1994a). A comparable, although wide range of 20–50% suppressive effects, were observed in brain slices with higher 2.5–5.0 mmol/L concentrations of HC (Sterling et al., 1981; Rícný and Tucek, 1982; Gibson and Peterson, 1983). It should be stressed that at such high concentrations, HC could exert weaker unspecific inhibitory effects on other enzymes of the citrate metabolism, as well as on PDHC and phosphofructokinase (Cheema-Dhadli et al., 1973; Szutowicz et al., 1981). In addition, they represent averaged data from multiple subcellular neuronal and glial compartments of acetyl-CoA metabolism, which might respond differentially to the same experimental conditions (Rícný and Tucek, 1982; Klimaszewska-Łata et al., 2015; Zyśk et al., 2017). These findings indicate that metabolic flux through ACL step influences both acetyl-CoA availability in cytoplasmic compartment and citrate homeostasis in neuronal cells (Szutowicz et al., 1976, 1981, 1994a; Rícný and Tucek, 1982).

ATP-Citrate Lyase Pathway and Cholinergic Metabolism

The rates of various extramitochondrial synthetic pathways may depend directly on the acetyl-CoA level, considering Km values of respective enzymes to this substrate as a putative regulatory factor (**Tables 1**, **2**). Hence, in brain synaptosomes and slices, HC brought about inhibition of ACh synthesis/release, roughly proportional to HC-evoked decreases of acetyl-CoA levels (Rícný and Tucek, 1981, 1982; Szutowicz et al., 1981, 1994a). In brains of suckling animals, HC caused non-proportionally greater, over 60% inhibition, of non-saponifiable lipids and fatty acid synthesis (Patel and Owen, 1976). These data indicate a significant role of the ACL pathway in regulation of both ACh and lipid synthesis in brain cell cytoplasmic compartments. However, differential inhibition of both synthetic pathways by HC suggests the existence of separate cytoplasmic sub-compartments in neuronal and glial cells, being lesser and more dependent on the supply of acetyl-CoA through the ACL pathway, respectively. Also HC-evoked inhibition of ACh synthesis varied regionally, being low (17%) in the hippocampus, intermediate (30%) in the caudate nucleus, and high (55%) in the septum (Rícný and Tucek, 1982; Gibson and Peterson, 1983). These data demonstrate that the fractional contribution of the ACL pathway providing acetyl-CoA for ACh synthesis may be significantly different in various regional subpopulations of brain cholinergic neurons (Sterling et al., 1981; Rícný and Tucek, 1982; Gibson and Peterson, 1983).

This specific demand for citrate as a precursor of cytoplasmic acetyl-CoA for ACh synthesis may be met due to preferential localization of ACL in cholinergic neurons (Szutowicz, 1979; Szutowicz et al., 1980, 1983; Tomaszewicz et al., 2003). There are highly significant, positive correlations between ChAT and ACL activities in cytosolic and synaptosomal fractions isolated from brain regions of variable density of cholinergic innervation (Szutowicz et al., 1980, 1982). Activities of ACL in

TABLE 1 | The acetyl-CoA Km values for acetyl-CoA consuming enzymes in different cellular compartments.

Enzyme	Tissue/cells	Compartment	Km (μmol/L)	Reference
Citrate synthase	Rat brain	Mitochondria	4.8	Matsuoka and Srere, 1973
Carnitine acetyltransferase	Human liver	Mitochondria	21.3	Bloisi et al., 1990
Aspartate acetyltransferase	Rat brain	Mitochondria	58	Madhavarao et al., 2003
Acetyl-CoA hydrolase	Rat liver	Cytoplasm	150	Suematsu and Isohashi, 2006
	Rat liver	Cytoplasm	60	Prass et al., 1980
	Rat liver	Peroxisomes	400	Hovik et al., 1991
Choline acetyltransferase	Rat brain	Cytoplasm	38	Rossier et al., 1977
	Human brain	Cytoplasm	32–200	Koshimura et al., 1988
	regions	Highly purified	46.5	Ryan and McClure, 1980
	Rat brain	Highly purified	16.5	
	Bovine brain			
Sphingosine kinase 1(COX2 acetyltransferase)	Mouse brain neurons	Cytoplasm	58.2	Lee et al., 2018
Acetyl-glutamate synthetase	Rat liver	Mitochondria	600	Coude et al., 1979
Acetyl-CoA carboxylase	Rat muscles	Cytoplasm	31.7 ± 1.5	Trumble et al., 1995
	Rat adipose tissue		21.5 ± 1.0	
Fatty acid synthase	Rat liver (purified)	Cytoplasm	4.4	Rendina and Cheng, 2005
Acetyl-CoA acetyltransferase	Rat liver	Peroxisomes	<200	Hovik et al., 1991
		Mitochondria	237	Middleton, 1974
3-hydroxy-3-methyl glutaryl coenzyme A synthase	Ox liver (purified)	Cytoplasm	158	Lowe and Tubbs, 1985
ER membrane acetyl-CoA transporter (AT-1)	CHO Cell culture	Endoplasmic reticulum	14	Constantini et al., 2007
Lysine acetyltransferase BACE1	CHO Cell culture	Endoplasmic reticulum	14	Puglielli (personal report)
Lysine acetyltransferase 8 KAT8 (histone 4)	Recombinant enzyme	Nucleus	1.1-4.8	Wapenaar et al., 2015
Histone acetyltransferase Tip 60	HeLa cell nuclear extract	Nucleus	2.0	Ghizzoni et al., 2012
Histone acetyltransferase p300/CPB associated factor	Recombinant from Sf21 cells	Nucleus	0.3	Balasubramanyam et al., 2003

non-cholinergic neurons, calculated from ACL/ChAT correlation plots, were found to be equal to 2–4 nmol/min/mg protein, respectively. On the other hand, the ACL activity in cholinergic neurons, calculated from regional and cholinergic lesions studies, was in the range of 40 nmol/min/mg protein (Szutowicz et al., 1982, 1983; Tomaszewicz et al., 2003). These calculations remain in accord with immunohistochemical studies demonstrating a strong co-expression of ACL with ChAT and VAChT-expressing neurons in mice hippocampus, fascial nucleus and medulla oblongata (Beigneux et al., 2004). The tight functional links of ACL with cholinergic metabolism were demonstrated by its ability to bind ataxia-related protein forming BNIP-H-ACL-ChAT complex leading to enhanced ACh release (Sun et al., 2015). In the newborn rat brain, activity of ACL in all regions was comparably high, serving as a provider of acetyl units for structural lipid synthesis during myelinisation (Szutowicz, 1979; Szutowicz and Łysiak, 1980; Dietschy and Turley, 2004). In the course of brain development ACL activity remained high in all cortical regions, in which ChAT/ACh increased due to maturation of cholinergic neurons.

On the other hand, ACL activity in the cerebellum, devoid of cholinergic elements, decreased several fold in parallel with a maturation-dependent decrease of fatty acid synthesis due to termination of myelin and plasma membrane proteo-lipid structures formation (Szutowicz, 1979; Szutowicz and Łysiak, 1980; Szutowicz et al., 1982; Dietschy and Turley, 2004). In addition, large non-cholinergic synaptosomes isolated from the brain cortex and cerebellum contained 4 – 5 times lower ACL activities than small cortical synaptosomes containing significant fraction of cholinergic elements (Kuhar and Rommelspacher, 1974; Szutowicz et al., 1983). Cultured S20 or SN56 neuronal cells expressing mature cholinergic phenotype were found to contain higher activities of ACL than non-cholinergic neuronal and micro or astroglial cells (Szutowicz et al., 1983; Klimaszewska-Łata et al., 2015). Such cholino-tropic developmental patterns of ACL would be compatible with the demand of maturing cholinergic neurons for optimal provision of acetyl-CoA for age-dependent elevations of ACh synthesis (Szutowicz and Łysiak, 1980). Such a claim is supported by studies showing significant 30% decreases of ACL and no changes in other enzymes of acetyl-CoA metabolism activities in hippocampal synaptosomes isolated from septum electro-lesioned rat brain (Szutowicz et al., 1982). Similar alterations of ACL were observed in the IgG192 saporin (cholinergic immunotoxin) lesioned brain cortex (Tomaszewicz et al., 2003). These changes remained in accord with 70–80% decays of ChAT activities and ACh synthesis indicating loss of cholinergic neurons (Szutowicz et al., 1982; Tomaszewicz et al., 2003).

TABLE 2 | Estimated molar concentrations of acetyl-CoA in different compartments of the brain and clonal cells of brain origin.

Experimental model	Calculated concentration (μmol/L cell water)	Reference
Rat cerebrum	7.0 ± 0.2	Schuberth et al., 1966
Rat whole brain cortex	6.6 ± 0.3	Guynn, 1976
Rat whole brain cortex	8.1 ± 0.5	Shea and Aprison, 1977
Rat whole thalamus	11.8 ± 0.8	
Rat whole hippocampus	9.2 ± 0.5	
Rat whole striatum	9.0 ± 0.5	
Rat whole cerebellum	7.8 ± 0.5	
Nucleus caudatus (slices)	5.3 ± 0.1	Rícný and Tucek, 1981
Rat whole brain newborn	4.5 ± 0.2	Mitzen and Koeppen, 1984
60 days old	2.5 ± 0.1	
Rat whole forebrain	8.5 ± 0.4	Szutowicz and Bielarczyk, 1987
Rat whole forebrain synaptosomes	7.7 ± 0.3	Bielarczyk and Szutowicz, 1989; Szutowicz et al., 1994a,b, 1998b
Rat synaptosomal mitochondria	7.5 ± 0.3	Bielarczyk et al., 1998;
Rat synaptosomal cytoplasm	6.3 ± 0.2	Tomaszewicz et al., 2003;
Rat Whole forebrain mitochondria	17.6 ± 0.5	Jankowska-Kulawy et al., 2010
Rat whole brain	3.4 ± 1.3	Pawlosky et al., 2010
Rat whole frontal cortex		Zimatkin et al., 2011
Rat ethanol susceptible	128 ± 9	
Rat ethanol resistant	99 ± 5	
Mice forebrain synaptosomes	9.5 ± 0.7	Bielarczyk et al., 2015
Mice forebrain synaptosomal mitochondria	14.1 ± 1.6	
Mice forebrain synaptosomal cytoplasm	13.5 ± 0.5	
Mice forebrain whole forebrain mitochondria	15.7 ± 0.4	
Mice neonatal brain crude mitochondria	28.5 ± 2.7	Sun et al., 2016
Rat whole brain	4.0 ± 1.5	Shurubor et al., 2017
Clonal cell lines		
SN56 cholinergic neuroblastoma	9.6 ± 0.2	Szutowicz et al., 2004, 2005;
Mitochondria	10.9 ± 0.4	Ronowska et al., 2010;
Cytoplasm	7.2 ± 0.2	Bizon-Zygmańska et al., 2011;
SHY5Y dopaminergic neuroblastoma	11.6 ± 0.9	Klimaszewska-Łata et al., 2015;
N9 microglial cells	15.9 ± 0.8	Zyśk et al., 2017
C6 astroglial cells	4.5 ± 0.4	

Molar concentrations of acetyl-CoA in whole brain were recalculated from original data expressed as nmol/g tissue or pmol/mg protein assuming water and protein contents in whole brain being equal to 77% and 107 mg/g of tissue, respectively (Szutowicz et al., 1982; Kozler et al., 2013). In subcellular fractions recalculations of pmol/mg protein data to molar concentrations were done assuming protein concentrations 150 and 350 mg/ml of water for cytoplasmic and mitochondrial fractions, respectively, (Nolin et al., 2016).

Rat hippocampal synaptosomes contain about 6% subfraction of cholinergic terminals (Kuhar and Rommelspacher, 1974). Therefore, one might estimate, that ACL activities in cholinergic terminals are 10–15 times higher than in non-cholinergic ones (Szutowicz, 1979; Szutowicz et al., 1982).

Thiamine deficiency (TD) in rats caused inhibition of metabolic flux of pyruvate through PDHC, reductions of ACL-dependent fractions of cytoplasmic acetyl-CoA, and quantal ACh release from their brain nerve terminals (Jankowska-Kulawy et al., 2010). When taken together, these data indicate that ACL is preferentially expressed in cholinergic neurons, where it plays a crucial role in adequate provision of acetyl-CoA to the site of ACh synthesis (Gibson and Shimada, 1980; Szutowicz et al., 1982, 1996, 2013; Tuček, 1983; Beigneux et al., 2004).

ATP-citrate lyase may form multiple discrete subdomains executing different metabolic functions in the cells. ACL forms BNIP-ACL-ChAT complex facilitating direct provision of acetyl-CoA to the site of ACh synthesis (Sun et al., 2015). ACL also constitutes extramitochondrial sub-fractions bound with microsomes and nuclear-chromatin (Linn and Srere, 1984; Zhao et al., 2016). As such, ACL could form microdomains providing acetyl-CoA directly to acetyl-CoA transporter (AT-1) located in ER membranes (Hirabayashi et al., 2013; Pietrocola et al., 2015). In the nucleus, ACL-derived acetyl-CoA could modulate gene expression through alterations in histone acetylations (Kouzarides, 2000; Mews et al., 2017). Adipocyte studies have revealed that ACL, through cytoplasmic acetyl-CoA synthesis, may suppress expression of ACS. In *ACLYgen* knock-out cells, deficits of glucose derived acetyl-CoA could be partially alleviated

by upregulation of ACS2 (Zhao et al., 2016). In such conditions acetate production by brain mitochondria exceeded that of citrate. This could increase the rate of metabolic flux through upregulated ACS2 (Łysiak et al., 1976; Zhao et al., 2016). In fact early data revealed that whole brain mitochondria incubated without oxaloacetate/malate produced several times greater amounts of acetate than those of citrate (Łysiak et al., 1976).

Acetyl-l-Carnitine and Direct Acetyl-CoA Transporting Pathways and Cholinergic Metabolism

Acetyl-l-carnitine is another metabolite involved in indirect transfer of acetyl-CoA from mitochondria to the cytoplasm through membrane-bound carnitine acetyl-transferases (Rícný et al., 1992; Szutowicz et al., 2005). This pathway seems to be independent of other ones described above, introducing some surplus of acetyl-CoA to the cytoplasmic compartment. Thanks to such a mode of action, acetyl-l-carnitine might exert neuroprotective effects and alleviate ACh deficits under different neurotoxic conditions, suppressing acetyl-CoA synthesis (Rícný et al., 1992; Sharman et al., 2002; Szutowicz et al., 2005).

Chronic, oral application of acetyl-l-carnitine to patients in early stages of AD improved their cognitive functions and increased brain energy phosphate levels against the placebo treated group (Pettegrew et al., 1995). In cultured cholinergic neuronal cells, acetyl-l-carnitine partially overcame the detrimental effects of neurotoxic agents through a reduction of acetyl-CoA deficits (Szutowicz et al., 2005).

In depolarized cultured cholinergic SN56 cells and brain nerve terminals, the acetyl-CoA could be also transported out of mitochondria directly through Ca-activated, verapamil-sensitive, high permeability anion channels (PTP) (Bielarczyk and Szutowicz, 1989; Szutowicz et al., 1998a, 2005). The mechanism of direct acetyl-CoA output was also found to exist in whole brain mitochondria derived mainly form glial cells (**Figure 1A**) (Rícný and Tucek, 1982; Szutowicz et al., 1998a). Analysis of our past reports revealed the existence of direct relationships between cytoplasmic and mitochondrial acetyl-CoA levels in SN56 cholinergic neuronal cells (**Figure 1D**). The use of different cytotoxic and cytoprotective agents revealed the existence of two - Ca–dependent and Ca-independent mechanisms of acetyl-CoA synthesis and distribution between mitochondrial and cytoplasmic compartments in the neurons (**Figure 1D**).

These diverse acetyl-CoA transporting pathways seem to be particularly important for depolarized cholinergic neurons. In such a functional state, cholinergic nerve terminals release quanta of ACh. This requires instant reconstitution of the ACh pool in presynaptic cholinergic terminals for continuation of neurotransmitter function. It has been shown that nerve terminals are capable of assuring an adequate provision of acetyl-CoA, and maintaining stable levels of ACh and transmission rate, even during prolonged excessive activation (Birks, 1977; Tuček, 1993; Szutowicz et al., 1996). On the other hand, decreases in cytoplasmic acetyl-CoA caused by diverse neurotoxic signals resulted in proportional suppressions of ACh content and the rate of its release from depolarized brain synaptosomes and cultured cholinergic neuronal cells (**Figure 1F**) (Szutowicz et al., 1998b, 2006, 2013).

ACETYL-CoA LEVELS IN THE BRAIN

Acetyl-CoA concentrations in brain compartments are usually much lower than the Km values for several acetyl-CoA utilizing enzymes (**Tables 1**, **2**). In such conditions, alterations in acetyl-CoA level may play a role of the primary factor regulating *in situ* activities of acetyl-CoA utilizing enzymes and thereby flow rates through respective metabolic pathways (Tuček, 1993; Szutowicz et al., 2013, 2017; Pietrocola et al., 2015). The analysis of acetyl-CoA determinations performed within a 50-year time span in different preparations of the brain using diverse methodologies demonstrates their strikingly good intrinsic comparability (**Table 2**). In general, acetyl-CoA concentration in whole brain tissue was reported to be below 0.01 mmol/L, with intramitochondrial levels being somewhat higher than those in the cytoplasmic compartment (**Table 2**). Some data presenting several times higher acetyl-CoA concentrations in the brain may correspond to the sum of CoA-SH + acetyl-CoA levels (**Table 2**) (Zimatkin et al., 2011). There are also indications that acetyl-CoA levels in neurons may be higher than in astroglial and lower than in microglial cells (**Table 2**) (Klimaszewska-Łata et al., 2015; Zyśk et al., 2017).

The heterogeneity of neuronal groups in the brain, as well as diversity of neurotransmitter systems and functions may imply differences in acetyl-CoA concentrations and pathways of its inter-compartmental redistribution (**Figure 2**) (Sterling et al., 1981; Szutowicz et al., 1981, 1996, 2017; Rícný and Tucek, 1982; Gibson and Peterson, 1983). Such a thesis is justified by studies of cholinergic neurons with high expression of the cholinergic phenotype, which displayed lower concentrations of acetyl-CoA than those with low expression of this phenotype, or non-cholinergic ones (Bielarczyk et al., 2003; Szutowicz et al., 2004, 2013; Zyśk et al., 2017). Moreover, cholinergic differentiation – despite a decrease of whole cell acetyl-CoA – was linked with its redistribution to the cytoplasmic compartment, resulting in a substrate-dependent increase in rate of ChAT reaction (**Figure 2**). It would also be compatible with the increased demand for acetyl groups for ACh synthesis in mature cholinergic neurons (Mitzen and Koeppen, 1984; Bielarczyk et al., 2003; Szutowicz et al., 2004, 2013). One may suspect that neurons of different neurotransmitter systems might contain variable profiles of intraneuronal compartmentation acetyl-CoA. Therefore, estimations of acetyl-CoA level in whole brain tissue may not adequately reflect the distribution of this metabolite between subcellular compartments in specific cell groups (**Table 2**) (Rícný and Tucek, 1982; Szutowicz et al., 1996, 2013; Pietrocola et al., 2015; Shurubor et al., 2017).

Metabolic Regulations Through Acetyl-CoA Levels Alterations

Mitochondrial Acetyl-CoA, Energy Production, and Neuronal Viability

The PDHC plays a principal role in adequate provision and maintenance of the proper level of acetyl-CoA in mitochondrial

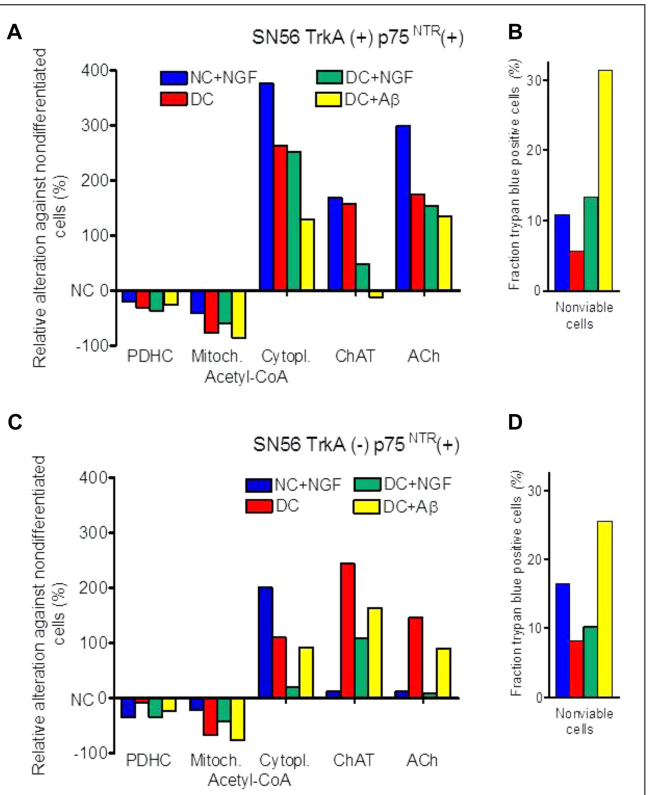

FIGURE 2 | Effects of cholinergic differentiation with dibutyryl-cAMP/RA (DC) and/or with nerve growth factor (NGF) and amyloid-β (Aβ) on PDHC and ChAT activities, acetyl-CoA distribution, acetylcholine content and loss of viability of **(A,B)** cholinergic neuroblastoma SN56 with surface TrkA(+) and p75^{NTR}(+) NGF receptors; **(C,D)** SN56 with TrkA(–) and p75^{NTR}(+) NGF receptors. Absolute values of enzyme activities and metabolite levels corresponding to 0 ordinate are given in **Table 3**.

TABLE 3 | Basal parameters of acetyl-CoA and ACh metabolism in TrkA(–) and TrkA(+) cholinergic SN56 neuronal cells.

Parameter	TrkA(+p75^{NTR}(+)	TrkA(–) p75^{NTR}(+)
PDHC activity *(nmol/min/mg protein)*	7.25 ± 0.31	7.60 ± 0.23
Mitochondrial acetyl-CoA *(pmol/mg protein)*	15.9 ± 2.1	14.2 ± 0.4
Cytoplasmic acetyl-CoA *(pmol/mg protein)*	20.1 ± 3.9	32.4 ± 3.6
Choline acetyltransferase *(nmol/min/mg protein)*	0.178 ± 0.017	0.188 ± 0.011
Acetylcholine level *(pmol/mg protein)*	149 ± 5.0	169 ± 6.0
Non-viable cell fraction *(%)*	5.5 ± 0.5	6.3 ± 0.4

Data for recalculations were taken from: Szutowicz (2001); Madziar et al. (2003), Szutowicz et al. (2004, 2005), Bielarczyk et al. (2005), Ronowska et al. (2007).

compartment of neurons, platelets and, presumably, in other cell types. The enzyme is sensitive to several neurotoxic signals both under *in vivo* and *in vitro* experimental models of neurodegeneration. Inhibitors and activators of PDHC caused decreases and increases of acetyl-CoA in mitochondrial compartment of brain nerve terminals and cultured cholinergic neuroblastoma cells, respectively (**Figures 1A,B**) (Szutowicz et al., 2013, 2017). Non-toxic, low nmolar concentrations of Aβ inhibited PDHC activity *in situ* in rat hippocampal cell culture through its hyper-phosphorylation which was activated o tau protein kinase I and glycogen synthase kinase 3 (Hoshi et al., 1996, 1997). Similar conditions may occur in the brains of AD 2576Tg and 3xTg mice, in which sub micromolar Aβ accumulation was accompanied by mental impairment, suppression of pyruvate uptake, a drop of acetyl-CoA content and ACh synthesis in nerve terminals at non-altered PDHC and ChAT activities (Yao et al., 2009; Bielarczyk et al., 2015). These findings are in accord with observations of different Tg models of AD demonstrating co-existence of diverse synaptosomal mitochondrial dysfunctions as well as cholinergic and/or behavioral deficits with amyloidosis (Perez et al., 2007; Rhein et al., 2009; Webster et al., 2014; Wang et al., 2016). On the other hand, no alterations of PDHC and KDHC activities, but an increase of pyruvate uptake, was observed in whole brain mitochondria originating predominately from non-neuronal cells (Bielarczyk et al., 2015). For the above reasons, the observations made on whole brain tissue may overlook the unique alteration of pyruvate metabolism in individual cellular compartments of the brain.

There is general agreement that the increase of Zn in postsynaptic neurons of gluzinergic synapses is one of earliest events of neurodegeneration (Sensi et al., 2009; Granzotto and Sensi, 2015). This cation, in combination with Ca shifts, is considered to be a critical factor in excitotoxic cascade yielding excessive production of NOS and ROS resulting in inhibition of PDHC and diverse enzymes of energy metabolism (Ronowska et al., 2007, 2010; Granzotto and Sensi, 2015; Zyśk et al., 2017). Common cytotoxic signals such as hypoxia/ischemia and neuroinflammation may inhibit PDHC activity both in astroglial and neuronal cells through activation of PDH kinase. Aging was found to activate c-JUN-N-terminal kinase, which inhibits PDHC activity through phosphorylation of E1α subunit leading to a decrease of ATP levels in aged brains (Zhou et al., 2009). The suppression of oxidative decarboxylation of pyruvate may result in hyperlactatemia, lactate was found to act as an intercellular signaling/messenger molecule modulating neuronal plasticity, neuron glia interactions and inflammatory pain (Halim et al., 2010; Jha et al., 2015, 2016). There is also a possibility that pyruvate may itself serve not only as an energy substrate but also as a neuroprotective agent. Chronic intraperitoneal application of large doses of pyruvate to 3xTg AD mice improved memory deficits by non-energy linked reductions of oxidative stress, hyperexcitability, and maintenance of Ca/Zn homeostasis without affecting Aβ/tau pathology (Isopi et al., 2015). Activation of brain PDHC by dichloroacetate (DCA) alleviated neurological complications and improved the survival of rats after cardiac arrest (Wang et al., 2017). There is also evidence that pyruvate derived acetyl-CoA is a direct modulator of neuronal viability. The rate of neuronal SN56 cell injury by multiple neurotoxic signals displayed strong direct correlation both with rates of pyruvate utilization and acetyl-CoA levels in neuronal mitochondria (**Figures 1A,B**) (Szutowicz et al.,

2013, 2017). The exogenous high energy compounds – ATP, phosphocreatine as well as acetyl-CoA – promoted physiological processing of APP and boosted survival in the cultured human SH-SY5Y neuronal cell (Sawmiller et al., 2012).

Therefore, one may assume that decreases in uptake F^{18}-deoxyglucose, binding of cholinergic ligands, and a drop of NAA level in MRI/PET images of AD patient's brains may be directly linked with acetyl-CoA deficits (**Figure 1**) (Zhong et al., 2014; Kumar et al., 2017; Schreiner et al., 2018). The regional pattern of these changes in individual AD patients matched well with specific clinical symptoms of their cognitive deficits (Mori et al., 2012; Jagust et al., 2015). These findings are compatible with postmortem studies of AD brains, revealing decreases of PDHC and TCA enzymes as well as cholinergic markers including ChAT, high affinity choline uptake (HACU), M_2 muscarinic autoreceptors, and VAChT (Terwel et al., 1998; Pappas et al., 2000; Bubber et al., 2005; Mufson et al., 2008; Potter et al., 2011; Jagust et al., 2015). These deficits could be also caused by direct, reversible inhibition of ChAT by Aβ oligomers, yielding cholinergic dysfunction without apparent structural impairment of neuronal terminals (Hoshi et al., 1996, 1997, Nunes-Tavares et al., 2012; Bielarczyk et al., 2015). However, some patients develop clinical symptoms of AD without accumulation of Aβ (Jagust et al., 2015). It is also apparent that ca. 80% of elderly subjects display AD-type amyloid deposits, but relatively few of them suffer from AD (Ferrer, 2012; Schreiner et al., 2018). These inconsistencies may be linked with the occurrence of different ApoE phenotypes in the AD population. Thus, 99% of AD $apoE4^+$ patients were also florbetapir positive, whereas in the AD apoE4- subgroup only 60% were florbetapir positive (Jagust et al., 2015). There is also a possibility that acetyl-CoA and energy deficits may appear much earlier and trigger the onset of different cholinergic encephalopathies, including AD (Szutowicz et al., 2013; Jagust et al., 2015). However, there is no data whether acetyl-CoA alterations might be involved in phenotypic diversity of AD.

The KDHC is an enzymatic complex of relatively low activity, thereby being a rate limiting step for the TCA cycle. Its inhibition seen in AD, TD, hepatic encephalopathy, and other brain pathologies has been identified as a primary factor responsible for energy deficits in neurodegenerating brains, being extensively reviewed elsewhere (Gibson et al., 2005; Butterworth, 2009).

Mitochondrial Acetyl-CoA and NAA Metabolism

In each type of brain cells, a major fraction of acetyl-CoA generated in mitochondria in PDHC reaction is utilized in the TCA cycle covering 98% of the energy demand. The alterations in rate of *in situ* pyruvate oxidation may bring about respective changes in levels of acetyl-CoA in the neuronal mitochondrial compartment. Inhibition of PDHC decreased availability of this substrate for the TCA cycle, yielding a decrease of ATP levels (**Figures 1A,B**) (Zyśk et al., 2017). Alterations in cytoplasmic acetyl-CoA levels correlated with its level and outward transport from the mitochondrial compartment as well as with viability of cholinergic neuronal cells (Szutowicz et al., 2013; Zyśk et al., 2017) (**Figure 1D**). In addition, 1–3% fraction of neuronal mitochondrial pool of this metabolite pool is converted intramitochondrially by aspartate *N*-acetyltransferase (AAT, EC 2.3.1.17) to NAA (Baslow, 2007; Zyśk et al., 2017). Therefore, neurons contain 98.5% of whole brain NAA. One may assume that at whole brain concentration of this amino acid, being in the range of 10 mmol/L, its intraneuronal level is likely to be several times higher (Baslow, 2007).

N-acetyl-l-aspartate is transferred from axons through axo-glial contact zones to oligodendrocytes and hydrolyzed to acetate by cytoplasmic *N*-acetyl aspartate aminohydrolase (EC 3.5.1.15) (Baslow, 2007; Moffett et al., 2013). This enzyme plays a significant role in myelination during brain ontogenesis, providing acetyl units for oligodendroglial energy production and fatty acid synthesis (Francis et al., 2016). Mutations in the aspartate aminohydrolase gene result in failure of myelin formation, manifested phenotypically as congenital pediatric leukodystrophy – Canavan's disease (Moffett et al., 2013; Francis et al., 2016). Postmortem studies of multiple sclerosis brains revealed decreased levels of NAA and acetate in gray matter from parietal and motor cortex. They suggest that mitochondrial dysfunction and reduced levels of acetyl-CoA might yield deficits of NAA in neurons, which in turn would decrease its transport to oligodendrocytes. That could result in insufficient availability of acetate compromising energy production and myelin formation in these cells (Li et al., 2013; Szutowicz et al., 2017).

Aspartate *N*-acetyltransferase, the enzyme synthesizing NAA is located exclusively in neuronal mitochondria (Baslow, 2007). Its Km values for acetyl-CoA and l-aspartate are equal to 58 and 580 μmol/L, whereas concentrations of these metabolites in the brain are estimated to be 7.5–14.0 and ca. 3500 μmol/L, respectively (**Tables 1**, **2**; Perry, 1982; Madhavarao et al., 2003; Papazisis et al., 2008). In such conditions, *in situ* metabolic flux through AAT reaction is estimated to be equal to ca. 16% of its maximal activity (Zyśk et al., 2017). Therefore, *in vivo*, at saturating levels of l-aspartate, the yield of AAT reaction may depend exclusively on acetyl-CoA concentration in the neuronal mitochondrial compartment. For instance, exposition of cholinergic SN56 neuronal cells to low-toxic Zn concentration, affected neither PDHC nor AAT levels/activities, but brought about similar ca. 50% decreases of pyruvate oxidation, acetyl-CoA, and NAA levels (**Figures 1B,C**). In these conditions, decreases in NAA levels strongly correlated with reductions of acetyl-CoA levels in whole cells and in mitochondrial compartment ($p < 0.001$) (**Figure 1C**) (Zyśk et al., 2017). This would be a first direct evidence for the thesis that alterations in NAA level in MRI imaging, seen in the gray matter of a neurodegenerating brain, may reflect changes in availability of acetyl-CoA in the neuronal compartment (**Figure 1C**) (Baslow, 2007; Moffett et al., 2013; Szutowicz et al., 2013, 2017; Schreiner et al., 2018).

Cytoplasmic Acetyl-CoA and ACh Metabolism

The functional and structural loss of cholinergic transmitter functions in the basal forebrain is a key feature of AD pathology and also includes acetyl-CoA deficits (Gelfo et al., 2013; Nell et al., 2014; Bielarczyk et al., 2015; Pepeu and Giovannini, 2017). The level of acetyl-CoA in the cytoplasmic compartment of neuronal cells is a result of the rates of its

synthesis and utilization in mitochondria and the rate of its efflux to the cytoplasm through different direct (Ca-dependent) and indirect (metabolic) mechanisms (Tuček, 1993; Szutowicz et al., 1996, 2013). Compounds altering acetyl-CoA synthesis in mitochondria and increasing their membrane permeability tend to yield higher levels of cytoplasmic acetyl-CoA (**Figure 1D**, green plot) than those not changing or inhibiting membrane permeability (**Figure 1D**, blue plot). The comparisons of Km values for acetyl-CoA against different enzymes utilizing this substrate indicate that the rates of metabolic fluxes through these metabolic steps *in situ* may be several times lower than the activities of respective enzymes estimated at saturating or suboptimal substrates concentrations (**Tables 1**, **2**).

The ChAT is expressed exclusively in brain cholinergic neurons, being a biomarker of their structural integrity and capacity to synthesize neurotransmitter ACh from choline and acetyl-CoA. Acetyl-CoA Km values for brain ChAT, reported in the literature, are in the range of 35–200 μmol/L (**Table 2**) and those of choline vary from 400 to 1500 μmol/L (Rossier et al., 1977; Ryan and McClure, 1980; Koshimura et al., 1988). On the other hand, averaged concentration of free choline in the brain was assessed to be ca. 60 μmol/L (Shea and Aprison, 1973; Brunello et al., 1982; Tuček, 1983, 1985; Klein et al., 1993), and that of acetyl-CoA to be close to 7 μmol/L, respectively (**Table 2**). Kinetic studies on ChAT preparations purified from rat brain revealed that in medium containing high phosphate – low chloride concentrations, characteristic for intracellular compartment, the Km's for acetyl-CoA and choline were equal to about 40 and 1000 μmol/L, respectively (**Table 1**) (Rossier et al., 1977; Ryan and McClure, 1980). They are several times higher than intracellular levels of these substrates (**Tables 1**, **2**). Considering such concentrations and kinetic constants for those metabolites, one may calculate that metabolic flux through ChAT in cholinergic neurons *in situ* is likely be equal to ca. 0.8% of maximal velocity of the enzyme, assessed at saturating concentrations of substrates (Szutowicz et al., 1982; Tuček, 1985; Koshimura et al., 1988). Such an approximation is compatible with rates of ACh synthesis in brain synaptosomes utilizing glucose or pyruvate, corresponding to 0.75–1.24% of their maximal ChAT activity (Szutowicz and Łysiak, 1980; Szutowicz et al., 1981; Bielarczyk and Szutowicz, 1989; Bielarczyk et al., 1998, 2015; Tomaszewicz et al., 2003).

The murine cholinergic SN56 neuroblastoma cells of septal origin, contain somewhat higher intracellular concentrations of acetyl-CoA and choline, of about 10 and 250 μmol/L, respectively (**Table 2**) (Lee et al., 1993). Based on the same equation, the calculated ChAT velocity in SN56 cells *in situ* should be equal to ca. 4% of its maximal rate (Jankowska et al., 2000; Szutowicz et al., 2004, 2006). Accordingly, K/Ca-induced rates of ACh synthesis in differentiated SN56 were found to vary from 1.9 to 3.5% of maximal ChAT activities, being close to its calculated *in situ* activities (Jankowska et al., 2000; Szutowicz et al., 2004, 2006; Bielarczyk et al., 2015). In such conditions the availability of acetyl-CoA in cytoplasmic compartment may be a primary factor limiting rate of ACh synthesis through concentration-dependent regulation ChAT activity (**Figures 1E,F**, **2**) (Tuček, 1983, 1985; Szutowicz et al., 2013, 2017). It is also certain that pyruvate, through PDHC step, is a main source of acetyl moieties for ACh synthesis (Lefresne et al., 1973; Gibson and Shimada, 1980; Sterling et al., 1981; Bielarczyk and Szutowicz, 1989). In fact, significant alterations in intraneuronal acetyl-CoA distribution were found to take place both in physiologic and neurotoxic conditions, differentially affecting mitochondrial synthesis, transport, and its utilization in cytoplasmic compartments of cultured neuronal cells and brain synaptosomes (**Figure 1**) (Szutowicz et al., 2013, 2017). In maturing cholinergic neurons, increases of cytoplasmic level of acetyl-CoA may combine with elevation of ChAT expression, yielding a non-proportionally higher increase in the rate of ACh synthesis. For instance, cAMP/RA-induced differentiation of cholinergic SN56 cells brought a ca. 110 and 40% increases of ChAT activity and cytoplasmic acetyl-CoA level, but a 290% activation of ACh synthesis, respectively (Bielarczyk et al., 2005). This suggests the existence of synergistic, positive cooperative interactions of independent elevations of ChAT activity and acetyl-CoA levels in the stimulation of neurotransmission in maturing cholinergic neurons (Bielarczyk et al., 2005). Studies on developing rat brains revealed that adequate provision of acetyl-CoA to cytoplasmic compartment in maturing cholinergic neurons may be supported by the increase of ACL activity (Szutowicz, 1979; Szutowicz et al., 1982).

Primary and secondary thiamine deficits disturb cholinergic transmission in the brain, impairing the cognitive and motor functions in affected individuals (Gibson et al., 1982; Butterworth, 2009; Jankowska-Kulawy et al., 2010). Thiamine-deficient rats displayed inhibition of ACh synthesis and release, despite the unchanged activities of ChAT – indicating the preservation of cholinergic neurons integrity in these conditions. Thus, TD-evoked inhibition of ACh metabolism resulted exclusively from *in situ* inhibition of pyruvate oxidation by PDHC, yielding decreased availability of acetyl-CoA in the mitochondria and its secondary deficits in the ACh synthesizing compartment. (**Figures 1A,E,F**). In these conditions, the rate of ACL-dependent fraction of ACh synthesis/release fell from 0.52 to 0.26% of maximal ChAT activity (Jankowska-Kulawy et al., 2010).

In addition, in cultured SN56 cholinergic cells acute Zn overload or amprolium-thiamine depletion caused inhibition of PDHC activity and proportional suppressions of cytoplasmic acetyl-CoA level and ACh synthesis without altering ChAT activity (**Figures 1A,E,F**) (Ronowska et al., 2010; Bizon-Zygmańska et al., 2011). In the early stages of Aβ encephalopathies, inhibition of cholinergic transmission may be brought about exclusively by deficits of acetyl-CoA within structurally preserved neurons (**Figures 1E,F**) (Hoshi et al., 1996, 1997; Cuadrado-Tejedor et al., 2013; Bielarczyk et al., 2015). Such reversible alterations may precede late structural losses of cholinergic neurons (Trushina et al., 2012; Szutowicz et al., 2013, 2017). In fact, persistent exposition of differentiated SN56 cells to Zn or NO excess, simulating chronic excitotoxic conditions, brought about their morphologic deterioration and death. Neurons surviving such treatments displayed irreversible loss of both PDHC and ChAT, yielding deficits of mitochondrial and cytoplasmic acetyl-CoA and ACh metabolism (Ronowska

et al., 2007; Klimaszewska-Łata et al., 2015; Zyśk et al., 2017). In latter experiments, suppressions of acetyl-CoA/ACh metabolism were caused by combination of functional and mal-adaptative structural alterations (Szutowicz et al., 2013, 2017).

One of the consequences of acetyl-CoA deficits in neuronal cytoplasm of AD brains may be decreased activity of cytoplasmic SphK1 (Ceccom et al., 2014; Bielarczyk et al., 2015). This enzyme, besides being protein kinase, also displays cyclooxygenase 2 transacetylase activity with Km for acetyl-CoA equal to 58.2 μM. This value is several times higher than neuronal levels of this metabolite (**Tables 1**, **2**) (Lee et al., 2018). Acetylation of COX2 stimulates secretion of specialized proresolving mediators, which increase phagocytosis by microglia different aberrant proteins, including Aβ. There is an inverse correlation between SphK1 activity and Aβ levels in the brains of AD patients (Ceccom et al., 2014). Hence, shortages of acetyl-CoA in cytoplasmic compartment might facilitate Aβ formation, due to decreased acetylating activity of SphK1 (Lee et al., 2018). Accumulating Aβ may further aggravate acetyl-CoA deficits, directly inhibiting PDHC activity (**Figures 2A,C**) (Hoshi et al., 1996, 1997).

Nerve Growth Factor and Neuronal Acetyl-CoA

Nerve growth factor (NGF) is a cholinotrophic cytokine that regulates the maturation, development, and maintenance of basal cholinergic neurons through retrograde signals mediated by high affinity specific TrkA and low affinity, non-specific $p75^{NTR}$ receptors (Szutowicz, 2001; Chao, 2003; Szutowicz et al., 2004; Boskovic et al., 2014; Isaev et al., 2017; Latina et al., 2017). Regional distribution of NGF protein and its mRNA correlate with density of cholinergic innervation (Korsching et al., 1985). Intracerebroventricular injections of NGF to neonatal rats increased in a dose-dependent manner ChAT and HACU activities in all groups of basal forebrain cholinergic neurons (Gnahn et al., 1983; Mobley et al., 1986; Auld et al., 2001). Similar cholinotrophic effects of NGF application were observed in adult animals (Williams and Rylett, 1990). Positive cholinotrophic effects of NGF were also observed *in vitro* in cultured hippocampal slices, primary cultures of septal and striatal neurons, as well as in PC12 and SN56 cholinergic cell lines. In each case NGF elevated expression of cholinergic phenotype bio-markers including; fractional content of ChAT positive cells, ChAT, HACU, VAChT levels/activities, as well as ACh contents and rates of its release (Martinez et al., 1985; Gähwiler et al., 1987; Szutowicz, 2001; Szutowicz et al., 2004; Madziar et al., 2008; Latina et al., 2017; Morelli et al., 2017). These adaptative positive cholinotrophic effects of NGF/BDNF are executed through TrkA/TrkB - CREB dependent signaling pathway yielding increased expression of the cholinergic locus and activation of Ca-accumulation/mobilization systems (Jiang et al., 1999; Finkbeiner, 2000; Chao, 2003). Similar differentiating effects are attained with diverse differentiation protocols acting through the mechanism of CREB activation (Szutowicz, 2001; Cheng et al., 2002). Impairment of TrkA/NGF signaling was involved in pathomechanism of early presynaptic dysfunction of cholinergic neurons (Latina et al., 2017). It was found to drive Aβ accumulation in cholinergic neurons (Triaca and Calissano, 2016). NGF administration prevented excitotoxic atrophy of cholinergic basal forebrain neurons (Charles et al., 1996). Treatment of neural stem cells *in vitro* with NGF stimulated their transformation toward fully functional cholinergic neuron-like cells which after transplantation into APP/PS1 transgenic mice corrected their cholinergic and behavioral deficits (Gu et al., 2015).

The $p75^{NTR}$ receptor is a non-specific receptor shared by all four neurotrophins (Chao, 2003). Its heterodimeric complex with TrkA increased affinity to NGF and augmented Ca influx, promoting maturation of basal cholinergic neurons (**Table 3**) (Jiang et al., 1999; Mamidipudi and Wooten, 2002; Zhang et al., 2003). On the other hand, occupancy of homodimeric form of $p75^{NTR}$ by NGF triggered ceramide-programed cell death (Carter and Lewin, 1997; Brann et al., 2002; Mamidipudi and Wooten, 2002). The excess of $p75^{NTR}$ signaling may aggravate cognitive deficits through phenotypic suppression of cholinergic neurons (Carter and Lewin, 1997; Mamidipudi and Wooten, 2002). *In vivo* knock down of $p75^{NTR}$ increased ChAT activity in aging rats (Barrett et al., 2016). The reduction of $p75^{NTR}$ expression ameliorated cognitive and cholinergic deficits in Tg2576 mice (Murphy et al., 2015).

Differentiation of both TrkA(+)$p75^{NTR}$(+) and TrkA(−)$p75^{NTR}$(+) septal cholinergic SN56 neurons with cAMP/RA increased the density of $p75^{NTR}$ receptors, apparently promoting their homo-dimerization (Szutowicz et al., 2004, 2006; Barrett et al., 2016). Such treatment also caused morphologic maturation and elevations of ChAT activity and ACh content in both TrkA (+)$p75^{NTR}$ (+) and TrkA (−)$p75^{NTR}$ (+) cells (**Table 3**). This was accompanied by a shift of acetyl-CoA from the mitochondria to their cytoplasm. The increased acetyl-CoA level in the cytoplasm was compatible with increased demand for acetyl units by activated ACh synthesis (**Table 3**) (Szutowicz et al., 2004, 2005). NGF application to non-differentiated cells increased ChAT/ACh only in cells with TrkA(+) but not with TrkA(−)phenotype. Moreover, NGF added either to cAMP/RA differentiated TrkA(+) and TrkA (−)cells caused parallel suppression of cytoplasmic acetyl-CoA levels and ChAT activities, as well as an increase of non-viable cell fractions (**Figures 2B,D**). It also aggravated the cytotoxic effects of Aβ or NO excess mediated by the increased density of $p75^{NTR}$ in DC (**Figure 2**) (Szutowicz et al., 2006). These negative alterations were alleviated by the simultaneous addition of anti-$p75^{NTR}$ antibodies (Szutowicz et al., 2004, 2005). These data indicate that both the cytoprotective/cholino-trophic and cholino-suppressive effects of NGF may be at least in part mediated through alterations of acetyl-CoA levels in mitochondrial and cytoplasmic compartments of cholinergic neurons, respectively.

Endoplasmic Reticulum and Nuclear Acetylations

Extramitochondrial acetyl-CoA directly affects acetylation levels of several proteins located in separate cytoplasmic, ER, and nuclear compartments. In peripheral tissues, starvation induces the depletion of cytoplasmic acetyl-CoA and protein deacetylation, being a principal signal triggering autophagy (Mariño et al., 2014). On the other hand, the replenishment of acetyl-CoA by DCA or lipoic acid inhibited autophagy through increased protein acetylations. The acetyltransferase EP300 was

required for autophagy suppression by high concentrations of acetyl-CoA (Mariño et al., 2014). Also, in the brain maintenance of a proper level of protein acetylation is achieved by diverse lysine acetyltransferases, including CREB-binding protein and F1A-associated protein p300. The latter seem to be crucial for normal neurodevelopment and cognitive processes (Valor et al., 2013). Both hypoacetylation and hyperacetylation may bring about a similar spectrum of dysfunctions and/or neurodegenerative disorders (Valor et al., 2013).

A small, yet unknown fraction of cytoplasmic acetyl-CoA has to be sub-distributed into ER/Golgi compartments to supply acetyl units for acetylation reactions of lysine residues in hundreds of structural proteins in order to regulate their turnover and activity (Kouzarides, 2000; Pehar and Puglielli, 2013; Ceccom et al., 2014). There is no acetyl-CoA synthesizing enzymes in ER lumen. However, ACS or ACL binding to ER may facilitate the provision of acetyl-CoA into their proximity (Linn and Srere, 1984; Mews et al., 2017). Such fine compartmentalization of these enzymes may assure the efficient transport of acetyl-CoA into ER by the specific membrane transporter (AT-1), a member of multiple transporters of the SLC33 family (Jonas et al., 2010; Hirabayashi et al., 2013). It would maintain acetyl-CoA on the level sufficient for activation of transient acetylations of lysine groups of different proteins in the ER lumen by specific lysine protein acetyltransferases (Constantini et al., 2007). They would include, among others, acetylations of β-amyloid precursor protein cleaving enzyme 1 (BACE 1), low density lipoproteins receptor (LDLR) or amyloid precursor protein (APP), and tubulin (Kouzarides, 2000; Jonas et al., 2010; Wong et al., 2018). Nuclear transacetylases were found to carry regulatory acetylations of histones and transcription factors modifying neuronal phenotype, plasticity, and memory/cognitive functions (Kouzarides, 2000; Mews et al., 2017).

The true level of acetyl-CoA in ER remains unknown, nevertheless it might be close or somewhat higher than that in the cytoplasmic compartment (**Table 2**). The Km values for acetyl-CoA for AT-1 transporter in ER membranes are in the range of 14 μmol/L, being higher than cytoplasmic concentrations of this metabolite (**Tables 1**, **2**; Constantini et al., 2007; Jonas et al., 2010). Therefore, the rate of acetyl-CoA influx into the ER compartment may be appropriately altered both by increases and decreases of cytoplasmic levels of this metabolite taking place during neuronal maturation or excitotoxic injury, respectively (**Figure 1**) (Szutowicz, 2001; Szutowicz et al., 2004, 2013; Constantini et al., 2007; Pehar and Puglielli, 2013).

On the other hand, the nuclear membrane seems to be fully permeable for acetyl-CoA. In addition, its provision directly to acetylation sites is thought to be conducted by nuclear subfractions of ACL and ACS2 (Wellen et al., 2009; Mews et al., 2017). The presence of nuclear PDHC was also documented by Sivanand et al. (2018). Such specific compartmentation of several acetyl-CoA producing enzymes drives preferential utilization of this metabolite for acetylations of nuclear proteins by numerous HAT (Kouzarides, 2000; Drazic et al., 2016; Sivanand et al., 2018). This process would be facilitated by the fact that affinities of nuclear HATs to acetyl-CoA were found to be very high, with Km values being in range of 0.3–4.8 μmol/L (**Table 1**) (Balasubramanyam et al., 2003; Ghizzoni et al., 2012; Wapenaar et al., 2015). Therefore, neuronal-cytoplasmic acetyl-CoA concentrations of 8–13 μmol/L may assure sub-maximal rates of metabolic fluxes through nuclear acetyltransferases (**Tables 1**, **2**). Consequently, the degree of nuclear histones acetylations might be regulated rather by amount/ratios of HATs and histone deacetylases than by acetyl-CoA concentration itself.

In fact, remarkable changes in proteins acetylations take place in different pathologic and physiologic conditions. Human brain autopsy revealed that increased acetylation of tau protein in AD and chronic traumatic encephalopathy brains may precede subsequent critical phosphorylation at lysine 280 (Lucke-Wold et al., 2017). On the other hand, deficient import of acetyl-CoA into ER lumen, in haploinsufficient mice carrying point mutation (S113R) in AT-1, was also associated with neurodegeneration, susceptibility to infections and increased risk of cancer (Peng et al., 2014). In another work, the same haploinsufficiency of AT-1 alleviated brain degeneration processes in ($APP_{695/swe}$) transgenic AD mice, but not in those with Huntington's disease (HD, R6/2) or ALS ($hSOD^{G93A}$) (Peng et al., 2016). This discrepancy may result from the fact that inhibition of ER acetylations improved autophagy-mediated disposal toxic protein in AD. On the other hand, removal of HD and ALS aggregates took place in the cytoplasm and could not be affected by ER acetylations (Peng et al., 2016). One of the sources of such discrepancies in these pathologies could be also variable alterations in PDHC activity, which was suppressed in AD and not altered in HD (Bubber et al., 2005; Naseri et al., 2015). That might also generate differences in acetyl-CoA availability in mitochondria yielding respective down-stream changes in extramitochondrial distribution of this metabolite (Szutowicz et al., 2013, 2017; Bielarczyk et al., 2015; Peng et al., 2016). Inhibitors of histone deacetylase could exert an indirect cytoprotective effect alleviating dysfunction of PDHC, suppressing its kinases (Naia et al., 2017). Tubastatin A, the inhibitor of histone deacetylase 6 alleviated stroke-induced infarction and functional deficits, preventing a decrease in α-tubulin acetylation evoked by occlusion of middle cerebral artery (Wang et al., 2016). Inhibition of this enzyme also prevented degeneration of pluripotent stem cells from ALS patients, increasing the level of α-tubulin acetylation and the integrity of ER and axonal transport (Guo et al., 2017).

Endogenous repair of neurons in the brain is impeded by chondroitin sulfate proteoglycans or myelin associated proteins, which were found to suppress α-tubulin acetyltransferase, thereby preventing axon regeneration and growth of primary cortical neurons (Wong et al., 2018). The reconstitution level of α-tubulin acetyltransferase by lentiviral expression or increase of Rho-associated kinase reversed tubulin acetylation and neuronal growth (Wong et al., 2018). The application of icariin, a plant flavonoid, to mice with traumatic brain injury increased the acetylation of histones and prevented loss of ChAT activity and ACh content in the hippocampus (Zhang et al., 2018). Injection of another deacetylase inhibitor trichostatin A into the hippocampal CA1 area of prenatally stressed rats prevented the development

of depressive behavior and reversed the suppression of AMPA glutamate receptors mRNA in the hippocampus (Lu et al., 2017). On the other hand, excessive expression of AT1/SLC33A1 in an AT-1 Tg mouse model affected dendritic branching, spine formation, and key metabolic pathways yielding cognitive deficits and autistic-like phenotype (Hullinger et al., 2016).

CONCLUSION

Pyruvate-derived acetyl-CoA and oxaloacetate are principal energy-precursor substrates feeding the TCA cycle in the brain mitochondria. A relatively small fraction of mitochondrial acetyl-CoA is utilized in a large number of diverse synthetic pathways taking place in different subcellular compartments. In addition, each type of brain neuronal and glial cells apparently possesses their own individual, unique metabolic profile of acetyl-CoA distribution, fitting their specific functions. At least four subcellular structural and functional acetyl-CoA compartments have been identified, which utilize this intermediate for synthesis of a diverse range of acetylated regulatory and signaling compounds. The concentrations of acetyl-CoA in different subcellular compartments are low and may change in a fairly broad range in the course of different physiologic and pathologic conditions. On the other hand, acetyl-CoA metabolizing enzymes display relatively low affinity to this substrate. Therefore, pathophysiologic alterations in intracellular compartmentation of acetyl-CoA may be early primary signals that deeply modify cell viability and function.

In the mitochondrial compartment of neurons, the rate of NAA synthesis by AAT correlates, with acetyl-CoA level, which also directly affects neuronal viability. The output of acetyl-CoA from mitochondrial to extramitochondrial compartments depends on the rate of its synthesis by PDHC and the capacity of transport systems in the mitochondrial membranes. In cholinergic neurons, mitochondrial levels of acetyl-CoA are lower and those in the cytoplasm are higher than in respective compartments of non-cholinergic cells. The high level of acetyl-CoA in mature cholinergic neurons cytoplasm is necessary for the maintenance rate of ACh synthesis adequate to its release. In different pathophysiological conditions, the rates of ACh synthesis and release directly correlated with the levels of acetyl-CoA in the cytoplasmic compartment of the neuron. The NGF-evoked, TrkA/$p75^{NTR}$ dependent maturation of cholinergic neurons and their susceptibility to injury may be mediated by changes in intracellular redistribution of acetyl-CoA. The provision of acetyl-CoA to ER and nuclear sub-compartments may play a key role in the development and maintenance of neuronal cells viability through alteration of the acetylation level of lysine residues of a very large range of regulatory proteins and peptides.

This review illustrates that alterations in concentration and intracellular compartmentalization of acetyl-CoA play a significant role in direct substrate-dependent regulation of multiple acetylation reactions velocities, as well as signaling molecule changing properties of several regulatory peptides and proteins. More research is required to uncover the role of acetyl-CoA in pathomechanisms and potential therapeutic approaches to neurodegenerative diseases.

AUTHOR CONTRIBUTIONS

AR writing most of whole chapter acetyl-CoA precursors in the brain. AS corresponding author, writing of introduction, conclusions, coordinator, main reviewer, tables and figures preparation. HB writing of subchapters introduction to acetyl-CoA levels in the brain, mitochondrial acetyl-CoA, energy production and neuronal viability. SG-H writing of endoplasmic reticulum and nuclear acetylations. JK-Ł writing of NGF and neuronal acetyl-CoA. AD writing of cytoplasmic acetyl-CoA and ACh metabolism. MZ writing of mitochondrial acetyl-CoA and NAA metabolism. AJ-K writing of subchapter acetate and brain acetyl-CoA.

FUNDING

This work was supported by St57 MUG project.

REFERENCES

Angielski, S., and Szutowicz, A. (1967). Tissue content of citrate and citrate-cleavage enzyme activity during starvation and refeeding. *Nature* 213, 1252–1253. doi: 10.1038/2131252a0

Auld, D. S., Mennicken, F., Day, J. C., and Quirion, R. (2001). Neurotrophins differentially enhance acetylcholine release, acetylcholine content and choline acetyltransferase activity in basal forebrain neurons. *J. Neurochem.* 77, 253–262. doi: 10.1046/j.1471-4159.2001.00234.x

Balasubramanyam, K., Swaminathan, V., Ranganathan, A., and Kundu, T. K. (2003). Small molecule modulators of histone acetyltransferase p300. *J. Biol. Chem.* 278, 19134–19140. doi: 10.1074/jbc.M301580200

Barrett, G. L., Naim, T., Trieu, J., and Huang, M. (2016). In vivo knockdown of basal forebrain p75 neurotrophin receptor stimulates choline acetyltransferase activity in the mature hippocampus. *J. Neurosci. Res.* 94, 389–400. doi: 10.1002/jnr.23717

Baslow, M. H. (2007). "N-acetylaspartate, and N-acetylaspartylglutamate," in *Handbook of Neurochemistry and Molecular Biology Amino acids and peptides in the nervous system*, 3rd Edn, eds S. S. Oja, A. Schousboe, and P. Saransaari (Berlin: Springer), 305–346.

Beigneux, A. P., Kosinski, C., Gavino, B., Horton, J. D., Skarnes, W. C., and Young, S. G. (2004). ATP-citrate lyase deficiency in the mouse. *J. Biol. Chem.* 279, 9557–9564. doi: 10.1074/jbc.M310512200

Bielarczyk, H., Jankowska-Kulawy, A., Gul, S., Pawełczyk, T., and Szutowicz, A. (2005). Phenotype dependent differentia effects of interleukin-1beta and amyloid-beta on viability and cholinergic phenotype of T17 neuroblastoma cells. *Neurochem. Int.* 47, 466–473. doi: 10.1016/j.neuint.2005.06.010

Bielarczyk, H., Jankowska-Kulawy, A., Höfling, C., Ronowska, A., Gul-Hinc, S., and Roßner, S. (2015). AβPP-transgenic 2576 mice mimic cell type-specific aspects of acetyl-CoA-linked metabolic deficits in Alzheimer's disease. *J. Alzheimers Dis.* 48, 1083–1094. doi: 10.3233/JAD-150327

Bielarczyk, H., and Szutowicz, A. (1989). Evidence for the regulatory function of synaptoplasmic acetyl-CoA in acetylcholine synthesis in nerve endings. *Biochem. J.* 262, 377–380. doi: 10.1042/bj2620377

Bielarczyk, H., Tomaszewicz, M., Madziar, B., Ćwikowska, J., Pawełczyk, T., and Szutowicz, A. (2003). Relationships between cholinergic phenotype and acetyl-CoA level in hybrid murine neuroblastoma cells of septal origin. *J. Neurosci. Res.* 73, 717–721. doi: 10.1002/jnr.10711

Bielarczyk, H., Tomaszewicz, M., and Szutowicz, A. (1998). Effect of aluminum on acetyl-CoA and acetylcholine metabolism in nerve terminals. *J. Neurochem.* 70, 1175–1181. doi: 10.1046/j.1471-4159.1998.70031175.x

Birks, R. I. (1977). A long-lasting potentiation of transmitter release related to an increase in transmitter stores in a sympathetic ganglion. *J. Physiol.* 271, 847–862. doi: 10.1113/jphysiol.1977.sp012028

Bizon-Zygmańska, D., Jankowska-Kulawy, A., Bielarczyk, H., Pawełczyk, H., Ronowska, A., and Marszałł, M. (2011). Acetyl-CoA metabolism in amprolium-evoked thiamine pyrophosphate deficits in cholinergic SN56 neuroblastoma cells. *Neurochem. Int.* 59, 208–216. doi: 10.1016/j.neuint.2011.04.018

Bloisi, W., Colombo, I., Garavaglia, B., Giardini, R., Finocchiaro, G., and Didonato, S. (1990). Purification and properties carnitine acetyltransferase from human liver. *Eur. J. Biochem.* 189, 539–546. doi: 10.1111/j.1432-1033.1990.tb15520.x

Boskovic, Z., Alfonsi, F., Rumballe, B. A., Fonseka, S., Windels, F., and Coulson, E. J. (2014). The role of p75NTR in cholinergic basal forebrain structure and function. *J. Neurosci.* 34, 13033–13038. doi: 10.1523/JNEUROSCI.2364-14.2014

Brann, A. B., Tcherpakov, M., Williams, I. M., Futerman, A. H., and Fainzilber, M. (2002). Nerve growth factor-induced p76-mediated death of cultured hippocampal neurons is age-dependent and transduced through ceramide generated by neutral sphingomyelinase. *J. Biol. Chem.* 277, 9812–9818. doi: 10.1074/jbc.M109862200

Brunello, N., Cheney, D. L., and Costa, E. (1982). Increase in exogenous choline fails to elevate the content or turnover rate of cortical, striatal or hippocampal acetylcholine. *J. Neurochem.* 38, 1160–1163. doi: 10.1111/j.1471-4159.1982.tb05364.x

Bubber, P., Haroutunian, V., Fisch, G., Blass, J. P., and Gibson, G. E. (2005). Mitochondrial abnormalities in Alzheimer brain: mechanistic implications. *Ann. Neurol.* 57, 695–703. doi: 10.1002/ana.20474

Buckley, B. M., and Williamson, D. H. (1973). Acetoacetate and brain lipogenesis: developmental pattern of acetoacetyl-coenzyme A synthetase in the soluble fraction of the brain. *Biochem. J.* 132, 653–656. doi: 10.1042/bj1320653

Butterworth, R. F. (2009). Thiamine deficiency-related brain dysfunction in chronic liver failure. *Metab. Brain Dis.* 24, 189–196. doi: 10.1007/s11011-008-9129-y

Camberos-Luna, L., Gerónimo-Olvera, C., Montiel, T., Rincon-Heredia, R., and Massieu, L. (2016). The ketone body, β-hydroxybutyrate stimulates autophagic flux and prevents neuronal death induced glucose deprivation in cortical cultured neurons. *Neurochem. Res.* 41, 600–609. doi: 10.1007/s11064-015-1700-4

Carlsson, C., and Chapman, A. G. (1981). The effect of diazepam on the cerebral metabolic state in rats and its interaction with nitrous oxide. *Anesthesiology* 54, 488–495. doi: 10.1097/00000542-198106000-00008

Carter, B. D., and Lewin, G. R. (1997). Neutrophins live or let die: does p75NTR decide? *Neuron* 18, 187–190. doi: 10.1016/S0896-6273(00)80259-7

Castellano, C. A., Nugent, S., Paquet, N., Tremblay, S., Bocti, C., and Lacombe, G. (2015). Lower brain 18F-fluorodeoxyglucose uptake but normal 11C-acetoacetate metabolism in mild Alzheimer's disease dementia. *J. Alzheimers Dis.* 43, 1343–1353. doi: 10.3233/JAD-141074

Ceccom, J., Loukh, N., Lauwers-Cances, V., Touriol, C., Nicaise, Y., and Gentil, C. (2014). Reduced sphigosine kinase-1 and enhanced sphingosine 1-phosphate lyase expression demonstrate dysregulated shingosine 1-phosphate signaling in Alzheimer's disease. *Acta Neuropathol. Commun.* 2:12. doi: 10.1186/2951-5960-2-12

Chao, M. V. (2003). Neurotrophins and their receptors: a convergence point for many signaling pathways. *Nat. Rev. Neurosci.* 4, 299–309. doi: 10.1038/nrn1078

Charles, V., Mufson, E. J., Friden, P. M., Bartus, R. T., and Kordower, J. H. (1996). Atrophy of cholinergic basal forebrain neurons following excitotoxic cortical lesions is reversed by intravenous administration of an NGF conjugate. *Brain Res.* 728, 193–203. doi: 10.1016/0006-8993(96)00398-8

Chechik, T., Roeder, L. M., Tildon, J. T., and Poduslo, S. E. (1987). Ketone body enzyme activities in purified neurons, astrocytes and oligodendrocytes. *Neurochem. Int.* 10, 95–99. doi: 10.1016/0197-0186(87)90179-3

Cheema-Dhadli, S., Halperin, M. L., and Leeznoff, C. C. (1973). Inhibition of enzymes which interact with citrate by (-)hydroxycitrate and 1.2,3,-tricarboxybenzene. *Eur. J. Biochem.* 38, 98–102. doi: 10.1111/j.1432-1033.1973.tb03038.x

Cheng, H. C., Shih, H. M., and Chern, Y. (2002). Essential role of cAMP-response element-binding protein activation by A2A adenosine receptors in rescuing the nerve growth factor-induced neurite outgrowth impaired by blockage of the MAPK cascade. *J. Biol. Chem.* 277, 33930–33942. doi: 10.1074/jbc.M201206200

Constantini, C., Ko, M. H., Jonas, M. C., and Puglielli, L. (2007). A reversible form of lysine acetylation in the ER and Golgi lumen controls the molecular stabilization of BACE1. *Biochem. J.* 407, 383–395. doi: 10.1042/BJ20070040

Coude, F. X., Sweetman, L., and Nyhan, W. L. (1979). Inhibition by propionyl-coenzyme A of N-acetylglutamate synthetase in rat liver mitochondria. *J. Clin. Invest.* 64, 1544–1551. doi: 10.1172/JCI109614

Cuadrado-Tejedor, M., Cabodevilla, J. F., Zamarbide, M., Gomez-Isla, T., Franco, R., and Perez-Mediavilla, A. (2013). Age-related mitochondrial alterations without neural loss in the hippocampus of a transgenic model of Alzheimer's disease. *Curr. Alzheimer Res.* 10, 390–405. doi: 10.2174/1567205011310040005

Cunnane, S., Nugent, S., Roy, M., Courchesne-Loyer, A., Croteau, E., and Tremblay, S. (2011). Brain fuel metabolism, aging and Alzheimer's disease. *Nutrition* 27, 3–20. doi: 10.1016/j.nut.2010.07.021

Dietschy, J. M., and Turley, S. D. (2004). Thematic review series: brain lipids. Cholesterol metabolism in the central nervous system during early development and in mature animal. *J. Lipid Res.* 45, 1375–1397. doi: 10.1194/jlr.R400004-JLR200

Drazic, A., Myklebust, L. M., Ree, R., and Arnesen, T. (2016). The world of protein acetylation. *Biochim. Biophys. Acta* 1864, 1372–1401. doi: 10.1016/j.bbapap.2016.06.007

Ferrer, I. (2012). Defining Alzheimer as a common age-related neurodegenerative process not inevitably leading to dementia. *Progr. Neurobiol.* 97, 38–51. doi: 10.1016/j.pneurobio.2012.03.005

Finkbeiner, S. (2000). CREB couples neurotrophin signals to survival messages. *Neuron* 25, 11–14. doi: 10.1016/S0896-6273(00)80866-1

Francis, J. S., Wojtas, I., Markov, V., Gray, S. J., McCown, T. J., and Samulski, R. J. (2016). N-acetylaspartate supports the energetic demands of developmental myelination via oligodendroglial aspartoacylase. *Neurobiol. Dis.* 96, 323–334. doi: 10.1016/j.nbd.2016.10.001

Gähwiler, B. H., Enz, A., and Hefti, F. (1987). Nerve growth factor promotes development of the rat septo-hippocampal cholinergic projection in vitro. *Neurosci. Lett.* 75, 6–10. doi: 10.1016/0304-3940(87)90066-8

Gelfo, F., Petrosini, L., Graziano, A., De Bartolo, P., Burello, L., and Vitale, E. (2013). Cortical metabolic deficits in a rat model of cholinergic basal forebrain degeneration. *Neurochem. Res.* 38, 2114–2123. doi: 10.1007/s11064-013-1120-2

Ghizzoni, M., Wu, J., Gao, T., Haisma, H. J., Dekker, F. J., and Zheng, G. Y. (2012). 6-alkylsalicylates are selective Tip60 inhibitors and target the acetyl-CoA binding. *Eur. J. Med. Chem.* 47, 337–344. doi: 10.1016/j.ejmech.2011.11.001

Gibson, G. E., Barclay, L., and Blass, J. (1982). The role of the cholinergic system in thiamin deficiency. *Ann. N. Y. Acad. Sci.* 378, 382–403. doi: 10.1111/j.1749-6632.1982.tb31213.x

Gibson, G. E., Blass, J. P., Beal, M. F., and Bunik, V. (2005). The α-ketoglutarate-dehydrogenase complex: a mediator between mitochondria and oxidative stress in neurodegeneration. *Mol. Neurobiol.* 31, 43–63. doi: 10.1385/MN:31:1-3:043

Gibson, G. E., and Peterson, C. (1983). Acetylcholine and oxidative metabolism in septum and hippocampus in vitro. *J. Biol. Chem.* 258, 1142–1145.

Gibson, G. E., and Shimada, M. (1980). Studies on metabolic pathway of the acetyl group for acetylcholine synthesis. *Biochem. Pharmacol.* 29, 167–174. doi: 10.1016/0006-2952(80)90325-1

Gnahn, H., Hefti, F., Heumann, R., Schwab, M. E., and Thoenen, H. (1983). NGF-mediated increase of choline acetyltransferase (ChAT) in the neonatal forebrain: evidence for a physiological role of NGF in the brain? *Brain Res.* 285, 45–52. doi: 10.1016/0165-3806(83)90107-4

Gnoni, G. V., Priore, P., Geelen, M. J., and Siculella, L. (2009). The mitochondrial citrate carrier: metabolic role and regulation of its activity and expression. *IUBMB Life* 61, 987–994. doi: 10.1002/iub.249

Granzotto, A., and Sensi, S. L. (2015). Intracellular zinc is a critical intermediate in the excitotoxic cascade. *Neurobiol. Dis.* 81, 25–37. doi: 10.1016/j.nbd.2015.04.010

Gu, G., Zhang, W., Li, M., Ni, J., and Wang, P. (2015). Transplantation of NSC-derived cholinergic neuron-like cells improves cognitive function in APP/PS1 transgenic mice. *Neuroscience* 291, 81–92. doi: 10.1016/j.neuroscience.2015.01.073

Guo, W., Naujock, M., Fumagalli, L., Vandoorne, T., Baatsen, P., and Boon, R. (2017). HDAC6 inhibition reverses axonal transport defects in motor neurons derived from FUS-ALS patients. *Nat. Commun.* 8:861. doi: 10.1038/s41467-017-00911-y

Guynn, R. W. (1976). Effect of ethanol on brain CoA and acetyl-CoA. *J. Neurochem.* 27, 303–304. doi: 10.1111/j.1471-4159.1976.tb01583.x

Halim, N. D., Mcfate, T., Mohyeldin, A., Okagaki, P., Korotchkina, L. G., and Patel, S. M. (2010). Phosphorylation status of pyruvate dehydrogenase distinguishes metabolic phenotypes of cultured rat brain astrocytes and neurons. *Glia* 58, 1168–1176. doi: 10.1002/glia.20996

Herculano-Houzel, S. (2011). Scaling of brain metabolism with fixed energy budget per neuron: implications for neuronal activity, plasticity and evolution. *PLoS One* 6:e17514. doi: 10.1371/journal.pone.0017514

Herculano-Houzel, S. (2014). The glia/neuron ratio: how it varies uniformly across brain structures and species and what that means for brain physiology and evolution. *Glia* 62, 1377–1391. doi: 10.1002/glia.22683

Hirabayashi, Y., Nomura, K. H., and Nomura, K. (2013). The acetyl-CoA transporter family SLC33. *Mol. Aspects Med.* 34, 586–589. doi: 10.1016/j.mam.2012.05.009

Hoshi, M., Takashima, A., Murayama, M., Yasutake, K., Yoshida, N., and Hoshino, T. (1997). Nontoxic amyloid beta peptide 1-42 suppresses acetylcholine synthesis. Possible role in cholinergic dysfunction in Alzheimer's disease. *J. Biol. Chem.* 272, 2038–2041. doi: 10.1074/jbc.272.4.2038

Hoshi, M., Takashima, A., Noguchi, K., Murayama, M., Sato, M., and Kondo, S. (1996). Regulation of mitochondrial pyruvate dehydrogenase activity by tau protein kinase I/glycogen synthase kinase 3beta in brain. *Proc. Natl. Acad. Sci. U.S.A.* 93, 2719–2723. doi: 10.1073/pnas.93.7.2719

Hovik, R., Brodal, B., Bartlett, K., and Osmundsen, H. (1991). Metabolism of acetyl-CoA by isolated peroxisomal fractions: formation of acetate and acetoacetyl-CoA. *J. Lipid Res.* 32, 993–999.

Hullinger, R., Li, M., Wang, J., Peng, Y., Dowell, J. A., Bomba-Warczak, E., et al. (2016). Increased expression of AT-1/SLC33A1 causes an autistic-like phenotype in mice by affecting dendritic branching and spine formation. *J. Exp. Med.* 213, 1267–1284. doi: 10.1084/jem.20151776

Isaev, N. K., Stelmashook, E. V., and Genrikhs, E. E. (2017). Role of nerve growth factor in plasticity of forebrain cholinergic neurons. *Biochemistry* 82, 291–300. doi: 10.1134/S0006297917030075

Isopi, E., Granzotto, A., Corona, C., Bomba, M., Ciavardelli, D., and Curcio, M. (2015). Pyruvate prevents the development of age-dependent cognitive deficits in a mouse model of Alzheimer's disease without reducing amyloid and tau pathology. *Neurobiol. Dis.* 81, 214–224. doi: 10.1016/j.nbd.2014.11.013

Jagust, W. J., Landau, S. M., Koeppe, R. A., Reiman, E. M., Chen, K., Mathis, C. A., et al. (2015). The Alzheimer's disease neuroimaging initiative 2PET Core: 2015. *Alzheimer's Dement.* 11, 757–771. doi: 10.1016/j.jalz.2015.05.001

Jankowska, A., Madziar, B., Tomaszewicz, M., and Szutowicz, A. (2000). Acute and chronic effects of aluminum on acetyl-CoA and acetylcholine metabolism in differentiated and nondifferentiated SN56 cholinergic cells. *J. Neurosci. Res.* 62, 615–622. doi: 10.1002/1097-4547(20001115)62:4<615::AID-JNR17>3.0.CO;2-1

Jankowska-Kulawy, A., Bielarczyk, H., Pawełczyk, T., Wróblewska, M., and Szutowicz, A. (2010). Acetyl-CoA and acetylcholine metabolism in nerve terminal compartment of thiamine deficient rat brain. *J. Neurochem.* 115, 333–342. doi: 10.1111/j.1471-4159.2010.06919.x

Jha, M. K., Lee, I. K., and Suk, K. (2016). Metabolic reprogramming by the pyruvate dehydrogenase kinase-lactic acid axis: linking metabolism and diverse neuropathophysiologies. *Neurosci. Biobehav. Rev.* 68, 1–19. doi: 10.1016/j.neubiorev.2016.05.006

Jha, M. K., Song, G. J., Lee, M. G., Jeoung, N. H., Go, Y., and Harris, R. A. (2015). Metabolic connection of inflammatory pain: pivotal role of a pyruvate dehydrogenase kinase-pyruvate dehydrogenase-lactic acid axis. *J. Neurosci.* 35, 14353–14369. doi: 10.1523/JNEUROSCI.1910-15.2015

Jiang, H., Takeda, K., Lazarovici, P., Katagiri, Y., Yu, Z.-X., Dickens, G., et al. (1999). Nerve growth factor (NGF)-induced calcium influx and intracellular calcium mobilization in 3T3 cells expressing NGF receptor. *J. Biol. Chem.* 274, 26209–26216. doi: 10.1074/jbc.274.37.26209

Jolivet, R., Magistretti, P. J., and Weber, B. (2009). Deciphering neuron-glia compartmentalization in cortical energy metabolism. *Front. Neuroenergetics* 1:4. doi: 10.3389/neuro.14.004.2009

Jonas, M. C., Pehar, M., and Puglielli, L. (2010). AT-1 is the ER membrane acetyl-CoA transporter and is essential for cell viability. *J. Cell Sci.* 123, 3378–3388. doi: 10.1242/jcs.068841

Kato, T., Inui, Y., Nakamura, A., and Ito, K. (2016). Brain fluorodeoxyglucose (FDG) PET in dementia. *Ageing Res. Rev.* 30, 73–84. doi: 10.1016/j.arr.2016.02.003

Klein, J., Gonzalez, R., Köppen, A., and Löffelholz, K. (1993). Free choline and choline metabolites in rat brain and body fluids: sensitive determination and implications for choline supply to the brain. *Neurochem. Int.* 22, 293–300. doi: 10.1016/0197-0186(93)90058-D

Klimaszewska-Łata, J., Gul-Hinc, S., Bielarczyk, H., Ronowska, A., Zyśk, M., and Grużewska, K. (2015). Differential effects of lipopolysaccharide on energy metabolism in murine microglial N9 and cholinergic SN56 neuronal cells. *J. Neurochem.* 133, 284–297. doi: 10.1111/jnc.12979

Kochunov, P., Coyle, T., Lancaster, J., Robin, D. A., Hardies, J., and Kochunov, V. (2010). Processing speed is correlated with cerebral health markers in the frontal lobes as quantified by neuroimaging. *Neuroimage* 49, 1190–1199. doi: 10.1016/j.neuroimage.2009.09.052

Korsching, S., Auburger, G., Heumann, R., Scott, J., and Thoenen, H. (1985). Levels of nerve growth factor and its mRNA in the central nervous system of the rat correlate with cholinergic innervation. *EMBO J.* 4, 1389–1393.

Koshimura, K., Nakamura, S., Miwa, S., Fujiwara, M., and Kameyama, M. (1988). Regional difference in the kinetics of choline acetyltransferase in brains of neurologically normal elderly people and those with Alzheimer-type dementia. *J. Neurol. Sci.* 84, 141–146. doi: 10.1016/0022-510X(88)90119-0

Kouzarides, T. (2000). Acetylation: a regulatory modification to rival phosphorylation? *EMBO J.* 19, 1176–1179. doi: 10.1093/emboj/19.6.1176

Kozler, P., Riljak, V., and Pokorny, J. (2013). Both water intoxication and osmotic BBB disruption increase brain water content in rats. *Physiol. Res.* 62(Suppl. 1), S75–S80.

Krikorian, R., Shidler, M. D., Dangelo, K., Couch, S. C., Benoit, S. C., and Clegg, D. J. (2012). Dietary ketosis enhances memory in mild cognitive impairment. *Neurobiol. Aging* 33, 425.e19–425.e27. doi: 10.1016/j.neurobiolaging.2010.10.006

Kuhar, M. J., and Rommelspacher, H. (1974). Acetylcholinesterase-staining synaptosomes from rat hippocampus: relative frequency and tentative estimation of internal concentration of free or 'labile bound' acetylcholine. *Brain Res.* 77, 85–96. doi: 10.1016/0006-8993(74)90806-3

Kumar, R., Kumar, A., Långström, M. B., and Darreh-Shori, T. (2017). Discovery of novel choline acetyltransferase inhibitors using structure-based virtual screening. *Sci. Rep.* 7:16287. doi: 10.1038/s41598-017-16033-w

Latina, V., Caioli, S., Zona, C., Ciotti, M. T., Amadoro, G., and Callisano, P. (2017). Impaired NGF/TrkA signaling causes early AD-linked presynaptic dysfunction in cholinergic primary neurons. *Front. Cell. Neurosci.* 11:68. doi: 10.3389/fncel.2017.00068

Lee, H. C., Fellenz-Maloney, M. P., Liscovitch, M., and Blusztajn, J. K. (1993). Phospholipase D-catalyzed hydrolysis of phosphatidylcholine provides the choline precursor for acetylcholine synthesis in human neuronal cell line. *Proc. Natl. Acad. Sci. U.S.A.* 90, 10086–10090. doi: 10.1073/pnas.90.21.10086

Lee, J. Y., Han, S. H., Park, M. H., Baek, B., Song, I. S., Choi, M. K., et al. (2018). Neuronal SphK1 acetylates COX2 and contributes to pathogenesis in a model of Alzheimer's disease. *Nat. Commun.* 9:1479. doi: 10.1038/s41467-018-03674-2

Lefresne, P., Guyenet, P., and Glowinski, J. (1973). Acetylcholine synthesis from (2-14C) pyruvate in rat striatal slices. *J. Neurochem.* 20, 1083–1097. doi: 10.1111/j.1471-4159.1973.tb00079.x

Li, S., Clements, R., Sulak, M., Gregory, R., Freeman, E., and McDonough, J. (2013). Decreased NAA in gray matter is correlated with decreased availability

of acetate in white matter in postmortem multiple sclerosis cortex. *Neurochem. Res.* 38, 2385–2396. doi: 10.1007/s11064-013-1151-8

Linn, T. C., and Srere, P. A. (1984). Binding of ATP citrate lyase to the microsomal fraction of rat liver. *J. Biol. Chem.* 259, 13379–13384.

Lowe, D. M., and Tubbs, P. K. (1985). 3-hydroxy-3-methylglutaryl-coenzyme A synthase from ox liver. Purification, molecular and catalytic properties. *Biochem. J.* 227, 591–599. doi: 10.1042/bj2270591

Lu, Y., Zhang, J., Zhang, L., Dang, S., Su, Q., and Zhang, H. (2017). Hippocampal acetylation may improve prenatal-stress-induced depression-like behavior of male offspring rats through regulating AMPARs expression. *Neurochem. Res.* 42, 3456–3464. doi: 10.1007/s11064-017-2393-7

Lucke-Wold, B., Seidel, K., Udo, R., Omalu, B., Ornstein, M., and Nolan, R. (2017). Role of tau acetylation in Alzheimer's disease and chronic traumatic encephalopathy: the way forward for successful treatment. *J. Neurol. Neurosurg.* 4:140.

Łysiak, W., Szutowicz, A., and Angielski, S. (1976). Pyruvate metabolism in rat brain mitochondria. *Acta Biochim. Polon.* 23, 325–333.

Madhavarao, C. N., Chinopoulos, C., Chandrasekaran, K., and Namboodiri, M. A. (2003). Characterization of the N-acetylaspartate biosynthetic enzyme from rat brain. *J. Neurochem.* 86, 824–835. doi: 10.1046/j.1471-4159.2003.01905.x

Madziar, B., Shah, S., Brock, M., Burke, R., Lopez-Coviela, I., and Nickel, A. C. (2008). Nerve growth factor regulates the expression of the cholinergic locus and the high-affinity choline transporter via the Akt/PKB signaling pathway. *J. Neurochem.* 107, 1284–1293. doi: 10.1111/j.1471-4159.2008.05681.x

Madziar, B., Tomaszewicz, M., Matecki, A., Bielarczyk, H., and Szutowicz, A. (2003). Interactions between p75 and TrkA receptors in differentiation and vulnerability of SN56 cholinergic cells to beta-amyloid. *Neurochem. Res.* 28, 461–465. doi: 10.1023/A:1022800802179

Mamidipudi, V., and Wooten, M. W. (2002). Dual role for p75(NTR) signaling in survival and cell death: can intracellular mediators provide an explanation? *J. Neurosci. Res.* 68, 373–384. doi: 10.1002/jnr.10244

Mangia, S., DiNuzzo, M., Giove, F., Carruthers, A., Simpson, I. A., and Vannucci, S. J. (2011). Response to comment on recent modeling studies of astrocyte-neuron metabolic interactions': much ado about nothing. *J. Cereb. Blood Flow Metab.* 31, 1346–1353. doi: 10.1038/jcbfm.2011.29

Mariño, G., Pietrocola, F., Eisenberg, T., Kong, Y., Malik, S. A., and Andryushkova, A. (2014). Regulation of autophagy by cytosolic acetyl-coenzyme A. *Mol. Cell.* 53, 710–725. doi: 10.1016/j.molcel.2014.01.016

Marosi, K., Kim, S. W., Moehl, K., Scheibye-Knudsen, M., Cheng, A., and Cutler, R. (2016). 3-Hydroxybutyrate regulates energy metabolism and induces BDNF expression in cerebral cortical neurons. *J. Neurochem.* 139, 769–781. doi: 10.1111/jnc.13868

Martinez, H. J., Dreyfus, C. F., Jonakait, G. M., and Black, I. B. (1985). Nerve growth factor promotes cholinergic development in brain striatal cultures. *Proc. Natl. Acad. Sci. U.S.A.* 82, 7777–7781. doi: 10.1073/pnas.82.22.7777

Matsuoka, Y., and Srere, P. A. (1973). Kinetic studies of citrate synthase from rat kidney and rat brain. *J. Biol. Chem.* 248, 8022–8030.

Mattson, M. P., Moehl, K., Ghena, N., Schmaedick, M., and Cheng, A. (2018). Intermittent metabolic switching, neuroplasticity and brain health. *Nat. Rev. Neurosci.* 19, 63–80. doi: 10.1038/nrn.2017.156

McKenna, M. C. (2012). Substrate competition studies demonstrate oxidative metabolism of glucose, glutamate, glutamine, lactate and 3-hydroxybutyrate in cortical astrocytes from rat brain. *Neurochem. Res.* 37, 2613–2626. doi: 10.1007/s11064-012-0901-3

Mews, P., Donahue, G., Drake, A. M., Luczak, V., Abel, T., and Berger, S. L. (2017). Acetyl-CoA synthetase regulates histone acetylation and hippocampal memory. *Nature* 546, 381–386. doi: 10.1038/nature22405

Middleton, B. (1974). The kinetic mechanism and properties of the cytoplasmic acetoacetyl-coenzyme A thiolase from rat liver. *Biochem. J.* 139, 109–121. doi: 10.1042/bj1390109

Mitzen, E. J., and Koeppen, A. H. (1984). Malonate, malonyl-CoA, and acetyl-coenzyme A in developing rat brain. *J. Neurochem.* 43, 499–506. doi: 10.1111/j.1471-4159.1984.tb00927.x

Mobley, W. C., Rutkowski, J. L., Tennekoon, G. I., Gemski, J., Buchanan, K., and Johnston, M. V. (1986). Nerve growth factor increases choline acetyltransferase activity in developing basal forebrain neurons. *Brain Res.* 387, 53–62. doi: 10.1016/0169-328X(86)90020-3

Moffett, J. R., Arun, P., Ariyannyr, P. S., and Namboodiri, A. M. (2013). N-acetylaspartate reductions in brain injury: impact on post-injury neuroenergetics, lipid synthesis, and protein acetylation. *Front. Neuroenergetics* 5:11. doi: 10.3389/fnene.2013.00011

Morelli, A., Sarchielli, E., Guarnieri, G., Coppi, E., Pantano, D., and Comeglio, P. (2017). Young human cholinergic neurons respond to physiological regulators and improve cognitive symptoms in an animal model of Alzheimer's disease. *Front. Cell. Neurosci.* 11:339. doi: 10.3389/fncel.2017.00339

Mori, T., Maeda, J., Shimada, H., Higuchi, M., Shinotoh, H., and Ueno, S. (2012). Molecular imaging of dementia. *Psychogeriatrics* 12, 106–114. doi: 10.1111/j.1479-8301.2012.00409.x

Mufson, E. J., Counts, S. E., Perez, S. E., and Ginsberg, S. D. (2008). Cholinergic system during the progression of Alzheimer's disease: therapeutic implications. *Expert Rev. Neurother.* 8, 1705–1718. doi: 10.1586/14737175.8.11.1703

Murphy, M., Wilson, Y. M., Vargas, E., Munro, K. M., Smith, B., and Huang, A. (2015). Reduction of p75 neurotrophin receptor ameliorates the cognitive deficits in a model of Alzheimer's disease. *Neurobiol. Aging* 36, 740–752. doi: 10.1016/j.neurobiolaging.2014.09.014

Naia, L., Cunha-Oliveira, T., Rodrigues, J., Rosenstock, T. R., Oliveira, A., and Ribeiro, M. (2017). Histone deacetylase inhibitors protect against pyruvate dehydrogenase dysfunction in Huntington's disease. *J. Neurosci.* 37, 2776–2794. doi: 10.1523/JNEUROSCI.2006-14.2016

Naseri, N. N., Xu, H., Bonica, J., Vonsattel, J. P., Corte, E. T., and Park, L. C. (2015). Abnormalities in the tricarboxylic acid cycle in Huntington disease and in a Huntington disease mouse model. *J. Neuropathol. Exp. Neurol.* 74, 527–537. doi: 10.1097/NEN.0000000000000197

Nell, H. J., Whitehead, S. N., and Cechetto, D. F. (2014). Age-dependent effect of β-amyloid toxicity on basal forebrain cholinergic neurons and inflammation in rat brain. *Brain Pathol.* 25, 531–542. doi: 10.1111/bpa.12199

Nolin, F., Michel, J., Wortham, L., Tchelidze, P., and Banchet, V. (2016). Stage-specific changes in water, Na +, Cl-, and K + contents of organelles during apoptosis, demonstrated by a targeted cryo correlative analytical approach. *PLoS One* 11:e0148727. doi: 10.1371/journal.pone.0148727

Nunes-Tavares, N., Santos, L. E., Stutz, B., Brito-Moreira, J., Klein, W. L., and Ferreira, S. T. (2012). Inhibition of choline acetyltransferase as a mechanism for cholinergic dysfunction induced by amyloid-β peptide oligomers. *J. Biol. Chem.* 287, 19377–19385. doi: 10.1074/jbc.M111.321448

Papazisis, G., Pourzitaki, C., Sardeli, C., Lallas, A., Amaniti, E., and Kouvelas, D. (2008). Deferoxamine decreases the excitatory amino acid levels and improves the histological outcome in the hippocampus of neonatal rats after hypoxia-ischemia. *Pharmacol. Res.* 57, 73–78. doi: 10.1016/j.phrs.2007.12.003

Pappas, B. A., Bayley, P. J., Bui, B. K., Hansen, L. A., and Thal, L. J. (2000). Choline acetyltransferase activity and cognitive domain scores of Alzheimer's patients. *Neurobiol. Aging* 21, 11–17. doi: 10.1016/S0197-4580(00)00090-7

Patel, M. S., and Owen, O. E. (1976). Lipogenesis from ketone bodies in rat brain. Evidence for conversion of acetoacetate into acetyl-coenzyme A in the cytosol. *Biochem. J.* 156, 603–607. doi: 10.1042/bj1560603

Pawlosky, R. J., Kashiwaya, Y., Srivastava, S., King, M. T., Cruthfield, C., and Volkov, N. (2010). Alterations in brain glucose utilization accompanying elevations in blood ethanol and acetate concentrations in the rat. *Alcoholism Clin. Exp. Res.* 34, 375–381. doi: 10.1111/j.1530-0277.2009.01099.x

Pawlosky, R. J., Kemper, M. F., Kashiwaya, Y., King, M. T., Mattson, M. P., and Veech, R. L. (2017). Effects of dietary ketone esters on hippocampal glycolytic and tricarboxylic acid cycle intermediates and amino acids in 3xTgAD mouse model of Alzheimer's disease. *J. Neurochem.* 141, 195–207. doi: 10.1111/jnc.13958

Pehar, M., and Puglielli, L. (2013). Lysine acetylation in the lumen of ER: a novel and essential function under the control of the UPR. *Biochim. Biophys. Acta* 1833, 686–697. doi: 10.1016/j.bbamcr.2012.12.004

Peng, Y., Kim, M. J., Hullinger, R., O'Riordan, K. J., Burger, C., Pehar, M., et al. (2016). Improved proteostasis in the secretory pathway rescues Alzheimer's disease in the mouse. *Brain* 139, 937–952. doi: 10.1093/brain/awv385

Peng, Y., Li, M., Clarkson, B. D., Pehar, M., Lao, P. J., and Hillmer, A. T. (2014). Deficient import of acetyl-CoA into the ER lumen causes neurodegeneration an propensity to infections, inflammation, and cancer. *J. Neurosci.* 34, 6772–6789. doi: 10.1523/JNEUROSCI.0077-14.2014

Pepeu, G., and Giovannini, G. M. (2017). The fate of the brain cholinergic neurons in neurodegenerative diseases. *Brain Res.* 1670, 173–184. doi: 10.1016/j.brainres.2017.06.023

Perez, S. E., Dar, S., Ikonomovic, M. D., DeKosky, S. T., and Mufson, E. J. (2007). Cholinergic forebrain degeneration in the APPswe/PS1DeltaE9 transgenic mouse. *Neurobiol. Dis.* 28, 3–15. doi: 10.1016/j.nbd.2007.06.015

Pérez-Escuredo, J., Van Hée, V. F., Sboarina, M., Falces, J., Payen, V. L., and Pellerin, L. (2016). Monocarboxylate transporters in the brain and in cancer. *Biochim. Biophys. Acta* 1863, 2481–2497. doi: 10.1016/j.bbamcr.2016.03.013

Perry, T. L. (1982). "Cerebral amino acid pools," in *Handbook of Neurochemistry Chemical*, 2nd Edn, ed. A. Lajtha (New York, NY: Plenum Press), 151–180.

Pettegrew, J. W., Klunk, W. E., Panchalingam, K., Kanfer, J. N., and McClure, R. J. (1995). Clinical and neurochemical effects of acetyl-L-carnitine in Alzheimer's disease. *Neurol. Aging* 16, 1–4. doi: 10.1016/0197-4580(95)80001-8

Pietrocola, F., Galluzzi, L., Bravo-San Pedro, J. M., Madeo, F., and Kroemer, G. (2015). Acetyl-CoA: central metabolite and second messenger. *Cell Metab.* 21, 805–821. doi: 10.1016/j.cmet.2015.05.014

Potter, P. E., Rauschkolb, P. K., Pandya, Y., Sue, L. I., Sabbagh, M. N., and Walker, D. G. (2011). Pre- and post-synaptic cortical cholinergic deficits are proportional to amyloid plaque presence and density at preclinical stages of Alzheimer's disease. *Acta Neuropathol.* 122, 49–60. doi: 10.1007/s00401-011-0831-1

Prass, R. L., Isohashi, F., and Utter, M. F. (1980). Purification and characterization of an extramitochondrial acetyl coenzyme A hydrolase from rat liver. *J. Biol. Chem.* 255, 5215–5223.

Rae, C., Fekete, A. D., Kashem, M. A., Nasrallah, F. A., and Bröer, S. (2012). Metabolism, compartmentation, transport and production of acetate in the cortical brain tissue slice. *Neurochem. Res.* 37, 2541–2553. doi: 10.1007/s11064-012-0847-5

Reijnierse, G. L., Veldstra, H., and Van den Berg, C. J. (1975). Short-chain fatty acid synthases in brain. Subcellular localization and changes during development. *Biochem. J.* 152, 477–484. doi: 10.1042/bj1520477

Rendina, A. N., and Cheng, D. (2005). Characterization of the inactiviation of rat fatty acid synthase by C75: inhibition of partial reactions and protection by substrates. *Biochem. J.* 388, 895–903. doi: 10.1042/BJ20041963

Rhein, V., Song, X., Wiesner, A., Ittner, L. M., Baysang, G., and Meier, F. (2009). Amyloid-beta and tau synergistically impair the oxidative phosphorylation system in triple transgenic Alzheimer's disease mice. *Proc. Natl. Acad. Sci. U.S.A.* 106, 20057–20062. doi: 10.1073/pnas.0905529106

Rícný, J., and Tucek, J. (1981). Acetyl coenzyme A and acetylcholine in slices of rat caudate nuclei incubated in the presence of metabolic inhibitors. *J. Biol. Chem.* 256, 4919–4923.

Rícný, J., and Tucek, S. (1982). Acetylcoenzyme A and acetylcholine in slices of rat caudate nuclei incubated with (-)hydroxycitrate, citrate and EGTA. *J. Neurochem.* 39, 668–673. doi: 10.1111/j.1471-4159.1982.tb07944.x

Rícný, J., and Tuěek, S. (1983). Ca2 + ions and the output of acetylcoenzyme A from brain mitochondria. *Gen. Physiol. Biophys.* 2, 27–37.

Rícný, J., Tucek, S., and Nováková, J. (1992). Acetylcarnitine, carnitine and glucose diminish the effect of muscarinic antagonist quinuclinyl benzilate on striatal acetylcholine content. *Brain Res.* 576, 215–219. doi: 10.1016/0006-8993(92)90683-Z

Ronowska, A., Dyś, A., Jankowska-Kulawy, A., Klimaszewska-Łata, J., Bielarczyk, H., and Romianowski, P. (2010). Short-term effects of zinc on acetylcholine metabolism and viability of SN56 cholinergic neuroblastoma cells. *Neurochem. Int.* 56, 143–151. doi: 10.1016/j.neuint.2009.09.012

Ronowska, A., Gul-Hinc, S., Bielarczyk, H., Pawełczyk, T., and Szutowicz, A. (2007). Effects of zinc on SN56 cholinergic neuroblastoma cells. *J. Neurochem.* 103, 972–983. doi: 10.1111/j.1471-4159.2007.04786.x

Rossier, J., Spantidakis, Y., and Benda, P. (1977). The effect of Cl- on choline acetyltransferase kinetic parameters and a proposed role for Cl- in the regulation of acetylcholine synthesis. *J. Neurochem.* 29, 1007–1012. doi: 10.1111/j.1471-4159.1977.tb06504.x

Rowlands, B. D., Klugmann, M., and Rae, C. D. (2017). Acetate metabolism does not reflect astrocytic activity, contributes directly to GABA synthesis, and is increased by silent information regulator 1 activation. *J. Neurochem.* 140, 903–918. doi: 10.1111/jnc.13916

Ryan, R., and McClure, W. O. (1980). Physical and kinetic properties of choline acetyl transferase from rat and bovine brain. *J. Neurochem.* 34, 395–403. doi: 10.1111/j.1471-4159.1980.tb06609.x

Sawmiller, D. R., Nguyen, H. T., Markov, O., and Chen, M. (2012). High-energy compounds promote physiological processing of Alzheimer's amyloid-β precursor protein and boost cell survival in culture. *J. Neurochem.* 123, 525–531. doi: 10.1111/j.1471-4159.2012.07923.x

Schreiner, S. J., Kirchner, T., Narkhede, A., Wyss, M., Van Bergen, J. M. G., and Steininger, S. C. (2018). Brain amyloid burden and cerebrovascular disease are synergistically associated with neurometabolism in cognitively unimpaired older adults. *Neurobiol. Aging* 63, 152–161. doi: 10.1016/j.neurobiolaging.2017.12.004

Schuberth, J., Sollenberg, J., Sundwall, A., and Sörbo, B. (1966). Acetyl-CoA in brain. The effect of centrally active drugs, insulin coma and hypoxia. *J. Neurochem.* 13, 819–822. doi: 10.1111/j.1471-4159.1966.tb05877.x

Sensi, S. L., Paoletti, P., Bush, A. I., and Sekler, I. (2009). Zinc in the physiology and pathology of the CNS. *Nat. Rev. Neurosci.* 10, 780–791. doi: 10.1038/nrn2734

Sharman, E. H., Vaziri, N. D., Ni, Z., Sharman, K. G., and Bondy, S. C. (2002). Reversal of biochemical and behavioral parameters of brain aging by melatonin and acetyl-L-carnitine. *Brain Res.* 957, 223–230. doi: 10.1016/S0006-8993(02)03551-5

Shea, P. A., and Aprison, M. H. (1973). An enzymatic method for measuring picomole quantities of acetylcholine and choline in CNS tissue. *Anal. Biochem.* 56, 165–177. doi: 10.1016/0003-2697(73)90181-4

Shea, P. A., and Aprison, M. H. (1977). The distribution of acetyl-CoA in specific areas of the CNS of the rat as measured by a modification of a radio-enzymatic assay for acetylcholine and choline. *J. Neurochem.* 28, 51–58. doi: 10.1111/j.1471-4159.1977.tb07707.x

Shurubor, Y. I., D'Aurelio, M., Clark-Matott, J., Isakova, E. P., Deryabina, Y. I., and Beal, M. F. (2017). Determination of coenzyme A and acetyl-coenzyme A in biological samples using HPLC with UV detection. *Molecules* 22:1388. doi: 10.3390/molecules22091388

Simpson, I. A., Carruthers, A., and Vanucci, S. (2007). Supply and demand in cerebral energy metabolism: the role of nutrient transporters. *J. Cereb. Blood Flow Metab.* 27, 1766–1791. doi: 10.1038/sj.jcbfm.9600521

Sivanand, S., Viney, I., and Wellen, K. E. (2018). Spatiotemporal control of acetyl-CoA metabolism in chromatin regulation. *Trends Biochem. Sci.* 43, 61–74. doi: 10.1016/j.tibs.2017.11.004

Srere, P. A. (1965). The molecular physiology of citrate. *Nature* 205, 766–770. doi: 10.1038/205766a0

Sterling, G. H., McCafferty, M. R., and O'Neil, J. J. (1981). β-Hydroxybutyrate as precursor to acetyl moiety of acetycholine. *J. Neurochem.* 37, 1250–1259. doi: 10.1111/j.1471-4159.1981.tb04675.x

Suematsu, N., and Isohashi, F. (2006). Molecular cloning and functional expression of human cytosolic acetyl-CoA hydrolase. *Acta Biochim. Polon.* 53, 553–561.

Sun, J., Pan, C. Q., Chew, T. W., Liang, F., Burmeister, M., and Low, B. C. (2015). BNIP-H recruits the cholinergic machinery to neurite terminals to promote acetylcholine signaling and neuritogenesis. *Dev. Cell.* 34, 555–568. doi: 10.1016/j.devcel.2015.08.006

Sun, Y., Li, T., Xie, C., Zhang, Y., Zhou, K., and Wang, X. (2016). Dichloroacetate treatment improves mitochondrial metabolism and reduces brain injury in neonatal mice. *Oncotarget* 7, 31708–31722. doi: 10.18632/oncotarget.9150

Szutowicz, A. (1979). "Regional and developmental correlations between choline acetyl transferase and ATP-citrate lyase in rat brain," in *Biological Aspects of Learning, Memory Formation and Ontogeny of the CNS*, eds H. Mathies, M. Krug, and N. Popov (Berlin: Akademie Verlag), 489–499.

Szutowicz, A. (2001). Aluminum, NO, and nerve growth factor neurotoxicity in cholinergic neurons. *J. Neurosci. Res.* 66, 1009–1018. doi: 10.1002/jnr.10040

Szutowicz, A., and Bielarczyk, H. (1987). Elimination of CoASH interference from acetyl-CoA cycling assay by maleic anhydride. *Anal. Biochem.* 164, 292–296. doi: 10.1016/0003-2697(87)90495-7

Szutowicz, A., Bielarczyk, H., Gul, S., Ronowska, A., Pawełczyk, T., and Jankowska-Kulawy, A. (2006). Phenotype-dependent susceptibility of cholinergic neuroblastoma cells to neurotoxic inputs. *Metab. Brain Dis.* 21, 149–161. doi: 10.1007/s11011-006-9007-4

Szutowicz, A., Bielarczyk, H., Gul, S., Zieliński, P., Pawełczyk, T., and Tomaszewicz, M. (2005). Nerve growth factor and acetyl-L-carnitine evoked

shifts in acetyl-CoA and cholinergic SN56 cell vulnerability to neurotoxic inputs. *J. Neurosci. Res.* 79, 185–192. doi: 10.1002/jnr.20276

Szutowicz, A., Bielarczyk, H., Jankowska-Kulawy, A., Pawełczyk, T., and Ronowska, A. (2013). Acetyl-CoA the key factor for survival or death of cholinergic neurons in course of neurodegenerative diseases. *Neurochem. Res.* 38, 1523–1542. doi: 10.1007/s11064-013-1060-x

Szutowicz, A., Bielarczyk, H., Kisielevski, Y., Jankowska, A., Madziar, B., and Tomaszewicz, M. (1998a). Effects of aluminium and calcium on acetyl-CoA metabolism in rat brain mitochondria. *J. Neurochem.* 71, 2447–2453.

Szutowicz, A., Bielarczyk, H., and Łysiak, W. (1981). The role of citrate derived from glucose in the acetylcholine synthesis in rat brain synaptosomes. *Int. J. Biochem.* 13, 887–892. doi: 10.1016/0020-711X(81)90014-8

Szutowicz, A., Bielarczyk, H., Sosnowska, D., and Ciszek, B. (1989). Regulation of citrate metabolism and acetycholine synthesis by Ca^{2+} in rat brain synaptosomes. *Neurochem. Int.* 15, 403–409. doi: 10.1016/0197-0186(89)90157-5

Szutowicz, A., Bielarczyk, H., and Skulimowska, H. (1994a). Effect of dichloroacetate on acetyl-CoA content and acetylcholine synthesis in rat brain synaptosomes. *Neurochem. Res.* 19, 1107–1112. doi: 10.1007/BF00965142

Szutowicz, A., Bielarczyk, H., Zyśk, M., Dyś, A., Ronowska, A., and Gul-Hinc, S. (2017). Early and late pathomechanisms in Alzheimer's disease. From zinc to amyloid-β neurotoxicity. *Neurochem. Res.* 42, 891–904. doi: 10.1007/s11064-016-2154-z

Szutowicz, A., Harris, N. F., Srere, P. A., and Crawford, I. L. (1983). ATP-citrate lyase and other enzymes of acetyl-CoA metabolism in fractions of small and large synaptosomes from rat brain hippocampus and cerebellum. *J. Neurochem.* 41, 1502–1505. doi: 10.1111/j.1471-4159.1983.tb00854.x

Szutowicz, A., Kabata, J., and Łysiak W. (1980). ATP citrate lyase and other enzymes of acetyl-CoA metabolism in developing rat cerebrum and cerebellum. *Int. J. Biochem.* 11, 545–549. doi: 10.1016/0020-711X(80)90263-3

Szutowicz, A., and Łysiak, W. (1980). Regional and subcellular distribution of ATP-citrate lyase and other enzymes of acetyl-CoA metabolism in rat brain. *J. Neurochem.* 35, 775–785. doi: 10.1111/j.1471-4159.1980.tb07073.x

Szutowicz, A., Madziar, B., Pawełczyk, T., Tomaszewicz, M., and Bielarczyk, H. (2004). Effects of NGF on acetylcholine, acetyl-CoA metabolism, and viability of differentiated and non-differentiated cholinergic neuroblastoma cells. *J. Neurochem.* 90, 952–961. doi: 10.1111/j.1471-4159.2004.02556.x

Szutowicz, A., Stepień, M., Bielarczyk, H., Kabata, J., and Łysiak, W. (1982). ATP citrate lyase in cholinergic nerve terminals. *Neurochem. Res.* 7, 799–810. doi: 10.1007/BF00965673

Szutowicz, A., Tomaszewicz, M., Bielarczyk, H., and Jankowska, A. (1998b). Putative significance of shifts in acetyl-CoA compartmentalization in nerve terminals for disturbances of cholinergic transmission in brain. *Dev. Neurosci.* 20, 485–492. doi: 10.1159/000017347

Szutowicz, A., Tomaszewicz, M., and Bielarczyk, H. (1996). Disturbances of acetyl-CoA, energy and acetylcholine metabolism in some encephalopathies. *Acta Neurobiol. Exp.* 56, 323–339.

Szutowicz, A., Tomaszewicz, M., Jankowska, A., and Kisielevski, Y. (1994b). Acetylcholine synthesis in nerve terminals of diabetic rats. *Neuroreport* 5, 2421–2424. doi: 10.1097/00001756-199412000-00004

Szutowicz, A., Stepień, M., Łysiak, W., and Angielski, S. (1976). Effect of (-)hydroxycitrate on the activities of ATP citrate lyase and enzymes of acetyl-CoA metabolism in rat brain. *Acta Biochim. Pol.* 23, 227–234.

Terwel, D., Bothmer, J., Wolf, E., Meng, F., and Jolles, J. (1998). Affected enzyme activities in Alzheimer's disease are sensitive to antemortem hypoxia. *J. Neurol. Sci.* 161, 47–56. doi: 10.1016/S0022-510X(98)00240-8

Thevenet, J., De Marchi, U., Santo Domingo, J., Christinat, N., and Bultot, L. (2016). Medium-chain fatty acids inhibit mitochondrial metabolism in astrocytes promoting astrocyte-neuron lactate and ketone body shuttle systems. *FASEB J.* 30, 1913–1926. doi: 10.1096/fj.201500182

Tomaszewicz, M., Bielarczyk, H., Jankowska, A., and Szutowicz, A. (1997). "Modification by nitric oxide of acetyl-CoA and acetylcholine metabolism in nerve terminals," in *Neurochemistry Cellular, Molecular, and Clinical Aspects*, eds A. Teelken and J. Korf (New York, NY: Plenum Press), 993–997.

Tomaszewicz, M., Rossner, S., Schliebs, R., Ćwikowska, J., and Szutowicz, A. (2003). Changes in cortical acetyl-CoA metabolism after selective basal forebrain cholinergic degeneration by 192IgG-saporin. *J. Neurochem.* 87, 318–324. doi: 10.1046/j.1471-4159.2003.01983.x

Triaca, V., and Calissano, P. (2016). Impairment of the nerve growth factor pathway driving amyloid accumulation in cholinergic neurons: the incipit of the Alzheimer's disease story? *Neural. Regen. Res.* 11, 1553–1556. doi: 10.4103/1673-5374.193224

Trumble, G. E., Smith, M. A., and Winder, W. W. (1995). Purification and characterization of rat skeletal muscle acetyl-CoA carboxylase. *Eur. J. Biochem.* 231, 192–198. doi: 10.1111/j.1432-1033.1995.0192f.x

Trushina, E., Nemutlu, E., Zhang, S., Christensen, T., Camp, J., and Mesa, J. (2012). Defects of mitochondrial dynamics and metabolomic signatures of evolving energetic stress in mouse models of familial Alzheimer's disease. *PLoS One* 7:e32737. doi: 10.1371/journal.pone.0032737

Tuček, S. (1983). "The synthesis of acetylcholine," in *ito. Handbook if Neurochemistry*, Vol. 4, ed. A. Lajtha (New York, NY: Plenum Press), 219–249.

Tuček, S. (1985). Regulation of acetylcholine synthesis in the brain. *J. Neurochem.* 44, 11–24. doi: 10.1111/j.1471-4159.1985.tb07106.x

Tuček, S. (1993). Short-term control of the synthesis of acetylcholine. *Prog. Biophys. Mol. Biol.* 60, 59–69. doi: 10.1016/0079-6107(93)90013-A

Valor, L. M., Viosca, J., Lopez-Atalaya, J. P., and Barco, A. (2013). Lysine acetyltransferases CBP and p300 as therapeutic targets in cognitive and neurodegenerative disorders. *Curr. Pharm. Design* 19, 5051–5064. doi: 10.2174/1381612811319990382

Veech, R. L., Bradshaw, P. C., Clarke, K., Curtis, W., Pawlosky, R., and King, M. T. (2017). Ketone bodies mimic the life span extending properties of caloric restriction. *IUBMB Life* 69, 305–314. doi: 10.1002/iub.1627

Vossel, K. A., Ranasinghe, K. G., Beagle, A. J., Mizurini, D., Honma, S. M., and Dowling, A. S. (2016). Incidence and impact of subclinical epileptiform activity in Alzheimer's disease. *Ann. Neurol.* 80, 858–870. doi: 10.1002/ana.24794

Waagepetersen, H. S., Schousboe, A., and Sonnewald, U. (2007). "Glutamine, glutamate, and GABA: metabolic aspects," in *Handbook of Neurochemistry and Molecular Biology*, 3rd Edn, eds S. S. Oja, A. Schousboe, and P. Saransaari (Berlin: Springer), 1–21.

Wang, L., Guo, L., Lu, L., Sun, H., Shao, M., and Beck, S. J. (2016). Synaptosomal mitochondrial dysfunction in 5xFAD mouse model of Alzheimer's disease. *PLoS One* 11:e0150441. doi: 10.1371/journal.pone.0150441

Wang, P., Chen, M., Yang, Z., Yu, T., Zhu, J., and Zhou, L. (2017). Activation of pyruvate dehydrogenase activity by bidichloroacetate improves survival and neurologic outcomes after cardiac arrest in rats. *Shock* 49, 704–711. doi: 10.1097/SHK.0000000000000971

Wang, Z., Leng, Y., Wang, J., Liao, H. M., Bergman, J., and Leeds, P. (2016). Tubastatin A, an HDAC6 inhibitor, alleviates stroke-induced brain infarction and functional deficits: potential roles of a α-tubulin acetylation and FGF-21 up-regulation. *Sci. Rep.* 6:19626. doi: 10.1038/srep19626

Wapenaar, H., van der Wouden, P. E., Groves, M. R., Rotili, D., Mai, A., and Dekker, F. J. (2015). Enzyme kinetics and inhibition of histone acetyltransferase KAT8. *Eur. J. Med. Chem.* 105, 289–296. doi: 10.1016/j.ejmech.2015.10.016

Webster, S. J., Bachstetter, A. D., Nelson, P. T., Schmitt, F. A., and Van Eldik, L. J. (2014). Using mice to model Alzheimer's dementia: an overview of the clinical disease and the preclinical behavioral changes in 10 mouse models. *Front. Genet.* 5:88. doi: 10.3389/fgene.2014.00088

Wellen, K. E., Hatzivassiliou, G., Sachdeva, U. M., Bui, T. V., Cross, J. R., and Thomson, C. B. (2009). ATP-citrate lyase links cellular metabolism to histone acetylation. *Science* 324, 1076–1080. doi: 10.1126/science.1164097

Williams, L. R., and Rylett, R. J. (1990). Exogenous nerve growth factor increases the activity of high-affinity choline uptake and choline acetyltransferase in brain of Fisher 344 male rats. *J. Neurochem.* 55, 1042–1049. doi: 10.1111/j.1471-4159.1990.tb04594.x

Wlassics, I. D., Stille, C., and Anderson, V. E. (1988). Coenzyme A dithioesters: synthesis, characterization and reaction with citrate synthase and acetyl-CoA:choline *O*-acetyltransferase. *Biochim. Biophys. Acta* 952, 269–276. doi: 10.1016/0167-4838(88)90126-4

Wohnsland, S., Burgers, H. F., Kuschinsky, W., and Maurer, M. H. (2010). Neurons and neuronal stem cells survive in glucose-free lactate and in high glucose cell culture medium during normoxia and anoxia. *Neurochem. Res.* 35, 1635–1642. doi: 10.1007/s11064-010-0224-1

Wong, V. S. C., Picci, C., Swift, M., Levinson, M., Willis, D., and Langley, B. (2018). α-Tubulin acetyltransferase is a novel target mediating neurite growth inhibitory effects of chondroitin sulfate proteoglycans and myelin-associated glycoprotein. *eNeuro* 5:ENEURO.0240-17.2018. doi: 10.1523/ENEURO.0240-17.2018

Yao, J., Irwin, R. W., Zhao, L., Nilsen, J., Hamilton, R. T., and Brinton, R. D. (2009). Mitochondrial bioenergetics deficit precedes Alzheimer's pathology in female mouse model of Alzheimer's disease. *Proc. Natl. Acad. Sci. U.S.A.* 106, 14670–14675. doi: 10.1073/pnas.0903563106

Yin, J. X., Maalouf, M., Han, P., Zhao, M., Gao, M., and Dharshaun, T. (2016). Ketones block amyloid entry and improve cognition in an Alzheimer's model. *Neurobiol. Aging* 39, 25–37. doi: 10.1016/j.neurobiolaging.2015.11.018

Zhang, Y., Hong, Y., Bounhar, Y., Blacker, M., Roucou, X., and Tounekti, O. (2003). p75 neurotrophin receptor protects primary cultures of human neurons against extracellular amyloid beta peptide cytotoxicity. *J. Neurosci.* 23, 7385–7394. doi: 10.1523/JNEUROSCI.23-19-07385.2003

Zhang, Z. G., Wang, X., Zai, J. H., Sun, C. H., and Yan, B. C. (2018). Icariin improves cognitive impairment after traumatic brain injury by enhancing hippocampal acetylation. *Chin. J. Integr. Med.* 2018, 1–6. doi: 10.1007/s11655-018-2823-z

Zhao, S., Torres, A., Henry, R. A., Trefely, S., Wallace, M., and Lee, J. V. (2016). ATP-citrate lyase controls a glucose-to-acetate metabolic switch. *Cell Rep.* 17, 1037–1052. doi: 10.1016/j.celrep.2016.09.069

Zhong, X., Shi, H., Shen, Z., Hou, L., Luo, X., and Chen, X. (2014). 1H-proton magnetic resonance spectroscopy differentiates dementia with Lewy bodies from Alzheimer's disease. *J. Alzheimer's Dis.* 40, 953–966. doi: 10.3233/JAD-131517

Zhou, Q., Lam, P. Y., Han, D., and Cadenas, E. (2009). Activation of c-Jun-N-terminal kinase and decline of mitochondrial pyruvate dehydrogenase activity during brain aging. *FEBS Lett.* 583, 1132–1140. doi: 10.1016/j.febslet.2009.02.043

Zimatkin, S. M., Oganesian, N. A., Kiselevski, Y. V., and Deitrich, R. A. (2011). Acetate-dependent mechanisms of inborn tolerance to ethanol. *Alcohol Alcohol.* 46, 233–238. doi: 10.1093/alcalc/agr014

Zyśk, M., Bielarczyk, H., Gul-Hinc, S., Dyś, A., Gapys, B., and Ronowska, A. (2017). Phenotype-dependent interactions between N-acetyl-L-aspartate and acetyl-CoA in septal SN56 cholinergic cells exposed to excess of zinc. *J. Alzheimer's Dis.* 56, 1145–1158. doi: 10.3233/JAD-160693

Conflict of Interest Statement: The authors declare that the research was conducted in the absence of any commercial or financial relationships that could be construed as a potential conflict of interest.

frontiers in Molecular Neuroscience

MINI REVIEW
published: 23 May 2018
doi: 10.3389/fnmol.2018.00169

The Role of Activity-Dependent DNA Demethylation in the Adult Brain and in Neurological Disorders

Gonca Bayraktar[1*†] *and Michael R. Kreutz*[1,2]

[1]*RG Neuroplasticity, Leibniz Institute for Neurobiology, Magdeburg, Germany,* [2]*Leibniz Group 'Dendritic Organelles and Synaptic Function', Center for Molecular Neurobiology (ZMNH), University Medical Center Hamburg-Eppendorf, Hamburg, Germany*

Over the last decade, an increasing number of reports underscored the importance of epigenetic regulations in brain plasticity. Epigenetic elements such as readers, writers and erasers recognize, establish, and remove the epigenetic tags in nucleosomes, respectively. One such regulation concerns DNA-methylation and demethylation, which are highly dynamic and activity-dependent processes even in the adult neurons. It is nowadays widely believed that external stimuli control the methylation marks on the DNA and that such processes serve transcriptional regulation in neurons. In this mini-review, we cover the current knowledge on the regulatory mechanisms controlling in particular DNA demethylation as well as the possible functional consequences in health and disease.

Keywords: DNA Methylation, GADD45B, gene expression, synaptic plasticity, TET enzymes, base excision repair (BER), neural disorders, neurons

OPEN ACCESS

Edited by:
Daniel Ortuño-Sahagún, Universidad de Guadalajara, Mexico

Reviewed by:
Ana M. M. Oliveira, Universität Heidelberg, Germany
Katja Kobow, Universitätsklinikum Erlangen, Germany
Xiaolu Zhang, Northern Jiangsu People's Hospital, China

****Correspondence:***
Gonca Bayraktar
gb581@medschl.cam.ac.uk

†Present address:
Gonca Bayraktar, UK Dementia Research Institute at the University of Cambridge, Clifford Allbutt Building, Cambridge Biomedical Campus, University of Cambridge, Cambridge, United Kingdom

Received: *08 March 2018*
Accepted: *04 May 2018*
Published: *23 May 2018*

Citation:
Bayraktar G and Kreutz MR (2018) The Role of Activity-Dependent DNA Demethylation in the Adult Brain and in Neurological Disorders. Front. Mol. Neurosci. 11:169. doi: 10.3389/fnmol.2018.00169

INTRODUCTION

Among several other epigenetic tags, methyl tags on the DNA were generally considered as repressive marks. However, an increasing number of studies showed that the DNA methylation at intergenic regions as well as gene regulatory regions might enhance gene expression (Bayraktar and Kreutz, 2017). How, the key enzymes in DNA methylation, DNA methyltransferases (DNMTs), are differentially regulated and perform the DNA methylation are well characterized (Goll and Bestor, 2005; Bayraktar and Kreutz, 2017). However, the removal of methyl tags from the DNA has been more perplexing. The reversal of DNA methylation can take place passively by diluting the DNA methylation of both copies of the genome following multiple rounds of cell division in the absence of maintenance of DNA methylation (Inoue and Zhang, 2011). In postmitotic neurons, other mechanisms must be in place. Current opinion disfavors the direct removal of the covalent bond between the methyl groups and cytosines (Ooi and Bestor, 2008). A unifying mechanistic process on how active DNA demethylation is still lacking. We, therefore, discuss how active DNA demethylation is achieved by the interplay of DNA oxidative reactions and repair mechanisms.

MECHANISMS OF ACTIVE DNA DEMETHYLATION

Several proteins have been identified that are part of neuronal demethylation machinery. These include Growth Arrest and DNA Damage-inducible (GADD) 45 proteins (GADD45A and GADD45B) that in neurons take part in active DNA demethylation processes (Barreto et al., 2007; Ma et al., 2009). Termed initially as the MyD118 (myeloid differentiation), *Gadd45b* was

identified as an immediate gene whose expression was induced following the induction of long-term potentiation (LTP) *in vivo* (Hevroni et al., 1998). GADD45B mediated activity-dependent demethylation was first shown for the promoter of fibroblast growth factor 1, isoform B (Fgf1B) and Brain-derived neurotrophic factor (Bdnf) 9. It is nowadays widely believed that GADD45B contributes to demethylation in conjunction with other modifiers which will be discussed below.

5-hydroxymethyl cytosine (5hmC) was first described in the 1972 (Penn et al., 1972) and more than three decades later enzymatic activity of Ten-eleven translocation (TET) proteins was discovered to biochemically convert 5mC to 5hmC (Tahiliani et al., 2009; Ito et al., 2010). The characterization of TET enzymes (Tahiliani et al., 2009; Ito et al., 2010) and 5hmC in the brain (Kriaucionis and Heintz, 2009) also advanced our understanding of active DNA demethylation in neurons. In successive oxidation steps 5mC is initially converted to 5hmC which is followed by the conversion to 5-formylcytosine (5fC) and subsequently 5-carboxylcytosine (5cC). Each of these steps requires one of the three TET enzymes (Ito et al., 2011; **Figure 1**). 5fC and 5caC can be recognized and excised by Thymine DNA Glycosylase (TDG) generating an apyrimidinic (AP) site (He et al., 2011; Maiti and Drohat, 2011). The AP site is then corrected by specific base-excision repair mechanism (BER) with the replacement of cytosine in mammals (Zhu, 2009). TDG depletion in embryonic stem cells causes enhanced levels of 5fC and 5caC at proximal and distal gene regulatory elements (Raiber et al., 2012; Shen et al., 2013). TDG knockout or catalytical inactivation leads to embryonic lethality in mice and hypermethylated CpG islands (Cortellino et al., 2011). Along these lines, the perturbation of BER enzymes by genetic and pharmacological inhibition results in the partial block of global DNA demethylation in mouse germ line (Hajkova et al., 2010). Collectively this evidence suggests that BER has an evolutionarily conserved role in active DNA demethylation.

The finding that TDG rapidly processes the oxidation products by TET enzymes corroborated the view of a TET-initiated, TDG-processed and BER-terminated active DNA demethylation mechanism. In support of this picture and the surmised recruiting function of GADD45B, Li et al. (2015) reported that GADD45A as well as GADD45B promote demethylation of an *in vitro* methylated promoter through TDG. TDG physically interacts with GADD45 and in the presence of the triple complex, GADD45B, TDG and TET2, a complete demethylation of reporters could be achieved (Li et al., 2015). TDG has several interesting and yet not well-understood features. It interacts with DNMT3A either via the PWWP or the catalytic domain of DNMT3A (see **Figure 2**). This interaction enhances TDG activity possibly by facilitating the binding of TDG to the mismatch sites while binding to TDG at the same time represses DNMT3A methyltransferase activity (Li et al., 2007). TDG is one of the two enzymes that together with the methyl-CpG binding domain protein 4 (MBD4) is known to initiate this repair mechanism (Hardeland et al., 2001; Krokan et al., 2002). Both TDG and MBD4 possess low levels of 5mC DNA glycosylase activity *in vitro* (Zhu et al., 2000a,b).

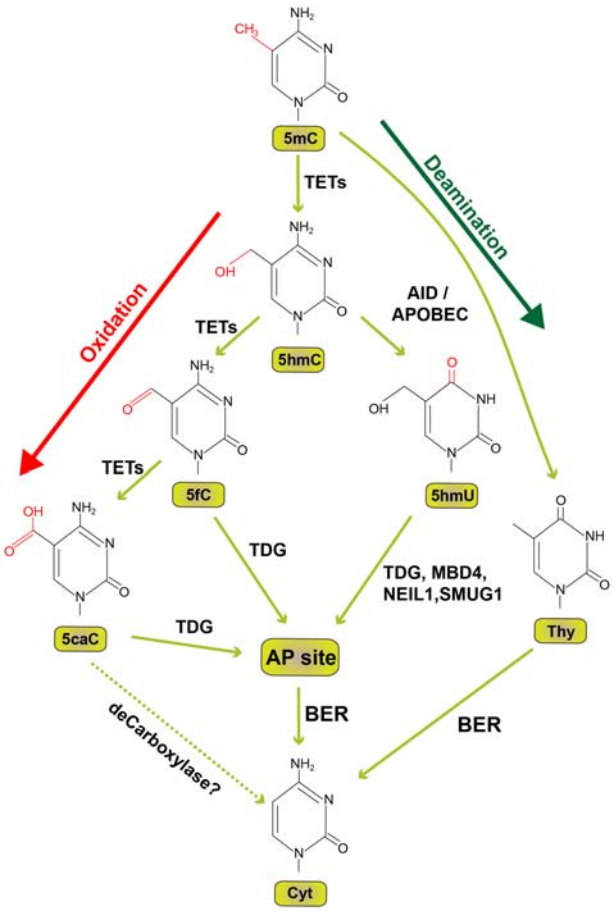

FIGURE 1 | Pathways of active DNA demethylation. Since the formerly hypothesized demethylase to directly convert 5-methylcytosine (5mC) to cytosine (Cyt) has not been identified, we depict here the current view how active DNA demethylation might take place. 5mC is oxidized by ten-eleven translocation (TET) family of dioxygenases to generate 5-hydroxymethylcytosine (5hmC). In successive steps TET enzymes further hydroxylate 5hmC to generate 5-formylcytosine (5fC) and 5-carboxylcytosine (5caC). Thymine DNA glycosylase (TDG) recognizes intermediate DNA forms 5fC and 5caC and excises the glycosidic bond resulting in an apyrimidinic (AP) site. In an alternative deamination pathway 5hmC can be deaminated by activity-induced cytidine deaminase/apolipoprotein B mRNA editing complex (AID/APOBEC) deaminases to form 5-hydroxymethyluracil (5hmU) or 5mC can be converted to Thymine (Thy). 5hmU can be cleaved by TDG, single-strand-selective monofunctional uracil-DNA glycosylase 1 (SMUG1), Nei-Like DNA Glycosylase 1 (NEIL1), or methyl-CpG binding protein 4 (MBD4). AP sites and T:G mismatches can be efficiently repaired by Base Excision Repair (BER) enzymes. Dotted lines indicate a proposed but not experimentally proven path.

Deamination of 5mC and 5hmC by Activity Induced Cytosine Deaminase (AID) or apolipoprotein B mRNA editing complex (APOBEC) is an alternative path to successive oxidation reactions by TET enzymes for the initiation of DNA demethylation (**Figure 1**). The modified nucleotide can then be replaced by BER. Shortly after the discovery of AID (Muramatsu et al., 1999), a functional role in DNA demethylation by

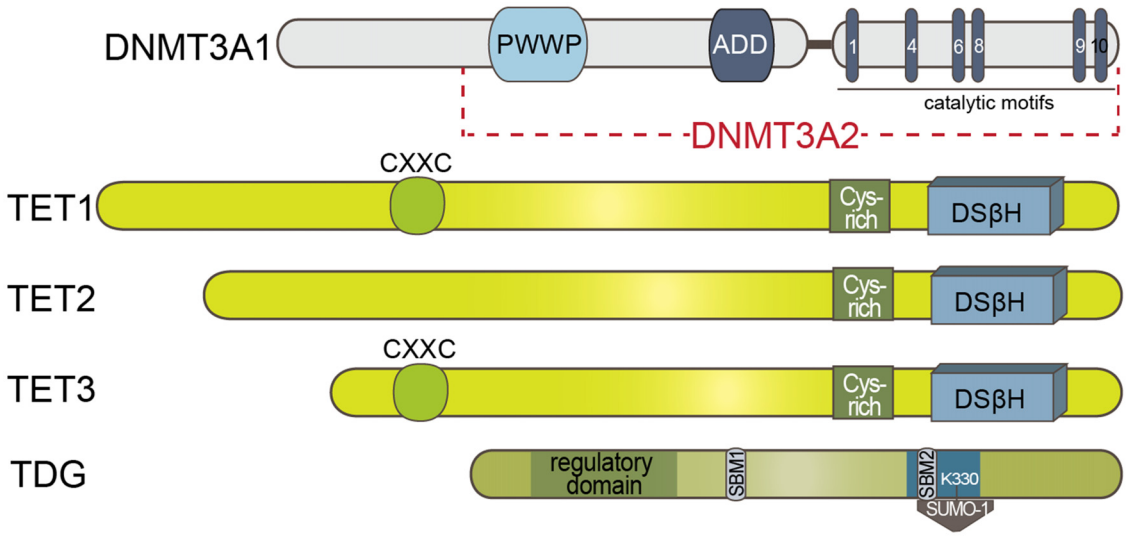

FIGURE 2 | Schematic presentation of the known domain structures of proteins involved in DNA methylation/demethylation. DNMT3A1/2: ADD domain of DNMT3A1/2 is involved in the allosteric control of the enzyme. TET enzymes: DNA binding CXXC motif is present in TET1 and TET3. Double-stranded β-helix (DSβH) is the fold core oxygenase domain is preceded by a cysteine (Cys)-rich domain. Sumo-binding motifs (SBM) and catalytic residues (in blue) of TDG is represented. PWWP: Pro-Trp-Trp-Pro; CXXC: Cys-X-X-Cys motif.

deamination was proposed (Rai et al., 2008; Bhutani et al., 2010). The identification of AID in a ternary complex with GADD45A and TDG also indicates a contribution of AID in the demethylation process (Cortellino et al., 2011). On the contrary, several independent studies revealed that 5mC and 5hmC are poorer substrates for AID as compared to cytosine (Larijani et al., 2005; Nabel et al., 2012; Rangam et al., 2012; Abdouni et al., 2013). The contribution of AID for the deamination pathway to demethylate 5mC in association with BER mechanism is rather elusive since the enzyme cannot efficiently deaminate 5mC (Wijesinghe and Bhagwat, 2012). However, the same study showed efficient 5mC deamination capability of APOBEC3 (Wijesinghe and Bhagwat, 2012). In conclusion, the role of AID in DNA demethylation particularly in the adult brain is still unclear (for review, see Bochtler et al., 2017).

REGULATION OF NEURONAL GENE EXPRESSION BY ACTIVE DNA DEMETHYLATION

In the long-lived nature of postmitotic neurons, genomic stability needs to be maintained for decades while at the same time their remarkable plasticity has to be kept at a poised state ready to respond (Baker-Andresen et al., 2013). How are stability and permissiveness for changes in DNA methylation achieved upon enhanced neuronal activity? It is tempting to speculate that due to its plastic nature the basal epigenomic state of hippocampal neuron determines the permissiveness for an initial wave of transcription of DNA modifiers, including demethylation machinery component expressions, which precedes effector gene expression (Oliveira, 2016). An example for a methylation mark keeping the gene in a silent but in a transcriptionally poised state is the promoter methylation of the *Bdnf* gene that is quite well investigated in the context of synaptic plasticity and learning (Miller and Sweatt, 2007; Lubin et al., 2008). In differentiated neurons, the *Bdnf* promoter is methylated at basal conditions and thereby kept in a repressed state by the occupation of repressor complex involving RE1-Silencing Transcription factor corepressor (CoRest), methyl CpG binding protein 2 (MeCP2), histone deacetylases (HDAC) 1 and 2. The repressor complex dissociates following phosphorylation of MeCP2 and nitrosylation of HDAC2 in response to Ca^{+2} influx (Chen et al., 2003; Nott et al., 2008). Activity-induced deaminase (AID) regulates the induced expression of *Bdnf IV* in a stimulus-dependent manner (Ratnu et al., 2014). However, the yet unclear status of AID in DNA demethylation makes it hard to directly link the effect of AID on Bdnf expression to activity-dependent DNA demethylation.

Unfortunately, conflicting reports have been published on the role of GADD45B in learning and memory processes. Fear conditioning induces *Gadd45b* gene expression (Keeley et al., 2006) and deletion of the gene results in hippocampus-dependent long-term memory deficits including fear conditioning (Leach et al., 2012). However, others found improved long-term memory following Gadd45b knockout mice employing a similar contextual fear-conditioning paradigm (Sultan et al., 2012). Of note, the mice strains used in the latter two studies had a different genetic background (C57BL/6 and B6:129VJ mice) which might account for the discrepant results. Moreover, targeted siRNA delivery to transiently knock down Gadd45b expression in the neonatal rat amygdala results in altered juvenile

behavior with consequences for the expression of Bdnf, MeCP2 and Reelin (Kigar et al., 2015). NF-κB, which is known to be important in hippocampus-dependent memory formation (Kaltschmidt and Kaltschmidt, 2015), was proposed to regulate Gadd45b gene expression and thereby DNA demethylation activity (Jarome et al., 2015). Interestingly, overexpression of TET1 leads to enhanced expression of several memory-related genes but surprisingly to impairment of contextual fear memory (Kaas et al., 2013). It is possible that TET proteins might have functions independent of DNA hydroxymethylation. TET3, for instance, was recently shown to have a functional role in scaling-down synaptic strength in hippocampal neurons (Yu et al., 2015).

Interestingly, 5hmC is not only an intermediate DNA demethylation form but also an epigenetic mark on its own, which is enriched within promoters and gene bodies (Kaas et al., 2013). This enrichment correlates with a depletion of 5mC in actively transcribed genes. Moreover, gene body 5mC and gene expression are inversely correlated (Mellen et al., 2012). Recent advances in whole epigenome analysis identified gradually accumulating non-CG methylation (mCH, H = A/C/T) from post-natal week one onwards in the genome peaking in the adult mouse brain (Xie et al., 2012; Lister et al., 2013) and at several hundred genomic positions in the adult human brain (Varley et al., 2013). Genes expressed in the mammalian brain are devoid of intragenic and promoter mCH (Xie et al., 2012) and mCH correlates with decreased gene expression in a highly cell type-specific manner (Mo et al., 2015). mCH accumulation is implicated in X chromosome inactivation and might therefore contribute to gender specific gene expression (Keown et al., 2017). Reconfiguration of the global DNA methylome during development coincides with synaptogenesis, a period in which mCH accumulates in neurons but not in glial cells (Lister et al., 2013). On the other hand, methylated CpG-rich DNA regions are not only found in transcription initiation sites but also in gene bodies and intergenic regions (Jones, 2012). Collectively these studies illustrate that it is important to identify the location and type of DNA methylation to assess its contribution to gene expression.

Another critical issue is cell-type specificity of DNA demethylation. In most studies brain tissue that contains different neuronal and glial cell types was used. The current knowledge on how the DNA demethylation machinery functions in different cell-types and responds to neuronal activity is therefore very limited. DNA methylation patterns vary between neurons and non-neuronal cells. Ventromedial prefrontal cortex neurons have higher global DNA methylation levels compared to non-neuronal cells (Li et al., 2014a). Early life stress (ELS) alters DNA methylation and Bdnf expression in medial prefrontal cortex neurons in a cell-type and sex-specific manner (Blaze and Roth, 2017). The expression of Bdnf IX and Fgf1B genes, which are crucially involved in neurogenesis and plasticity, is also regulated by Gadd45b in an activity-dependent manner in granule cells of the dentate gyrus (Ma et al., 2009). Furthermore, Halder et al. (2016) showed that DNA methylation and changes in histone acetylation occur in parallel following contextual fear conditioning learning and alterations in DNA methylation may also arise in non-neuronal cells potentially supporting an epigenetic code for memory formation. Interestingly, in contrast to hippocampal neurons, TET3 but not TET1 is expressed in cortical neurons in an activity-dependent manner (Li et al., 2014b). Gephyrin stabilizes GABA receptors to postsynaptic membrane and takes part in fear extinction (Chhatwal et al., 2005). Li et al. (2014b) further validated the enhanced expression of TET3 on the gephyrin locus where they showed increased occupancy of TET3 in association with an accumulation of the demethylation intermediate mark 5hmC.

ROLE OF DNA DEMETHYLATION IN NEUROLOGICAL DISORDERS

Given the principal functions of chromatin modifications in regulating gene transcription programs, it's not surprising that the number of studies, which report the involvement of DNA demethylation machinery in neurological disorders, is steadily increasing. Enhanced GADD45B levels were reported in two different cohorts of major psychotic patients (Gavin et al., 2012). However, reduced occupancy of GADD45B on the *Bdnf IX* promoter was found, which is in line with reduced *Bdnf IX* expression (Gavin et al., 2012). Recently, GADD45B expression was shown to be regulated by transforming growth factor beta (TGFB) signaling and protein levels of GADD45B are reduced in a model of chronic mild stress (Grassi et al., 2017). Moreover, a reduction in expression levels of the immediate early gene *Arc* was also associated with reduced levels of GADD45B and DNA demethylation in this stress model (Grassi et al., 2017). Although its neurobiological underpinnings have not been fully understood, electroconvulsive therapy (ECT) is currently in clinical practice for the treatment of several psychiatric diseases including depression (Singh and Kar, 2017). In an animal model ECT reduces the methylation levels of Bdnf 9 promoter, hence inducing the mRNA expression of the gene, however, in the transgenic mice model in which Gadd45b was knocked out the effect of ECT on the *Bdnf IX* promoter methylation level is abolished and mRNA expression is perturbed (Ma et al., 2009). Prenatally stressed mice exhibit not only similar behavioral traits like psychotic patients but also similar epigenetic signatures (Dong et al., 2015). DNA methyltransferase1 and TET1 enzyme level increase in prenatally stressed mice correlates with enhanced 5mC and 5hmC in the regulatory DNA regions and hence decreased *Bdnf* gene expression (Dong et al., 2015). Samples from patients that suffered from bipolar disorder and schizophrenia show enhanced methylation of associated gene promoters resulting in suppressed expression (Grayson and Guidotti, 2013). This is linked to the enhanced expression of DNMTs (Veldic et al., 2004; Zhubi et al., 2009). However, it's not clear whether the lack of active DNA demethylation can also be responsible for the disease etiology in some cases. The contribution of methylation and active DNA demethylation in Alzheimer's disease (AD) remains to be determined. The varying global methylation levels

reported in the postmortem brain samples can be region specific (Roubroeks et al., 2017). There are conflicting studies on the increase in 5mC and 5hmC in the hippocampus whereas no changes in the entorhinal cortex in AD as compared to controls were reported (Bradley-Whitman and Lovell, 2013; Lashley et al., 2015). Contradictory evidence on the global decrease in methylation levels in the hippocampus and entorhinal cortex was published by others (Mastroeni et al., 2010; Chouliaras et al., 2013). In a complex disease like AD, the readout from brain samples and genome-wide association studies on various chromatin modifiers is hard to interpret because of the readout's variability due to the initiation, progression or terminal stage of the disease.

CONCLUDING REMARKS

Based on the initial GADD45B-dependent demethylation hypothesis (Gavin et al., 2012), current data suggest that active demethylation in postmitotic neurons is initiated by TET family enzymes in conjunction with TDG. While GADD45B apparently lacks enzymatic activity, it seems to recruit demethylation machinery components to certain promoters by yet unknown mechanisms. The cascade of events in active DNA demethylation finally requires the contribution of BER mechanism to generate mark-free cytosine. There are several gaps in our understanding of the DNA demethylation pathway in neurons. For instance, how are the DNA demethylation components targeted to specific genomic sites? Finally, it is yet unclear how one can interfere with this machinery to regulate activity-dependent gene expression and whether this machinery has druggable pathways in the context of neurological disorders.

AUTHOR CONTRIBUTIONS

GB and MK are invited to contribute to the article collection for the special issue of the "Epigenetic Mechanisms Regulating Neural Plasticity". GB outlined the mini review and GB and MK wrote the manuscript.

FUNDING

This work was supported by grants from the Deutsche Forschungsgemeinschaft (DFG; Kr1879/5-1/6-1/SFB 779 TPB8), BMBF "Energi" FKZ: 01GQ1421B, The EU Joint Programme—Neurodegenerative Disease Research (JPND) project STAD and Leibniz Foundation to MK.

REFERENCES

Abdouni, H., King, J. J., Suliman, M., Quinlan, M., Fifield, H., and Larijani, M. (2013). Zebrafish AID is capable of deaminating methylated deoxycytidines. *Nucleic Acids Res.* 41, 5457–5468. doi: 10.1093/nar/gkt212

Baker-Andresen, D., Ratnu, V. S., and Bredy, T. W. (2013). Dynamic DNA methylation: a prime candidate for genomic metaplasticity and behavioral adaptation. *Trends Neurosci.* 36, 3–13. doi: 10.1016/j.tins.2012.09.003

Barreto, G., Schäfer, A., Marhold, J., Stach, D., Swaminathan, S. K., Handa, V., et al. (2007). Gadd45a promotes epigenetic gene activation by repair-mediated DNA demethylation. *Nature* 445, 671–675. doi: 10.1038/nature05515

Bayraktar, G., and Kreutz, M. R. (2017). Neuronal DNA methyltransferases: epigenetic mediators between synaptic activity and gene expression? *Neuroscientist* 24, 171–185. doi: 10.1177/1073858417707457

Bhutani, N., Brady, J. J., Damian, M., Sacco, A., Corbel, S. Y., and Blau, H. M. (2010). Reprogramming towards pluripotency requires AID-dependent DNA demethylation. *Nature* 463, 1042–1047. doi: 10.1038/nature08752

Blaze, J., and Roth, T. L. (2017). Caregiver maltreatment causes altered neuronal DNA methylation in female rodents. *Dev. Psychopathol.* 29, 477–489. doi: 10.1017/s0954579417000128

Bochtler, M., Kolano, A., and Xu, G. L. (2017). DNA demethylation pathways: additional players and regulators. *Bioessays* 39, 1–13. doi: 10.1002/bies.201600178

Bradley-Whitman, M. A., and Lovell, M. A. (2013). Epigenetic changes in the progression of Alzheimer's disease. *Mech. Ageing Dev.* 134, 486–495. doi: 10.1016/j.mad.2013.08.005

Chen, W. G., Chang, Q., Lin, Y., Meissner, A., West, A. E., Griffith, E. C., et al. (2003). Derepression of BDNF transcription involves calcium-dependent phosphorylation of MeCP2. *Science* 302, 885–889. doi: 10.1126/science.1086446

Chhatwal, J. P., Myers, K. M., Ressler, K. J., and Davis, M. (2005). Regulation of gephyrin and GABAA receptor binding within the amygdala after fear acquisition and extinction. *J. Neurosci.* 25, 502–506. doi: 10.1523/JNEUROSCI.3301-04.2005

Chouliaras, L., Mastroeni, D., Delvaux, E., Grover, A., Kenis, G., Hof, P. R., et al. (2013). Consistent decrease in global DNA methylation and hydroxymethylation in the hippocampus of Alzheimer's disease patients. *Neurobiol. Aging* 34, 2091–2099. doi: 10.1016/j.neurobiolaging.2013.02.021

Cortellino, S., Xu, J., Sannai, M., Moore, R., Caretti, E., Cigliano, A., et al. (2011). Thymine DNA glycosylase is essential for active DNA demethylation by linked deamination-base excision repair. *Cell* 146, 67–79. doi: 10.1016/j.cell.2011.06.020

Dong, E., Ruzicka, W. B., Grayson, D. R., and Guidotti, A. (2015). DNA-methyltransferase1 (DNMT1) binding to CpG rich GABAergic and BDNF promoters is increased in the brain of schizophrenia and bipolar disorder patients. *Schizophr. Res.* 167, 35–41. doi: 10.1016/j.schres.2014.10.030

Gavin, D. P., Sharma, R. P., Chase, K. A., Matrisciano, F., Dong, E., and Guidotti, A. (2012). Growth arrest and DNA-damage-inducible, β (GADD45b)-mediated DNA demethylation in major psychosis. *Neuropsychopharmacology* 37, 531–542. doi: 10.1038/npp.2011.221

Goll, M. G., and Bestor, T. H. (2005). Eukaryotic cytosine methyltransferases. *Annu. Rev. Biochem.* 74, 481–514. doi: 10.1146/annurev.biochem.74.010904.153721

Grassi, D., Franz, H., Vezzali, R., Bovio, P., Heidrich, S., Dehghanian, F., et al. (2017). Neuronal activity, TGFβ-signaling and unpredictable chronic stress modulate transcription of Gadd45 family members and DNA methylation in the hippocampus. *Cereb. Cortex* 27, 4166–4181. doi: 10.1093/cercor/bhx095

Grayson, D. R., and Guidotti, A. (2013). The dynamics of DNA methylation in schizophrenia and related psychiatric disorders. *Neuropsychopharmacology* 38, 138–166. doi: 10.1038/npp.2012.125

Hajkova, P., Jeffries, S. J., Lee, C., Miller, N., Jackson, S. P., and Surani, M. A. (2010). Genome-wide reprogramming in the mouse germ line entails the base excision repair pathway. *Science* 329, 78–82. doi: 10.1126/science.1187945

Halder, R., Hennion, M., Vidal, R. O., Shomroni, O., Rahman, R. U., Rajput, A., et al. (2016). DNA methylation changes in plasticity genes accompany the formation and maintenance of memory. *Nat. Neurosci.* 19, 102–110. doi: 10.1038/nn.4194

Hardeland, U., Bentele, M., Lettieri, T., Steinacher, R., Jiricny, J., and Schar, P. (2001). Thymine DNA glycosylase. *Prog. Nucleic Acid Res. Mol. Biol.* 68, 235–253. doi: 10.1016/S0079-6603(01)68103-0

He, Y. F., Li, B. Z., Li, Z., Liu, P., Wang, Y., Tang, Q., et al. (2011). Tet-mediated formation of 5-carboxylcytosine and its excision by TDG in mammalian DNA. *Science* 333, 1303–1307. doi: 10.1126/science.1210944

Hevroni, D., Rattner, A., Bundman, M., Lederfein, D., Gabarah, A., Mangelus, M., et al. (1998). Hippocampal plasticity involves extensive gene induction and multiple cellular mechanisms. *J. Mol. Neurosci.* 10, 75–98. doi: 10.1007/bf02737120

Inoue, A., and Zhang, Y. (2011). Replication-dependent loss of 5-hydroxymethylcytosine in mouse preimplantation embryos. *Science* 334:194. doi: 10.1126/science.1212483

Ito, S., D'Alessio, A. C., Taranova, O. V., Hong, K., Sowers, L. C., and Zhang, Y. (2010). Role of Tet proteins in 5mC to 5hmC conversion, ES-cell self-renewal and inner cell mass specification. *Nature* 466, 1129–1133. doi: 10.1038/nature09303

Ito, S., Shen, L., Dai, Q., Wu, S. C., Collins, L. B., Swenberg, J. A., et al. (2011). Tet proteins can convert 5-methylcytosine to 5-formylcytosine and 5-carboxylcytosine. *Science* 333, 1300–1303. doi: 10.1126/science.1210597

Jarome, T. J., Butler, A. A., Nichols, J. N., Pacheco, N. L., and Lubin, F. D. (2015). NF-κB mediates Gadd45β expression and DNA demethylation in the hippocampus during fear memory formation. *Front. Mol. Neurosci.* 8:54. doi: 10.3389/fnmol.2015.00054

Jones, P. A. (2012). Functions of DNA methylation: islands, start sites, gene bodies and beyond. *Nat. Rev. Genet.* 13, 484–492. doi: 10.1038/nrg3230

Kaas, G. A., Zhong, C., Eason, D. E., Ross, D. L., Vachhani, R. V., Ming, G. L., et al. (2013). TET1 controls CNS 5-methylcytosine hydroxylation, active DNA demethylation, gene transcription and memory formation. *Neuron* 79, 1086–1093. doi: 10.1016/j.neuron.2013.08.032

Kaltschmidt, B., and Kaltschmidt, C. (2015). NF-KappaB in long-term memory and structural plasticity in the adult mammalian brain. *Front. Mol. Neurosci.* 8:69. doi: 10.3389/fnmol.2015.00069

Keeley, M. B., Wood, M. A., Isiegas, C., Stein, J., Hellman, K., Hannenhalli, S., et al. (2006). Differential transcriptional response to nonassociative and associative components of classical fear conditioning in the amygdala and hippocampus. *Learn. Mem.* 13, 135–142. doi: 10.1101/lm.86906

Keown, C. L., Berletch, J. B., Castanon, R., Nery, J. R., Disteche, C. M., Ecker, J. R., et al. (2017). Allele-specific non-CG DNA methylation marks domains of active chromatin in female mouse brain. *Proc. Natl. Acad. Sci. U S A* 114, E2882–E2890. doi: 10.1073/pnas.1611905114

Kigar, S. L., Chang, L., and Auger, A. P. (2015). Gadd45b is an epigenetic regulator of juvenile social behavior and alters local pro-inflammatory cytokine production in the rodent amygdala. *Brain Behav. Immun.* 46, 60–69. doi: 10.1016/j.bbi.2015.02.018

Kriaucionis, S., and Heintz, N. (2009). The nuclear DNA base 5-hydroxymethylcytosine is present in Purkinje neurons and the brain. *Science* 324, 929–930. doi: 10.1126/science.1169786

Krokan, H. E., Drablos, F., and Slupphaug, G. (2002). Uracil in DNA—occurrence, consequences and repair. *Oncogene* 21, 8935–8948. doi: 10.1038/sj.onc.1205996

Larijani, M., Frieder, D., Sonbuchner, T. M., Bransteitter, R., Goodman, M. F., Bouhassira, E. E., et al. (2005). Methylation protects cytidines from AID-mediated deamination. *Mol. Immunol.* 42, 599–604. doi: 10.1016/j.molimm.2004.09.007

Lashley, T., Gami, P., Valizadeh, N., Li, A., Revesz, T., and Balazs, R. (2015). Alterations in global DNA methylation and hydroxymethylation are not detected in Alzheimer's disease. *Neuropathol. Appl. Neurobiol.* 41, 497–506. doi: 10.1111/nan.12183

Leach, P. T., Poplawski, S. G., Kenney, J. W., Hoffman, B., Liebermann, D. A., Abel, T., et al. (2012). Gadd45b knockout mice exhibit selective deficits in hippocampus-dependent long-term memory. *Learn. Mem.* 19, 319–324. doi: 10.1101/lm.024984.111

Li, X., Baker-Andresen, D., Zhao, Q., Marshall, V., and Bredy, T. W. (2014a). Methyl CpG binding domain ultra-sequencing: a novel method for identifying inter-individual and cell-type-specific variation in DNA methylation. *Genes Brain Behav.* 13, 721–731. doi: 10.1111/gbb.12150

Li, X., Wei, W., Zhao, Q. Y., Widagdo, J., Baker-Andresen, D., Flavell, C. R., et al. (2014b). Neocortical Tet3-mediated accumulation of 5-hydroxymethylcytosine promotes rapid behavioral adaptation. *Proc. Natl. Acad. Sci. U S A* 111, 7120–7125. doi: 10.1073/pnas.1318906111

Li, Z., Gu, T. P., Weber, A. R., Shen, J. Z., Li, B. Z., Xie, Z. G., et al. (2015). Gadd45a promotes DNA demethylation through TDG. *Nucleic Acids Res.* 43, 3986–3997. doi: 10.1093/nar/gkv283

Li, Y. Q., Zhou, P. Z., Zheng, X. D., Walsh, C. P., and Xu, G. L. (2007). Association of Dnmt3a and thymine DNA glycosylase links DNA methylation with base-excision repair. *Nucleic Acids Res.* 35, 390–400. doi: 10.1093/nar/gkl1052

Lister, R., Mukamel, E. A., Nery, J. R., Urich, M., Puddifoot, C. A., Johnson, N. D., et al. (2013). Global epigenomic reconfiguration during mammalian brain development. *Science* 341:1237905. doi: 10.1126/science.1237905

Lubin, F. D., Roth, T. L., and Sweatt, J. D. (2008). Epigenetic regulation of BDNF gene transcription in the consolidation of fear memory. *J. Neurosci.* 28, 10576–10586. doi: 10.1523/JNEUROSCI.1786-08.2008

Ma, D. K., Jang, M. H., Guo, J. U., Kitabatake, Y., Chang, M. L., Pow-Anpongkul, N., et al. (2009). Neuronal activity-induced Gadd45b promotes epigenetic DNA demethylation and adult neurogenesis. *Science* 323, 1074–1077. doi: 10.1126/science.1166859

Maiti, A., and Drohat, A. C. (2011). Thymine DNA glycosylase can rapidly excise 5-formylcytosine and 5-carboxylcytosine: potential implications for active demethylation of CpG sites. *J. Biol. Chem.* 286, 35334–35338. doi: 10.1074/jbc.C111.284620

Mastroeni, D., Grover, A., Delvaux, E., Whiteside, C., Coleman, P. D., and Rogers, J. (2010). Epigenetic changes in Alzheimer's disease: decrements in DNA methylation. *Neurobiol. Aging* 31, 2025–2037. doi: 10.1016/j.neurobiolaging.2008.12.005

Mellen, M., Ayata, P., Dewell, S., Kriaucionis, S., and Heintz, N. (2012). MeCP2 binds to 5hmC enriched within active genes and accessible chromatin in the nervous system. *Cell* 151, 1417–1430. doi: 10.1016/j.cell.2012.11.022

Miller, C. A., and Sweatt, J. D. (2007). Covalent modification of DNA regulates memory formation. *Neuron* 53, 857–869. doi: 10.1016/j.neuron.2007.02.022

Mo, A., Mukamel, E. A., Davis, F. P., Luo, C., Henry, G. L., Picard, S., et al. (2015). Epigenomic signatures of neuronal diversity in the mammalian brain. *Neuron* 86, 1369–1384. doi: 10.1016/j.neuron.2015.05.018

Muramatsu, M., Sankaranand, V. S., Anant, S., Sugai, M., Kinoshita, K., Davidson, N. O., et al. (1999). Specific expression of activation-induced cytidine deaminase (AID), a novel member of the RNA-editing deaminase family in germinal center B cells. *J. Biol. Chem.* 274, 18470–18476. doi: 10.1074/jbc.274.26.18470

Nabel, C. S., Jia, H., Ye, Y., Shen, L., Goldschmidt, H. L., Stivers, J. T., et al. (2012). AID/APOBEC deaminases disfavor modified cytosines implicated in DNA demethylation. *Nat. Chem. Biol.* 8, 751–758. doi: 10.1038/nchembio.1042

Nott, A., Watson, P. M., Robinson, J. D., Crepaldi, L., and Riccio, A. (2008). S-Nitrosylation of histone deacetylase 2 induces chromatin remodelling in neurons. *Nature* 455, 411–415. doi: 10.1038/nature07238

Oliveira, A. M. (2016). DNA methylation: a permissive mark in memory formation and maintenance. *Learn. Mem.* 23, 587–593. doi: 10.1101/lm.042739.116

Ooi, S. K., and Bestor, T. H. (2008). The colorful history of active DNA demethylation. *Cell* 133, 1145–1148. doi: 10.1016/j.cell.2008.06.009

Penn, N. W., Suwalski, R., O'Riley, C., Bojanowski, K., and Yura, R. (1972). The presence of 5-hydroxymethylcytosine in animal deoxyribonucleic acid. *Biochem. J.* 126, 781–790. doi: 10.1042/bj1260781

Rai, K., Huggins, I. J., James, S. R., Karpf, A. R., Jones, D. A., and Cairns, B. R. (2008). DNA demethylation in zebrafish involves the coupling of a deaminase, a glycosylase and gadd45. *Cell* 135, 1201–1212. doi: 10.1016/j.cell.2008.11.042

Raiber, E. A., Beraldi, D., Ficz, G., Burgess, H. E., Branco, M. R., Murat, P., et al. (2012). Genome-wide distribution of 5-formylcytosine in embryonic stem cells is associated with transcription and depends on thymine DNA glycosylase. *Genome Biol.* 13:R69. doi: 10.1186/gb-2012-13-8-r69

Rangam, G., Schmitz, K. M., Cobb, A. J., and Petersen-Mahrt, S. K. (2012). AID enzymatic activity is inversely proportional to the size of cytosine C5 orbital cloud. *PLoS One* 7:e43279. doi: 10.1371/journal.pone.0043279

Ratnu, V. S., Wei, W., and Bredy, T. W. (2014). Activation-induced cytidine deaminase regulates activity-dependent BDNF expression in post-mitotic cortical neurons. *Eur. J. Neurosci.* 40, 3032–3039. doi: 10.1111/ejn.12678

Roubroeks, J. A. Y., Smith, R. G., van den Hove, D. L. A., and Lunnon, K. (2017). Epigenetics and DNA methylomic profiling in Alzheimer's disease and other neurodegenerative diseases. *J. Neurochem.* 143, 158–170. doi: 10.1111/jnc.14148

Shen, L., Wu, H., Diep, D., Yamaguchi, S., D'Alessio, A. C., Fung, H. L., et al. (2013). Genome-wide analysis reveals TET- and TDG-dependent 5-

methylcytosine oxidation dynamics. *Cell* 153, 692–706. doi: 10.1016/j.cell.2013.04.002

Singh, A., and Kar, S. K. (2017). How electroconvulsive therapy Works?: understanding the neurobiological mechanisms. *Clin. Psychopharmacol. Neurosci.* 15, 210–221. doi: 10.9758/cpn.2017.15.3.210

Sultan, F. A., Wang, J., Tront, J., Liebermann, D. A., and Sweatt, J. D. (2012). Genetic deletion of Gadd45b, a regulator of active DNA demethylation, enhances long-term memory and synaptic plasticity. *J. Neurosci.* 32, 17059–17066. doi: 10.1523/JNEUROSCI.1747-12.2012

Tahiliani, M., Koh, K. P., Shen, Y., Pastor, W. A., Bandukwala, H., Brudno, Y., et al. (2009). Conversion of 5-methylcytosine to 5-hydroxymethylcytosine in mammalian DNA by MLL partner TET1. *Science* 324, 930–935. doi: 10.1126/science.1170116

Varley, K. E., Gertz, J., Bowling, K. M., Parker, S. L., Reddy, T. E., Pauli-Behn, F., et al. (2013). Dynamic DNA methylation across diverse human cell lines and tissues. *Genome Res.* 23, 555–567. doi: 10.1101/gr.147942.112

Veldic, M., Caruncho, H. J., Liu, W. S., Davis, J., Satta, R., Grayson, D. R., et al. (2004). DNA-methyltransferase 1 mRNA is selectively overexpressed in telencephalic GABAergic interneurons of schizophrenia brains. *Proc. Natl. Acad. Sci. U S A* 101, 348–353. doi: 10.1073/pnas.2637013100

Wijesinghe, P., and Bhagwat, A. S. (2012). Efficient deamination of 5-methylcytosines in DNA by human APOBEC3A, but not by AID or APOBEC3G. *Nucleic Acids Res.* 40, 9206–9217. doi: 10.1093/nar/gks685

Xie, W., Barr, C. L., Kim, A., Yue, F., Lee, A. Y., Eubanks, J., et al. (2012). Base-resolution analysis of sequence and parent-of-origin dependent DNA methylation in the mouse genome. *Cell* 148, 816–831. doi: 10.1016/j.cell.2011.12.035

Yu, H., Su, Y., Shin, J., Zhong, C., Guo, J. U., Weng, Y. L., et al. (2015). Tet3 regulates synaptic transmission and homeostatic plasticity via DNA oxidation and repair. *Nat. Neurosci.* 18, 836–843. doi: 10.1038/nn.4008

Zhu, J. K. (2009). Active DNA demethylation mediated by DNA glycosylases. *Annu. Rev. Genet.* 43, 143–166. doi: 10.1146/annurev-genet-102108-134205

Zhu, B., Zheng, Y., Angliker, H., Schwarz, S., Thiry, S., Siegmann, M., et al. (2000a). 5-methylcytosine DNA glycosylase activity is also present in the human MBD4 (G/T mismatch glycosylase) and in a related avian sequence. *Nucleic Acids Res.* 28, 4157–4165. doi: 10.1093/nar/28.21.4157

Zhu, B., Zheng, Y., Hess, D., Angliker, H., Schwarz, S., Siegmann, M., et al. (2000b). 5-methylcytosine-DNA glycosylase activity is present in a cloned G/T mismatch DNA glycosylase associated with the chicken embryo DNA demethylation complex. *Proc. Natl. Acad. Sci. U S A* 97, 5135–5139. doi: 10.1073/pnas.100107597

Zhubi, A., Veldic, M., Puri, N. V., Kadriu, B., Caruncho, H., Loza, I., et al. (2009). An upregulation of DNA-methyltransferase 1 and 3a expressed in telencephalic GABAergic neurons of schizophrenia patients is also detected in peripheral blood lymphocytes. *Schizophr. Res.* 111, 115–122. doi: 10.1016/j.schres.2009.03.020

Conflict of Interest Statement: The authors declare that the research was conducted in the absence of any commercial or financial relationships that could be construed as a potential conflict of interest.

frontiers in Cellular Neuroscience

ORIGINAL RESEARCH
published: 17 May 2018
doi: 10.3389/fncel.2018.00131

Altered Regulation of KIAA0566, and Katanin Signaling Expression in the Locus Coeruleus With Neurofibrillary Tangle Pathology

Pol Andrés-Benito[1], *Raul Delgado-Morales*[2] *and Isidro Ferrer*[1,3,4,5]*

[1] Neuropathology, Pathologic Anatomy Service, Bellvitge Biomedical Research Institute, Hospitalet de Llobregat, Bellvitge University Hospital, Barcelona, Spain, [2] Cancer Epigenetics Group, Cancer Epigenetics and Biology Program, Bellvitge Biomedical Research Institute, L'Hospitalet de Llobregat, Spain, [3] Department of Pathology and Experimental Therapeutics, University of Barcelona, L'Hospitalet de Llobregat, Spain, [4] Institute of Neurosciences, University of Barcelona, L'Hospitalet de Llobregat, Spain, [5] Biomedical Network Research Centre of Neurodegenerative Diseases, National Institute of Health Carlos III, L'Hospitalet de Llobregat, Spain

The locus coeruleus (LC), which contains the largest group of noradrenergic neurons in the central nervous system innervating the telencephalon, is an early and constantly vulnerable region to neurofibrillary tangle (NFT) pathology in aging and Alzheimer's disease (AD). The present study using whole genome bisulfite sequencing and Infinium Human Methylation 450 BeadChip was designed to learn about DNA methylation profiles in LC with age and NFT pathology. This method identified decreased DNA methylation of Katanin-Interacting Protein gene (*KIAA0566)* linked to age and presence of NFT pathology. *KIAA0566* mRNA expression demonstrated with RT-qPCR significantly decreased in cases with NFT pathology. Importantly, KIAA0566 immunoreactivity was significantly decreased only in LC neurons with NFTs, but not in neurons without tau pathology when compared with neurons of middle-aged individuals. These changes were accompanied by a similar pattern of selective p80-katanin reduced protein expression in neurons with NFTs. In contrast, p60-katanin subunit expression levels in the neuropil were similar in MA cases and cases with NFT pathology. Since katanin is a major microtubule-severing protein and KIAA0566 binds and interacts with katanin, de-regulation of the katanin-signaling pathway may have implications in the regulation of microtubule homeostasis in LC neurons with NFTs, thereby potentially interfering with maintenance of the cytoskeleton and transport.

Keywords: Alzheimer's disease, locus coeruleus, neurofibrillary tangles, methylation, katanin, KIAA0556, microtubules

OPEN ACCESS

Edited by:
Daniel Ortuño-Sahagún, Universidad de Guadalajara, Mexico

Reviewed by:
Michela Ferrucci, Università degli Studi di Pisa, Italy
Annamaria Confaloni, Istituto Superiore di Sanità, Italy

***Correspondence:**
Isidro Ferrer
8082ifa@gmail.com

Received: *27 January 2018*
Accepted: *26 April 2018*
Published: *17 May 2018*

Citation:
Andrés-Benito P, Delgado-Morales R and Ferrer I (2018) Altered Regulation of KIAA0566, and Katanin Signaling Expression in the Locus Coeruleus With Neurofibrillary Tangle Pathology. Front. Cell. Neurosci. 12:131. doi: 10.3389/fncel.2018.00131

INTRODUCTION

Studies of Alzheimer's disease (AD) are mainly focused on the entorhinal cortex, hippocampus, and neocortex because of the massive accumulation with disease progression of β-amyloid deposits (diffuse and senile plaques) and hyper-phosphorylated tau-containing neurofibrillary tangles (NFTs), neuropil threads, and dystrophic neurites in these regions. Recently, the study of the brainstem in AD has captivated attention as (a) several nuclei of the brain stem such as the raphe nuclei and locus ceruleus (LC) are early and constantly affected in AD by abnormal

neuronal deposition and formation of NFTs; (b) these nuclei are the main source of serotoninergic and noradrenergic innervations of the telencephalon including cerebral cortex; and (c) several functions dependent on the integrity of these nuclei such as arousal, attention, sleep-awake cycles, emotional states (control of panic, anxiety, and depression), autonomic function, memory and learning, stress responses, and motor coordination, among others, are altered in AD (Rüb et al., 2001; Aston-Jones and Cohen, 2005; Grinberg et al., 2009; Simic et al., 2009; Šimić et al., 2016; Attems et al., 2012; Szabadi, 2013). Whole-transcriptome arrays in LC reveal up-regulation of genes coding for proteins associated with heat shock protein binding and genes associated with ATP metabolism, and down-regulation of genes coding for DNA-binding proteins and members of the small nucleolar RNA family in LC neurons at early stages of NFT pathology (Andrés-Benito et al., 2017). MicroRNA expression is altered in the LC at early stages of NFT pathology (Llorens et al., 2017). These observations indicate alterations in the mechanisms leading to gene transcription and protein translation in LC at early stages of AD-related pathology.

DNA methylation and other epigenetic mechanisms which are modulators of gene transcription are altered in several neurodegenerative diseases including AD (Jakovcevski and Akbarian, 2012; Lu et al., 2013; Sanchez-Mut et al., 2014; Lardenoije et al., 2015; Blanch et al., 2016; Watson et al., 2016; Wen et al., 2016; Nicolia et al., 2017; Roubroeks et al., 2017; Smith and Lunnon, 2017). Epigenetic deregulation of brainstem nuclei has been postulated as one of the primary mechanisms in the pathogenesis of AD (Iatrou et al., 2017). The present work focuses on the study of DNA methylation in dissected LC in cases with NFT pathology compared with middle-aged individuals. Since one of the differentially methylated genes is *KIAA0556*, which encodes katanin-Interacting Protein, the study is then redirected to the analysis of expression of KIAA0556 mRNA and protein, and the proteins katanin subunit 60 and katanin subunit 80 (p60-katanin and p80-katanin, respectively) to assess possible alterations in katanin pathway signaling linked to NFT pathology in LC.

MATERIALS AND METHODS

Human Brain Samples

Human brain samples were obtained from the Institute of Neuropathology Brain Bank (HUB-ICO-IDIBELL Biobank) following the guidelines of the Spanish legislation on this matter (Real Decreto 1716/2011) and approval by the local ethics committee of the Bellvitge University Hospital-IDIBELL. The post-mortem interval between death and tissue processing was between 2 h 45 min and 15 h. This interval permits the study of RNA and protein expression as assessed elsewhere (Ferrer et al., 2008). One hemisphere was immediately cut in coronal sections, 1 cm thick, and selected areas of the encephalon were rapidly dissected, frozen on metal plates over dry ice, placed in individual air-tight plastic bags, and stored at −80°C until use. The other hemisphere was fixed by immersion in 4% buffered formalin for 3 weeks. The brain stem was cut on tangential sections 2 mm thick which were alternately frozen at −80°C or fixed in buffered formalin for 3 weeks. The neuropathological study for diagnosis was carried out with selected 4 μm-thick de-waxed paraffin sections of representative brain regions processed for immunohistochemistry as detailed elsewhere (Ferrer, 2014). Neuropathological diagnosis was based on the Braak and Braak stages of neurofibrillary tangle (NFT) pathology (Braak and Braak, 1991; Braak et al., 2006) and Thal phases of β-amyloid deposits (Thal et al., 2002). Cases with combined pathologies, excepting small blood vessel disease, and cases with metabolic syndrome, hypoxia, seizures, and long agonic state, were excluded. Since early stages of sporadic AD may show only NFT pathology without β-amyloid deposition Ferrer, 2012; Braak and Del Tredici, 2015), and these changes are similar to those seen in Primary age-related tauopathy (PART) (Crary et al., 2014; Duyckaerts et al., 2015), no attempt was made here to distinguish between early AD and PART, thus considering as pathological cases those containing NFTs grade according to Braak categorization stages. Cases were divided in two series. One series was used for DNA methylation studies; the LC of both sides was dissected from frozen samples. These cases were as follows: middle-aged cases (MA): $n = 3$, mean age: 50 ± 1 years; NFT pathology stages I-II, $n = 4$, age: 68 ± 6.3; NFT pathology stages III-IV, $n = 7$, age 85.1 ± 7.0; NFT pathology stages V-VI, $n = 6$, age: 76.3 ± 12.5 years. The second series was used for RT-qPCR after dissection of LC from frozen sections, and immunofluorescence and confocal microscopy carried out on serial sections containing the LC fixed in buffered formalin. These cases were the following: MA, $n = 9$, age: 51.0 ± 6.1; NFT pathology stages I-II, $n = 9$, age: 64.6 ± 5.7; and NFT pathology stages III-IV, $n = 13$, age: 78.1 ± 8.0. Cases in the second series were not affected by β-amyloid deposits, as phases 1 and 2 of Thal do not affect the LC.

Cases are summarized in **Table 1**. No differences in gender distribution were observed in these series. See comments below about age differences among groups.

Regarding clinical phenotype, MA cases and cases with NFT pathology stages I-III were normal; some cases at stage IV (cases 20, 40 and 41) had suffered from mild cognitive impairment, and cases at stages V-VI were categorized as dementia of AD type.

DNA Extraction and Illumina Infinium Human MethylationEPIC BeadChip

Cases used for DNA methylation are detailed in **Table 1**. Total DNA was isolated from microdissected LC with DNeasy Blood and Tissue Kit (Qiagen, Madrid, Spain) according to the manufacturer's instructions. All DNA samples were assessed for integrity, quantity, and purity with electrophoresis in a 1.3% agarose gel, with picogreen quantification and nanodrop measurements. Bisulfite conversion of 500 ng of genomic DNA was performed using EZ DNA methylation kit (Zymo Research, Irvine, CA, USA) following the manufacturer's instructions. 200 ng of bisulfite-converted DNA was used for hybridization on the Illumina Infinium Human MethylationEPIC BeadChip (Illumina Inc., San Diego, CA, USA). Briefly, samples were whole genome-amplified, followed by an enzymatic end-point fragmentation, precipitation, and re-suspension. The re-suspended samples were hybridized onto the bead-chip for

TABLE 1 | Summary of cases analyzed in the present series.

Case	Age	Sex	Thal	Braak	PMD	RIN	RTqPCR	Methylation
1	64	M	1	I	04 h 35 min	6.2	X	-
2	73	M	0	I	07 h 05 min	6.6	X	-
3	56	W	1	I	08 h 00 min	6.3	X	-
4	67	M	0	I	14 h 40 min	5.9	X	-
5	70	M	1	I	02 h 00 min	7.6	X	-
6	61	M	0	I	04 h 30 min	6.9	X	-
7	66	M	0	I	12 h 10 min	5.8	X	-
8	68	W	1	II	04 h 30 min	6.7	X	-
9	57	M	0	II	04 h 30 min	6.7	X	-
10	90	W	1	III	04 h 00 min	7.1	X	-
11	78	W	A	III	06 h 00 min	6.8	X	-
12	69	M	0	III	13 h 10 min	7.2	X	-
13	64	M	2	III	06 h 00 min	7.0	X	-
14	90	W	1	III	04 h 00 min	7.1	X	-
15	73	M	0	III	04 h 15 min	8.0	X	-
16	75	M	1	III	03 h 25 min	6.2	X	-
17	76	M	1	III	06 h 00 min	5.8	X	-
18	76	M	1	III	06 h 00 min	5.8	X	-
19	78	W	2	III	06 h 00 min	6.8	X	-
20	74	M	2	IV	04 h 45 min	6.2	X	-
21	84	M	2	IV	10 h 50 min	7.0	X	-
22	89	M	2	IV	03 h 20 min	7.0	X	-
23	44	M	0	0	06 h 40 min	6.7	X	-
24	52	M	0	0	03 h 00 min	6.8	X	-
25	52	M	0	0	04 h 40 min	7.6	X	-
26	52	W	0	0	05 h 45 min	6.4	X	-
27	41	M	0	0	11 h 35 min	5.9	X	-
28	60	W	0	0	11 h 30 min	5.8	X	-
29	59	M	0	0	08 h 30 min	6.6	X	-
30	51	W	0	0	04 h 00 min	5.9	X	-
31	48	W	0	0	14 h 30 min	6.1	X	-
32	64	M	0	I	08 h 00 min	-	-	X
33	68	M	0	I	10 h 55 min	-	-	X
34	77	M	1	I	06 h 55 min	-	-	X
35	63	M	0	I	02 h 45 min	-	-	X
36	79	W	2	III	03 h 40 min	-	-	X
37	82	W	2	III	03 h 05 min	-	-	X
38	81	M	1	III	05 h 50 min	-	-	X
39	90	W	1	IV	09 h 55 min	-	-	X
40	81	W	3	IV	05 h 00 min	-	-	X
41	99	W	2	IV	05 h 00 min	-	-	X
42	84	M	2	IV	12 h 15 min	-	-	X
43	74	W	2	V	05 h 30 min	-	-	X
44	95	M	3	V	03 h 00 min	-	-	X
45	81	W	3	V	05 h 15 min	-	-	X
46	75	M	3	V	11 h 30 min	-	-	X
47	77	M	3	V	16 h 00 min	-	-	X
48	56	W	4	VI	07 h 00 min	-	-	X
49	59	M	0	0	06 h 25 min	-	-	X
50	53	M	0	0	07 h 25 min	-	-	X
51	46	M	0	0	15 h 00 min	-	-	X

Age in years; M, man; W, woman; Thal phases of β-amyloid deposition; Braak stages of neurofibrillary tangle pathology; PMD, post-mortem delay; RIN, RNA integrity number; RTqPCR, cases used for RT-qPCR and immunofluorescence; Methylation, cases assessed for DNA methylation. Cases 23-31 and 49–51 were considered middle-aged (MA) individuals with no NFT and plaque pathology.

16 h at 48°C and then washed. A single nucleotide extension with labeled dideoxy-nucleotides was performed, and repeated rounds of staining were applied with a combination of fluorescently labeled antibodies differentiating between biotin and DNP. Fluorescent signal from the microarray was measured with a HiScan scanner (Illumina Inc.,) using iScan Control Software (V 3.3.29). A three-step-based normalization procedure was performed using a package available for Bioconductor (Gentleman et al., 2004), under the R statistical environment, consisting of color bias adjustment, background level adjustment, and quantile normalization across arrays (Du et al., 2008). Methylation level (β-value) for each of the 866,836 CpG sites was calculated as the ratio of methylated signal divided by the sum of methylated and unmethylated signals plus 100. All beta values with an associated $p \geq 0.01$ were removed from the analysis.

Gene Expression Validation

Samples used for RT-qPCR analysis are detailed in **Table 1**. RNA from frozen dissected LC was extracted following the instructions of the supplier (RNeasy Mini Kit; Qiagen GmbH, Hilden, GE). RNA integrity number (RIN) and 28/18 S ratios were determined with the Agilent Bioanalyzer (Agilent Technologies, Santa Clara, CA, USA) to assess RNA quality; RNA concentration was evaluated using a NanoDropTM Spectrophotometer (Thermo Fisher Scientific, Carlsbad, CA, USA). RIN (RNA integrity number) values varied from 5.8 to 7.6 with no significant differences among groups. Retro-transcription reaction of RNA samples was carried out with the high-capacity cDNA archive kit (Applied Biosystems, Foster City, CA, USA) following the guidelines provided by the manufacturer and using Gene Amp 9700 PCR System thermocycler (Applied Biosystems). One sample of RNA was processed in parallel in the absence of reverse transcriptase to rule out DNA contamination.

Quantitative real-time polymerase chain reaction (RT-qPCR) assays were conducted in duplicate on cDNA samples obtained from the retro-transcription reaction diluted 1:10 in 384-well optical plates (Kisker Biotech, Steinfurt, GE) utilizing the ABI Prism 7900 HT Sequence Detection System (Applied Biosystems). TaqMan probes (Thermo Fisher Scientific) were Hs00390731_m1 (*KIAA0556* probe) and Hs01125994_m1 (*UTRN* probe). The mean value of four house-keeping genes, alanyl-transfer RNA synthase (AARS) (Hs00609836_m1), glucuronidase Beta (*GUS-β*) (Hs00939627_m1), hypoxanthine-guanine phosphoribosyltransferase (*HPRT1*) (Hs02800695_m1), and X-prolyl amino-peptidase (aminopeptidase P) 1 (*XPNPEP1*) (Hs00958026_m1), were used as internal controls for normalization of LC samples (Barrachina et al., 2006; Durrenberger et al., 2012). DDCT values were obtained from the DCT of each sample minus the mean DCT of the population of control samples (calibrator samples). The fold change was determined using the equation 2DDCT. Mean fold change values in each group were analyzed with the Students *t*-test using the Statgraphics Statistical Analysis and Data Visualization Software version 5.1.

Double-Labeling Immunofluorescence and Confocal Microscopy

Cases used for immunofluorescence are named 10–31 in **Table 1** (stages I-II were not examined). Three de-waxed sections, 4 μm thick, per selected cases were stained with a saturated solution of Sudan black B (Merck, Barcelona, Spain) for 15 min to block the auto-fluorescence of lipofuscin granules present in cell bodies, and then rinsed in 70% ethanol and washed in distilled water. The sections were incubated at 4°C overnight with combinations of primary antibodies: anti-KIAA0556 diluted 1:250 (NBP1-91006, NovusBiologicals, USA), anti-p60 katanin subunit diluted 1:250 (MAB7100, R&D systems, USA), anti-p80 katanin subunit diluted 1:150 (ab224171, Abcam, UK), and antibody AT8 diluted 1:50 (MN1020, ThermoFisher, USA). After washing, the sections were incubated with Alexa488 or Alexa546 (1:400; Molecular Probes, Eugene, OR, USA) fluorescence secondary antibodies against the corresponding host species. Nuclei were stained with DRAQ5^{TM} (1:2,000; Biostatus, Shepshed, UK). After washing, the sections were mounted in Immuno-Fluore mounting medium (ICN Biomedicals, Santa Clara, CA, USA), sealed, and dried overnight. Sections were examined with a Leica TCS-SL confocal microscope (Leica, Barcelona, Spain), and the images were acquired with Leica confocal software. Densitometry of the immunoreaction signal in LC positive cells for KIAA0556 and p80 was performed using Photoshop software in three different sections per case. Comparisons were made between control and diseased cases, and between neurons with and without NFT pathology in pathological cases. Densitometry of p60 immunostaining was performed in the whole neuropil of the LC due to punctate characteristics of p60 immunostaining.

Statistical Analysis

The effect of age and NFT pathology were determinant in DNA methylation and RT-qPCR expression. These aspects were further interpreted on the basis of immunohistochemical studies and quantification of data.

The normality of the data was assessed with the Shapiro-Wilk test or Kolmogorov–Smirnov test when required. DNA methylation data and RT-qPCR data were compared with one-way analysis of variance (ANOVA) followed by Tukey post-test. Statistical analysis and graphic design were performed with GraphPad Prism version 5.01 (La Jolla, CA, USA). Outliers were detected using the GraphPad software QuickCalcs ($p < 0.05$). Significance levels were set at $^{*}p < 0.05$ and $^{**}p < 0.01$. Statistical analysis of densitometric protein levels between groups, as revealed by immunofluorescence, was performed using t-student's test or one-way analysis of variance (ANOVA) followed by Tukey post-test when required using the SPSS software (IBM Corp. Released 2013, IBM SPSS Statistics for Windows, Version 21.0. Armonk, NY: IBM Corp.). Outliers were detected using the GraphPad software QuickCalcs ($p < 0.05$). All data were expressed as mean values ± SEM. Differences between middle-aged and NFT(+) were considered statistically significant at $^{*}p < 0.05$, $^{**}p < 0.01$, $^{***}p < 0.001$, and set at $\$ p < 0.05$ and $\$\$ p < 0.01$ when comparing NFT(–) and NFT(+) neurons.

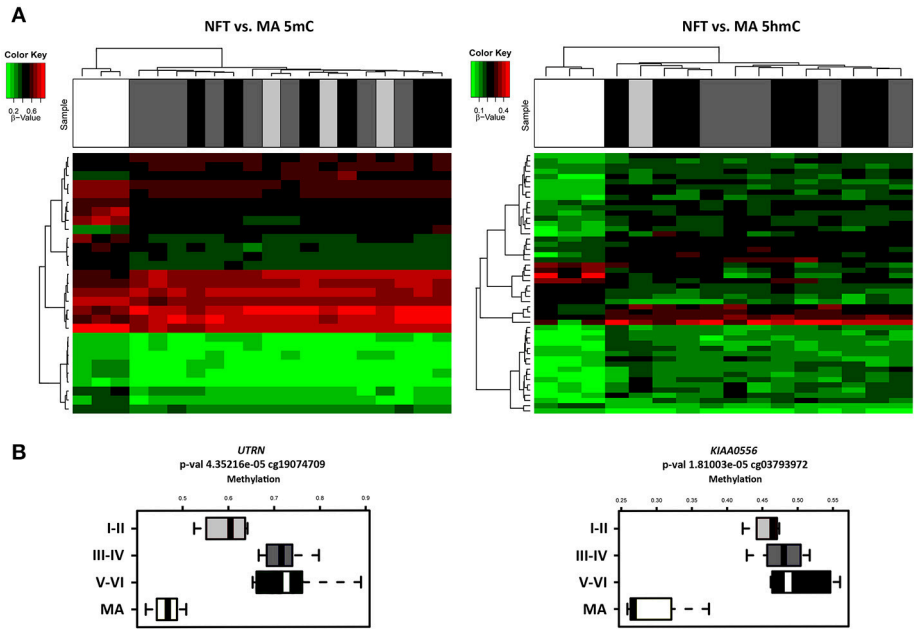

FIGURE 1 | (A) Hierarchical clustering heat map of methylation (5mC) (left) and hydroxmethylation (5hmC) (right) array showing differential methylation profile in LC in cases with neurofibrillary tangle (NFT) pathology and middle-aged individuals (MA). Differences between groups are here considered statistically significant at an adjusted $p < 0.05$ in methylation study and at an unadjusted $p < 0.05$ in hydroxymethylation study. **(B)** Box plot of CpG methylation differences between MA and cases at different stages of NFT pathology (I-II, III-IV, and V-VI) in *UTRN* (left) and *KIAA0556* (right) genes. Significant differences in *KIAA0556* DNA 5mC are seen between MA and all stages of NFT pathology. Abbreviations: 5mC: methylation; 5hmC: hydroxymethylation, *UTRN*: utrophin; *KIAA0556*: Katanin-interacting protein. Samples color code: gray: MA cases; black: cases with NFT pathology.

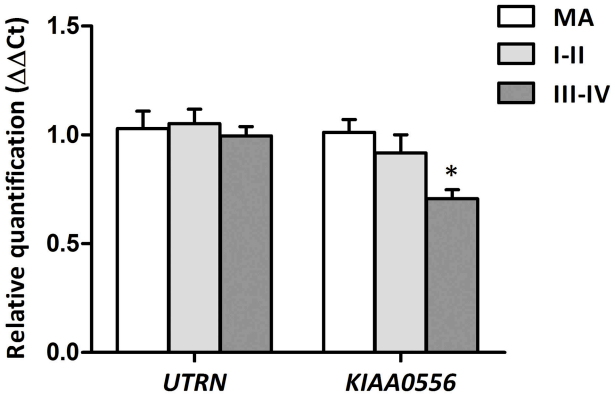

FIGURE 2 | Gene expression levels of *UTRN* and *KIAA0556* genes in LC in MA and cases with NFT pathology at stages I-II and III-IV. *$p < 0.05$ when comparing MA with NFT III-IV.

RESULTS

Differential Methylation Regions

Illumnia Infinium Human MethylationEPIC BeadChip Kit was used, covering over 850,000 methylation sites quantitatively across the genome at single-nucleotide resolution, which permits discrimination between 5mC and 5hmC. DNA methylation profiles obtained from this platform showed a few differential methylation regions (DMRs) when comparing MA individuals with cases showing various stages of NFT pathology. After the *Lumi* software analysis, coding DMRs showing significant differences at an adjusted $p < 0.05$ were sorted and ranked according to their CpG mean differences and significance (Supplementary Table 1). In contrast, 5hmC data obtained when comparing NFT stages with MA cases did not reveal significant differences following the same adjusted *p*-value established for 5mC (**Figure 1A**). For this reason no further attempt was made to analyze gene expression of suspected hydroximethylated genes. Enrichment analysis against the "Go Ontology" database did not identify significant clusters for coding DMRs in ases with NFT pathology. Two significant DMRs, *UTRN* and *KIAA0556* genes, coding for utrophin and katanin-Interacting Protein, respectively, were differentially hypo-methylated in cases with NFT pathology when compared with MA individuals. Differences were more marked for *KIAA0556* when comparing MA with early stages of NFT pathology (**Figure 1B**).

Gene Expression Validation

RT-qPCR was performed to evaluate *UTRN* and *KIAA0556* mRNA expression. *UTRN* mRNA expression did not significantly differ in MA and cases with NFT pathology. In contrast, *KIAA0556* mRNA expression was significantly reduced at stages III-IV of NFT pathology when compared with MA individuals ($p = 0.002$; **Figure 2**).

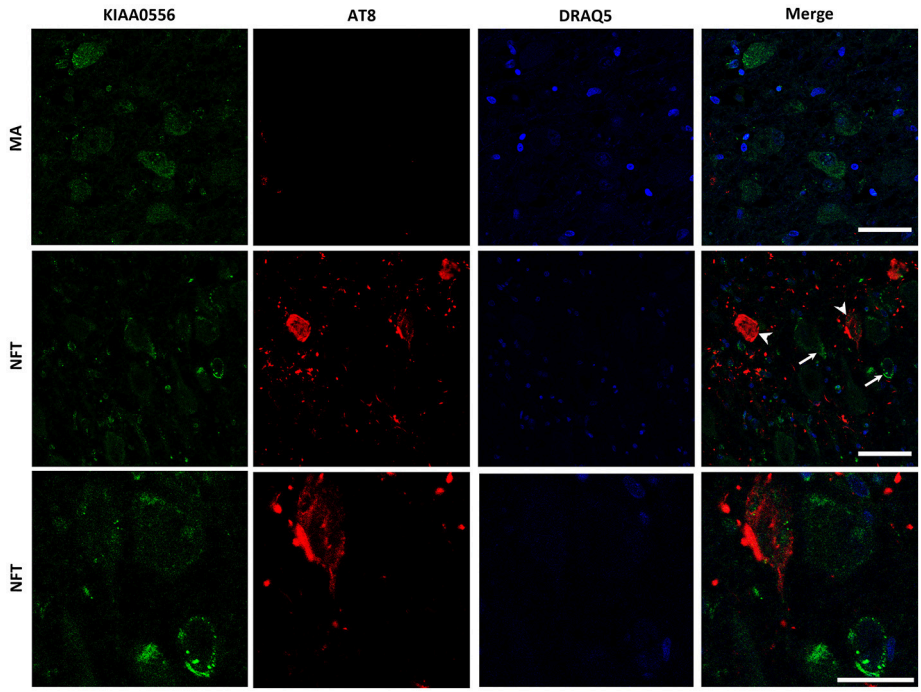

FIGURE 3 | Double-labeling immunofluorescence and confocal microscopy to KIAA0556 (green) and hyper-phosphorylated tau (clone AT8: red) in MA and in one case with NFT pathology stage IV. Note decreased KIAA0556 restricted to neurons containing NFT (arrowhead: only red; arrows: only green). Lower row: higher magnification of the upper right corner showing decreased KIAA0556 immunoreactivity in one neuron containing NFT. Paraffin sections; nuclei stained with DRAQ5TM (blue); bar in the two upper rows = 50 μm; bar in the lower row = 25 μm.

Protein Expression of KIAA0556, and Katanin p80 and p60 Subunits in LC

Double-labeling immunofluorescence and confocal microscopy to selected proteins and hyperphosphorylated tau (antibody AT8) were used to a: identify localization of KIAA0556, and katanin p80 and p60 subunits in LC; b: assess modified expression levels of these proteins in cases with NFT pathology; and c: analyze the relationship, if any, between KIAA0556, and katanin p80 and p60, in relation to tau deposition in neurons and neuropil of the LC.

KIAA0556 immunoreactivity was observed in the cytoplasm of neurons in MA and in cases with NFT pathology; the immunoreactivity was similar in neurons from MA cases and in neurons without NFTs in cases with NFT pathology. But KIAA0556 immunoreactivity was markedly reduced in neurons with NFTs, as revealed by double-labeling immunofluorescence and confocal microscopy (**Figure 3**). Quantitative studies showed no differences in the amount of protein in neurons of the LC in MA individuals and in non-containing NFT neurons in cases with NFT pathology stages III-IV. However, significant reduction of KIAA0556 immunoreactivity was verified in neurons containing hyper-phosphorylated tau deposits when compared with neurons not bearing NFTs in the same tissue section ($p = 0.002$) (**Figure 6A**).

To further learn about KIAA0556-associated proteins, double-labeling immunofluorescence to p60- and p80-katanin subunits was assessed. p60-katanin immunoreactivity was localized as punctuate, synaptic-like deposits in the neuropil in MA and cases at stages III-IV of NFT pathology, which was consistent with the localization of this protein in distal neuronal processes. Double-staining of p60-katanin and AT8 showed no apparent decrease in p60-katanin immunoreactivity in the neuropil of the LC in cases with NFT pathology when compared with MA (**Figure 4**). Densitometry revealed no significant differences between the two groups ($p = 0.62$; **Figure 6B**).

Finally, p80-katanin protein expression was localized in the cytoplasm of LC neurons. p80-katanin immunoreactivity was selectively reduced in neurons of the LC containing hyperphosphorylated tau deposits (**Figure 5**). Densitometric analysis further demonstrated no differences between MA neurons and neurons without tau deposits in cases with NFT pathology, but significant reduction of p80-katanin immunoreactivity in neurons with NFTs when compared with neurons without NFTs in the same tissue section ($p = 0.000$; **Figure 6C**).

DISCUSSION

DNA methylation at 5-methylcytosine (5mC) is an epigenetic mechanism associated primarily with transcriptional repression,

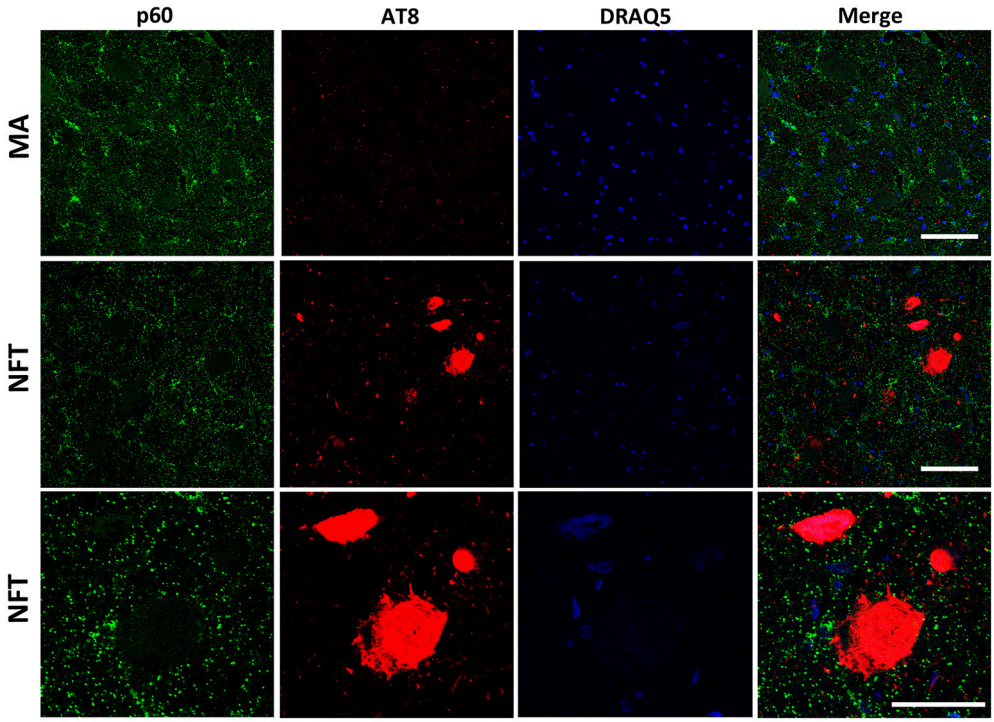

FIGURE 4 | Double-labeling immunofluorescence and confocal microscopy to p60-katanin (green) and hyper-phosphorylated tau (clone AT8: red) in MA and in one case with NFT pathology stage IV. Lower row: higher magnification of the upper right corner showing preserved p60-katanin immunoreactivity in the neuropil in NFT case when compared with MA. Paraffin sections; nuclei stained with DRAQ5TM (blue); bar in the two upper rows = 50 μm; bar in the lower row = 25 μm.

whereas methylation at 5-hydroxymethylcytosine (5hmC) has opposite effects. Here we used hybridization on the Illumina Infinium Human MethylationEPIC BeadChip to identify differences in DNA methylation of dissected LC of cases with NFT pathology compared with MA individuals without NFTs. The age of the two groups was different, with cases with NFT pathology being older than MA individuals. This is not a rare situation as 85% of human beings aged 65 years and older show NFT pathology defined, minimally, as stages I-II of Braak in the entorhinal cortex (EC). Most of them, if not all, have hyper-phosphorylated tau deposits in the LC (Braak et al., 2011; Ferrer, 2012). Indeed, tau pathology in certain nuclei of the brain stem, including LC, precedes tau pathology in the EC (Rüb et al., 2001; Grinberg et al., 2009; Simic et al., 2009; Attems et al., 2012). For this reason, the MA group was selected on the basis of the absence of tau pathology in LC. It can be argued that the present design is biased by age differences between the two main groups. This objection may be true in other situations, but present observations geared to learning about the association of NFT pathology and abnormal gene expression in neurons of the LC proved it not to be here.

Using restrictive conditions, two DNA hypo-methylated genes were selected for further study; *UTRN* and *KIAA0556* genes, coding for utrophin and katanin-Interacting Protein, were differentially hypo-methylated in cases with NFT pathology when compared with MA individuals. RT-qPCR showed no differences in *UTRN* mRNA expression between the two groups. However, *KIAA0556* mRNA expression was significantly reduced in cases with NFT pathology when compared with MA. Lack of correlation between degree of DNA methylation of CpG islands as revealed by the bisulphate methods and gene transcription is not a rare phenomenon in diseases of the nervous system (Nicolia et al., 2017).

Altered *KIAA0556* mRNA expression in neurons with NFT may have implications in microtubule pathology in neurons bearing hyper-phosphorylated tau in LC. Microtubules are hollow polymers of α- and β-tubulin subunits with one end, the plus-end, favored by the addition and subtraction of subunits, while the minus-end has limited turnover capacity; β-tubulins predominate at the plus-end and α-tubulins at the minus-end (Baas and Lin, 2011; Baas, 2013; Kapitein and Hoogenaad, 2015; Baas et al., 2016). This structure permits high plasticity; long microtubules shape the morphology and stability of dendrites and axons, and serve as a means to transport distinct molecules over long distances; short microtubules permit the growth of microtubules and the transport of tubulins (Baas et al., 2016). Stability of microtubules is in part related to tubulin polyamination catalyzed by transglutaminases (Song et al., 2013; Song and Brady, 2015). Several proteins bind to microtubules and modulate stabilization of microtubules; tau and other microtubule-associated proteins (MAPs) have repeats of microtubule-binding domains and prevent de-polymerization of microtubules (Mandelkow and Mandelkow, 1995; Kadavath et al., 2015). Tau hyper-phosphorylation, as occurs in NFTs,

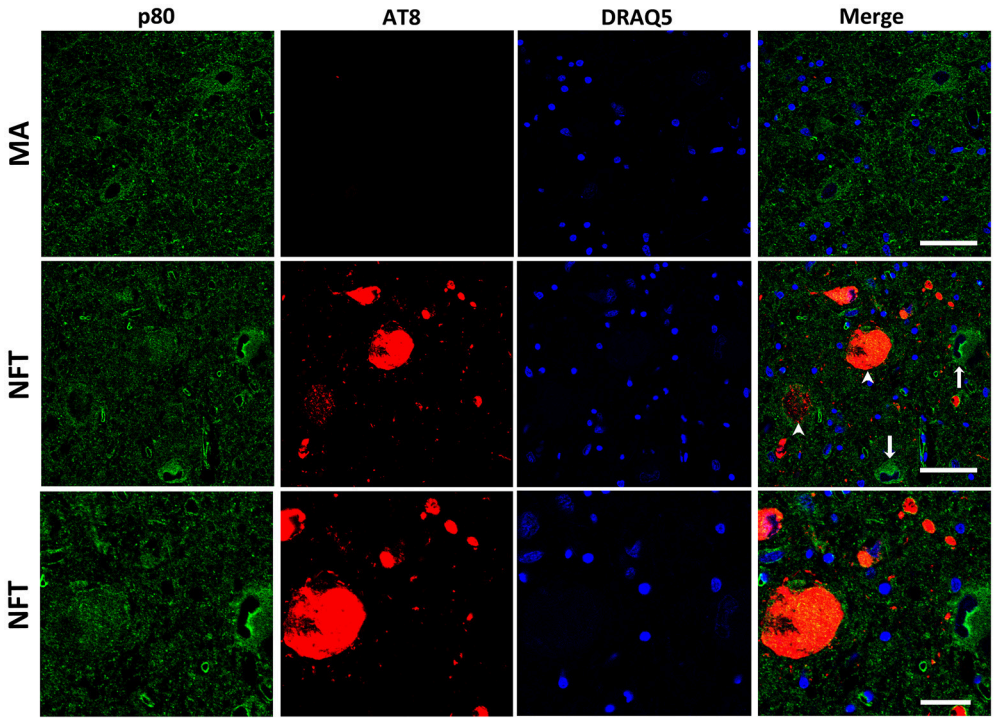

FIGURE 5 | Double-labeling immunofluorescence and confocal microscopy to p80-katanin (green) and hyper-phosphorylated tau (clone AT8: red) in MA and in one case with NFT pathology stage IV. Note decreased p80-katanin restricted to neurons containing NFT (arrowhead: only red; arrows: only green). Lower row: higher magnification of the upper right corner showing decreased p80-katanin immunoreactivity in one neuron containing NFT. Paraffin sections; nuclei stained with DRAQ5TM (blue); bar in the two upper rows = 50 μm; bar in the lower row = 25 μm.

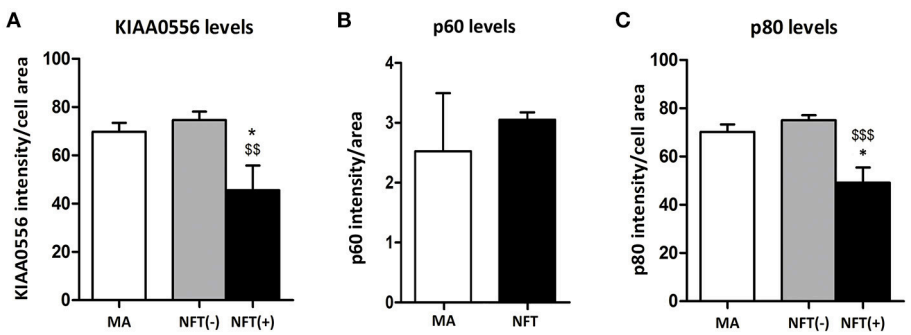

FIGURE 6 | Densitometric study showing no differences in p60 protein expression between LC neurons in MA cases and tau non-bearing neurons in cases with NFT pathology **(B)**, but significant KIAA0556 **(A)**, and p80-katanin (p80) **(C)** reduction in NFT-containing neurons when compared with non-tau containing neurons in the same sections. *$p < 0.05$ when comparing MA with NFT, and \$\$$p < 0.01$ and \$\$\$$p < 0.001$ when comparing NFT(–) and NFT(+) neurons in cases with NFT pathology.

results in tau dissociation from microtubules and aberrant formation of paired helical filaments (Alonso et al., 1999; Buée and Delacourte, 2001; Avila, 2006; Goedert et al., 2006; Wang and Liu, 2008; Duan et al., 2012; Matamoros and Bass, 2016).

Microtubule-severing proteins are proteins which form hexamers on the surface of microtubules and break the microtubules into fragments that can be transported to distinct places of the cytoplasm, axon, and dendrites to produce new microtubules, as only short microtubules are able to be transported (Wang and Brown, 2002; Baas et al., 2006; Roll-Mecak and McNally, 2010). Katanin is one of the most abundant microtubule-severing proteins in brain and plays an important role in axonal growth and dendrite branching during development due to its participation in the generation of microtubules (Ahmad et al., 1999; Yu et al., 2005, 2008; Roll-Mecak and Vale, 2006). Increased activity of microtubule-severing proteins also has noxious effects as it is accompanied by degradation of the neuronal cytoskeleton (Yu et al., 2005; Sudo

and Baas, 2011). p60-katanin is localized in neuronal processes and severs microtubules whereas p80-katanin is localized in the cytoplasm at the centrosomes (McNally et al., 2000; Yu et al., 2005). Tau seems to protect microtubules in the axon from severing by katanin (Qiang et al., 2006). Following on from this posit, it has been suggested that hyper-phosphorylated tau loses its function as protector and randomly enables microtubule severing by katanin (Qiang et al., 2006; Sudo and Baas, 2011).

KIAA0556 co-localizes with α-tubulin, and binds to p60- and p80-katanin subunits (Sanders et al., 2015). Moreover, KIAA0556 seems to negatively regulate katanin severing (Sanders et al., 2015). Mutations of KIAA0556 gene are causative of Joubert syndrome, which is manifested by several malformations including brain (Sanders et al., 2015; Roosing et al., 2016).

Considering all these data, the expression of proteins KIAA0556, and p60- and p80-katanin was considered a next step in the study of possible alterations of this pathway in the LC in neurons with NFT pathology. Double-labeling immunofluorescence with antibodies to these proteins, and to phosphorylated tau, disclosed no differences in the expression of KIAA0556 and p80-katanin in LC neurons of MA cases and in neurons without hyper-phosphorylated tau deposits in cases with NFT pathology. Moreover, no significant differences were seen in p60-katenin expression in the neuropil of cases with and without NFT pathology. These findings support the idea that age, *per se*, is not a determining factor in the altered expression of KIAA0556 and p80-katanin in LC neurons. Yet it is the presence of NFTs which makes the difference; KIAA0556 and p80-katanin protein are reduced only in neurons with NFTs.

Together, the present findings show association of decreased KIAA0556 and p80-katanin subunits in LC neurons with NFTs, and suggest that altered microtubule homeostasis in those neurons is linked to deregulation of the katanin-signaling pathway.

AUTHOR CONTRIBUTIONS

PA-B: RT-qPCR, immunohistochemistry; RD-M: DNA methylation studies; IF: Design of the study, sample selection, data interpretation, and writing of the manuscript.

FUNDING

This study was supported by grants from the Institute of Health Carlos III, and co-funded by the European Regional Development Fund (ERDF)–a way to build Europe, FIS grants PIE 14/00034 and PI17/00809, and IFI15/00035 fellowship to PA-B.

ACKNOWLEDGMENTS

We wish to thank T. Yohannan for editorial help.

SUPPLEMENTARY MATERIAL

The Supplementary Material for this article can be found online at: https://www.frontiersin.org/articles/10.3389/fncel.2018.00131/full#supplementary-material

REFERENCES

Ahmad, F. J., Yu, W., McNally, F. J., and Bass, P. W. (1999). An essential role for katanin in severing microtubules in the neuron. *J. Cell Biol.* 145, 305–315. doi: 10.1083/jcb.145.2.305

Alonso, A. C., Grundke-Iqbal, I., and Iqbal, K. (1999). Alzheimer's disease hyperphosphorylated tau sequesters normal tau into tangles of filaments and disassembles microtubules. *Nat. Med.* 2, 783–787. doi: 10.1038/nm0796-783

Andrés-Benito, P., Fernández-Dueñas, V., Carmona, M., Escobar, L. A., Torrejón-Escribano, B., Aso, E., et al. (2017). Locus coeruleus at asymptomatic early and middle Braak stages of neurofibrillary tangle pathology. *Neuropathol. Appl. Neurobiol.* 43, 373–392. doi: 10.1111/nan.12386

Aston-Jones, G., and Cohen, J. D. (2005). An integrative theory of locus coeruleus-norepinephrine function: adaptive gain and optimal performance. *Annu. Rev. Neurosci.* 28, 403–450. doi: 10.1146/annurev.neuro.28.061604.135709

Attems, J., Thal, D. R., and Jellinger, K. A. (2012). The relationship between subcortical tau pathology and Alzheimer's disease. *Biochem. Soc. Trans.* 40, 711–715. doi: 10.1042/BST20120034

Avila, J. (2006). Tau phosphorylation and aggregation in Alzheimer's disease pathology. *FEBS Lett.* 580, 2922–2927. doi: 10.1016/j.febslet.2006.2.067

Baas, P. W. (2013). Microtubule stability in the axon: new answers to an old mystery. *Neuron* 78, 3–5. doi: 10.1016/j.neuron.2013.03.012

Baas, P. W., and Lin, S. (2011). Hooks and comets: the history of microtubule polarity orientation in the neuron. *Dev. Neurobiol.* 71, 403–418. doi: 10.1002/dneu.20818

Baas, P. W., Rao, A. N., Matamoros, A. J., and Leo, L. (2016). Stability properties of neuronal microtubules. *Cytoskeleton* 73, 442–460. doi: 10.1002/cm.21286

Baas, P. W., Vidya Nadar, C., and Myers, K. A. (2006). Axonal transport of microtubules: the long and short for it. *Traffic* 7, 490–498. doi: 10.1111/j.1600-0854.2006.00392.x

Barrachina, M., Castaño, E., and Ferrer, I. (2006). TaqMan PCR assay in the control of RNA normalization in human post-mortem brain tissue. *Neurochem. Int.* 49, 276–284. doi: 10.1016/j.neuint.2006.01.018

Blanch, M., Mosquera, J. L., Ansoleaga, B., Ferrer, I., and Barrachina, M. (2016). Altered mitochondrial DNA methylation pattern in Alzheimer disease-related pathology and in Parkinson disease. *Am. J. Pathol.* 186, 385–397. doi: 10.1016/j.ajpath.2015.10.004

Braak, H., Alafuzoff, I., Arzberger, T., Kretzschmar, H., and Del Tredici, K. (2006). Staging of Alzheimer disease-associated neurofibrillary pathology using paraffin sections and immunocytochemistry. *Acta Neuropathol.* 112, 389–404. doi: 10.1007/s00401-006-0127-z

Braak, H., and Braak, E. (1991). Neuropathological staging of Alzheimer-related changes. *Acta Neuropathol.* 82, 239–259. doi: 10.1007/BF00308809

Braak, H., and Del Tredici, K. (2015). The preclinical phase of the pathological process underlying sporadic Alzheimer's disease. *Brain* 138(Pt 10), 2814-2833. doi: 10.1093/brain/awv236

Braak, H., Thal, D. R., Ghebremedhin, E., and del Tredici, K. (2011). Stages of the pathologic process in Alzheimer disease: age categories from 1 to 100 years. *J. Neuropathol. Exp. Neurol.* 70, 960–969. doi: 10.1097/NEN.0b013e318232a379

Buée, L., and Delacourte, A. (2001). "Tau phosphorylation," in *Functional Neurobiology of Aging*, eds P. R. Hof and C. V. Mobbs (San Diego, CA; San Francisco, CA; New York, NY; Boston, MA; London; Sydney, NSW; Tokyo: Academic Press), 315–332.

Crary, J. F., Trojanowski, J. Q., Schneider, J. A., Abisambra, J. F., Abner, E. L., Alafuzoff, I., et al. (2014). Primary age-related tauopathy. (PART): a common

pathology associated with human aging. *Acta Neuropathol.* 128, 755–766. doi: 10.1007/s00401-014-1349-0

Du, P., Kibbe, W. A., and Lin, S. M. (2008). Lumi: a pipeline for processing Illumina microarray. *Bioinformatics* 24, 1547–1548. doi: 10.1093/bioinformatics/btn224

Duan, Y., Dong, S., Gu, F., Hu, Y., and Zhao, Z. (2012). Advances in the pathogenesis of Alzheimer's disease focusing on tau-mediated neurodegeneration. *Trans. Neurodeg* 1:24 doi: 10.1186/2047-9158-1-24

Durrenberger, P. F., Fernando, F. S., Magliozzi, R., Kashefi, S. N., Bonnert, T. P., Ferrer, I., et al. (2012). Selection of novel reference genes for use in the human central nervous system: a BrainNet Europe Study. *Acta Neuropathol.* 124, 893–903. doi: 10.1007/s00401-012-1027-z

Duyckaerts, C., Braak, H., Brion, J. P., Buée, L., Del Tredici, K., Goedert, M., et al. (2015). PART is part of Alzheimer disease. *Acta Neuropathol.* 129, 749–756. doi: 10.1007/s00401-015-1390-7

Ferrer, I. (2012). Defining Alzheimer as a common age-related neurodegenerative process not inevitably leading to dementia. *Prog. Neurobiol.* 97, 38–51. doi: 10.1016/j.pneurobio.2012.03.005

Ferrer, I. (2014). "Brain banking," in *Encyclopedia of the Neurological Sciences*, *2nd Edn*, Vol. 1, eds M. J. Aminoff and R. B. Daroff (Oxford: Academic Press), 467–473.

Ferrer, I., Martinez, A., Boluda, S., Parchi, P., and Barrachina, M. (2008). Brain banks: benefits, limitations and cautions concerning the use of post-mortem brain tissue for molecular studies. *Cell Tissue Bank.* 9, 181–194. doi: 10.1007/s10561-008-9077-0

Gentleman, R. C., Carey, V. J., Bates, D. M., Bolstad, B., Dettling, M., Dudoit, S., et al. (2004). Bioconductor: open software development for computational biology and bioinformatics. *Genome Biol.* 5:R80. doi: 10.1186/gb-2004-5-10-r80

Goedert, M., Klug, A., and Crowther, R. A. (2006). Tau protein, the paired helical filament and Alzheimer's disease. *J. Alzheimers Dis.* 9, 195–207. doi: 10.3233/JAD-2006-9S323

Grinberg, L. T., Rüb, U., Ferretti, R. E. L., Nitrini, R., Farfel, J. M., Polichiso, L., et al. (2009). The dorsal raphe nucleus shows phospho-tau neurofibrillary changes before the transentorhinal region in Alzheimer's disease. A precocious onset? *Neuropathol. Appl. Neurobiol.* 35, 406–416. doi: 10.1111/j.1365-2990.2008.00997.x

Iatrou, A., Kenis, G., Rutten, B. P., Lunnon, K., and van den Hove, D. L. (2017). Epigenetic dysregulation of brainstem nuclei in the pathogenesis of Alzheimer's disease: looking in the correct place at the right time? *Cell. Mol. Life Sci.* 74, 509–523. doi: 10.1007/s00018-016-2361-4

Jakovcevski, M., and Akbarian, S. (2012). Epigenetic mechanisms in neurological disease. *Nat. Med.* 18, 1194–1204. doi: 10.1038/nm.2828

Kadavath, H., Hofele, R. W., Biernat, J., Kumar, S., Tepper, K., Urlaub, H., et al. (2015). Tau stabilizes microtubules by binding at the interface between tubulin heterodimers. *Proc. Natl. Acad. Sci. U.S.A.* 112, 7501–7506. doi: 10.1073/pnas.1504081112

Kapitein, L. C., and Hoogenaad, C. C. (2015). Building the neuronal microtubule cytoskeleton. *Neuron* 87, 492–506. doi: 10.1016/j.neuron.2015.05.046

Lardenoije, R., Iatrou, A., Kenis, G., Kompotis, K., Steinbusch, H. W., Mastroeni, D., et al. (2015). The epigenetics of aging and neurodegeneration. *Prog. Neurobiol.* 131, 21–64. doi: 10.1016/j.pneurobio.2015.05.002

Llorens, F., Thüne, K., Andrés-Benito, P., Tahir, W., Ansoleaga, B., Hernández-Ortega, K., et al. (2017). MicroRNA expression in the locus coeruleus, entorhinal cortex, and hippocampus at early and middle stages of Braak neurofibrillary tangle pathology. *J. Mol. Neurosci.* 63, 206–215. doi: 10.1007/s12031-017-0971-4

Lu, H., Liu, X., Deng, Y., and Qing, H. (2013). DNA methylation, a hand behind neurodegenerative diseases. *Front. Aging Neurosci.* 5:85. doi: 10.3389/fnagi.2013.00085

Mandelkow, E., and Mandelkow, E. M. (1995). Microtubules and microtubule-associated proteins. *Curr. Opin. Cell Biol.* 7, 72–81. doi: 10.1016/0955-0674(95)80047-6

Matamoros, A. J., and Bass, P. W. (2016). Microtubules in health and disease of the nervous system. *Brain Res. Bull.* 126, 217–225 doi: 10.1016/j.brainresbull.2016.06.016

McNally, K. P., Bazirgan, O. A., and McNally, F. J. (2000). Two domains of p80 katanin regulate microtubule severing and spindle pole targeting by p60 katanin. *J. Cell Sci.* 113, 1623–1633.

Nicolia, V., Cavallaro, R. A., López-González, I., Maccarrone, M., Scarpa, S., Ferrer, I., et al. (2017). DNA Methylation profiles of selected pro-inflammatory cytokines in Alzheimer disease. *J. Neuropathol. Exp. Neurol.* 76, 27–31. doi: 10.1093/jnen/nlw099

Qiang, L., Yu, W., Andreadis, A., Luo, M., and Baas, P. W. (2006). Tau protects microtubules in thed axon from severing by katanin. *J. Neurosci.* 26, 3120–3129. doi: 10.1523/JNEUROSCI.5392-05.2006

Roll-Mecak, A., and McNally, F. J. (2010). Microtubule-severing enzymes. *Curr. Opin. Cell Biol.* 22, 96–103. doi: 10.1016/j.ceb.2009.11.001

Roll-Mecak, A., Vale, R. D. (2006). Making more microtubules by severing: a common theme of noncentrosomal microtubule arrays? *J. Cell Biol.* 175, 849–851. doi: 10.1083/jcb.200611149

Roosing, S., Rosti, R. O., Rosti, B., de Vrieze, E., Silhavy, J. L., van Wijk, E., et al. (2016). Identification of a homozygous nonsense mutation in KIAA0556 in a consanguineous family displaying Joubert syndrome. *Hum. Genet.* 135, 919–921 doi: 10.1007/s00439-016-1689-z

Roubroeks, J. A. Y., Smith, R. G., van den Hove, D. L. A., and Lunnon, K. (2017). Epigenetics and DNA methylomic profiling in Alzheimer's disease and other neurodegenerative diseases. *J. Neurochem.* 143, 158–170. doi: 10.1111/jnc.14148

Rüb, U., Del Tredici, K., Schultz, C., Thal, D. R., Braak, E., and Braak, H. (2001). The autonomic higher order processing nuclei of the lower brain stem are among the early targets of the Alzheimer's disease-related cytoskeletal pathology. *Acta Neuropathol.* 101, 555–564. doi: 10.1007/s004010000320

Sanchez-Mut, J. V., Aso, E., Heyn, H., Matsuda, T., Bock, C., Ferrer, I., et al. (2014). Promoter hypermethylation of the phosphatase DUSP22 mediates PKA-dependent TAU phosphorylation and CREB activation in Alzheimer's disease. *Hippocampus* 24, 363–368. doi: 10.1002/hipo.22245

Sanders, A. A., de Vrieze, E., Alazami, A. M., Alzahrani, F., Malarkey, E. B., Sorusch, N., et al. (2015). KIAA0556 is a novel ciliary basal body component mutated in Joubert syndrome. *Genome Biol.* 16, 293. doi: 10.1186/s13059-015-0858-z

Šimić, G., Babić Leko, M., Wray, S., Harrington, C. R., Delalle, I., Jovanov-Milošević, N., et al. (2016). Monoaminergic neuropathology in Alzheimer's disease. *Prog. Neurobiol.* 151, 101–138. doi: 10.1016/j.pneurobio.2016.04.001

Simic, G., Stanic, G., Mladinov, M., Jovanov-Milosevic, N., Kostovic, I., and Hof, P. R. (2009). Does Alzheimer's disease begin in the brainstem? *Neuropathol. Appl. Neurobiol.* 35, 532–554. doi: 10.1111/j.1365-2990.2009.01038.x

Smith, R. G., and Lunnon, K. (2017). DNA Modifications and Alzheimer's disease. *Adv. Exp. Med. Biol.* 978, 303–319. doi: 10.1007/978-3-319-53889-1_16

Song, Y., and Brady, S. T. (2015). Post-translational modifications of tubulin: pathways to functional diversity of microtubules. *Trends Cell Biol.* 25, 125–136. doi: 10.1016/j.tcb.2014.10.004

Song, Y., Kirkpatrick, L. L., Schilling, A. B., Helseth, D. L., Chabot, N., Keillor, J. W., et al. (2013). Transglutaminase and polyamination of tubulin: post-translational modification for stabilizing axonal microtubules. *Neuron* 78, 109–123. doi: 10.1016/j.neuron.2013.01.036

Sudo, H., and Baas, P. W. (2011). Strategies for diminishing katanin-based loss of microtubules in tauopathic neurodegenerative diseases. *Hum. Mol. Genet.* 20, 763–778. doi: 10.1093/hmg/ddq521

Szabadi, E. (2013). Functional neuroanatomy of the central noradrenergic system. *J. Psychopharmacol. (Oxford).* 27, 659–693. doi: 10.1177/0269881113490326

Thal, D., Rüb, U., Orantes, M., and Braak, H. (2002). Phases of Aβ-deposition in the human brain and its relevance for the development of AD. *Neurology* 58, 1791–1800. doi: 10.1212/WNL.58.12.1791

Wang, J. Z., and Liu, F. (2008). Microtubule-associated protein tau in development, degeneration and protection of neurons. *Prog. Neurobiol.* 85, 148–175. doi: 10.1016/j.pneurobio.2008.03.002

Wang, L., and Brown, A. (2002). Rapid movement of microtubules in axons. *Curr. Biol.* 12, 1496–1501. doi: 10.1016/S0960-9822(02)01078-3

Watson, C. T., Roussos, P., Garg, P., Ho, D. J., Azam, N., Katsel, P. L., et al. (2016). Genome-wide DNA methylation profiling in the superior temporal gyrus reveals epigenetic signatures associated with Alzheimer's disease. *Genome Med.* 8:5. doi: 10.1186/s13073-015-0258-8

Wen, K. X., Miliç, J., El-Khodor, B., Dhana, K., Nano, J., Pulido, T., et al. (2016). The Role of DNA Methylation and histone modifications in neurodegenerative diseases: a systematic review. *PLoS ONE* 11:e0167201. doi: 10.1371/journal.pone.0167201

Yu, W., Qiang, L., Solowska, J. M., Karabay, A., Korulu, S., and Baas, P. W. (2008). The microtubule-severing proteins spastin and katanin participate differently in the formation of axonal branches. *Mol. Biol. Cell* 19, 1485–1498. doi: 10.1091/mbc.E07-09-0878

Yu, W., Solowska, J. M., Qiang, L., Karabay, A., Baird, D., and Baas, P. W. (2005). Regulation of microtubule severing by katanin subunits during neuronal development. *J. Neurosci.* 25, 5573–5583. doi: 10.1523/JNEUROSCI.0834-05.2005

Conflict of Interest Statement: The authors declare that the research was conducted in the absence of any commercial or financial relationships that could be construed as a potential conflict of interest.

frontiers in Cellular Neuroscience

REVIEW
published: 07 June 2018
doi: 10.3389/fncel.2018.00158

Epigenetic Modifications Associated to Neuroinflammation and Neuropathic Pain After Neural Trauma

Clara Penas[1,2] *and Xavier Navarro*[1,2]*

[1] *Institut de Neurociències, Departament de Biologia Cellular, Fisiologia i Immunologia, Universitat Autònoma de Barcelona, Barcelona, Spain,* [2] *Centro de Investigación Biomédica en Red sobre Enfermedades Neurodegenerativas, Madrid, Spain*

Accumulating evidence suggests that epigenetic alterations lie behind the induction and maintenance of neuropathic pain. Neuropathic pain is usually a chronic condition caused by a lesion, or pathological change, within the nervous system. Neuropathic pain appears frequently after nerve and spinal cord injuries or diseases, producing a debilitation of the patient and a decrease of the quality of life. At the cellular level, neuropathic pain is the result of neuronal plasticity shaped by an increase in the sensitivity and excitability of sensory neurons of the central and peripheral nervous system. One of the mechanisms thought to contribute to hyperexcitability and therefore to the ontogeny of neuropathic pain is the altered expression, trafficking, and functioning of receptors and ion channels expressed by primary sensory neurons. Besides, neuronal and glial cells, such as microglia and astrocytes, together with blood borne macrophages, play a critical role in the induction and maintenance of neuropathic pain by releasing powerful neuromodulators such as pro-inflammatory cytokines and chemokines, which enhance neuronal excitability. Altered gene expression of neuronal receptors, ion channels, and pro-inflammatory cytokines and chemokines, have been associated to epigenetic adaptations of the injured tissue. Within this review, we discuss the involvement of these epigenetic changes, including histone modifications, DNA methylation, non-coding RNAs, and alteration of chromatin modifiers, that have been shown to trigger modification of nociception after neural lesions. In particular, the function on these processes of EZH2, JMJD3, MeCP2, several histone deacetylases (HDACs) and histone acetyl transferases (HATs), G9a, DNMT, REST and diverse non-coding RNAs, are described. Despite the effort on developing new therapies, current treatments have only produced limited relief of this pain in a portion of patients. Thus, the present review aims to contribute to find novel targets for chronic neuropathic pain treatment.

Keywords: traumatic injury, inflammation, neuronal hyperexcitability, neuropathic pain, epigenetic enzymes

OPEN ACCESS

Edited by:
Merce Pallas,
Universitat de Barcelona, Spain

Reviewed by:
Hee Kee Kim,
The University of Texas MD Anderson Cancer Center, United States
Stefania Ceruti,
Università degli Studi di Milano, Italy

***Correspondence:**
Xavier Navarro
xavier.navarro@uab.cat

Received: *30 January 2018*
Accepted: *22 May 2018*
Published: *07 June 2018*

Citation:
Penas C and Navarro X (2018) Epigenetic Modifications Associated to Neuroinflammation and Neuropathic Pain After Neural Trauma. Front. Cell. Neurosci. 12:158. doi: 10.3389/fncel.2018.00158

INTRODUCTION

Neuropathic pain appears as a consequence of a lesion or disease affecting the CNS or PNS (Freynhagen and Bennett, 2009). It is estimated that around 6–8% of general population suffers of chronic pain with neuropathic characteristics (Torrance et al., 2006; Bouhassira et al., 2008). Neuropathic pain is characterized by presenting pain under non-painful stimulus (allodynia), increased pain after painful stimulus (hyperalgesia) and spontaneous pain without stimuli. Neuropathic pain is considered the result of neural plasticity, produced by both an increase in the sensitivity and excitability of primary sensory neurons in PNS, and an increase in the activity and excitability of nociceptive neurons in the spinal cord and the brain (Woolf and Salter, 2000; Julius and Basbaum, 2001). Thus, injury to the PNS or CNS induces maladaptive changes in neurons along the nociceptive pathway that can cause neuropathic pain. The cellular and molecular alterations underlying such pain have been described at different locations within the nociceptive pathways. So far, changes have been reported in the peripheral nerve, the DRG, the dorsal horn, the brainstem, particularly in the nucleus raphe magnus, the thalamic relay nuclei, and the brain cortex (Geranton and Tochiki, 2015). Despite the nature of the neural traumatic injury, there is an alteration of similar structures triggering peripheral and central sensitization. Several mice models of human neuropathic pain have been developed to try to understand these processes (Colleoni and Sacerdote, 2010). Despite the effort on developing new therapies, current treatments have only produced limited relief of this pain in a portion of patients (Dworkin et al., 2003; Costigan et al., 2009) and there is a significant proportion of patients showing resistance to medication. For example, a reduced responsiveness to opioid analgesics is typically seen in patients with neuropathic pain (Campbell and Meyer, 2006).

Spinal cord glial cells, microglia and astrocytes, together with blood borne macrophages, play a critical role in the induction and maintenance of neuropathic pain by releasing powerful neuromodulators such as pro-inflammatory cytokines and chemokines (McMahon et al., 2005). Cytokines and chemokines regulate synaptic transmission and plasticity (Gao and Ji, 2010), and enhance neuronal excitability after neural lesions. Inflammation, and the neural injury *per se*, contribute to hyperexcitability and therefore to the development of neuropathic pain, inducing the altered expression, trafficking and functioning of ion channels expressed by sensitized sensory neurons (Hains and Waxman, 2007; Dib-Hajj et al., 2009; Tibbs et al., 2016). Then, positive feedback loops between enhanced electrical activity of neurons and combined activation of peripheral and central inflammatory cells help to sustain neuroinflammation and chronic neuropathic pain (Miller et al., 2009; Xie et al., 2009; Walters, 2012). The pathophysiological changes that underlie the generation and maintenance of neuropathic pain could be summarized in two sections. On one side, the induction of pro-inflammatory neuromodulator expression, mainly released by glial cells and macrophages. On the other side, the altered expression of channels, receptors, transporters and neurotransmitters by neuronal cells.

There is strong evidence that the molecular changes developing pain states after traumatic injuries of the nervous system, are governed by epigenetic mechanisms. Epigenetic mechanisms are inherited and reversible modifications to nucelotides or chromosomes that alter gene expression without changing DNA sequence. Epigenetic mechanisms are capable to sustain the long-lasting effects on gene activity in response to environmental stimuli, observed in neuropathic pain. Epigenetic mechanisms are alterations that produce changes in gene expression that occur without alteration in DNA sequence. These non-genetic alterations are regulated by two major epigenetic modifications: chemical modifications of DNA (DNA methylation) and covalent modification of histones associated with DNA (histone modifications). These alterations change the chromatin state between euchromatin or heterochromatin, which are transcriptionally accessible/active, or inaccessible/inactive states of chromatin, respectively. More recently, a third system included is non-coding RNA (ncRNA)-associated gene silencing and microRNA alteration. DNA methylation, produced by DNMTs, is linked to transcriptional silencing. It produces gene repression by physically impeding the binding of transcriptional proteins to the gene and because methylated DNA may be bound by proteins can modify histones, thereby forming heterochromatin. Methylation of histones can either increase or decrease transcription of genes, depending on which amino acids in the histones are methylated, and how many methyl groups are attached. Methylation events that weaken chemical attractions between histone tails and DNA increase transcription, because they enable the DNA to uncoil from nucleosomes, and thus forming euchromatin. Histone acetylation in lysine residues is promoted by HATs, and deacetylation by HDACs. The lysine residues have a positive charge that binds tightly to the negatively charged DNA and form closed chromatin structure, inaccessible to transcription factors (Jenuwein and Allis, 2001; Ruthenburg et al., 2007). Thus, acetylation removes positive charges of histones, opens the condensed chromatin structure, and allows transcriptional machines easier access to promoter regions. Finally, histone methylation is associated with either transcriptional activation, inactivation, or silent genomic regions (Jenuwein and Allis, 2001; Consortium et al., 2007). A summary

Abbreviations: 5-AZA, 5-azacytidine; 5-aza-dC, 5-aza-2′-deoxycytidine; BBB, blood-brain barrier; BDNF, brain-derived neurotrophic factor; BET, bromodomain and extra terminal domain; CBP, CREB-binding protein; CCI, chronic constriction injury; CCL/MCP, C-C motif chemokine ligand/monocyte chemoattractant protein; CNS, central nervous system; COX2, cyclooxygenase-2; CREP, cyclic AMP response element-binding protein; CXCR, C-X-C motif chemokine receptor; DNMTs, DNA methyltransferases; DOR, δ-opioid receptor; DRG, dorsal root ganglia; EHMT2 or G9a, euchromatic histone-lysine *N*-methyltransferase; EZH2, enhancer of zeste 2 polycomb repressive complex 2 subunit; H3K27me2/3, histone 3 lysine 27 di and trimethylation; H3K4me3, histone 3 lysine 4 trimethylation; H3K4me3, trimetilation H3K4; H3K9Ac, H3K9 acetylation; H3K9Ac, histone 3 lysine 9 acetylation; HATs, histone acetyltransferase enzymes; HDACs, histone deacetylases; JMJD3 or KDM6b, jumonji domain containing 3; KOR, κ-opioid receptor; MeCP2, methyl-CpG-binding protein 2; mGLU, metabotropic glutamate receptor; MOR, μ-opioid receptor; NF-κB, nuclear factor-kappa B; NGF, nerve growth factor; NMDA, *N*-methyl-D-aspartate; Orpm1, opioid mu receptor gene; PNS, peripheral nervous system; PRC2, polycomb repressive complex 2; PSL, partial sciatic nerve ligation; (REST, also known as Neuron-Restrictive Silencer Factor, NRSF), RE1-Silencing Transcription factor; SAHA, voronistat; SIRT, sirtuin; TSA, trichostatin A; VEGF, vascular endothelial growth factor.

of epigenetic marks associated to transcriptional activation or gene inactivation or silencing is shown in **Table 1**. Besides, non-coding RNAs play also an important role. From these, microRNAs contribute to inhibit translation and/or degradation of mRNAs (Grishok et al., 2001; Bartel, 2004; He and Hannon, 2004).

Within this review, we describe the major epigenetic enzyme alterations observed after traumatic neural injuries that affect the expression of pro-inflammatory neuromodulators, and intrinsic neuronal excitability, promoting neuropathic pain. Although the importance of epigenetics in traumatic injuries is becoming evident, the discoveries in this field are still limited, and further research needs to be done to clarify the molecular pathways underlying these events. That we are at this initial point is clearly evident when in the literature there is no agreement, and certain contradictory findings are described. The present review tries to shed light onto these mechanisms that may be useful to develop therapeutic interventions for reducing neuropathic pain.

INDUCTION OF PRO-INFLAMMATORY NEUROMODULATOR EXPRESSION

Diverse causes of neuropathic pain are associated with excessive inflammation in both the PNS and CNS, which may contribute to the initiation and maintenance of persistent pain (Ellis and Bennett, 2013). Inflammation is produced by the release of neuromodulators, including cytokines, chemokines, vasoactive peptides, lipid mediators, and proteolytic enzymes. Such chemical mediators produce the sensitization of central neurons and nociceptors, and are released by both resident cells (microglia, astrocytes, Schwann cells) and infiltrating cells (neutrophils, macrophages). Several studies suggest that after traumatic injuries, the expression of these mediators is altered by the dysregulation of epigenetic enzymes (**Figure 1**). These enzymes are methyltransferases and demethylases, as well as HDACs and HATs, which alter the promoter state of these neuromodulators. Therefore, epigenetic enzymes contribute to create chemical mediator promoter accessibility to the transcription machinery, enhancing gene expression. Inhibition of these enzymes has been described to produce a decrease of inflammation as well as neuropathic pain.

Besides, microRNAs play also an important role on the generation of neuropathic pain. Genome or micro-array data of several investigations report that microRNAs are differentially regulated in neuropathic pain models in DRG neurons, sciatic nerve, spinal cord and nucleus accumbens (Imai et al., 2011; Kusuda et al., 2011; Genda et al., 2013; Bali et al., 2014; Chang et al., 2017). These non-coding RNAs seem to affect both inflammation and excitability after neural trauma.

TABLE 1 | Major epigenetic marks of active and repressive gene expression.

Epigenetic markers	Euchromatin (active expression)	Heterochromatin (repressed expression)
DNA methylation	Hypomethylation	Hypermethylation
Histone methylation	H3K4me2/3, H3K9me	H3K27 me2/3, H3K9me2/3
Histone acetylation	Hypercetylated H3 and H4	Hypoacetylated H3 and H4

Histone and DNA Methylation

After traumatic injury, there is altered expression of the histone methyltransferase EZH2, the histone demethylase JMJD3 or KDM6b and the transcriptional repressor MeCP2. EZH2 and JMJD3 have opposite actions on the H3K27me2/3, which is a repressive biomarker that induces chromatin compaction and thus gene inactivation. However, literature reports indicate that both enzymes have an inflammatory action causing neuropathic pain. Thus, intriguing molecular events onto the cross-talk between opposite enzymes need to be clarified.

EZH2

EZH2, is a subunit of the polycomb repressive complex 2 (PRC2), and catalyzes the di- and tri-methylation of histone H3 on lysine 27 (H3K27Me2/3), resulting in gene silencing. Although increases of PRC2 complex may contribute to protect neurons against neurodegeneration (von Schimmelmann et al., 2016), very recently, a couple of investigations indicate that the methyltransferase EZH2 is involved in the generation and maintenance of neuropathic pain by inflammatory mechanisms.

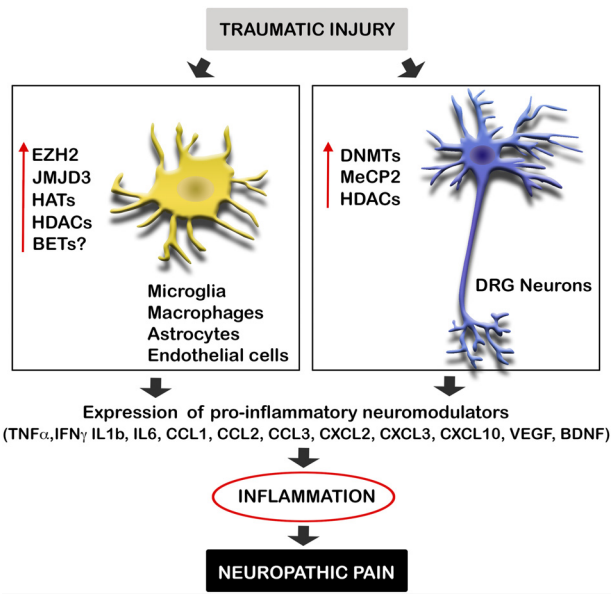

FIGURE 1 | Traumatic injuries of the nervous system induce epigenetic alterations triggering inflammation and neuropathic pain. Neural injuries produce an increase of the expression of several epigenetic enzyme in microglia, macrophages, astrocytes, endothelial cells, and neurons of the DRG after neural injuries. These enzymes alter the promoter state of several pro-inflammatory neuromodulators inducing their expression. Enhanced gene expression of these cytokines, chemokines, and neurotrophic factors, produce inflammation, and consequent neuropathic pain. BET, bromodomain and extra terminal domain; DNMTs, DNA methyltransferases; EZH2, enhancer of zeste 2 polycomb repressive complex 2 subunit; HAT, histone acetyltransferase enzymes; HDAC, histone deacetylases; JMJD3, jumonji domain containing 3; MeCP2, methyl-CpG-binding protein 2.

EZH2 is expressed by neurons of the dorsal horn in normal conditions. After PSL, EZH2 expression is increased in neurons of the spinal cord dorsal horn in lesioned rats with neuropathic pain (Yadav and Weng, 2017). Besides, the number of microglia with EZH2 expression is drastically increased by more than sevenfold (Yadav and Weng, 2017). Inhibition of EZH2 attenuates the expression of inflammatory mediators (**Table 2**) and the development and maintenance of mechanical and thermal hyperalgesia in rats with PSL. In agreement with this study, Arifuzzaman et al. (2017) described that the use of EPZ-6438, an EZH2 inhibitor, dose-dependently inhibits LPS induced inflammatory gene expression in microglial cells *in vitro*. Genes found to be decreased by EZH2 inhibition after LPS activation were linked to cytokines, chemokines, enzymes, and transcription factors (Arifuzzaman et al., 2017). Thus, targeting the EZH2 signaling pathway could be an effective approach for the management of neuropathic pain, through immunomodulation.

JMJD3

The histone demethylase that specifically demethylates H3K27me2/3 producing de-repression, JMJD3, seems also to be involved in inflammatory mechanisms which contribute to the physiopathology after CNS injury. For example, it has been described that spinal cord injury (SCI) produces an increase of JMJD3 in endothelial cells, inducing an increased expression of the cytokine IL-6 by demethylating its promoter (Lee et al., 2012). This event has been corroborated *in vitro*, JMJD3 siRNA inhibits the expression of IL-6 in response to oxygen/glucose deprivation (Lee et al., 2012). The acutely expressed IL-6 from endothelial cells after injury, may play a central role in early processes after a CNS lesion, since it influences the BBB integrity (Brett et al., 1995; Tinsley et al., 2009). Thus, JMJD3 is certainly related with the acute processes after a lesion on the CNS. However, a direct contribution of IL-6-induced by JMJD3 to neuropathic mechanisms, has still not been proven.

Further studies *in vitro* confirm the relation of JMJD3 on inflammation. JMJD3 expression increases after inflammatory stimuli such as LPS, and has been found to activate the expression of genes associated with inflammation in microglial and macrophage cultures through transcriptional regulation of Stat1 and Stat 3 (Lee et al., 2014; Przanowski et al., 2014). Besides JMJD3 contribution to inflammatory processes, can be also related through modulation of the expression of BDNF in DRG neurons after nerve lesions. BDNF has been found to increase in DRG after peripheral nerve injury, contributing to neuropathic pain. Thermal hyperalgesia and mechanical allodynia are inhibited with an antibody against BDNF administered intrathecally (Uchida et al., 2013). Usually, BDNF gene is silenced by PRC2, which contains as a catalytic subunit EZH2. After neuronal stimulation with NMDA *in vitro*, JMJD3 is recruited to the BDNF promoter, inducing demethylation of BDNF promoter. Thus, the de-repression of the promoter contributes to increase BDNF expression in mature neurons (Palomer et al., 2016). Besides promoter de-repression, BDNF expression is also enhanced through acetylation mechanisms, through the action of the CREB kinase/CBP. Thus, the epigenetic modification of the BDNF promoter has a crucial role in neuronal activation *in vitro* and may contribute to BDNF increased levels observed

TABLE 2 | Epigenetic enzymes related to inflammation after injury.

Enzyme	Alteration after injury	Molecular effect	Effect on gene expression	Genes altered	Direct relation to pain	Reference
EZH2	Increased	Di- and tri-methylation of H3K27	Gene silencing	Indirect increase of TNF-α, IL-1β, and MCP-1	Yes	Arifuzzaman et al., 2017; Yadav and Weng, 2017
JMJD3	Increased	Demethylation of H3K27me2/3	De-repression	IL-6, BDNF	No	Lee et al., 2012; Palomer et al., 2016
MeCP2	Increased	Binding to CpG	Gene silencing	Indirect increase of IL-6, TNF-α, CXCL2, CXCL3, and CSF3	Yes	Wang et al., 2011; Tochiki et al., 2012; Cronk et al., 2015
DNMT3B	Decreased	CpG methylation	Gene silencing	CXC3R3	Yes	Jiang et al., 2017
HATs	Increased	H3K9 acetylation	Gene expression	CCL2 (MCP-1), CCL3 (MIP-1a), MiP-2, VEGFA, CXCR2, CXCR1/CXRR5, VEGFR, BDNF, COX2	Yes	Kiguchi et al., 2012, 2013, 2014; Sun et al., 2013; Zhu et al., 2014
HDAC1	Increased	H3K9 hypoacetylation	Reduction of gene expression		Yes	Kami et al., 2016
SIRT1	Decreased	H3 deacetylation	Reduction of gene expression	IL-6, INF-γ, IL-1β, TNF-α, and nuclear factor-kappa B (NF-κB) p65 activation	Yes	Yin et al., 2013; He et al., 2014; Shao et al., 2014; Gui et al., 2015
SIRT2	Decreased	H3 deacetylation	Reduction of gene expression	TNF-α, IL-1β, and IL-6, and acetylation of the NF-κB p65	Yes	Zhang and Chi, 2017
BET proteins	Unkown	Binding to acetylated histones	Gene expression	Cytokines, chemokines	No	Huang et al., 2009; Nicodeme et al., 2010; Gallagher et al., 2014

after neuronal injury *in vitro*. JMJD3 might be a therapeutic target to reduce neuropathic pain after a neural traumatic lesion by decreasing inflammation and neurotrophic factor expression.

MeCP2

MeCP2, which belongs to a transcriptional repressor complex together with a subset of HDACs, has been related to neuropathic pain after several nerve injuries. Priming for MeCP2 binding to DNA is DNA methylation at CpG, implemented by DNMTs. Once MeCP2 binds to the DNA, produces gene silencing. MeCP2 it is highly expressed in neurons of the dorsal horn and DRG, but also, in a lower extent in oligodendrocytes and astrocytes within the spinal horn (Wang et al., 2011; Tochiki et al., 2012). Increased DNMT, MeCP2 and HDACs expression has been observed after different pain states, paralleled by changes in MeCP2 target genes (Wang et al., 2011; Tochiki et al., 2012; Pollema-Mays et al., 2014). The neuropathic pain observed is markedly attenuated by the DNMT inhibitor 5-AZA treatment (Wang et al., 2011), which reduces DNA methylation and reactivate silenced genes (Holliday and Ho, 2002). Thus 5-AZA may alleviate neuropathic pain by upregulating the expression of some DNA methylation-dependent anti-nociceptive genes in the lumbar spinal cord in CCI rats. Although in the study authored by Wang et al., the molecular mechanisms by which MeCP2 may promote neuropathic pain where not described, it may be in part by promoting inflammatory mechanisms. It has been observed that MeCP2 is an important epigenetic regulator of macrophage response to stimuli and stressors (**Table 2**) (Cronk et al., 2015). Also, MeCP2 has been observed to be important for the expression of the opioid receptor, which will be commented later on.

However, controversial studies show that MeCP2 is decreased in the lumbar spinal cord, in DRG (Tochiki et al., 2012), and in the prefrontal cortex and amygdala (Tajerian et al., 2013) of mice after SNI, a lesion that produces persistent pain. These levels are reversed by environmental enrichment and correlated with decreased levels of hyperalgesia (Tajerian et al., 2013). These discrepancies may be related to the time window studied or methodologies used. In any case, further studies should be performed analyzing the DNA methylation and MeCP2 binding on specific genes related to nociception (reviewed in Geranton and Tochiki, 2015). Similarly, it has also been described that spinal nerve ligation (SNL) downregulates the expression of DNMT3b, which may cause demethylation of *C-X-C motif chemokine receptor 3 (Cxcr3)* gene promoter and increase CXCR3 expression in spinal neurons. CXCR3 is a receptor for the chemokine CXCL10, and binding of this chemokine facilitates excitatory synaptic transmission and contribute to the maintenance of neuropathic pain. The upregulated CXCR3 may contribute to neuropathic pain by facilitating central sensitization (Jiang et al., 2017).

Thus, literature has a discrepancy about the role of MeCP2 and DNMTs in neuropathic pain after traumatic injuries. Giving the importance of these events, further studies should be performed to clarify the molecular events underlying these epigenetic alterations.

Histone Acetylation

Several studies suggest that modifications in histone tails (H3 and H4), acetylation and methylation, produce the transcription of inflammatory molecules, such as cytokines and chemokines, being the reason of chronic inflammatory diseases. In these case, HATs seem to be related to the chemokine expression, whereas HDACs are related to cytokine expression.

Histone Acetyltransferases

Nerve injury induces increased expression of chemokines and their receptors in infiltrated macrophages and neutrophils on the lesioned nerve, leading to neuropathic pain (**Table 2**). The induced expression of these proteins is concomitant with an increased H3K9Ac and tri-methylation of H3K4 (H3K4me3) and on their promoters (Kiguchi et al., 2012, 2013, 2014). Several studies demonstrated that the increased expression of CCL2, CCL3, MiP-2, CXCR2, and CXCR1/CXRR5 were suppressed by the HAT inhibitor anacardic acid, suggesting that these chemokines are upregulated through histone acetylation of H3K9. Moreover, this treatment also decreased the neuropathic pain associated to the nerve injury. Furthermore, another study observed an increased expression of CXCR2 and CCL1 by H3K9Ac in the spinal cord, being responsible of neuropathic pain induced after injury. Blocking CXCR2 reverses mechanical hypersensitivity after lesion (Sun et al., 2013). In agreement with this, treatment with suberoylanilide hydroxamic acid (a HDAC inhibitor) significantly exacerbated mechanical sensitization after incision (Sun et al., 2013). Similarly, Curcumin, which has been recognized as a p300/CBP inhibitor of the HAT activity, has been observed to have an anti-nociceptive role in the CCI rat model of neuropathic pain, through down-regulating p300/CBP HAT activity-mediated gene expression of BDNF and COX2 (Zhu et al., 2014). Thus, inhibition of HAT activity has been proven to reduce inflammation and neuropathic pain.

Histone Deacetylases

Recent studies have shown that HDAC inhibitors can alleviate inflammatory pain (Chiechio et al., 2009; Bai et al., 2010; Zhang et al., 2011) and attenuate the development of hypersensitivity in models of neuropathic pain (Zhang et al., 2011; Denk et al., 2013; Kukkar et al., 2014; Capasso et al., 2015). Since, HDACs inhibitors have demonstrated suppression of cytokine expression (Leoni et al., 2005; Kukkar et al., 2014; Khangura et al., 2017), decreased neuropathic pain through HDAC inhibitors may be related to suppression of inflammation through pro-inflammatory cytokine suppression.

Searching for specific HDACs, it has been described that neuropathic pain maintenance involves HDAC1, since the use of a HDAC1 specific inhibitor (LG325) dose-dependently ameliorated mechanical allodynia of SNI mice. Nerve injury increases HDAC1 as well as hypoacetylation of H3K9 within microglia of the dorsal horn (Kami et al., 2016). Furthermore, running exercise is to reduce HDAC1, increase H3K9Ac and reverse hyperalgesia in the mice (Kami et al., 2016). In another study, Baicalin, a natural compound, administration reversed H3 and HDAC1 expression in spinal cord, paralleled by a decrease

of neuropathic pain after SNL (Cherng et al., 2014). Conversely, the HDAC1-HDAC6 inhibitor LG322, showed a less favorable antinociceptive profile (Sanna et al., 2017).

The histone deacetylase SIRT1 has a special interest. It has been observed that SIRT1 is decreased in the L4/L5 segments of the spinal cord after CCI, (Gui et al., 2015). Natural compounds that attenuate neuropathic pain, increase its expression within the spinal cord as well as decrease acetyl-histone H3 (Yin et al., 2013; He et al., 2014; Gui et al., 2015), reduce microglia activation, and expression of inflammatory modulators (**Table 2**) (Tillu et al., 2012; Gui et al., 2015; Wang et al., 2016). Reversion of mechanical and thermal hyperalgesia was observed with an specific SIRT1 inhibitor (Shao et al., 2014). Similarly, SIRT2 is downregulated in the DRG after CCI in rats. Overexpression of SIRT2 markedly alleviates mechanical allodynia and thermal hyperalgesia in CCI rats associated with inhibition of NF-κB signaling and inflammation (**Table 2**). Additionally, treatment with a SIRT2 specific inhibitor significantly aggravated neuropathic pain and attenuated the inhibitory effect of SIRT2 overexpression on neuropathic pain development. Therefore, SIRT2 and SIRT 1 may serve as potential therapeutic targets for treatment of neuropathic pain (Zhang and Chi, 2017).

BET Proteins

The BET protein family is comprised of BRD2, BRD3, BRD4 and BRDT, and regulates RNA Polymerase II (Pol II)-dependent gene expression by recruiting transcriptional regulatory complexes to poly-acetylated chromatin. Recently, BET proteins have been intensively studied as epigenetic regulators of cell cycle and inflammation in many disorders such as cancer and arthritis. However, virtually nothing is known about the role of BET proteins during the injury response after CNS trauma. It has been described that BET inhibition reduces the expression of pro-inflammatory cytokines/chemokines in macrophages after LPS stimulation (Nicodeme et al., 2010). In several contexts, NF-κB-mediated inflammatory signaling is disrupted after BET inhibition treatment (Huang et al., 2009; Gallagher et al., 2014). Therefore, there is a clear link between BET proteins and NF-κB-mediated inflammatory signaling, which can be targeted for therapeutic purposes. Thus, the BET proteins have an important role in inflammation and cell proliferation. However, its implication in neuropathic pain remains unknown.

Non-coding RNAs

Most of the studied non-coding RNAs related to pain are microRNAs (**Table 3**). For example, diverse microRNAs directly regulate the levels of the regulator of inflammation named suppressor of cytokine signaling 1 (SOCS1), and thus control neuropathic pain by modulating inflammation. SOCS1 mRNA is a direct target of miR-221, miR-155 and miR-19a. After CCI these microRNAs increase, producing decreased levels of SOCS1. Inhibition of these microRNAs abrogate SOCS1 depletion, and mechanical and thermal hyperalgesia (Tan et al., 2015; Wang et al., 2015; Xia et al., 2016). Similarly, downregulation of microRNA-218 by a specific inhibitor relieves neuropathic pain by regulating suppressor of cytokine signaling 3 (SOCS3) after CCI in rats (Li and Zhao, 2016).

The levels of BDNF are also important in neuropathic pain formation and maintenance, and are linked to microRNA expression. On one side, miRNA microarray analysis reveals that 167 miRNAs are altered in DRG after following BDNF gene deletion (Neumann et al., 2016). On the other side, microRNAs tightly regulate the levels of BDNF. BDNF is controlled by miR-206 in DRG (Neumann et al., 2015), and by miR-1 in sciatic nerve (Sun W. et al., 2017), following CCI. Both microRNAs decrease after injury and induce BDNF expression, producing mechanical and thermal hyperalgesia. Inhibition of miR-206, which directly interacts at the 3′-UTR of BDNF, also decreases pro-inflammatory cytokine expression and neuropathic pain development (Sun W. et al., 2017).

Besides, there are several others upregulated microRNAs that regulate neuropathic pain and inflammation. Nerve injury induces upregulated expression of miR-21 in DRG neurons (Sakai and Suzuki, 2013), and miR-32-5p (Yan et al., 2018) and miR-195 (Shi et al., 2013) in spinal microglia. Investigations related to the increased miR-32-5p in spinal microglia after SNL, revealed Dual-specificity phosphatase 5 (Dusp5) as a direct target of this microRNA, which is involved in mediating the effects on neuropathic pain and neuroinflammation (Yan et al., 2018). Interestingly, miR-195 aggravates inflammation and neuropathic pain by inhibiting autophagy after SNL (Shi et al., 2013).

Finally, it is important to mention that not all the microRNAs have a pathogenic effect. In fact, injury induces the reduction of several microRNAs, and intrathecal delivery of some of them, may be a therapeutically effective on reducing pain symptoms. miR-124 levels are associated with M1/M2 microglia phenotype, and inflammatory signaling. Intrathecal miR-124 treatment reverses the persistent hyperalgesia induced and mechanical allodynia several models of chronic neuropathic pain in mice (Willemen et al., 2012). miRNA-146a-5p attenuates neuropathic pain via suppressing TNF receptor associated factor-6 (TRAF6) and its downstream signaling JNK/CCL2 in the spinal cord (Lu et al., 2015). There is also decreased miR-93 in the spinal cord of CCI rats compared with sham rats, which directly targets the signal transducer and activator of transcription 3 (STAT3), an important regulator of inflammation. Overexpression of miR-93 markedly suppresses the expression of STAT3 *in vitro* and *in vivo*, and significantly alleviates inflammation and neuropathic pain development in CCI rats (Yan et al., 2017).

ALTERED GENE EXPRESSION RELATED TO NEURONAL HYPEREXCITABILITY

Traumatic injuries produce neuronal hyperexcitability. Although the exact mechanisms vary depending on site and pathology, peripheral and central sensitization lead to the development of neuropathic pain (reviewed in Cohen and Mao, 2014; Ligon et al., 2016). After nerve injury, the pain pathway involves the activation of primary nociceptive afferents within the periphery, which then send impulses to the dorsal horn of the spinal cord, where second order nociceptive neurons convey ascending

TABLE 3 | miRNAs related to inflammation and neuropathic pain after traumatic injury.

miRNA	Expression after injury	Site	Genes altered	Reference
miR-221, miR-155, miR-19a	Increased	Microglia	SOCS1	Tan et al., 2015; Wang et al., 2015; Xia et al., 2016
miR-221	Increased	Microglia	TNF-α, IL-1β, IL-6, NF-κB, p38 MAPK activation	Xia et al., 2016
microRNA-218	Increased	Microglia	SOCS3	Li and Zhao, 2016
miR-206	Increased	DRG	BDNF	Neumann et al., 2015
miR-1	Increased	Sciatic nerve	BDNF	Sun W. et al., 2017
miR-21	Increased	DRG	Unknown	Sakai and Suzuki, 2013
miR-32-5p	Increased	Microglia	Dusp5	Yan et al., 2018
miR-195	Increased	Microglia	Indirect effect on IL-1β, TNF-α, iNOS	Shi et al., 2013
miR-124	Decreased	Microglia	Unknown	Willemen et al., 2012
MicroRNA-146a-5p	Decreased	Spinal cord	TRAF6, JNK/CCL2	Lu et al., 2015
miR-93	Decreased	Spinal cord	STAT3	Yan et al., 2017

signals to the thalamus, amygdala, and the brain cortex. If the injury occurs in the spinal cord, signals descend to nociceptors at the dorsal horn, as well as ascend to supraspinal regions. These lesions produce also the loss of inhibitory control from supraspinal regions onto primary afferent neurons, which contributes to exacerbate pain. In any case, neuronal sensitization is promoted through changes in gene regulation that shift the balance of channels, receptors, neurotransmitters or transporters, leading to an increased excitably of the neuron. Most of these gene expression alterations are produced by changes in histone or DNA methylation in their promoters, although some changes in promoter acetylation are also described. In particular, it has been clearly demonstrated that injury in the nervous system triggers an increase of promoter methylation producing gene silencing.

Histone and DNA Methylation

Nerve injury produces the upregulation of the methyltransferases such as EHMT2 or G9a, DNA methyltransferase 3 alpha (DNMT3a), and the repressive complex RE1-Silencing Transcription factor (REST, also known as Neuron-Restrictive Silencer Factor, NRSF), that produce gene silencing. There is a clear effect of these over-expressed epigenetic enzymes on the silencing of similar target genes (**Figure 2**). Besides, several microRNAs have been described to alter neuronal excitability after neural injury.

G9a

G9a (encoded by Ehmt2), is a H3K9 methyltransferase, responsible of gene silencing and it has been clearly demonstrated that it contributes to transcriptional repression in primary sensory neurons contributing to neuropathic pain. Nerve injury consistently increases the enrichment of H3K9me2 in the promoters of potassium channels, producing their silencing. A study demonstrated that the specific knockout of G9a in sensory neurons of the DRG blocked gene silencing of potassium channels (**Table 4**) and the promotion of neuropathic pain after peripheral nerve lesion (Laumet et al., 2015).

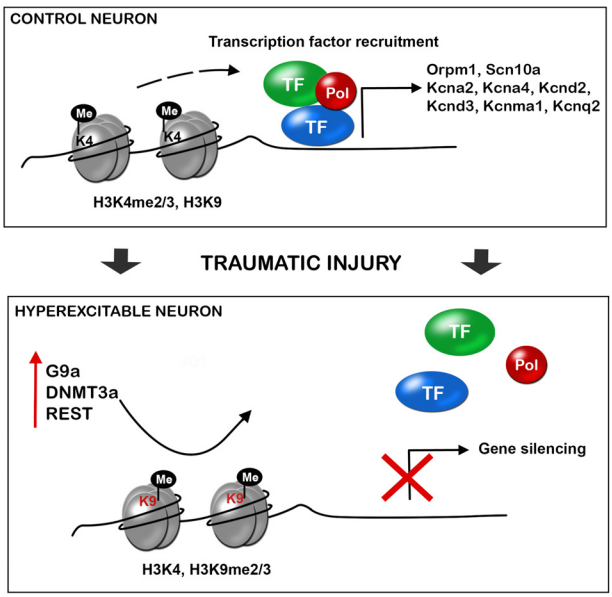

FIGURE 2 | Traumatic injuries of the nervous system induce gene expression alteration in neurons triggering hyperexcitability and neuropathic pain. During control conditions, the promoter state of genes codifying for ion channels, receptors and other important neuronal genes allow the recruitment of transcription factors, and thus gene expression. After a traumatic injury of the nervous system, there is an increased expression of methyltransferases (G9a, histone-lysine *N*-methyltransferase; DNMT3a, DNA methyltransferase a), and the repressor complex REST (RE1-silencing transcription factor), with decrease H3K4 methylation and increase H3K9 methylation. This alteration of the promoter state does not allow transcription factor recruitment and there is silencing of several neuronal genes. De-balanced expression of ion channel, receptors, transporters, and other neuronal genes triggers neuronal hyperexcitability and consequent neuropathic pain.

Other studies demonstrated that targeting G9a reverses the silencing of the Orpm1 gene, which encodes the MOR, and restores the effect of morphine on the hypersensitivity induced by peripheral nerve lesions (Zhou et al., 2014; Zhang et al., 2016).

TABLE 4 | Epigenetic enzymes related to neuronal hyperexcitability after injury.

Enzyme	Expression after injury	Molecular effect	Effect on gene expression	Genes altered	Direct relation to pain	Reference
G9a	Increased	H3K9 methyltransferase	Gene silencing	Kcna4, Kcnd2, Kcnq2 and Kcnma1, Orpm1	Yes	Zhou et al., 2014; Zhang et al., 2016
DNMT3a	Increased	CpG methyltransferase	Gene silencing	Orpm1 (MOR), Oprk1 (KOR), channel expression as Kcna2	Yes	Shao et al., 2017; Sun L. et al., 2017; Zhao et al., 2017
REST	Increased	H3K4 demethylation and histone deacetylation	Gene silencing	Kcnd3, Kcnq2 and Scn10a, Oprm1 and Gad2	Yes	Uchida et al., 2010a; Zhang et al., 2011
HDAC	Increased	H3 and H4 deacetylation	Gene silencing	Gad65, mGlu2, MOR, DOR and Nav1.8	Yes	Chiechio et al., 2006, 2010; Uchida et al., 2010a; Zhang et al., 2011; Matsushita et al., 2013; Zammataro et al., 2014; Tao et al., 2016; Hou et al., 2017

Opioids are the gold standard for pharmacological treatment of pain, but their analgesic effects are unsatisfactory in conditions of neuropathic pain, due in part to nerve injury–induced downregulation of opioid receptors in DRG and spinal neurons. Nerve lesion produces a decreased expression of MOR in DRG, by increasing H3K9me2 in its promoter, reducing the opioid effect on neuropathic pain (Zhou et al., 2014; Zhang et al., 2016). The knockout of G9a reverses the expression of MOR in lesioned DRG and potentiates the effect of morphine after lesion (Zhang et al., 2016). Similarly, treatment with the inhibitor of DNA methylation 5-aza-dC, inhibited the increased methylation of MOR gene and prevented their decreased expression in DRG, thereby improving systemic, spinal and peripheral morphine analgesia (Zhou et al., 2014).

DNA Methyltransferases

Similar to the histone methyltransferase G9a, the DNA methyltransferases DNMT3a has been found to have similar effects on MOR and ionic channel expression. Nerve injury induces increased expression of DNMT3a in lesioned DRG neurons and represses expression of Orpm1 and Oprk1 genes which encode for MOR and KOR (Shao et al., 2017; Sun L. et al., 2017). Blocking this increase with a DNMT3a shRNA-adenoviral vector, restored MOR and KOR expression as well as restored morphine analgesic effects. Mechanistically, DNMT3a regulation of Oprm1 gene expression required the methyl-CpG–binding protein 1, MBD1, as MBD1 knockout resulted in the decreased binding of DNMT3a to the Oprm1 gene promoter and blocked the DNMT3a-triggered repression of Oprm1 gene expression in DRG neurons (Sun L. et al., 2017).

Besides, increased DNMT3a expression in the injured DRG neurons by SNL promotes the decrease of the voltage-dependent potassium channel subunit Kcna2. Blocking this increase with a DNMT3a shRNA-adenoviral vector, prevents nerve injury-induced methylation of the subunit Kcna2 promoter region, rescues Kcna2 expression in the injured DRG and attenuates neuropathic pain (Zhao et al., 2017). In agreement with this observation, in the absence of nerve injury, mimicking the increase of DNMT3a reduces the Kcna2 promoter activity, diminishes Kcna2 expression, decreases potassium current, increases excitability in DRG neurons and leads to spinal cord central sensitization and neuropathic pain symptoms (Zhao et al., 2017). These findings suggest that DNMT3a may contribute to neuropathic pain by repressing MOR, KOR and Kcna2 expression in the DRG (Zhao et al., 2017). Consistently, DNA methylation by DNMTs alters voltage gated and Ca2+ ion channels, affecting neuronal excitability (Meadows et al., 2016).

REST

The enzymatic core of the REST repressor complex contains REST, CoREST, LSD1, BHC80, and BRAF35 (Mosammaparast and Shi, 2010). The REST complex also recruits additional silencing molecular machineries, such as HDAC1/2, MeCP2 and G9a, to consolidate the suppression (Ballas et al., 2005). The REST complex suppresses gene expression by removing active histone marks, such as H3K4 methylation or various histone acetylation. REST suppresses the expression of genes important for the acquisition and preservation of neuronal specificity. Thus, in the adult brain, neurons exhibit low levels of REST (Gao et al., 2011). The decrease of REST expression during neuronal differentiation, allows the expression of genes that activate a large variety of processes such as axonal growth, establishment of synaptic contacts and membrane excitability (Paquette et al., 2000; Aoki et al., 2012). Conversely, the levels of REST are high in the majority of non-neuronal cells (Prada et al., 2011).

In several pathologic conditions, REST is induced in neurons, which is associated with the repression of specific neuronal genes (Baldelli and Meldolesi, 2015). This increase of REST expression has been observed in the CNS after ischemia, epileptic seizures, as well as in the PNS after nerve lesions, and *in vitro* after prolonged neuronal depolarization (Hara et al., 2009; Uchida et al., 2010a; Roopra et al., 2012; Schweizer et al., 2013; Bersten et al., 2014; Baldelli and Meldolesi, 2015). If these increases of REST are protective or detrimental is still controversial. However,

it is clearly demonstrated that neuropathic pain is associated with REST overexpression in the PNS.

Studies using the PNL of the sciatic nerve in the mouse, showed an increase of the REST mRNA and protein in DRG, which is maintained during weeks after lesion (Uchida et al., 2010a,b; Rose et al., 2011). The expression levels of target genes for REST such as Kcnd3, Kcnq2 and Scn10a (that respectively encode for the channels Kv4.3, Kv7.2 and Nav1.8), as well as Oprm1 and Gad2 are repressed in response to the increased levels of REST (**Table 4**). The repression of these target genes is associated with persistent dysfunction of nociceptive C-fibers and disruption of H and M currents, that facilitate the neuropathic excitability of the peripheral sensory fibers. Thus, increased REST expression enhances the generation and maintenance of neuropathic pain. REST knockdown with antisense nucleotides is sufficient to rescue the expression levels of several target genes, as well as C-nociceptive fiber function (Uchida et al., 2010a; Zhang et al., 2011).

Acetylation

Finally, some studies indicate that HDAC inhibition or acetylation in histones in neuropathic pain models have analgesic effects. Most of these studies have their target in inflammation, as they have been explained in a previous section. However, other studies have demonstrated that HDAC inhibition also affects channel expression in neurons. For example, induced inflammation produces a decrease of acetilated-H3 in *Gad65* promoter, decreasing the expression of GAD65. GAD65 is an essential enzyme for GABAergic neuron function in the dorsal horn of the spinal cord and in the raphe nucleus in the brain. Administration of TSA or SAHA restores *Gad65* acetylation and relieve sensitive pain behavior in raphe nucleus (Zhang et al., 2011).

Another analgesic effect of HDAC inhibitors is through increasing metabotropic glutamate 2 receptors (mGLU2). mGLU2 receptors are at the synapses between primary afferent fibers and neurons in the dorsal horn of the spinal cord, in the peripheral nociceptors, and in pain-regulatory centers of the brainstem and forebrain. Activation of these receptors inhibits pain transmission. HDAC inhibitors transcriptionally increase mGLU receptors via the acetylation-promoted activation of the p65/RELA transcription factor (Chiechio et al., 2006, 2010). Thus, HDAC inhibitors increase acetylated p65 in the DRG and spinal cord dorsal horn, which regulates p65 retention in the nucleus, increasing NF-κB function on mGLU2 transcriptional activation (Chiechio et al., 2006, 2009) after CCI or inflammatory-induced pain. Induction of analgesia is inhibited by the mGLU2/3 receptor antagonist, LY341495 (Chiechio et al., 2002; Descalzi et al., 2015). Moreover, the analgesic effect of a mGLU2/3 agonist was enhanced after HDAC inhibitor treatment (SAHA) (Zammataro et al., 2014).

Additional evidence for the importance of histone acetylation has been related to MOR, DORs and Nav1.8 expression. The expression of these receptors and channels is reduced under neuropathic pain states (Uchida et al., 2010a; Tao et al., 2016), produced by a reduction of acetylation in its promoters. Treatment with HDAC inhibitors, such as TSA, VPA and SAHA treatments, that increase acetylation at the regulatory sequence of these genes, promotes C-fiber related hypoesthesia and restores peripheral and systemic morphine analgesia (Matsushita et al., 2013; Uchida et al., 2015; Hou et al., 2017). These results suggest that HDAC inhibitors could serve as adjuvant analgesics to morphine for the management of neuropathic pain.

Non-coding RNAs

Several miRNas have been observed to change their expression in models of neuropathic pain. For instance, miR-7a is the most robustly decreased microRNA in the injured DRG, and is associated to neuropathic pain through regulation of neuronal excitability. Overexpression of this microRNA, suppresses established neuropathic pain, and downregulation is sufficient to cause pain-related behaviors in intact rats. miR-7a targets b2 subunit of the voltage-gated sodium channel. Thus, after injury decreased miR-7a allows b2 subunit protein expression, triggering hyperexcitability of nociceptive neurons (Sakai et al., 2013). Sodium voltage gated channels have been observed to me regulated by other miRNAs. For example, miRN-96 inhibits Nav1.3 expression and alleviates neuropathic pain after CCI. Injury increases Nav1.3 expression and intrathecal administration of miR-96 suppresses this expression (Chen et al., 2014). Similarly, miR-30b controls the expression of Nav1.7 after SNI. miR-30b over-expression in spared nerve injury rats inhibits SCN9A transcription, resulting in pain relief. In addition, miR-30b knockdown significantly increased hypersensitivity to pain in naive rats (Shao et al., 2016).

It has been established also, that the cluster of microRNAs that includes miR-96, -182, and -183, has a reduced expression in primary afferent neurons DRG in a model of SNL. The redistribution of microRNAs is associated with altered distribution of the stress granule protein TIA-1, which may have a significant impact on regulatory activity of microRNAs (Bhattacharyya et al., 2006; Vasudevan and Steitz, 2007; Aldrich et al., 2009). Specifically, the microRNA-183 cluster in mice controls more than 80% of neuropathic pain–regulated genes and scales basal mechanical sensitivity and mechanical allodynia. For example, controls voltage-gated calcium channel subunits α2δ-1 and α2δ-2 and TrkB+ light-touch mechanoreceptors (Peng et al., 2017). Besides, another microRNA that controls calcium voltage-gated channels is miR-103, which regulates the expression of the three subunits forming Cav1.2-comprising L-type calcium channel (LTC). This regulation is bidirectional since knocking-down or over-expressing miR-103, respectively, up- or down-regulate the level of Cav1.2-LTC translation. Besides, miR-103 knockdown in intact rats results in hypersensitivity to pain. This miRNA, is downregulated in neuropathic pain animals, and its intrathechal administration relieve pain after SNL (Favereaux et al., 2011).

CONCLUSION

Epigenetic alterations produced after injury of the CNS or PNS contribute to the generation and maintenance of neuropathic pain. Current literature describes clear effects of

DNA methylation, histone methylation and acetylation, and microRNAs on the expression of ion channels, receptors and neurotransmitters in neurons. HATs affect chemokine expression whereas HDACs affect cytokine expression within glial and macrophage cells that are reactive to neuronal damage. However, there is no agreement regarding histone and DNA methylation effects on inflammatory mechanisms that sustain pain states. Although increasing interest is shown within this epigenetic field, we are still at the initial steps of understanding these processes. Thus, further research needs to be performed to evaluate novel therapies that might be effective on patients that suffer from neuropathic conditions.

AUTHOR CONTRIBUTIONS

CP and XN reviewed the bibliography, wrote the text, and drew the figures of the present review.

FUNDING

This work was supported by CIBERNED (CB06/05/1105) and TERCEL (RD16/0011/0014) funds from the Instituto de Salud Carlos III of Spain. CP holds a fellowship of the P-SPHERE program funded by the MSC COFUND Action.

REFERENCES

Aldrich, B. T., Frakes, E. P., Kasuya, J., Hammond, D. L., and Kitamoto, T. (2009). Changes in expression of sensory organ-specific microRNAs in rat dorsal root ganglia in association with mechanical hypersensitivity induced by spinal nerve ligation. *Neuroscience* 164, 711–723. doi: 10.1016/j.neuroscience.2009.08.033

Aoki, H., Hara, A., Era, T., Kunisada, T., and Yamada, Y. (2012). Genetic ablation of Rest leads to in vitro-specific derepression of neuronal genes during neurogenesis. *Development* 139, 667–677. doi: 10.1242/dev.072272

Arifuzzaman, S., Das, A., Kim, S. H., Yoon, T., Lee, Y. S., Jung, K. H., et al. (2017). Selective inhibition of EZH2 by a small molecule inhibitor regulates microglial gene expression essential for inflammation. *Biochem. Pharmacol.* 137, 61–80. doi: 10.1016/j.bcp.2017.04.016

Bai, G., Wei, D., Zou, S., Ren, K., and Dubner, R. (2010). Inhibition of class II histone deacetylases in the spinal cord attenuates inflammatory hyperalgesia. *Mol. Pain* 6:51. doi: 10.1186/1744-8069-6-51

Baldelli, P., and Meldolesi, J. (2015). The transcription repressor REST in adult neurons: physiology, pathology, and diseases. *eNeuro* 2:ENEURO.0010-ENEURO.15. doi: 10.1523/ENEURO.0010-15.2015

Bali, K. K., Hackenberg, M., Lubin, A., Kuner, R., and Devor, M. (2014). Sources of individual variability: miRNAs that predispose to neuropathic pain identified using genome-wide sequencing. *Mol. Pain* 10:22. doi: 10.1186/1744-8069-10-22

Ballas, N., Grunseich, C., Lu, D. D., Speh, J. C., and Mandel, G. (2005). REST and its corepressors mediate plasticity of neuronal gene chromatin throughout neurogenesis. *Cell* 121, 645–657. doi: 10.1016/j.cell.2005.03.013

Bartel, D. P. (2004). MicroRNAs: genomics, biogenesis, mechanism, and function. *Cell* 116, 281–297. doi: 10.1016/S0092-8674(04)00045-5

Bersten, D. C., Wright, J. A., McCarthy, P. J., and Whitelaw, M. L. (2014). Regulation of the neuronal transcription factor NPAS4 by REST and microRNAs. *Biochim. Biophys. Acta* 1839, 13–24. doi: 10.1016/j.bbagrm.2013.11.004

Bhattacharyya, S. N., Habermacher, R., Martine, U., Closs, E. I., and Filipowicz, W. (2006). Relief of microRNA-mediated translational repression in human cells subjected to stress. *Cell* 125, 1111–1124. doi: 10.1016/j.cell.2006.04.031

Bouhassira, D., Lanteri-Minet, M., Attal, N., Laurent, B., and Touboul, C. (2008). Prevalence of chronic pain with neuropathic characteristics in the general population. *Pain* 136, 380–387. doi: 10.1016/j.pain.2007.08.013

Brett, F. M., Mizisin, A. P., Powell, H. C., and Campbell, I. L. (1995). Evolution of neuropathologic abnormalities associated with blood-brain barrier breakdown in transgenic mice expressing interleukin-6 in astrocytes. *J. Neuropathol. Exp. Neurol.* 54, 766–775. doi: 10.1097/00005072-199511000-00003

Campbell, J. N., and Meyer, R. A. (2006). Mechanisms of neuropathic pain. *Neuron* 52, 77–92. doi: 10.1016/j.neuron.2006.09.021

Capasso, K. E., Manners, M. T., Quershi, R. A., Tian, Y., Gao, R., Hu, H., et al. (2015). Effect of histone deacetylase inhibitor JNJ-26481585 in pain. *J. Mol. Neurosci.* 55, 570–578. doi: 10.1007/s12031-014-0391-7

Chang, H. L., Wang, H. C., Chunag, Y. T., Chou, C. W., Lin, I. L., Lai, C. S., et al. (2017). miRNA expression change in dorsal root ganglia after peripheral nerve injury. *J. Mol. Neurosci.* 61, 169–177. doi: 10.1007/s12031-016-0876-7

Chen, H. P., Zhou, W., Kang, L. M., Yan, H., Zhang, L., Xu, B. H., et al. (2014). Intrathecal miR-96 inhibits Nav1.3 expression and alleviates neuropathic pain in rat following chronic construction injury. *Neurochem. Res.* 39, 76–83. doi: 10.1007/s11064-013-1192-z

Cherng, C. H., Lee, K. C., Chien, C. C., Chou, K. Y., Cheng, Y. C., Hsin, S. T., et al. (2014). Baicalin ameliorates neuropathic pain by suppressing HDAC1 expression in the spinal cord of spinal nerve ligation rats. *J. Formos. Med. Assoc.* 113, 513–520. doi: 10.1016/j.jfma.2013.04.007

Chiechio, S., Caricasole, A., Barletta, E., Storto, M., Catania, M. V., Copani, A., et al. (2002). L-Acetylcarnitine induces analgesia by selectively up-regulating mGlu2 metabotropic glutamate receptors. *Mol. Pharmacol.* 61, 989–996. doi: 10.1124/mol.61.5.989

Chiechio, S., Copani, A., De Petris, L., Morales, M. E., Nicoletti, F., and Gereau, R. W. T. (2006). Transcriptional regulation of metabotropic glutamate receptor 2/3 expression by the NF-kappaB pathway in primary dorsal root ganglia neurons: a possible mechanism for the analgesic effect of L-acetylcarnitine. *Mol. Pain* 2:20.

Chiechio, S., Copani, A., Zammataro, M., Battaglia, G., Gereau, R. W. T., and Nicoletti, F. (2010). Transcriptional regulation of type-2 metabotropic glutamate receptors: an epigenetic path to novel treatments for chronic pain. *Trends Pharmacol. Sci.* 31, 153–160. doi: 10.1016/j.tips.2009.12.003

Chiechio, S., Zammataro, M., Morales, M. E., Busceti, C. L., Drago, F., Gereau, R. W. T., et al. (2009). Epigenetic modulation of mGlu2 receptors by histone deacetylase inhibitors in the treatment of inflammatory pain. *Mol. Pharmacol.* 75, 1014–1020. doi: 10.1124/mol.108.054346

Cohen, S. P., and Mao, J. (2014). Neuropathic pain: mechanisms and their clinical implications. *BMJ* 348:f7656. doi: 10.1136/bmj.f7656

Colleoni, M., and Sacerdote, P. (2010). Murine models of human neuropathic pain. *Biochim. Biophys. Acta* 1802, 924–933. doi: 10.1016/j.bbadis.2009.10.012

Consortium, E. P., Birney, E., Stamatoyannopoulos, J. A., Dutta, A., Guigo, R., Gingeras, T. R., et al. (2007). Identification and analysis of functional elements in 1% of the human genome by the ENCODE pilot project. *Nature* 447, 799–816. doi: 10.1038/nature05874

Costigan, M., Scholz, J., and Woolf, C. J. (2009). Neuropathic pain: a maladaptive response of the nervous system to damage. *Annu. Rev. Neurosci.* 32, 1–32. doi: 10.1146/annurev.neuro.051508.135531

Cronk, J. C., Derecki, N. C., Ji, E., Xu, Y., Lampano, A. E., Smirnov, I., et al. (2015). Methyl-CpG Binding Protein 2 regulates microglia and macrophage gene expression in response to inflammatory stimuli. *Immunity* 42, 679–691. doi: 10.1016/j.immuni.2015.03.013

Denk, F., Huang, W., Sidders, B., Bithell, A., Crow, M., Grist, J., et al. (2013). HDAC inhibitors attenuate the development of hypersensitivity in models of neuropathic pain. *Pain* 154, 1668–1679. doi: 10.1016/j.pain.2013.05.021

Descalzi, G., Ikegami, D., Ushijima, T., Nestler, E. J., Zachariou, V., and Narita, M. (2015). Epigenetic mechanisms of chronic pain. *Trends Neurosci.* 38, 237–246. doi: 10.1016/j.tins.2015.02.001

Dib-Hajj, S. D., Black, J. A., and Waxman, S. G. (2009). Voltage-gated sodium channels: therapeutic targets for pain. *Pain Med.* 10, 1260–1269. doi: 10.1111/j.1526-4637.2009.00719.x

Dworkin, R. H., Backonja, M., Rowbotham, M. C., Allen, R. R., Argoff, C. R., Bennett, G. J., et al. (2003). Advances in neuropathic pain: diagnosis, mechanisms, and treatment recommendations. *Arch. Neurol.* 60, 1524–1534. doi: 10.1001/archneur.60.11.1524

Ellis, A., and Bennett, D. L. (2013). Neuroinflammation and the generation of neuropathic pain. *Br. J. Anaesth.* 111, 26–37. doi: 10.1093/bja/aet128

Favereaux, A., Thoumine, O., Bouali-Benazzouz, R., Roques, V., Papon, M. A., Salam, S. A., et al. (2011). Bidirectional integrative regulation of Cav1.2 calcium channel by microRNA miR-103: role in pain. *EMBO J.* 30, 3830–3841. doi: 10.1038/emboj.2011.249

Freynhagen, R., and Bennett, M. I. (2009). Diagnosis and management of neuropathic pain. *BMJ* 339:b3002. doi: 10.1136/bmj.b3002

Gallagher, S. J., Mijatov, B., Gunatilake, D., Gowrishankar, K., Tiffen, J., James, W., et al. (2014). Control of NF-kB activity in human melanoma by bromodomain and extra-terminal protein inhibitor I-BET151. *Pigment Cell Melanoma Res.* 27, 1126–1137. doi: 10.1111/pcmr.12282

Gao, Y. J., and Ji, R. R. (2010). Chemokines, neuronal-glial interactions, and central processing of neuropathic pain. *Pharmacol. Ther.* 126, 56–68. doi: 10.1016/j.pharmthera.2010.01.002

Gao, Z., Ure, K., Ding, P., Nashaat, M., Yuan, L., Ma, J., et al. (2011). The master negative regulator REST/NRSF controls adult neurogenesis by restraining the neurogenic program in quiescent stem cells. *J. Neurosci.* 31, 9772–9786. doi: 10.1523/JNEUROSCI.1604-11.2011

Genda, Y., Arai, M., Ishikawa, M., Tanaka, S., Okabe, T., and Sakamoto, A. (2013). microRNA changes in the dorsal horn of the spinal cord of rats with chronic constriction injury: a TaqMan(R) Low Density Array study. *Int. J. Mol. Med.* 31, 129–137. doi: 10.3892/ijmm.2012.1163

Geranton, S. M., and Tochiki, K. K. (2015). Regulation of gene expression and pain states by epigenetic mechanisms. *Prog. Mol. Biol. Transl. Sci.* 131, 147–183. doi: 10.1016/bs.pmbts.2014.11.012

Grishok, A., Pasquinelli, A. E., Conte, D., Li, N., Parrish, S., Ha, I., et al. (2001). Genes and mechanisms related to RNA interference regulate expression of the small temporal RNAs that control *C. elegans* developmental timing. *Cell* 106, 23–34. doi: 10.1016/S0092-8674(01)00431-7

Gui, Y., Li, A., Chen, F., Zhou, H., Tang, Y., Chen, L., et al. (2015). Involvement of AMPK/SIRT1 pathway in anti-allodynic effect of troxerutin in CCI-induced neuropathic pain. *Eur. J. Pharmacol.* 769, 234–241. doi: 10.1016/j.ejphar.2015.11.023

Hains, B. C., and Waxman, S. G. (2007). Sodium channel expression and the molecular pathophysiology of pain after SCI. *Prog. Brain Res.* 161, 195–203. doi: 10.1016/S0079-6123(06)61013-3

Hara, D., Fukuchi, M., Miyashita, T., Tabuchi, A., Takasaki, I., Naruse, Y., et al. (2009). Remote control of activity-dependent BDNF gene promoter-I transcription mediated by REST/NRSF. *Biochem. Biophys. Res. Commun.* 384, 506–511. doi: 10.1016/j.bbrc.2009.05.007

He, L., and Hannon, G. J. (2004). MicroRNAs: small RNAs with a big role in gene regulation. *Nat. Rev. Genet.* 5, 522–531. doi: 10.1038/nrg1379

He, X., Ou, P., Wu, K., Huang, C., Wang, Y., Yu, Z., et al. (2014). Resveratrol attenuates morphine antinociceptive tolerance via SIRT1 regulation in the rat spinal cord. *Neurosci. Lett.* 566, 55–60. doi: 10.1016/j.neulet.2014.02.022

Holliday, R., and Ho, T. (2002). DNA methylation and epigenetic inheritance. *Methods* 27, 179–183. doi: 10.1016/S1046-2023(02)00072-5

Hou, X., Weng, Y., Ouyang, B., Ding, Z., Song, Z., Zou, W., et al. (2017). HDAC inhibitor TSA ameliorates mechanical hypersensitivity and potentiates analgesic effect of morphine in a rat model of bone cancer pain by restoring μ-opioid receptor in spinal cord. *Brain Res.* 1669, 97–105. doi: 10.1016/j.brainres.2017.05.014

Huang, B., Yang, X. D., Zhou, M. M., Ozato, K., and Chen, L. F. (2009). Brd4 coactivates transcriptional activation of NF-kappaB via specific binding to acetylated RelA. *Mol. Cell. Biol.* 29, 1375–1387. doi: 10.1128/MCB.01365-08

Imai, S., Saeki, M., Yanase, M., Horiuchi, H., Abe, M., Narita, M., et al. (2011). Change in microRNAs associated with neuronal adaptive responses in the nucleus accumbens under neuropathic pain. *J. Neurosci.* 31, 15294–15299. doi: 10.1523/JNEUROSCI.0921-11.2011

Jenuwein, T., and Allis, C. D. (2001). Translating the histone code. *Science* 293, 1074–1080. doi: 10.1126/science.1063127

Jiang, B. C., He, L. N., Wu, X. B., Shi, H., Zhang, W. W., Zhang, Z. J., et al. (2017). Promoted interaction of C/EBPalpha with demethylated Cxcr3 gene promoter contributes to neuropathic pain in mice. *J. Neurosci.* 37, 685–700. doi: 10.1523/JNEUROSCI.2262-16.2016

Julius, D., and Basbaum, A. I. (2001). Molecular mechanisms of nociception. *Nature* 413, 203–210. doi: 10.1038/35093019

Kami, K., Taguchi, S., Tajima, F., and Senba, E. (2016). Histone acetylation in microglia contributes to exercise-induced hypoalgesia in neuropathic pain model mice. *J. Pain* 17, 588–599. doi: 10.1016/j.jpain.2016.01.471

Khangura, R. K., Bali, A., Jaggi, A. S., and Singh, N. (2017). Histone acetylation and histone deacetylation in neuropathic pain: an unresolved puzzle? *Eur. J. Pharmacol.* 795, 36–42. doi: 10.1016/j.ejphar.2016.12.001

Kiguchi, N., Kobayashi, Y., Kadowaki, Y., Fukazawa, Y., Saika, F., and Kishioka, S. (2014). Vascular endothelial growth factor signaling in injured nerves underlies peripheral sensitization in neuropathic pain. *J. Neurochem.* 129, 169–178. doi: 10.1111/jnc.12614

Kiguchi, N., Kobayashi, Y., Maeda, T., Fukazawa, Y., Tohya, K., Kimura, M., et al. (2012). Epigenetic augmentation of the macrophage inflammatory protein 2/C-X-C chemokine receptor type 2 axis through histone H3 acetylation in injured peripheral nerves elicits neuropathic pain. *J. Pharmacol. Exp. Ther.* 340, 577–587. doi: 10.1124/jpet.111.187724

Kiguchi, N., Kobayashi, Y., Saika, F., and Kishioka, S. (2013). Epigenetic upregulation of CCL2 and CCL3 via histone modifications in infiltrating macrophages after peripheral nerve injury. *Cytokine* 64, 666–672. doi: 10.1016/j.cyto.2013.09.019

Kukkar, A., Singh, N., and Jaggi, A. S. (2014). Attenuation of neuropathic pain by sodium butyrate in an experimental model of chronic constriction injury in rats. *J. Formos. Med. Assoc.* 113, 921–928. doi: 10.1016/j.jfma.2013.05.013

Kusuda, R., Cadetti, F., Ravanelli, M. I., Sousa, T. A., Zanon, S., De Lucca, F. L., et al. (2011). Differential expression of microRNAs in mouse pain models. *Mol. Pain* 7:17. doi: 10.1186/1744-8069-7-17

Laumet, G., Garriga, J., Chen, S. R., Zhang, Y., Li, D. P., Smith, T. M., et al. (2015). G9a is essential for epigenetic silencing of K(+) channel genes in acute-to-chronic pain transition. *Nat. Neurosci.* 18, 1746–1755. doi: 10.1038/nn.4165

Lee, H. T., Kim, S. K., Kim, S. H., Kim, K., Lim, C. H., Park, J., et al. (2014). Transcription-related element gene expression pattern differs between microglia and macrophages during inflammation. *Inflamm. Res.* 63, 389–397. doi: 10.1007/s00011-014-0711-y

Lee, K., Na, W., Lee, J. Y., Na, J., Cho, H., Wu, H., et al. (2012). Molecular mechanism of Jmjd3-mediated interleukin-6 gene regulation in endothelial cells underlying spinal cord injury. *J. Neurochem.* 122, 272–282. doi: 10.1111/j.1471-4159.2012.07786.x

Leoni, F., Fossati, G., Lewis, E. C., Lee, J. K., Porro, G., Pagani, P., et al. (2005). The histone deacetylase inhibitor ITF2357 reduces production of pro-inflammatory cytokines in vitro and systemic inflammation in vivo. *Mol. Med.* 11, 1–15. doi: 10.2119/2006-00005.Dinarello

Li, L., and Zhao, G. (2016). Downregulation of microRNA-218 relieves neuropathic pain by regulating suppressor of cytokine signaling 3. *Int. J. Mol. Med.* 37, 851–858. doi: 10.3892/ijmm.2016.2455

Ligon, C. O., Moloney, R. D., and Greenwood-Van Meerveld, B. (2016). Targeting epigenetic mechanisms for chronic pain: a valid approach for the development of novel therapeutics. *J. Pharmacol. Exp. Ther.* 357, 84–93. doi: 10.1124/jpet.115.231670

Lu, Y., Cao, D. L., Jiang, B. C., Yang, T., and Gao, Y. J. (2015). MicroRNA-146a-5p attenuates neuropathic pain via suppressing TRAF6 signaling in the spinal cord. *Brain Behav. Immun.* 49, 119–129. doi: 10.1016/j.bbi.2015.04.018

Matsushita, Y., Araki, K., Omotuyi, O., Mukae, T., and Ueda, H. (2013). HDAC inhibitors restore C-fibre sensitivity in experimental neuropathic pain model. *Br. J. Pharmacol.* 170, 991–998. doi: 10.1111/bph.12366

McMahon, S. B., Cafferty, W. B., and Marchand, F. (2005). Immune and glial cell factors as pain mediators and modulators. *Exp. Neurol.* 192, 444–462. doi: 10.1016/j.expneurol.2004.11.001

Meadows, J. P., Guzman-Karlsson, M. C., Phillips, S., Brown, J. A., Strange, S. K., Sweatt, J. D., et al. (2016). Dynamic DNA methylation regulates neuronal intrinsic membrane excitability. *Sci. Signal.* 9:ra83. doi: 10.1126/scisignal.aaf5642

Miller, R. J., Jung, H., Bhangoo, S. K., and White, F. A. (2009). Cytokine and chemokine regulation of sensory neuron function. *Handb. Exp. Pharmacol.* 194, 417–449. doi: 10.1007/978-3-540-79090-7_12

Mosammaparast, N., and Shi, Y. (2010). Reversal of histone methylation: biochemical and molecular mechanisms of histone demethylases. *Annu. Rev. Biochem.* 79, 155–179. doi: 10.1146/annurev.biochem.78.070907.103946

Neumann, E., Brandenburger, T., Santana-Varela, S., Deenen, R., Kohrer, K., Bauer, I., et al. (2016). MicroRNA-1-associated effects of neuron-specific brain-derived neurotrophic factor gene deletion in dorsal root ganglia. *Mol. Cell. Neurosci.* 75, 36–43. doi: 10.1016/j.mcn.2016.06.003

Neumann, E., Hermanns, H., Barthel, F., Werdehausen, R., and Brandenburger, T. (2015). Expression changes of microRNA-1 and its targets Connexin 43 and brain-derived neurotrophic factor in the peripheral nervous system of chronic neuropathic rats. *Mol. Pain* 11:39. doi: 10.1186/s12990-015-0045-y

Nicodeme, E., Jeffrey, K. L., Schaefer, U., Beinke, S., Dewell, S., Chung, C. W., et al. (2010). Suppression of inflammation by a synthetic histone mimic. *Nature* 468, 1119–1123. doi: 10.1038/nature09589

Palomer, E., Carretero, J., Benvegnu, S., Dotti, C. G., and Martin, M. G. (2016). Neuronal activity controls Bdnf expression via Polycomb de-repression and CREB/CBP/JMJD3 activation in mature neurons. *Nat. Commun.* 7:11081. doi: 10.1038/ncomms11081

Paquette, A. J., Perez, S. E., and Anderson, D. J. (2000). Constitutive expression of the neuron-restrictive silencer factor (NRSF)/REST in differentiating neurons disrupts neuronal gene expression and causes axon pathfinding errors in vivo. *Proc. Natl. Acad. Sci. U.S.A.* 97, 12318–12323. doi: 10.1073/pnas.97.22.12318

Peng, C., Li, L., Zhang, M. D., Bengtsson Gonzales, C., Parisien, M., Belfer, I., et al. (2017). miR-183 cluster scales mechanical pain sensitivity by regulating basal and neuropathic pain genes. *Science* 356, 1168–1171. doi: 10.1126/science.aam7671

Pollema-Mays, S. L., Centeno, M. V., Apkarian, A. V., and Martina, M. (2014). Expression of DNA methyltransferases in adult dorsal root ganglia is cell-type specific and up regulated in a rodent model of neuropathic pain. *Front. Cell Neurosci.* 8:217. doi: 10.3389/fncel.2014.00217

Prada, I., Marchaland, J., Podini, P., Magrassi, L., D'Alessandro, R., Bezzi, P., et al. (2011). REST/NRSF governs the expression of dense-core vesicle gliosecretion in astrocytes. *J. Cell Biol.* 193, 537–549. doi: 10.1083/jcb.201010126

Przanowski, P., Dabrowski, M., Ellert-Miklaszewska, A., Kloss, M., Mieczkowski, J., Kaza, B., et al. (2014). The signal transducers Stat1 and Stat3 and their novel target Jmjd3 drive the expression of inflammatory genes in microglia. *J. Mol. Med.* 92, 239–254. doi: 10.1007/s00109-013-1090-5

Roopra, A., Dingledine, R., and Hsieh, J. (2012). Epigenetics and epilepsy. *Epilepsia* 53(Suppl. 9), 2–10. doi: 10.1111/epi.12030

Rose, K., Ooi, L., Dalle, C., Robertson, B., Wood, I. C., and Gamper, N. (2011). Transcriptional repression of the M channel subunit Kv7.2 in chronic nerve injury. *Pain* 152, 742–754. doi: 10.1016/j.pain.2010.12.028

Ruthenburg, A. J., Li, H., Patel, D. J., and Allis, C. D. (2007). Multivalent engagement of chromatin modifications by linked binding modules. *Nat. Rev. Mol. Cell Biol.* 8, 983–994. doi: 10.1038/nrm2298

Sakai, A., Saitow, F., Miyake, N., Miyake, K., Shimada, T., and Suzuki, H. (2013). miR-7a alleviates the maintenance of neuropathic pain through regulation of neuronal excitability. *Brain* 136, 2738–2750. doi: 10.1093/brain/awt191

Sakai, A., and Suzuki, H. (2013). Nerve injury-induced upregulation of miR-21 in the primary sensory neurons contributes to neuropathic pain in rats. *Biochem. Biophys. Res. Commun.* 435, 176–181. doi: 10.1016/j.bbrc.2013.04.089

Sanna, M. D., Guandalini, L., Romanelli, M. N., and Galeotti, N. (2017). The new HDAC1 inhibitor LG325 ameliorates neuropathic pain in a mouse model. *Pharmacol. Biochem. Behav.* 160, 70–75. doi: 10.1016/j.pbb.2017.08.006

Schweizer, S., Meisel, A., and Marschenz, S. (2013). Epigenetic mechanisms in cerebral ischemia. *J. Cereb. Blood Flow Metab.* 33, 1335–1346. doi: 10.1038/jcbfm.2013.93

Shao, C., Gao, Y., Jin, D., Xu, X., Tan, S., Yu, H., et al. (2017). DNMT3a methylation in neuropathic pain. *J. Pain Res.* 10, 2253–2262. doi: 10.2147/JPR.S130654

Shao, H., Xue, Q., Zhang, F., Luo, Y., Zhu, H., Zhang, X., et al. (2014). Spinal SIRT1 activation attenuates neuropathic pain in mice. *PLoS One* 9:e100938. doi: 10.1371/journal.pone.0100938

Shao, J., Cao, J., Wang, J., Ren, X., Su, S., Li, M., et al. (2016). MicroRNA-30b regulates expression of the sodium channel Nav1.7 in nerve injury-induced neuropathic pain in the rat. *Mol. Pain* 12:1744806916671523.

Shi, G., Shi, J., Liu, K., Liu, N., Wang, Y., Fu, Z., et al. (2013). Increased miR-195 aggravates neuropathic pain by inhibiting autophagy following peripheral nerve injury. *Glia* 61, 504–512. doi: 10.1002/glia.22451

Sun, L., Zhao, J. Y., Gu, X., Liang, L., Wu, S., Mo, K., et al. (2017). Nerve injury-induced epigenetic silencing of opioid receptors controlled by DNMT3a in primary afferent neurons. *Pain* 158, 1153–1165. doi: 10.1097/j.pain.0000000000000894

Sun, W., Zhang, L., and Li, R. (2017). Overexpression of miR-206 ameliorates chronic constriction injury-induced neuropathic pain in rats via the MEK/ERK pathway by targeting brain-derived neurotrophic factor. *Neurosci. Lett.* 646, 68–74. doi: 10.1016/j.neulet.2016.12.047

Sun, Y., Sahbaie, P., Liang, D. Y., Li, W. W., Li, X. Q., Shi, X. Y., et al. (2013). Epigenetic regulation of spinal CXCR2 signaling in incisional hypersensitivity in mice. *Anesthesiology* 119, 1198–1208. doi: 10.1097/ALN.0b013e31829ce340

Tajerian, M., Alvarado, S., Millecamps, M., Vachon, P., Crosby, C., Bushnell, M. C., et al. (2013). Peripheral nerve injury is associated with chronic, reversible changes in global DNA methylation in the mouse prefrontal cortex. *PLoS One* 8:e55259. doi: 10.1371/journal.pone.0055259

Tan, Y., Yang, J., Xiang, K., Tan, Q., and Guo, Q. (2015). Suppression of microRNA-155 attenuates neuropathic pain by regulating SOCS1 signalling pathway. *Neurochem. Res.* 40, 550–560. doi: 10.1007/s11064-014-1500-2

Tao, W., Zhou, W., Wang, Y., Sun, T., Wang, H., Zhang, Z., et al. (2016). Histone deacetylase inhibitor-induced emergence of synaptic delta-opioid receptors and behavioral antinociception in persistent neuropathic pain. *Neuroscience* 339, 54–63. doi: 10.1016/j.neuroscience.2016.09.015

Tibbs, G. R., Posson, D. J., and Goldstein, P. A. (2016). Voltage-Gated ion channels in the PNS: novel therapies for neuropathic pain? *Trends Pharmacol. Sci.* 37, 522–542. doi: 10.1016/j.tips.2016.05.002

Tillu, D. V., Melemedjian, O. K., Asiedu, M. N., Qu, N., De Felice, M., Dussor, G., et al. (2012). Resveratrol engages AMPK to attenuate ERK and mTOR signaling in sensory neurons and inhibits incision-induced acute and chronic pain. *Mol. Pain* 8:5. doi: 10.1186/1744-8069-8-5

Tinsley, J. H., Hunter, F. A., and Childs, E. W. (2009). PKC and MLCK-dependent, cytokine-induced rat coronary endothelial dysfunction. *J. Surg. Res.* 152, 76–83. doi: 10.1016/j.jss.2008.02.022

Tochiki, K. K., Cunningham, J., Hunt, S. P., and Geranton, S. M. (2012). The expression of spinal methyl-CpG-binding protein 2, DNA methyltransferases and histone deacetylases is modulated in persistent pain states. *Mol. Pain* 8:14. doi: 10.1186/1744-8069-8-14

Torrance, N., Smith, B. H., Bennett, M. I., and Lee, A. J. (2006). The epidemiology of chronic pain of predominantly neuropathic origin. Results from a general population survey. *J. Pain* 7, 281–289. doi: 10.1016/j.jpain.2005.11.008

Uchida, H., Ma, L., and Ueda, H. (2010a). Epigenetic gene silencing underlies C-fiber dysfunctions in neuropathic pain. *J. Neurosci.* 30, 4806–4814. doi: 10.1523/JNEUROSCI.5541-09.2010

Uchida, H., Matsushita, Y., Araki, K., Mukae, T., and Ueda, H. (2015). Histone deacetylase inhibitors relieve morphine resistance in neuropathic pain after peripheral nerve injury. *J. Pharmacol. Sci.* 128, 208–211. doi: 10.1016/j.jphs.2015.07.040

Uchida, H., Matsushita, Y., and Ueda, H. (2013). Epigenetic regulation of BDNF expression in the primary sensory neurons after peripheral nerve injury: implications in the development of neuropathic pain. *Neuroscience* 240, 147–154. doi: 10.1016/j.neuroscience.2013.02.053

Uchida, H., Sasaki, K., Ma, L., and Ueda, H. (2010b). Neuron-restrictive silencer factor causes epigenetic silencing of Kv4.3 gene after peripheral nerve injury. *Neuroscience* 166, 1–4. doi: 10.1016/j.neuroscience.2009.12.021

Vasudevan, S., and Steitz, J. A. (2007). AU-rich-element-mediated upregulation of translation by FXR1 and Argonaute 2. *Cell* 128, 1105–1118. doi: 10.1016/j.cell.2007.01.038

von Schimmelmann, M., Feinberg, P. A., Sullivan, J. M., Ku, S. M., Badimon, A., Duff, M. K., et al. (2016). Polycomb repressive complex 2 (PRC2) silences genes responsible for neurodegeneration. *Nat. Neurosci.* 19, 1321–1330. doi: 10.1038/nn.4360

Walters, E. T. (2012). Nociceptors as chronic drivers of pain and hyperreflexia after spinal cord injury: an adaptive-maladaptive hyperfunctional state hypothesis. *Front. Physiol.* 3:309. doi: 10.3389/fphys.2012.00309

Wang, C., Jiang, Q., Wang, M., and Li, D. (2015). MiR-19a targets suppressor of cytokine signaling 1 to modulate the progression of neuropathic pain. *Int. J. Clin. Exp. Pathol.* 8, 10901–10907.

Wang, L. L., Shi, D. L., Gu, H. Y., Zheng, M. Z., Hu, J., Song, X. H., et al. (2016). Resveratrol attenuates inflammatory hyperalgesia by inhibiting glial activation in mice spinal cords. *Mol. Med. Rep.* 13, 4051–4057. doi: 10.3892/mmr.2016.5027

Wang, Y., Liu, C., Guo, Q. L., Yan, J. Q., Zhu, X. Y., Huang, C. S., et al. (2011). Intrathecal 5-azacytidine inhibits global DNA methylation and methyl- CpG-binding protein 2 expression and alleviates neuropathic pain in rats following chronic constriction injury. *Brain Res.* 1418, 64–69. doi: 10.1016/j.brainres.2011.08.040

Willemen, H. L., Huo, X. J., Mao-Ying, Q. L., Zijlstra, J., Heijnen, C. J., and Kavelaars, A. (2012). MicroRNA-124 as a novel treatment for persistent hyperalgesia. *J. Neuroinflammation* 9:143. doi: 10.1186/1742-2094-9-143

Woolf, C. J., and Salter, M. W. (2000). Neuronal plasticity: increasing the gain in pain. *Science* 288, 1765–1769. doi: 10.1126/science.288.5472.1765

Xia, L., Zhang, Y., and Dong, T. (2016). Inhibition of MicroRNA-221 alleviates neuropathic pain through targeting suppressor of cytokine signaling 1. *J. Mol. Neurosci.* 59, 411–420. doi: 10.1007/s12031-016-0748-1

Xie, Y. F., Huo, F. Q., and Tang, J. S. (2009). Cerebral cortex modulation of pain. *Acta Pharmacol. Sin.* 30, 31–41. doi: 10.1038/aps.2008.14

Yadav, R., and Weng, H. R. (2017). EZH2 regulates spinal neuroinflammation in rats with neuropathic pain. *Neuroscience* 349, 106–117. doi: 10.1016/j.neuroscience.2017.02.041

Yan, T., Zhang, F., Sun, C., Sun, J., Wang, Y., Xu, X., et al. (2018). miR-32-5p-mediated Dusp5 downregulation contributes to neuropathic pain. *Biochem. Biophys. Res. Commun.* 495, 506–511. doi: 10.1016/j.bbrc.2017.11.013

Yan, X. T., Ji, L. J., Wang, Z., Wu, X., Wang, Q., Sun, S., et al. (2017). MicroRNA-93 alleviates neuropathic pain through targeting signal transducer and activator of transcription 3. *Int. Immunopharmacol.* 46, 156–162. doi: 10.1016/j.intimp.2017.01.027

Yin, Q., Lu, F. F., Zhao, Y., Cheng, M. Y., Fan, Q., Cui, J., et al. (2013). Resveratrol facilitates pain attenuation in a rat model of neuropathic pain through the activation of spinal Sirt1. *Reg. Anesth. Pain Med.* 38, 93–99. doi: 10.1097/AAP.0b013e3182795b23

Zammataro, M., Sortino, M. A., Parenti, C., Gereau, R. W. T., and Chiechio, S. (2014). HDAC and HAT inhibitors differently affect analgesia mediated by group II metabotropic glutamate receptors. *Mol. Pain* 10:68. doi: 10.1186/1744-8069-10-68

Zhang, Y., Chen, S. R., Laumet, G., Chen, H., and Pan, H. L. (2016). Nerve injury diminishes opioid analgesia through lysine methyltransferase-mediated transcriptional repression of mu-opioid receptors in primary sensory neurons. *J. Biol. Chem.* 291, 8475–8485. doi: 10.1074/jbc.M115.711812

Zhang, Y., and Chi, D. (2017). Overexpression of SIRT2 alleviates neuropathic pain and neuroinflammation through deacetylation of transcription factor nuclear Factor-Kappa B. *Inflammation* 41, 569–578. doi: 10.1007/s10753-017-0713-3

Zhang, Z., Cai, Y. Q., Zou, F., Bie, B., and Pan, Z. Z. (2011). Epigenetic suppression of GAD65 expression mediates persistent pain. *Nat. Med.* 17, 1448–1455. doi: 10.1038/nm.2442

Zhao, J. Y., Liang, L., Gu, X., Li, Z., Wu, S., Sun, L., et al. (2017). DNA methyltransferase DNMT3a contributes to neuropathic pain by repressing Kcna2 in primary afferent neurons. *Nat. Commun.* 8:14712. doi: 10.1038/ncomms14712

Zhou, X. L., Yu, L. N., Wang, Y., Tang, L. H., Peng, Y. N., Cao, J. L., et al. (2014). Increased methylation of the MOR gene proximal promoter in primary sensory neurons plays a crucial role in the decreased analgesic effect of opioids in neuropathic pain. *Mol. Pain* 10:51. doi: 10.1186/1744-8069-10-51

Zhu, X., Li, Q., Chang, R., Yang, D., Song, Z., Guo, Q., et al. (2014). Curcumin alleviates neuropathic pain by inhibiting p300/CBP histone acetyltransferase activity-regulated expression of BDNF and cox-2 in a rat model. *PLoS One* 9:e91303. doi: 10.1371/journal.pone.0091303

Conflict of Interest Statement: The authors declare that the research was conducted in the absence of any commercial or financial relationships that could be construed as a potential conflict of interest.

frontiers in Cellular Neuroscience

REVIEW
published: 24 September 2018
doi: 10.3389/fncel.2018.00317

Potential Effects of MSC-Derived Exosomes in Neuroplasticity in Alzheimer's Disease

*Edwin E. Reza-Zaldivar[1], Mercedes A. Hernández-Sapiéns[1], Benito Minjarez[2], Yanet K. Gutiérrez-Mercado[1], Ana L. Márquez-Aguirre[1] and Alejandro A. Canales-Aguirre[1,3]**

[1]Unidad de Evaluación Preclínica, Biotecnología Médica y Farmacéutica, CONACYT Centro de Investigación y Asistencia en Tecnología y Diseño del Estado de Jalisco (CIATEJ), Guadalajara, Mexico, [2]Centro Universitario de Ciencias Biológicas y Agropecuarias (CUCBA), Universidad de Guadalajara, Guadalajara, Mexico, [3]Profesor del programa de Maestría en Ciencias de la Salud Ambiental, Centro Universitario de Ciencias Biológicas y Agropecuarias (CUCBA), Universidad de Guadalajara, Guadalajara, Mexico

Alzheimer's disease (AD) is the most common type of dementia affecting regions of the central nervous system that exhibit synaptic plasticity and are involved in higher brain functions such as learning and memory. AD is characterized by progressive cognitive dysfunction, memory loss and behavioral disturbances of synaptic plasticity and energy metabolism. Cell therapy has emerged as an alternative treatment of AD. The use of adult stem cells, such as neural stem cells and Mesenchymal Stem Cells (MSCs) from bone marrow and adipose tissue, have the potential to decrease cognitive deficits, possibly by reducing neuronal loss through blocking apoptosis, increasing neurogenesis, synaptogenesis and angiogenesis. These processes are mediated primarily by the secretion of many growth factors, anti-inflammatory proteins, membrane receptors, microRNAs (miRNA) and exosomes. Exosomes encapsulate and transfer several functional molecules like proteins, lipids and regulatory RNA which can modify cell metabolism. In the proteomic characterization of the content of MSC-derived exosomes, more than 730 proteins have been identified, some of which are specific cell type markers and others are involved in the regulation of binding and fusion of exosomes with adjacent cells. Furthermore, some factors were found that promote the recruitment, proliferation and differentiation of other cells like neural stem cells. Moreover, within exosomal cargo, a wide range of miRNAs were found, which can control functions related to neural remodeling as well as angiogenic and neurogenic processes. Taking this into consideration, the use of exosomes could be part of a strategy to promote neuroplasticity, improve cognitive impairment and neural replacement in AD. In this review, we describe how exosomes are involved in AD pathology and discuss the therapeutic potential of MSC-derived exosomes mediated by miRNA and protein cargo.

Keywords: exosomes, Alzheimer's disease, neuroplasticity, exosomal cargo, proteomics, miRNA

OPEN ACCESS

Edited by:
Merce Pallas,
University of Barcelona, Spain

Reviewed by:
Albert Rizvanov,
Kazan Federal University, Russia
Consuelo Morgado-Valle,
Universidad Veracruzana, Mexico

****Correspondence:***
Alejandro A. Canales-Aguirre
acanales@ciatej.mx

Received: *06 March 2018*
Accepted: *30 August 2018*
Published: *24 September 2018*

Citation:
Reza-Zaldivar EE, Hernández-Sapiéns MA, Minjarez B, Gutiérrez-Mercado YK, Márquez-Aguirre AL and Canales-Aguirre AA (2018) Potential Effects of MSC-Derived Exosomes in Neuroplasticity in Alzheimer's Disease. Front. Cell. Neurosci. 12:317. doi: 10.3389/fncel.2018.00317

INTRODUCTION

Alzheimer's disease (AD) is characterized by the progressive deposition of β-amyloid (Aβ) around neurons and the intracellular accumulation of neurofibrillary tangles (NFT) of hyperphosphorylated tau, mainly in areas implicated in memory and learning, such as the prefrontal cortex and hippocampus. In advanced stages of the disease, aggregates of Aβ are present in

motor areas, cerebrospinal fluid, as well as in eyes and neuromuscular joints (Reiss et al., 2018).

Presently there is no effective treatment for AD hence, stem cell therapy has been proposed to be a promising therapeutic option for this neurological disorder. Cell therapies for brain restoration generally target multiple cells of the brain parenchyma such as endothelial cells, neural stem cells (also named neural progenitors) and oligodendrocyte precursor cells. The interaction between the administered cells and resident cells promote neuroplastic events such angiogenesis stimulation, neurogenesis and axonal remodeling, result in a neurological recovery (Xin et al., 2017a; Xiong et al., 2017).

Several studies have demonstrated the effectiveness of Mesenchymal Stem Cells (MSCs) treatment in several neurodegenerative diseases (Wei et al., 2013). These cells have typical stem cell characteristics like the potential to differentiate into multiple cell lineages under different physiological conditions, including the ability to selectively migrate towards damage sites (homing) and interact with brain parenchyma cells. This interaction stimulate the production of neurotrophins such as vascular endothelial growth factor (VEGF), hepatocyte growth factor (HGF), nerve growth factor (NGF), brain-derived neurotrophic factor (BDNF) and neurotrophin-3 (Li et al., 2002; Kurozumi et al., 2004; Kim et al., 2010; Matthay et al., 2017) which increase neuritic development, promote neurorestoration and neurological recovery (Xiong et al., 2017; Harting et al., 2018).

Among the main functions of MSCs are their ability to limit inflammation environments through the release of soluble factors such as HGF, prostaglandin E2, transforming growth factor β1, indoleamine 2,3 dioxygenase, interleukin 10 and nitric oxide. This immunomodulatory environment allows the expression of growth factors, high immunomodulatory protein secretion and the enhancement of endogenous cellular repair processes (Nguyen et al., 2013; Phinney and Pittenger, 2017).

A central hypothesis has been proposed, in which MSCs are implied to exert a dynamic homeostatic response that supports tissue preservation as well as function recovery (Harting et al., 2018). The main mechanism by which MSCs mediate this activity is not the cellular implant and its subsequent differentiation, but the paracrine activity of the secretome (Nakano et al., 2016; Yang Y. et al., 2017). This phenomenon was demonstrated in studies where conditioned medium of MSCs was administered and therapeutic effects similar to those already reported for MSCs were produced in different animal models of diseases (Timmers et al., 2007; Mitsialis and Kourembanas, 2016). A subsequent fractionation of this conditioned medium was performed and an active component of approximately 50–150 nm was found. Biophysical studies categorized these compounds as exosomes (Lai et al., 2010; Phinney and Pittenger, 2017). Consequently, it was established that one of the critical parameters that regulate the paracrine activity of MSC is the generation of exosomes (Drommelschmidt et al., 2017; Phinney and Pittenger, 2017). Therefore, exosomes may be a therapeutic option in the treatment of AD because they exert therapeutic effects like MSCs.

Biogenesis of Exosomes

Exosomes are small (30–150 nm diameter) membrane-enclosed vesicles of endosomal origin, released by a variety of cell types, capable of transferring biologically active macromolecules, such as proteins, lipids and RNA, to other cells (Bang and Thum, 2012). Exosomes are originated as intraluminal vesicles within the multivesicular bodies (MVB) by inward budding of the late endosomal membrane (Colombo et al., 2014). The Endosomal Sorting Complex Required for Transport (ESCRT) machinery is important in this process. ESCRT consist of approximately 20 proteins that assemble four different complexes; ESCRT-0, -I, -II, -III and the associated AAA ATPase vacuolar protein sorting 34 (Vps4) complex (Henne et al., 2013). ESCRT-0 recognizes and sequesters ubiquitylated proteins in the endosomal membrane, ESCRT-I and -II are responsible for membrane budding as well as recruiting of ESCRT-III that finally drive vesicle scission (Hurley and Hanson, 2010). The dissociation and recycling of the ESCRTs require the AAA ATPase Vps4 complex. Transport of MVB towards plasma membrane depends on interaction with the cytoskeleton, this interaction is mediated mainly by Rab GTPases and SNARE proteins, although precise mechanism of action in this process is not known (Ostrowski et al., 2009; Beer and Wehman, 2017). MVB subsequently fuse with the plasma membrane and release those intraluminal vesicles such as exosomes (Camacho et al., 2013; Abels and Breakefield, 2016). Some studies also suggest that MVB biogenesis can occur without ESCRTs. It has been shown that despite simultaneously silencing key subunits of all four ESCRTs, intraluminal vesicles are still formed in MVB, indicating the presence of a mechanism independent of ESCRT (Stuffers et al., 2009). Tetraspanins (Escola et al., 1998) and lipids (mainly ceramide; Trajkovic et al., 2008) could be essential players in exosome biogenesis due to the formation of microdomains that coalescence into larger domains that promote membrane budding.

As mentioned above, exosomes contain different proteins, lipids and nucleic acids (DNA, mRNA, microRNAs (miRNA), lncRNA), however, determining the exact composition and content of the exosomal content (cargo) produced by different cell types is hard to establish due to differences in the conditions which the cells are found. It should be mentioned that cellular homeostasis is an important factor that controls exosome cargo and secretion, therefore the exosomes will present characteristics that reflect its cellular origin (de Jong et al., 2012; Harting et al., 2018). Mechanisms for sorting cargo molecules into exosomes are still poorly understood. However, the ubiquitination is considered the main sorting signal for protein cargo entry into exosomes. Ubiquitinated proteins are recognized by receptors such as ESCRT subunits responsible for binding and directing cargo towards intraluminal vesicles (Piper and Katzmann, 2007). Usually these vesicles contain proteins that are involved in its biogenesis mechanisms, for example, ESCRT system components such as tetraspanins CD63, CD81 and CD9, as well as ALIX, TSG10, likewise proteins associated with their secretion as RAB27A, RAB11 and ARF6 (Wu et al., 2015; Abels and Breakefield, 2016). There are different pathways for miRNA sorting, which include: (I) neutral

sphingomyelinase 2 pathway demonstrated by Kosaka et al. (2010), in where they found that overexpression of neutral sphingomyelinase 2 increased the amount of miRNA into exosomes, while its chemical inhibition reduced the number of miRNAs; (II) the miRNA motif and sumoylated heterogeneous nuclear ribonucleoproteins (hnRNPs) pathway reported by Villarroya-Beltri et al. (2013), identified a short sequence motifs in miRNAs (GGAG) in the portion 3′ that is recognized by exosomal sumoylated hnRNPs, this hnRNP-miRNA binding control the miRNA loading into exosomes; (III) the miRNA induced silencing complex (miRSC) pathway. Components of miRSC include miRNA, miRNA repressible mRNA, and proteins GW182 and AGO2; Guduric-Fuchs et al. (2012) discovered that knockout of AGO2 decreases the abundance of miRNA exported by exosomes. Besides AGO2, others components of miRSC like GW182 were found to be colocalized with MVB (Guduric-Fuchs et al., 2012). Despite this evidence of exosomal cargo sorting, the underlying mechanisms remain unclear.

Concerning lipid composition of the exosomal membrane, there are some lipids such as sphingomyelin, cholesterol, ganglioside GM3, phosphatidylserine and ceramide that form lipid raft domains that are more abundant in the exosomal membrane than in the cell of origin (Angeloni et al., 2016). In contrast, phosphatidylcholine and diacylglycerol are scarce in the membrane of exosomes compared to the cell membrane (Abels and Breakefield, 2016).

Exosomes as Intercellular Communication Mediators

There is evidence suggesting that exosomes are internalized into recipient cells (Mulcahy et al., 2014). However, elucidation of the mechanisms of exosome targeting and uptake by recipient cells remains an important challenge. Exosomes could bear combinations of ligands that would engage different cell-surface receptors simultaneously, therefore different mechanisms have been proposed by which a cell can interact and uptake these nanovesicles. This communication could be through membrane receptors and the subsequent exosome membrane fusion with the cell membrane to exchange proteins and cytosol components. An other mechanism is through endocytosis, among which are clathrin-mediated endocytosis, caveolin-mediated endocytosis (Svensson et al., 2013), phagocytosis mediated mainly by phosphatidylserine, and micropinocytosis. The uptake mechanism used may depend on proteins and glycoproteins found on the surface of both the nanovesicle and the target cell.

Different studies establish that exosomes are mediators of intercellular communication, since they reach biological fluids such as blood, cerebrospinal fluid and urine among others, and act as paracrine messengers through the transference of bioactive lipids, mRNAs, miRNA, lncRNAs, and can also transfer genomic DNA and mitochondrial DNA and different proteins (Kalra et al., 2012; Keerthikumar et al., 2016). This transference of bioactive molecules establishing cell-cell communication processes can in an epigenetic way, alter the activity of the cells both in physiological and pathological conditions (Xiong et al., 2017; Harting et al., 2018).

Interestingly, the evidence shows that exosomes are released more under pathological conditions (Cheng et al., 2017). In this way, the most studied pathogenic components that use exosomes as infection route are the prion proteins (Vella et al., 2008), responsible for transmissible neurodegenerative diseases such as bovine spongiform encephalopathy and α-synuclein (Emmanouilidou et al., 2010), involved in Parkinson's disease pathology. Prion diseases are fatal neurodegenerative disorders associated with the conversion of the cellular prion protein into the scrapie prion protein, an abnormal conformational state that tends to form amyloid deposits in brain tissue leading to dementia (Vingtdeux et al., 2012). On the other hand, exosomes released from cells that have an overproduction of α-synuclein can transfer this protein to normal cells and promote the overproduction by alterations in the ESCRT system that result in an increased exocytosis of exosomes with α-synuclein (Spencer et al., 2016). In AD, it has been proposed that exosomes have a key pathological function in the progression of the disease, and are involved in Aβ and tau dissemination, since an accumulation of exosomes has been found in amyloid plaques (Rajendran et al., 2006) and hyperphosphorylated tau tangles (Saman et al., 2012, 2014; Levy, 2017).

ALZHEIMER'S DISEASE

AD is the most common neurodegenerative disease characterized by neuron loss and impairment of memory, cognition and functions of daily living. In many cases, death results from the loss of fine motor skills and incapacitation (Koelsch, 2017; Mroczko et al., 2018). The main pathological markers of AD are the accumulation of Aβ plaques and the formation of NFT, composed of hyperphosphorylated tau protein (Eitan et al., 2016). In early stages, these pathological changes are primarily localized within the medial temporal lobe and are spread through the neocortex (Braak and Braak, 1996).

Accumulation of Aβ in oligomers is one of the earliest events in the disease process, occurring 10–20 years prior to the onset of memory loss and other clinical symptoms (Reiman et al., 2012). Amyloid plaque formation are the result of Aβ peptides deposition that takes place in early endosomes, this process involves sequential hydrolysis of the amyloid precursor protein (APP) by β and γ-secretases (Rajendran et al., 2006). The β-site APP cleaving enzyme 1 (BACE1) is a transmembrane type I aspartyl protease that is located in endosomes as an immature precursor protein, and later in lysosomes and Golgi complex as a mature protein that catalyzes the initial amyloidogenic cleavage at β-site of APP while the membrane-associated 99 amino acid carboxyl-terminal fragment β remains (Munro et al., 2016; Yan et al., 2016). The γ-secretase has been identified as a multimeric protein complex containing presenilin 1, presenilin 2 associated with nicastrin, Aph-1 and Pen-2. The carboxyl-terminal fragment β is cleaved by γ-secretase releasing Aβ peptides (Sharples et al., 2008). The Aβ peptides released have pathophysiological impacts on synaptic function through

inhibition of transmission of the synaptic signal leading neuronal death (Mroczko et al., 2018).

On the other hand, NFTs are formed by massive accumulations of abnormal insoluble polymers, referred to as paired helical filaments (Wischik et al., 1985, 1988). The main structural component of this filaments is tau, a microtubule-associated protein (Kosik et al., 1986). The physiological function of tau is to stabilize microtubules in the cell cytoskeleton, an activity regulated by its phosphorylation (Grundke-Iqbal et al., 1986). It has been suggested that abnormal phosphorylation is an early molecular event that may lead to a sequence of structural changes in the tau molecule, such as conformational changes like truncations (Luna-Muñoz et al., 2007) and is thought that hyperphosphorylation and its aggregation are related to the disassembling of neuronal microtubules, that consequently affect axonal transport and result in cell death (Stoothoff and Johnson, 2005). Hyperphosphorylation of tau primarily occurs at Ser-Pro or Thr-Pro motifs, suggesting that proline-directed kinases such as the MAPK, GSK3β and CDK5 are directly involved (Mandelkow et al., 1992; Baumann et al., 1993; Greenberg et al., 1994). Other kinases are also able to modify the tau molecule, including CAMK, PKA and PKC (Correas et al., 1992; Scott et al., 1993; Ghosh and Giese, 2015).

Dissemination of Aβ and tau has been suggested to be mediated through release of extracellular vesicles (EVs; Nath et al., 2012). EV are small membrane vesicles which result from the budding of the plasma membrane as microvesicles (also called ectosomes) or from the exocytosis of MVB as exosomes. EV is considered one of the distant extracellular communication agents due to its capacity to carry and deliver different types of components to target cells (Zhang and Yang, 2018). A relationship between EV and progression of AD has been proposed because most of the Aβ and tau oligomers are colocalized with late endosome/lysosome markers, mainly MVB (Nath et al., 2012; Joshi et al., 2015). During disease progression, both these histopathological hallmarks extend throughout the brain with characteristic patterns reaching limbic and association areas (Cho et al., 2016).

Role of Exosomes in Alzheimer's Disease

Although the origin of the disease remains unknown, several investigations have postulated prion-like mechanisms in AD progression and dissemination, including direct cell communication through gap junctions, synaptic transmission and exacerbated paracrine signaling due to alterations of endosomal/lysosomal secretion system, in which exosomes play a fundamental role in the distribution of neuropathological components between neuronal cells (Gauthier et al., 2017; Xiao et al., 2017; Laulagnier et al., 2018).

Subcellular location of neuronal Aβ was identified using immunoelectron microscopy by Takahashi et al. (2002), they found that Aβ42 is localized predominantly within MVB of the neurons. Accumulation of Aβ inside neurons is prevented by autophagy, an event occurring in the endosomal/lysosomal system where Aβ within endosomes are destroyed by lysosomes (Mizushima and Komatsu, 2011). A key regulator of this system is phosphatidylinositol-3-phosphate (PI3P), a phospholipid synthesized mainly by class III PI3-kinase Vps34 (Jaber et al., 2016). Miranda et al. (2018) showed that disruption of neuronal Vps34 (a retromer complex component) function impairs autophagy, lysosomal degradation as well as lipid metabolism. This promotes the secretion of unique exosomes enriched with undigested lysosomal substrates, including Aβ, APP and the enzymes that process APP in an amyloidogenic way (Malm et al., 2016). In addition, this accumulation increases with aging and it is associated with abnormal synaptic morphology (Takahashi et al., 2002). Overall, inhibiting neutral sphingomyelinase 2, a key regulatory enzyme in ceramide synthesis and exosome biogenesis, reduced the number of exosomes in the brain and serum and further reduced Aβ plaque load in 5×FAD mice (Dinkins et al., 2016). These observations suggest that MVB is essential for APP metabolism and Aβ secretion (Takahashi et al., 2002; Joshi et al., 2015). Furthermore, other studies demonstrated that transference of damaged neuronal cell-derived exosomes with APP, γ/β secretases, Aβ peptides, APP-CTF, ubiquitins, modified ubiquitin ligases and tau protein to adjacent neurons can lead to AD propagation (Chen et al., 2017; Yuyama and Igarashi, 2017; Zheng et al., 2017; Miranda et al., 2018).

An interactome analysis demonstrated that inhibition of γ-secretase activity results in a significant increase of exosomes enriched with APP-CTF suggesting the association of γ-secretase in exosome membrane. Also, it was shown that exosomes tetraspanins CD9 and CD81 interact with the γ-secretase complex regulating their activity in a positive way. Using neutralizing antibodies against CD9 and CD81 result in the disruption of Aβ generation and lead to an accumulation of the APP-CTF (Wakabayashi et al., 2009). Likewise, tetraspanin 6 enrichment in exosomal membrane allows the accumulation of Aβ, CTF-APP and BACE1 in exosomes, and independently of ESCRT, increases biogenesis of exosomes and secretion of this type of cargo, as well as inhibits the degradation of these nanovesicles by the lysosomal system (Guix et al., 2017). Thereby, these studies suggest the involvement of the tetraspanin web protein in the up and down regulation of Aβ generation.

It has been reported that the endosomal localization of BACE1 is regulated by the ACG sequence and the retromer, a multiprotein complex required for the recycling of transmembrane proteins from the endosomes to the trans-Golgi network (Tan and Evin, 2012). Kizuka et al. (2015) showed that BACE1 is modified with bisecting N-acetylglucosamine, a sugar modification highly expressed in the brain of AD patients, by GnT-III. They reported that lack of this modification directs BACE1 to late/lysosomes where it is less colocalized with APP, however, the glycan modification is protective for lysosomal degradation.

Furthermore, the Aβ peptides already present in extracellular space can interact with the exosomal membrane through their glycosphingolipids and the cellular prion protein (PrP^C), forming aggregates of Aβ (Rajendran et al., 2006; Zappulli et al., 2016; Yuyama and Igarashi, 2017; Zheng et al., 2017). This was demonstrated in the histological analysis performed in brains of AD patients were an enrichment of exosomal markers Alix and flotillin-1 was found around neuritic plaques; this suggested that exosomes function as nucleation centers

for amyloid plaque formation (Xiao et al., 2017). A recent publication by Falker et al. (2016) showed that PrP^C is highly enriched on exosomes membranes and distinct Aβ oligomers bind PrP^C with high affinity via its flexible N-terminus. This bind drives Aβ fibrillation and may be involved in the extracellular deposition of Aβ. However, there is a debate about if PrP^C is required for Aβ-mediated synaptotoxicity and suppression of long-term potentiation (Lauren et al., 2009; Kessels et al., 2010).

On the other hand, it has been proposed that the spread of tau can occur through neuronal synaptic connections, but the mechanism underlying this process remains unknown (Wang Y. et al., 2017). However, it also has been reported that monomers and oligomers of tau hyperphosphorylated are encapsulated within the exosomes (Shi et al., 2016), which are then transferred through synaptic contact with other neurons, and like the exosomes that interact with Aβ, can promote nucleation centers for hyperphosphorylated tau aggregation (Saman et al., 2012, 2014).

In addition to neural cell interaction, exosomes from damaged cells also interact with glial cells. Consequently, astrocytes not only fail to support neurons but also generate a toxic environment that is detrimental to neurons and astrocytes themselves through promoting secondary apoptosis of adjacent cells (Wang et al., 2012). Wang et al. (2012) found that the astrocytic-mediated apoptosis is associated with the secretion of PAR-4/ceramide containing exosomes in the adjacent cells even if they were not exposed to Aβ. It has been demonstrated that astrocytes tend to interact more with exosomes and accumulate large amounts of Aβ42 protofibers, subsequently, this storage results in endosomal/lysosomal system alterations which induce exosome secretion with a neurotoxic cargo (Nikitidou et al., 2017). Astrocyte-derived exosomes of patients with AD had up to 20-fold higher concentrations of β/γ-secretase and sAPPβ than neuron-derived exosomes (Goetzl et al., 2016). Moreover, Chiarini et al., 2017 presented evidence showing that tau and its hyperphosphorylated form are expressed by untransformed astrocytes in culture exposed to Aβ, the release is mediated by exosomes to the extracellular medium.

In addition, microglia also participates in the internalization of exosomes derived from damaged cells, Ikezu et al. (2016) found that microglia transduces tau aggregates into nearby neuronal cells via exosome secretion, tau aggregates propagate from cortical neurons to dentate granular cells and this propagation is sensitive to exosome inhibition or microglial depletion. In AD, Aβ phagocytosis by microglia is one of the principal mechanisms for a level decrease of these peptides. Exosome phagocytosis is a process mediated by phosphatidylserine; as well as in apoptotic cells, exosomal phosphatidylserine is found in the outer layer of the membrane, so it can be recognized by microglia phosphatidylserine receptor (Yuyama and Igarashi, 2017). However, in AD, microglia activity is markedly diminished, therefore, when Aβ interacts with exosomes, it initiates the formation of large aggregates in the form of plaques (Zheng et al., 2017).

Since AD has a long asymptomatic latency period, many investigators are searching for biomarkers that can detect the disease early on, particularly in its pre-symptomatic and early stages. Different studies show that deregulation in miRNA expression and its traffic via exosomes has repercussions on AD pathogenesis (Lugli et al., 2015). miRNAs are endogenous, short, noncoding RNAs of 18–25 nucleotides which act as important post-transcriptional regulators of gene expression by binding with their target mRNA (Liu C. G. et al., 2014). Currently there are about 2,650 different miRNAs identified in all human tissues and only 34–40 miRNA are abundant in the brain (Jaber et al., 2017), among them, there are different miRNAs that bind specifically to key genes that determine the expression of APP and β-secretase, such as miR-193b, miR-101 and miR-29c respectively, these miRNAs negatively influence the generation of Aβ (Lei et al., 2015; Chen et al., 2017). Nevertheless, it has been found that expression of these miRNAs decreased with AD progression (Liu C. G. et al., 2014). Lugli et al. (2015) performed an exosomal miRNAs analysis samples of people with AD and control people. They indicated that 20 miRNAs showed differential expression in AD, and miR-342-3p, miR-141-3p, miR-342-5p, miR-23b-3p, miR-24-3p, miR-125b-5p and miR-152-3p were selected as most predictive for AD group identity. Furthermore, miR-9, miR-125b, miR-191-5p, miR-181c and let-7g-5p are thought to be the best candidates for early biomarkers (Trotta et al., 2018).

As mentioned above, defects in protein transport are closely related with neurodegeneration. In this context, it has been reported that genes like SEC22B and SEC63 which participate in protein transport and regulation of cell motion are downregulated by miR-206 in the AD, the increase of this miRNA leads to a disequilibrium of proteostasis in the brain that could result in Aβ accumulation (Zhao et al., 2016b).

On the other hand, it has been shown that the miR-132/miR-212 cluster regulates tau expression. Smith et al. (2015) showed that miR-132/miR-212 deficiency in mice leads to increased tau expression, phosphorylation and aggregation, an effect associated with an autophagy dysfunction. Conversely, treatment of AD mice with miR-132/miR-212 restore, in part, memory dysfunction and tau metabolism.

Some miRNAs like miR-139 over express in AD, this overexpression impairs the hippocampus-dependent learning and memory formation by targeting the cannabinoid receptor type 2 (Tang et al., 2017), a membrane marker of activated microglial cells, which triggers pathophysiological events involved in synaptic plasticity and neuroprotection but is also implicated in diverse roles in regulating memory, depending on memory types and brain areas (Li and Kim, 2016).

However, due to the high degree of heterogeneity in miRNAs, further in-depth investigation is required to provide easily identifiable biomarkers of AD that can be isolated from blood or its components. It is also important to consider is the possibility of using miRNA approaches like the modulation of these miRNAs for the treatment of AD.

FOCUS ON MSC-DERIVED EXOSOMES AND THEIR ROLE IN NEUROPLASTICITY

MSCs have multipotent mesodermal differentiation potential, but more importantly, they have demonstrated the ability

to promote tissue repair through the release of paracrine factors, mainly a variety of growth factors, immunomodulatory cytokines and other trophic mediators, which make them an attractive therapeutic strategy for applications in inflammatory and chronic-degenerative diseases (Donders et al., 2018). In general, administration of MSCs or conditioned media from MSCs induce structural and functional benefits that reduce apoptosis at the lesion site, module proinflammatory response, provide a permissive environment for axonal extension, enhance neurogenesis and ameliorate neurological deficits (Cantinieaux et al., 2013; Qu and Zhang, 2017; Harris et al., 2018).

The composition of exosomal cargo determines the therapeutic potential of exosomes, and the fact that these vesicles were produced by cells with a therapeutic activity already described (like MSCs), increases this potential. Besides, MSCs are the most efficient exosome producing cells (Hall et al., 2016). Based on these facts and the paracrine hypothesis which establishes that the beneficial effect of stem cell therapy is due to stimulation of resident cell by secretion of bioactive molecules and release of EV, the use of exosomes could offer several advantages over MSCs such as a superior safety profile. Since these vesicles do not replicate they are exempted from uncontrolled division, unlike MSC, which during its isolation and expansion there is a risk of genetic damage which can lead to proliferation issues and spontaneous differentiation promoting tumor formation. Furthermore, exosomes lack metabolism, so the environment where they are administered will have no impact, also, they have a nanometric size, which decreases the possibility of microvascular thrombotic events, they can be sterilized by filtration, can be stored for long periods without presenting functional loss, and above all, have similar effects to those that MSCs exert with no side effects (Nakano et al., 2016; Ophelders et al., 2016; Gomzikova and Rizvanov, 2017; Xiong et al., 2017).

Many studies have shown that exosomes derived from MSCs can reduce cognitive problems associated with various neurological disorders models such as Traumatic Brain Injury (TBI; Xiong et al., 2017), Parkinson's disease and stroke (Yang Y. et al., 2017). It has been hypothesized that these vesicles act as paracrine activity effectors of MSCs by encapsulating and transferring many functional factors, including regulatory RNAs, proteins and lipids, however, exosome release is considered a cellular adaptation mechanism and its composition, biogenesis and secretion will depend on microenvironment with which cells interact (Xin et al., 2017a). An example of this cellular adaptation was reported by Harting et al. (2018) in a coculture of MSCs with ischemic tissue extracts, which demonstrated that MSCs can respond to an inflammatory stimulus by producing exosomes with a high anti-inflammatory capacity.

Recent studies show that proteins and regulatory RNAs within MSC-derived exosomes have synergistic effects in crucial processes such as metabolism, neuroinflammation, migration of cellular precursors and processes related to angiogenesis, neurogenesis and synaptogenesis, all activated after injuries (Nakano et al., 2016; Börger et al., 2017; Collino et al., 2017). In a study conducted by Li et al. (2017) in a TBI model, it was reported that dental pulp MSC-derived exosomes alter M1 microglia polarization and promote the transition to M2 phenotype. The M1/M2 transition inhibits the proinflammatory activity of M1 and increases M2 production of anti-inflammatory factors, which decreases neuroinflammation and promotes the functional recovery of rodents; however, the mechanisms that mediates these events remains unknown (Xin et al., 2013a; Doeppner et al., 2015; Li et al., 2017). Nakano et al. (2016) showed that neurological alterations caused by streptozotocin are restored by administration of MSC-derived exosomes, nevertheless, it was reported that there was no generation of new neurons, instead, these vesicles restore and protect the function of remaining neurons by increasing neuritic density and inhibiting oxidative stress damage, mainly lipid peroxidation of neuronal membranes.

In the last years, different studies demonstrated that MSC-derived exosomes promoted neurogenesis in different mice models of disease (Xin et al., 2013b; Doeppner et al., 2015; Zhang Y. et al., 2017). In these studies, treatment with exosomes increased the number of new-born neurons in neurogenic niches (the subventricular zone (SVZ) and dentate gyrus (DG)). However, the concrete cellular and molecular mechanism of this neurogenic process still unclear.

This demonstrates the multimodal therapeutic capabilities of the MSC-derived exosomes as MSC paracrine activity effectors, although the mechanisms remain unknown.

MSC-Derived Exosomes miRNAs

As mentioned above, exosomes can transfer different RNAs to adjacent cells. Among RNAs, miRNAs are the most widely studied (Cheng et al., 2018). miRNAs are a class of non-coding RNAs that functionally inhibit their respective messenger RNAs target by binding to the 3′ untranslated regions (3′ UTR) and are implicated in many biological processes such as embryonic development, proliferation, differentiation and apoptosis (Stevanato et al., 2016). It has been described that approximately 60% of genes are more than 1,000 miRNAs targets, and 70% of those miRNAs are expressed in the brain, where they regulate different neural and glial functions (Lei et al., 2015). Also, it was demonstrated that the proportion of miRNA is higher in exosomes than in their parent cells (Zhang et al., 2015). The number and type of miRNA within the exosomes is not a random process, instead, the cells selectively group the miRNAs, however, the process of packing RNAs into exosomes is poorly understood (Stevanato et al., 2016). Nevertheless, there are potential ways of sorting miRNAs into exosomes like the neural sphingomyelinase 2, the miRNA induced silencing complex and the miRNA motif sumoylation pathways, however, the underlying mechanisms remain unclear (Zhang et al., 2015).

Several *in vitro* and *in vivo* studies indicate that MSC exosomes transfer functional miRNAs to neural cells and promote neuritic remodeling and plasticity, as well as inhibit apoptosis, which subsequently promotes functional recovery (Xin et al., 2013b, 2017b; Cheng et al., 2018). Few studies have identified a single exosome cargo component that contributes to observed effects (Börger et al., 2017). For example, Xin et al. (2017b) demonstrated that exosomes enriched with miR-133b promote neurovascular plasticity and also reported that this

miRNA increases secondary release of exosomes from astrocytes, which considerably enhances neuritic growth, however, they do not exclude the possibility that other cells are influenced by miR-133b. Baglio et al. (2015) analyzed MSC miRNA profiles of bone marrow and adipose tissue, among these miRNAs, there are some that are involved in MSC biology, such as miR-486 that regulates cellular senescence, or miR-143 with a key role in MSC immune response modulation, additionally, other miRNAs were identified, such as miR-191, miR-222, miR-21 and let-7a related to cell cycle progression, proliferation and angiogenesis modulation (Chen et al., 2010; Clark et al., 2014; Baglio et al., 2015).

On the other hand, it has been reported that exosomes also contain miR-98, miR-155 and miR-125a which have antiapoptotic activity (Ma et al., 2016; Cheng et al., 2018). Cheng et al. (2018), showed that in chronic inflammation and apoptotic conditions, miR-21 levels decrease considerably, however, MSCs in this condition secrete exosomes with high levels of miR21, which reduce apoptosis of cells that are in an environment of chronic inflammation. Furthermore, they demonstrated that miR-21 can bind to messenger RNA 3′ UTR of PTEN, main inhibitor of the PI3K/Akt survival pathway in apoptosis mediated by p53 and phosphatidylinositol. Therefore miR-21 possibly promotes cell survival by inhibiting PTEN during apoptosis, triggering the activation of Akt and Bcl-2 and the decrease of Bad, Bax and caspase-3, eventually inhibiting apoptosis.

The miRNA-miR-17-92 cluster, formed by miR-17, miR-18a, miR-19a, miR-19b, miR-20a and miR-92a, has shown to be implicated in neuritic remodeling and neurogenesis as established by Xin et al. (2017a). This cluster, like miR21, targets PTEN, allowing the activation of Akt and mTOR, which phosphorylate GSK-3β, inhibiting its function. GSK-3β inactivation has been reported to stimulate axonal growth and central nervous system recovery (Eldar-Finkelman and Martinez, 2011; Xin et al., 2017a). Moreover, it has been described that MSC exosomes assist in neural differentiation by miR-124 delivering to neural precursor cells (NPCs). This miRNA suppresses Sox9 expression, implied in NPC multipotent capacity and maintenance, hence the effect of miR-124 on Sox9 promotes NPC differentiation (Lee et al., 2014; Yang J. et al., 2017).

Understanding miRNA-regulated molecular mechanisms and their impact on the brain can likely be translated into therapies with positive clinical impact for AD and other neurodegenerative disorders in the future.

MSC-Derived Exosomes Proteins

Similar to miRNAs, proteins from exosomal cargo are important effectors of these vesicles. Currently, more than 900 proteins have been identified within MSC-derived exosomes (Kalra et al., 2012; Keerthikumar et al., 2016). Exosomal proteins can act as signaling molecules, receptors, cell adhesion molecules among other functions. For example, the expression of proteins such as nestin, neuro-D, growth-associated protein 43, synaptophysins, VEGF, FGF promote events such as neural development, synaptogenesis and angiogenesis (Chopp and Li, 2002). Katsuda et al. (2013) indicated that MSC exosomes from adipose tissue contain neprilysin, an enzyme capable of degrading Aβ, and in co-culture with cells designed for Aβ exacerbated production, these exosomes significantly reduced levels of Aβ1–40 and 1–42.

In different neurodegenerative disease models, it has been reported that MSCs interact with NPC in neurogenic niches of SVZ of lateral ventricles and the hippocampus DG through exosomes (Lee et al., 2013; Zhang and Chopp, 2015; Xin et al., 2017b; Yang Y. et al., 2017). However, the mechanisms by which exosomes interact with NPC and modify their behavior to promote neurogenesis, among other neuroplastic events, have not yet been determined. Nevertheless, some authors have associated some components with the activation (see **Table 1**), of the chemokine ligand (motif cc) 2 (CCL2), that functions as a neuronal activity modulator. MSCs release CCL2 to stimulate proliferation, migration and differentiation of NPC to neural and glial cells (Liu et al., 2007; Lee et al., 2013).

Another identified component is Sirtuin1 (SIRT1), which regulates transcription factors and cofactor deacetylation involved in angiogenesis, inflammation, response to oxidative stress and in neural development, associated with NPC proliferation and differentiation (Hu et al., 2014). SIRT1 forms a complex with Hairy/enhancer of Split 1 (Hes1), a transcriptional repressor of Mash1, responsible for the activation of neuronal specific transcription program. Under oxidizing conditions, this SIRT1/Hes1 complex deacetylates Mash1 promoter and recruits other co-repressors such as TLE1, which block neuronal differentiation, whereas under reducing conditions the SIRT1/Hes1 complex is not formed, therefore Hes1 recruits transcriptional activators such as the CREB binding protein to the Mash1 promoter, resulting in a neural destiny of NPC (Libert et al., 2008).

McBride et al. (2017) found that MSC-derived exosomes transport Wnt3a proteins associated with the outer face of the exosomal membrane. This allows the activation of the Wnt/β catenin signaling pathway, the main canonical signaling process that regulates adult neurogenesis (Yin et al., 2007). It has been reported that this signaling increases in the hippocampus DG after the administration of MSC in TBI models and improves cognitive deficits, as a result of potentiation of neurogenesis. It has been described that this signaling increases in hippocampus DG after MSC administration in TBI models and improves cognitive deficits, associated with the potentiation of neurogenesis (Zhao et al., 2016a; McBride et al., 2017). Wnt3a and its active form β-catenin expression promote NPC expansion and differentiation into synaptically active neurons, whereas the absence of Wnt3a inhibits the differentiation of NPC to neurons (Yin et al., 2007).

Rodriguez-Grande et al. (2015) studied the effect of Pentraxin 3 (PTX3) protein on neurogenesis using a stroke model and reported that PTX3 is a key regulator of angiogenesis and neurogenesis, however, the molecular mechanisms involved have not been described yet. PTX3 is a protein with direct involvement in neuroinflammation in acute phases (Ummenthum et al., 2016). The inhibition of PTX3 reduces the number of capillaries in reperfusion areas after ischemia as well as the formation of new neurons (Rodriguez-Grande et al., 2015).

In the exosomal cargo, ephrins, are a pivotal regulator of the developmental process of axon guidance, cell migration, synapse

TABLE 1 | Polypeptides identified in exosomes derivate from Mesenchymal Stem Cells (MSC).

Protein name	Gene	UniProtKB[a] Acc. No.	MW[b] (kDa)	pI[C]
1. C-C motif chemokine 2 (CCL2)	*CCL2*	P13500	11.02	9.40
2. NAD-dependent protein deacetylase sirtuin-1	*SIRT1*	Q96EB6	81.68	4.55
3. Protein Wnt-3a	*WNT3A*	P56704	39.36	8.52
4. Pentraxin-related protein PTX3	*PTX3*	P26022	41.97	4.94
5. Thrombospondin-1	*THBS1*	P07996	129.38	4.71
6. Growth/differentiation factor 15	*GDF15*	Q99988	34.14	9.79
7. Cell division control protein 42	*CDC42*	P60953	21.25	6.16
8. Dihydropyrimidinase-related protein 2	*DPYSL2*	Q17555	62.29	5.95
9. Prosaposin	*PSAP*	P07602	58.11	5.06
10. Brain-derived neurotrophic factor	*BDNF*	P23560	27.81	9.01
11. Nerve growth factor	*NGF*	P01138	26.95	9.94
12. Fibroblast growth factor 2	*FGF2*	P09038	30.77	11.18
13. Stromal cell-derived factor 1	*CXCL12*	P48061	10.66	9.92
14. Ephrin A-2	*EFNA2*	O43921	23.87	6.99
15. Vascular endothelial growth factor	*VEGFA*	P15692	27.04	9.21
16. Microtubule-associated protein tau	*MAPT*	P10636	78.92	6.25
17. Beta-secretase 1	*BACE1*	P56817	55.76	5.31
18. Amyloid-beta A4 protein	*APP*	P05067	86.94	4.73
19. Prion protein	*PRNP*	P04156	27.66	9.13
20. CD81	*CD81*	P60033	25.80	5.09
21. Tetraspanin-6	*TSPAN6*	O43657	27.56	8.44
22. CD9	*CD9*	P21926	25.41	6.80
23. Neutral sphingomyelinase 2	*SMPD3*	Q9NY59	71.03	5.52

[a]*UniProtKB Acc. Numb., UniProt Knowledgebase Accession Number.* [b]*MW, Molecular weight.* [C]*pI, Isoelectric point.*

formation and vascular formation but it is unknown the role they play in the adult organism (Wilkinson, 2001), to this account Holmberg et al. (2005) studied the role of A-class ephrins in the neural stem cell niche, and reported that ephrin-A2 (EFNA2) negatively regulates neural progenitor proliferation. Lack of expression EFNA2 and its receptor Eph7A result in active and ongoing neurogenesis, suggesting that neural cell replacement therapies may be achieved by modification of ephrin signaling pathways.

Dihydropyrimidinase-like 2 (DPYSL2) best known as collapsing response mediator protein 2 also is found in the exosomal cargo. DPYSL2 is a member of a family named for their roles in axonal growth cone collapse. Its main function is stabilizing microtubules, promoting neuritic outgrowth and modulating signaling processes (Pham et al., 2016). In the process of NPC senescence, the expression of DPYSL2 decreases with the age, consistent with the involvement in the neurodegeneration processes (Wang et al., 2016).

Prosaposin (PSAP) is another protein found in exosomes (Li et al., 2010). PSAP is suggested to be an essential neurotrophic factor since its secretion stimulates proliferation and maturation of immature neurons in the hippocampus DG, as well as provides protection against apoptosis. It was reported that deficiency of PSAP precedes massive neuronal loss in neurotoxic environments (Morishita et al., 2014; Nabeka et al., 2017).

It has been recently demonstrated that THBS1 is present in the secretome of MSC and exosomes (Maumus et al., 2017). Blake et al. (2008) show that thrombospondin-1 (THBS1) is a physiological ligand for ApoER2 like Reelin. This study demonstrated that the first alternative physiological ligand for ApoER2 and VLDLR is capable of inducing Dab1 phosphorylation, but no other key events of the Reelin signaling pathway. Blake et al. (2008) also showed that THBS1 increases the length of neuronal precursor chains and stabilizes the structure of established chains along the rostral migratory stream. These functions of THBS1 in neuronal migration could help replace neural cells in injured zones and ameliorate neurological deficits through the administration of exosomes.

An analysis of a bioinformatic database was performed in order to identify and classify exosomal cargo of MSC according to their biologic function and their interaction in the secretome. The 23 proteins described in **Table 1** were classified by Protein Analysis Through Evolutionary Relationships (PANTHER) system (Mi et al., 2017) and were grouped according to their involvement in the different cellular biological processes. In this first approach, we found 12 different biological processes (**Figure 1**; a protein can participate in more than one cellular process). From these 12 biological processes, four main groups are mentioned as; (a) cellular processes with 17 members; (b) response to a stimulus with 12 members; (c) biological regulation with 11 members; and (d) development processes with nine members.

In the cellular processes group, there are 13 proteins involved in cellular communication and four proteins with a role in the movement of cellular components. The main proteins implicated in cellular communication are members of CXC chemokine family such as CCL2 (UniProt code P13500) and CXCL2 (UniProt code P19875; The UniProt Consortium, 2018). A recent work in murine models of neurodegeneration has associated these two proteins in cellular migration processes and enhanced proliferation and differentiation of neural precursors (Hong et al., 2015; Wang F. et al., 2017). In addition, another member of this family, CXCR4 expressed by neurons (UniProt code P61073) has been linked to inflammatory processes by activating microglia expressing CCR2 (UniProt

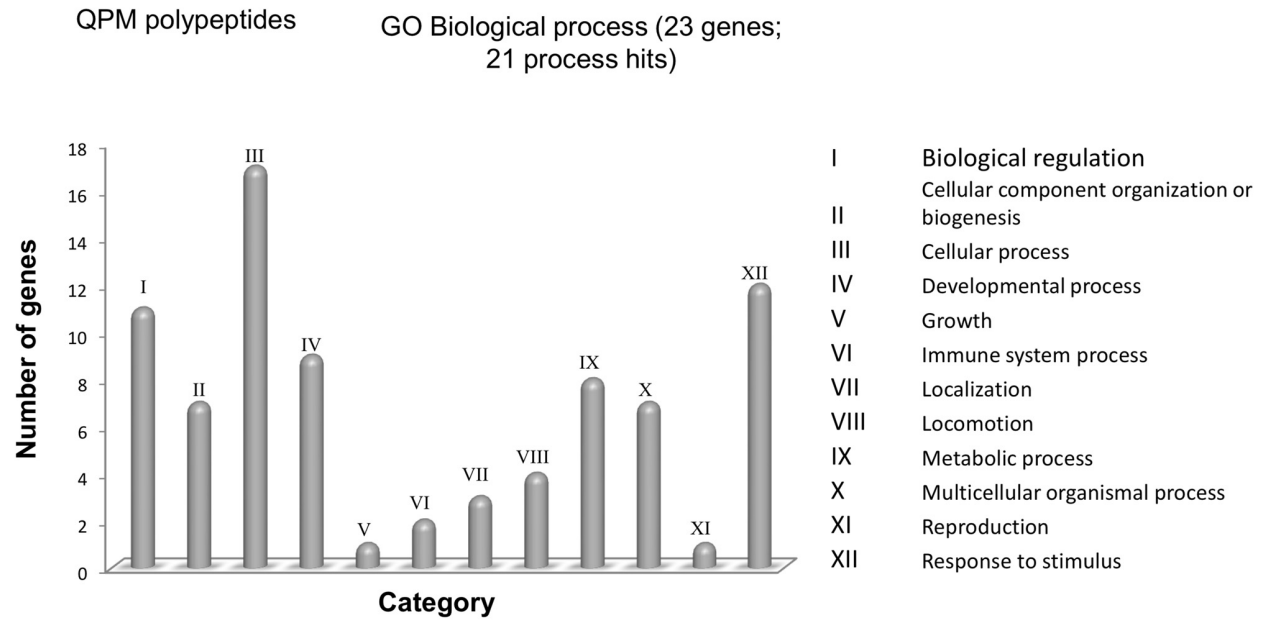

FIGURE 1 | Functional classification with PANTHER of the polypeptides found in exosomes. The UniProtKB IDs of proteins were submitted to the PANTHER database for their classification in Gene Ontology (GO) according to Biological. *X*-axis, categories of proteins. *Y*-axis, number of genes contained in each category.

code P41597; Liu C. et al., 2014). One study showed that knockout of CCR2 in an AD transgenic mouse model decreases microglia activation and increases Aβ accumulation (Kiyota et al., 2013). This demonstrates the role of microglia in Aβ clearance and how its deficiency could speed up AD progression.

The second most important biological process was response to stimuli, mainly the regulation of protein phosphorylation, where the neurotrophic factors VEGF (UniProt code P15692), NGF (UniProt code P01138) and BDNF (UniProt code P23560) that modulate cell death cascades, increase production of proteins responsible for proliferation and maintenance of neurons. These factors also have roles in the outgrowth of dendrites and stabilizing synapses between neurons. In recent years, these neurotrophins have been considered as key regulators of adult neurogenesis and the changes in expression have been related to occurrence and development of cognitive impairments, even though the molecular mechanism is not completely elucidated (Ke and Zhang, 2013; Budni et al., 2015; Vilar and Mira, 2016). However, more data and support are needed to elucidate the mechanisms of neurotrophin imbalance and dysregulation in AD as well as possible therapeutic applications.

On the other hand, the main molecular functions identified for these molecules are related to catalytic activity, signal transduction and protein binding. In these cases, protein binding activity is the most representative molecular function for 12 proteins implied. In this group neurotrophins can also be found, due to their activity, which is mediated mainly by receptor phosphorylation which subsequently promotes the expression of proteins involved in the proliferation of the NPC, maintenance of the cell and ensuring neuronal survival (Bolijn and Lucassen, 2015).

This classification allowed us to generate a network of known and predicted protein-protein interaction using the STRING program (Szklarczyk et al., 2017). The interactome network represented in **Figure 2** describes the interactome with a minimum required interaction score of 0.70 (high confidence) and highlights the biological processes in the regulation of axon extension (shown in red) with seven members in it and a false discovery rate (FDR) of $4.78e^{-09}$.

The second most important process for our analysis is axonogenesis with 10 members and an FDR of $8.91e^{-08}$, shown in blue. Interesting members related to axonogenesis are tau (MAPT UniProt code P10636) and cell division control protein 42 (CDC42 UniProt code P60953). It is known that tau is accumulated in the growth cone and its presence persists during the axonal elongation, however, understand the role of tau in axonogenesis is complicated because tau exists in different phosphorylation states and these states influence the subsequent localization of tau within neurons without implication of its role in the progression of AD (Zmuda and Rivas, 2000). CDC42 has roles in axon guidance and neurite formation particularly on growth cone through Robo signaling activation and actin filaments regulation (Matsuura et al., 2004). The CXCL12 and the neurotrophins BDNF and NGF are also associated with axonogenesis. Almost all proteins exert their function by acting as ligands (shown in green with an FDR $4.02e^{-08}$).

The proteins of interactome network are usually found in the extracellular space (shown in pink with an FDR $1.8e^{-06}$) where they can modulate the processes like the responses to stimuli previously described. The main pathway of this interactome

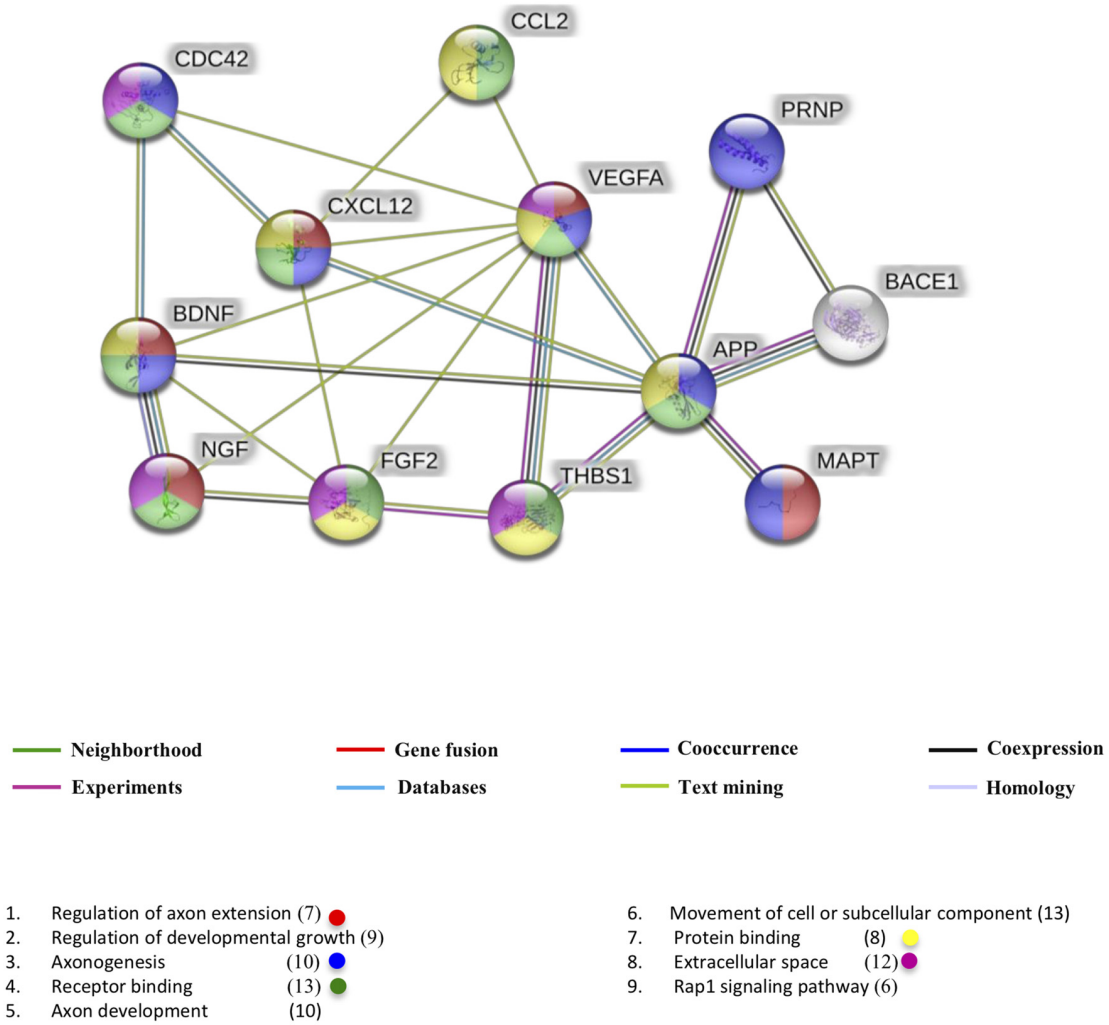

FIGURE 2 | Interactome of polypeptides found in common exosomes related with a beta and tau protein. UniProtKB accession numbers were submitted to the String program to identify the predicted functional network. Lines in color represent different pieces of evidence for each identified interaction: red line, fusion; green line, neighborhood; blue line, cooccurrence; purple line, experimental; yellow line, text mining; light blue line, database; black line, coexpression.

network was the Rap1 signaling pathway (FDR $2.3e^{-05}$) which has been reported to regulate vesicle secretion, cytoskeletal dynamics, proliferation and cell adhesion, (Shibasaki et al., 2007; van Hooren et al., 2012; Zhang Y.-L. et al., 2017). Possibly this way of signaling supports the delivery of the exosomal cargo.

On the other hand, it is interesting that VEGF participates in all analyzed processes. It has been reported that this neurotrophic factor evokes elements of brain plasticity like neurogenesis and neural progenitor cells migration (Chen et al., 2005). According to the interaction diagram, VEGF has synergistic effects with some neurotrophins and with components that mediate axonal guidance such as CDC42 and THBS1 (UniProt code P07996). This leads us to think that possibly the synergy of the exosomal cargo promotes better therapeutic responses compared to those that a single isolated component could. It would be important to study the effects of the composition of the exosomal charge on the progression of AD in both interactions with Aβ and the tau protein, as well as the effects it could have on neuroplastic events, mainly neurogenesis and synaptogenesis.

CONCLUSION AND PERSPECTIVES

Despite the great advances in AD research, the molecular mechanisms underlying this devastating disease have not been fully unveiled. However, remarkable neuropathological studies have provided the largest contribution to the knowledge of the mechanisms involved in the pathological amyloidogenic processing of Aβ as well as hyperphosphorylated tau aggregation into paired helical filaments. Unfortunately, there remains a need to find an accurate diagnosis, in addition to generating really effective treatments; thus, it is necessary to use novel approaches to understand the molecular and cellular mechanisms of AD in order to identify new

therapeutic strategies that allow to delay, reverse or, in the best case, to avoid the normal pathological processing of this disease.

The use of proteomic study technologies plus the advent of induced pluripotent stem cells and three-dimensional culture technologies, has made it possible to generate novel *in vitro* 3D neural cell culture models that replicate AD pathologies, allowing us to explore new perspectives on the origin of the disease and its progression, for example the influence of some proteins in the misfolding of Aβ and the tau protein and its resistance to degradation. These *in vitro* 3D neural cell culture models also could explore the biochemical composition and modulation of exosomes and their role in disease progression. These advances have revolutionized the potential to generate novel platforms that can be used to study the mechanisms of pathology or to develop novel diagnostic and therapeutic tools in a brain-like environment.

Currently, MSC therapy has emerged as a promising strategy for treating different neurodegenerative disorders via tissue repair, however, the risks of tumor formation, cellular rejection and thrombosis in MSCs transplantation remain unresolved. Currently, the cell-free therapy using MSC-derived exosomes might constitute an alternative because of their advantages over MSCs. There are different studies indicating that exosomes act as an important mediator of the information exchange between MSCs and NPC. The exchange of miRNA and proteins between cell to cell through exosomes can reduce the neuroinflammation, promote neurogenesis and angiogenesis rescue learning impairments and improve functional recovery. However, the concrete mechanisms involved in the positive effects induced by MSCs-derived exosomes in AD are still unclear. Given a variety of functions and multiple molecules in exosomal cargo, is necessary that other studies analyze all interaction and understand the relation between the intrinsic potential that is glimpsed in the combination of the use of exosome therapy and the participation of their cargo (miRNA and/or proteins) combined with the proteomic and bioinformatic analysis of those pathways that participate in this therapeutic modulation.

The bioinformatic analysis performed, allowed us to focus on possible candidates with an important role in neurogenesis and neuroplasticity or even identify some potential pathways implicated in AD's patient's progress. This would allow us to use exosomes with different therapeutic approaches, for example, the modification of exosomes with some classes of proteins or miRNAs, with effects on tissue repair, maintenance of cellular homeostasis or impairing the disease progression.

AUTHOR CONTRIBUTIONS

ER-Z, MH-S, BM, YG-M, AM-A and AC-A: equal contribution for the literature search, writing and correcting of this review article.

FUNDING

The present work was sponsored by CONACYT scholarship #487713 and by FondoMixto de Ciencia y Tecnología del Estado de Jalisco grant JAL-2014-0-250508.

ACKNOWLEDGMENTS

We also would like to thank Ean Hundley and Estefanía Vázquez from CIATEJ/Peace Corps and University of Guadalajara, respectively for their valuable efforts in editing the English language of the manuscript.

REFERENCES

Abels, E. R., and Breakefield, X. O. (2016). Introduction to extracellular vesicles: biogenesis, RNA cargo selection, content, release, and uptake. *Cell. Mol. Neurobiol.* 36, 301–312. doi: 10.1007/s10571-016-0366-z

Angeloni, N. L., McMahon, K. M., Swaminathan, S., Plebanek, M. P., Osman, I., Volpert, O. V., et al. (2016). Pathways for modulating exosome lipids identified by high-density lipoprotein-like nanoparticle binding to scavenger receptor type B-1. *Sci. Rep.* 6:22915. doi: 10.1038/srep22915

Baglio, S. R., Rooijers, K., Koppers-Lalic, D., Verweij, F. J., Pérez Lanzón, M., Zini, N., et al. (2015). Human bone marrow- and adipose-mesenchymal stem cells secrete exosomes enriched in distinctive miRNA and tRNA species. *Stem Cell Res. Ther.* 6:127. doi: 10.1186/s13287-015-0116-z

Bang, C., and Thum, T. (2012). Exosomes: new players in cell-cell communication. *Int. J. Biochem. Cell Biol.* 44, 2060–2064. doi: 10.1016/j.biocel.2012.08.007

Baumann, K., Mandelkow, E.-M., Biernat, J., Piwnica-Worms, H., and Mandelkow, E. (1993). Abnormal Alzheimer-like phosphorylation of tau-protein by cyclin-dependent kinases cdk2 and cdk5. *FEBS Lett.* 336, 417–424. doi: 10.1016/0014-5793(93)80849-p

Beer, K. B., and Wehman, A. M. (2017). Mechanisms and functions of extracellular vesicle release *in vivo*—What we can learn from flies and worms. *Cell Adh. Migr.* 11, 135–150. doi: 10.1080/19336918.2016.1236899

Blake, S. M., Strasser, V., Andrade, N., Duit, S., Hofbauer, R., Schneider, W. J., et al. (2008). Thrombospondin-1 binds to ApoER2 and VLDL receptor and functions in postnatal neuronal migration. *EMBO J.* 27, 3069–3080. doi: 10.1038/emboj.2008.223

Bolijn, S., and Lucassen, P. J. (2015). How the body talks to the brain; peripheral mediators of physical activity-induced proliferation in the adult hippocampus. *Brain Plasticity* 1, 5–27. doi: 10.3233/bpl-150020

Börger, V., Bremer, M., Ferrer-Tur, R., Gockeln, L., Stambouli, O., Becic, A., et al. (2017). Mesenchymal stem/stromal cell-derived extracellular vesicles and their potential as novel immunomodulatory therapeutic agents. *Int. J. Mol. Sci.* 18:E1450. doi: 10.3390/ijms18071450

Braak, H., and Braak, E. (1996). Evolution of the neuropathology of Alzheimer's disease. *Acta Neurol. Scand. Suppl.* 165, 3–12. doi: 10.1111/j.1600-0404.1996.tb05866.x

Budni, J., Bellettini-Santos, T., Mina, F., Garcez, M. L., and Zugno, A. I. (2015). The involvement of BDNF, NGF and GDNF in aging and Alzheimer's disease. *Aging Dis.* 6, 331–341. doi: 10.14336/ad.2015.0825

Camacho, L., Guerrero, P., and Marchetti, D. (2013). MicroRNA and protein profiling of brain metastasis competent cell-derived exosomes. *PLoS One* 8:e73790. doi: 10.1371/journal.pone.0073790

Cantinieaux, D., Quertainmont, R., Blacher, S., Rossi, L., Wanet, T., Noël, A., et al. (2013). Conditioned medium from bone marrow-derived mesenchymal stem cells improves recovery after spinal cord injury in rats: an original strategy to avoid cell transplantation. *PLoS One* 8:e69515. doi: 10.1371/journal.pone.0069515

Chen, T. S., Lai, R. C., Lee, M. M., Choo, A. B., Lee, C. N., and Lim, S. K. (2010). Mesenchymal stem cell secretes microparticles enriched in pre-microRNAs. *Nucleic Acids Res.* 38, 215–224. doi: 10.1093/nar/gkp857

Chen, J., Zhang, C., Jiang, H., Li, Y., Zhang, L., Robin, A., et al. (2005). Atorvastatin induction of VEGF and BDNF promotes brain plasticity after stroke in mice. *J. Cereb. Blood Flow Metab.* 25, 281–290. doi: 10.1038/sj.jcbfm.9600034

Chen, J. J., Zhao, B., Zhao, J., and Li, S. (2017). Potential roles of exosomal micrornas as diagnostic biomarkers and therapeutic application in Alzheimer's disease. *Neural Plast.* 2017:7027380. doi: 10.1155/2017/7027380

Cheng, L., Wu, S., Zhang, K., Qing, Y., and Xu, T. (2017). A comprehensive overview of exosomes in ovarian cancer: emerging biomarkers and therapeutic strategies. *J. Ovarian Res.* 10:73. doi: 10.1186/s13048-017-0368-6

Cheng, X., Zhang, G., Zhang, L., Hu, Y., Zhang, K., Sun, X., et al. (2018). Mesenchymal stem cells deliver exogenous miR-21 via exosomes to inhibit nucleus pulposus cell apoptosis and reduce intervertebral disc degeneration. *J. Cell. Mol. Med.* 22, 261–276. doi: 10.1111/jcmm.13316

Chiarini, A., Armato, U., Gardenal, E., Gui, L., and Dal Prà, I. (2017). Amyloid β-exposed human astrocytes overproduce phospho-tau and overrelease it within exosomes, effects suppressed by calcilytic NPS 2143-further implications for Alzheimer's therapy. *Front. Neurosci.* 11:217. doi: 10.3389/fnins.2017.00217

Cho, H., Choi, J. Y., Hwang, M. S., Kim, Y. J., Lee, H. M., Lee, H. S., et al. (2016). *In vivo* cortical spreading pattern of tau and amyloid in the Alzheimer disease spectrum. *Ann. Neurol.* 80, 247–258. doi: 10.1002/ana.24711

Chopp, M., and Li, Y. (2002). Treatment of neural injury with marrow stromal cells. *Lancet Neurol.* 1, 92–100. doi: 10.1016/s1474-4422(02)00040-6

Clark, E. A., Kalomoiris, S., Nolta, J. A., and Fierro, F. A. (2014). Concise review: MicroRNA function in multipotent mesenchymal stromal cells. *Stem Cells* 32, 1074–1082. doi: 10.1002/stem.1623

Collino, F., Pomatto, M., Bruno, S., Lindoso, R. S., Tapparo, M., Sicheng, W., et al. (2017). Exosome and microvesicle-enriched fractions isolated from mesenchymal stem cells by gradient separation showed different molecular signatures and functions on renal tubular epithelial cells. *Stem Cell Rev.* 13, 226–243. doi: 10.1007/s12015-016-9713-1

Colombo, M., Raposo, G., and Théry, C. (2014). Biogenesis, secretion, and intercellular interactions of exosomes and other extracellular vesicles. *Annu. Rev. Cell Dev. Biol.* 30, 255–289. doi: 10.1146/annurev-cellbio-101512-122326

Correas, I., Díaz-Nido, J., and Avila, J. (1992). Microtubule-associated protein tau is phosphorylated by protein kinase C on its tubulin binding domain. *J. Biol. Chem.* 267, 15721–15728.

de Jong, O. G., Verhaar, M. C., Chen, Y., Vader, P., Gremmels, H., Posthuma, G., et al. (2012). Cellular stress conditions are reflected in the protein and RNA content of endothelial cell-derived exosomes. *J. Extracell. Vesicles* 1:18396. doi: 10.3402/jev.v1i0.18396

Dinkins, M. B., Enasko, J., Hernandez, C., Wang, G., Kong, J., Helwa, I., et al. (2016). Neutral sphingomyelinase-2 deficiency ameliorates Alzheimer's disease pathology and improves cognition in the 5XFAD mouse. *J. Neurosci.* 36, 8653–8667. doi: 10.1523/JNEUROSCI.1429-16.2016

Doeppner, T. R., Herz, J., Görgens, A., Schlechter, J., Ludwig, A. K., Radtke, S., et al. (2015). Extracellular vesicles improve post-stroke neuroregeneration and prevent postischemic immunosuppression. *Stem Cells Transl. Med.* 4, 1131–1143. doi: 10.5966/sctm.2015-0078

Donders, R., Bogie, J. F. J., Ravanidis, S., Gervois, P., Vanheusden, M., Marée, R., et al. (2018). Human wharton's jelly-derived stem cells display a distinct immunomodulatory and proregenerative transcriptional signature compared to bone marrow-derived stem cells. *Stem Cells Dev.* 27, 65–84. doi: 10.1089/scd.2017.0029

Drommelschmidt, K., Serdar, M., Bendix, I., Herz, J., Bertling, F., Prager, S., et al. (2017). Mesenchymal stem cell-derived extracellular vesicles ameliorate inflammation-induced preterm brain injury. *Brain Behav. Immun.* 60, 220–232. doi: 10.1016/j.bbi.2016.11.011

Eitan, E., Suire, C., Zhang, S., and Mattson, M. P. (2016). Impact of lysosome status on extracellular vesicle content and release. *Ageing Res. Rev.* 32, 65–74. doi: 10.1016/j.arr.2016.05.001

Eldar-Finkelman, H., and Martinez, A. (2011). GSK-3 inhibitors: preclinical and clinical focus on CNS. *Front. Mol. Neurosci.* 4:32. doi: 10.3389/fnmol.2011.00032

Emmanouilidou, E., Melachroinou, K., Roumeliotis, T., Garbis, S. D., Ntzouni, M., Margaritis, L. H., et al. (2010). Cell-produced α-synuclein is secreted in a calcium-dependent manner by exosomes and impacts neuronal survival. *J. Neurosci.* 30, 6838–6851. doi: 10.1523/JNEUROSCI.5699-09.2010

Escola, J. M., Kleijmeer, M. J., Stoorvogel, W., Griffith, J. M., Yoshie, O., and Geuze, H. J. (1998). Selective enrichment of tetraspan proteins on the internal vesicles of multivesicular endosomes and on exosomes secreted by human B-lymphocytes. *J. Biol. Chem.* 273, 20121–20127. doi: 10.1074/jbc.273.32.20121

Falker, C., Hartmann, A., Guett, I., Dohler, F., Altmeppen, H., Betzel, C., et al. (2016). Exosomal cellular prion protein drives fibrillization of amyloid β and counteracts amyloid β-mediated neurotoxicity. *J. Neurochem.* 137, 88–100. doi: 10.1111/jnc.13514

Gauthier, S. A., Pérez-González, R., Sharma, A., Huang, F. K., Alldred, M. J., Pawlik, M., et al. (2017). Enhanced exosome secretion in Down syndrome brain—a protective mechanism to alleviate neuronal endosomal abnormalities. *Acta Neuropathol. Commun.* 5:65. doi: 10.1186/s40478-017-0466-0

Ghosh, A., and Giese, K. P. (2015). Calcium/calmodulin-dependent kinase II and Alzheimer's disease. *Mol. Brain* 8:78. doi: 10.1186/s13041-015-0166-2

Goetzl, E. J., Mustapic, M., Kapogiannis, D., Eitan, E., Lobach, I. V., Goetzl, L., et al. (2016). Cargo proteins of plasma astrocyte-derived exosomes in Alzheimer's disease. *FASEB J.* 30, 3853–3859. doi: 10.1096/fj.201600756r

Gomzikova, M. O., and Rizvanov, A. A. (2017). Current trends in regenerative medicine: from cell to cell-free therapy. *BioNanoScience* 7, 240–245. doi: 10.1007/s12668-016-0348-0

Greenberg, S. M., Koo, E. H., Selkoe, D. J., Qiu, W. Q., and Kosik, K. S. (1994). Secreted β-amyloid precursor protein stimulates mitogen-activated protein kinase and enhances tau phosphorylation. *Proc. Natl. Acad. Sci. U S A* 91, 7104–7108. doi: 10.1073/pnas.91.15.7104

Grundke-Iqbal, I., Iqbal, K., Tung, Y. C., Quinlan, M., Wisniewski, H. M., and Binder, L. I. (1986). Abnormal phosphorylation of the microtubule-associated protein tau (tau) in Alzheimer cytoskeletal pathology. *Proc. Natl. Acad. Sci. U S A* 83, 4913–4917. doi: 10.1073/pnas.83.13.4913

Guduric-Fuchs, J., O'Connor, A., Camp, B., O'Neill, C. L., Medina, R. J., and Simpson, D. A. (2012). Selective extracellular vesicle-mediated export of an overlapping set of microRNAs from multiple cell types. *BMC Genomics* 13:357. doi: 10.1186/1471-2164-13-357

Guix, F. X., Sannerud, R., Berditchevski, F., Arranz, A. M., Horré, K., Snellinx, A., et al. (2017). Tetraspanin 6: a pivotal protein of the multiple vesicular body determining exosome release and lysosomal degradation of amyloid precursor protein fragments. *Mol. Neurodegener.* 12:25. doi: 10.1186/s13024-017-0165-0

Hall, J., Prabhakar, S., Balaj, L., Lai, C. P., Cerione, R. A., and Breakefield, X. O. (2016). Delivery of therapeutic proteins via extracellular vesicles: review and potential treatments for Parkinson's disease, glioma, and schwannoma. *Cell. Mol. Neurobiol.* 36, 417–427. doi: 10.1007/s10571-015-0309-0

Harris, V. K., Stark, J., Vyshkina, T., Blackshear, L., Joo, G., Stefanova, V., et al. (2018). Phase I trial of intrathecal mesenchymal stem cell-derived neural progenitors in progressive multiple sclerosis. *EBioMedicine* 29, 23–30. doi: 10.1016/j.ebiom.2018.02.002

Harting, M. T., Srivastava, A. K., Zhaorigetu, S., Bair, H., Prabhakara, K. S., Toledano Furman, N. E., et al. (2018). Inflammation-stimulated mesenchymal stromal cell-derived extracellular vesicles attenuate inflammation. *Stem Cells* 36, 79–90. doi: 10.1002/stem.2730

Henne, W. M., Stenmark, H., and Emr, S. D. (2013). Molecular mechanisms of the membrane sculpting ESCRT pathway. *Cold Spring Harb. Perspect. Biol.* 5:a016766. doi: 10.1101/cshperspect.a016766

Holmberg, J., Armulik, A., Senti, K.-A., Edoff, K., Spalding, K., Momma, S., et al. (2005). Ephrin-A2 reverse signaling negatively regulates neural progenitor proliferation and neurogenesis. *Genes Dev.* 19, 462–471. doi: 10.1101/gad.326905

Hong, Y. R., Lee, H., Park, M. H., Lee, J. K., Lee, J. Y., Suh, H. D., et al. (2015). CCL2 induces neural stem cell proliferation and neuronal differentiation in Niemann-Pick type C mice. *J. Vet. Med. Sci.* 77, 693–699. doi: 10.1292/jvms.14-0352

Hu, B., Guo, Y., Chen, C., Li, Q., Niu, X., Guo, S., et al. (2014). Repression of SIRT1 promotes the differentiation of mouse induced pluripotent stem cells into neural stem cells. *Cell. Mol. Neurobiol.* 34, 905–912. doi: 10.1007/s10571-014-0071-8

Hurley, J. H., and Hanson, P. I. (2010). Membrane budding and scission by the ESCRT machinery: it's all in the neck. *Nat. Rev. Mol. Cell Biol.* 11, 556–566. doi: 10.1038/nrm2937

Ikezu, T., Ikezu, S., Varnum, M., Wolozin, B., Butovsky, O., Kügler, S., et al. (2016). Microglial exosomes propagate tau protein from the entorhinal cortex to the

hippocampus: an early pathophysiology of Alzheimer's disease. *Alzheimers Dement.* 12, P339–P340. doi: 10.1016/j.jalz.2016.06.624

Jaber, N., Mohd-Naim, N., Wang, Z., DeLeon, J. L., Kim, S., Zhong, H., et al. (2016). Vps34 regulates Rab7 and late endocytic trafficking through recruitment of the GTPase-activating protein Armus. *J. Cell Sci.* 129, 4424–4435. doi: 10.1242/jcs.192260

Jaber, V., Zhao, Y., and Lukiw, W. J. (2017). Alterations in micro RNA-messenger RNA (miRNA-mRNA) coupled signaling networks in sporadic Alzheimer's disease (AD) hippocampal CA1. *J. Alzheimers Dis. Parkinsonism* 7:312. doi: 10.4172/2161-0460.1000312

Joshi, P., Benussi, L., Furlan, R., Ghidoni, R., and Verderio, C. (2015). Extracellular vesicles in Alzheimer's disease: friends or foes? Focus on Aβ-vesicle interaction. *Int. J. Mol. Sci.* 16, 4800–4813. doi: 10.3390/ijms16034800

Kalra, H., Simpson, R. J., Ji, H., Aikawa, E., Altevogt, P., Askenase, P., et al. (2012). Vesiclepedia: a compendium for extracellular vesicles with continuous community annotation. *PLoS Biol.* 10:e1001450. doi: 10.1371/journal.pbio.1001450

Katsuda, T., Tsuchiya, R., Kosaka, N., Yoshioka, Y., Takagaki, K., Oki, K., et al. (2013). Human adipose tissue-derived mesenchymal stem cells secrete functional neprilysin-bound exosomes. *Sci. Rep.* 3:1197. doi: 10.1038/srep01197

Ke, X.-J., and Zhang, J.-J. (2013). Changes in HIF-1α, VEGF, NGF and BDNF levels in cerebrospinal fluid and their relationship with cognitive impairment in patients with cerebral infarction. *J. Huazhong Univ. Sci. Technolog. Med. Sci.* 33, 433–437. doi: 10.1007/s11596-013-1137-4

Keerthikumar, S., Chisanga, D., Ariyaratne, D., Al Saffar, H., Anand, S., Zhao, K., et al. (2016). ExoCarta: a web-based compendium of exosomal cargo. *J. Mol. Biol.* 428, 688–692. doi: 10.1016/j.jmb.2015.09.019

Kessels, H. W., Nguyen, L. N., Nabavi, S., and Malinow, R. (2010). The prion protein as a receptor for amyloid-β. *Nature* 466, E3–E4; discussion E4–E5. doi: 10.1038/nature09217

Kim, H. J., Lee, J. H., and Kim, S. H. (2010). Therapeutic effects of human mesenchymal stem cells on traumatic brain injury in rats: secretion of neurotrophic factors and inhibition of apoptosis. *J. Neurotrauma* 27, 131–138. doi: 10.1089/neu.2008.0818

Kiyota, T., Gendelman, H. E., Weir, R. A., Higgins, E. E., Zhang, G., and Jain, M. (2013). CCL2 affects β-amyloidosis and progressive neurocognitive dysfunction in a mouse model of Alzheimer's disease. *Neurobiol. Aging* 34, 1060–1068. doi: 10.1016/j.neurobiolaging.2012.08.009

Kizuka, Y., Kitazume, S., Fujinawa, R., Saito, T., Iwata, N., Saido, T. C., et al. (2015). An aberrant sugar modification of BACE1 blocks its lysosomal targeting in Alzheimer's disease. *EMBO Mol. Med.* 7, 175–189. doi: 10.15252/emmm.201404438

Koelsch, G. (2017). BACE1 function and inhibition: implications of intervention in the amyloid pathway of Alzheimer's disease pathology. *Molecules* 22:E1723. doi: 10.3390/molecules22101723

Kosaka, N., Iguchi, H., Yoshioka, Y., Takeshita, F., Matsuki, Y., and Ochiya, T. (2010). Secretory mechanisms and intercellular transfer of microRNAs in living cells. *J. Biol. Chem.* 285, 17442–17452. doi: 10.1074/jbc.M110.107821

Kosik, K. S., Joachim, C. L., and Selkoe, D. J. (1986). Microtubule-associated protein tau (tau) is a major antigenic component of paired helical filaments in Alzheimer disease. *Proc. Natl. Acad. Sci. U S A* 83, 4044–4048. doi: 10.1073/pnas.83.11.4044

Kurozumi, K., Nakamura, K., Tamiya, T., Kawano, Y., Kobune, M., Hirai, S., et al. (2004). BDNF gene-modified mesenchymal stem cells promote functional recovery and reduce infarct size in the rat middle cerebral artery occlusion model. *Mol. Ther.* 9, 189–197. doi: 10.1016/j.ymthe.2003.10.012

Lai, R. C., Arslan, F., Lee, M. M., Sze, N. S., Choo, A., Chen, T. S., et al. (2010). Exosome secreted by MSC reduces myocardial ischemia/reperfusion injury. *Stem Cell Res.* 4, 214–222. doi: 10.1016/j.scr.2009.12.003

Laulagnier, K., Javalet, C., Hemming, F. J., Chivet, M., Lachenal, G., Blot, B., et al. (2018). Amyloid precursor protein products concentrate in a subset of exosomes specifically endocytosed by neurons. *Cell. Mol. Life Sci.* 75, 757–773. doi: 10.1007/s00018-017-2664-0

Lauren, J., Gimbel, D. A., Nygaard, H. B., Gilbert, J. W., and Strittmatter, S. M. (2009). Cellular prion protein mediates impairment of synaptic plasticity by amyloid-β oligomers. *Nature* 457, 1128–1132. doi: 10.1038/nature07761

Lee, H. K., Finniss, S., Cazacu, S., Xiang, C., and Brodie, C. (2014). Mesenchymal stem cells deliver exogenous miRNAs to neural cells and induce their differentiation and glutamate transporter expression. *Stem Cells Dev.* 23, 2851–2861. doi: 10.1089/scd.2014.0146

Lee, H., Kang, J. E., Lee, J. K., Bae, J. S., and Jin, H. K. (2013). Bone-marrow-derived mesenchymal stem cells promote proliferation and neuronal differentiation of Niemann-Pick type C mouse neural stem cells by upregulation and secretion of CCL2. *Hum. Gene Ther.* 24, 655–669. doi: 10.1089/hum.2013.001

Lei, X., Lei, L., Zhang, Z., Zhang, Z., and Cheng, Y. (2015). Downregulated miR-29c correlates with increased BACE1 expression in sporadic Alzheimer's disease. *Int. J. Clin. Exp. Pathol.* 8, 1565–1574.

Levy, E. (2017). Exosomes in the diseased brain: first insights from *in vivo* studies. *Front. Neurosci.* 11:142. doi: 10.3389/fnins.2017.00142

Li, Y., Chen, J., Chen, X. G., Wang, L., Gautam, S. C., Xu, Y. X., et al. (2002). Human marrow stromal cell therapy for stroke in rat: neurotrophins and functional recovery. *Neurology* 59, 514–523. doi: 10.1212/wnl.59.4.514

Li, Y., and Kim, J. (2016). CB2 cannabinoid receptor knockout in mice impairs contextual long-term memory and enhances spatial working memory. *Neural Plast.* 2016:9817089. doi: 10.1155/2016/9817089

Li, N., Sarojini, H., An, J., and Wang, E. (2010). Prosaposin in the secretome of marrow stroma-derived neural progenitor cells protects neural cells from apoptotic death. *J. Neurochem.* 112, 1527–1538. doi: 10.1111/j.1471-4159.2009.06565.x

Li, Y., Yang, Y. Y., Ren, J. L., Xu, F., Chen, F. M., and Li, A. (2017). Exosomes secreted by stem cells from human exfoliated deciduous teeth contribute to functional recovery after traumatic brain injury by shifting microglia M1/M2 polarization in rats. *Stem Cell Res. Ther.* 8:198. doi: 10.1186/s13287-017-0648-5

Libert, S., Cohen, D., and Guarente, L. (2008). Neurogenesis directed by Sirt1. *Nat. Cell Biol.* 10, 373–374. doi: 10.1038/ncb0408-373

Liu, C., Cui, G., Zhu, M., Kang, X., and Guo, H. (2014). Neuroinflammation in Alzheimer's disease: chemokines produced by astrocytes and chemokine receptors. *Int. J. Clin. Exp. Pathol.* 7, 8342–8355.

Liu, C. G., Song, J., Zhang, Y. Q., and Wang, P. C. (2014). MicroRNA-193b is a regulator of amyloid precursor protein in the blood and cerebrospinal fluid derived exosomal microRNA-193b is a biomarker of Alzheimer's disease. *Mol. Med. Rep.* 10, 2395–2400. doi: 10.3892/mmr.2014.2484

Liu, X. S., Zhang, Z. G., Zhang, R. L., Gregg, S. R., Wang, L., Yier, T., et al. (2007). Chemokine ligand 2 (CCL2) induces migration and differentiation of subventricular zone cells after stroke. *J. Neurosci. Res.* 85, 2120–2125. doi: 10.1002/jnr.21359

Lugli, G., Cohen, A. M., Bennett, D. A., Shah, R. C., Fields, C. J., Hernandez, A. G., et al. (2015). Plasma exosomal miRNAs in persons with and without alzheimer disease: altered expression and prospects for biomarkers. *PLoS One* 10:e0139233. doi: 10.1371/journal.pone.0139233

Luna-Muñoz, J., Chávez-Macías, L., García-Sierra, F., and Mena, R. (2007). Earliest stages of tau conformational changes are related to the appearance of a sequence of specific phospho-dependent tau epitopes in Alzheimer's disease. *J. Alzheimers Dis.* 12, 365–375. doi: 10.3233/jad-2007-12410

Ma, J. F., Zang, L. N., Xi, Y. M., Yang, W. J., and Zou, D. (2016). MiR-125a Rs12976445 polymorphism is associated with the apoptosis status of nucleus pulposus cells and the risk of intervertebral disc degeneration. *Cell. Physiol. Biochem.* 38, 295–305. doi: 10.1159/000438630

Malm, T., Loppi, S., and Kanninen, K. M. (2016). Exosomes in Alzheimer's disease. *Neurochem. Int.* 97, 193–199. doi: 10.1016/j.neuint.2016.04.011

Mandelkow, E. M., Drewes, G., Biernat, J., Gustke, N., Van Lint, J., Vandenheede, J. R., et al. (1992). Glycogen synthase kinase-3 and the Alzheimer-like state of microtubule-associated protein tau. *FEBS Lett.* 314, 315–321. doi: 10.1016/0014-5793(92)81496-9

Matsuura, R., Tanaka, H., and Go, M. J. (2004). Distinct functions of Rac1 and Cdc42 during axon guidance and growth cone morphogenesis in *Drosophila*. *Eur. J. Neurosci.* 19, 21–31. doi: 10.1046/j.1460-9568.2003.03084.x

Matthay, M. A., Pati, S., and Lee, J. W. (2017). Concise review: mesenchymal stem (Stromal) cells: biology and preclinical evidence for therapeutic potential for organ dysfunction following trauma or sepsis. *Stem Cells* 35, 316–324. doi: 10.1002/stem.2551

Maumus, M., Manferdini, C., Toupet, K., Chuchana, P., Casteilla, L., Gachet, M., et al. (2017). Thrombospondin-1 partly mediates the cartilage protective effect

of adipose-derived mesenchymal stem cells in osteoarthritis. *Front Immunol.* 8:1638. doi: 10.3389/fimmu.2017.01638

McBride, J. D., Rodriguez-Menocal, L., Guzman, W., Candanedo, A., Garcia-Contreras, M., and Badiavas, E. V. (2017). Bone marrow mesenchymal stem cell-derived CD63^{+} exosomes transport Wnt3a exteriorly and enhance dermal fibroblast proliferation, migration and angiogenesis *in vitro*. *Stem Cells Dev.* 26, 1384–1398. doi: 10.1089/scd.2017.0087

Mi, H., Huang, X., Muruganujan, A., Tang, H., Mills, C., Kang, D., et al. (2017). PANTHER version 11: expanded annotation data from Gene Ontology and Reactome pathways and data analysis tool enhancements. *Nucleic Acids Res.* 45, D183–D189. doi: 10.1093/nar/gkw1138

Miranda, A. M., Lasiecka, Z. M., Xu, Y., Neufeld, J., Shahriar, S., Simoes, S., et al. (2018). Neuronal lysosomal dysfunction releases exosomes harboring APP C-terminal fragments and unique lipid signatures. *Nat. Commun.* 9:291. doi: 10.1038/s41467-017-02533-w

Mitsialis, S. A., and Kourembanas, S. (2016). Stem cell-based therapies for the newborn lung and brain: possibilities and challenges. *Semin. Perinatol.* 40, 138–151. doi: 10.1053/j.semperi.2015.12.002

Mizushima, N., and Komatsu, M. (2011). Autophagy: renovation of cells and tissues. *Cell* 147, 728–741. doi: 10.1016/j.cell.2011.10.026

Morishita, M., Nabeka, H., Shimokawa, T., Miyawaki, K., Doihara, T., Saito, S., et al. (2014). Temporal changes in prosaposin expression in the rat dentate gyrus after birth. *PLoS One* 9:e95883. doi: 10.1371/journal.pone.0095883

Mroczko, B., Groblewska, M., Litman-Zawadzka, A., Kornhuber, J., and Lewczuk, P. (2018). Amyloid β oligomers (AβOs) in Alzheimer's disease. *J. Neural Transm.* 125, 177–191. doi: 10.1007/s00702-017-1820-x

Mulcahy, L. A., Pink, R. C., and Carter, D. R. (2014). Routes and mechanisms of extracellular vesicle uptake. *J. Extracell. Vesicles* 3:24641. doi: 10.3402/jev.v3.24641

Munro, K. M., Nash, A., Pigoni, M., Lichtenthaler, S. F., and Gunnersen, J. M. (2016). Functions of the Alzheimer's disease protease BACE1 at the synapse in the central nervous system. *J. Mol. Neurosci.* 60, 305–315. doi: 10.1007/s12031-016-0800-1

Nabeka, H., Saito, S., Li, X., Shimokawa, T., Khan, M. S. I., Yamamiya, K., et al. (2017). Interneurons secrete prosaposin, a neurotrophic factor, to attenuate kainic acid-induced neurotoxicity. *IBRO Rep.* 3, 17–32. doi: 10.1016/j.ibror.2017.07.001

Nakano, M., Nagaishi, K., Konari, N., Saito, Y., Chikenji, T., Mizue, Y., et al. (2016). Bone marrow-derived mesenchymal stem cells improve diabetes-induced cognitive impairment by exosome transfer into damaged neurons and astrocytes. *Sci. Rep.* 6:24805. doi: 10.1038/srep24805

Nath, S., Agholme, L., Kurudenkandy, F. R., Granseth, B., Marcusson, J., and Hallbeck, M. (2012). Spreading of neurodegenerative pathology via neuron-to-neuron transmission of β-amyloid. *J. Neurosci.* 32, 8767–8777. doi: 10.1523/JNEUROSCI.0615-12.2012

Nguyen, T. M., Arthur, A., Hayball, J. D., and Gronthos, S. (2013). EphB and Ephrin-B interactions mediate human mesenchymal stem cell suppression of activated T-cells. *Stem Cells Dev.* 22, 2751–2764. doi: 10.1089/scd.2012.0676

Nikitidou, E., Khoonsari, P. E., Shevchenko, G., Ingelsson, M., Kultima, K., and Erlandsson, A. (2017). Increased release of apolipoprotein E in extracellular vesicles following amyloid-β protofibril exposure of neuroglial co-cultures. *J. Alzheimers Dis.* 60, 305–321. doi: 10.3233/jad-170278

Ophelders, D. R., Wolfs, T. G., Jellema, R. K., Zwanenburg, A., Andriessen, P., Delhaas, T., et al. (2016). Mesenchymal stromal cell-derived extracellular vesicles protect the fetal brain after hypoxia-ischemia. *Stem Cells Transl. Med.* 5, 754–763. doi: 10.5966/sctm.2015-0197

Ostrowski, M., Carmo, N. B., Krumeich, S., Fanget, I., Raposo, G., Savina, A., et al. (2009). Rab27a and Rab27b control different steps of the exosome secretion pathway. *Nat. Cell Biol.* 12, 19–30. doi: 10.1038/ncb2000

Pham, X., Song, G., Lao, S., Goff, L., Zhu, H., Valle, D., et al. (2016). The DPYSL2 gene connects mTOR and schizophrenia. *Transl. Psychiatry* 6:e933. doi: 10.1038/tp.2016.204

Phinney, D. G., and Pittenger, M. F. (2017). Concise review: MSC-derived exosomes for cell-free therapy. *Stem Cells* 35, 851–858. doi: 10.1002/stem.2575

Piper, R. C., and Katzmann, D. J. (2007). Biogenesis and function of multivesicular bodies. *Annu. Rev. Cell Dev. Biol.* 23, 519–547. doi: 10.1146/annurev.cellbio.23.090506.123319

Qu, J., and Zhang, H. (2017). Roles of mesenchymal stem cells in spinal cord injury. *Stem Cells Int.* 2017:5251313. doi: 10.1155/2017/5251313

Rajendran, L., Honsho, M., Zahn, T. R., Keller, P., Geiger, K. D., Verkade, P., et al. (2006). Alzheimer's disease β-amyloid peptides are released in association with exosomes. *Proc. Natl. Acad. Sci. U S A* 103, 11172–11177. doi: 10.1073/pnas.0603838103

Reiman, E. M., Quiroz, Y. T., Fleisher, A. S., Chen, K., Velez-Pardo, C., Jimenez-Del-Rio, M., et al. (2012). Brain imaging and fluid biomarker analysis in young adults at genetic risk for autosomal dominant Alzheimer's disease in the presenilin 1 E280A kindred: a case-control study. *Lancet Neurol.* 11, 1048–1056. doi: 10.1016/S1474-4422(12)70228-4

Reiss, A. B., Arain, H. A., Stecker, M. M., Siegart, N. M., and Kasselman, L. J. (2018). Amyloid toxicity in Alzheimer's disease. *Rev. Neurosci.* 29, 613–627. doi: 10.1515/revneuro-2017-0063

Rodriguez-Grande, B., Varghese, L., Molina-Holgado, F., Rajkovic, O., Garlanda, C., Denes, A., et al. (2015). Pentraxin 3 mediates neurogenesis and angiogenesis after cerebral ischaemia. *J. Neuroinflammation* 12:15. doi: 10.1186/s12974-014-0227-y

Saman, S., Kim, W., Raya, M., Visnick, Y., Miro, S., Saman, S., et al. (2012). Exosome-associated tau is secreted in tauopathy models and is selectively phosphorylated in cerebrospinal fluid in early Alzheimer disease. *J. Biol. Chem.* 287, 3842–3849. doi: 10.1074/jbc.M111.277061

Saman, S., Lee, N. C., Inoyo, I., Jin, J., Li, Z., Doyle, T., et al. (2014). Proteins recruited to exosomes by tau overexpression implicate novel cellular mechanisms linking tau secretion with Alzheimer's disease. *J. Alzheimers Dis.* 40, S47–S70. doi: 10.3233/jad-132135

Scott, C. W., Spreen, R. C., Herman, J. L., Chow, F. P., Davison, M. D., Young, J., et al. (1993). Phosphorylation of recombinant tau by cAMP-dependent protein kinase. Identification of phosphorylation sites and effect on microtubule assembly. *J. Biol. Chem.* 268, 1166–1173.

Sharples, R. A., Vella, L. J., Nisbet, R. M., Naylor, R., Perez, K., Barnham, K. J., et al. (2008). Inhibition of γ-secretase causes increased secretion of amyloid precursor protein C-terminal fragments in association with exosomes. *FASEB J.* 22, 1469–1478. doi: 10.1096/fj.07-9357com

Shi, M., Kovac, A., Korff, A., Cook, T. J., Ginghina, C., Bullock, K. M., et al. (2016). CNS tau efflux via exosomes is likely increased in Parkinson's disease but not in Alzheimer's disease. *Alzheimers Dement.* 12, 1125–1131. doi: 10.1016/j.jalz.2016.04.003

Shibasaki, T., Takahashi, H., Miki, T., Sunaga, Y., Matsumura, K., Yamanaka, M., et al. (2007). Essential role of Epac2/Rap1 signaling in regulation of insulin granule dynamics by cAMP. *Proc. Natl. Acad. Sci. U S A* 104, 19333–19338. doi: 10.1073/pnas.0707054104

Smith, P. Y., Hernandez-Rapp, J., Jolivette, F., Lecours, C., Bisht, K., Goupil, C., et al. (2015). miR-132/212 deficiency impairs tau metabolism and promotes pathological aggregation *in vivo*. *Hum. Mol. Genet.* 24, 6721–6735. doi: 10.1093/hmg/ddv377

Spencer, B., Kim, C., Gonzalez, T., Bisquertt, A., Patrick, C., Rockenstein, E., et al. (2016). α-Synuclein interferes with the ESCRT-III complex contributing to the pathogenesis of Lewy body disease. *Hum. Mol. Genet.* 25, 1100–1115. doi: 10.1093/hmg/ddv633

Stevanato, L., Thanabalasundaram, L., Vysokov, N., and Sinden, J. D. (2016). Investigation of content, stoichiometry and transfer of miRNA from human neural stem cell line derived exosomes. *PLoS One* 11:e0146353. doi: 10.1371/journal.pone.0146353

Stoothoff, W. H., and Johnson, G. V. (2005). Tau phosphorylation: physiological and pathological consequences. *Biochim. Biophys. Acta* 1739, 280–297. doi: 10.1016/j.bbadis.2004.06.017

Stuffers, S., Sem Wegner, C., Stenmark, H., and Brech, A. (2009). Multivesicular endosome biogenesis in the absence of ESCRTs. *Traffic* 10, 925–937. doi: 10.1111/j.1600-0854.2009.00920.x

Svensson, K. J., Christianson, H. C., Wittrup, A., Bourseau-Guilmain, E., Lindqvist, E., Svensson, L. M., et al. (2013). Exosome uptake depends on ERK1/2-heat shock protein 27 signaling and lipid Raft-mediated endocytosis negatively regulated by caveolin-1. *J. Biol. Chem.* 288, 17713–17724. doi: 10.1074/jbc.M112.445403

Szklarczyk, D., Morris, J. H., Cook, H., Kuhn, M., Wyder, S., Simonovic, M., et al. (2017). The STRING database in 2017: quality-controlled protein-

protein association networks, made broadly accessible. *Nucleic Acids Res.* 45, D362–D368. doi: 10.1093/nar/gkw937

Takahashi, R. H., Milner, T. A., Li, F., Nam, E. E., Edgar, M. A., Yamaguchi, H., et al. (2002). Intraneuronal Alzheimer Aβ42 accumulates in multivesicular bodies and is associated with synaptic pathology. *Am. J. Pathol.* 161, 1869–1879. doi: 10.1016/s0002-9440(10)64463-x

Tan, J., and Evin, G. (2012). β-site APP-cleaving enzyme 1 trafficking and Alzheimer's disease pathogenesis. *J. Neurochem.* 120, 869–880. doi: 10.1111/j.1471-4159.2011.07623.x

Tang, Y., Bao, J. S., Su, J. H., and Huang, W. (2017). MicroRNA-139 modulates Alzheimer's-associated pathogenesis in SAMP8 mice by targeting cannabinoid receptor type 2. *Genet. Mol. Res.* 16, 10–4238. doi: 10.4238/gmr16019166

The UniProt Consortium. (2018). UniProt: the universal protein knowledgebase. *Nucleic Acids Res.* 46, 2699–2699. doi: 10.1093/nar/gky092

Timmers, L., Lim, S. K., Arslan, F., Armstrong, J. S., Hoefer, I. E., Doevendans, P. A., et al. (2007). Reduction of myocardial infarct size by human mesenchymal stem cell conditioned medium. *Stem Cell Res.* 1, 129–137. doi: 10.1016/j.scr.2008.02.002

Trajkovic, K., Hsu, C., Chiantia, S., Rajendran, L., Wenzel, D., Wieland, F., et al. (2008). Ceramide triggers budding of exosome vesicles into multivesicular endosomes. *Science* 319, 1244–1247. doi: 10.1126/science.1153124

Trotta, T., Panaro, M. A., Cianciulli, A., Mori, G., Di Benedetto, A., and Porro, C. (2018). Microglia-derived extracellular vesicles in Alzheimer's disease: a double-edged sword. *Biochem. Pharmacol.* 148, 184–192. doi: 10.1016/j.bcp.2017.12.020

Ummenthum, K., Peferoen, L. A., Finardi, A., Baker, D., Pryce, G., Mantovani, A., et al. (2016). Pentraxin-3 is upregulated in the central nervous system during MS and EAE, but does not modulate experimental neurological disease. *Eur. J. Immunol.* 46, 701–711. doi: 10.1002/eji.201545950

van Hooren, K. W., van Agtmaal, E. L., Fernandez-Borja, M., van Mourik, J. A., Voorberg, J., and Bierings, R. (2012). The Epac-Rap1 signaling pathway controls cAMP-mediated exocytosis of Weibel-Palade bodies in endothelial cells. *J. Biol. Chem.* 287, 24713–24720. doi: 10.1074/jbc.M111.321976

Vella, L. J., Sharples, R. A., Nisbet, R. M., Cappai, R., and Hill, A. F. (2008). The role of exosomes in the processing of proteins associated with neurodegenerative diseases. *Eur. Biophys. J.* 37, 323–332. doi: 10.1007/s00249-007-0246-z

Vilar, M., and Mira, H. (2016). Regulation of neurogenesis by neurotrophins during adulthood: expected and unexpected roles. *Front. Neurosci.* 10:26. doi: 10.3389/fnins.2016.00026

Villarroya-Beltri, C., Gutiérrez-Vázquez, C., Sánchez-Cabo, F., Pérez-Hernández, D., Vázquez, J., Martin-Cofreces, N., et al. (2013). Sumoylated hnRNPA2B1 controls the sorting of miRNAs into exosomes through binding to specific motifs. *Nat. Commun.* 4:2980. doi: 10.1038/ncomms3980

Vingtdeux, V., Sergeant, N., and Buee, L. (2012). Potential contribution of exosomes to the prion-like propagation of lesions in Alzheimer's disease. *Front. Physiol.* 3:229. doi: 10.3389/fphys.2012.00229

Wakabayashi, T., Craessaerts, K., Bammens, L., Bentahir, M., Borgions, F., Herdewijn, P., et al. (2009). Analysis of the γ-secretase interactome and validation of its association with tetraspanin-enriched microdomains. *Nat. Cell Biol.* 11, 1340–1346. doi: 10.1038/ncb1978

Wang, F., Baba, N., Shen, Y., Yamashita, T., Tsuru, E., Tsuda, M., et al. (2017). CCL11 promotes migration and proliferation of mouse neural progenitor cells. *Stem Cell Res. Ther.* 8:26. doi: 10.1186/s13287-017-0474-9

Wang, Y., Balaji, V., Kaniyappan, S., Krüger, L., Irsen, S., Tepper, K., et al. (2017). The release and trans-synaptic transmission of Tau via exosomes. *Mol. Neurodegener.* 12:5. doi: 10.1186/s13024-016-0143-y

Wang, G., Dinkins, M., He, Q., Zhu, G., Poirier, C., Campbell, A., et al. (2012). Astrocytes secrete exosomes enriched with proapoptotic ceramide and prostate apoptosis response 4 (PAR-4): potential mechanism of apoptosis induction in Alzheimer disease (AD). *J. Biol. Chem.* 287, 21384–21395. doi: 10.1074/jbc.M112.340513

Wang, X., Dong, C., Sun, L., Zhu, L., Sun, C., Ma, R., et al. (2016). Quantitative proteomic analysis of age-related subventricular zone proteins associated with neurodegenerative disease. *Sci. Rep.* 6:37443. doi: 10.1038/srep37443

Wei, X., Yang, X., Han, Z. P., Qu, F. F., Shao, L., and Shi, Y. F. (2013). Mesenchymal stem cells: a new trend for cell therapy. *Acta Pharmacol. Sin.* 34, 747–754. doi: 10.1038/aps.2013.50

Wilkinson, D. G. (2001). Multiple roles of EPH receptors and ephrins in neural development. *Nat. Rev. Neurosci.* 2, 155–164. doi: 10.1038/35058515

Wischik, C. M., Crowther, R. A., Stewart, M., and Roth, M. (1985). Subunit structure of paired helical filaments in Alzheimer's disease. *J. Cell Biol.* 100, 1905–1912. doi: 10.1083/jcb.100.6.1905

Wischik, C. M., Novak, M., Edwards, P. C., Klug, A., Tichelaar, W., and Crowther, R. A. (1988). Structural characterization of the core of the paired helical filament of Alzheimer disease. *Proc. Natl. Acad. Sci. U S A* 85, 4884–4888. doi: 10.1073/pnas.85.13.4884

Wu, Y., Deng, W., and Klinke, D. J. II. (2015). Exosomes: improved methods to characterize their morphology, RNA content, and surface protein biomarkers. *Analyst* 140, 6631–6642. doi: 10.1039/c5an00688k

Xiao, T., Zhang, W., Jiao, B., Pan, C. Z., Liu, X., and Shen, L. (2017). The role of exosomes in the pathogenesis of Alzheimer' disease. *Transl. Neurodegener.* 6:3. doi: 10.1186/s40035-017-0072-x

Xin, H., Katakowski, M., Wang, F., Qian, J. Y., Liu, X. S., Ali, M. M., et al. (2017a). MicroRNA cluster miR-17–92 cluster in exosomes enhance neuroplasticity and functional recovery after stroke in rats. *Stroke* 48, 747–753. doi: 10.1161/STROKEAHA.116.015204

Xin, H., Wang, F., Li, Y., Lu, Q. E., Cheung, W. L., Zhang, Y., et al. (2017b). Secondary release of exosomes from astrocytes contributes to the increase in neural plasticity and improvement of functional recovery after stroke in rats treated with exosomes harvested from MicroRNA 133b-overexpressing multipotent mesenchymal stromal cells. *Cell Transplant.* 26, 243–257. doi: 10.3727/096368916x693031

Xin, H., Li, Y., Cui, Y., Yang, J. J., Zhang, Z. G., and Chopp, M. (2013a). Systemic administration of exosomes released from mesenchymal stromal cells promote functional recovery and neurovascular plasticity after stroke in rats. *J. Cereb. Blood Flow Metab.* 33, 1711–1715. doi: 10.1038/jcbfm.2013.152

Xin, H., Li, Y., Liu, Z., Wang, X., Shang, X., Cui, Y., et al. (2013b). MiR-133b promotes neural plasticity and functional recovery after treatment of stroke with multipotent mesenchymal stromal cells in rats via transfer of exosome-enriched extracellular particles. *Stem Cells* 31, 2737–2746. doi: 10.1002/stem.1409

Xiong, Y., Mahmood, A., and Chopp, M. (2017). Emerging potential of exosomes for treatment of traumatic brain injury. *Neural Regen. Res.* 12, 19–22. doi: 10.4103/1673-5374.198966

Yan, R., Fan, Q., Zhou, J., and Vassar, R. (2016). Inhibiting BACE1 to reverse synaptic dysfunctions in Alzheimer's disease. *Neurosci. Biobehav. Rev.* 65, 326–340. doi: 10.1016/j.neubiorev.2016.03.025

Yang, Y., Ye, Y., Su, X., He, J., Bai, W., and He, X. (2017). MSCs-derived exosomes and neuroinflammation, neurogenesis and therapy of traumatic brain injury. *Front. Cell. Neurosci.* 11:55. doi: 10.3389/fncel.2017.00055

Yang, J., Zhang, X., Chen, X., Wang, L., and Yang, G. (2017). Exosome mediated delivery of miR-124 promotes neurogenesis after ischemia. *Mol. Ther. Nucleic Acids* 7, 278–287. doi: 10.1016/j.omtn.2017.04.010

Yin, Z. S., Zhang, H., Wang, W., Hua, X. Y., Hu, Y., Zhang, S. Q., et al. (2007). Wnt-3a protein promote neuronal differentiation of neural stem cells derived from adult mouse spinal cord. *Neurol. Res.* 29, 847–854. doi: 10.1179/016164107x223539

Yuyama, K., and Igarashi, Y. (2017). Exosomes as carriers of Alzheimer's amyloid-ß. *Front. Neurosci.* 11:229. doi: 10.3389/fnins.2017.00229

Zappulli, V., Friis, K. P., Fitzpatrick, Z., Maguire, C. A., and Breakefield, X. O. (2016). Extracellular vesicles and intercellular communication within the nervous system. *J. Clin. Invest.* 126, 1198–1207. doi: 10.1172/jci81134

Zhang, Z. G., and Chopp, M. (2015). Promoting brain remodeling to aid in stroke recovery. *Trends Mol. Med.* 21, 543–548. doi: 10.1016/j.molmed.2015.07.005

Zhang, Y., Chopp, M., Zhang, Z. G., Katakowski, M., Xin, H., Qu, C., et al. (2017). Systemic administration of cell-free exosomes generated by human bone marrow derived mesenchymal stem cells cultured under 2D and 3D conditions improves functional recovery in rats after traumatic brain injury. *Neurochem. Int.* 111, 69–81. doi: 10.1016/j.neuint.2016.08.003

Zhang, J., Li, S., Li, L., Li, M., Guo, C., Yao, J., et al. (2015). Exosome and exosomal microRNA: trafficking, sorting, and function. *Genomics Proteomics Bioinformatics* 13, 17–24. doi: 10.1016/j.gpb.2015.02.001

Zhang, Y.-L., Wang, R.-C., Cheng, K., Ring, B. Z., and Su, L. (2017). Roles of Rap1 signaling in tumor cell migration and invasion. *Cancer Biol. Med.* 14, 90–99. doi: 10.20892/j.issn.2095-3941.2016.0086

Zhang, G., and Yang, P. (2018). A novel cell-cell communication mechanism in the nervous system: exosomes. *J. Neurosci. Res.* 96, 45–52. doi: 10.1002/jnr.24113

Zhao, Y., Gibb, S. L., Zhao, J., Moore, A. N., Hylin, M. J., Menge, T., et al. (2016a). Wnt3a, a protein secreted by mesenchymal stem cells is neuroprotective and promotes neurocognitive recovery following traumatic brain injury. *Stem Cells* 34, 1263–1272. doi: 10.1002/stem.2310

Zhao, Y., Tan, W., Sheng, W., and Li, X. (2016b). Identification of biomarkers associated With Alzheimer's disease by bioinformatics analysis. *Am. J. Alzheimers Dis. Other Demen.* 31, 163–168. doi: 10.1177/1533317515588181

Zheng, T., Pu, J., Chen, Y., Mao, Y., Guo, Z., Pan, H., et al. (2017). Plasma exosomes spread and cluster around β-amyloid plaques in an animal model of Alzheimer's disease. *Front. Aging. Neurosci.* 9:12. doi: 10.3389/fnagi.2017.00012

Zmuda, J. F., and Rivas, R. J. (2000). Actin disruption alters the localization of tau in the growth cones of cerebellar granule neurons. *J. Cell Sci.* 113, 2797–2809. doi: 10.1002/1097-4695(20000615)43:4<313::aid-neu1>3.0.co;2-2

Conflict of Interest Statement: The authors declare that the research was conducted in the absence of any commercial or financial relationships that could be construed as a potential conflict of interest.

frontiers in Cellular Neuroscience

ORIGINAL RESEARCH
published: 24 April 2018
doi: 10.3389/fncel.2018.00103

Ovarian Function Modulates the Effects of Long-Chain Polyunsaturated Fatty Acids on the Mouse Cerebral Cortex

Jose L. Herrera[1], Lara Ordoñez-Gutierrez[2,3], Gemma Fabrias[4], Josefina Casas[4], Araceli Morales[1], Guadalberto Hernandez[1], Nieves G. Acosta[5], Covadonga Rodriguez[1,5], Luis Prieto-Valiente[6], Luis M. Garcia-Segura[7], Rafael Alonso[1]* and Francisco G. Wandosell[2,3]**

[1] Departamento de Ciencias Médicas Básica and Instituto de Tecnologías Biomédicas, Centro de Investigaciones Biomédicas de Canarias, Universidad de La Laguna, La Laguna, Spain, [2] Centro de Biología Molecular "Severo Ochoa" (CSIC-UAM), Universidad Autónoma de Madrid, Madrid, Spain, [3] Centro de Investigación Biomédica en Red de Enfermedades Neurodegenerativas, Madrid, Spain, [4] Instituto de Química Avanzada de Cataluña (IQAC-CSIC), Barcelona, Spain, [5] Departamento de Biología Animal, Edafología y Geología, and Instituto de Tecnologías Biomédicas, Centro de Investigaciones Biomédicas de Canarias, Universidad de La Laguna, Tenerife, Spain, [6] Unidad de Estadística Médica, Universidad Católica de Murcia, Murcia, Spain, [7] Instituto Cajal (CSIC) and Centro de Investigación Biomédica en Red de Fragilidad y Envejecimiento Saludable, Madrid, Spain

OPEN ACCESS

Edited by:
Merce Pallas, Universitat de Barcelona, Spain

Reviewed by:
Mustapha Umar Imam, Zhengzhou University, China
Amy Christensen, University of Southern California, United States

***Correspondence:**
Francisco G. Wandosell
fwandosell@cbm.csic.es
Rafael Alonso
ralonsosolis@gmail.com
Luis M. Garcia-Segura
lmgs@cajal.csic.es

Received: 28 November 2017
Accepted: 29 March 2018
Published: 24 April 2018

Citation:
Herrera JL, Ordoñez-Gutierrez L, Fabrias G, Casas J, Morales A, Hernandez G, Acosta NG, Rodriguez C, Prieto-Valiente L, Garcia-Segura LM, Alonso R and Wandosell FG (2018) Ovarian Function Modulates the Effects of Long-Chain Polyunsaturated Fatty Acids on the Mouse Cerebral Cortex. Front. Cell. Neurosci. 12:103. doi: 10.3389/fncel.2018.00103

Different dietary ratios of *n*−6/*n*−3 long-chain polyunsaturated fatty acids (LC-PUFAs) may alter brain lipid profile, neural activity, and brain cognitive function. To determine whether ovarian hormones influence the effect of diet on the brain, ovariectomized and sham-operated mice continuously treated with placebo or estradiol were fed for 3 months with diets containing low or high *n*−6/*n*−3 LC-PUFA ratios. The fatty acid (FA) profile and expression of key neuronal proteins were analyzed in the cerebral cortex, with intact female mice on standard diet serving as internal controls of brain lipidome composition. Diets containing different concentrations of LC-PUFAs greatly modified total FAs, sphingolipids, and gangliosides in the cerebral cortex. Some of these changes were dependent on ovarian hormones, as they were not detected in ovariectomized animals, and in the case of complex lipids, the effect of ovariectomy was partially or totally reversed by continuous administration of estradiol. However, even though differential dietary LC-PUFA content modified the expression of neuronal proteins such as synapsin and its phosphorylation level, PSD-95, amyloid precursor protein (APP), or glial proteins such as glial fibrillary acidic protein (GFAP), an effect also dependent on the presence of the ovary, chronic estradiol treatment was unable to revert the dietary effects on brain cortex synaptic proteins. These results suggest that, in addition to stable estradiol levels, other ovarian hormones such as progesterone and/or cyclic ovarian secretory activity could play a physiological role in the modulation of dietary LC-PUFAs on the cerebral cortex, which may have clinical implications for post-menopausal women on diets enriched with different proportions of *n*−3 and *n*−6 LC-PUFAs.

Keywords: cerebral cortex lipidome, long-chain polyunsaturated fatty acids (LC-PUFAs), docosahexaenoic acid (DHA), sphingolipids, ovarian hormones, synaptic proteins

INTRODUCTION

Phospholipids are major components of neural cell membranes, playing critical roles in synaptic transmission and neuronal signaling through interactions with specific membrane proteins (Bazan, 2014). The brain's complement of phospholipids and other complex lipids contains large amounts of long-chain polyunsaturated fatty acids (LC-PUFAs) such as arachidonic acid (ARA; 20:4*n*−6) and docosahexaenoic acid (DHA; 22:6*n*−3), but low levels of other omega-3 LC-PUFAs, especially eicosapentaenoic acid (EPA; 20:5*n*−3) (Brenna and Diau, 2007; Chen et al., 2009). While saturated and monounsaturated fatty acids can be synthesized *de novo* within the brain, LC-PUFAs are mainly supplied by the blood and are synthesized from two dietary precursors: linoleic acid (LNA; 18:2*n*−6) and α-linoleic acid (ALA; 18:3*n*−3) (Carrié et al., 2000; Williard et al., 2001; Bazinet and Layé, 2014). Even though the specific mechanisms involved in phospholipid signaling are not completely understood, several pro-resolving lipid mediators (SPMs) have been identified, including 17S-hydroxy-DHA (17S-DHA), neuroprotectin D1 (NPD-1), resolvin D5 (RvD5), 14S-HDHA and maresin 1 (MaR1) (Orr et al., 2013; Serhan, 2014). LC-PUFAs and SPMs participate in a plethora of signaling processes, such as cell survival and neuroinflammation, neurotransmission, and cognitive function (Bannenberg and Serhan, 2010; Serhan and Chang, 2013). One of the best-characterized SPMs is NPD-1, which is synthesized in response to brain injury and may have therapeutic potential in a wide range of neurological conditions (Bazan et al., 2011a,b, 2013).

In rodents, daily intake of omega-3 LC-PUFAs (*n*−3 LC-PUFAs) is necessary for neural development and maintenance of synaptic circuitry (Brenna and Diau, 2007; Dyall and Michael-Titus, 2008; Bazan et al., 2011a,b). In addition, experimental and clinical data support that their dietary inclusion has positive effects on numerous pathological conditions (Gorjão et al., 2009; Mozaffarian and Wu, 2012; Russell and Bürgin–Maunder, 2012). Diets enriched in *n*−3 LC-PUFAs have been associated with a lower incidence of dementia and neurological disorders (Mazza et al., 2007), while diets containing low percentage of DHA may be linked to cognitive impairment (Ikemoto et al., 2001; Catalan et al., 2002). Interestingly, the ratio of *n*−3 to *n*−6 LC- PUFA in the diet appears to be a critical factor for the effect on the brain lipidome (Bourre et al., 1984; Jumpsen et al., 1997; Carrié et al., 2000). On the other hand, women have significantly lower blood levels of docosapentaenoic acid (DPA; 22:5-3) and EPA, but significantly higher levels of DHA than men (Metherel et al., 2009). In studies with female mice, it has been reported that the effect of diet on the brain lipidome may be partially dependent on circulating levels of gonadal hormones (Díaz et al., 2016). Furthermore, experimental evidence has indicated that estrogen may modulate neuronal signaling through interactions with specific estrogen receptors in neural membrane microdomains, such as lipid rafts (Herrera et al., 2011; Marín et al., 2013).

The aim of this study was to investigate the putative synergistic interaction between estradiol and differential dietary fatty acid (FA) supplementation, and observe how this combination may affect the long-term lipid and protein profile in the brain. A multifactorial design was established to investigate the effects of diets containing two different ratios of *n*−3 and *n*−6 LC-PUFAs, specifically EPA and DHA, and their potential interaction with reproductive status in placebo and estradiol-treated ovariectomized mice. At the end point, analysis of the cerebral cortex showed that both diets modified the brain lipidome when compared to standard diet, and may influence neural function by modifying the content of several proteins involved in intracellular signaling and synaptic transmission. In addition, some of these effects were sensitive to the presence or absence of the ovaries and, at least partially, to circulating levels of estradiol.

MATERIALS AND METHODS

Animals and Husbandry

Female C57BL/6J mice (*Mus musculus*) were purchased from Charles River Laboratories, and housed under constant temperature (22 ± 2°C) and humidity (50 ± 5%) and a 12:12 h light-dark cycle in specific pathogen–free conditions. Mice (10 per cage) were housed in cages fitted with microbarrier filter tops, and allowed access to food (A03/R03, SAFE-Panlab) and tap water *ad libitum*. One month after birth, the standard laboratory food was gradually replaced in all animals with the experimental diets (see below) at a rate of 25% per week; all mice were fed with 100% experimental diet from the age of 2 months until the time of sacrifice. For lipid analysis, a group of intact females fed with standard laboratory food was used as a control. La Laguna University Animal Care and Use Committee approved the protocol for this study.

Ovariectomy and Hormone Treatments

In preliminary experiments it was found that ovariectomized mice implanted with 0.05 mg estradiol pellets (Innovative Research of America, Sarasota, Florida) for 90 days showed plasma estradiol levels of 7.2 ± 4.54 pg/ml (mean ± SEM) as determined by RIA (Architect System, ref #B7K720, Abbot, Germany). Since these values are within the range of those found in cycling animals of the same age at proestrus (20.9 ± 6.03 pg/ml) and estrus (1.8 ± 4.54 pg/ml), this dose of estradiol was chosen for the dietary experiments. Thus, female mice were anesthetized with inhaled isoflurane (2 ± 0.5%) after analgesic injection (buprenorphine hydrochloride, Buprex), and then bilaterally ovariectomized or sham-operated at 90 ± 1 days-of-age through a 1 cm dorsal incision that was closed with surgical clips. The day after ovariectomy mice received a 3 mm pellet containing a 90-day timed-release 0.05 mg 17β-estradiol or placebo. The pellet was subcutaneously implanted in the subscapular region by using a trocar according to manufacturer's instructions. Animals still showing inflammation around the implantation area 13 days after receiving the pellet were discarded. Mice were then housed according to the different diets and hormonal treatments until the end-point 90 days later, as shown in **Table 1**.

TABLE 1 | Design of experimental groups.

Reproductive status	Diet
Intact sham-operated females (CO)	Standard laboratory food (SF)
	High *n*−6/*n*−3 ratio diet –(DI)
	Low *n*−6/*n*−3 ratio diet– (DII)
Ovariectomized-placebo treated (OVX)	High *n*−6/*n*−3 ratio diet–(DI)
	Low *n*−6/*n*−3 ratio diet– (DII)
Ovariectomized-estradiol treated (OVX-E)	High *n*−6/*n*−3 ratio diet– (DI)
	Low *n*−6/*n*−3 ratio diet– (DII)

Diets

Two specific experimental diets were used in these experiments. The high *n*−6/*n*−3 ratio diet (DI) containing safflower oil, which had undetectable levels of EPA (20:5*n*−3) and DHA (22:6*n*−3), had abundant oleic acid (18:1*n*−9) and linoleic acid (18:2*n*−6), but was poor in α-linolenic acid (18:3*n*−3). The low *n*−6/*n*−3 ratio diet (DII) had the same basic composition, but was supplemented with extra EPA and DHA in a proportion of 7 g/kg of diet, added in the form of fish oil as a lipid source to give a particularly high DHA content. These diets were designed in the Instituto de Nutrición y Tecnología de los Alimentos at the University of Granada, Spain, and produced by Mucedola (Mucedola srl, Milano, Italy). Both diets and the standard laboratory food (SF) were subsequently lab-analyzed to determine the final percentage and absolute quantity (g/kg) of each FA (**Table 2**). Summarizing the main diet differences: (a) DI had a *n*−6/*n*−3 ratio 13–14 times higher than that of SF and 59 times higher than that of DII; (b) DII had a *n*−6/*n*−3 ratio 4–5 times lower than that of SF; (c) DI did not have traces of either DHA or EPA, while DII contained relevant amounts of both LC-PUFAs (**Table 2**). For simplicity, high and low *n*−6/*n*−3 LC-PUFA ratio diets are referred to in the text and graphics as DI and DII, respectively. Mice were fed these diets *ad libitum* for 90 days until the time of sacrifice.

TABLE 2 | Main fatty acid composition of experimental diets (Mean ± *SD*, g/kg fresh weight).

Fatty acids	SF	DI	DII
C 14: 0	0.05 ± 0.00	0.21 ± 0.01	1.50 ± 0.00
C 16: 0	4.13 ± 0.14	4.68 ± 0.31	6.33 ± 0.04
C 16:1 *n*−7	0.09 ± 0.01	0.17 ± 0.01	1.55 ± 0.01
C 18:0	0.75 ± 0.04	1.55 ± 0.08	1.77 ± 0.01
C 18:1 *n*−9	13.15 ± 0.35	12.04 ± 0.81	6.15 ± 0.05
C 18:1 *n*−7	0.34 ± 0.06	0.59 ± 0.07	0.98 ± 0.02
C 18:2 *n*−6	10.63 ± 0.78	28.84 ± 0.42	16.23 ± 0.00
C 18:3 *n*−3	1.01 ± 0.13	0.15 ± 0.03	0.44 ± 0.00
C 18:4 *n*−3	0.00 ± 0.00	0.00 ± 0.00	0.66 ± 0.01
C 20:0	0.11 ± 0.01	0.18 ± 0.00	0.24 ± 0.00
C 20:1 *n*−9	0.18 ± 0.00	0.12 ± 0.00	1.09 ± 0.07
C 20:4 *n*−6 (ADA)	0.00 ± 0.00	0.00 ± 0.00	0.20 ± 0.00
C 20:4 *n*−3	0.00 ± 0.00	0.00 ± 0.00	0.24 ± 0.01
C 20:5 *n*−3 (EPA)	0.00 ± 0.00	0.00 ± 0.00	2.29 ± 0.02
C 22:0	0.18 ± 0.01	0.10 ± 0.01	0.13 ± 0.02
C 22:1 *n*−11	0.05 ± 0.02	0.10 ± 0.06	0.74 ± 0.04
C 22: 5 *n*−6 (DPA)	0.00 ± 0.00	0.00 ± 0.00	0.11 ± 0.01
C 22: 5 *n*−3	0.05 ± 0.00	0.06 ± 0.03	0.43 ± 0.01
C 22: 6 *n*−3 (DHA)	0.00 ± 0.00	0.00 ± 0.00	3.47 ± 0.01
TOTALS			
Saturates	5.42 ± 0.16	6.83 ± 0.37	10.41 ± 0.06
Monoenes	14.00 ± 0.39	13.41 ± 1.03	11.24 ± 0.09
PUFAs	11.69 ± 0.91	29.05 ± 0.47	24.07 ± 0.08
n−9	13.47 ± 0.33	12.35 ± 0.86	7.85 ± 0.10
n−6	10.63 ± 0.78	28.84 ± 0.42	16.55 ± 0.09
n−3	1.06 ± 0.13	0.22 ± 0.06	7.52 ± 0.01
n−3 LC-PUFAs	0.05 ± 0.00	0.06 ± 0.03	6.43 ± 0.02
n−6 LC-PUFAs	0.00 ± 0.00	0.00 ± 0.00	0.32 ± 0.01
RATIOS			
n−3/*n*−6	0.10 ± 0.01	0.01 ± 0.00	0.45 ± 0.00
n−6/*n*−3	10.04 ± 0.52	138.37 ± 33.71	2.20 ± 0.02
Total FA content	31.53 ± 1.67	49.84 ± 2.10	46.43 ± 0.45
% Lipids (fresh weight)	5.48 ± 0.11	6.45 ± 0.55	6.31 ± 0.00
% Moisture	9.79 ± 0.09	8.65 ± 0.27	7.85 ± 0.00
% Lipids (dry weight)	6.07 ± 0.12	7.06 ± 0.59	6.85 ± 0.00

FA; fatty acids. Totals include some minor components not shown. The most common LC-PUFAs mentioned in the text are bold marked.

Tissue Processing and Sample Preparation

Mice were sacrificed using CO_2 90 days after ovariectomy or sham operation, and their brains were collected. Cerebral cortex tissue for western blot analysis was homogenized in 3 volumes of ice-cold lysis buffer containing 20 mM HEPES, 100 mM NaCl, 100 mM NaF, 1 mM Na_3VO_4, 5 mM EDTA, 1% Triton X100 plus protease inhibitor cocktail (Roche Diagnostic) and 1 μM Okadaic acid (Calbiochem). Homogenates were centrifuged at 16,000 × g for 20 min at 4°C, and supernatants were stored at −80°C. Protein concentration was measured using BioRad DC Protein Assay (BioRad) following the manufacturer's protocol. Buffer containing 10% sodium dodecyl sulfate (SDS), 0.5 mM dithiothreitol, 325 mM Tris HCl, pH 6.8, 87% glycerol and bromophenol blue was added to samples before loading into polyacrylamide gels for electrophoresis. For all samples Western blot determinations were repeated 3–4 times. For lipid analysis, tissues were homogenized at a concentration of 5 mg/ml in PBS with 0.01% 3,5-Di-tert-4-butylhydroxytoluene (HBT) as an antioxidant.

Western Blot Analysis

Cerebral cortex tissue extracts were resolved by SDS-PAGE and transferred onto nitrocellulose (Whatman) or PVDF (Millipore) membranes, and subsequently blocked by incubation in 10% non-fat milk for 1 h at room temperature. Membranes were incubated overnight at 4°C with appropriate primary antibodies (**Table 3**), then washed in 0.1% Tween–PBS and incubated with secondary horseradish peroxide-conjugated antibody (Santa Cruz Biotechnology, Santa Cruz, CA, USA). Antibody binding was detected with *SuperSignal*^{TM} (Thermo-Fisher Scientific),

TABLE 3 | Antibodies used in western blot analysis.

Antibody	Source	Dilution	References
P120	Mouse	1:1,000	#610133 BD Transduction Lab, USA
PSD95	Rabbit	1:1,000	#3450 Cell Signaling, USA
Phospho-Synapsin (Ser-9)	Rabbit	1:1,000	#2311 Cell Signaling, USA
Synapsin	Rabbit	1:1,000	#2312 Cell Signaling, USA
Synaptophysin (SY38)	Mouse	1:20,000	#10701 Progen, UK
β-catenin	Mouse	1:1,000	#610153 BD, USA
βAmyloid, 1-16 (6E10)	Mouse	1:1,000	#SIG-39320 Covance, USA
BACE (D10E5)	Rabbit	1:1,000	#5606 Cell Signaling, USA
Tau1	Mouse	1:1,000	#MAB3420 Chemicon, USA
Tau5	Mouse	1:1,000	#AHB0042 Invitrogen, USA
PHF1	Mouse	1:1,000	Dr. P. Davies, USA
GFAP	Rabbit	1:1,000	#G5601 Promega, USA
β-actin	Mouse	1:10,000	#A4441 Sigma-Aldrich, USA
Anti-mouse IgG-HRP	Goat	1:5,000	#sc-2005 St Cruz Biotech, Germany
Anti-rabbit IgG-HRP	Goat	1:5,000	#sc-2004 St Cruz Biotech, Germany

using β-actin as internal loading control. Densitometry analysis was performed using a GS-800 Calibrated Densitometer (Bio-Rad).

Lipid Analysis

Lipid extraction from dietary samples and cerebral tissue was performed using a modification of the Folch's method (Folch et al., 1957). Dietary FA profiles (g FA/kg diet fresh weight) were obtained by means of acid-catalyzed transmethylation of the lipid fractions followed by GC-MS analysis (Fabelo et al., 2014). Similarly, the cerebral cortex lipid fractions were subjected to further analysis of FA and complex lipids as previously described (Cingolani et al., 2014). Sphingolipids were analyzed by HPLC-MS (Garanto et al., 2013) by using 0.2 nmol of C17-sphinganine, *N*–dodecanoylsphingosine, *N*–dodecanoylglucosylsphingosine, and *N*–dodecanoyl sphingosylphosphorylcholine as internal standards. Sphingolipids were annotated as <lipid subclass> <total fatty acyl chain length>:<total number of unsaturated bonds>. If the sphingoid base residue was dihydrosphingosine, the lipid class contained a <DH> prefix. Since our chromatographic separation did not discriminate between dh-glucosylceramides (GlcdhCer) and dh-galactosylceramides (GaldhCer), their mixture was represented as monohesoxylceramides (MHC). In all cases, the final tissue data was indicated as pmol/mg of protein, except in the case of total FA, which were calculated as pmol equivalents *per* mg of protein with respect to C12 ceramide. For statistical analysis, all lipids were shown as percentage of variation relative to its content in brain tissue from animals fed with SF.

Statistical Analysis

For lipidomic outcomes, we performed a 2×3 factorial analysis with an extra control group. General ANOVA was performed, followed by linear contrasts to answer the questions posed during the design phase of the study. Regardless, no more than 6 contrasts were performed. In this way, 12 response variables were tested in addition to the "multi-testing effect," whose accurate quantification is unfeasible. A reasonable approach to take this into account is to consider only those effects or interactions in which the p-value of the test is <0.01. However, when any interaction was found to be significant in several of the analyzed lipids, it is discussed, even if the p-value of the test is slightly higher than 0.01. In addition, the 95% confidence interval was calculated for all effects and interactions of interest.

In the case of changes in cerebral cortex protein expression levels, since the effect of diet under each reproductive status was monitored in different electrophoresis gels, it was not feasible to evaluate possible effects of each hormone condition. However, we were still able to evaluate the interaction of the hormonal condition with the effect of the diet. Thus, for each reproductive status and within the same gel, we calculated the percentage of variation induced by DII vs. DI diets. Then, in order to estimate effects and interactions between the different factors, we ran a saturated regression model which includes the dichotomous variable diet and the polytomous variable hormone condition with three levels (Armitage et al., 2004). The latter entered the model as two dummy variables, the first with a value of "1" in ovariectomized animals receiving placebo pellets, and the second with value "1" in ovariectomized mice treated with estradiol. Intact, sham-operated controls had a value of "0" in each dummy variable. This model provides us with confidence intervals and tests for the three effects of the diet conditioned to the hormonal status and the interaction between the two factors, adding up to the 5 comparisons "a priori" expected in the experimental design. Although there are four animals per group, the 2×3 factorial design includes $6 \times 4 = 24$ animals, which allows us to estimate the intragroup population variance with $6 \times 3 = 18$ degrees of freedom (df). In this way, any contrast that compares two means follows a t-Student distribution with 18 df. This provides a higher statistical power than the simple comparison of two groups with 4 animals per group.

For all tests, actual p-values are given for each comparison and the significance of the main effects detected by the analysis. The statistical software used was Stata 14 (StataCorp LLC, College Station, Texas) for inference factorial analysis and GraphPad Prisma 7 (GraphPad Software, Inc., San Diego, California) for graphic representations.

RESULTS

The Cerebral Cortex Lipidome Is Affected by Dietary Differences in the Ratio of *n*−3 and *n*−6 LC-PUFAs

In intact, sham-operated females (CO), both experimental diets (DI and DII) induced a dramatic rise in total brain cortex FAs (**Figure 1** and **Table 4A**), compared with animals fed with SF

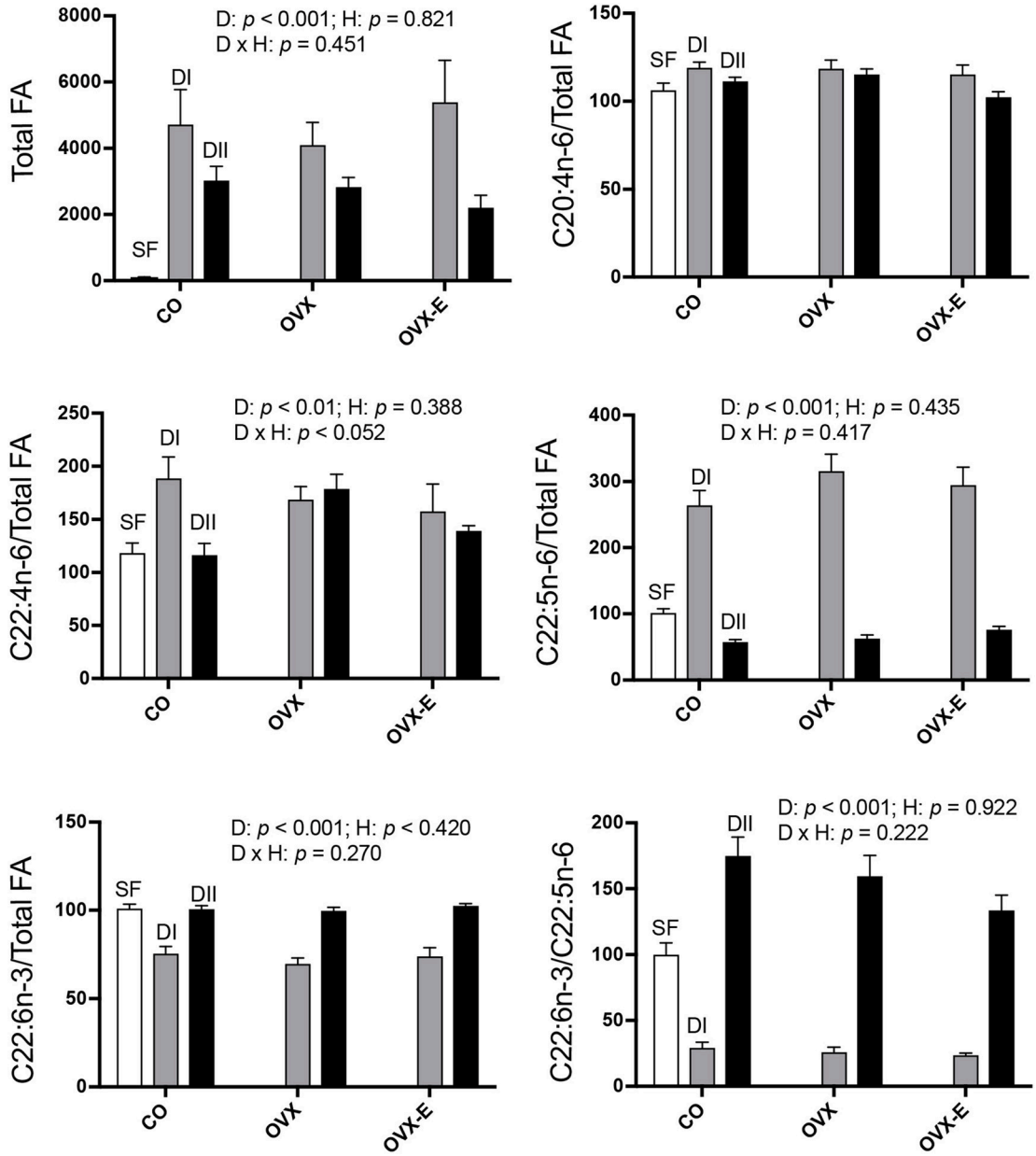

FIGURE 1 | Differential effects of dietary LC-PUFAs on the relative cerebral cortex fatty acid content in female mice under different reproductive conditions. Fatty acid (FA) composition of each diet is shown in **Table 1**. The FAs from brain cortex were obtained and analyzed as described in section Materials and Methods. White bars represent the relative FA content from cerebral cortex of intact animals fed with standard food (SF). Gray and black bars represent the data from animals fed with DI or DII *n*−6/*n*−3 LC-PUFA diets, respectively. Vertical axis represents the percentage of variation induced by each diet relative to SF. Data are represented as mean ± SEM of 4 animals per group, except those fed with SF ($n = 3$). Horizontal axis indicates the different reproductive status: CO, intact, sham-operated; OVX, ovariectomized, placebo-treated; OVX-E, ovariectomized, estradiol-treated. Only some representative *p*-values for the main effects of diet (D), hormone status (H) and their interaction (D × H) were indicated in each graph and the remaining data were detailed in **Table 4**.

(DI: $p = 0.0001$; DII: $p = 0.015$) and the effect of DI was even higher than that of DII ($p = 0.004$). The effect of diet was not significantly affected by reproductive status ($p = 0.821$), and no significant interaction was detected ($p = 0.451$). Thus, cerebral cortex levels of total FAs were altered by changes in the ratios of dietary *n*−3 and *n*−6 LC-PUFAs, apparently regardless of the presence of ovaries and circulating levels of estradiol.

With regard to the LC-PUFAs analyzed, each was significantly altered by both experimental diets compared to their levels in animals fed with SF ($p < 0.01$ or $p < 0.001$). In the case of C20:4*n*−6 (arachidonic acid, ARA) almost no modifications were seen (**Figure 1** and **Table 4B**), in parallel with the dietary content of its precursor, C18:2*n*−6 (linoleic acid), which had the lowest levels in mice fed with SF, and the highest in those fed with DI

TABLE 4 | Linear contrasts of the differential effects of dietary *n*−6/*n*−3 ratio on cerebral cortex fatty acid content under different reproductive conditions.

Lipid class	Main effects	*p*-value	95% CI
A. Total FAs	DI-SF (CO)	**0.0001**	**2618.3, 6650.0**
	DII-SF (CO)	**0.0154**	**558.5, 4631.7**
	DI-DII (CO)	**0.0041**	**730.7, 3350.4**
B. C20:4*n*−6	DI-SF (CO)	0.0288	1.3, 12.4
	DII-SF (CO)	0.4942	−6.8, 13.6
	DI-DII (CO)	0.0194	1.4, 14.5
C. C22:4*n*−6	DI-SF (CO)	**0.0091**	**19.7, 121.2**
	[DI-DII (CO)] - [DI-DII (OVX)]	**0.0194**	**16.1, 148.9**
D. C33:5*n*−6	DI-SF (CO)	**>0.00001**	**142.7, 237.8**
	DII-SF (CO)	0.1375	−83.7, 12.5
	DI-DII (CO)	**>0.00001**	**195.0, 256.8**
E. C22:6*n*−3	DI-DII (CO+OVX+OVX–E)	**>0.00001**	**−33.4, −22.4**
F. C22:6*n*−3 /C22:5*n*−6	[SF (CO)] - [DI (CO+OVX+OVX–E)]	**>0.00001**	**47.8, 99.8**
	[DII (CO)] - [SF (CO)]	**0.0001**	**29.7, 82.3**

DI: High dietary n−6/n−3 ratio; DII: Low n−6/n−3 ratio; SF: Standard food. CO: Intact control female mice; OVX: Ovariectomized, placebo-treated female mice; OVX–E: Ovariectomized, estradiol-treated female mice. Data represented in ***Figure 1*** *were analyzed by 2 × 3 factorial ANOVA. In cases where the influence of reproductive status on diet action was absent and significant interaction between the factors was not detected, data from those animals were grouped to emphasize the main dietary effects. The most significant p-values and 95% confidence intervals are highlighted.*

(**Table 2**). In contrast, levels of C22:4*n*−6 (adrenic acid; ADA) and C22:5*n*−6 (DPA) were elevated in animals fed with DI (high *n*−6/*n*−3 ratio) when compared to mice fed with SF or DII (with lower *n*−6/*n*−3 ratio), as shown in **Figure 1**, **Table 4C** ($p = 0.0091$) and **Table 4D** ($p < 0.0001$). Regarding the levels of C22:6*n*−3 (DHA), they were reduced in animals fed with DI (high *n*−6/*n*−3 ratio) compared to mice fed with either SF or DII (low *n*−6/*n*−3 ratio), as shown in **Figure 1** and **Table 4E** ($p < 0.0001$). However, no significant differences were found between the levels of DHA in animals fed with SF and those fed with DII, in agreement with the high amount of its precursor, C18:3*n*−3 (α-linolenic acid) in both. Despite its high concentration in diet DII, we were unable to detect any trace of 20:5*n*−3 (EPA), the most direct DHA biosynthetic precursor. Interestingly, the ratio between C22:6*n*−3 (DHA) and C22:5*n*−6 (DPA) was found to be significantly reduced in animals fed with DI and elevated in those fed with DII as shown in **Figure 1** and **Table 4F** ($p < 0.0001$, and $p = 0.0001$), in correlation with their higher *n*−6/*n*−3 and lowest *n*−6/*n*−3 ratios, respectively.

In addition to the effect of dietary composition on brain FA content, we studied its possible dependence on reproductive status. As shown in **Figure 1**, no clear effect was found in either ovariectomized or estradiol-treated mice, and only in the case of C22:4*n*−6 (ADA) was a nearly significant interaction detected ($p = 0.052$). In addition, when comparing the differential effect of DI and DII in control (CO) vs. ovariectomized (OVX) mice, a truly significant difference was found (**Table 4C**: $p = 0.0194$). Since the effect of diet was quite similar under all reproductive conditions for the rest of FAs analyzed, we grouped the data from CO, OVX, and OVX-E mice to emphasize the effect and ratio of DI and DII in the case of C22:5*n*−6 (DPA) and C22:6*n*−3 (DHA) (**Tables 4E,F**). It was found that, irrespective of reproductive condition, the effect of each diet on cortical levels of these LC-PUFAs correlated comparatively more with the total amount of FAs or relatively with the amount of linoleic acid in the diet (**Table 2**).

Results from the analysis of complex lipids are shown in **Figure 2** and **Table 5**; for all lipids analyzed, the global effect of diet was highly significant ($p \leq 0.001$–0.0001). Thus, control animals fed alternative diets had increased cerebral cortex complex lipids compared to those fed SF, although the effect was significantly, quantitatively higher in mice fed with DI ($p \leq 0.0001$) than those fed with DII ($p \leq 0.02$–0.003). On the other hand, though no significant effect of hormone status was observed, certain interactions between diet and reproductive condition (D × H) were detected (**Figure 2**), a finding that justified further comparisons of the differences between the effects of both diets under each reproductive condition (**Table 5**; *p*-values and 95% confidence intervals). In all cases, the differences between the DI and DII effects observed in control animals were also significant in ovariectomized, estradiol-treated mice, and were even more evident when data from CO and OVX-E groups were combined. In contrast, the effects of DI and DII were similar in ovariectomized, placebo-treated females and no significant differences were detected for any of the different lipids analyzed. Furthermore, when comparing the dietary effect observed in CO animals (intact ovaries) plus OVX-E animals (continuous estradiol treatment) with that of OVX mice, a reasonable level of significance was found in all cases (**Tables 5A–F**, $p \leq 0.025$).

As an indication of the levels of estradiol, the dry uterine weight was determined at the endpoint. Intact females showed similar uterine weights, with independence of being fed with DI or DII (DI: 16.00 ± 2.40 mg; DII: 18.40 ± 2.00 mg). Also, OVX animals treated with estradiol showed similar uterine weights with the two diets (DI: 38.40 ± 8.00 mg; DII: 34.40 ± 3.20 mg). In contrast, OVX mice treated with placebo and fed with DI had uterine weights significantly higher than those fed with DII (DI: 8.00 ± 1.20 mg; DII: 4.00 ± 0.40 mg; $p < 0.001$).

In summary, these findings suggest interaction of diet and ovarian hormones on the levels of complex lipids in the mouse cerebral cortex, even though the presence or absence of ovaries and normal circulating estradiol levels do not appear to significantly modify the main effect of each diet.

The Expression of Synaptic Proteins in the Cerebral Cortex Are Affected by Dietary Differences in the Ratio of *n*−3 and *n*−6 LC-PUFAs

Brain lipids constitute a basic component of neural organization and play a critical role in the interactions of membrane proteins that are involved in cell signaling and synaptic functions (Bazan, 2014), processes that are also regulated by circulating levels of reproductive hormones and locally-synthesized steroids

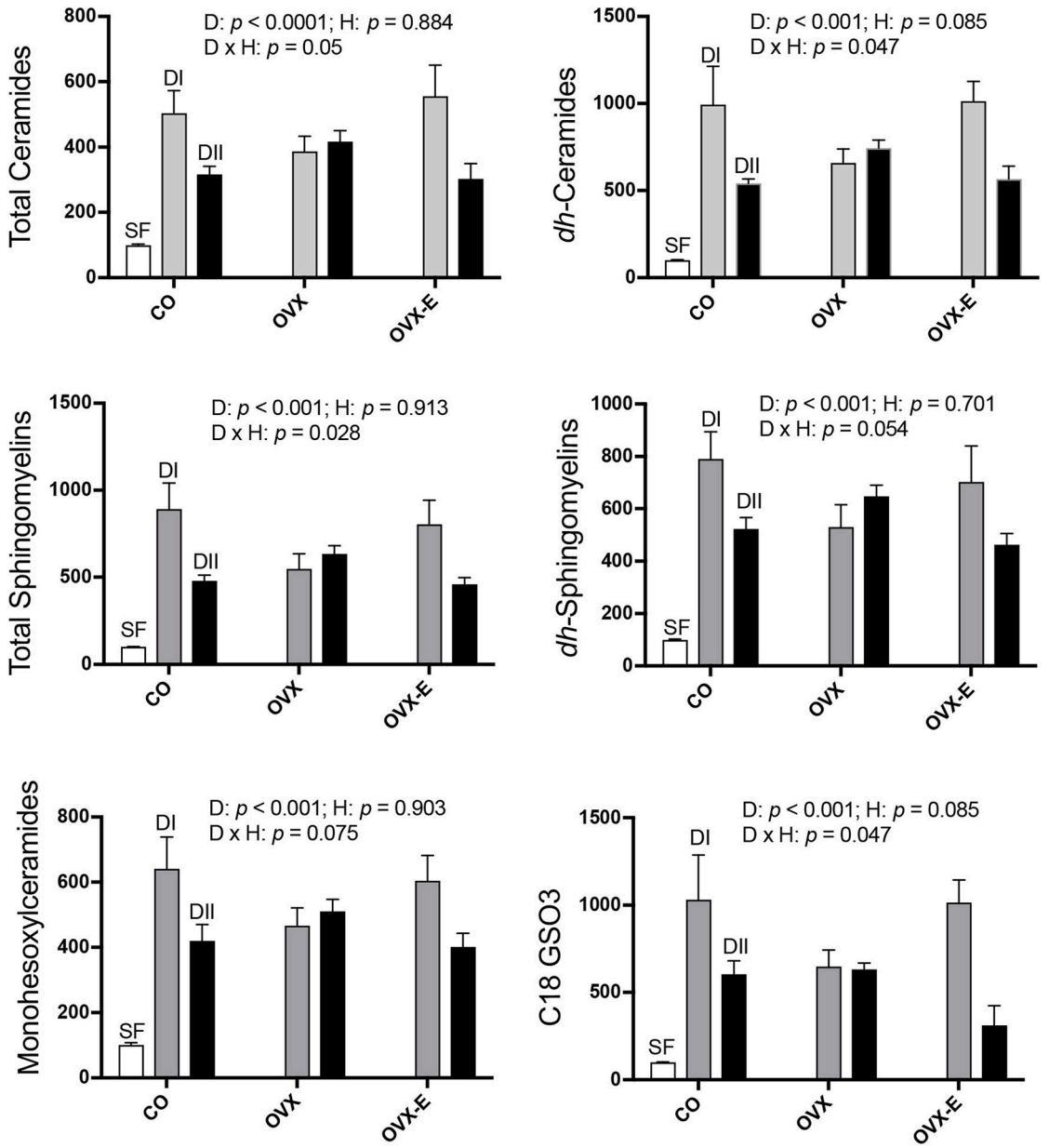

FIGURE 2 | Differential effects of dietary LC-PUFAs on the relative complex lipid content in the cerebral cortex of female mice under different reproductive conditions. Some sphingolipids and complex lipids were obtained and analyzed as described in section Materials and Methods. White bars represent the relative lipid content from cerebral cortex of intact animals fed with standard laboratory food (SF). Gray and black bars represent the same data from animals fed with DI or DII $n-6/n-3$ LC-PUFA diets, respectively. Vertical axis represents the percentage of variation induced by each diet relative to SF. Data are represented as mean ± SEM of 4 animals per group, except for those fed with SF ($n = 3$). Horizontal axis indicates the different reproductive status: CO, intact, sham-operated; OVX, ovariectomized, placebo-treated; OVX-E, ovariectomized, estradiol-treated The data were analyzed as previously described, and only some representative p-values for the main effects of diet (D), hormone status (H) and their interaction (D × H) were indicated in each graph, the remaining data were detailed in **Table 5**.

(Varea et al., 2009; Arevalo et al., 2015). Thus, it was interesting to explore whether differences in dietary $n-6/n-3$ LC-PUFA ratios affect expression and/or phosphorylation of synaptic proteins and key neuronal markers. Statistical analyses of observed changes for each protein were performed as follows: (a) the effect of differences in dietary content of LC-PUFAs in control animals; (b) the global interaction between the effect of diet and reproductive status; and (c) the specific differences between the effect of diet in controls and those observed in OVX or OVX-E mice.

CO mice fed a low $n-6/n-3$ ratio diet (DII) showed higher levels of both synapsin ($p = 0.023$) and PSD-95 ($p = 0.006$) than those fed with a high $n-6/n-3$ ratio diet (DI) (**Figure 3** and **Tables 6A, D**). In both cases, a global interaction between diet

TABLE 5 | Linear contrasts of the differential effects of dietary *n*−6/*n*−3 ratio on cerebral cortex lipid content under different reproductive conditions.

Lipid class	Main effects	*p*-value	95% CI
A. Total Ceramides	DI-SF (CO)	**0.0001**	**230.1, 578.3**
	DII-SF (CO)	**0.018**	**41.3, 389.5**
	DI-DII (CO)	**0.024**	**27.6, 350.0**
	DI-DII (OVX)	0.707	−190.6, 13.8
	DI-DII (OVX–E)	**0.007**	**78.8, 427.1**
	DI-DII (CO+OVX–E)	**0.001**	**102.2, 339.5**
	[DI-DII (CO+OVX–E)]-[DI-DII (OVX)]	**0.017**	**50.1, 450.4**
B. *dh*-Ceramides	DI-SF (CO)	**>0.00001**	**551.9, 1236.4**
	DII-SF (CO)	**0.014**	**99.3, 783.8**
	DI-DII (CO)	**0.008**	**135.7, 769.5**
	DI-DII (OVX)	0.577	−402.9, 230.8
	DI-DII (OVX–E)	**0.013**	**104.6, 789.1**
	DI-DII (CO+OVX–E)	**0.001**	**216.5, 682.9**
	[DI-DII (CO+OVX–E)]-[DI-DII (OVX)]	**0.010**	**142.3, 929.2**
C. Total Sphingomyelins	DI-SF (CO)	**>0.00001**	**500.9, 1082.9**
	DII-SF (CO)	**0.013**	**88.0, 669.9**
	DI-DII (CO)	**0.005**	**143.5, 682.3**
	DI-DII (OVX)	0.512	−355.5, 183.3
	DI-DII (OVX–E)	**0.023**	**54.4, 636.4**
	DI-DII (CO+OVX–E)	**0.001**	**180.9, 577.4**
	[DI-DII (CO+OVX–E)] - [DI-DII (OVX)]	**0.009**	**130.7, 799.7**
E. MHC	DI-SF (CO)	**>0.00001**	**432.0, 948.6**
	DII-SF (CO)	**0.003**	**165.7, 682.3**
	DI-DII (CO)	**0.031**	**27.2, 505.4**
	DI-DII (OVX)	0.323	−355.1, 123.2
	DI-DII (OVX–E)	0.067	−18.9, 497.7
	DI-DII (CO+OVX–E)	**0.007**	**76.8, 428.8**
	[DI-DII (CO+OVX–E)] - [DI-DII (OVX)]	**0.018**	**71.8, 665.7**
E. MHC	DI-SF (CO)	**>0.00001**	**346.9, 734.7**
	DII-SF (CO)	**0.003**	**126.8, 514.6**
	DI-DII (CO)	**0.019**	**40.6, 399.6**
	DI-DII (OVX)	0.589	−226.6, 132.4
	DI-DII (OVX–E)	**0.041**	**8.8, 396.6**
	DI-DII (CO+OVX–E)	**0.003**	**79.3, 343.5**
	[DI-DII (CO+OVX–E)] - [DI-DII (OVX)]	**0.025**	**35.6, 481.4**
F. C18 GSO3	DI-SF (CO)	**0.0001**	**519.4, 1343.0**
	DII-SF (CO)	**0.019**	**93.1, 916.6**
	DI-DII (CO)	**0.030**	**45.1, 807.6**
	DI-DII (OVX)	0.934	−366.0, 396.5
	DI-DII (OVX–E)	**0.001**	**321.0, 1083.5**
	DI-DII (CO+OVX–E)	**0.0001**	**294.7, 833.9**
	[DI-DII (CO+OVX–E)] - [DI-DII (OVX)]	**0.024**	**82.1, 1016.0**

*DI: High dietary n−6/n−3 ratio; DII: Low n−6/n−3 ratio; SF: Standard food. CO: Intact control female mice; OVX: Ovariectomized, placebo-treated female mice; OVX–E: Ovariectomized, estradiol-treated female mice. Data represented in **Figure 2** were analyzed by 2 × 3 factorial ANOVA. In cases where the influence of reproductive status on diet action was absent and significant interaction between the factors was not detected, data from those animals were grouped to emphasize the main dietary effects. The most significant p-values and 95% confidence intervals are highlighted.*

and reproductive status was observed ($p = 0.013$ and $p = 0.001$, respectively). Significant differences were also found in the effect of diet on the levels of synapsin (**Table 6A**: $p = 0.001$ and $p = 0.009$) and PSD-95 (**Table 6D**: $p = 0.0004$ and $p = 0.004$) when intact (CO) mice were compared with ovariectomized (OVX) or ovariectomized, estradiol-treated animals (OVX-E), respectively. These findings suggest that the presence of ovaries may be necessary for the effect of dietary lipid composition on the expression of these synaptic proteins, and that continuous treatment with estradiol alone was not able to compensate for ovariectomy. In contrast, levels of p-synapsin were reduced in animals fed with a low *n*−6/*n*−3 ratio diet (DII) compared to those fed with a high *n*−6/*n*−3 ratio diet (DI), regardless of reproductive status (**Figure 3** and **Table 6B**: $p = 0.015$). These differences in p-synapsin were additionally confirmed by a supplementary Western blots from the three diets (DI, DII and SF), and using PDK1 and Actin as internal controls (Supplementary Figure 1). No significant effects were found in the case of synaptophysin (**Figure 3** and **Table 6C**), P120 or β-catenin (**Tables 6E,F**, respectively). The slight effect observed in synaptophysin in the case of OVX-E animals fed DII when compared to CO mice was not considered significant as it was quantitatively small, and the 95% confidence intervals did not allow further accurate interpretation of the results. Neither significant effects of diet nor reproductive status were found in the case of several neuronal markers such as BACE, PHF1, Tau1, and Tau5 (data not shown). However, CO mice fed with low *n*−6/*n*−3 ratio diet (DII) showed higher levels of APP and GFAP than those fed with high *n*−6/*n*−3 ratio diet (DI) (**Figure 4** and **Table 7**; $p = 0.003$ and $p < 0.0012$, respectively). These effects were partially affected by reproductive status, as certain global interaction was detected, albeit of a small magnitude. Significant differences were also detected in the effect of diet on both APP and GFAP between controls and ovariectomized animals (**Tables 7A,B**; $p = 0.018$ and $p = 0.029$, respectively), which was partially compensated by continuous estradiol treatment.

DISCUSSION

Experimental evidence has suggested that the ratio between *n*−6 and *n*−3 LC-PUFAs is a critical factor for their developmental

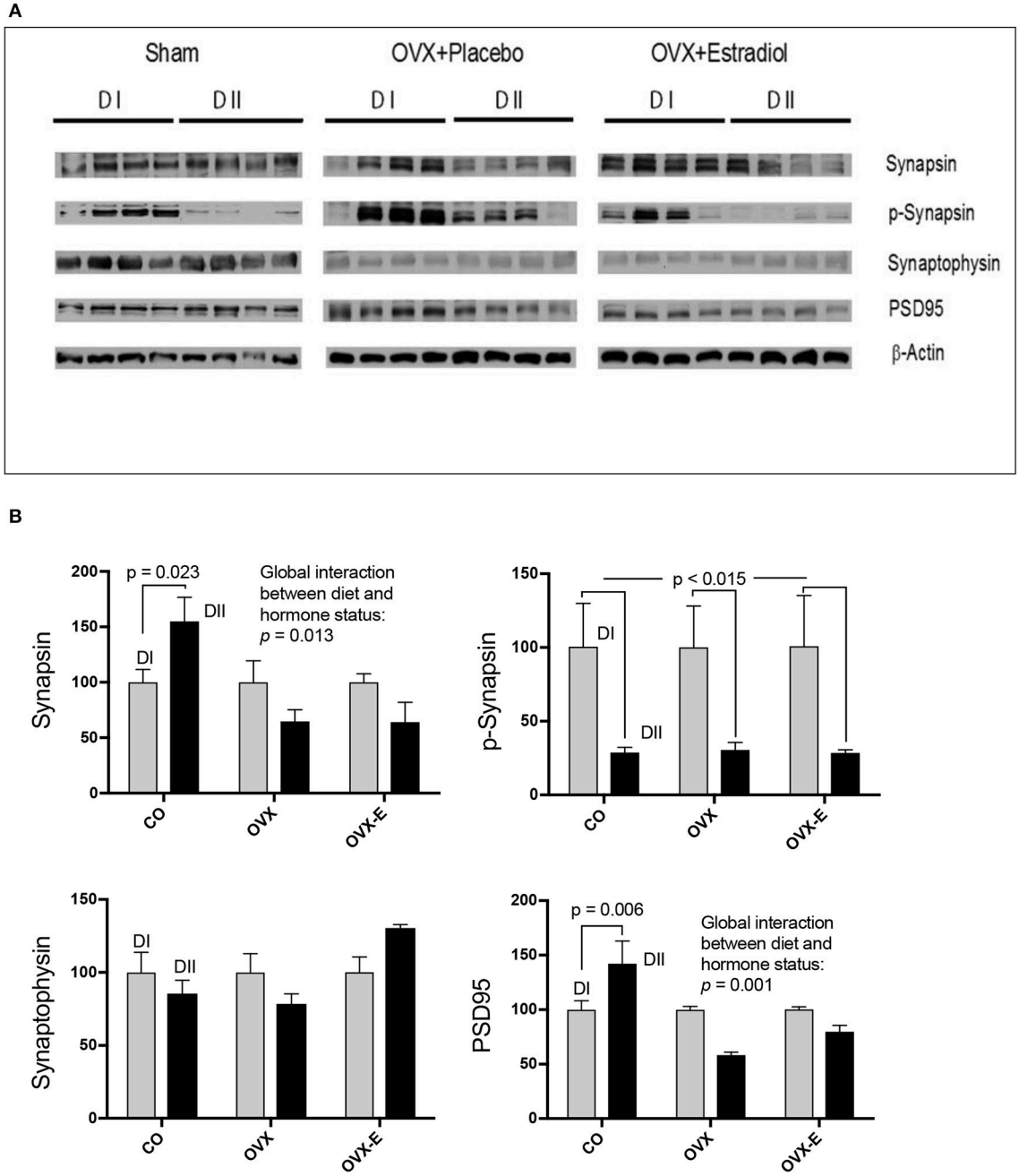

FIGURE 3 | Differential effects of dietary LC-PUFAs on the expression of synaptic proteins (synapsin, synaptophysin, and PSD95) in the cerebral cortex of female mice under different reproductive conditions. **(A)** Represents the Western blots, and **(B)** represents means ± SEM of densitometric quantification (4 mice per group). Western blots were quantified and normalized with respect to the loading control, actin. The normalized data corresponding to intact, sham-operated mice from the DI diet was arbitrarily considered 100 relative units. Vertical axis represents the percentage of variation induced by DII vs. DI *n*−6/*n*−3 LC-PUFA ratio diet. Horizontal axis indicates the different reproductive status as follows: CO, intact, sham-operated; OVX, ovariectomized, placebo-treated; OVX-E, ovariectomized, estradiol-treated. The data were statistically analyzed as previously described, and for simplicity, only the main effects of diet are given in the figure, as well as the interaction between diet and reproductive status. Other details of the analysis including the differences between the effect of diet in controls and ovariectomized mice treated with either placebo or estradiol were presented in **Table 6**.

and neuroprotective activity (Miller et al., 2016; Dyall, 2017). Therefore, the present study tested the effects of two experimental diets, DI and DII, whose major difference in composition was the global ratio of *n*−6 and *n*−3 LC-PUFAs. In addition, the two diets contained higher total levels of FA content (DI: 158%; DII: 147%) compared to the standard diet (SF), which explains the dramatic

TABLE 6 | Linear contrasts of the differential effects of dietary *n*−6/*n*−3 ratio on the expression of synaptic proteins in the cerebral cortex of female mice under different reproductive conditions.

Protein	Main effects	*p*-value	95 % CI
A. synapsin	DI-DII (CO)	**0.023**	**8.5, 101.4**
	[DI-DII (CO)] - [D-DII (OVX)]	**0.001**	**−155.7, −24.4**
	[DI-DII (CO)] - [DI-DII (OVX–E)]	**0.009**	**−156.4, −25.1**
B. p-synapsin	DI-DII (CO)	**0.014**	**−191.9, −25.3**
	[DI-DII (CO)] - [DI-DII (OVX)]	0.988	−117.0, 118.7
	[DI-DII (CO)] - [DI-DII (OVX–E)]	0.478	−77.2, 158.5
C. synaptophysin	DI-DII (CO)	0.321	−44.3, 15.4
	[DI-DII (CO)] - [DI-DII (OVX)]	0.730	−49.2, 35.1
	[DI-DII (CO)] - [DI-DII (OVX–E)]	**0.039**	**2.5, 86.9**
D. PSD-95	DI-DII (CO)	**0.006**	**13.8, 70.8**
	[DI-DII (CO)] - [DI-DII (OVX)]	**0.0004**	**−124.3, −43.6**
	[DI-DII (CO)] - [DI-DII (OVX–E)]	**0.004**	**−103.0, −22.3**
E. P120	DI-DII (CO)	0.440	−33.8, 74.4
	[DI-DII (CO)] - [DI-DII (OVX)]	0.293	−115.9, 37.1
	[DII-DII (CO)] - [DI-DII (OVX–E)]	0.830	−84.4, 68.6
F. β-catenin	DI-DII (CO)	0.217	−82.2, 20.0
	[DI-DII (CO)] - [DI-DII (OVX)]	0.142	−19.5, 125.0
	[DI-DII (CO)] - [DI-DII (OVX–E)]	0.122	−16.4, 128.1

The effect of diet under each reproductive status was calculated as a percentage of variation induced by DII (Low n−6/n−3 ratio) vs. DI (High dietary n−6/n−3 ratio). CO: Intact, sham-operated female mice; OVX: Ovariectomized, placebo-treated; OVX-E: Ovariectomized, estradiol-treated. Data represented in ***Figure 3*** *were analyzed by 2 × 3 factorial ANOVA and saturated regression models; the most significant p values and their corresponding 95% confidence intervals are highlighted.*

increases of total FAs observed in the cerebral cortex of mice fed with both experimental diets.

As expected, DI had increased percentages of *n*−6 FAs including C22:4*n*−6 (ADA) and C22:5*n*−6 (DPA), and reduced levels of C22:6*n*−3 (DHA). In addition, both diets caused minor elevation in C20:4*n*−6 (ARA) levels in the cerebral cortex, though the effect of DI was slightly higher, in agreement with the dietary content of its precursor, linoleic acid. Since ARA is a critical intermediate in the biosynthesis of thromboxanes, prostaglandins, and leukotrienes, which play an essential role in the inflammatory/anti-inflammatory response (Stables and Gilroy, 2011), some regulatory mechanisms to maintain balanced levels may exist. On the other hand, levels of DHA were higher in the cortex of mice fed with DII than in those fed with DI, in good correlation with the absence of DHA and the extremely low levels of its precursor, C18:3*n*−3 (ALA) in the composition of DI. Interestingly, the levels of DHA in animals fed with DII were similar to those fed with SF, despite the absence of DHA in the standard diet. However, the fact that the SF diet contains twice as much of the DHA precursor indicates that ALA-derived DHA may be sufficient to maintain brain DHA levels and preserve its function, as it has been suggested (Anderson et al., 2005; André et al., 2005). Furthermore, this interpretation is in agreement with evidence from animal models that brain DHA levels are similar when fed with diets with ALA as the only PUFA compared to those fed with DHA or ALA+DHA (reviewed in Barcelo-Coblijn and Murphy, 2009). Regarding other LC-PUFA intermediates in DHA biosynthesis, such as eicosatetranoic acid (ETA, C20:4*n*−3) or EPA (C20:5*n*−3), we did not find detectable amounts of either in brain samples, in agreement with previous reports (Miller et al., 2016; Harauma et al., 2017).

In summary, the most relevant finding regarding the effect of DI and DII on LC-PUFAs was a dramatic reduction in the ratio between C22:6*n*−3 and C22:5*n*−6 in animals fed with DI, and a marked increase in those fed with DII. However, this effect does not seem to be due to DHA enrichment in DII, but rather to the differential dietary levels of LNA (DI) and ALA (DII), in agreement with other reports (Domenichiello et al., 2016). Interestingly, no significant effects of reproductive status were detected for the dietary effects on cerebral cortex LC-PUFA levels, since the *p*-values obtained from the factorial analysis did not support relevant interactions between diet and gonadal conditions.

Our findings also show that the two experimental diets induced profound and highly significant elevations in the levels of all complex lipids analyzed, though for all of them the effect was stronger in animals fed a diet with the highest *n*−6/*n*−3 LC-PUFA ratio. Interestingly, the effects of DI and DII on cortical ceramide levels observed in control mice were not detected in ovariectomized mice. Furthermore, the differential effect in all complex lipids of each diet was reverted in ovariectomized animals receiving continuous estradiol treatment. These results suggest a synergistic action between dietary PUFAs and ovarian hormones on the cerebral cortex lipidome, which would be in agreement with other reports using hippocampal tissue from female mice and multivariate statistical approaches (Díaz et al., 2016).

The influence of ovarian hormones on the dietary effects on cortical ceramides is highly relevant given the important function of these lipids in a wide range of cell processes including growth, differentiation, apoptosis, and oncogenesis (Kashara and Sanai, 2000; Simons and Toomre, 2000; Anderson and Jacobson, 2002; Sengupta et al., 2007; Pruett et al., 2008). Increase in ceramide concentration in cell membranes affects not only the structural organization and dynamic properties of lipid rafts (Cremesti et al., 2002) but also myelin formation and stability (Pan et al., 2005; Susuki et al., 2007), neural differentiation (Wang and Yu, 2013; Wang et al., 2014), synapse formation (Hering et al., 2003; Mendez-Otero and Santiago, 2003), synaptic plasticity and transmission, neurotoxicity, and neurodegeneration (Hering et al., 2003; Besshoh et al., 2005; Ferrer, 2009; Fabelo et al., 2014; Attiori Essis et al., 2015; Sonnino and Prinetti, 2016; Marín et al., 2017). In addition to experimental evidence in rodents, a number of postmortem studies support the role of age-dependent or genetic alterations of ceramide and sphingolipid metabolism in several neurological disorders, including Alzheimer's (AD) and Parkinson's diseases (He et al., 2010; Fabelo et al., 2011; Gegg et al., 2012; Bouti et al., 2016; Olsen and Færgeman, 2017). However, despite the importance of ceramide and sphingolipids for brain function, the effect of dietary interventions on their levels in the cerebral cortex has not been previously explored.

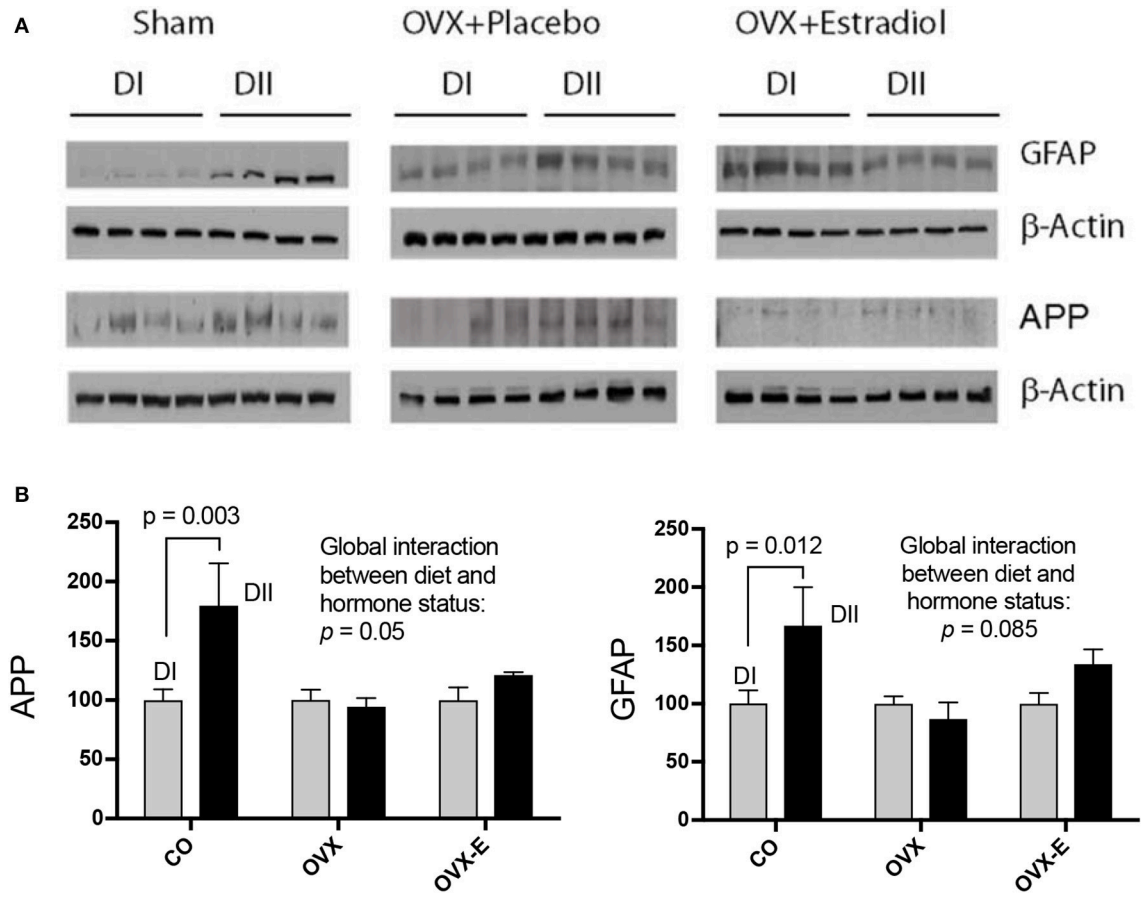

FIGURE 4 | Differential effects of dietary LC-PUFAs on the expression of APP and GFAP in the cerebral cortex of female mice under different reproductive conditions. **(A)** Represent the western blots, and **(B)** represent the densitometric data as means ± SEM of relative densitometric quantification (4 mice per group). Vertical axis represents the percentage of variation induced by DII vs. DI *n*−6/*n*−3 LC-PUFA ratio diet. Horizontal axis indicates the different reproductive status as follows: CO, intact, sham-operated; OVX, ovariectomized, placebo-treated; OVX-E, ovariectomized, estradiol-treated. Western blots were quantified and normalized with respect to the loading control, β-Actin. The normalized data corresponding to intact, sham-operated mice from the DI diet was arbitrarily considered 100 relative units. The data were statistically analyzed as previously described, and only some relevant data are included in this Figure whereas the remaining data was presented in **Table 7**.

In addition, neuronal lipid microdomains are also targets for estrogen hormones that act via classical estrogen receptors or membrane-associated receptors to trigger a variety of signaling pathways (Marín et al., 2003, 2005, 2007; Guerra et al., 2004). Activation of these pathways is involved in the regulation of brain development, neuronal survival and synaptic plasticity, which are the basis for the neuroprotective role of estrogens (Marín et al., 2005; Herrera et al., 2011; Arevalo et al., 2015). Therefore, dietary and estrogen-induced modification of brain sphingolipid composition may be expected to alter the expression of specific signaling and synaptic proteins. Thus, the second aim of this work was to determine whether circulating ovarian hormones could interact with the effects of dietary lipid composition, altering expression of neuronal proteins in the mouse cerebral cortex. We analyzed the levels of key neuronal proteins such as P120, PSD-95, β-catenin, synaptophysin, and synapsin. Though no significant effects were detected on the expression of P120, β-catenin, or synaptophysin, both PSD-95 and synapsin were found to be sensitive to the different dietary *n*−6/*n*−3 ratios. In addition, the effect of diet was blocked by ovariectomy, suggesting a potential synergy between diet and reproductive hormones at both presynaptic and postsynaptic levels.

Synapsins are a family of presynaptic proteins that interact with synaptic vesicles through phosphorylation-dependent processes (Chi et al., 2003; Cousin et al., 2003; Menegon et al., 2006; Sun et al., 2006; Giachello et al., 2010; Messa et al., 2010). In this work, a diet with a low *n*−6/*n*−3 LC-PUFA ratio (with relatively high levels of DHA and EPA) induced higher expression of synapsin, but lower levels of p-synapsin (Ser-9) than a diet with a higher *n*−6/*n*−3 ratio (lacking supplemental DHA and EPA). Interestingly, regarding total synapsin, it was found that ovariectomy blocked the dietary effect, and that continuous estradiol-treatment neither reverted nor prevented the effect of ovariectomy, suggesting that,

TABLE 7 | Linear contrasts of the differential effects of dietary *n*−6/*n*−3 ratio on the expression of APP and the glial marker GFAP, in the cerebral cortex of female mice under different reproductive conditions.

Protein	Main effects	*p*-value	95 % CI
A. APP	DI-DII (CO)	**0.003**	**31.1, 128.3**
	DI-DII (CO) - DI-II (OVX)	**0.018**	**−154.2, −16.7**
	DI-DII (CO) - DI-DII (OVX–E)	0.090	−127.4, 10.1
B. GFAP	DI-DII (CO)	**0.012**	**16.7, 117.0**
	DI-DII (CO) - DI-II (OVX)	**0.029**	**−150.7, −9.0**
	DI-DII (CO) - DI-DII (OVX–E)	0.344	−103.7, 38.1

The effect of diet under each reproductive status was calculated as percentage of variation induced by DII (Low n−6/n−3 ratio) vs. DI (High dietary n−6/n−3 ratio). CO: Intact, sham-operated female mice; OVX: Ovariectomized, placebo-treated; OVX-E: Ovariectomized, estradiol-treated. Data represented in ***Figure 4*** *were analyzed by 2 × 3 factorial ANOVA and saturated regression model; the most significant p-values and their corresponding 95% confidence intervals are highlighted.*

in addition to estradiol, other ovarian secretions might be involved. In this respect, estrogen-progesterone interactions in the modulation of synaptic plasticity and the expression of both pre-and post-synaptic proteins in several brain regions of monkeys and rodents have been reported (Choi et al., 2003; Foy et al., 2008; Williams et al., 2011; Baudry et al., 2013). On the contrary, the profound dietary effect observed for p-synapsin was not influenced by ovariectomy. It should be pointed out that synapsin phosphorylation is a short-term regulated event at the level of presynaptic terminals which depends on action potential firing, activation dynamics of highly localized voltage-dependent calcium channels, and a complex interplay between several Ca^{++}-dependent protein kinases (Chi et al., 2003; Menegon et al., 2006; Sun et al., 2006; Giachello et al., 2010). Thus, protein-lipid interactions at the level of presynaptic membranes can be expected to depend on dietary lipid composition and being additionally influenced by ovarian function. However, rapid modulation of short-term presynaptic phenomena, such as those involved in p-synapsin phosphorylation and its potential dependence on ovarian hormone levels, must be difficult to be observed under our experimental approach.

PSD-95 is an integral component of the postsynaptic density that participates in neurotransmission (Cho et al., 1992; Kim and Sheng, 2004; Berry and Nedivi, 2017), synaptic plasticity and learning (Migaude et al., 1998; EI-Husseini et al., 2000; Schnell et al., 2002; Ehrlich and Malonow, 2004; Ehrlich et al., 2007). In intact female mice, we found that a diet with a low *n*−6/*n*−3 LC-PUFA ratio (enriched in DHA and EPA) induced higher expression levels of PSD-95 in the cerebral cortex than a diet with a higher *n*−6/*n*−3 ratio (lacking DHA or EPA enrichment). This is in agreement with previous reports of reduced PSD-95 expression in aged mice fed with DHA-deficient diets (Sidhu et al., 2016). This effect was not observed in ovariectomized animals, indicating that circulating ovarian hormones might interact with brain dietary inputs for regulation of the synaptic proteome. However, administration of estradiol alone was unable to either revert or prevent the effect of ovariectomy. Even though we cannot reach clear conclusions from these findings, they suggest that, in addition to estradiol, oscillations in other cyclic ovarian secretions may play a physiological role in the modulation of brain cortex synaptic proteins by dietary differences in *n*−6/*n*−3 ratios. In this respect, as mentioned above, there are several reports supporting the potential effect of estrogen-progesterone interactions on synaptic plasticity and post-synaptic proteins (Foy et al., 2008; Baudry et al., 2013; for review see Williams et al., 2011).

The second group of proteins analyzed were those involved in some neurodegenerative pathologies like AD and other taupathies, such as APP, Tau, BACE or GFAP (for review see Laird et al., 2005; LaFerla and Green, 2012; Rosenberg et al., 2016). Our data indicate that only APP and GFAP were differentially expressed in the cerebral cortex of female mice fed with either DI or DII. In both cases, ovariectomy blocked the differential effect of DII, even though only a slight estradiol-induced reversion was observed. It is tantalizing to suggest that the increase of APP expression induced by DII over DI might be a positive response to certain stress, influencing the balance of neuronal-glia interactions. It will be interesting to further studying the effects of these dietary and reproductive manipulations in specific mouse models of neurodegenerative disorders.

The results of the current work indicate that different dietary *n*−6/*n*−3 LC-PUFA ratios are able to remodel the lipidome in the cerebral cortex of female mice, and that these effects are partially influenced by the circulating levels of ovarian hormones. A variety of results from animal models of neurodegenerative diseases have suggested that dietary interventions may be useful therapeutic tools against several neurodegenerative disorders (Lim et al., 2005; Green et al., 2007; Bazan et al., 2011a,b; Bazan, 2014). However, the potential for these therapeutic approaches in human health and disease is still unclear, and the current dietary recommendations have been considered specific to particular age groups and physiological conditions (Zárate et al., 2017). The interactions between the effect of dietary lipid composition and reproductive status shown here indicate the importance the specific *n*−6/*n*−3 composition in therapeutic diets, which must also be well-balanced in regards to the hormonal context and physiological situations of age-associated impairment of reproductive function, such as menopause.

AUTHOR CONTRIBUTIONS

JH performed the animal experiments and was in charge of most experimental manipulations, hormone treatments, and collection of brain samples; JH and LO-G prepared brain samples and western blotting analysis; AM and GH participated in experimental designs, animal treatments, and collection of samples; GF and JC performed the lipidomic analysis of brain samples; NA and CR analyzed the lipid composition of the experimental diets; CR collaborated in the interpretation of results; LP-V performed statistical analysis of quantitative results; RA conceived and designed the experiments and contributed

together with LP-V to the design of the specific statistical analysis; LG-S, RA, and FW were in charge of the final interpretation of results and wrote the paper.

FUNDING

RA was supported in part by SAF2007-66148-C02-01 & FP7-REGPOT-2012-31637-IMBRAIN grants. LG-S was supported by BFU2014-51836-C2-1-R grant, CIBERFES and Fondos Feder. FW was supported by grants from the MICINN (SAF2012-39148-C03-0), the European Union (EU-FP7-2009-CT222887), CAM (B2017/BMD-3700), Centro de Investigación Biomédica en Red sobre Enfermedades Neurodegenerativas (CIBERNED), CIBERNED Proyectos Colaborativos (PI2016/01), and by an institutional grant from the Fundación Ramón Areces to CBMSO and Fondos FEDER.

ACKNOWLEDGMENTS

The authors gratefully acknowledge Mario Diaz (Universidad de La Laguna) and Emilio Martinez de la Victoria (Instituto de Nutrición y Tecnología de los Alimentos, Universidad de Granada) for their advice in the design of experimental diets, and Maria Rosa Arnaiz for her help in the management of mice in the University of La Laguna animal facility. The antibody PHF-1 was generously provided by Prof. P. Davies (The Feinstein Institute for Medical Research, NY, USA).

SUPPLEMENTARY MATERIAL

The Supplementary Material for this article can be found online at: https://www.frontiersin.org/articles/10.3389/fncel.2018.00103/full#supplementary-material

REFERENCES

Anderson, G. J., Neuringer, M., Lin, D. S., and Connor, W. E. (2005). Can prenatal *N*−3 fatty acid defficiency be completely reversed after birth? Effects on retinal and brain biochemistry and visual function in Rhesus monkeys. *Pediatr. Res.* 58, 865–872. doi: 10.1203/01.pdr.0000182188.31596.5a

Anderson, R. G., and Jacobson, K. (2002). A role for lipid shells in targetting proteins to caveolae, rafts, and other lipid domains. *Science* 296, 1821–1825. doi: 10.1126/science.1068886

André A, Juanéda, P., Sébédio, J. L., and Chardigny, J. M. (2005). Effects of aging and dietary *n*−3 fatty acids on rat brain phospholipids: focus on plasmalogens. *Lipids* 40, 799–806. doi: 10.1007/s11745-005-1441-x

Arevalo, M. A., Azcoitia, I., and Garcia-Segura, L. M. (2015). The neuroprotective actions of oestradiol and oestrogen receptors. *Nat. Rev. Neurosci.* 16, 17–29. doi: 10.1038/nrn3856

Armitage, P., Berry, G., and Mathews, J. N. S. (2004). *Statistical Methods in Medical Research*. London: Wiley-Blackwell.

Attiori Essis, S., Laurier-Laurin, M. E., Pépin, É., Cyr, M., and Massicote, G. (2015). GluN2B-containing NMDA receptors are upregulated in plasma membranes by the sphingosine-1-phosphate analog FTY720P. *Brain Res.* 1624, 349–358. doi: 10.1016/j.brainres.2015.07.055

Bannenberg, G., and Serhan, C. N. (2010). Specialized pro-resolving lipid mediators in the inflamatory response: an update. *Biochem. Biophys. Acta* 1891, 1260–1273. doi: 10.1016/j.bbalip.2010.08.002

Barcelo-Coblijn, G., and Murphy, E. J. (2009). Alpha-linoleic acid and its conversion to longer chain *n*−3 fatty acids: benefits for human health and a role in maintaining tissue *n*−3 fatty acid levels. *Prog. Lipid Res.* 48, 355–374. doi: 10.1016/j.plipres.2009.07.002

Baudry, M., Xiaoning, B., and Aguirre, C. (2013). Progesterone-estrogen interactions in synaptic plasticity and neuroprotection. *Neuroscience* 239, 280–294. doi: 10.1016/j.neuroscience.2012.10.051

Bazan, N. G. (2014). Is there a molecular logic that sustains neuronal functional integrity and survival?: lipid signaling is necessary for neuroprotective neuronal transcriptional programs. *Mol. Neurobiol.* 50, 1–5. doi: 10.1007/s12035-014-8897-0

Bazan, N. G., Calandria, J. M., and Gordon, W. C. (2013). Docosahexanoic acid and its derivative neuroprotectin D1 display neuroprotective properties in the retina, brain and central nervous system. *Nestle Nutr. Inst. Workshop Ser.* 77, 121–131. doi: 10.1159/000351395

Bazan, N. G., Molina, M. F., and Gordon, W. C. (2011a). Docosahexaenoic acid signalolipidomics in nutrition: significance in aging, neuroinflamation, macular degeneration, Alzheimer's, and other neurodegenerative diseases. *Ann. Rev. Nutr.* 31, 321–351. doi: 10.1146/annurev.nutr.012809.104635

Bazan, N. G., Musto, A. E., and Knott, E. J. (2011b). Endogenous signaling by omega-3 docosahexanoic acid-derived mediators sustains homeostatic synaptic and circuitry integrity. *Mol. Neurobiol.* 44, 216–222. doi: 10.1007/s12035-011-8200-6

Bazinet, R. P., and Layé, S. (2014). Polyunsaturated fatty acids and their metabolites in brain function and disease. *Nat. Rev. Neurosci.* 15, 771–785. doi: 10.1038/nrn3820

Berry, K. P., and Nedivi, E. (2017). Spine dynamics: are they all the same? *Neuron* 27, 43–55. doi: 10.1016/j.neuron.2017.08.008

Besshoh, S., Bawa, D., Teves, L., Wallace, M. C., and Gurd, J. W. (2005). Increased phosphorylation and redistribution of NMDA receptors between synaptic lipid rafts and postsynaptic densities following transient global ischemia in the rat brain. *J. Neurochem.* 93, 186–194. doi: 10.1111/j.1471-4159.2004.03009.x

Bourre, J. M., Pascal, G., Durand, G., Masson, M., Dumont, O., and Piciotti, M. (1984). Alterations in the fatty acid composition of rat brain cells (neurons, astrocytes, and oligodendrocytes) and of subcellular fractions (myelin ans synaptosomes) induced by a diet devoid of *n*−3 fatty acids. *J. Neurochem.* 43, 342–348. doi: 10.1111/j.1471-4159.1984.tb00906.x

Bouti, M., Sun, Y., Shacka, J. J., and Auray-Blais, C. (2016). Tandem mass spectometry multiplex analysis of glucoceramide and galactosyceramide isoforms in brain tissues at different stages of Parkinson disease. *Anal Chem.* 88, 1856–1863. doi: 10.1021/acs.analchem.5b04227

Brenna, J. T., and Diau, G.-Y. (2007). The influence of dietary docosahexanoic acid and arachdonic acid on central nervous system polyunsaturated fatty acid composition. *Prostaglandins Leukot. Essent. Fatty Acids.* 77, 247–250. doi: 10.1016/j.plefa.2007.10.016

Carrié, I., Clément, M., de Javel, D., Francès, H., and Bourre, J.-M. (2000). Specific phospholipid fatty acid composition of brain regions in mice: effects of *n*−3 polyunsaturated fatty acid deficiency and phospholipid supplementation. *J. Lipid Res.* 41, 465–472.

Catalan, J., Moriguchi, T., Slotnick, B., Murthy, M., Greiner, R. S., and Salem Jr, N. (2002). Cognitive deficits in docosahexanoic acid-deficiency rats. *Behav. Neurosci.* 116, 1022–1031. doi: 10.1037/0735-7044.116.6.1022

Chen, C. T., Liu, Z., Ouellet, M., Calon, F., and Bazinet, R. P. (2009). Rapid beta-oxidation of eicosapentanoic acid in mouse brain: an *in situ* study. *Prostaglandins Leukot. Essent. Fatty Acids.* 80, 157–163. doi: 10.1016/j.plefa.2009.01.005

Chi, P., Greengard, P., and Ryan, T. A. (2003). Synaptic vesicle mobilization is regulated by distinct synapsin I phosphorylation pathways at different frequencies. *Neuron* 38, 69–78. doi: 10.1016/S0896-6273(03)00151-X

Cho, K. O., Hunt, C. A., and Kennedy, M. B. (1992). The rat brain postsynaptic density fraction contains a homolog of the *Drosophila* discs-large tumor suppressor protein. *Neuron* 9, 929–942. doi: 10.1016/0896-6273(92)90245-9

Choi, J. M., Romeo, R. D., Brake, W. G., Bethea, C. L., Rosenwaks, Z., and McEwen, B. S. (2003). Estradiol increases pre- and post-synaptic proteins in the CA1 region of the hippocampus in female Rhesus macaques (*Macaca mulata*). *Endocrinology* 144, 4734–4738. doi: 10.1210/en.2003-0216

Cingolani, F., Casasampere, M., Sanllehi, P., Casas, J., Bujons, J., and Fabrias, G. (2014). Inhibition of dihydroceramide desaturase activity by the sphingosine kinase inhibitor SKII. *J. Lipid Res.* 55, 1711–1720. doi: 10.1194/jlr.M049759

Cousin, M. A., Maladi, C. S., Tan, T. C., Raymond, C. R., Smillie, K. J., and Robinson, P. J. (2003). Synapsin I-associated phosphatidylinositol 3-kinase mediates synaptic vesicle delivery to the readily releasable pool. *J. Biol. Chem.* 278, 29065–29071. doi: 10.1074/jbc.M302386200

Cremesti, A. E., Goni, F. M., and Kolesnick, R. (2002). Role of sphingomyelinase and ceramide in regulationg rafts: do biophysical properties determine biologic outcomes? *FEBS Lett.* 531, 47–53. doi: 10.1016/S0014-5793(02)03489-0

Díaz, M., Fabelo, N., Casañas-Sánchez, V., Marin, R., Gómez, T., Quinto-Alemany, D., et al. (2016). Hippocampal lipid homeostasis in APP/PS1 mice is modulated by a complex interplay between dietary DHA and estrogens: relevance for Alzheimer's disease. *J. Alzheimers Dis.* 49, 459–481. doi: 10.3233/JAD-150470

Domenichiello, A. F., Kitson, A. P., Chen, C. T., Trépanier, M. O., Stavro, P. M., and Bazinet, R. P. (2016). The effect of linoleic acid on the whole body synthesis rates of polyunsaturated fattu acids from α-linolenic and linoleic acid in free-living rats. *J. Nutr. Biochem.* 30, 167–176. doi: 10.1016/j.jnutbio.2015.11.016

Dyall, S. C. (2017). Interplay between $n-3$ and $n-6$ long-chain polyunsaturated fatty acids and the endocannabinoid system in brain protection and repair. *Lipids* 52, 885–900. doi: 10.1007/s11745-017-4292-8

Dyall, S. C., and Michael-Titus, A. T. (2008). Neurological benefits of omega-3 fatty acids. *Neuromol. Med.* 10, 219–235. doi: 10.1007/s12017-008-8036-z

Ehrlich, I., Klein, M., Rumpel, S., and Malinow, R. (2007). PSD-95 is required for activity-driven synapse stabilization. *Proc. Natl. Acad. Sci. U.S.A.* 104, 4176–4181. doi: 10.1073/pnas0609307104

Ehrlich, I., and Malonow, R. (2004). Postsynaptic density 95 controls AMP receptor incorporation during long-term potentiation and experienced-driven synaptic plasticity. *J. Neurosci.* 24, 916–927. doi: 10.1523/JNEUROSCI.4733-03.2004

EI-Husseini, A. E., Schnell, E., Chetkovich, D. M., Nicoll, R. A., and Bredt, D.S. (2000). PSD-95 involvement in maduration of excitatory synapses. *Science* 290, 1364–1368.

Fabelo, N., Martín, V., Marín, R., Moreno, D., Ferrer, I., and Díaz, M. (2014). Altered lipid composition in cortical lipid rafts occurs at early stages of sporadic Alzheimer's diseas and facilitates APP/BACE1 interactions. *Neurobiol. Aging.* 35, 1801–1812. doi: 10.1016/j.neurobiolaging.2014.02.005

Fabelo, N., Martin, V., Santpere, G., Marín, R., Torrent, L., Ferrer, I., et al. (2011). Severe alterations in lipid composition of frontal cortex lipid rafts from Parkinson's disease and incidental Parkinson's disease. *Mol. Med.* 17, 1107–1118. doi: 10.2119/molmed.2011.00119

Ferrer, I. (2009). Altered mitochondria, energy metabolism, voltage-dependent anion channel, and lipid rafts converge to exaust neurons in Alzheimer's disease. *J. Bioenerg. Biomembr.* 41, 425–431. doi: 10.1007/s10863-009-9243-5

Folch, J., Lees, M., and Sloane Stanley, G. H. (1957). A simple method for the isolation and purification of total lipids from animal tissues. *J. Biol. Chem.* 226, 497–509.

Foy, M. R., Akopian, G., and Thompson, R. F. (2008). Progesterone regulation of synaptic transmission and plasticity in rodent hippocampus. *Learn. Mem.* 15, 820–822. doi: 10.1101/lm.1124708

Garanto, A., Mandal, N. A., Egido-Gabás, M., Marfany, G., Fabriàs, G., Anderson, R. E., et al. (2013). Specific spjingolipid content decrease in Cerkl knockdown mouse retinas. *Exp. Eye Res.* 110, 96–106. doi: 10.1016/j.exer.2013.03.003

Gegg, M. E., Burke, D., Heales, S. J., Cooper, J. M., Hardy, J., Wood, N. W., et al. (2012). Glucocerebrosidade deficiency in substantia nigra of Parkinson disease brains. *Ann. Neurol.* 72, 455–463. doi: 10.1002/ana.23614

Giachello, C. N., Fiumara, F., Giacomini, C., Corradi, C., Milanese, C., Ghirardi, M., et al. (2010). MAPK/Erk-dependent phosphorylation of synapsin mediates formation of functional synapses and short-term homosynaptic plasticity. *J. Cell Sci.* 123, 881–893. doi: 10.1242/jcs.056846

Gorjão, R., Acevedo-Martins, A. K., Rodrigues, H. G., Abdulkader, F., Arcisio-Miranda, M., Procopio, J., et al. (2009). Comparative effects of DHA and EPA on cell function. *Pharmacol. Ther.* 122, 56–64. doi: 10.1016/j.pharmthera.2009.01.004

Green, K. N., Martinez-Coria, H., Khahwji, H., Hall, E. B., Yurko-Mauro, K. A., Ellis, L., et al. (2007). Dietary docosahexaenoic acid and docosapentaenoic acid ameliorate amyloid-βand tau pathology via a mechanism involving presenelin 1 levels. *Neurobiol. Dis.* 27, 4385–4395. doi: 10.1523/JNEUROSCI.0055-07.2007

Guerra, B., Díaz, M., Alonso, R., and Marín, R. (2004). Plasma membrane oestrogen receptor mediates neuroprotection against β-amyloid toxicity through activation of Raf-1/MEK/ERK cascade. *J. Neurochem.* 91, 99–109. doi: 10.1111/j.1471-4159.2004.02695.x

Harauma, A., Yasuda, H., Hatanaka, E., Nakamura, M., Salem Jr, N., and Moriguchi, T. (2017). The essentiality of arachidonic acid in addition to docosahexaenoic acid for brain growth and function. *Prostaglandins Leukot. Essent. Fatty Acids* 116, 9–18. doi: 10.1016/j.plefa.2016.11.002

He, X., Huang, Y., Li, B., Gong, C. X., and Schuchman, E. H. (2010). Deregulation of sphingolipid metabolism in Alzheimer's disease. *Neurobiol. Aging* 31, 398–408. doi: 10.1016/j.neurobiolaging.2008.05.010

Hering, H., Lin, C. C., and Sheng, M. (2003). Lipid rafts in the maintenance of synapses, dendritic spines, and surface AMPA receptor stability. *J. Neurosci.* 23, 3262–3271.

Herrera, J. L., Díaz, M., Hernández-Fernaud, J. R., Salido, E., Alonso, R., Fernandez, C., et al. (2011). Voltage-dependent anion channel (VDAC) as a resident protein of lipid rafts: post-transductional regulation by estrogens and involvement in neuronal preservation against Alzheimer's disease. *J. Neurochem.* 116, 820–827. doi: 10.1111/j.1471-4159.2010.06987.x

Ikemoto, A., Ohishi, M., Sato, Y., Hata, N., Misawa, Y., Fujii, Y., et al. (2001). Okuyama, H. Reversibility of $n-3$ fatty acid deficiency-induced alterations of learning nehaviour in the rat: level of $n-6$ fatty acids as another critical factor. *Lipid Res.* 42, 1655–1663.

Jumpsen, J., Elien, E., Goh, Y., and Clandinin, M. (1997). Small changes of dietary ($n-6$) and ($n-3$)/fatty acid content ratio alter phosphatidylethanolamine and phosphatidylcholine fatty acid composition during development of neuronal and glial cells in rats. *J. Nutr.* 127, 724–731. doi: 10.1093/jn/127.5.724

Kashara, K., and Sanai, Y. (2000). Functional roles of glycospingolipids in signal transduction via lipid rafts. *Glyconj J.* 17, 153–162. doi: 10.1023/A:1026576804247

Kim, E., and Sheng, M. (2004). PDZ domain proteins of synapses. *Nat. Rev. Neurosci.* 5, 771–781. doi: 10.1038/nrn1517

LaFerla, F. M., and Green, K. N. (2012). Animal models of Alzheimer disease. *Cold Spring Harb. Perspect. Med.* 11:a005329. doi: 10.1101/cshperspect.a006320

Laird, F. M., Huaibi, C., Savonenko, A. V., Farah, M. H., He, K., Melnikova, T., et al. (2005). BACE1, a major determinant of selective vulnerability of the brain to amlyoid-β amyloidogenesis, is essential for dognitive, emotional, and synaptic function. *J. Neurosci.* 25, 111693–111709. doi: 10.1523/JNEUROSCI.2766-05.2005

Lim, G. P., Calon, F., Morihara, T., Yang, F., Teter, B., Ubeda, O., et al. (2005). A diet enriched with the omega-3 fatty acid docosahexaenoic acid reduces amyloid burden in an aged Alzheimer mouse model. *J. Neurosci.* 25, 3032–3040. doi: 10.1523/JNEUROSCI.4225-04.2005

Marín, R., Casañas, V., Pérez, J. A., Fabelo, N., Fernández, C. E., and Díaz, M. (2013). Oestrogens as modulators of neuronal signalosomes and brain lipid homeostasis related to protection against neurodegeneration. *J. Neuroendocrinol.* 25, 1104–1115. doi: 10.1111/jne.12068

Marín, R., Fabelo, N., Martín, V., García-Esparcia, P., Ferrer, I., Quinto-Alemany, D., et al. (2017). Anomalies occurring in lipid profiles and protein distribution in frontal cortex lipid rafts in dementia with Lewy bodies disclose neurochemical traits partially shared by Alzheimer's and Parkinson's disease. *Neurobiol. Aging.* 49, 52–59. doi: 10.1016/j.neurobiolaging.2016.08.027

Marín, R., Guerra, B., Alonso, R., Ramírez, C. M., and Díaz, M. (2005). Estrogen activates classical and alternative mechanisms to orchestrate neuroprotection. *Curr. Neurovasc. Res.* 2, 287–301. doi: 10.2174/156720205774322629

Marín, R., Guerra, B., Morales, A., Diaz, M., and Alonso, R. (2003). An estrogen membrane receptor participates in the neuroprotective action of estradiol against amyloid β-peptide$_{1-40}$-induced toxicity in SN56 neurons. *J. Neurochem.* 85, 1180–1189. doi: 10.1046/j.1471-4159.2003.01767.x

Marín, R., Ramírez, C., Morales, A., González, M., González-Muñoz, E., Zorzano, A., et al. (2007). Voltage-dependent anion channel (VDAC) participates in amiloid beta-induced toxicity and interacts with plasma membrane estrogen receptor α in septal and hippocampal neurons. *Mol. Membr. Biol.* 24, 148–160. doi: 10.1080/09687860601055559

Mazza, M., Pomponi, M., Janiri, L., Bria, P., and Mazza, S. (2007). Omega-3 fatty acids and antioxidant in neurological and psychiatric diseases: an overview. *Progr. Neuropsychopharmacol. Biol. Psychiatr.* 31, 12–26. doi: 10.1016/j.pnpbp.2006.07.010

Mendez-Otero, R., and Santiago, M. F. (2003). Functional role of a specific ganglioside in neuronal migration and neurite outgrowth. *Braz. J. Med. Biol. Res.* 36, 1003–1013. doi: 10.1590/S0100-879X2003000800006

Menegon, A., Bonanomi, D., Albertinazzi, C., Lotti, F., Ferrari, G., Kao, H. T., et al. (2006). Protein kinase A-mediated synapsin I phosphorylation is a central modulator of Ca^{2+}-dependent synapticactivity. *J. Neurosci.* 26, 11670–11681. doi: 10.1523/JNEUROSCI.3321-06.2006

Messa, M., Congia, S., Defranchi, E., Valtorta, F., Fassio, A., Onofri, F., et al. (2010). Benfenati, F. Tyrosine phosphorylation of synapsin I by Src regulates synaptic-vesicle trafficking. *J. Cell Sci.* 123, 2256–2265. doi: 10.1242/jcs.068445

Metherel, A. H., Armstrong, J. M., Patterson, A. C., and Stark, K. D. (2009). Assesment of blood measurements of *n*−3 polyunsaturated fatty acids with acute fish oil supplementation and washout in men and women. *Prostaglandins Leukot. Essent. Fatty Acids* 81, 23–29. doi: 10.1016/j.plefa.2009.05.018

Migaude, M., Charlesworth, P., Dempster, M., Webster, L. C., Watabe, A. M., Makhinson, M., et al. (1998). Enhanced long-term potentiation and impaired learning in mice with mutant postsynaptic density-95 protein. *Nature* 396, 433–439. doi: 10.1038/24790

Miller, L. R., Jorgensen, M. J., Kaplan, J. R., Seeds, M. C., Rahbar, E., Morgan, T. M., et al. (2016). Alterations in levels and ratios of *n*−3 and *n*−6 polyunsaturated fatty acids in the temporal cortex and liver of Vernet monkeys from brith to adulhood. *Physiol. Behav.* 156, 71–78. doi: 10.1016/j.physbeh.2015.12.009

Mozaffarian, D., and Wu, J. H. Y. (2012). (*n*−3) fatty acids and cardiovascular health: are effects of EPA and DHA shared or complementary? *J. Nutr.* 142, 614S−625S. doi: 10.3945/jn.111.149633

Olsen, A. S. B., and Færgeman, N. J. (2017). Sphingolipids: membrane microdomains in brain development, function and neurological diseases. *Open Biol.* 7:170069. doi: 10.1098/rsob.170069

Orr, S. K., Palumbo, S., Bosetti, F., Mount, H. T., Kang, J. X., Greenwood, C. E., et al. (2013). Unesterified docosahexaenoic acid is protective in neuroinflammation. *J. Neurochem.* 213, 378–393. doi: 10.1111/jnc.12392

Pan, B., Frombolt, S. E., Hess, E. J., Crawford, T. O., Griffin, J. W., Sheikh, K. A., et al. (2005). Myelin–associated glycoproteins and complementary axonal ligands, gangliosides, mediate axonal stability in the CNS and PNS: neuropathology and behavioral deficits in single- and double-null mice. *Exp. Neurol.* 195, 208–217. doi: 10.1016/j.expneurol.2005.04.017

Pruett, S. T., Bushnev, A., Hagedorn, K., Adiga, M., Haynes, C. A., Sullards, M. C., et al. (2008). Biodiversity of sphingoid bases ("sphingosines") and related aminoalcoholes. *Lipid Res.* 49, 1621–1639. doi: 10.1194/jlr.R800012-JLR200

Rosenberg, R. N., Lambracht-Washington, D., Yu, G., and Xia, W. (2016). Genomics of Alzheimer disease: a review. *JAMA Neurol.* 73, 867–874. doi: 10.1001/jamaneurol.2016.0301

Russell, F. D., and Bürgin–Maunder, C. S. (2012). Distinguishing health benefits of eicosapentaenoic and docosahexaenoic acids. *Mar. Drugs* 10, 2535–2559. doi: 10.3390/md10112535

Schnell, E., Sizemore, M., Karimzadegan, S., Chen, L., Bredt, D. S., and Nicholl, R. A. (2002). Direct interaction betweeb PSD-95 and stargazing control synaptic AMPA receptor number. *Proc. Natl. Acad. Sci. U.S.A.* 99, 13902–13907. doi: 10.1073/pnas.172511199

Sengupta, P., Barird, B., and Holowka, D. (2007). Lipid rafts, fluid/fluid phase separation, and their relevance to plasma membrane structure and function. *Semin. Cell. Dev. Biol.* 18, 583–590. doi: 10.1016/j.semcdb.2007.07.010

Serhan, C. N. (2014). Pro-resolving lipid mediators are leads for resolution physiology. *Nature* 510, 92–101. doi: 10.1038/nature13479

Serhan, C. N., and Chang, N. (2013). Resolution phase lipid mediators of inflamation: agonists of resolution. *Curr. Opin. Pharmacol.* 13, 632–640. doi: 10.1016/j.coph.2013.05.012

Sidhu, V. K., Huang, B. X., Desai, A., Kevala, K., and Kim, H.-Y. (2016). Role of DHA in aging-related change in mouse brain synaptic plasma membrane proteome. *Neurobiol. Aging* 41, 73–85. doi: 10.1016/j.neurobiolaging.2016.02.007

Simons, K., and Toomre, D. (2000). Lipid rafts and signal transduction. *Nat. Rev. Mol. Cell. Biol.* 1, 31–39. doi: 10.1038/35036052

Sonnino, S., and Prinetti, A. (2016). The role of sphingolipids in neural plasticity of the brain. *J. Neurochem.* 137, 485–488. doi: 10.1111/jnc.13589

Stables, M. J., and Gilroy, D. W. (2011). Old and new generation lipid mediators in acute inflammation and resolution. *Progr. Lipid Res.* 50, 35–51. doi: 10.1016/j.plipres.2010.07.005

Sun, J., Bronk, P., Liu, X., Han, W., and Sudhof, T. C. (2006). Synapsins regulate use-dependent synaptic plasticity in the calyx of Held by a Ca^{2+}/calmodul*in*–dependent pathway. *Proc. Natl. Acad. Sci. U.S.A.* 103, 2880–2885. doi: 10.1073/pnas.0511300103

Susuki, K., Baba, H., Tohyama, K., Kanai, K., Kuwabara, S., Hirata, K., et al. (2007). Gangliosides contribute to stability of paranodal junctions and ion channel clusters in myelinated nerve fibers. *Glia* 55, 746–757. doi: 10.1002/glia.20503

Varea, O., Garrido, J. J., Dopazo, A., Mendez, P., Garcia-Segura, L. M., and Wandosell, F. (2009). Estradiol activates beta-catenin dependent transcription in neurons. *PLoS ONE* 4:e5153. doi: 10.1371/journal.pone.0005153

Wang, J., Cheng, A., Wakade, C., and Yu, R. K. (2014). Ganglioside GD3 is required for neurogenesis and long-term maintenance of neural stem cells in the postnatal mouse brain. *J. Neurosci.* 34, 13790–13800. doi: 10.1523/JNEUROSCI.2275-14.2014

Wang, J., and Yu, R. K. (2013). Interaction of ganglioside GD3 with n EGF receptor sustains the self-renewal ability of mouse neural stem cells *in vitro*. *Proc. Natl. Acad. Sci. U.S.A.* 110, 137–142. doi: 10.1073/pnas.1307224110

Williams, T. J., Mitterling, K. L., Thompson, L. I., Torres-Reveron, A., Waters, E. M., McEwen, B. S., et al. (2011). Age- and hormone-regulation of opiod peptides and synaptic proteins in the rat dorsal hippocampal formation. *Brain Res.* 1379, 71–85. doi: 10.1016/j.brainres.2010.08.103

Williard, D. E., Harmon, S. D., Kaduce, T. L., Preuss, M., Moore, S. A., Robbins, M. E. C., et al. (2001). Docosahexanoic acid synthesis from *n*−3 polyunsaturated fatty acids in differentiated rat brain astrocytes. *J. Lipid Res.* 42, 1368–1376.

Zárate, R., El Jaber-Vazdekis, N., Tejera, N., Pérez, J. A., and Rodríguez, C. (2017). Significance of long chanin polyunsaturated fatty acids in human health. *Clin. Trans. Med.* 6, 25. doi: 10.1186/s40169-017-0153-6

Conflict of Interest Statement: The authors declare that the research was conducted in the absence of any commercial or financial relationships that could be construed as a potential conflict of interest.

frontiers in Molecular Neuroscience

ORIGINAL RESEARCH
published: 28 March 2018
doi: 10.3389/fnmol.2018.00090

miRNA Long-Term Response to Early Metabolic Environmental Challenge in Hypothalamic Arcuate Nucleus

*Charlotte Benoit†, Soraya Doubi-Kadmiri†, Xavier Benigni, Delphine Crepin, Laure Riffault, Ghislaine Poizat, Claire-Marie Vacher, Mohammed Taouis, Anne Baroin-Tourancheau and Laurence Amar**

Centre National de la Recherche Scientifique UMR 9197/Institut de Neurosciences, Université Paris-Sud, Université Paris-Saclay, Orsay, France

Epidemiological reports and studies using rodent models indicate that early exposure to nutrient and/or hormonal challenges can reprogram metabolism at adulthood. Hypothalamic arcuate nucleus (ARC) integrates peripheral and central signals to adequately regulate energy homeostasis. microRNAs (miRNAs) participate in the control of gene expression of large regulatory networks including many signaling pathways involved in epigenetics regulations. Here, we have characterized and compared the miRNA population of ARC of adult male rats continuously exposed to a balanced metabolic environment to the one of adult male rats exposed to an unbalanced high-fat/high-carbohydrate/moderate-protein metabolic environment during the perinatal period and/or at adulthood that consequently displayed hyperinsulinemia and/or hyperleptinemia. We identified more than 400 miRNA species in ARC of adult male rats. By comparing the miRNA content of six biological replicates in each of the four perinatal/adult environments/rat groups, we identified the 10 miRNAs specified by clusters miR-96/182/183, miR-141/200c, and miR-200a/200b/429 as miRNAs of systematic and uncommonly high variation of expression. This uncommon variation of expression may underlie high individual differences in aging disease susceptibilities. By comparing the miRNA content of the adult ARC between the rat groups, we showed that the miRNA population was not affected by the unbalanced adult environment while, in contrast, the expression of 11 miRNAs was repeatedly impacted by the perinatal unbalanced environment. Our data revealed a miRNA response of adult ARC to early metabolic environmental challenge.

Keywords: aging, brain, Illumina sequencing, metabolic environment, metabolic programming, miRNA expression, miRNome

OPEN ACCESS

Edited by:
Daniel Ortuño-Sahagún, Universidad de Guadalajara, Mexico

Reviewed by:
Valery Grinevich, Deutsches Krebsforschungszentrum (DKFZ), Germany
Laura Maria Frago, Universidad Autonoma de Madrid, Spain

***Correspondence:**
Laurence Amar
laurence.amar@u-psud.fr

†These authors have contributed equally to this work.

Received: *02 February 2018*
Accepted: *08 March 2018*
Published: *28 March 2018*

Citation:
Benoit C, Doubi-Kadmiri S, Benigni X, Crepin D, Riffault L, Poizat G, Vacher C-M, Taouis M, Baroin-Tourancheau A and Amar L (2018) miRNA Long-Term Response to Early Metabolic Environmental Challenge in Hypothalamic Arcuate Nucleus. Front. Mol. Neurosci. 11:90. doi: 10.3389/fnmol.2018.00090

INTRODUCTION

The arcuate nucleus (ARC) of the hypothalamus is central for the regulation of the energy balance through adequate neuro/endocrine responses (Timper and Brüning, 2017). The ARC receives information from blood via multiple specialized transporters of nutrients and hormones. Glucose, fatty acids, amino acids, insulin, and ghrelin indicate immediate fuel availability while leptin is indicative of long-term energy store. The ARC also receives information from the cerebrospinal

fluid that releases products filtered and/or produced by the choroid plexus. In addition, the ARC receives information from the brainstem that integrates signals from blood through neurons of the postrema area, an area harboring fenestrated capillaries (Rodríguez et al., 2010), and from the gastrointestinal tract through the vagus nerve (Sobrino Crespo et al., 2017). The control of food intake and energy expenditure by the ARC mainly involves two populations of neurons, the orexigenic Agouti-related peptide/Neuropeptide Y (AgRP/NPY) neurons and anorexigenic pro-opiomelanocortin/cocaine-amphetamine-related transcript (POMC/CART) neurons. The ultimate molecular mechanisms whereby the ARC integrates these signals and conveys them to other hypothalamic and non-hypothalamic areas need further investigations, in particular in cases of diabetes and/or obesity.

Epidemiological analyses identified adult unbalanced metabolic environments as one causal factor of metabolic diseases such as obesity and type 2 diabetes. In addition retrospective epidemiological analyses strongly suggested that unbalanced metabolic environments during early-life may potentiate these diseases later at adulthood (Hanson and Gluckman, 2014). Numerous studies conducted in mouse or

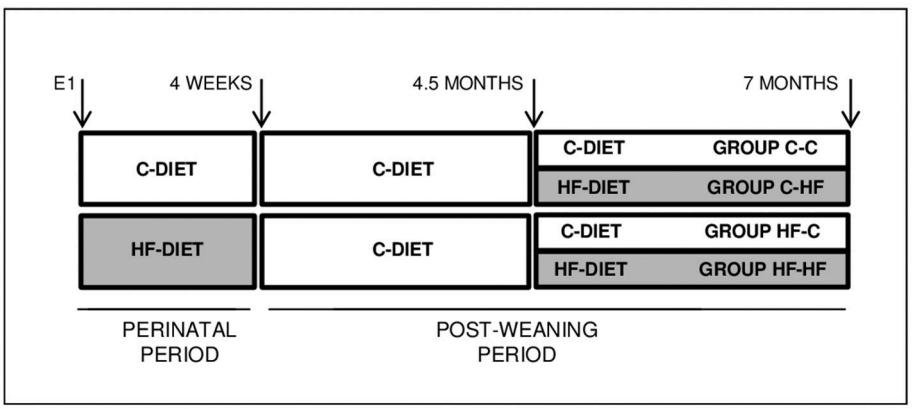

FIGURE 1 | Experimental scheme. Wistar female rats were fed a balanced C-diet (18, 23, and 59% of the energy content derived from lipids, proteins and carbohydrates, respectively) or unbalanced HF-diet (46, 16, and 38% of the energy content derived from lipids, proteins, and carbohydrates, respectively) during the whole perinatal period, from day 1 of gestation up till postnatal week 4. Pups were weaned on the C-diet. Adults of 4.5 months were either maintained on the C-diet or shifted to the HF-diet for 10 weeks. Animals were euthanazied at the age of 7-months after a 14–16-h overnight fasting. Groups were named according to their respective perinatal and adult diets, i.e., C-C, C-HF, HF-C, and HF-HF.

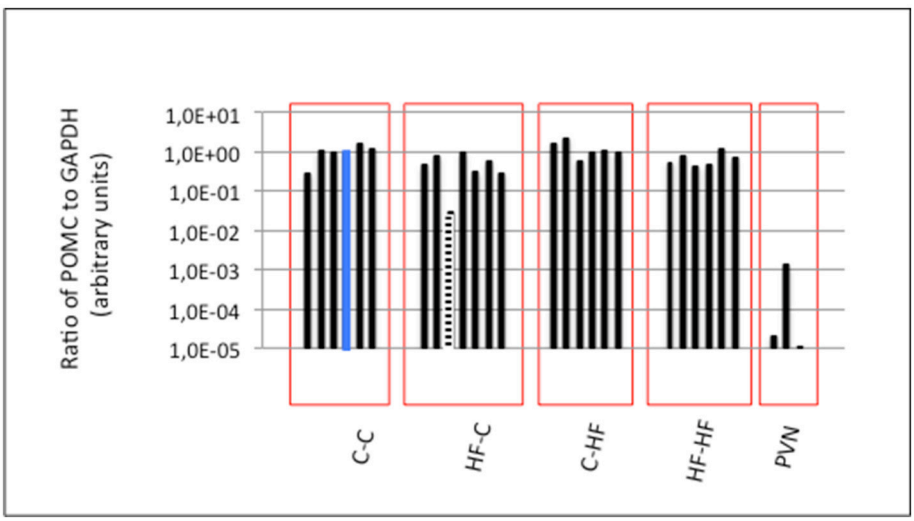

FIGURE 2 | ARC molecular characterization. The ARC harbors a neuronal population specifically expressing POMC transcripts when compared to the surrounding hypothalamic nuclei including the PVN. GAPDH and POMC expression were analyzed by RT-qPCR. POMC expression was normalized to GAPDH expression in each ARC and PVN. Ratio in one ARC of Group C-C (blue bar) was taken as the reference ratio. Ratios are shown using a $\log_{10}$ scale. All ARCs displayed POMC to GAPDH ratios at least a hundred-fold higher than those characterizing the PVNs except one ARC of Group HF-C (hatched bar) that was excluded from further analyses. Twenty-four ARCs (six ARCs/group) were conserved for analyses of miRNA populations.

rat demonstrated, by means of inappropriate diets, the impact of adult and/or perinatal unbalanced metabolic environments on the development of high levels of circulating leptin, insulin, glucose, and/or lipids, contributing then to overweight/obesity and/or insulin resistance/type 2 diabetes at adulthood (Ainge et al., 2011). How unbalanced metabolic environments in early life and/or at adulthood alter mechanisms controlling the energy homeostasis in the central nervous system are currently active research fields.

microRNAs (miRNAs) are small RNAs of 20–24 nucleotides modulating the expression of networks of tens/hundreds of targeted genes (Bartel, 2009; Ha and Kim, 2014). miRNAs and targeted mRNAs form imperfect duplexes that decrease mRNA translation efficiency and/or stability, reducing then the levels of the corresponding proteins. Each miRNA is predicted to control the expression of several hundreds of protein-coding genes because of the short size of miRNA:mRNA heteroduplexes and large amount of putative targets in mRNA transcriptomes. Bioinformatics analyses also predicted that targeted mRNAs might be controlled by multiple miRNAs. In human, mouse and rat genomes, miRNAs are encoded by several hundreds of genes (miR genes). A large fraction of the miR genes is expressed in brain generating highly complex miRNA populations (miRNomes). Different miRNAs have been related to peripheral controls of metabolisms (Vienberg et al., 2017). miRNA involvement in such functions at the ARC level has started to be explored and the possibility that miRNAs of ARC participate in the central control of energy homeostasis has yet to be characterized (Amar et al., 2012; Baroin-Tourancheau et al., 2014; Doubi-Kadmiri et al., 2016). Here, we have identified miRNA expression responses of ARC of adult male rats that had been submitted to perinatal and/or adult metabolic environmental challenges and consequently displayed differences in circulating levels of nutrients and hormones.

MATERIALS AND METHODS

Animals

All animals were maintained under a 12/12 Light/Dark cycle (lights on at 8 a.m.) with stable temperature (22 ± 1°C). Virgin females Wistar of 4 weeks and males Wistar of 8 weeks from CERJ Janvier, France, have been habituated to our facilities for 4 weeks before breeding. Standard balanced diet (C-diet) (18, 23, and 59% of the energy content derived from lipids, proteins, and carbohydrates, respectively, Safe, France) and water were provided *ad libitum*. From day 1 of pregnancy and until weaning, dams were either maintained on the standard diet or shifted to an unbalanced diet (HF-diet) (46, 16, and 38% of the energy content derived from lipids, proteins, and carbohydrates, respectively,

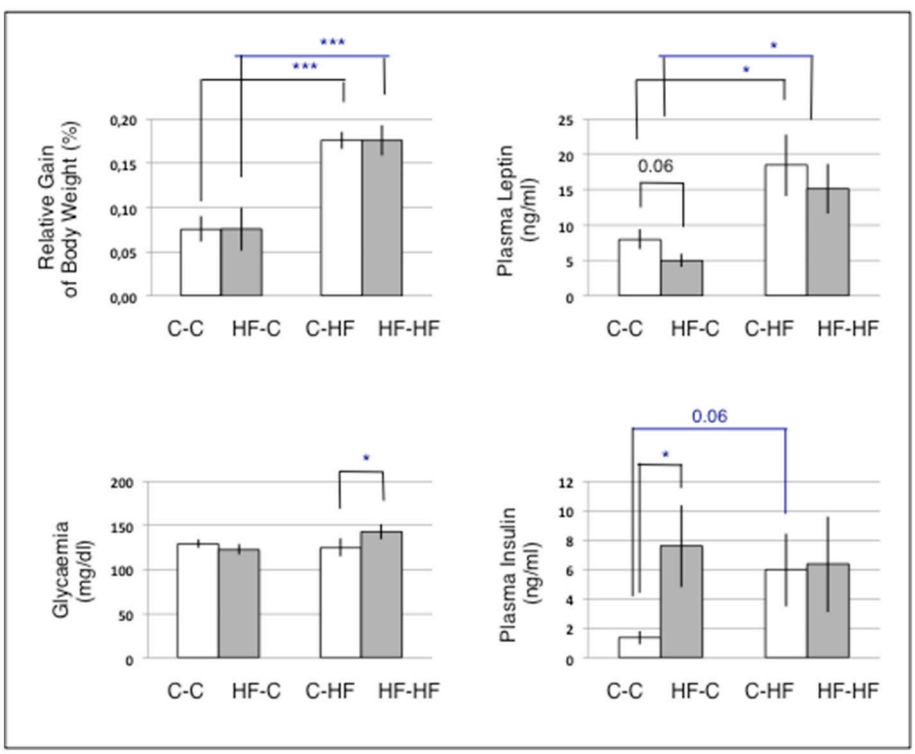

FIGURE 3 | Body weight gains and plasma parameters. For each animal, the gain of body weight was calculated relatively to the body weight at the age of 4.5 months at which animals had been either maintained on the C-diet or shifted to the HF-diet. $n = 6$/group. Statistics were performed using Mann and Whitney tests. Data are given as mean ± SEM. $^{*}p < 0.05$; $^{***}p < 0.001$. Challenging the perinatal and/or adult diet resulted in differences in circulating nutrients and hormones involved in the lipid and carbohydrate metabolisms.

Safe, France) (**Figure 1**). At birth, litters were sized to 10 pups to prevent lactation under- or over-nutrition. Upon weaning, animals were fed the C-diet. At the age of 4.5 months, and for the next 10 weeks, they were either maintained under the C-diet or shifted to the HF-diet. At 7 months adults were submitted to an overnight fasting of 14–16-h before being anesthesied with isoflurane, weighted and killed by decapitation. Brains were removed, frozen in isopentane at −40°C for 2 min and stored at −80°C. Bloods were collected in the presence of 50 µl/ml of 160 U/ml heparin. All procedures were conducted according to the guidelines of laboratory animal care and were approved by the local governmental commission for animal research: Ethic Committee for animal experimentation of Paris Center and South # 59 (France), with authorization # 91-467.

TABLE 1 | miRNA expression profiles.

		C-C	C-HF	HF-C	HF-HF
miRNAs (N)		**417**	**380**	**446**	**440**
MAX/MIN	MEAN	2.6	3.5	3.2	2.2
	STD	2.9	6.1	4.2	1.6
	MEAN + 2 STD	8.3	15.7	11.6	5.5
	miRNAs with MAX/MIN >8.3 (N)	**15**	**21**	**25**	**6**
	miRNAs with MAX/MIN >8.3 (%)	**3.6**	**5.5**	**5.6**	**1.4**
CV	MEAN	0.28	0.29	0.32	0.24
	STD	0.18	0.16	0.20	0.13

Statistics. Expression profiles of male adult ARCs display complex populations of 380–446 miRNAs. We analyzed the variation of expression of each miRNA between the six profiles of groups C-C, C-HF, HF-C, or HF-HF by calculating its maximal to minimal ratio (MAX/MIN) and standard deviation to mean ratio (coefficient of variation; CV). Only a minor fraction of the miRNA population of each group displays MAX/MIN values higher than the value of 8.3 that corresponds to mean + 2 STD in group C-C: 1.1, 3.6, 5.5, and 5.6% in groups HF-HF, C-C, C-HF, and HF-C, respectively. Extensive intra-group homogeneity of miRNA expression in all groups is an important feature for sound analyses of inter-group differential expression.

Insulin and Leptin Measurements

Insulin and leptin plasma levels were measured using Elisa according to the manufacturer's protocol (Millipore). Twenty-five microliters of plasma were used for each point.

ARC Dissection, RNA Extraction, and Purification of Short RNAs

ARC is ventrally adjacent to the 3rd ventricle. A 2–3 mm section was cut from brains, 1 mm rostral to the optic chiasma, and ARC was punched with relation to the ventral part of the 3rd ventricle. ARC-containing punches (ARC punches) were stored individually in Ceramic Bead tubes (Ozyme) at −80°C. The paraventricular nucleus (PVN) that was used as a non-POMC expressing tissue is located dorsally and laterally to the 3rd ventricle. A 1 mm section was cut from brains immediately

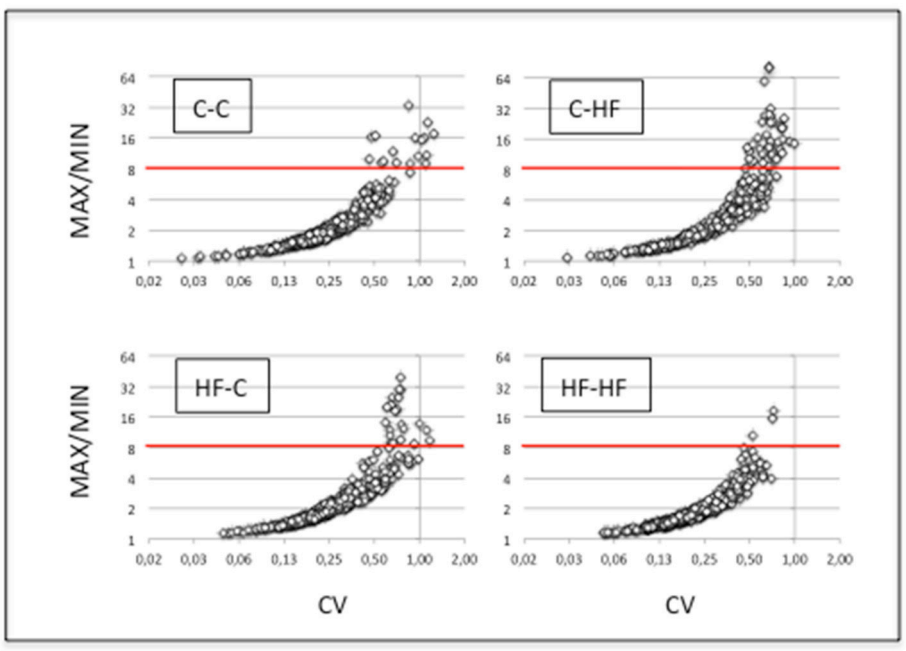

FIGURE 4 | miRNA expression displays high intra-group homogeneity. We characterized complex populations of some 400 miRNAs. In each group and for each miRNA, we analyzed the variation of expression between the six profiles by calculating the maximal to minimal ratio (MAX/MIN) and the standard deviation to mean ratio (coefficient of variation; CV). For each group, scatter plots of MAX/MINs against CVs are drawn. Note that X- and Y-axes used a $\log_2$ scale. Red lines identify the threshold value of mean + 2 STD in group C-C (i.e., 8.3). More than 94% of the miRNAs displayed close MAX/MINs and/or CVs in each group indicative of extensive intra-group homogeneity of miRNA expression.

rostral to the optic chiasma. The PVN was punched with relation to the dorsal part of the 3rd ventricle. PVN-containing punches (PVN punches) were stored as described above.

TABLE 2 | miRNAs specified by clusters miR-96/182/183, miR-141/200c, and miR-200a/200b/429 display hypervariable expression.

	MAX/MIN			
miRNA	**C-C**	**C-HF**	**HF-C**	**HF-HF**
miR-200a-3p	5.9	2.7	**39.3**	4.9
miR-200a-5p				
miR-200b-3p	**16.0**	**12.1**	**24.8**	**4.0**
miR-200b-5p	**22.6**	**17.5**	**20.8**	**7.3**
miR-200c-3p	**11.1**	**24.4**	**19.1**	**6.1**
miR-200c-5p				
miR-182	**10.8**	**27.2**	**18.7**	**6.7**
miR-183-3p	**15.5**	**70.1**	**29.4**	**5.4**
miR-183-5p	**9.1**	**31.7**	**14.1**	**7.8**
miR-141-3p	4.5	1.9	**25.0**	**5.6**
miR-141-5p				
miR-429	**9.1**	**27.0**	**11.8**	**4.8**
miR-96-5p	**11.7**	**25.6**	**20.0**	**5.0**

Clusters miR-96/182/183, miR-141/200c, and miR-200a/200b/429 specify 10 miRNAs in male adult ARC. Eight miRNAs displayed MAX/MINs higher than the value of 8.3 (i.e., mean + 2 STD) in group C-C as well in groups C-HF, HF-C, and HF-HF (Bold numbers). miRNAs miR-200a-3p and miR-141-3p displayed MAX/MINs higher than the value of 8.3 in groups HF-C and/or HF-HF.

On purpose, ARC- or PVN-containing Ceramic Bead tubes were added QIAzol lysis reagent (Qiagen) (700 µl) and immediately homogeneized using a PreCellys homogenizer (PreCellys 24/Cryolys) for 20 s at room temperature. After addition of chloroform (150 µl), homogenates were centrifugated 15 min at 13,200 rpm to separate the organic and aqueous phases. The latter was recovered and nucleic acids, precipitated by adding one volume of isopropanol. Pellets were centrifuged, rinsed twice with ethanol 70%, and resuspended in RNase-free H_2O (20 µl). The yield of total RNA was consistently around 1–2 µg.

To check the quality of the hypothalamic nucleus dissection, we took advantage of the presence of a neuronal population specifically producing POMC transcripts in the ARC when compared to the surrounding hypothalamic nuclei including the PVN. We determined the level of POMC transcripts relatively to that of Glyceraldehyde 3-phosphate dehydrogenase (GAPDH) transcripts using DNA-free RNAs and RT-qPCRs (**Figure 2**). Three independent hypothalamic PVNs of adult males were taken as POMC-non-expressing controls. Taking the ratio of POMC to GAPDH transcripts of one ARC of group C-C as the reference ratio, all ARCs but one displayed ratios at least ten-fold higher than ratios characterizing PVNs (low amounts of POMC mRNAs identified in PVNs were due to mRNA axonal transport from ARC to PVN). The low POMC-expressing ARC was discarded and 24 ARCs (6 ARCs/group) were conserved for expression analyses of miRNA populations.

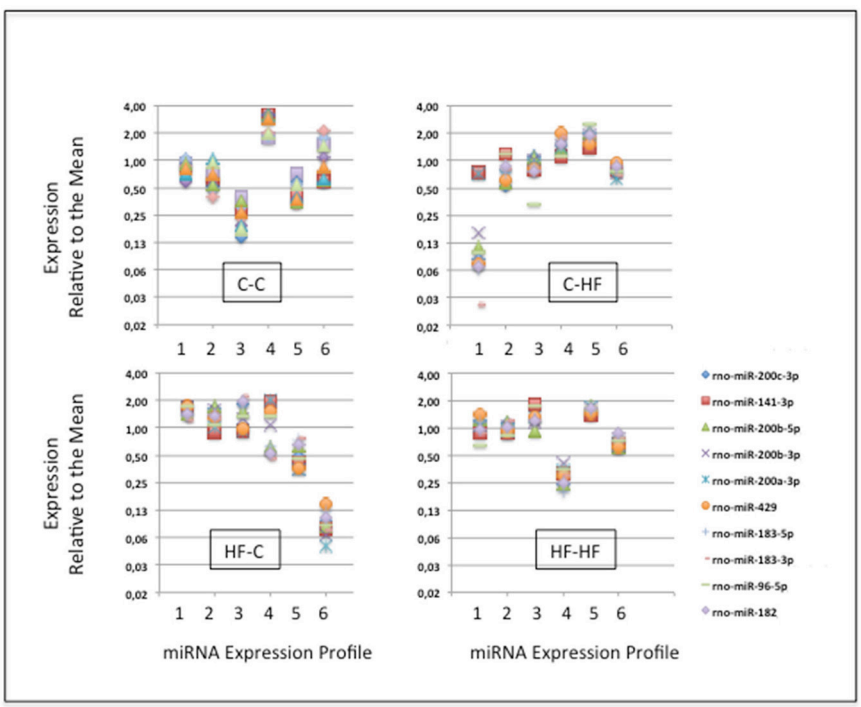

FIGURE 5 | The specific case of the miRNAs specified by clusters miR-96/182/183, miR-141/200c, and miR-200a/200b/429. Ten miRNAs are produced by clusters miR-96/182/183, miR-141/200c, and miR-200a/200b/429. In each group, in each of the six profiles, and for each miRNA, we calculated the expression relative to the mean by dividing individual miRNA read counts by the mean miRNA read count. The expression of the 10 miRNAs co-varies in each profile.

Two-thirds of total RNAs were added an equal volume of formamide, heated at 70°C for 3 min, and loaded on a denaturing urea (8 M) polyacrylamide (17%) gel for size-fractionation. In all cases, the high quality of RNAs was checked by a lack of any smear and the fact that the tRNAs, 5S RNA and 5.8S RNA migrated as discrete bands. Small RNAs of 18–36 nucleotides were eluted from the corresponding slices by overnight incubation in NaCl 0.4 M (0.8 ml) at 4°C under gentle shaking. Eluats were precipitated by adding 2.5 volumes of ethanol in the presence of glycogen (10 ng), rinsed twice with ethanol 70%, and resuspended in RNase-free H_2O (10 μl).

cDNA Library Construction

Individual cDNA libraries were built following an Illumina-like protocol in which 3′- and 5′-adapters were sequentially ligated at the 3′- and 5′-ends of small RNAs, respectively, to allow for their reverse transcription (RT) and amplification by polymerase chain reaction (PCR) as previously described (Doubi-Kadmiri et al., 2016). The 3′-Adaptor was first adenylated by using 25 pmoles of oligonucleotides, 2 × Quick Ligation reaction buffer (New England Biolabs), and 1,600 U of T4 DNA ligase (New England Biolabs), in a volume of 50 μl and by overnight incubation at 37°C. The adenylated and non-adenylated adaptors were size-fractioned on a denaturing urea (8 M) polyacrylamide (20%) gel. The adenylated adaptor was eluted as described above. [0.25 μM] adenylated 3′-adaptor (0.5 μl) was then added to small RNAs (5 μl) in 0.2 ml Thermo-Tubes (Thermo Scientific). To prevent secondary structures, mixes were heated for 3 min at 70°C, then kept on ice while adding [50%] PEG 8000 (2.4 μl), [200 U/μL] truncated T4 RNA ligase 2 (0.4 μl), and 10X truncated T4 RNA ligase 2 buffer (all provided by New England Biolabs) (1.0 μl). Mixes were incubated for 90 min at 25°C. After the addition of [1 μM] 5′-adaptor (0.5 μl) and a new 70°C/ice cycle, mixes were added with [20 U/μl] T4 RNA ligase 1 (0.75 μl) (New England Biolabs) and [10 μM] ATP (1 μl) and incubated for 90 min at 25°C. In a third step, mixes were added with [100 μM] RT-primer (0.5 μl), submitted to a 70°C/ice cycle, then added with [0.1 M] DTT (1 μl), [10 μM each] dNTP (1 μl), 10X buffer (4 μl), and [200 U/μl] of Superscript III reverse transcriptase (0.65 μl) (all from Life Technologies, ThermoFischer Scientific) and incubated for 90 min at 50°C. Finally, mixes were added with [100 μM] 3′-PCR-primer (0.6 μl), [100 μM] 5′-PCR-primer (0.3 μl), and 2X Master Mix Phusion enzyme (15 μl) (New England Biolabs). Reaction mixes were split into two tubes to enhance thermic exchange, denaturated for 1 min at 98°C, and submitted to 16 cycles of 20 s at 98°C, 30 s at 55°C, 25 s at 72°C. PCR products were size-fractionated on a 6% polyacrylamide gel so that ∼100-bp cDNAs could be separated from the 75-bp byproducts corresponding to primer dimers. We used a set of 3′-PCR-primers with whole complementarity to the 3′-adaptor but a bulge of two nucleotides at position 22 that were showed not to introduce any bias in control cDNA libraries built from RNAs of one ARC. cDNA libraries built from biological replicates were barcoded with the same 3′-PCR-primer and sequenced in different lanes of an Illumina's genome analyzer GAIIX (Baroin-Tourancheau et al., 2016).

miRNA Expression Profiling

Sequencing quality was ascertained using the FASTQC program (http://www.bioinformatics.babraham.ac.uk/projects/fastqc). cDNA libraries were demultiplexed using our scripts on the basis of the first 11 nucleotides of the 3′ adaptor and reads were trimmed from the 3′ adaptor sequence. Sequencing reads <15 nucleotides which could not be mapped on the genome were discarded. Duplicate reads >15 nucleotides were collapsed into unique sequences and analyzed with the sRNAbench tool on the sRNAtoolbox server (http://bioinfo5.ugr.es/srnatoolbox) to build individual miRNA expression profiles (Rueda et al., 2015). This server used the miRBase database version 21 (http://www.mirbase.org) to identify miRNA sequences (Griffiths-Jones et al., 2008). miRNA expression profiles were normalized using the DESeq procedure (Anders and Huber, 2010).

Statistical Measures

Individual group statistics were calculated using Mann and Whitney tests and corrected for multiple testing when necessary according to the false discovery rate method described by Benjamini and Hochberg (1995).

RESULTS

Metabolic Responses to Early and/or Adult Environmental Challenges

All male and female rats have been mated while fed a balanced control diet (C-diet). Then, pregnant females were fed either the same C-diet or shifted to an unbalanced diet rich in fat and carbohydrates and moderate in protein (HF-diet) from the first day of gestation until pup weaning (see **Figure 1**). Pups were fed the C-diet until the age of 4.5 months. For the next 10 weeks, animals were either maintained under the C-diet or shifted to the HF-diet. Animal groups were named according to their respective perinatal (1st capital letter) and adult (2nd capital letter) diets. For each group, i.e., C-C, C-HF, HF-C, and HF-HF, we used six male rats obtained from three different litters in order to avoid breeding and/or housing bias.

Animal groups fed the C-diet at adulthood (C-C and HF-C) displayed similar body weight gains ($p = 0.31$) and slight difference in plasma leptin levels (C-C: 8 ± 1 ng/ml; HF-C: 5 ± 1 ng/ml, $p = 0.06$) (**Figure 3**). Both groups displayed similar levels of glycaemia ($p = 0.36$) but significant difference in plasma insulin levels (C-C: 1.4 ± 0.5 ng/ml; HF-C: 7.6 ± 2.8 ng/ml, $p = 0.03$).

Animal groups fed the HF-diet at adulthood (C-HF and HF-HF) displayed similar body weight gains ($p = 0.32$) and plasma leptin levels ($p = 0.29$). Those body weight gains and plasma leptin levels were significantly increased when compared to those of groups fed the C-diet ($p < 1.0E\text{-}3$ and 0.03, respectively). Plasma insulin levels were similar in groups C-HF and HF-HF ($p = 0.39$). This contrasted with a significant difference in glycaemia (C-HF: 123 ± 5.9 ng/ml; HF-HF: 143 ± 8.7 ng/ml; $p = 0.03$). Plasma insulin levels of groups C-HF and HF-HF were similar to that of group HF-C.

Challenging the perinatal and/or adult diet produced, as expected, four groups of adult rats differing in circulating

nutrients and hormones involved in lipid and carbohydrate metabolisms.

miRNA Expression Displays High Intra-Group Homogeneity

Molecular characterization of ARCs was performed in order to check the quality of the dissection (see **Figure 2**) and small RNAs (16–36 nucleotides) were used for the construction of individual cDNA libraries (Supplemental Table S1) (see section Materials and Methods). A miRNA expression profile was built for each ARC (Supplemental Table S2) (see section Materials and Methods). In each group, the six profiles were then normalized (Supplemental Table S3). Using a mean normalized expression threshold of 10 reads, we characterized complex populations of 380–446 miRNAs in groups C-C, C-HF, HF-C, and HF-HF. In each group we analyzed miRNA expression variation between the six profiles. For each miRNA, we plotted the maximal to minimal ratio (MAX/MIN) against the standard deviation to mean ratio (coefficient of variation; CV) (**Table 1**, **Figure 4**).

In group C-C taken as the reference, a large fraction of the miRNAs displayed close MAX/MINs (mean ± STD-values = 2.6 ± 2.9) and CVs (0.28 ± 0.18). Indeed more than 96% of the miRNAs had MAX/MINs lower than the value of mean + 2 STD (i.e., 8.3) taken as a threshold value for identifying hypervariable miRNAs (see **Table 1**). Among the 15 (3.6%) miRNAs displaying MAX/MINs larger than this value, 8 were produced from three miR gene clusters, namely the miR-96/182/183 cluster and the two evolutionary-related clusters miR-141/200c and miR-200a/200b/429 (**Table 2**). Noticeably these 8 miRNAs as well as the other 2 miRNAs produced from the three miR gene clusters displayed co-variation of expression in each profile (**Figure 5**).

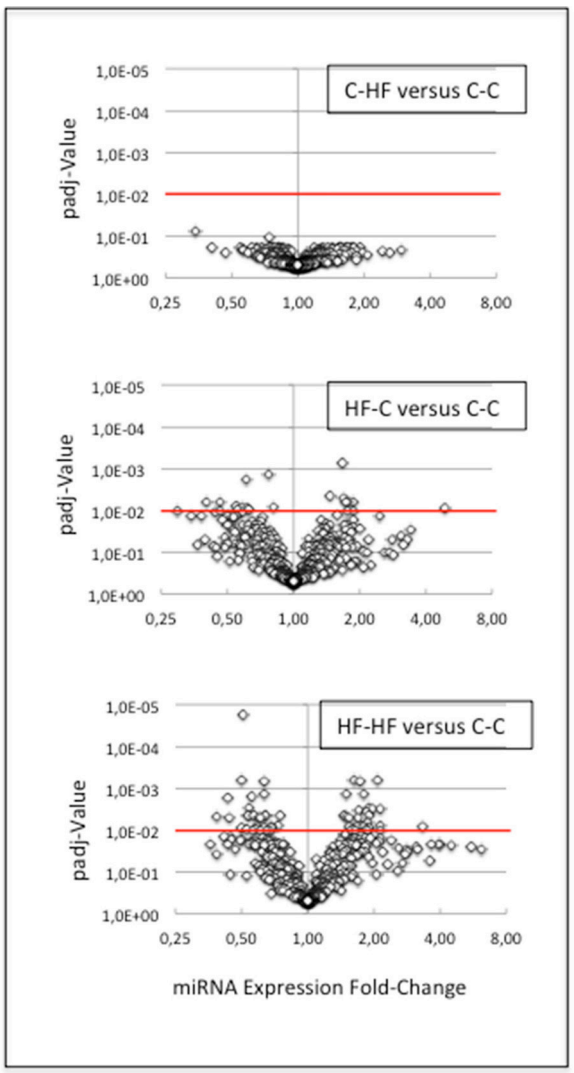

FIGURE 6 | miRNA response to metabolic challenge. We compared miRNA expressions between groups C-C and C-HF, HF-C, or HF-HF. For each comparison, the volcano plot displays padj-values plotted against expression fold-changes. X- and Y-axes are drawn using $\log_2$ and $\log_{10}$ scales, respectively. Values higher than 1 on the X-axis denote up-regulated miRNAs in groups C-HF, HF-C, or HF-HF, and values lower than 1, down-regulated miRNAs. Red lines identify the threshold padj-value of 1.0E-2. **(Upper Plot)** C-HF vs. C-C comparison. All padj-values were higher than 7.0E-2. miRNAs did not display any expression difference. **(Middle Plot)** HF-C vs. C-C comparison. Eighteen miRNAs displayed significant difference of expression. **(Lower Plot)** HF-HF vs. C-C comparison. Sixty miRNAs displayed significant difference of expression. The expression of several miRNAs was impacted by the perinatal only, or perinatal and adult, unbalanced environment.

TABLE 3 | miRNA and partner-miRNA expression in groups HF-C vs. C-C.

miRNAs Differentially Expressed Between Groups C-C and HF-C					
miRNA	**FCE**	**Padj-value**	**Partner-miRNA**	**FCE**	**Padj-value**
let-7i-5p	1.9	6.5E-03	let-7i-3p	1.5	3.1E-01
miR-107-3p	0.6	9.3E-03			
miR-1188-5p	0.4	7.0E-03			
miR-132-3p	1.7	5.1E-03	miR-132-5p	1.3	2.5E-01
miR-140-5p	1.7	6.5E-03	miR-140-3p	0.9	1.9E-01
miR-28-5p	1.7	6.9E-03	miR-28-3p	0.8	9.3E-02
miR-221-5p	1.9	1.0E-02	miR-221-3p	1.6	6.2E-02
miR-323-5p	0.5	6.5E-03	miR-323-3p	0.5	1.1E-02
miR-338-5p	1.5	4.2E-03	miR-338-3p	1.4	3.1E-01
miR-3585-5p	4.8	9.3E-03	miR-3585-3p	3.4	3.1E-02
miR-433-3p	0.6	1.0E-02	miR-433-5p	0.6	4.7E-02
miR-485-3p	0.6	1.8E-03	miR-485-5p	0.8	4.2E-02
miR-543-3p	0.8	6.9E-03	miR-543-5p	0.6	2.2E-02
miR-668	0.6	9.3E-03			
miR-673-5p	0.5	6.5E-03			
miR-708-5p	1.6	7.7E-04	miR-708-3p	0.9	3.4E-01
miR-770-3p	0.6	1.0E-02	miR-770-5p	0.6	1.2E-02
miR-92a-3p	0.8	1.8E-03			

Eighteen miRNAs displayed expression differences with padj-values = < 1.0E-2 between groups C-C and HF-C. Ratios of HF-C to C-C expressions (Fold-Changes of Expression; FCEs) are expected to occur with similar levels and associated padj-values for the miRNA and second strand (Partner-miRNA) derived from the same RNA duplex precursor. Thirteen miRNAs were identified along with their Partner-miRNAs. Six Partner-miRNAs, i.e., miR-323-5p, −3585-5p, −433-3p, −485-3p, −543-5p, and −770-3p displayed close FCEs and padj-values = <5.0E-2. Seven Partner-miRNAs (shaded Partner-miRNAs) displayed similar FCEs but padj-values >5.0E-2. miRNAs are listed by alphabetical order.

In groups C-HF, HF-C, and HF-HF, more than 94% of miRNAs also displayed close MAX/MINs and CVs with 5.5, 5.6, and 1.3% of the miRNAs having MAX/MINs larger than the threshold value of 8.3, respectively. In these groups, miRNAs produced from clusters miR-96/182/183, miR-141/200c, miR-200a/200b/429 also appeared as hypervariable miRNAs (see **Table 2**). In groups C-HF, HF-C, and HF-HF as in group C-C, the expression of the 10 miRNAs expressed by these clusters co-varies in each profile (see **Figure 5**).

The extensive intra-group homogeneity of miRNA expression profiles of each group is an important feature for sound inter-group differential expression analyses.

miRNA Expression Profiles Are Impacted by Perinatal Metabolic Environments

We then compared miRNA expressions between groups C-C and C-HF, HF-C, or HF-HF (Supplemental Table S4). The 24 expression profiles were normalized together, *p*-values were calculated and corrected for false discovery rates (see section Materials and Methods). The padj-value of 1.0E-2 was retained as the first threshold significant value.

miRNAs did not display any expression difference between groups C-C and C-HF: all padj-values were higher than 0.07 (**Figure 6**).

In contrast, 18 out of 433 miRNAs (4%) displayed significant difference of expression between groups C-C and HF-C (padj-value = < 1.0E-2) (see **Figure 6**) (**Table 3**). Fold-changes of expression (FCEs) ranged from 0.4 to 2 except in the case of miR-3585-5p that displayed a FCE of 4.8. FCEs are expected to occur with similar levels and associated padj-values in cases where miRNAs are specified by tightly linked genes transcribed as one RNA unit. This is the case for 1 of the 18 miRNAs. miR-3585-5p and -547-3p maturate from the same precursor and miR-547-3p did display similar FCE (3.3) and padj-value (5.0E-2).

miRNAs maturate from imperfect duplexes of some 22 basepairs, themselves arisen from RNA imperfect hairpins of some 70 nucleotides. miRNA maturation involves the incorporation of one duplex strand/miRNA into a RNA-induced silencing complex (RISC). For almost all duplexes, each strand can be incorporated within a RISC. Depending on the duplex, incorporation can display similar or highly different efficiencies between the two strands designed as miRNA-3p and miRNA-5p according to the hairpin arm from which they arise. We reasoned that FCEs of miRNA-3p and miRNA-5p derived from the same duplex are expected to vary similarly for all or almost all duplexes and used this feature to validate FCEs observed between groups C-C and HF-C.

Thirteen of the eighteen miRNAs differentially expressed between groups C-C and HF-C maturated in parallel with the second duplex strand (hereafter named Partner-miRNA) (see **Table 3**). Those 13 miRNAs and Partner-miRNAs displayed highly correlated FCEs (R^2 = 0.92) (**Figure 7**). In six cases, i.e., miR-323-3p, −3585-3p, −433-5p, −485-5p, −543-3p, and −770-5p, Partner-miRNAs, 323-5p, −3585-5p, −433-3p, −485-3p, −543-5p, and −770-3p, also displayed very close padj-values (<5.0E-2). Therefore 13 miRNAs, i.e., the two strands specified by genes miR-323, −3585, −433, −485, −543, and −770 as well as the miR-547-3p strand appeared impacted by the perinatal unbalanced environment. All these miRNAs except miR-543-5p also displayed significant changes of expression (padj-value =< 5.2E-02) between groups C-C and HF-HF (**Table 4**). miRNA FCEs between profiles of groups C-C and HF-C highly correlated

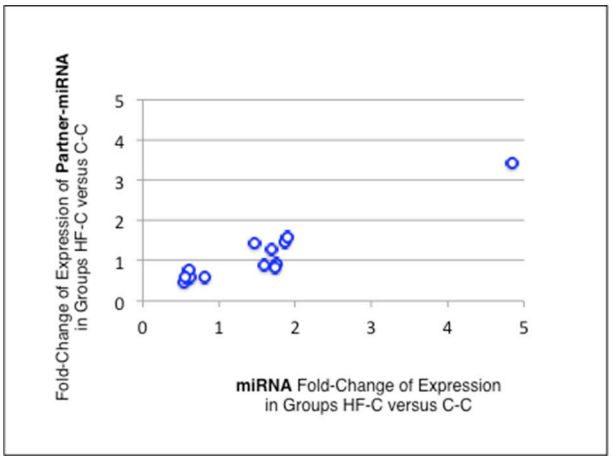

FIGURE 7 | miRNA and partner-miRNA differential expression in groups HF-C vs. C-C. Thirteen miRNAs differentially expressed between groups C-C and HF-C maturated in parallel with the second strand of their RNA duplex precursor (Partner-miRNA). Ratios of HF-C to C-C expressions (Fold-Change of Expression; FCE) are expected to occur with similar levels for a miRNA and its Partner-miRNA. FCEs of miRNA-Partners were plotted against FCEs of miRNAs. Both FCEs displayed high correlation (R^2 = 0.92).

TABLE 4 | miRNA expression in groups HF-C and HF-HF.

	miRNAs Differentially Expressed Between			
miRNA	**Groups C-C and HF-C**		**Groups C-C and HF-HF**	
miRNA	FCE	Padj-value	FCE	Padj-value
miR-323-3p	0.5	1.1E-02	0.4	5.3E-03
miR-323-5p	0.5	6.5E-03	0.7	5.3E-03
miR-3585-3p	3.4	3.1E-02	3.2	2.4E-02
miR-3585-5p	4.8	9.3E-03	4.6	2.3E-02
miR-433-3p	0.6	1.0E-02	0.6	2.0E-03
miR-433-5p	0.6	4.7E-02	0.5	1.7E-02
miR-485-3p	0.6	1.8E-03	0.5	5.1E-04
miR-485-5p	0.8	4.2E-02	0.8	2.2E-02
miR-543-3p	0.8	6.9E-03	0.5	1.7E-05
miR-543-5p	0.6	2.2E-02	1.0	4.2E-01
miR-547-3p	3.3	5.0E-02	3.6	5.2E-02
miR-770-3p	0.6	1.0E-02	0.5	5.3E-03
miR-770-5p	0.6	1.2E-02	0.7	1.1E-02

*Thirteen miRNAs, i.e., the two strands specified by the genes miR-323, −3585, −433, −485, −543, and −770 as well as the miR-547-3p strand were differently expressed in groups HF-C vs. CC (see **Table 3**). Remarkably all these miRNAs except miR-543-5p (shaded miRNA) also displayed significant changes of expression (padj-value = < 5.2E-02) between groups C-C and HF-HF, thus defining a subset of miRNAs repeatedly impacted by the perinatal unbalanced environment. miRNAs are listed by alphabetical order.*

with miRNA FCEs between profiles of groups C-C and HF-HF (R^2 =0.98) (**Figure 8**). Based on these criteria, 11 miRNAs, i.e., the two strands specified by the genes miR-323, −3585, −433, −485, and −770 as well as the 3p strand defined by the gene miR-547 defined a subset of miRNAs repeatedly impacted by the perinatal unbalanced environment.

Finally, when comparing profiles of groups C-C and HF-HF, 49 additional miRNAs displayed significant difference of expression (padj-value = < 1.0E-2) (**Table 5**). Thirty-four of these miRNAs maturated in parallel with the second duplex strand (see **Table 5**). Those 34 miRNAs and Partner-miRNAs displayed low correlated FCEs (R^2 = 0.15) (**Figure 9**). In nine cases, i.e., miR-127-3p, −139-3p, −140-5p, 145-5p, 27a-3p, 29a-3p, −344-b1-3p, 369-5p, and −409a-5p, miRNAs and Partner-miRNAs displayed close FCEs and padj-values (=<5.0E-2). For miR-145-5p, −27a-3p, −29a-3p, −344b-3p, −369-5p, and −409a-5p that lay within miR gene clusters potentially transcribed as single RNA units, we noted that associated miRNAs displayed similar FCEs and padj-values.

Comparisons of the expression profiles of groups C-C, HF-C, C-HF, and HF-HF showed that the expression of 29 miRNAs/Partner-miRNAs of the ARC of adult rats was impacted by the perinatal unbalanced environment. For 18 miRNAs/Partner-miRNAs, this impact relied on consecutive perinatal and adult exposures to an unbalanced metabolic environment.

DISCUSSION

Here, we extensively characterized miRNA populations in ARC of adult male rats of four metabolic statuses resulting from

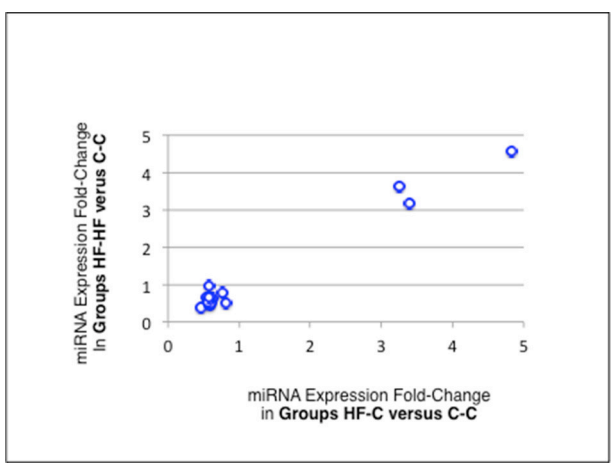

FIGURE 8 | miRNA differential expression in groups HF-C or HF-HF vs. C-C. miRNAs and Partner-miRNAs specified by the genes miR-323,−3585,−433,−485, and−770 as well as the miRNA miR-547-3p appeared significantly impacted by the sole perinatal unbalanced environment (padj-value < 5.2E-02; see **Table 3**). For each of these miRNAs, the Fold-Change of Expression (FCE) in Groups HF-HF vs. C-C was plotted against the FCE in Groups HF-C vs. C-C. Both FCEs displayed high correlation (R^2 = 0.98) indicating that the 11 miRNAs defined a subset of miRNAs repeatedly impacted by the perinatal unbalanced environment.

TABLE 5 | miRNA and partner-miRNA expression in groups HF-HF vs. C-C.

miRNAs Differentially Expressed Between Groups C-C and HF-HF					
miRNA	**FCE**	**Padj-value**	**Partner miRNA**	**FCE**	**Padj-value**
let-7a-1-3p	1.9	4.0E-03	let-7a-5p	0.7	6.5E-02
let-7i-5p	1.6	6.4E-03	let-7i-3p	1.4	5.6E-02
miR-1188-5p	0.4	5.7E-03			
miR-1224	0.5	5.1E-03			
miR-127-3p	0.7	9.2E-03	miR-127-5p	0.7	2.3E-02
miR-132-3p	1.9	6.6E-03	miR-132-5p	1.1	2.8E-01
miR-134-3p	1.8	8.1E-03	miR-134-5p	0.9	6.3E-02
miR-139-3p	0.6	5.7E-03	miR-139-5p	0.7	2.3E-02
miR-140-5p	2.1	3.0E-04	miR-140-3p	1.1	3.3E-02
miR-145-5p	3.4	8.1E-03	miR-145-3p	2.1	1.8E-02
miR-149-5p	0.6	5.1E-03			
miR-153-3p	1.9	9.7E-03	miR-153-5p	1.2	1.8E-01
miR-154-5p	1.5	4.9E-03	miR-154-3p	0.8	6.5E-02
miR-1843b-3p	0.6	9.1E-03			
miR-185-5p	1.5	4.5E-03			
miR-192-5p	1.7	2.9E-03			
miR-212-3p	1.9	3.1E-03	miR-212-5p	1.3	5.1E-02
miR-23a-3p	2.0	3.0E-03	miR-23a-5p	0.8	2.1E-01
miR-25-3p	1.6	5.7E-03	miR-25-5p	0.7	1.5E-02
miR-27a-3p	2.1	1.0E-02	miR-27a-5p	2.6	2.7E-02
miR-27b-3p	1.8	5.7E-03	miR-27b-5p	1.4	8.1E-02
miR-28-5p	1.7	5.1E-03	miR-28-3p	0.9	3.3E-01
miR-298-3p	0.4	2.0E-02	miR-298-5p	1.1	2.7E-01
miR-29a-3p	1.6	9.7E-03	miR-29a-5p	1.7	2.1E-02
miR-3068-5p	1.8	8.1E-04	miR-3068-3p	1.0	4.8E-01
miR-329-3p	0.7	9.7E-03	miR-329-5p	1.0	4.8E-01
miR-335	1.5	2.0E-03			
miR-344b-1-3p	0.5	9.7E-03	miR-344b-5p	0.7	2.1E-02
miR-34a-5p	2.1	2.9E-02			
miR-34c-5p	1.9	2.9E-03	miR-34c-3p	1.2	2.2E-01
miR-369-5p	0.8	5.3E-03	miR-369-3p	0.7	4.4E-02
miR-376b-3p	0.6	9.7E-03	miR-376b-5p	1.0	4.4E-01
miR-376c-3p	1.8	7.0E-04			
miR-409a-5p	0.6	9.9E-03	miR-409a-3p	0.7	2.5E-02
miR-410-3p	0.5	9.5E-03			
miR-434-3p	0.7	9.7E-03	miR-434-5p	1.3	5.9E-02
miR-487b-3p	0.6	5.3E-03			
miR-493-5p	0.6	9.7E-03	miR-493-3p	1.8	1.7E-02
miR-495	0.6	2.0E-03			
miR-504	0.6	6.7E-04			
miR-505-5p	0.7	1.0E-02	miR-505-3p	1.2	4.0E-02
miR-539-3p	2.2	7.7E-03	miR-539-5p	0.9	1.5E-01
miR-652-5p	1.9	7.8E-03	miR-652-3p	1.1	2.6E-01
miR-668	0.6	5.8E-03			
miR-708-5p	1.6	3.6E-04	miR-708-3p	0.9	3.1E-01
miR-760-3p	0.5	2.9E-03			
miR-7a-1-3p	1.7	8.1E-03	miR-7a-5p	1.2	2.0E-01
miR-7a-2-3p	1.7	1.0E-02	miR-7a-5p	1.2	2.0E-01
miR-872-5p	1.6	9.7E-03	miR-872-3p	1.1	2.7E-01

Forty-nine additional miRNAs displayed expression differences with padj-values = <1.0E-2 between groups C-C and HF-HF. Thirty-four miRNAs were identified along with their Partner-miRNAs. Nine Partner-miRNAs displayed close FCEs and padj-values = <5.0E-2. Twenty-five Partner-miRNAs (shaded Partner-miRNAs) displayed different FCEs and/or padj-values >5.0E-2. miRNAs are listed by alphabetical order.

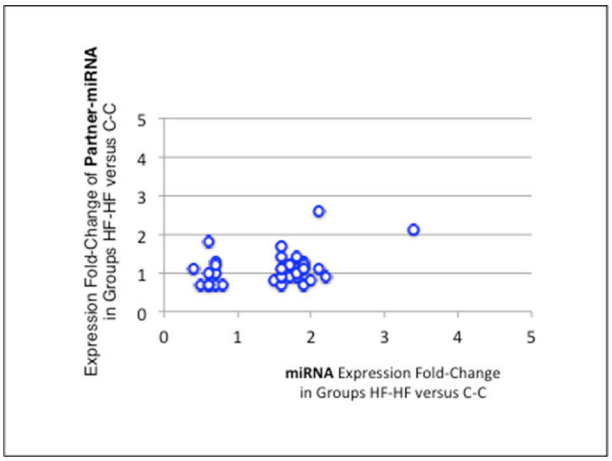

FIGURE 9 | miRNA and partner-miRNA differential expression in groups HF-HF vs. C-C. Thirty-four miRNAs specifically differentially expressed between groups C-C and HF-HF maturated in parallel with the second strand of their RNA duplex precursor (Partner-miRNA). Ratios of expressions (Fold-Change of Expression; FCE) of Partner-miRNAs were plotted against FCEs of miRNAs. Both FCEs displayed low correlation ($R^2 = 0.15$).

early and/or adult, balanced and/or unbalanced metabolic environments. We show that the ARC of adults holds a population of about 400 miRNA species that is as complex as the one of the first weeks of life (Doubi-Kadmiri et al., 2016). More than 94% of the miRNAs displayed homogeneous expression in the four groups C-C, C-HF, HF-C, and HF-HF. For 29 of those miRNAs, the perinatal environment impacts the expression.

The Specific Case of Clusters miR-96/182/183, miR-141/200c, and miR-200a/200b/429

In each metabolic status, a dozen of miRNAs exhibited hyper-variable expression. Among those miRNAs were all the 10 miRNAs produced from miR gene clusters miR-96/182/183, miR-141/200c, and miR-200a/200b/429. The 10 miRNAs co-varied in each profile demonstrating that the expression variability was due to true biological variations of expression rather than to experimental changes. Co-variation of miRNA expression also demonstrated that the transcription and maturation of clusters miR-96/182/183, miR-141/200c, and miR-200a/200b/429 are co-regulated in ARC.

miRNAs interact with targeted mRNAs primarily through nucleotides 2–7 (the seed region). In some cases, miRNA:mRNA interactions involve additional nucleotides. miRNA-5ps specified by the three clusters displayed low sequence identity and have four seed regions. miRNA-3ps specified by the three clusters displayed extensive sequence identity all along although the seed region of miR-141-3p and −200a-3p differs by one nucleotide at position 4 with that of miR-200b-3p, −200c-3p, and −429-3p. Large differences in the level of the seed regions of the miRNAs specified by the three clusters are expected to promote different levels of proteins encoded by targeted mRNAs. This may underlie differences in adult functions of ARC and, later, in individual susceptibilities to aging effects.

miRNAs specified by clusters miR-96/182/183, miR-141/200c, and miR-200a/200b/429 have been identified as miRNAs of functional importance in sensory organs. Punctual mutation or deletion in cluster miR-96/182/183 produces ear or retina disorders while loss of function of the miR-200 family leads to defects in the terminal differentiation of olfactory precursors (Choi et al., 2008; Kuhn et al., 2011; Lumayag et al., 2013). Whether expression of those miRNAs in sensory organs also varies between individuals deserves investigation.

Adult Unbalanced Metabolic Environment Has No Impact on miRNA Expression in ARC

miRNAs of the ARC of rats exposed to the unbalanced metabolic environment at the sole adulthood period display similar expression as those of rats exposed to the balanced environment. This absence of effect is observed although rats exposed to the unbalanced environment had two- and three-fold more circulating leptin and insulin, respectively, than rats exposed to the balanced environment. Levels of circulating fat are also probably highly different. Indeed, adult rats subjected to similar balanced or unbalanced metabolic environment have been reported to exhibit a seven-fold difference in plasma triglycerides (Auberval et al., 2014). This demonstrates that the transcription of the miRNA precursors of adult ARC is not affected by differences of such orders in circulating fat, leptin and insulin, even though leptin and insulin signaling pathways are known to include the activation of several transcription factors. Our work also suggests that miRNAs of adult ARC are not crucial for setting up carbohydrate and lipid peripheral metabolisms appropriate to balanced or unbalanced metabolic environment.

Early Unbalanced Metabolic Environment Affects miRNA Expression in Adult ARC

Eleven miRNAs of ARC of adult rats that have been exposed to the unbalanced metabolic environment during the perinatal period regularly displayed expression changes (**Figure 10A**). The five miRNAs miR-323-3p, −3585-3p, −433-5p, −485-5p, and −770-5p, the five Partner-miRNAs, 323-5p, −3585-5p, −433-3p, −485-3p, and−770-3p and the closely linked miRNA miR-547-3p defined a subset of miRNAs repeatedly impacted by the perinatal unbalanced environment.

Additionally, 18 miRNAs displayed expression differences in ARC of rats consecutively exposed to an unbalanced environment during the perinatal and adult periods, i.e., the nine miRNAs miRs-127-3p, −139-3p, −140-5p, −145-5p, −27a-3p, −29a-3p, −344b-3p, −369-5p, and −409a-5p, and nine Partner-miRNAs miRs-127-5p, −139-5p, −140-3p, −145-3p, −27a-5p, −29a-5p, −344b-5p, −369-3p, and −409a-3p (**Figure 10B**). Consecutive exposure to an unbalanced environment during the perinatal and adult periods led to slightly higher levels of circulating glucose

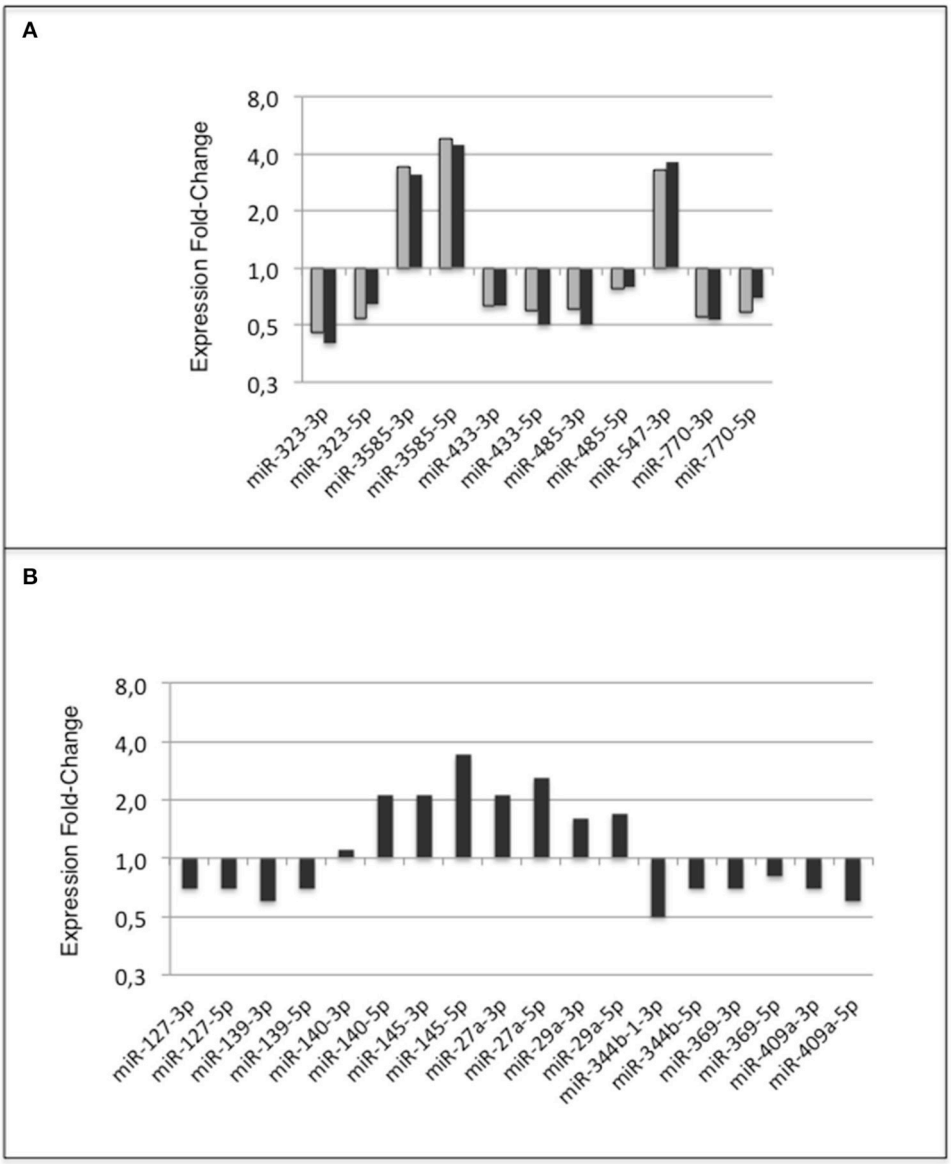

FIGURE 10 | miRNA response of adult ARC to metabolic environment. Summary **(A)** miRNA response to early metabolic challenge. Fold-Changes of Expression (FCE) were observed in Groups HF-C vs. C-C (gray bars) and Groups HF-HF vs. C-C (black bars); **(B)** Additional miRNA response to consecutive adult metabolic challenge observed in Groups HF-HF relatively to C-C. FCEs are shown using a $\log_2$ scale.

(see **Figure 3**). Glucose controls the expression of a glucose-responsive transcription factor (ChREBP) that regulates fatty acid synthesis and glycolysis in liver and adipose tissue. The role of ChREBP in the hypothalamus is still unknown.

We previously reported a significant ($p < 5.0E-2$) expression difference of miR-125a-3p, −200a-3p, and −409-5p in the hypothalamus of male adult rats fed a HF-diet for their last 4 weeks of life (this study used the same C- and HF-diets than the ones used here) in relation to differences in their postnatal environment (Benoit et al., 2013). Rats that had received a daily injection of a pegylated rat leptin antagonist (pRLA) from day 2 to day 13, displayed a slight enhancement of expression of the three miRNAs at the age of 4 months when compared to rats injected saline (FCEs ranged from 1.2 to 1.5).

In our study, miR-125a-3p displayed similar expression between the four groups (padj-values > 1.2E-01 in all comparisons; see Supplemental Table S5). In contrast, miR-200a-3p and −409-5p displayed trends to expression differences (padj-values > 1.0E-2 but < 5.0E-2) between groups C-C or C-HF on one hand and groups HF-C or HF-HF on the other hand. Along with miR-200a-3p, the miRNAs miR-200a-5p, −200b-3p, −200b-5p, and −429 that are specified by the same gene cluster displayed similar FCEs (ranging

from 2.0 to 3.4) and padj-values. Of note, the miRNAs miR-429, −182, −183-3p, −183-5p, and −96-5p which expression co-varied with that of with miR-200a-3p in all expression profiles (see above) also displayed similar FCEs (ranging from 2.8 to 6.2) and padj-values (>1.0E-2 but <5.0E-2). Similarly, along with miR-409a-5p, the miRNAs miR-409a-3p, −412-3p, and −412-5p that are specified by the same gene cluster displayed similar FCEs (ranging from 0.3 to 0.7) and padj-values when comparing group HF-C or HF-HF vs. group C-C.

Unbalanced perinatal metabolic environment and daily postnatal injection of pRLA have therefore different consequences on miR-125a-3p (constant expression vs. up-regulation, respectively) and −409-5p expression (down- vs. up-regulation, respectively). This may be due to differences in the experimental protocol itself, origin of miRNAs (the ARC vs. the whole hypothalamus) or age of animal (7 vs. 4 months). In contrast, miR-200a-3p expression, and potentially the expression of all miRNAs specified by the three clusters miR-96/182/183, miR-141/200c, and miR-200a/200b/429, tend to be up-regulated with similar FCEs in both experimental conditions.

We also reported up-regulation of miR-200a-3p,−200b-3p, and−409 in the hypothalamus of Lep^{ob}/Lep^{ob} mice deficient in leptin production when compared to Lep^{ob}/Lep^{+} or Lep^{+}/Lep^{+} mice (Crépin et al., 2014). In this study we also showed that daily intra-peritoneal injections of leptin significantly reduced hypothalamic expression of the three miRNAs in Lep^{ob}/Lep^{ob} but not in Lep^{ob}/Lep^{+} mice. On the other hand, intra-cerebroventricular (ICV) infusion of anti-miR-200a-3p to Lep^{ob}/Lep^{ob} mice restored the hypothalamic expression of *Irs-2* and *Lepr*, and up-regulated the hypothalamic expression of *Zfpm2*, *Insr, Pomc*, and *Npy*. *Pomc* and miR-200a-3p expressions did not display any correlation or anti-correlation in groups C-C, C-HF, HF-C, and HF-HF of our study ($R^2 = 0.09$). The increase of *Pomc* expression in infused mouse hypothalami may be due to the use of over-physiological quantities of anti-miR-200a-3p. Alternatively *Pomc* expression may be under different controls in mouse and rat.

Altogether our new and previous findings point to a trend to the long-term overexpression of clusters miR-96/182/183, miR-141/200c, and miR-200a/200b/429 in the ARC of adult rats and mice having experienced low levels of leptin/leptin signaling during the perinatal period.

Long-term consumption of a HFD-diet has been shown to induce microglia activation in hypothalamus of rats and mice (Thaler et al., 2012). Indeed the expression of several pro-inflammatory genes was increased by approximately 50% in the hypothalamus of adult male rats subjected to a HFD-diet of 4–20 weeks relatively to control rats fed a standard diet. Changes of microglial accumulation and cell size were limited to the ARC/Median eminence area. miR-146a and miR-155 appeared to play specific roles in brain inflammatory responses (Cardoso et al., 2016). miR-146a and miR-155 displayed similar expression between groups C-C and C-HF of our study (see Supplemental Table 4; padj-values > 3.0E-01). This suggests that adult HF-diet *per se,* at least the one we used, promotes low or no brain inflammatory response. miR-146a and −155 however displayed trends of up-regulation in groups HF-C and HF-HF when compared to group C-C (FCEs: 1.7–2.0; padj-values < 7.0E-02). The perinatal HF-diet may therefore induce long-term inflammation of ARC.

CONCLUSION

miRNAs participate in the control of many signaling pathways, many of which are involved in epigenetics regulations. Our findings reveal that miRNA expression in ARC at adulthood can change as a consequence of the quality of the early metabolic environment. Which among high fat, high carbohydrate, and/or moderate protein content in early life is responsible for miRNA differential expression in adult ARC needs to be determined. miRNA expression changes were modest with fold-changes lower than two except for a few miRNAs. *In vivo* identification of the mRNAs targeted by the differentially expressed miRNAs and characterization of the impact of miRNA expression differences on the synthesis of the mRNA-encoded proteins will determine whether and how these changes alter ARC functions.

ACCESSION CODES

Raw data files have been submitted at the SRA database (NCBI) under the study accession number SRP058705.

AUTHOR CONTRIBUTIONS

CB, SD-K, C-MV, MT, AB-T, and LA: Conceived and designed the experiments; SD-K, CB, DC, GP, LR, C-MV, MT, AB-T, and LA: Performed the experiments; XB: Developed the algorithms; SD-K, CB, XB, AB-T, and LA: Analyzed the data; AB-T and LA: Wrote the paper. All authors reviewed the manuscript.

ACKNOWLEDGMENTS

This work was supported by the Centre National de la Recherche Scientifique, the University Paris-Sud/Paris-Saclay and a grant from Danone/FRM 2011. XB was supported by a grant from FRM. Sequencing has benefited from the facilities and expertise of the high throughput sequencing platform of IMAGIF (Centre de Recherche de Gif, www.imagif.cnrs.fr).

SUPPLEMENTARY MATERIAL

The Supplementary Material for this article can be found online at: https://www.frontiersin.org/articles/10.3389/fnmol.2018.00090/full#supplementary-material

REFERENCES

Ainge, H., Thompson, C., Ozanne, S. E., and Rooney, K. B. (2011). A systematic review on animal models of maternal high fat feeding and offspring glycaemic control. *Int. J. Obes.* 35, 325–335. doi: 10.1038/ijo.2010.149

Amar, L., Benoit, C., Beaumont, G., Vacher, C. M., Crepin, D., Taouis, M., et al. (2012). MicroRNA expression profiling of hypothalamic arcuate and paraventricular nuclei from single rats using Illumina sequencing technology. *J. Neurosci. Methods.* 209, 134–143. doi: 10.1016/j.jneumeth.2012.05.033

Anders, S., and Huber, W. (2010). Differential expression analysis for sequence count data. *Genome Biol.* 11:R106. doi: 10.1186/gb-2010-11-10-r106

Auberval, N., Dal, S., Bietiger, W., Pinget, M., Jeandidier, N., Maillard-Pedracini, E., et al. (2014). Metabolic and oxidative stress markers in Wistar rats after 2 months on a high-fat diet. *Diabetol. Metab. Syndr.* 6:130. doi: 10.1186/1758-5996-6-130

Baroin-Tourancheau, A., Benigni, X., Benoit, C., Doubi-Kadmiri, S., Vacher, C. M., Taouis, M., et al. (2014). Keys for microRNA expression profiling of single rat hypothalamic nuclei and multiplex sequencing strategies. *Exp. Physiol.* 99, 72–77. doi: 10.1113/expphysiol.2013.072546

Baroin-Tourancheau, A., Benigni, X., Doubi-Kadmiri, S., Taouis, M., and Amar, L. (2016). Lessons from microRNA sequencing using Illumina technology. *Adv. Biol. Biotechnol.* 7, 319–328. doi: 10.4236/abb.2016.77030

Bartel, D. P. (2009). MicroRNAs: target recognition and regulatory functions. *Cell* 13, 215–233. doi: 10.1016/j.cell.2009.01.002

Benjamini Y., and Hochberg Y. (1995). Controlling the False Discovery Rate: a practical and powerful approach to multiple testing. *J. R. Stat. Soc. Ser. B* 57, 289–300. doi: 10.2307/2346101

Benoit, C., Ould-Hamouda, H., Crepin, D., Gertler, A., Amar, L., and Taouis, M. (2013). Early leptin blockade predisposes fat-fed rats to overweight and modifies hypothalamic microRNAs. *J. Endocrinol.* 218, 35–47. doi: 10.1530/JOE-12-0561

Cardoso, A. L., Guedes, J. R., and de Lima, M. C. (2016). Role of microRNAs in the regulation of innate immune cells under neuroinflammatory conditions. *Curr. Opin. Pharmacol.* 26, 1–9. doi: 10.1016/j.coph.2015.09.001

Choi, P. S., Zakhary, L., Choi, W. Y., Caron, S., Alvarez-Saavedra, E., Miska, E. A., et al. (2008). Members of the miRNA-200 family regulate olfactory neurogenesis. *Neuron* 57, 41–55. doi: 10.1016/j.neuron.2007.11.018

Crépin, D., Benomar, Y., Riffault, L., Amine, H., Gertler, A., and Taouis, M. (2014). The over-expression of miR-200a in the hypothalamus of ob/ob mice is linked to leptin and insulin signaling impairment. *Mol. Cell. Endocrinol.* 384, 1–11. doi: 10.1016/j.mce.2013.12.016

Doubi-Kadmiri, S., Benoit, C., Benigni, X., Beaumont, G., Vacher, C. M., Taouis, M., et al. (2016). Substantial and robust changes in microRNA transcriptome support postnatal development of the hypothalamus in rat. *Sci. Rep.* 6:24896. doi: 10.1038/srep24896

Griffiths-Jones, S., Saini, H. K., van Dongen, S., and Enright, A. J. (2008). miRBase: tools for microRNA genomics. *Nucleic Acids Res.* 36, D154–D158. doi: 10.1093/nar/gkm952

Ha, M., and Kim, V. N. (2014). Regulation of microRNA biogenesis. *Nat. Rev. Mol. Cell Biol.* 8, 509–524. doi: 10.1038/nrm3838

Hanson, M. A., and Gluckman, P. D. (2014). Early developmental conditioning of later health and disease: physiology or pathophysiology? *Physiol. Rev.* 94, 1027–1076. doi: 10.1152/physrev.00029.2013

Kuhn, S., Johnson, S. L., Furness, D. N., Chen, J., Ingham, N., Hilton, J. M., et al. (2011). miR-96 regulates the progression of differentiation in mammalian cochlear inner and outer hair cells. *Proc. Natl. Acad. Sci. U.S.A.* 108, 2355–2360. doi: 10.1073/pnas.1016646108

Lumayag, S., Haldin, C. E., Corbett, N. J., Wahlin, K. J., Cowan, C., Turturro, S., et al. (2013). Inactivation of the microRNA-183/96/182 cluster results in syndromic retinal degeneration. *Proc. Natl. Acad. Sci. U.S.A.* 110, E507–E516. doi: 10.1073/pnas.1212655110

Rodríguez, E. M., Blázquez, J. L., and Guerra, M. (2010). The design of barriers in the hypothalamus allows the median eminence and the arcuate nucleus to enjoy private milieus: the former opens to the portal blood and the latter to the cerebrospinal fluid. *Peptides* 31, 757–776. doi: 10.1016/j.peptides.2010.01.003

Rueda, A., Barturen, G., Lebron, R., Gomez-Martin, C., Aldanza, A., Oliver, J. L., et al. (2015). sRNAtoolbox: an integrated collection of small RNA research tool. *Nucl. Acids Res.* 43, W467–W473. doi: 10.1093/nar/gkv555

Sobrino Crespo, C., Perianes Cachero, A., Puebla Jiménez, L., Barrios, V., and Arilla Ferreiro, E. (2017). Peptides and food intake. *Front. Endocrinol.* 5:58. doi: 10.3389/fendo.2014.00058

Thaler, J. P., Yi, C. X., Schur, E. A., Guyenet, S. J., Hwang, B. H., Dietrich, M. O., et al. (2012). Obesity is associated with hypothalamic injury in rodents and humans. *J. Clin. Invest.* 22, 153–162. doi: 10.1172/JCI59660

Timper, K., and Brüning, J. C. (2017). Hypothalamic circuits regulating appetite and energy homeostasis: pathways to obesity. *Dis. Model. Mech.* 10, 679–689. doi: 10.1242/dmm.026609

Vienberg, S., Geiger, J., Madsen, S., and Dalgaard, L. T. (2017). MicroRNAs in metabolism. *Acta Physiol.* 219, 346–361. doi: 10.1111/apha.12681

Conflict of Interest Statement: The authors declare that the research was conducted in the absence of any commercial or financial relationships that could be construed as a potential conflict of interest.

frontiers in Cellular Neuroscience

ORIGINAL RESEARCH
published: 15 August 2018
doi: 10.3389/fncel.2018.00224

Environmental Enrichment Improves Cognitive Deficits, AD Hallmarks and Epigenetic Alterations Presented in 5xFAD Mouse Model

*Christian Griñán-Ferré[1], Vanesa Izquierdo[1], Eduard Otero[1], Dolors Puigoriol-Illamola[1], Rubén Corpas[2], Coral Sanfeliu[2], Daniel Ortuño-Sahagún[3] and Mercè Pallàs[1]**

[1]Department of Pharmacology and Therapeutic Chemistry, Institut de Neurociències, University of Barcelona, Barcelona, Spain, [2]Institut d'Investigacions Biomèdiques de Barcelona (IIBB), CSIC, IDIBAPS and CIBERESP, Barcelona, Spain, [3]Laboratorio de Neuroinmunomodulación Molecular, Instituto de Investigación en Ciencias Biomédicas (IICB), Centro Universitario de Ciencias de las Salud (CUCS), Universidad de Guadalajara, Guadalajara, Mexico

Cumulative evidence shows that modifications in lifestyle factors constitute an effective strategy to modulate molecular events related to neurodegenerative diseases, confirming the relevant role of epigenetics. Accordingly, Environmental Enrichment (EE) represents an approach to ameliorate cognitive decline and neuroprotection in Alzheimer's disease (AD). AD is characterized by specific neuropathological hallmarks, such as β-amyloid plaques and Neurofibrillary Tangles, which severely affect the areas of the brain responsible for learning and memory. We evaluated EE neuroprotective influence on 5xFAD mice. We found a better cognitive performance on EE vs. Control (Ct) 5xFAD mice, until being similar to Wild-Type (Wt) mice group. Neurodegenerative markers as β-CTF and tau hyperphosphorylation, reduced protein levels whiles APPα, postsynaptic density 95 (PSD95) and synaptophysin (SYN) protein levels increased protein levels in the hippocampus of 5xFAD-EE mice group. Furthermore, a reduction in gene expression of *Il-6, Gfap, Hmox1 and Aox1* was determined. However, no changes were found in the gene expression of neurotrophins, such as Brain-derived neurotrophic factor (*Bdnf*), Nerve growth factor (*Ngf*), Tumor growth factor *(Tgf)* and Nerve growth factor inducible (*Vgf*) in mice with EE. Specifically, we found a reduced DNA-methylation level (5-mC) and an increased hydroxymethylation level (5-hmC), as well as an increased histone H3 and H4 acetylation level. Likewise, we found changes in the hippocampal gene expression of some chromatin-modifying enzyme, such as *Dnmt3a/b*, *Hdac1*, and *Tet2*. Extensive molecular analysis revealed a correlation between neuronal function and changes in epigenetic marks after EE that explain the cognitive improvement in 5xFAD.

Keywords: behavior, cognition, environmental enrichment, epigenetics, APP, Tau, oxidative stress, inflammation

OPEN ACCESS

Edited by:
Lavinia Alberi, SICHH, Switzerland

Reviewed by:
Debomoy K. Lahiri, Indiana University, Purdue University Indianapolis, United States
Nicola Berretta, Fondazione Santa Lucia (IRCCS), Italy

****Correspondence:***
Mercè Pallàs
pallas@ub.edu

Received: *04 March 2018*
Accepted: *10 July 2018*
Published: *15 August 2018*

Citation:
Griñán-Ferré C, Izquierdo V, Otero E, Puigoriol-Illamola D, Corpas R, Sanfeliu C, Ortuño-Sahagún D and Pallàs M (2018) Environmental Enrichment Improves Cognitive Deficits, AD Hallmarks and Epigenetic Alterations Presented in 5xFAD Mouse Model. Front. Cell. Neurosci. 12:224. doi: 10.3389/fncel.2018.00224

INTRODUCTION

Emerging evidence indicates that the aberrant transcriptional regulation of memory-related genes reflects epigenetic landscape modifications because of changes in environmental factors (Puckett and Lubin, 2011; Duncan et al., 2014; Maloney and Lahiri, 2016). On the other hand, the main driving force of senescence process is the differential regulation of gene expression by epigenetic mechanisms (López-Otín et al., 2013). Moreover, a distinctive and critical influence of diet, Environmental Enrichment (EE) or exercise have emerged as strategies that correlate preventing cognitive decline and improving quality of life (Ricci et al., 2018).

Alzheimer disease (AD) and other dementias are strongly associated with aging (Delgado-Morales et al., 2017). AD involves degeneration of certain regions of the brain, which results in memory loss and declining in cognition, functions and behavior. The neuropathological hallmarks comprise the accumulation and deposition of β-amyloid in the senile plaques, and hyperphosphorylated tau (p-Tau) protein, a microtubule assembly protein formation of Neurofibrillary Tangles (NFTs; Bloom, 2014). Additionally, there are other key pathological changes such as oxidative stress, neuroinflammation and neuronal loss (Agostinho et al., 2010).

Epigenetic could act as the primary mechanism contributing to the pathogenesis of AD, with a critical role in the interaction between the genome and the environment (Spiegel et al., 2014; McCreary and Metz, 2016). In particular, modifications in DNA methylation (5-mC) and hydroxymethylation (5-hmC) are seen in the brain tissues of AD mouse model (Chouliaras et al., 2010; Lunnon et al., 2014; Griñán-Ferré et al., 2016c). Furthermore, deregulation of histone acetylation has been implicated in various neurodegenerative disorders such as AD (Bahari-Javan et al., 2012). Likewise, alterations in microRNA (miRNA) expression were found in the hippocampus of both demented patients (Lau et al., 2013) and AD mouse models (Barak et al., 2013; Cosín-Tomás et al., 2014). Specifically, dysregulation in *miR-101* (Long and Lahiri, 2011), *miR-153* (Long et al., 2012) and *miR-339-5* (Long et al., 2014), downregulates the APP expression in mouse *in vitro* and *in vivo* models and AD patients. In fact, several miRNAs have been proposed as biomarkers for AD (Yılmaz et al., 2016).

EE is an excellent experimental paradigm able to induce oxidative stress reduction (Pusic et al., 2016), a curbing in inflammation (Jurgens and Johnson, 2012) and epigenetic changes (Irier et al., 2014). EE is based on housing conditions that provide a combination of social interactions, cognitive, sensory and motor stimulation (Rosenzweig and Bennett, 1996; van Praag et al., 2000; Mora et al., 2007). In fact, it has been widely described the influence of the environment on behavior and cognition (Nathianantharajah and Hannan, 2006). For instance, a number of studies have demonstrated that rodent AD models maintained under EE conditions show better cognitive performance correlated with beneficial changes in the brain (Griñán-Ferré et al., 2016a,b; Hüttenrauch et al., 2016). Nevertheless, the mechanisms by which EE alters brain structure and function are not well understood. Since Hebb's first EE experiments, the two main mechanisms described were that EE promoted changes at the anatomical and electrophysiological level (Irvine et al., 2006; Eckert and Abraham, 2010). An alternative mechanism was that EE promoted neural plasticity through increasing levels of growth factors such as brain-derived neurotrophic factor (BDNF) and nerve growth factor (NGF), among others, in the brain (Ickes et al., 2000; Angelucci et al., 2009). There is also evidence that EE attenuates both oxidative stress (Herring et al., 2010; Cechetti et al., 2012) and inflammatory process (McQuaid et al., 2013).

Recent studies have demonstrated that EE promotes changes in DNA methylation states at the global level or at specific loci while changing the expression of DNA MethylTransferases (DNMTs; Madrigano et al., 2011; Barrès et al., 2012; Griñán-Ferré et al., 2016b). Other global changes in histone acetylation H3/H4 have been seen in AD mouse model (Fischer et al., 2007; Griñán-Ferré et al., 2016c; Vierci et al., 2016). Besides, it has been reported changes in DNA methylation of *Bdnf* promoter in rat hippocampus, caused increases in gene expression after EE (Gomez-Pinilla et al., 2011).

5xFAD represents an important transgenic murine model of AD, which develops early and aggressive hallmarks of amyloid burden and cognitive loss (Oakley et al., 2006; Devi and Ohno, 2010; Girard et al., 2013). Additional AD pathologies exhibited by the 5xFAD model include age-dependent synaptic degeneration (Wang et al., 2016), mitochondrial dysfunction (Devi and Ohno, 2012), increase in oxidative stress (Griñán-Ferré et al., 2016c), and microglial activation (Landel et al., 2014). On the other hand, epigenetic alterations in the 5xFAD model were also described (Anderson et al., 2015). Remarkably, recent studies revealed a correlation among cognitive deficits, Aβ pathology and epigenetic alterations (Griñán-Ferré et al., 2016c), demonstrating the key role of epigenetics in this mouse model.

The present work aimed to confirm the association between EE and cognitive improvement in 5xFAD mice and the molecular changes observed. Besides, we went deep to highlight the putative correlation between epigenetic alterations and the mechanisms underlying the neurodegenerative process in AD.

MATERIALS AND METHODS

Animals and Housing Conditions

Female Wild-Type (Wt-Ct, n = 24) and 5xFAD (n = 24) mice were used to carry out cognitive. Animals had free access to food and water and were kept under standard temperature conditions (22 ± 2°C) and 12 h:12 h light-dark cycles (300 lux/0 lux).

The animals were maintained until 4-month-old with standard conditions, and afterward were separated into treatment groups at up to 6-month-old. Twelve Wt and 5xFAD were employed for the EE group during 8 weeks (Wt-EE and 5xFAD-EE), and 12 were maintained under standard conditions as Control mice (Wt-Ct and 5xFAD-Ct). In the present study, we utilized the novel objects paradigm to accomplish EE conditions. Therefore, plastic tubes (20 cm long and 2.5 cm in diameter) were placed in EE cages, in addition to plastic dolls or toys, which were added, extracted, or changed each week (**Figure 1**).

This study was carried out in accordance with the recommendations of European Community Council Directive 86/609/EEC and the procedures established by the Department d'Agricultura, Ramaderia i Pesca of the Generalitat de Catalunya, Spain. Every effort was made to minimize animal suffering and to reduce the number of animals.

Behavioral Tests

Elevated Plus Maze

The Elevated Plus Maze (EPM) was performed as previously described (Griñán-Ferré et al., 2016a). Forty-eight mice (n = 12 per group) were placed on the central platform, facing an open arm, and allowed to explore the apparatus for 5 min. After

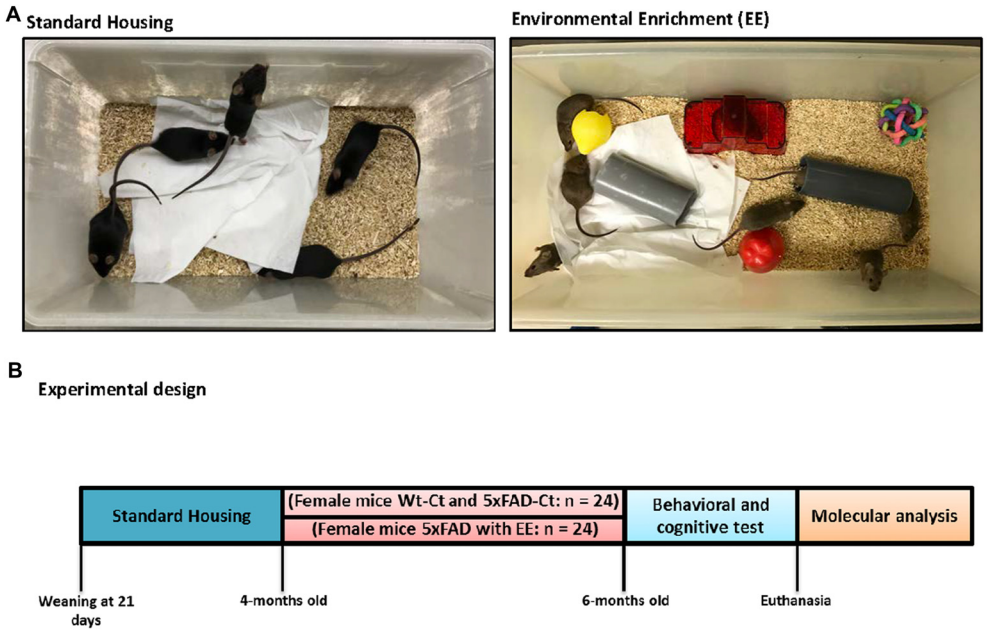

FIGURE 1 | Housing conditions and experimental design. Exemplary pictures of standard (Control, Ct) and enriched (Environmental Enrichment, EE) housing conditions **(A)**. Mice were housed in groups of 5–6. Enriched cages were equipped with tunnels, houses, and toys. At 4-month-old 5xFAD were randomly allocated to either Ct or EE conditions for 8 weeks. With 6-month-old, mice were tested in behavioral and memory tests followed by euthanasia and tissue collection **(B)**.

the 5-min test, each mouse was returned to their home cages, and the EPM apparatus was cleaned with 70% ethyl alcohol and allowed to dry between tests. Behavior was scored with SMART ver. 3.0 software and each trial were recorded for later analysis. Parameters recorded included time spent on open arms, time spent on closed arms, time spent in the center zone, rearings, defecation and urination.

Open Field Test

The Open Field Test (OFT) was performed as previously described (Griñán-Ferré et al., 2016a). Forty-eight mice (n = 12 per group) were individually placed at the center and allowed to explore the white polywood box (50 × 50 × 25 cm) for 5 min. Behavior was scored with SMART® ver.3.0 software and each trial was recorded for later analysis. The parameters scored included center-staying duration, rearings, defecations and the distance traveled.

Novel Object Recognition Test

The Novel Object Recognition Test (NORT) protocol employed was a modification of Ennaceur and Delacour (1988) and Ennaceur and Meliani (1992). In brief, 48 mice (n = 12 per group) were placed in a 90°, two-arm, 25-cm-long, 20-cm-high, 5-cm-wide black maze. Before performing the test, mice were individually habituated to the apparatus for 10 min during 3 days. On day 4, the animals were submitted to a 10-min acquisition trial (first trial), during which they were placed in the maze in the presence of two identical, novel objects at the end of each arm. After a delay (2 h and 24 h), the animal was exposed to two objects one old object and one novel object. The time that mice explored the Novel object (TN) and Time that mice explored the Old object (TO) were measured. A Discrimination Index (DI) was defined as (TN − TO)/(TN + TO). In order to avoid object preference biases, objects were counterbalanced.

T-Maze Spontaneous Alternation

T-Maze spontaneous alternation from 48 samples (n = 12 per group) was tested as previously described (Fragkouli et al., 2005). The protocol we followed consisted of one forced and 10 consecutive free-choice trials on the same day. Briefly, on the first trial, mice were individually placed on the central stem of the T-maze allowing to explore the central stem and one of the goal arms of the maze. After entering the goal arm, exit from the arm was blocked, and mice were left to explore the arm for 30 s. Animals were then retrieved, and the testing cycle started again 10 min later with another free-choice trial. The percentage of alternation (number of turns in each goal arm) and total trial duration are recorded and calculated.

Immunodetection Experiments

Brain Processing

Mice were euthanized by cervical dislocation one day after the behavioral test finished. Brains were immediately removed from the skull. The hippocampus was then isolated and frozen in powdered dry ice. They were maintained at −80°C for further use. Tissue samples were homogenized in lysis buffer containing phosphatase and protease inhibitors (Cocktail II, Sigma). Total protein levels were obtained and protein concentration was determined by the method of Bradford.

Protein Levels Determination by Western Blotting

For Western Blotting (WB), aliquots of 15 μg of hippocampal protein were used. Protein samples from 12 samples (n = 4 per group) were separated by SDS-PAGE (8%–12%) and transferred onto PVDF membranes (Millipore). Afterwards, membranes were blocked in 5% non-fat milk in 0.1% Tween20 TBS (TBS-T) for 1 h at room temperature, followed by overnight incubation at 4°C with the primary antibodies listed in **Supplementary Table S1**.

Afterward, membranes were washed and incubated with secondary antibodies for 1 h at room temperature. Immunoreactive proteins were viewed with a chemiluminescence-based detection kit, following the manufacturer's protocol (ECL Kit; Millipore) and digital images were acquired using a ChemiDoc XRS+ System (BioRad). Semi-quantitative analyses were carried out using ImageLab software (BioRad) and results were expressed in Arbitrary Units (AU), considering control protein levels as 100%. Immunodetection of GAPDH, or β-Actin routinely monitored protein loading.

Determination of Oxidative Stress in Hippocampus

Hydrogen peroxide from 12 samples (n = 4 per group) was measured as an indicator of oxidative stress, and it was quantified using the Hydrogen Peroxide Assay Kit (Sigma-Aldrich, St. Louis, MI) according to the manufacturer's instructions.

Global DNA Methylation and Hydroxymethylation Quantification

Isolation of genomic DNA from 12 samples (n = 4 per group) was conducted using the FitAmpTM Blood and Cultured Cell DNA Extraction Kit according to the manufacturer's instructions. Then, Methylflash Methylated DNA Quantification Kit (Epigentek, Farmingdale, NY, USA) and MethylFlash HydroxyMethylated DNA Quantification Kit were used in order to detect methylated and hydroxymethylated DNA. Briefly, these kits are based on specific antibody detection of 5-mC and 5-hmC residues, which trigger an ELISA-like reaction that allows colorimetric quantification by reading absorbance at 450 nm using a Microplate Photometer.

Global Histone Acetylation H3 and H4 Quantification

Histone extracts from 12 samples (n = 4 per group) were prepared by using a total histone extraction kit (Epigentek) according to the manufacturer's protocol. Detection of global histone H3/H4 acetylation status was performed using the EpiQuik^{TM} global histone H3/H4 acetylation assay kit (Cat. P-4008-96/P-4009-96, Epigentek Group Inc., NY, USA), following the manufacturer's recommendations. Briefly, histone proteins (1–2 μg) were added to the strip wells. Acetylated histone H3/H4 was detected with a high-affinity antibody, and the ratios and amounts of acetylated histone H3/H4 were displayed with a horseradish peroxidase-conjugated secondary anti-body color development system. The color was measured by reading absorbance at 450 nm using a Microplate Photometer.

RNA Extraction and Gene Expression Determination

Total RNA isolation from 12 samples (n = 4 per group) was carried out by means of TRIzol® reagent following the manufacturer's instructions. The yield, purity, and quality of RNA were determined spectrophotometrically with a NanoDrop^{TM} ND-1000 (Thermo Scientific) apparatus and an Agilent 2100B Bioanalyzer (Agilent Technologies). RNAs with 260/280 ratios and RIN higher than 1.9 and 7.5, respectively, were selected. Reverse Transcription-Polymerase Chain Reaction (RT-PCR) was performed as follows: 2 μg of messenger RNA (mRNA) was reverse-transcribed using the High Capacity cDNA Reverse Transcription Kit (Applied Biosystems). Real-time quantitative PCR (qPCR) was employed to quantify the mRNA expression of a set of chromatin-modifying enzyme genes, oxidative stress genes, inflammatory genes, neurotrophin genes. Normalization of expression levels was performed with actin for SYBER Green and TATA-binding protein (*Tbp*) for TaqMan. Primers and TaqMan probes are listed in **Supplementary Table S2**.

SYBR® Green real-time PCR was performed in a Step One Plus Detection System (Applied-Biosystems) employing SYBR® Green PCR Master Mix (Applied-Biosystems). Each reaction mixture contained 7.5 μL of complementary DNA (cDNA; which concentration was 2 μg), 0.75 μL of each primer (which concentration was 100 nM), and 7.5 μL of SYBR® Green PCR Master Mix (2×).

TaqMan-based real-time PCR (Applied Biosystems) was also performed in a Step One Plus Detection System (Applied-Biosystems). Each 20 μL of TaqMan reaction contained 9 μL of cDNA (25 ng), 1 μL 20× probe of TaqMan Gene Expression Assays and 10 μL of 2× TaqMan Universal PCR Master Mix.

Data were analyzed utilizing the comparative Cycle threshold (Ct) method (ΔΔCt), where the housekeeping gene level was used to normalize differences in sample loading and preparation. Normalization of expression levels was performed with *actin* for SYBR® Green-based real-time PCR results and TATA-binding protein *(Tbp)* for TaqMan-based real-time PCR. Each sample was analyzed in duplicate, and the results represent the n-fold difference of the transcript levels among different groups.

Data Analysis

The statistical analysis was conducted using GraphPad Prism ver. 6 statistical software. Data are expressed as the mean ± Standard Error of the Mean (SEM) of at least four samples per group. Means were compared with one-way analysis of variance (ANOVA), followed by Tukey *post hoc* test. Statistical significance was considered when a p-values were <0.05. The statistical outliers were determined with Grubbs' test and subsequently removed from the analysis.

RESULTS

Effect of EE, in Locomotor Activity and Motivational in 5xFAD Mice

5xFAD-EE group restored the locomotor activity in comparison with Wt-Ct group (**Figure 2A**). Time spent in the center zone was higher in 5xFAD-EE, although did not reach significance

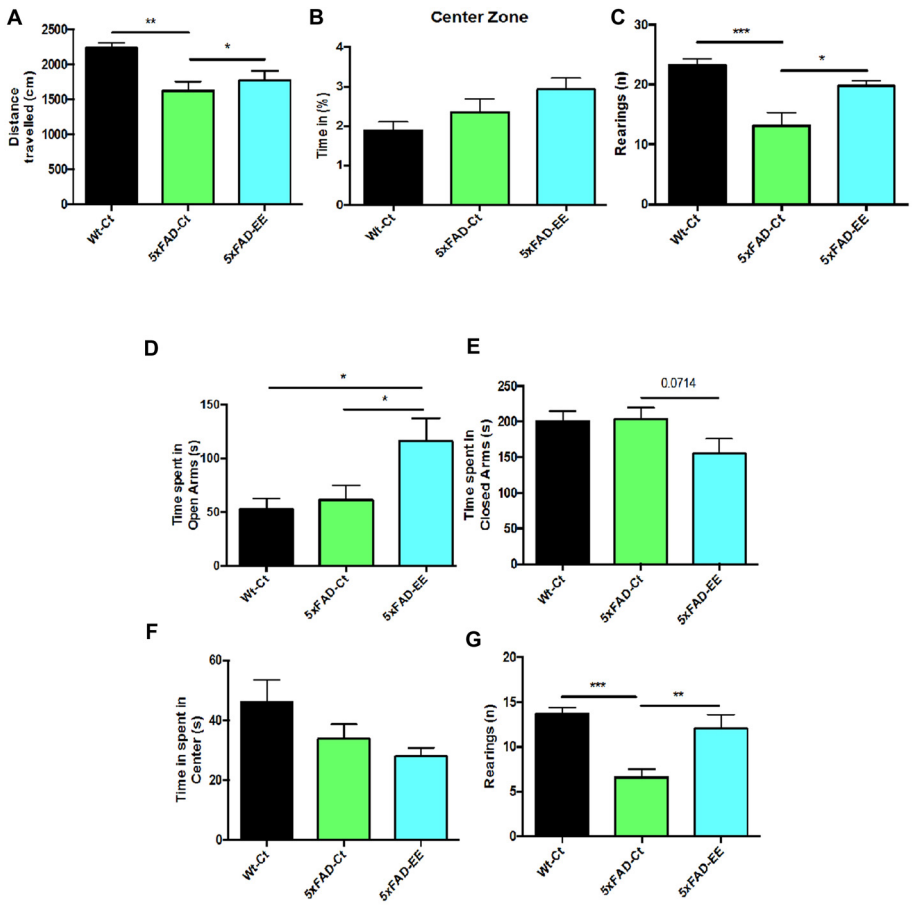

FIGURE 2 | Results of Open Field Test (OFT) in female mice at 4-month-old wild-type (Wt)-Ct and 5xFAD-Ct mice groups and 5xFAD mice group after 8 weeks with EE. Distance traveled **(A)**, percentage of time spent in Center zone **(B)** and Rearings **(C)**. Results of Elevated Plus Maze (EPM) in female mice at 4-month-old Wt-Ct and 5xFAD-Ct mice groups and 5xFAD mice group after 8 weeks with EE. Time spent in Open Arms **(D)**. Time spent in Closed Arms **(E)**. Time spent in Center **(F)** and Rearings **(G)**. Values represented are mean ± Standard error of the mean (SEM); $^{*}p < 0.05$; $^{**}p < 0.01$; $^{***}p < 0.001$.

(**Figure 2B**) as compared with controls. Furthermore, a significant increase in vertical activity, quantified by the number of rearings, in comparison with the 5xFAD-Ct was found (**Figure 2C**). Results obtained in the OFT exhibited changes in fear behavior and motor activity. Additional parameters measured in the EPM are presented in **Supplementary Table S3**.

The specific anxiety value obtained in the EPM, time spent in opened arms, showed a significant increase in 5xFAD-EE compared to 5xFAD-Ct (**Figure 2D**); time spent in closed arms by 5xFAD-EE mice group was slightly lower than other groups (**Figure 2E**). Furthermore, time spent in the center was lower in 5xFAD-EE, although did not reach significance (**Figure 2F**) as compared with controls. Finally, accordingly with OFT results, a significant increase in 5xFAD-EE vertical activity compared to 5xFAD-Ct was found (**Figure 2G**). Results obtained in the EPM demonstrated changes in fear-anxiety-like behavior. Additional parameters measured in the EPM are presented in **Supplementary Table S4**.

EE Reduced Cognitive Deficits Presented by 5xFAD Mice

NORT analysis showed, as described (Griñán-Ferré et al., 2016c) an impaired short- and long-memory in 5xFAD mice in comparison with age mated Wt (**Supplementary Figure S1**). However, EE intervention did not modify memory capabilities in Wt mice (**Supplementary Figure S1**). By contrast, NORT analysis demonstrated that 5xFAD-EE mice exhibited significantly reduced cognitive deficits in both short- and long-term memory (**Figures 3A,B**), obtaining highest DI than 5xFAD-Ct. Moreover, we found significant differences in spontaneous alternation between Wt-Ct and 5xFAD-Ct (**Figure 3C**) and between 5xFAD-EE and 5xFAD-Ct (**Figure 3C**), but not for Wt-EE (**Supplementary Figure S1**). The absence of changes in cognitive parameters in Wt mice, conducted us to evaluate only epigenetic marks in this strain (**Supplementary Figure S2**).

Finally, the polygonal graph depicts differences between 5xFAD mice with EE and control mice group by graphing several OF parameters, EPM parameters, DI of NORT and

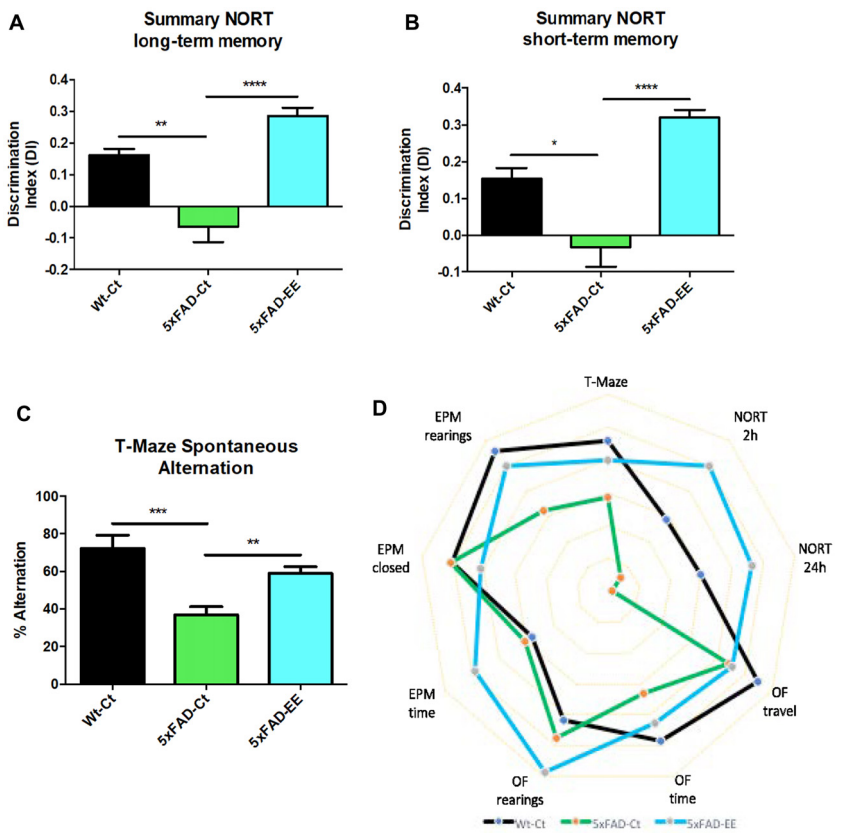

FIGURE 3 | Results of Discrimination Index (DI) of Novel Object Recognition Test (NORT) in female mice at 4-month-old Wt-Ct and 5xFAD-Ct mice groups and 5xFAD mice group after 8 weeks with EE. Summary from short-term memory **(A)**, and from summary long-term memory **(B)**. Results of Spontaneous Alternation T-Maze in female mice at 4-month-old Wt-Ct and 5xFAD-Ct mice groups and 5xFAD mice group after 8 weeks with EE. Percentage successful spontaneous alternations in a T-Maze **(C)**. Polygonal graph presented complete parameters obtained by OF, EPM, NORT and T-Maze **(D)**. Values represented are mean ± Standard error of the mean (SEM); $*p < 0.05$; $**p < 0.01$; $***p < 0.001$; $****p < 0.0001$.

spontaneous alternation of T-Maze (**Figure 3D**), demonstrating that EE intervention improved cognitive performance in 5xFAD mouse model in comparison with Control, approaching it to Wt.

Hippocampal Global Changes in DNA Methylation and Hydroxymethylation and Its Machinery After EE

To depict a landscape on global methylation affectation by EE we evaluate methylation and hydroxymethylation. 5-methylcytosine levels were significantly reduced in 5xFAD-EE in comparison with control mice (**Figure 4A**). In parallel, 5-hmC levels were increased in 5xFAD-EE. Because changes in methylation were determined, DNMTs family and Translocation family (TETs), members of DNA hydroxylase family gene expression, were studied; significant increases in *Dnmt3a* and *Dnmt3b* were found in the 5xFAD-EE mice group (**Figure 4B**). Results showed significant increases in *Tet2*, but not in *Tet1* in the 5xFAD-EE mice group in comparison with control group (**Figure 4B**). Similar changes in methylation and hydroxymethylation were also determined in Wt-EE mice in comparison with Wt-Ct, accompanied by variations in gene expression levels in enzymes (**Supplementary Figure S2**).

Hippocampal Global Changes in Histone Acetylation Levels and Chromatin-Modifying Enzymes After EE

Histone acetylation is another epigenetic marker that can modify gene expression. Acetylated H3 and H4 protein levels were significantly increased in 5xFAD-EE compared to 5xFAD-Ct (**Figure 5A**). Increased gene expression in *Hdac1* but no changes of *Hdac2* were found in 5xFAD-EE in comparison with control mice group (**Figure 5B**).

Reduction in Oxidative Stress and Inflammation Markers in 5xFAD Mice

Increases in oxidative stress as well as neuroinflammation are hallmarks of AD. Beneficial effects of EE depicted on a significant reduction in *Hmox1* and *Aox1* between 5xFAD-EE group compared to 5xFAD-Ct (**Figure 6A**). Likewise, a significant increase in *Hmox1* gene expression (**Figure 6A**) and SOD1 protein levels (**Figures 6B,C**) between 5xFAD-Ct in

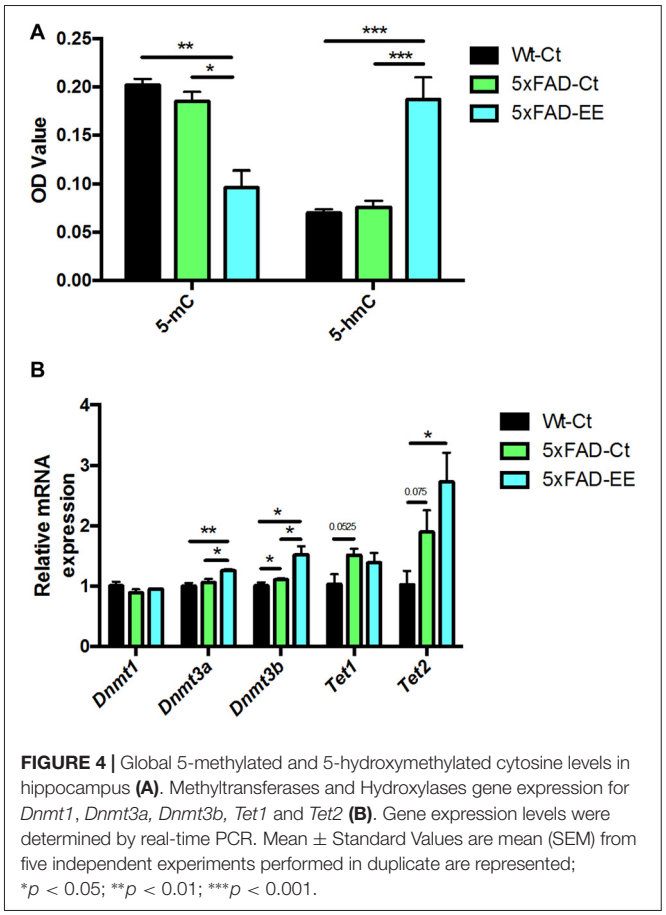

FIGURE 4 | Global 5-methylated and 5-hydroxymethylated cytosine levels in hippocampus **(A)**. Methyltransferases and Hydroxylases gene expression for *Dnmt1*, *Dnmt3a, Dnmt3b, Tet1* and *Tet2* **(B)**. Gene expression levels were determined by real-time PCR. Mean ± Standard Values are mean (SEM) from five independent experiments performed in duplicate are represented; $^{*}p < 0.05$; $^{**}p < 0.01$; $^{***}p < 0.001$.

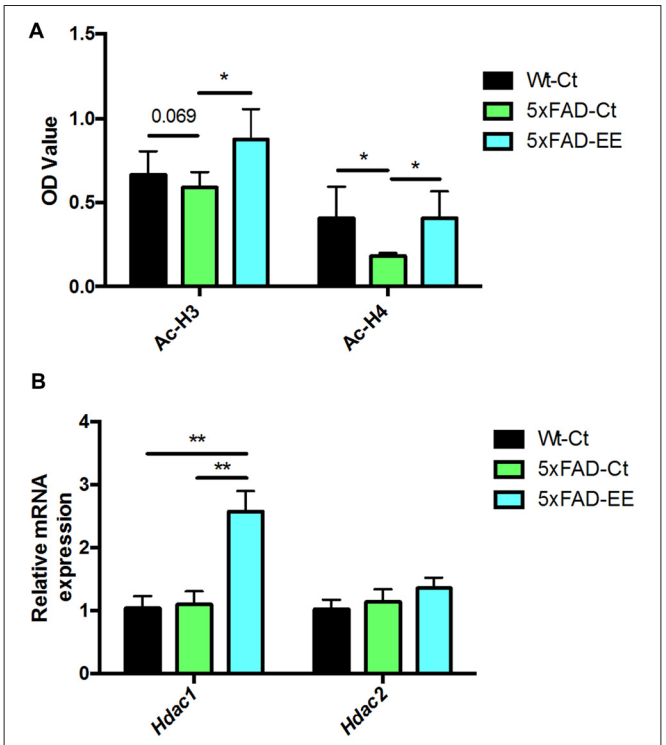

FIGURE 5 | Global histone H3/H4 acetylation levels in hippocampus **(A)**. Deacetylases gene expression related to memory for *Hdac1* and *Hdac2* **(B)**. For Gene expression levels were determined by real-time PCR. Mean ± Standard error of the mean (SEM) from five independent experiments performed in duplicate are represented; $^{*}p < 0.05$; $^{**}p < 0.01$.

comparison with Wt-Ct was found. Moreover, a slight but not significant decrease in *Cox2* gene expression in the 5xFAD-EE was observed when compared to the control group (**Figure 6A**). Finally, analysis of hydrogen peroxide levels in homogenates of hippocampus tissue showed a significant decrease in ROS levels in 5xFAD-EE compared to 5xFAD-Ct (**Figure 6D**). Interestingly, the highest ROS levels were observed in 5xFAD-Ct.

On the other hand, EE induced a significant reduction in *Il-6* and *Tnf-α* gene expression compared to control groups (**Figure 6E**). Decreased GFAP protein levels were found in 5xFAD-EE compared to control groups (**Figures 6F,G**). In addition, Wt-Ct and 5xFAD-EE presented a slight, although not significant, diminution in *Gfap* gene expression compared to 5xFAD-Ct (**Figure 6E**).

Increased Synaptic Marker Protein Levels but Not in Neurotrophins Gene Expression After EE

Synaptic damage and neurotrophin expression alteration have been described in 5xFAD. A significant increase in postsynaptic density 95 (PSD95) protein levels was found in 5xFAD-EE compared to 5xFAD-Ct reaching Wt-Ct levels (**Figures 7A,B**). Albeit did not reach significance, EE increased synaptophysin (SYN) protein levels (**Figures 7C,D**). However, no significant differences were observed in *Bdnf*, *Ngf*, *Tgf*, and *Vgf* gene expression after EE or among 5xFAD and control mice groups (**Figure 7E**).

EE Changed Alzheimer's Disease Markers in 5xFAD Mice

As mentioned, 5xFAD mice is an established AD model with changes in amyloid cascade and tauopathy. Prevention by EE of these two AD hallmarks was studied. To this end, we evaluate tau hyperphosphorylation and APP processing in 5xFAD under EE. Western blot analysis revealed that EE produced a significant decrease in both p-Tau Ser396 in 5xFAD reaching WT-Ct levels (**Figures 8A,B**). Additionally, a tendency to increase in sAPPα protein levels was found in 5xFAD-EE reaching Wt-Ct levels (**Figures 8C,D**), whereas β-CTF (the fragment delivered by β-secretase) was diminished after EE intervention (**Figures 8E,F**).

DISCUSSION

The present study aimed to evaluate, whether an EE intervention is effective in 5xFAD mouse model, modifying behavioral, cognitive and molecular AD hallmarks present in this transgenic mouse model. To this end, changes in oxidative stress, inflammation, tau hyperphosphorylation, and APP processing markers were determined. Besides, some epigenetic markers were studied to elucidate a possible epigenetic mechanism linking EE,

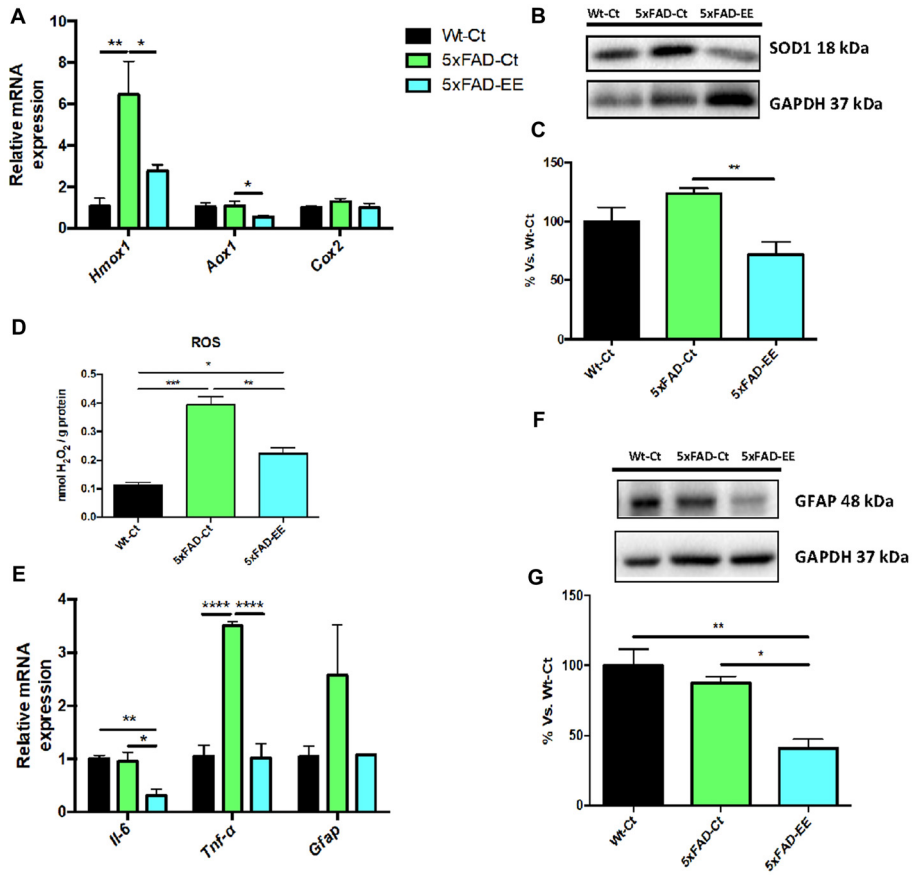

FIGURE 6 | Representative gene expression of antioxidant enzymes for *Hmox1*, *Aox1*, *Cox2* **(A)**. Representative Western blot for SOD1 protein levels **(B)** and quantification **(C)**. Representative Oxidative stress measured as hydrogen peroxide concentration in homogenates of hippocampus tissue **(D)**. Proinflammatory markers *Il-6*, *Tnf-α* and *Gfap* gene expression **(E)**. GFAP protein levels **(F)** and quantification **(G)**. Mean ± Standard error of the mean (SEM) from five independent experiments performed in duplicate are represented; $^{*}p < 0.05$; $^{**}p < 0.01$; $^{***}p < 0.001$; $^{****}p < 0.0001$.

molecular changes and better cognition status. The enrichment was started at the age of 4-month-old, when cognitive deficit appear in 5xFAD mice (Girard et al., 2013), and was continued until the age of 6-month-old.

Alterations in epigenetics contribute to gene expression deregulation, resulting in the development of different pathologies in mouse models and human beings, including unhealthy aging and AD (Hook et al., 2018; Griñán-Ferré et al., 2018). In previous reports, changes in cognition and molecular pathways were found after exercise or EE in a mouse model for senescence and early-AD. Modification of those parameters related to neurodegeneration was correlated with epigenetic modifications (Cosín-Tomás et al., 2014; Griñán-Ferré et al., 2016b). There are a number of works describing epigenetic alterations induced by EE and controlling several molecular pathways such as neuroplasticity and neuroinflammation (Williamson et al., 2012; Yang et al., 2012).

Our group described epigenetic modifications in 5xFAD (Griñán-Ferré et al., 2016c) and demonstrated that behavioral, biochemical and molecular changes in this AD mice model correlated with epigenetic changes. Although many studies related to beneficial effects of EE have been described in 5xFAD mice (Hüttenrauch et al., 2016; Ziegler-Waldkirch et al., 2018), this is, to our knowledge, the first time that EE has been connected to epigenetic mechanisms intervention with beneficial effects on cognition in 5xFAD mice.

EE for 8 weeks was enough to induce better cognitive performance in 5xFAD, including an improvement in spatial and recognition memory (Griñán-Ferré et al., 2016b; Hüttenrauch et al., 2016), in concordance to other works in different transgenic strain and with exercise (García-Mesa et al., 2016), that is other enrichment paradigm. In fact, the action of EE depends on the type of EE, experimental design with different duration of exposure, the severity of AD mouse model phenotype, age, and gender, among others. Besides, behavioral task analysis showed more active and less anxiety-like behavior gated to 5xFAD mice under EE.

As mentioned above, 5-mC is a stable epigenetic mark that alters the neuronal function to promote changes in gene expression through environment interactions such as behavior, stress, hormones, and EE that can participate in

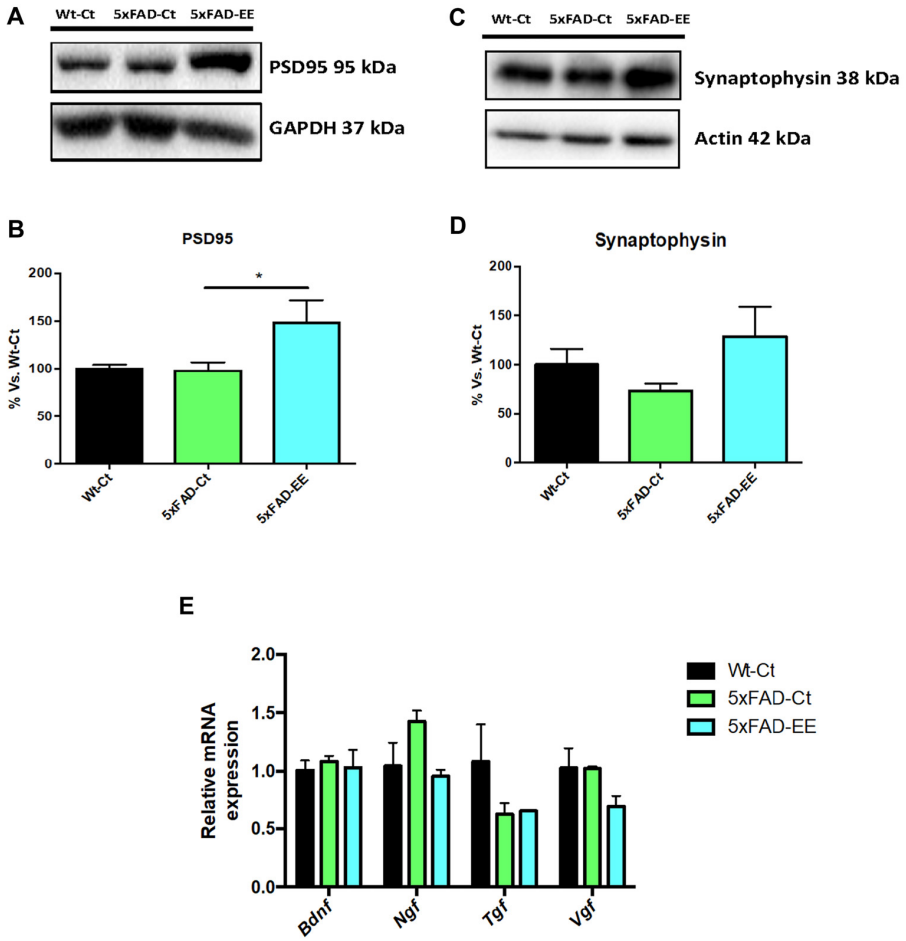

FIGURE 7 | Neuroplasticity markers in female mice at 4-month-old Wt-Ct and 5xFAD-Ct mice groups and 5xFAD mice group after 8 weeks with EE. Representative Western blot for postsynaptic density 95 (PSD95) protein levels protein levels **(A)** and quantification **(B)**, synaptophysin (SYN; **C**) and quantification **(D)**. Values in bar graphs are adjusted to 100% for protein levels of control (Wt-Ct). Representative gene expression for *Brain-derived neurotrophic factor (BDNF), Nerve growth factor (NGF), Tgf* and *Vgf* **(E)**. Gene expression levels were determined by real-time PCR. Values are mean ± Standard error of the mean (SEM); $^*p < 0.05$.

memory function (Keil and Lein, 2016). DNA methylation and hydroxymethylation constitute epigenetic markers that can alter neuronal function influencing gene expression. Accordingly, cognitive and behavioral changes after EE in Wt and 5xFAD were reflected in epigenetic marks 5-mC and 5-hmC changes.

Recent data suggest an aberrant 5-mC formation is linked to neurodegeneration and apoptotic neuronal death (Chestnut et al., 2011; Hernandez et al., 2011). Likewise, altered expression levels and pathological activity DNMT have been observed in aging and neurodegenerative disorders (Johnson et al., 2012). After EE, 5-mC levels were reduced in 5xFAD, but, conversely, *Dnmt3a/b* gene expressions were increased, whereas *Dnmt1* gene expression was not modified. In fact, DNA methylation changes by DNMT activity are necessary for memory formation and storage (Day and Sweatt, 2010). For instance, it was reported that elimination of DNMT1 in mice brain causes a hypomethylation in cortical and hippocampal neurons, resulting in the neurodegenerative process with deficits learning and memory (Hutnick et al., 2009). In addition, Oliveira et al. (2012) found in aged mice that increased gene expression of *Dnmt3a2* was associated with cognitive decline prevention, accordingly with results obtained in 5xFAD-EE.

5-hmC, an oxidative product of DNA demethylation is another epigenetic mark catalyzed by the TET family that exists at high levels within the brain (Irier et al., 2014). In our study, EE exposure increased 5-hmC levels and *Tet2* gene expression in 5xFAD mice. Indeed, these results are consistent with those reported recently by Irier et al. (2014) in mice. Besides, it has been described that loss of *TET2* induces DNA hypermethylation in a similar way to oxidative stress, reducing global 5-hmC (Zhang et al., 2017). In contrast, no changes in *Tet1* expression were found after EE, although in other experimental study were described (Irier et al., 2014); different timing and duration of the EE and also for the strain and age can explain differences.

Histone acetylation is one of the epigenetic modifications, which play a vital role in the etiopathogenesis of AD (Lu et al.,

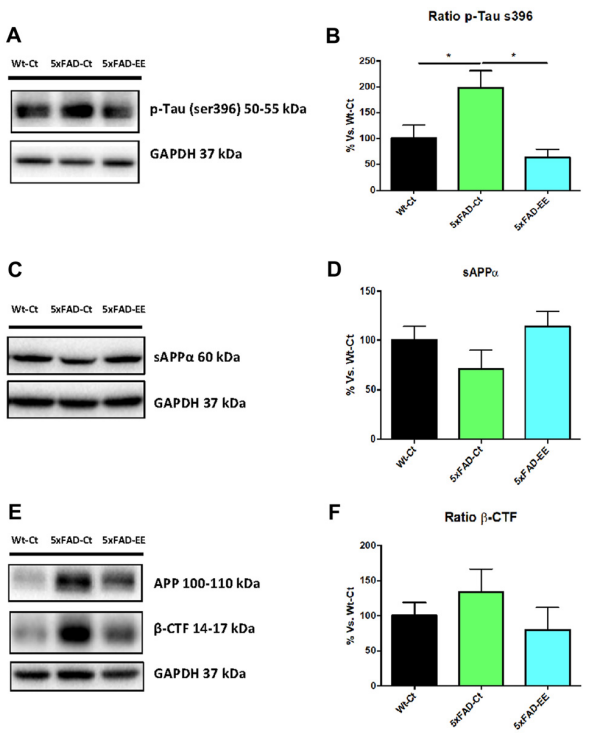

FIGURE 8 | Alzheimer's disease markers in female mice at 4-month-old Wt-Ct and 5xFAD-Ct mice groups and 5xFAD mice group after 8 weeks with EE. Representative Western blot for pTau ser396 protein levels **(A)** and quantifications **(B)**, protein levels of sAPPα and β-CTF **(C,E)** and quantifications **(D,F)**. Values in bar graphs are adjusted to 100% for protein levels of control Wild-Type (Wt-Ct); $^{*}p < 0.05$.

2015). Overall, HDAC inhibition increases histone acetylation H3/H4 and rescued learning and memory deficits in AD animal models, showing neuroprotective effects (Lu et al., 2015; Neidl et al., 2016). Here, we indeed reported a significant increase in H3 and H4 acetylation levels after EE in 5xFAD. Besides, the participation of histone acetylases and HDACs in AD is controversial. For example, it has been reported that HDAC2, but not HDAC1 or HDAC3, is up-regulated in AD mouse models (Broide et al., 2007), but other reported differential changes in HDAC family levels, for example, the SAMP8 mouse model (Griñán-Ferré et al., 2016b). In contrast with this last report, an increase of *Hdac1* expression in the 5xFAD-EE whereas no changes in *Hdac2* expression were found.

Thus, it can be hypothesized that epigenetic changes induced by EE should lead to a relaxed chromatin structure, allowing gene expression increase and protein synthesis essential for learning and memory (Kim and Kaang, 2017). These results suggest the role of EE in epigenetic modifications restoring learning and memory in an AD mouse model.

Besides cognitive and behavioral improvement induced by EE in 5xFAD mice, molecular and biochemical pathways related to AD pathogenic mechanism had been studied. Oxidative stress is accepted to have a key role in Aβ-induced neurotoxicity (Cheignon et al., 2018). The oxidative stress occurs when the balance between antioxidant enzymes and ROS are disrupted (Birben et al., 2012; Poljsak et al., 2013). Up-regulation of antioxidant enzymes might confer protection against oxidative insults (Chen et al., 2011). Specifically, changes in SOD1 expression and HMOX1 (Sugawara et al., 2002; Guo et al., 2010) were found, in response to a wide variety of oxidative stress stimuli. EE reduced H_2O_2 levels indicating oxidative stress diminution, and accompanied by lower SOD1 protein levels. Moreover, we observed a reduction in gene expression of the antioxidant enzymes *Hmox1* and *Aox1*.

Likewise, there is evidence that neuroinflammation plays a role in aging and the pathophysiology of AD (Liu et al., 2015; Raj et al., 2017). Significant differences in proinflammatory chemokines secreted by astrocytes have been proved between AD patients and normal aged people (Liu et al., 2015). A reduction in gene expression for *Il-6* and *Tnf-α* in 5xFAD-EE mice suggested a reduction in the inflammatory process in 5xFAD (Gurel et al., 2018). The lower inflammation after EE was also reinforced by a diminution in astroglial activation after EE demonstrated a significant decrease in *Gfap* gene expression and protein levels (Brahmachari et al., 2006). Evidence concerning food containing natural antioxidant and anti-inflammatory compounds open the avenue to potentiate a lifestyle based on diet, exercise and a healthy environment to underlying neurophysiological mechanisms in AD or neurodegenerative diseases, as a non-pharmacological strategy to face the cognitive impairment (Businaro et al., 2018; Francis and Stevenson, 2018).

As aforementioned, EE induced experience-dependent synaptic plasticity (Nithianantharajah et al., 2004), increased synapse and spine density (Jung and Herms, 2014) and memory consolidation through increased expression of synaptic proteins (Hu et al., 2010) and growth factors (Ickes et al., 2000). Accordingly, several reports in which an EE intervention showed improvements on hippocampal-dependent task (Jurgens and Johnson, 2012; Stein et al., 2016; Cortese et al., 2018) increased levels of both proteins PSD95 (postsynaptic) and SYN (presynaptic) in the hippocampus were found in 5xFAD-EE, indicating a neuroprotective role of EE intervention.

In our study, we were unable to determine any effect on gene expression of neurotrophic factors (NTFs) such as *Bdnf, Ngf, Tgf* and *Vgf* in 5xFAD with EE. Previous reports highlighted the influence of EE on molecular mediators of synaptic plasticity in AD mice models is inconsistent. While several studies found an increase in NTFs (Tong et al., 2001; Angelucci et al., 2009; Jha et al., 2016), others did not found differences in some of them (Hüttenrauch et al., 2016). There are several NTFs that are involved in neuroprotective effects of EE, and it is probable that experimental conditions such as type and duration of EE modifies growing factors. By last, about AD hallmarks, EE diminished p-Tau (Ser396) in the hippocampus of the 5xFAD.

In conclusion, our results confirm previous data were supporting the beneficial effects of EE in AD mouse models. Concretely, improvements in cognitive performance associated with changes in oxidative stress, inflammation, synaptic plasticity, and AD hallmarks were found in 5xFAD mice. Remarkably, those changes paralleled with epigenetic mechanisms in 5xFAD, as described previously in the non-transgenic model of cognitive impairment and senescence

(Griñán-Ferré et al., 2016a,b), disentangling a link between epigenetics, lifestyle and neurodegeneration.

It has been proposed that epigenetic mechanisms can modify the onset, latency period and progression of neurodegenerative diseases and this work give support to this claim that has emerged in the last decade (Tsankova et al., 2007). Strengthening the mechanistic understanding of neurodegeneration and its correlation with epigenetics, as is demonstrated in the 5xFAD model, will likely provide new insights pointing out the importance for the healthy lifestyle in the individuals at risk for AD. Results obtained in animal models must be validated in human beings but, noteworthy confirmation for epigenetic alterations in AD patients (Narayan and Dragunow, 2017) and the goodness of an improved lifestyle (diet, exercise, etc; Chouliaras et al., 2010; Ricci et al., 2018) is day by day more robust, evidencing the interrelation between neurodegeneration and epigenetics.

AUTHOR CONTRIBUTIONS

CG-F, EO and DP-I carried out the experimental intervention. CG-F and EO performed behavior experiments. RC and DP-I performed Western blot analysis. CG-F and VI performed the RT-PCR experiments. CG-F, DO-S and CS analyzed the data and drafted the manuscript. MP designed the experiments and supervised the study. All authors read and approved the final manuscript.

FUNDING

This study was supported by Ministerio de Economía y Competitividad of Spain SAF2016-33307. Authors belong to 2017SGR106 (Agencia de Gestió d'Ajuts Universitaris i de Recerca, AGAUR, Catalonia).

ACKNOWLEDGMENTS

We thank Maggie Brunner, M.A., for revising the language and style of the manuscript.

SUPPLEMENTARY MATERIAL

The Supplementary Material for this article can be found online at: https://www.frontiersin.org/articles/10.3389/fncel.2018.00224/full#supplementary-material

REFERENCES

Agostinho, P., Cunha, R. A., and Oliveira, C. (2010). Neuroinflammation, oxidative stress and the pathogenesis of Alzheimer's disease. *Curr. Pharm. Des.* 16, 2766–2778. doi: 10.2174/138161210793176572

Anderson, K. W., Mast, N., Pikuleva, I. A., and Turko, I. V. (2015). Histone H3 Ser57 and Thr58 phosphorylation in the brain of 5XFAD mice. *FEBS Open Bio.* 5, 550–556. doi: 10.1016/j.fob.2015.06.009

Angelucci, F., De Bartolo, P., Gelfo, F., Foti, F., Cutuli, D., Bossù, P., et al. (2009). Increased concentrations of nerve growth factor and brain-derived neurotrophic factor in the rat cerebellum after exposure to environmental enrichment. *Cerebellum* 8, 499–506. doi: 10.1007/s12311-009-0129-1

Bahari-Javan, S., Maddalena, A., Kerimoglu, C., Wittnam, J., Held, T., Bähr, M., et al. (2012). HDAC1 regulates fear extinction in mice. *J. Neurosci.* 32, 5062–5073. doi: 10.1523/JNEUROSCI.0079-12.2012

Barak, B., Shvarts-Serebro, I., Modai, S., Gilam, A., Okun, E., Michaelson, D. M., et al. (2013). Opposing actions of environmental enrichment and Alzheimer's disease on the expression of hippocampal microRNAs in mouse models. *Transl. Psychiatry* 3:e304. doi: 10.1038/tp.2013.77

Barrès, R., Yan, J., Egan, B., Treebak, J. T., Rasmussen, M., Fritz, T., et al. (2012). Acute exercise remodels promoter methylation in human skeletal muscle. *Cell Metab.* 15, 405–411. doi: 10.1016/j.cmet.2012.01.001

Birben, E., Sahiner, U. M., Sackesen, C., Erzurum, S., and Kalayci, O. (2012). Oxidative stress and antioxidant defense. *World Allergy Organ. J.* 5, 9–19. doi: 10.1097/WOX.0b013e3182439613

Bloom, G. S. (2014). Amyloid-β and tau: the trigger and bullet in Alzheimer disease pathogenesis. *JAMA Neurol.* 71, 505–508. doi: 10.1001/jamaneurol.2013.5847

Brahmachari, S., Fung, Y. K., and Pahan, K. (2006). Induction of glial fibrillary acidic protein expression in astrocytes by nitric oxide. *J. Neurosci.* 26, 4930–4939. doi: 10.1523/JNEUROSCI.5480-05.2006

Broide, R. S., Redwine, J. M., Aftahi, N., Young, W., Bloom, F. E., and Winrow, C. J. (2007). Distribution of histone deacetylases 1–11 in the rat brain. *J. Mol. Neurosci.* 31, 47–58. doi: 10.1007/bf02686117

Businaro, R., Corsi, M., Asprino, R., Di Lorenzo, C., Laskin, D., Corbo, R. M., et al. (2018). Modulation of inflammation as a way of delaying Alzheimer's disease progression: the diet's role. *Curr. Alzheimer Res.* 15, 363–380. doi: 10.2174/1567205014666170829100100

Cechetti, F., Worm, P. V., Lovatel, G., Moysés, F., Siqueira, I. R., and Netto, C. A. (2012). Environmetal enrichment prevents behavioural deficits and oxidative stress caused by chronic cerebral hyperfusion in the rat. *Life Sci.* 91, 29–36. doi: 10.1016/j.lfs.2012.05.013

Cheignon, C., Tomas, M., Bonnefont-Rousselot, D., Faller, P., Hureau, C., and Collin, F. (2018). Oxidative stress and the amyloid beta peptide in Alzheimer's disease. *Redox Biol.* 14, 450–464. doi: 10.1016/j.redox.2017.10.014

Chen, H., Yoshioka, H., Kim, G. S., Jung, J. E., Okami, N., Sakata, H., et al. (2011). Oxidative stress in ischemic brain damage: mechanisms of cell death and potential molecular targets for neuroprotection. *Antioxid. Redox Signal.* 14, 1505–1517. doi: 10.1089/ars.2010.3576

Chestnut, B. A., Chang, Q., Price, A., Lesuisse, C., Wong, M., and Martin, L. J. (2011). Epigenetic regulation of motor neuron cell death through DNA methylation. *J. Neurosci.* 31, 16619–16636. doi: 10.1523/JNEUROSCI.1639-11.2011

Chouliaras, L., Rutten, B. P., Kenis, G., Peerbooms, O., Visser, P. J., Verhey, F., et al. (2010). Epigenetic regulation in the pathophysiology of Alzheimer's disease. *Prog. Neurobiol.* 90, 498–510. doi: 10.1016/j.pneurobio.2010.01.002

Cortese, G. P., Olin, A., O'Riordan, K., Hullinger, R., and Burger, C. (2018). Environmental enrichment improves hippocampal function in aged rats by enchancing learning and memory, LTP, and mGluR5-Homer1c activity. *Neurobiol. Aging* 63, 1–11. doi: 10.1016/j.neurobiolaging.2017.11.004

Cosín-Tomás, M., Alvarez-López, M. J., Sanchez-Roige, S., Lalanza, J. F., Bayod, S., Sanfeliu, C., et al. (2014). Epigenetic alterations in hippocampus of SAMP8 senescent mice and modulation by voluntary physical exercise. *Front. Aging Neurosci.* 6:51. doi: 10.3389/fnagi.2014.00051

Day, J. J., and Sweatt, J. D. (2010). DNA methylation and memory formation. *Nat. Neurosci.* 13, 1319–1323. doi: 10.1038/nn.2666

Delgado-Morales, R., Agís-Balboa, R. C., Esteller, M., and Berdasco, M. (2017). Epigenetic mechanisms during aging and neurogenesis as novel therapeutic avenues in human brain disorders. *Clin. Epigenetics* 9:67. doi: 10.1186/s13148-017-0365-z

Devi, L., and Ohno, M. (2010). Genetic reductions of β-site amyloid precursor protein-cleaving enzyme 1 and amyloid-β ameliorate impairment of conditioned taste aversion memory in 5XFAD Alzheimer's disease model mice. *Eur. J. Neurosci.* 31, 110–118. doi: 10.1111/j.1460-9568.2009.07031.x

Devi, L., and Ohno, M. (2012). Mitochondrial dysfunction and accumulation of the β-secretase-cleaved C-terminal fragment of APP in Alzheimer's disease transgenic mice. *Neurobiol. Dis.* 45, 417–424. doi: 10.1016/j.nbd.2011.09.001

Duncan, E. J., Gluckman, P. D., and Dearden, P. K. (2014). Epigenetics, plasticity, and evolution: how do we link epigenetic change to phenotype? *J. Exp. Zool. B Mol. Dev. Evol.* 322, 208–220. doi: 10.1002/jez.b.22571

Eckert, M. J., and Abraham, W. C. (2010). Physiological effects of enriched environment exposure and LTP induction in the hippocampus *in vivo* do not transfer faithfully to *in vitro* slices. *Learn. Mem.* 17, 480–484. doi: 10.1101/lm.1822610

Ennaceur, A., and Delacour, J. (1988). A new one-trial test for neurobiological studies of memory in rats. 1: behavioral data. *Behav. Brain Res.* 31, 47–59. doi: 10.1016/0166-4328(88)90157-x

Ennaceur, A., and Meliani, K. (1992). A new one-trial test for neurobiological studies of memory in rats. III. Spatial vs. non-spatial working memory. *Behav. Brain Res.* 51, 83–92. doi: 10.1016/s0166-4328(05)80315-8

Fischer, A., Sananbenesi, F., Wang, X., Dobbin, M., and Tsai, L.-H. (2007). Recovery of learning and memory is associated with chromatin remodelling. *Nature* 447, 178–182. doi: 10.1038/nature05772

Fragkouli, A., Hearn, C., Errington, M., Cooke, S., Grigoriou, M., Bliss, T., et al. (2005). Loss of forebrain cholinergic neurons and impairment in spatial learning and memory in LHX7-deficient mice. *Eur. J. Neurosci.* 21, 2923–2938. doi: 10.1111/j.1460-9568.2005.04141.x

Francis, H. M., and Stevenson, R. J. (2018). Potential for diet to prevent and remediate cognitive deficits in neurological disorders. *Nutr. Rev.* 76, 204–217. doi: 10.1093/nutrit/nux073

García-Mesa, Y., Colie, S., Corpas, R., Cristòfol, R., Comellas, F., Nebreda, A. R., et al. (2016). Oxidative stress is a central target for physical exercise neuroprotection against pathological brain aging. *J. Gerontol. A Biol. Sci. Med. Sci.* 71, 40–49. doi: 10.1093/gerona/glv005

Girard, S. D., Baranger, K., Gauthier, C., Jacquet, M., Bernard, A., Escoffier, G., et al. (2013). Evidence for early cognitive impairment related to frontal cortex in the 5XFAD mouse model of Alzheimer's disease. *J. Alzheimers Dis.* 33, 781–796. doi: 10.3233/JAD-2012-120982

Gomez-Pinilla, F., Zhuang, Y., Feng, J., Ying, Z., and Fan, G. (2011). Exercise impacts brain-derived neurotrophic factor plasticity by engaging mechanisms of epigenetic regulation. *Eur. J. Neurosci.* 33, 383–390. doi: 10.1111/j.1460-9568.2010.07508.x

Griñán-Ferré, C., Corpas, R., Puigoriol-Illamola, D., Palomera-Ávalos, V., Sanfeliu, C., and Pallàs, M. (2018). Understanding epigenetics in the neurodegeneration of Alzheimer's disease: SAMP8 mouse model. *J. Alzheimers Dis.* 62, 943–963. doi: 10.3233/JAD-170664

Griñán-Ferré, C., Pérez-Cáceres, D., Gutiérrez-Zetina, S. M., Camins, A., Palomera-Avalos, V., Ortuño-Sahagún, D., et al. (2016a). Environmental enrichment improves behavior, cognition, and brain functional markers in young senescence-accelerated prone mice (SAMP8). *Mol. Neurobiol.* 53, 2435–2450. doi: 10.1007/s12035-015-9210-6

Griñán-Ferré, C., Puigoriol-Illamola, D., Palomera-Ávalos, V., Pérez-Cáceres, D., Companys-Alemany, J., Camins, A., et al. (2016b). Environmental enrichment modified epigenetic mechanisms in SAMP8 mouse hippocampus by reducing oxidative stress and inflammaging and achieving neuroprotection. *Front. Aging Neurosci.* 8:241. doi: 10.3389/fnagi.2016.00241

Griñán-Ferré, C., Sarroca, S., Ivanova, A., Camins, A., Puigoriol-Illamola, D., Aguado, F., et al. (2016c). Epigenetic mechanisms underlying cognitive impairment and Alzheimer disease hallmarks in 5xFAD mice. *Aging* 8, 664–684. doi: 10.18632/aging.100906

Guo, Y., Duan, W., Li, Z., Huang, J., Yin, Y., Zhang, K., et al. (2010). Decreased GLT-1 and increased SOD1 and HO-1 expression in astrocytes contribute to lumbar spinal cord vulnerability of SOD1–G93A transgenic mice. *FEBS Lett.* 584, 1615–1622. doi: 10.1016/j.febslet.2010.03.025

Gurel, B., Cansev, M., Sevinc, C., Kelestemur, S., Ocalan, B., Cakir, A., et al. (2018). Early stage alterations in CA1 extracellular region proteins indicate dysregulation of IL6 and iron homeostasis in the 5XFAD Alzheimer's disease mouse model. *J. Alzheimers Dis.* 61, 1399–1410. doi: 10.3233/JAD-170329

Hernandez, D. G., Nalls, M. A., Gibbs, J. R., Arepalli, S., van der Brug, M., Chong, S., et al. (2011). Distinct DNA methylation changes highly correlated with chronological age in the human brain. *Hum. Mol. Genet.* 20, 1164–1172. doi: 10.1093/hmg/ddq561

Herring, A., Blome, M., Ambrée, O., Sachser, N., Paulus, W., and Keyvani, K. (2010). Reduction of cerebral oxidative stress following environmental enrichment in mice with Alzheimer-like pathology. *Brain Pathol.* 20, 166–175. doi: 10.1111/j.1750-3639.2008.00257.x

Hook, M., Roy, S., Williams, E. G., Bou Sleiman, M., Mozhui, K., Nelson, J. F., et al. (2018). Genetic cartography of longevity in humans and mice: current landscape and horizons. *Biochim. Biophys. Acta* doi: 10.1016/j.bbadis.2018.01.026 [Epub ahead of print].

Hu, Y.-S., Xu, P., Pigino, G., Brady, S. T., Larson, J., and Lazarov, O. (2010). Complex environment experience rescues impaired neurogenesis, enhances synaptic plasticity, and attenuates neuropathology in familial Alzheimer's disease-linked APPswe/PS1ΔE9 mice. *FASEB J.* 24, 1667–1681. doi: 10.1096/fj.09-136945

Hutnick, L. K., Golshani, P., Namihira, M., Xue, Z., Matynia, A., Yang, X. W., et al. (2009). DNA hypomethylation restricted to the murine forebrain induces cortical degeneration and impairs postnatal neuronal maturation. *Hum. Mol. Genet.* 18, 2875–2888. doi: 10.1093/hmg/ddp222

Hüttenrauch, M., Brauß, A., Kurdakova, A., Borgers, H., Klinker, F., Liebetanz, D., et al. (2016). Physical activity delays hippocampal neurodegeneration and rescues memory deficits in an Alzheimer disease mouse model. *Transl. Psychiatry* 6:e800. doi: 10.1038/tp.2016.65

Ickes, B. R., Pham, T. M., Sanders, L. A., Albeck, D. S., Mohammed, A. H., and Granholm, A. C. (2000). Long-term environmental enrichment leads to regional increases in neurotrophin levels in rat brain. *Exp. Neurol.* 164, 45–52. doi: 10.1006/exnr.2000.7415

Irier, H., Street, R. C., Dave, R., Lin, L., Cai, C., Davis, T. H., et al. (2014). Environmental enrichment modulates 5-hydroxymethylcytosine dynamics in hippocampus. *Genomics* 104, 376–382. doi: 10.1016/j.ygeno.2014.08.019

Irvine, G. I., Logan, B., Eckert, M., and Abraham, W. C. (2006). Enriched environment exposure regulates excitability, synaptic transmission, and LTP in the dentate gyrus of freely moving rats. *Hippocampus* 16, 149–160. doi: 10.1002/hipo.20142

Jha, S., Dong, B. E., Xue, Y., Delotterie, D. F., Vail, M. G., and Sakata, K. (2016). Antidepressive and BDNF effects of enriched environment treatment across ages in mice lacking BDNF expression through promoter IV. *Transl. Psychiatry* 6:e896. doi: 10.1038/tp.2016.160

Johnson, A. A., Akman, K., Calimport, S. R. G., Wuttke, D., Stolzing, A., and de Magalhães, J. P. (2012). The role of DNA methylation in aging, rejuvenation, and age-related disease. *Rejuvenation Res.* 15, 483–494. doi: 10.1089/rej.2012.1324

Jung, C. K., and Herms, J. (2014). Structural dynamics of dendritic spines are influenced by an environmental enrichment: an *in vivo* imaging study. *Cereb. Cortex* 24, 377–384. doi: 10.1093/cercor/bhs317

Jurgens, H. A., and Johnson, R. W. (2012). Environmental enrichment attenuates hippocampal neuroinflammation and improves cognitive function during influenza infection. *Brain Behav. Immun.* 26, 1006–1016. doi: 10.1016/j.bbi.2012.05.015

Keil, K. P., and Lein, P. J. (2016). DNA methylation: a mechanism linking environmental chemical exposures to risk of autism spectrum disorders? *Environ. Epigenet.* 2:dvv012. doi: 10.1093/eep/dvv012

Kim, S., and Kaang, B.-K. (2017). Epigenetic regulation and chromatin remodeling in learning and memory. *Exp. Mol. Med.* 49:e281. doi: 10.1038/emm.2016.140

Landel, V., Baranger, K., Virard, I., Loriod, B., Khrestchatisky, M., Rivera, S., et al. (2014). Temporal gene profiling of the 5xFAD transgenic mouse model highlights the importance of microglial activation in Alzheimer's disease. *Mol. Neurodegener.* 9:33. doi: 10.1186/1750-1326-9-33

Lau, P., Bossers, K., Janky, R., Salta, E., Frigerio, C. S., Barbash, S., et al. (2013). Alteration of the microRNA network during the progression of Alzheimer's disease. *EMBO Mol. Med.* 5, 1613–1634. doi: 10.1002/emmm.201201974

Liu, B., Le, K. X., Park, M. A., Wang, S., Belanger, A. P., Dubey, S., et al. (2015). *In vivo* detection of age- and disease-related increases in neuroinflammation by ^{18}F-GE180 TSPO MicroPET imaging in wild-type and Alzheimer's transgenic mice. *J. Neurosci.* 35, 15716–15730. doi: 10.1523/JNEUROSCI.0996-15.2015

Long, J. M., and Lahiri, D. K. (2011). MicroRNA-101 downregulates Alzheimer's amyloid-β precursor protein levels in human cell cultures and is differentially expressed. *Biochem. Biophys. Res. Commun.* 404, 889–895. doi: 10.1016/j.bbrc.2010.12.053

Long, J. M., Ray, B., and Lahiri, D. K. (2012). MicroRNA-153 physiologically inhibits expression of amyloid-β precursor protein in cultured human fetal brain cells and is dysregulated in a subset of Alzheimer disease patients. *J. Biol. Chem.* 287, 31298–31310. doi: 10.1074/jbc.M112.366336

Long, J. M., Ray, B., and Lahiri, D. K. (2014). MicroRNA-339–5p down-regulates protein expression of β-site amyloid precursor protein-cleaving enzyme 1 (BACE1) in human primary brain cultures and is reduced in brain tissue specimens of Alzheimer disease subjects. *J. Biol. Chem.* 289, 5184–5198. doi: 10.1074/jbc.M113.518241

López-Otín, C., Blasco, M. A., Partridge, L., Serrano, M., and Kroemer, G. (2013). The hallmarks of aging. *Cell* 153, 1194–1217. doi: 10.1016/j.cell.2013.05.039

Lu, X., Wang, L., Yu, C., Yu, D., and Yu, G. (2015). Histone acetylation modifiers in the pathogenesis of Alzheimer's disease. *Front. Cell. Neurosci.* 9:226. doi: 10.3389/fncel.2015.00226

Lunnon, K., Smith, R., Hannon, E., De Jager, P. L., Srivastava, G., Volta, M., et al. (2014). Methylomic profiling implicates cortical deregulation of ANK1 in Alzheimer's disease. *Nat. Neurosci.* 17, 1164–1170. doi: 10.1038/nn.3782

Madrigano, J., Baccarelli, A., Mittleman, M. A., Wright, R. O., Sparrow, D., Vokonas, P. S., et al. (2011). Prolonged exposure to particulate pollution, genes associated with glutathione pathways, and DNA methylation in a cohort of older men. *Environ. Health Perspect.* 119, 977–982. doi: 10.1289/ehp.1002773

Maloney, B., and Lahiri, D. K. (2016). Epigenetics of dementia: understanding the disease as a transformation rather than a state. *Lancet Neurol.* 15, 760–774. doi: 10.1016/S1474-4422(16)00065-X

McCreary, J. K., and Metz, G. A. S. (2016). Environmental enrichment as an intervention for adverse health outcomes of prenatal stress. *Environ. Epigenet.* 2:dvw013. doi: 10.1093/eep/dvw013

McQuaid, R. J., Audet, M. C., Jacobson-Pick, S., and Anisman, H. (2013). Environmental enrichment influences brain cytokine variations elicited by social defeat in mice. *Psychoneuroendocrinology* 38, 987–996. doi: 10.1016/j.psyneuen.2012.10.003

Mora, F., Segovia, G., and del Arco, A. (2007). Aging, plasticity and environmental enrichment: structural changes and neurotransmitter dynamics in several areas of the brain. *Brain Res. Rev.* 55, 78–88. doi: 10.1016/j.brainresrev.2007.03.011

Narayan, P., and Dragunow, M. (2017). Alzheimer's disease and histone code alterations. *Adv. Exp. Med. Biol.* 978, 321–336. doi: 10.1007/978-3-319-53889-1_17

Nathianantharajah, J., and Hannan, A. J. (2006). Enriched environments, experience-dependent plasticity, and disorders of the nervous system. *Nat. Rev. Neurosci.* 7, 697–709. doi: 10.1038/nrn1970

Neidl, R., Schneider, A., Bousiges, O., Majchrzak, M., Barbelivien, A., Pereira de Vasconcelos, A., et al. (2016). Late-life environmental enrichment induces acetylation events and nuclear factor κB-dependent regulations in the hippocampus of aged rats showing improved plasticity and learning. *J. Neurosci.* 36, 4351–4361. doi: 10.1523/JNEUROSCI.3239-15.2016

Nithianantharajah, J., Levis, H., and Murphy, M. (2004). Environmental enrichment results in cortical and subcortical changes in levels of synaptophysin and PSD-95 proteins. *Neurobiol. Learn. Mem.* 81, 200–210. doi: 10.1016/j.nlm.2004.02.002

Oakley, H., Cole, S. L., Logan, S., Maus, E., Shao, P., Craft, J., et al. (2006). Intraneuronal beta-amyloid aggregates, neurodegeneration, and neuron loss in transgenic mice with five familial Alzheimer's disease mutations: potential factors in amyloid plaque formation. *J. Neurosci.* 26, 10129–10140. doi: 10.1523/JNEUROSCI.1202-06.2006

Oliveira, A. M., Hemstedt, T. J., and Bading, H. (2012). Rescue aging-associated decline in Dnmt32 expression restores cognitive abilities. *Nat. Neurosci.* 15, 1111–1113. doi: 10.1038/nn.3151

Poljsak, B., Šuput, D., and Milisav, I. (2013). Achieving the Balance between ROS and antioxidants: when to use the synthetic antioxidants. *Oxid. Med. Cell. Longev.* 2013:956792. doi: 10.1155/2013/956792

Puckett, R. E., and Lubin, F. D. (2011). Epigenetic mechanisms in experience-driven memory formation and behavior. *Epigenomics* 3, 649–664. doi: 10.2217/epi.11.86

Pusic, K. M., Pusic, A. D., and Kraig, R. P. (2016). Environmental enrichment stimulates immune cell secretion of exosomes that promote cns myeliation and may regulate inflammation. *Cell. Mol. Neurobiol.* 36, 313–325. doi: 10.1007/s10571-015-0269-4

Raj, D., Yin, Z., Breur, M., Doorduin, J., Holtman, I. R., Olah, M., et al. (2017). Increased white matter inflammation in aging- and Alzheimer's disease brain. *Front. Mol. Neurosci.* 10:206. doi: 10.3389/fnmol.2017.00206

Ricci, P., Massoni, F., Ricci, L., Onofri, E., Donato, G., and Ricci, S. (2018). Quality of life in dementia sufferers: the role of diet and exercise. *Curr. Alzheimer Res.* 15, 400–407. doi: 10.2174/1567205014666170925151614

Rosenzweig, M. R., and Bennett, E. L. (1996). Psychobiology of plasticity: effects of training and experience on brain and behavior. *Behav. Brain Res.* 78, 57–65. doi: 10.1016/0166-4328(95)00216-2

Spiegel, A. M., Sewal, A. S., and Rapp, P. R. (2014). Epigenetic contributions to cognitive aging: disentangling mindspan and lifespan. *Learn. Mem.* 21, 569–574. doi: 10.1101/lm.033506.113

Stein, L. R., O'Dell, K. A., Funatsu, M., Zorumski, C. F., and Izumi, Y. (2016). Short-term environmental enrichment enhances synaptic plasticity in hippocampal slices from aged rats. *Neuroscience* 329, 294–305. doi: 10.1016/j.neuroscience.2016.05.020

Sugawara, T., Noshita, N., Lewén, A., Gasche, Y., Ferrand-Drake, M., Morita-Fujimura, Y., et al. (2002). Overexpression of cooper/zing superoxide dismutase in transgenic rats protects vulnerable neurons against ischemic damage by blocking the mitochondrial pathway of caspase activation. *J. Neurosci.* 22, 209–217. doi: 10.1523/JNEUROSCI.22-01-00209.2002

Tong, L., Shen, H., Perreau, V. M., Balazs, R., and Cotman, C. W. (2001). Effects of exercise on Gene-expression profile in the rat hippocampus. *Neurobiol. Dis.* 8, 1046–1056. doi: 10.1006/nbdi.2001.0427

Tsankova, N., Renthal, W., Kumar, A., and Nestler, E. J. (2007). Epigenetic regulation in psychiatric disorders. *Nat. Rev. Neurosci.* 8, 355–367. doi: 10.1038/nrn2132

van Praag, H., Kempermann, G., and Gage, F. H. (2000). Neural consequences of environmental enrichment. *Nat. Rev. Neurosci.* 1, 191–198. doi: 10.1038/35044558

Vierci, G., Pannunzio, B., Bornia, N., and Rossi, F. M. (2016). H3 and H4 lysine acetylation correlates with developmental and experimentally induced adult experience-dependent plasticity in the mouse visual cortex. *J. Exp. Neurosci.* 10, 49–64. doi: 10.4137/jen.s39888

Wang, L., Guo, L., Lu, L., Sun, H., Shao, M., Beck, S. J., et al. (2016). Synaptosolmal mitochondrial dysfunction in 5xFAD mouse model of Alzheimer's disease. *PLoS One* 11:e0150441. doi: 10.1371/journal.pone.0150441

Williamson, L. L., Chao, A., and Bilbo, S. D. (2012). Environmental enrichment alters glial antigen expression and neuroimmune function in the adult rat hippocampus. *Brain Behav. Immun.* 26, 500–510. doi: 10.1016/j.bbi.2012.01.003

Yang, S., Lu, W., Zhou, D. S., and Tang, Y. (2012). Enriched environment and White matter in aging brain. *Anat. Rec.* 295, 1406–1414. doi: 10.1002/ar.22526

Yılmaz, Ş. G., Erdal, M. E., Özge, A. A., and Sungur, M. A. (2016). Can peripheral microrna expression data serve as epigenomic (upstream) biomarkers of Alzheimer's disease? *OMICS* 20, 456–461. doi: 10.1089/omi.2016.0099

Zhang, Y. W., Wang, Z., Xie, W., Cai, Y., Xia, L., Easwaran, H., et al. (2017). Acetylation enhances TET2 function in protecting against abnormal DNA methylation during oxidative stress. *Mol. Cell* 65, 323–335. doi: 10.1016/j.molcel.2016.12.013

Ziegler-Waldkirch, S., d'Errico, P., Sauer, J. F., Erny, D., Savanthrapadian, S., Loreth, D., et al. (2018). Seed-induced Aβ deposition is modulated by microglia under environmental enrichment in a mouse model of Alzheimer's disease. *EMBO J.* 37, 167–182. doi: 10.15252/embj.201797021

Conflict of Interest Statement: The authors declare that the research was conducted in the absence of any commercial or financial relationships that could be construed as a potential conflict of interest.

frontiers in Molecular Neuroscience

ORIGINAL RESEARCH
published: 06 August 2018
doi: 10.3389/fnmol.2018.00251

MicroRNA Profiling and Bioinformatics Target Analysis in Dorsal Hippocampus of Chronically Stressed Rats: Relevance to Depression Pathophysiology

*Mauricio Muñoz-Llanos[1†‡], María A. García-Pérez[1†], Xiaojiang Xu[2†], Macarena Tejos-Bravo[1], Elena A. Vidal[3,4], Tomás C. Moyano[4], Rodrigo A. Gutiérrez[4], Felipe I. Aguayo[1], Aníbal Pacheco[1], Gonzalo García-Rojo[1], Esteban Aliaga[5], Paulina S. Rojas[6], John A. Cidlowski[2] and Jenny L. Fiedler[1]**

[1] Laboratory of Neuroplasticity and Neurogenetics, Faculty of Chemical and Pharmaceutical Sciences, Department of Biochemistry and Molecular Biology, Universidad de Chile, Santiago, Chile, [2] National Institute of Environmental Health Sciences, National Institutes of Health, Department of Health and Human Services, Durham, NC, United States, [3] Centro de Genómica y Bioinformática, Facultad de Ciencias, Universidad Mayor, Santiago, Chile, [4] Millennium Institute for Integrative Biology (iBio), FONDAP Center for Genome Regulation, Departamento de Genética Molecular y Microbiología, Pontificia Universidad Católica de Chile, Santiago, Chile, [5] Department of Kinesiology, Faculty of Health Sciences, Universidad Católica del Maule, Talca, Chile, [6] Escuela de Química y Farmacia, Facultad de Medicina, Universidad Andres Bello, Santiago, Chile

OPEN ACCESS

Edited by:
Merce Pallas,
University of Barcelona, Spain

Reviewed by:
Anne Albrecht,
Leibniz Institute for Neurobiology, Germany
Boldizsar Czeh,
University of Pécs, Hungary

***Correspondence:**
Jenny L. Fiedler
jfiedler@ciq.uchile.cl

[†] These authors have contributed equally to this work.

[‡] **Present address:**
Mauricio Muñoz-Llanos,
Escuela de Química y Farmacia,
Facultad de Medicina, Universidad Andres Bello, Concepción, Chile

Received: 25 February 2018
Accepted: 03 July 2018
Published: 06 August 2018

Citation:
Muñoz-Llanos M, García-Pérez MA, Xu X, Tejos-Bravo M, Vidal EA, Moyano TC, Gutiérrez RA, Aguayo FI, Pacheco A, García-Rojo G, Aliaga E, Rojas PS, Cidlowski JA and Fiedler JL (2018) MicroRNA Profiling and Bioinformatics Target Analysis in Dorsal Hippocampus of Chronically Stressed Rats: Relevance to Depression Pathophysiology. Front. Mol. Neurosci. 11:251. doi: 10.3389/fnmol.2018.00251

Studies conducted in rodents subjected to chronic stress and some observations in humans after psychosocial stress, have allowed to establish a link between stress and the susceptibility to many complex diseases, including mood disorders. The studies in rodents have revealed that chronic exposure to stress negatively affects synaptic plasticity by triggering changes in the production of trophic factors, subunit levels of glutamate ionotropic receptors, neuron morphology, and neurogenesis in the adult hippocampus. These modifications may account for the impairment in learning and memory processes observed in chronically stressed animals. It is plausible then, that stress modifies the interplay between signal transduction cascades and gene expression regulation in the hippocampus, therefore leading to altered neuroplasticity and functioning of neural circuits. Considering that miRNAs play an important role in post-transcriptional-regulation of gene expression and participate in several hippocampus-dependent functions; we evaluated the consequences of chronic stress on the expression of miRNAs in dorsal (anterior) portion of the hippocampus, which participates in memory formation in rodents. Here, we show that male rats exposed to daily restraint stress (2.5 h/day) during 7 and 14 days display a differential profile of miRNA levels in dorsal hippocampus and remarkably, we found that some of these miRNAs belong to the miR-379-410 cluster. We confirmed a rise in miR-92a and miR-485 levels after 14 days of stress by qPCR, an effect that was not mimicked by chronic administration of corticosterone (14 days). Our *in silico* study identified the top-10 biological functions influenced by miR-92a, nine of which were shared with miR-485: Nervous system development and function, Tissue development, Behavior,

Embryonic development, Organ development, Organismal development, Organismal survival, Tissue morphology, and Organ morphology. Furthermore, our *in silico* study provided a landscape of potential miRNA-92a and miR-485 targets, along with relevant canonical pathways related to axonal guidance signaling and cAMP signaling, which may influence the functioning of several neuroplastic substrates in dorsal hippocampus. Additionally, the combined effect of miR-92a and miR-485 on transcription factors, along with histone-modifying enzymes, may have a functional relevance by producing changes in gene regulatory networks that modify the neuroplastic capacity of the adult dorsal hippocampus under stress.

Keywords: restraint stress, dorsal hippocampus, miRNA, neuroplasticity, mood disorder

INTRODUCTION

Neuroplasticity is considered a continuous process that permits short- to long-term brain remodeling in response to an experience and changing environment (McEwen and Gianaros, 2010). This process involves several mechanisms, ranging from synaptic remodeling to functional modification of synapses and neural circuitries (McEwen and Gianaros, 2010). In general, any acute threat to an individual, either physical or emotional in nature, triggers the activation of the stress system, including the sympathetic nervous system and the hypothalamic–pituitary–adrenal (HPA) axis and release of adrenal glucocorticoids, which are all responses that allow the organism to adapt (Chrousos and Harris, 1998; McEwen and Gianaros, 2010). Nonetheless, prolonged stress response may lead to a maladaptive response by favoring the onset or exacerbation of several stress-related disorders, including major depressive disorder (MDD) (Pittenger and Duman, 2008; Fernandez-Guasti et al., 2012). Depressed subjects show hippocampal volume reduction (Malykhin and Coupland, 2015) and cognitive deficits associated with altered hippocampal and prefrontal cortex functioning, along with a reduced complexity of dendritic trees; nonetheless, little is known about the mechanisms involved (Pittenger and Duman, 2008). One hypothesis considers that exposure to stressors alters neuroplasticity processes required for the maintenance and reestablishment of neuro-circuitry functioning (Pittenger and Duman, 2008).

Studies conducted in rodents under chronic stress models that recapitulate several symptoms of MDD have revealed changes in several forms of hippocampal neuroplasticity (Kim et al., 2015). Chronically stressed rodents show several cyto-architecture modifications in the hippocampus, including dendritic arbor simplification (Pinto et al., 2015) and dendritic spine loss in CA1 pyramidal neurons (Castaneda et al., 2015; Garcia-Rojo et al., 2017), changes that have been linked to reduced expression of the brain derived neurotrophic factor (BDNF) (Smith et al., 1995). Furthermore, chronic stress impairs hippocampus-dependent memory (Conrad et al., 1996), which can be associated with changes in the two forms of synaptic efficacy; i.e., long-term potentiation (LTP) and long-term depression (LTD) (Kim et al., 2015). All of these stress-induced neuroplasticity modifications in rodents can explain the impairment of learning and memory associated with hippocampal functioning (Conrad et al., 1996), which may be related to stress-related changes in gene expression.

Significant research has unveiled that microRNAs (miRNAs) mediate post-transcriptional gene silencing, playing a crucial role in brain development, synaptic plasticity, and neuropathology (Aksoy-Aksel et al., 2014). Emerging evidence recently reviewed has shown that miRNA expression can be differentially modulated by the extent of stress exposure (Hollins and Cairns, 2016). For instance, acute stress triggers variations in a higher number of miRNAs compared to subchronic stress in the prefrontal cortex of mice (Rinaldi et al., 2010). Moreover, evidences have also shown that acute stress produces the opposite effect when contrasted to chronic stress (Meerson et al., 2010). Some studies have evaluated the effect of chronic stress on the expression of miRNAs in the hippocampus. For instance, chronic restraint stress in male rats increases the expression of miR-138 (Castaneda et al., 2015). At least *in vitro*, this miRNA reduces the size of dendritic spines in cultured hippocampal neurons (Siegel et al., 2009), an effect that may be linked to the reduction in spine density observed in CA1 pyramidal neurons of chronically stressed rats (Castaneda et al., 2015). Chronic unpredictable mild stress (CUMS) triggers a rise in miR-182 levels at the hippocampus in rats and its overexpression exacerbates stress-induced depression-like behavior, a modification associated with a reduction in the levels of BDNF and cAMP responsive element binding protein 1 (CREB1) transcription factor (Li et al., 2016). Another study using microarray chip analyses and subsequent confirmation by RT-qPCR revealed that 35 days of CUMS mainly up-regulates a few miRNAs (miR-382-3p, miR-183-5p, miR-3573-5p, miR-202-3p, miR-493-3p) in male rats (Zhou et al., 2017). The miRNA target prediction and functional analysis conducted in this study revealed enrichment in numerous gene

Abbreviations: ALS, Amyotrophic Lateral Sclerosis; ARC, activity-regulated cytoskeleton-associated protein; BDNF, brain derived neurotrophic factor; CORT, corticosterone; CPEB3, the cytoplasmic polyadenylation protein; CREB1, cAMP responsive element binding protein 1; CUMS, chronic unpredictable mild stress; DG, dentate gyrus; EPH, EPHRINS; EPHS, EPHRIN receptor; GLUA2, AMPA receptor subunit 2; GRIN, glutamate ionotropic receptor NMDA type subunit 1; HDAC, histone deacetylase; KCC2, K-Cl co-transporter-2; LTP, long-term potentiation; MAPT, microtubule associated protein Tau; MDD, major depressive disorder; MEF2D, myocyte enhancer factor 2D; miRNAs, microRNAs; mTOR, mammalian target of rapamycin; NCOR1, nuclear receptor co-repressor 1; NFAT, nuclear factor of activated T-cells; PI3K, phosphatidylinositol-3-kinase; PTEN, phosphatase and tensin homolog; SEMA, semaphorin; SGK1, serum glucocorticoid dependent kinase 1; SNCA, synuclein alpha; TP53, tumor protein 53.

ontology terms and signaling related with depressive disorder (Zhou et al., 2017). However, in this study, authors used left hippocampal tissues after behavioral testing (Zhou et al., 2017) that may produce some biases in the study.

To date there is no study evaluating whether stress exposure chronicity (defined as days of stress exposure) determines a profile of miRNA expression, especially in dorsal hippocampus, an area that has a pivotal role in learning and memory in rodents (Fanselow and Dong, 2010). This portion of the hippocampus has called our attention because it is particularly sensitive to chronic stress, displaying an impairment of LTP induction (Miller et al., 2018) and reduction of dendritic spine density (Castaneda et al., 2015; Garcia-Rojo et al., 2017), reductions in NR1 and NR2A NMDA receptor subunit levels (Pacheco et al., 2017) and BDNF expression (Bravo et al., 2009); changes that altogether, indicate dorsal hippocampus dysfunction. Considering all these antecedents, we hypothesized that stress chronicity exposure determines a particular profile of miRNA expression in dorsal hippocampus that may influence several aspects of neuroplasticity in this structure.

By microarray analyses, the present study evaluates the effect of stress chronicity exposure on: physiological stress-related markers and miRNA expression profile in rat dorsal hippocampus, and by gene prediction and functional annotation analysis, we propose how these miRNAs may influence neuroplasticity mechanisms in the hippocampus.

MATERIALS AND METHODS

Animals

Adult male Sprague-Dawley rats maintained at the Faculty of Chemical and Pharmaceutical Sciences, Universidad de Chile, were used in this study. Efforts were made to reduce both the number of animals used and their suffering. The rats were handled in compliance with the National Institutes of Health Guide for Care and Use of Laboratory Animals (NIH Publication, eighth Edition, 2011) under an experimental protocol approved by the Ethical Committee of the Faculty of Chemical and Pharmaceutical Sciences, Universidad de Chile (CBE2011-7-4), and the Science and Technology National Commission (CONICYT). Two-month-old Sprague Dawley rats (320–350 g) were given free access to water and pelleted food and were maintained at 22°C with humidity of 55% and photoperiod cycle of 12 h (lights on from 7:00 am to 7:00 pm).

Chronic Stress Procedure and Tissue Collection

Prior to the experimental procedures, rats were handled once per day for a 1-week period, during the light phase of the photoperiod cycle. In the case of the stress experimental group, the rats were housed in a group of three to four rats and maintained in the experimental room. The stress procedure was conducted between 9:00 am and 12:00, as previously reported (Pacheco et al., 2017). In brief, the rats were introduced in transparent acrylic tubes (25 cm × 8 cm) during 2.5 h during 7 days (n = 9) or 14 days (n = 17). During the restraint, animals were placed in a cage in groups of three to four rats and the fecal pellet output during the stress session was evaluated. After this procedure, the stressed group of animals was placed in the home cage with new bedding. On the other hand, and considering that animal isolation may trigger a stress response, control animals (n = 16) were kept in the groups of three to four rats in the animal room located away from the experimental room. In order to determine the fecal output in control group, the bedding was changed each morning and after 2.5 h, the cage was inspected for fecal output quantification every day during 14 consecutive days. Hence, the estimation of fecal output corresponds to the mean value for a control group.

Rats were decapitated rapidly 24 h after the last stress exposure (between 9:00 am and 12:00 am) and trunk blood was collected for corticosterone (CORT) determination in serum, as previously described (Pacheco et al., 2017) (**Figure 1**). The dorsal hippocampi relative to bregma −3.10 to −4.44 mm coordinates (Paxinos, 1982) were rapidly dissected at 4°C and frozen under liquid N_2 and kept at −80°C until processing for RNA isolation and protein extract. Adrenal glands were rapidly dissected and weighed (**Figure 1**). We conducted two experimental series groups in which the first series was used for the microarrays, and the second one to: (i) validate the miRNAs, (ii) quantify some mRNAs by qPCR, and (iii) quantify protein levels by western blot analysis.

Corticosterone Administration

Hormone administration was conducted as previously described (Ulloa et al., 2010). In brief, rats were injected s.c. once per day with a 30 mg/kg/day dose of CORT (Sigma-Aldrich, St. Louis, MO, United States) suspended in propylene glycol (CORT group, n = 5) every day for 14 days and control animals (n = 5) were injected with a similar volume of vehicle. Rats were decapitated 24 h after the last CORT administration and a blood sample was collected for hormone determination as we have previously described (Pacheco et al., 2017).

RNA Isolation

Purified RNAs from dorsal hippocampi of the rat were isolated as we have previously described (Castaneda et al., 2015) by using the RNeasy Mini Kit ([1]QIAGEN, Hilden, Germany), that allows the separation of RNAs according to their size (RNAs < 200 nt and >200 nt). RNA concentration and purity were determined at OD260/280 and samples with an absorbance ratio between 1.8 and 2.0 were chosen. RNA integrity was evaluated by nondenaturing agarose gel electrophoresis.

Chip-Based miRNA Expression Analysis and Target Genes Network Analysis

Analysis of miRNA expression was conducted using Affymetrix GeneChip™ Version 3 miRNA arrays (680 mature rat and 486 rat pre-miRNA probe sets), following the Affymetrix hybridization protocols. Purified RNAs (<200 nt) were labeled using the Affymetrix FlashTag™ Biotin HSR kit, according to the manufacturer's protocol. Each sample was then

[1]https://www.qiagen.com

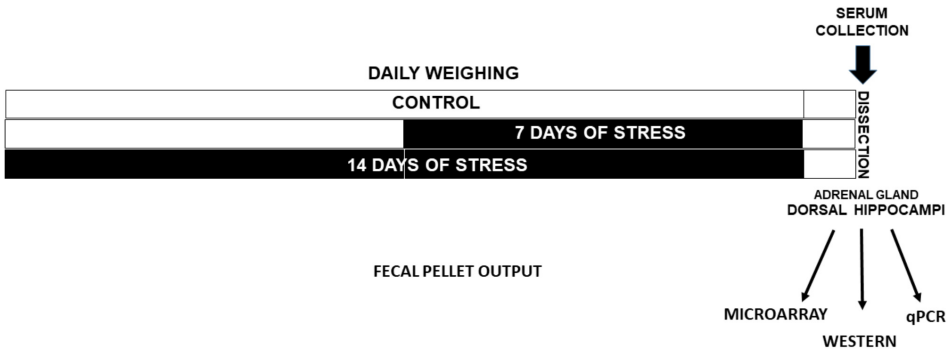

FIGURE 1 | Experimental design. Adult male rats were weighed every day in the morning. One group was stressed during 14 days (Stress-14d) and after 7 days other was stressed during 7 days (Stress-7d). Fecal output during the restraint stress procedure (2.5 h/day) was registered. Twenty four hours after the last treatment, animals were decapitated and a blood sample was taken to determine serum corticosterone levels. Adrenal glands were removed and weighed, and the dorsal hippocampi were dissected and rapidly frozen in liquid N_2.

hybridized under standardized conditions (16 h at 48°C) in a hybridization oven (Affymetrix) and array slides were stained with streptavidin/phycoerythrin and washed according to the manufacturer's protocol. Finally, arrays were scanned using the Affymetrix GCS 3000 7G and GeneChip® Operating Software (AGCC; Version 3.2). The microarray data are available in the Gene Expression Omnibus repository at the National Center for Biotechnology Information with the accession number GSE117046.[2]

To further analyze the microarray datasets, two tools were utilized: (1) Differential Expression Analysis using LIMMA-Bioconductor with R software[3] and (2) the Analysis in Partek® Genomics Suite™ (Partek, Inc., St. Louis, MO, United States). For both tools, a single log scale normalized expression measure was obtained for each probe set after background correction and normalization between samples. In order to evaluate the quality of the microarray data and to identify any unusual data in the array slides, several plots (Box plots, density plots, MA plots) were generated for both raw and normalized data. For the method based in R software, the statistical significance *P*-value of the log ratio for each probe was determined by a modification of the standard *t*-test by using an empirical Bayesian approach. For Partek, ANOVA was used to identify differentially expressed probes. Probes that had $P < 0.05$ were considered to be differentially expressed between experimental groups and controls. Among the significant probes, only rat miRNA probes were kept. To further refine the selection of significant genes, common significant genes found with the two biostatistical tools were used for downstream analysis. Heat maps were generated using BioConductor package HeatPlus. Dendrograms of samples (columns) and genes (row) were generated by hierarchical clustering. Color scale was from threefold lower (log2-fold = −1.585) than the mean (blue) to threefold higher (log2-fold = 1.585) than the mean (red).

Validated miRNAs were further analyzed for their mRNA targets using the Ingenuity Pathway Analysis (IPA) tool (version 21249400) (Ingenuity Systems, Redwood City, CA, United States), as previously described (Kadmiel et al., 2016). The IPA tool allows to access both experimentally validated and predicted mRNA targets from TargetScan and TarBase. Enrichment or overlapping was determined by IPA using Fisher's exact test ($P < 0.05$). The target genes were further analyzed with IPA core analysis module for functional enrichment of target genes to understand their putative impact in several biological functions and canonical pathways.

Determination of miRNA and mRNAs Levels in Dorsal Hippocampus by RT-qPCR

Validation of miRNAs

RNA < 200 nt (100 ng) was polyadenylated and, at the same time, reverse transcribed using the miScript II RT kit (see footnote 1, QIAGEN, Hilden, Germany), according to the manufacturer's instructions. This reaction was carried out for 1 h at 37°C and the enzyme was then inactivated by heating at 95°C for 5 min. The qPCR experiments were conducted as previously described on a Stratagene Mx3000p thermocycler (Stratagene, Agilent), using a denaturation step (95°C for 15 min), followed by 40 cycles of 94°C for 15 s, 55°C for 15 s and 70°C for 15 s (Castaneda et al., 2015). Each reaction was carried out in duplicate in a final volume of 25 μL and contained 12.5 μL miScript SYBR Green PCR, 2.5 μL of universal primer (see footnote 1, QIAGEN, Hilden, Germany), 2.5 μL of specific Primer Assay (QIAGEN, Hilden, Germany) and 200 pg of cDNA. A melting curve analysis was conducted afterward by heating the samples at 1°C per second from 70 to 95°C in order to detect PCR products. Designed primers were obtained from QIAGEN (Hilden, Germany). Primer sequences were 5′-UAUUGCACUUGUCCCGGCCUG-3′ for miR-92 and 5′-AGAGGCUGGCCGUGAUGAAUUC-3′ for miR-485, with an amplification efficiency of 89.5 and 86.8%, respectively. The relative abundance of these miRNAs was normalized to the levels of small nucleolar RNA SNO95, using standard primers (see footnote 1, QIAGEN, Hilden, Germany, cat # MS00033726,

[2]http://www.ncbi.nlm.nih.gov/geo/info/linking.html

[3]www.rproject.org

efficiency 97.3%), as we previously described (Castaneda et al., 2015). Relative miRNA levels were calculated based on the $2^{-\Delta\Delta CT}$, normalized to that of the SNO95 gene cDNA, and then relativized to control unstressed animals (Castaneda et al., 2015). All RT and qPCR reactions included water and RNA without the RT reaction as controls.

Determination of mRNA Levels in Dorsal Hippocampus

RNAs > 200 nt were reverse transcribed into cDNA by using Superscript II (Invitrogen, Carlsbad, CA, United States), following the manufacturer's instructions, but in the presence of RNAsin® (40 U, Promega Corporation, Madison, United States) as RNAase inhibitor. The qPCR was conducted in duplicate with 10 μL Brilliant II Ultra-fast SYBR Green QPCR Master Mix (Agilent Technologies), a suitable dilution of cDNA and 0.12 μM of primers from Integrated DNA Technologies (Coralville, IA, United States) and designed with Primer-Blast, NCBI. To determine CREB mRNA levels, we used a forward primer 5′-GAGAACAGAGTGGCAGTGCT and a reverse primer 5′-GGTCCTTAAGTGCTTTTAGCTCC (XM_017596652.1) that generate an amplicon of 70 bp. Additionally, we determined β-actin housekeeping gene mRNA levels by using the following forward primer 5′-TTGTCCCTGTATGCCTCTGGTC-3′ and reverse primer 5′-ACCGCTCATTGCCGATAGTG-3′ (NM_031144.3), which generate an amplicon of 346 bp. The efficiency of each primer set was obtained with several inputs of cDNA, and specificity was validated through melting curve analyses. Relative mRNA levels were calculated based on the $2^{-\Delta\Delta CT}$ and normalized to that of β-actin mRNA.

Determination of CREB Protein Levels in Dorsal Hippocampus

Dorsal hippocampi were homogenized as we previously described (Pacheco et al., 2017), in the presence of 0.32 M sucrose, 1 mM calcium-magnesium chelators (EDTA/EGTA), protease inhibitor (Complete™ EDTA-free, Sigma-Aldrich), and phosphatase inhibitor (PhosStop™, Sigma Aldrich) buffered with 10 mM HEPES at pH 7.4. Samples were then centrifuged at low speed (430 × *g* for 10 min at 4°C) to obtain a pellet (fraction enriched in nuclei) and a supernatant, which corresponds to a fraction of homogenate without nuclei. These fractions were mixed with loading buffer and then boiled during 10 min as described previously (Pacheco et al., 2017). Proteins (30 μg) were resolved on 10% SDS–PAGE and then blotted onto 0.2 μm PVDF membranes (2 h at 350 mA). Membranes were then incubated during 1 h at room temperature in 1% non-fat milk dissolved in PBS with 0.1% Tween-20 (PBS-T) and incubated overnight with a 1:500 dilution of CREB rabbit monoclonal antibody (catalog No 9197, Cell Signaling Technology). The blots were rinsed with PBS-T three times (each during 5 min) and then incubated at room temperature for 2 h with peroxidase-conjugated anti-rabbit secondary antibody (1:10,000, Thermo Scientific, Waltham, MA, United States). Membranes were then incubated with enhanced chemiluminescence Detection Kit for peroxidase (catalog No 20-500-120 Biological Industries, Israel Beit Haemek Ltd.) and signals were detected with a chemiluminescence imager (Syngene, United Kingdom). Blots were then treated with ReBlotPlus Mild Antibody Stripping Solution (Sigma-Aldrich, St. Louis, MO, United States) during 10 min and after were washed with PBS. Blots containing homogenate samples were blocked in 3% non-fat milk in PBS-T during 1 h and then incubated overnight with β-actin antibody in blocking solution (1:5000, Catalog No A5316, Sigma-Aldrich). Blots containing nuclear fraction were blocked in the presence of 1% BSA in PBS during 1 h and then incubated with antibody for Lamin B1 (LB1, monoclonal, 1:300, Catalog No sc-365962, Santa Cruz). Levels of β-actin and LB1 were used as loading controls for the homogenate fraction without nuclei and for the nuclear fraction, respectively. After capturing the images, band intensity was determined with the UN SCAN IT software ([4]RR ID: SCR_013725). Data represent the relative intensity ratio between CREB and respective loading controls (CREB/β-actin and CREB/LB1).

Statistical Analysis

Statistical analyses were conducted using GraphPad Prism (GraphPad Software Inc., San Diego, CA, United States). Data represent the mean ± SEM. Considering that data did not show normality test distribution (D'Agostino-Pearson omnibus and Shapiro–Wilk test), the data were analyzed either by the non-parametric Kruskal–Wallis test, followed by Dunn's *post hoc* test (for comparison between three groups) or the Mann–Whitney *U* test (to compare two experimental groups).

RESULTS

Effectiveness of Repeated Restraint Stress Through Evaluation of Physiological Markers

The effectiveness of repeated stress was confirmed by using several physiological parameters, and the data represent pooled animals that were used for miRNA array, RT-qPCR analyses and western-blot analysis. **Figure 2A** shows body weight gain at the experimental end-point. Kruskal–Wallis analysis revealed differences between groups ($P < 0.0001$) and Dunn's *posthoc* test revealed that controls increased their initial weight by 35%; in contrast to stressed animals during 7 (Stress-7d) and 14 days (Stress-14d), that gained approximately 17% ($P < 0.001$) and 18% ($P < 0.001$), respectively. We also determined fecal output every day during the stress procedure as a readout of stress effectiveness (Nakade et al., 2007), and estimated the mean *per* stress session. We found significant differences between groups (Kruskal–Wallis, $P = 0.0002$) and Dunn's *post hoc* test indicated a rise in the number of fecal pellets voided in both stress groups (both $P < 0.001$), compared to unstressed animals (**Figure 2B**). Furthermore, we determined that the weight of adrenal glands did not show differences among groups (Kruskal–Wallis, $P > 0.1$); nonetheless, we did observe an increase in Stress-14d when compared to controls (Mann–Whitney test, **Figure 2C**, $^{\#}P < 0.05$). Blood samples for CORT

[4]http://www.silkscientific.com

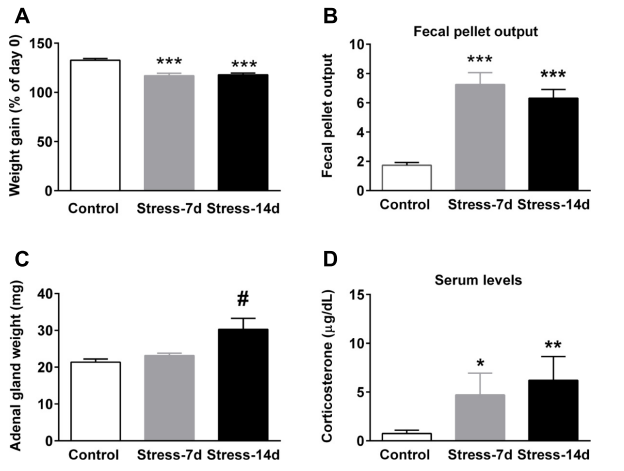

FIGURE 2 | Effect of restraint stress on body weight gain, fecal pellet output, adrenal gland weight, and baseline corticosterone levels. **(A)** Variation of body weight gain was evaluated at the end point of treatment. All rats were weighed daily and one group was stressed during 14 consecutive days. The graph represents the change in body weight as a percentage of the initial weight. **(B)** Fecal output was determined every day in control (2.5 h) and stressed animals during the stress session. Data represent the mean value/day. **(C)** Adrenal gland weight of control and stressed animals. **(D)** Serum corticosterone levels in control and stressed animals. Blood was sampled between 9:30 and 11:00 a.m. All data represent mean ± SEM of Control, $n = 16$ and animals subjected to restraint stress during 7 (Stress-7d, $n = 9$) and 14 days (Stress-14d, $n = 17$). Dunn's *post hoc* test: $^{***}P < 0.001$, $^{**}P < 0.01$, $^{*}P < 0.05$, Mann–Whitney test two-tail, $^{\#}P < 0.05$.

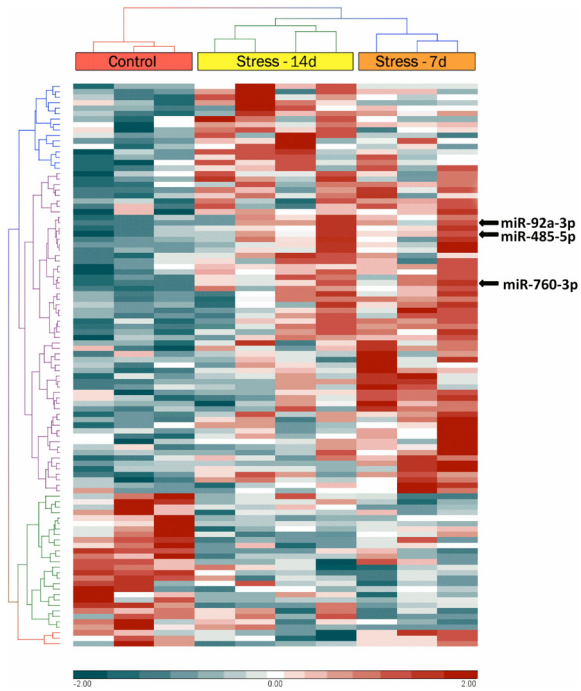

FIGURE 3 | Hierarchical cluster analysis of microRNAs (miRNAs) with significantly altered expression in rat dorsal hippocampus, representing the time evolution of stress treatment. Hierarchical clustering was performed on all samples of miRNAs differentially expressed between control dorsal hippocampi samples with fold changes greater than 2 (red) or less than –2 (blue). The top bar indicates experimental group [red: control ($n = 3$); orange: stressed animals during 7 days (Stress-7d, $n = 3$); yellow: stressed animals during14 days (Stress-14d, $n = 4$). Each row identifies one miRNA (not listed).

determination were obtained 24 h after the last stress session and in basal conditions (blood sampled between 9:30 and 11:00 a.m.). Kruskal–Wallis analysis revealed significant differences between groups ($P = 0.005$) and Dunn's *post hoc* test showed that both the Stress-7d and -14d groups had high baseline CORT levels compared to the control group ($P < 0.05$ and $P < 0.01$, respectively; **Figure 2D**). Altogether, these data indicate that restraint stress triggers the activation of the HPA axis and that the rats did not adapt when exposed daily to the homotypic stressor.

The miRNAs Are Up- and Down-Regulated in Dorsal Hippocampi of Stressed Animals

Dorsal hippocampi obtained 24 h after the last stress session were used for microarray analyses to detect the miRNA expression profile. A two-way hierarchical clustering analysis of controls and stressed animals showed significant variations of 103 miRNAs (P-value < 0.05) (**Figure 3**). This analysis segregated animals in two main clusters: one branch included control animals and the other one, stressed animals (during 7 and 14 days). We noticed that the miRNA profile of stressed animals during 7 days was very different from that of the controls, but more similar to the profile corresponding to animals stressed during 14 days (**Figure 3**). We used two bioinformatic tools in order to refine the search for significant miRNAs. Limma analysis revealed that after 7 days of stress, only 92 miRNAs changed their levels; on the other hand, Partek analysis detected changes in 78 miRNAs. To make the analysis more robust, we only selected those miRNAs that merged common to both analyses, thus detecting 71 miRNAs (**Supplementary Table S1**). Interestingly, our analysis revealed variations in the levels of 51 mature miRNAs and 20 precursor miRNAs (stem-loop). Most stem-loops (15 out of 20) increased their levels, and only a few were accompanied by changes in the levels of its respective mature form (miR-3594-3p; miR-598-5p). Similarly, many mature miRNAs increased their levels (54 out of 71) after 7 days of stress. Limma analysis also showed that after 14 days of stress, 64 precursors and miRNAs vary significantly, 55 of which were also found under Partek analysis (**Supplementary Table S2**). We found that 17 of these correspond to stem-loop (8 increased and 9 were reduced) and that the remnant are mature forms (12 increased and 26 were decreased). We also detected that variations in stem-loop miRNAs levels were correlated with significant variations in their mature forms (miR-24-1-5p, miR-296-5p, and miR-328a-3p). Interestingly, we detected variations in the levels of several miRNAs that belong to the miR-370-410 cluster at both stress periods.

These data indicate that a lower number of miRNAs changed their levels after 14 days of stress, in comparison to 7 days of stress. Thus, it is possible that stress triggers changes in the expression, processing and/or turnover of particular miRNAs. We segregated 10 miRNAs according to their maximal variation

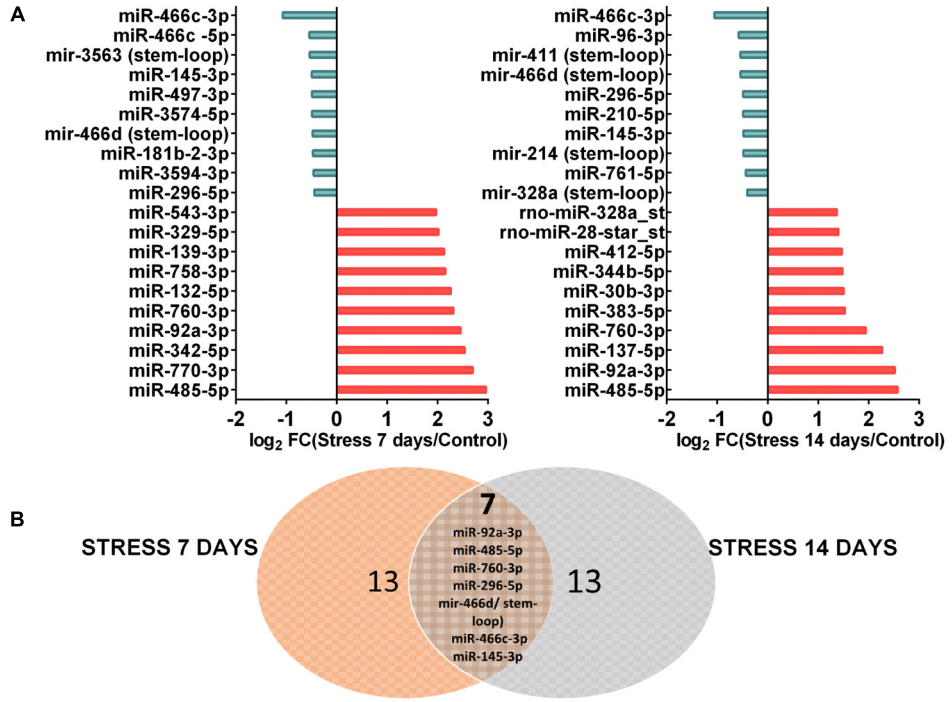

FIGURE 4 | Top 10 miRNAs most differentially expressed in dorsal hippocampi after 7 and 14 days of stress. **(A)** Distributions of Top 10 up-regulated miRNAs and down-regulated miRNAs after 7 and 14 days of stress in comparison to control animals, expressed as log2 FC. **(B)** The Venn diagram showing the overlapping between dorsal hippocampus of stressed animals during 7 days (left, orange circle) and 14 days (right, light blue circle).

respective to control. These top-10 miRNAs are shown in **Figure 4A**, which indicates that the magnitude of reduction in their levels ($\log_2$ FC) was lower than that of increase. It is noteworthy that at both stress periods, the miRNAs that reduced their levels were different. Furthermore, Venn diagram revealed seven common miRNAs that changed their levels at both stress periods (**Figure 4B**). Of those, three miRNAs (miR-296-5p, miR-466c-3p, miR-145-3p) and one precursor (miR-466d/stem-loop) decreased their levels; in contrast, three miRNAs (miR-760, miR-92a, and miR-485) increased their levels in dorsal hippocampus after both 7 and 14 days of stress (**Figures 3**, **4**). Thus, it is plausible that the chronicity of the stressor establishes waves of miRNA expression, and that some changes persist after 7 days of stress.

Validation of Selected miRNAs by qPCR

We next validated the changes in miR-760-3p, miR-92a-3p, and miR-485-5p by qPCR on independent biological samples obtained after 7 and 14 days of stress, using RNA expression of SNO95 gene as normalizer, as we previously validated (Castaneda et al., 2015). We detected that miR-760 levels were insensitive to both stress periods (**Figure 5A**). In contrast, the analysis of miR-92a levels showed differences between groups (Kruskal–Wallis $P < 0.005$) and we found that the levels of miR-92a in stressed animals during 14 days increased twofold in comparison to controls (Dunn's post-test $P < 0.01$, **Figure 5B**). Similarly, the expression of miR-485 was different among experimental groups (Kruskal–Wallis, $P < 0.01$), and we detected a rise of almost threefold in animals stressed during 14 days in comparison to controls (Dunn's post-test $P < 0.01$, **Figure 5C**). However, the difference between controls and animals stressed during 7 days was only detected by Mann–Whitney analysis, and indicated a 1.5 fold increase in miR-485 levels (one-tailed test $P < 0.05$).

In order to understand whether some of the stress mediators have a role in the expression of miR-92a and miR-485, we next examined the effect of chronic exogenous CORT administration (14 days) at a dose that we previously reported to induce an increased immobility time in the forced swimming test; i.e., similarly to our chronic stress model (Ulloa et al., 2010). Compared with vehicle control rats, CORT administration induced a reduction in both weight gain and adrenal gland weight, which is indicative of CORT effects (see **Supplementary Figure S1**). As shown in **Figure 6**, neither miR-92a nor miR-485 vary their expression under this CORT administration regimen. In whole, these results indicate that 14 days of stress triggers changes in the expression of miR-92a and miR-485 in dorsal hippocampi; variations that are not mimicked by CORT administration.

In silico Studies to Search Targets and Putative Pathways Regulated by miR-92a-3p and miR-485-5p

The miRNA Target Filter from IPA was used to gain insight about the gene products interaction network, their participation in canonical pathways, biologic functions, and cellular processes

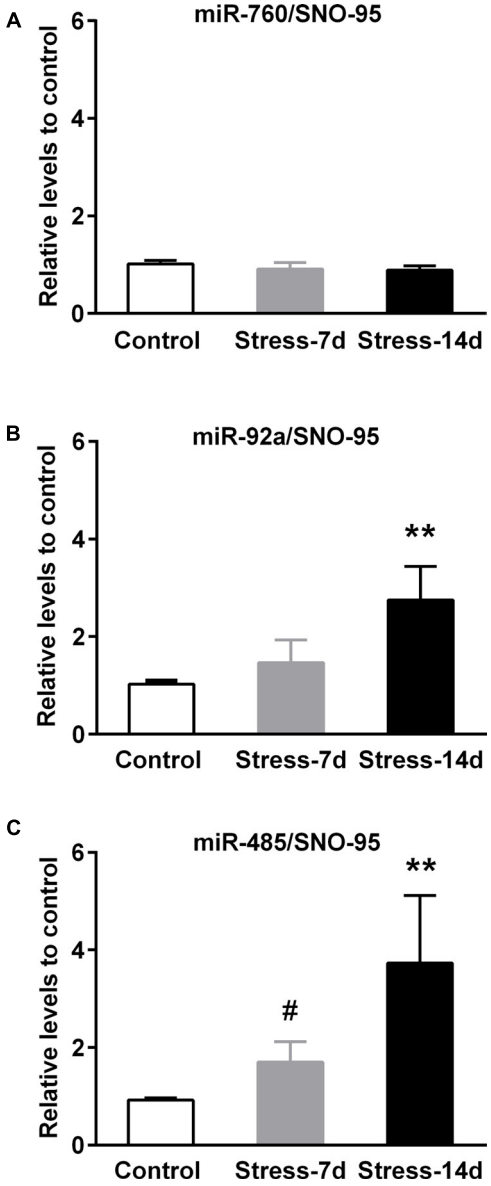

FIGURE 5 | Validation of stress-induced miRNAs expression in dorsal hippocampus. The miR-760, miR-92a, and miR-485 levels were determined by quantitative real-time PCR (qPCR) after 7 and 14 days of restraint stress. **(A)** Levels of miR-760 in dorsal hippocampi of Control (n = 7), Stress-7d (n = 5) and Stress-14d (n = 7) animals. **(B)** Levels of miR-92a in Control (n = 7), Stress-7d (n = 4) and Stress-14d (n = 8) group. **(C)** Levels of miR-485 in Control (n = 4), Stress-7d (n = 5) and Stress-14d (n = 5). Data were analyzed by Kruskal–Wallis test followed by Dunn's *post hoc* test, $^{**}P < 0.01$. Mann–Whitney test two-tail, $^{\#}P < 0.05$.

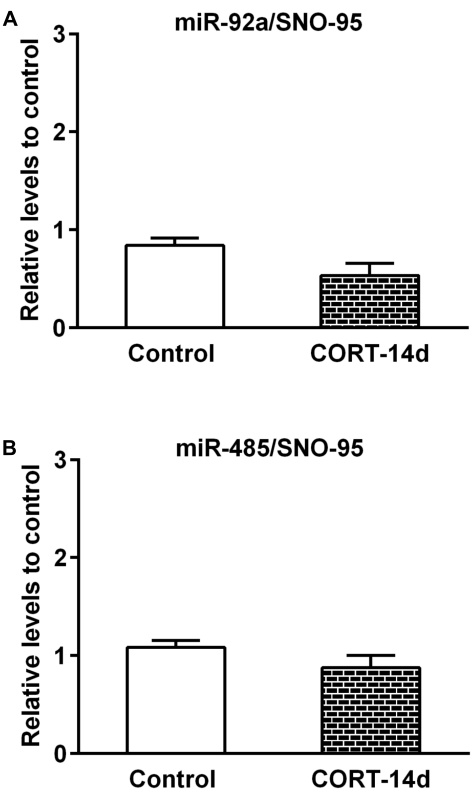

FIGURE 6 | Effect of corticosterone administration during 14 days on miR-92a and miR-485 expression in dorsal hippocampus. The miRNAs levels were determined by quantitative real-time PCR (qPCR) after daily 30 mg/kg s.c. administration of corticosterone (CORT) or vehicle (Propylene glycol). **(A)** Levels of miR-92a in Control (n = 5) and CORT-treated (n = 5) animals. **(B)** Levels of miR-485 in control (n = 6) and CORT-treated (n = 5) animals.

modulated by miRNA actions. From a total of 103 targets, we found 12 mRNAs with a moderate prediction, 86 with high prediction, and 5 experimental validated targets of miR-92a-3p (**Supplementary Table S3**). These targets were segregated according to their corresponding cellular compartments; 7 gene products were present at the extracellular space and correspond to peptides that are involved in cell polarity, and others correspond to secreted enzymes involved in matrix remodeling. Another main group of targets corresponded to proteins located at the plasma membrane, such as G-coupled receptors, subunits of channel receptors, scaffold proteins, and enzymes, among others (**Figure 7**). Furthermore, another group included targets located in the cytosol compartment, including phosphatases and other enzymes (**Figure 7**). Moreover, miR-92a had 13 predictive targets that correspond to transcription factors (**Figure 7**). *In silico* analysis revealed that the top-10 biological functions of miR-92a were related to: Nervous System Development and Function, Tissue Development, Behavior, Embryonic Development, Organ Development, Organismal Development, Organismal Survival, Tissue Morphology, Digestive System Development and Function, and Organ Morphology (**Figure 8A**). Target analysis revealed a large number of genes associated with canonical pathways related to Axonal Guidance Signaling, Synaptic Long-Term Potentiation, Calcium signaling, G-protein Coupled Receptor Signaling, cAMP-mediated signaling, PKA signaling, neuropathic pain signaling, cardiac β-adrenergic signaling, Phospholipase C signaling, and Dopamine-DARPP32 feedback in cAMP signaling (**Figure 8B**).

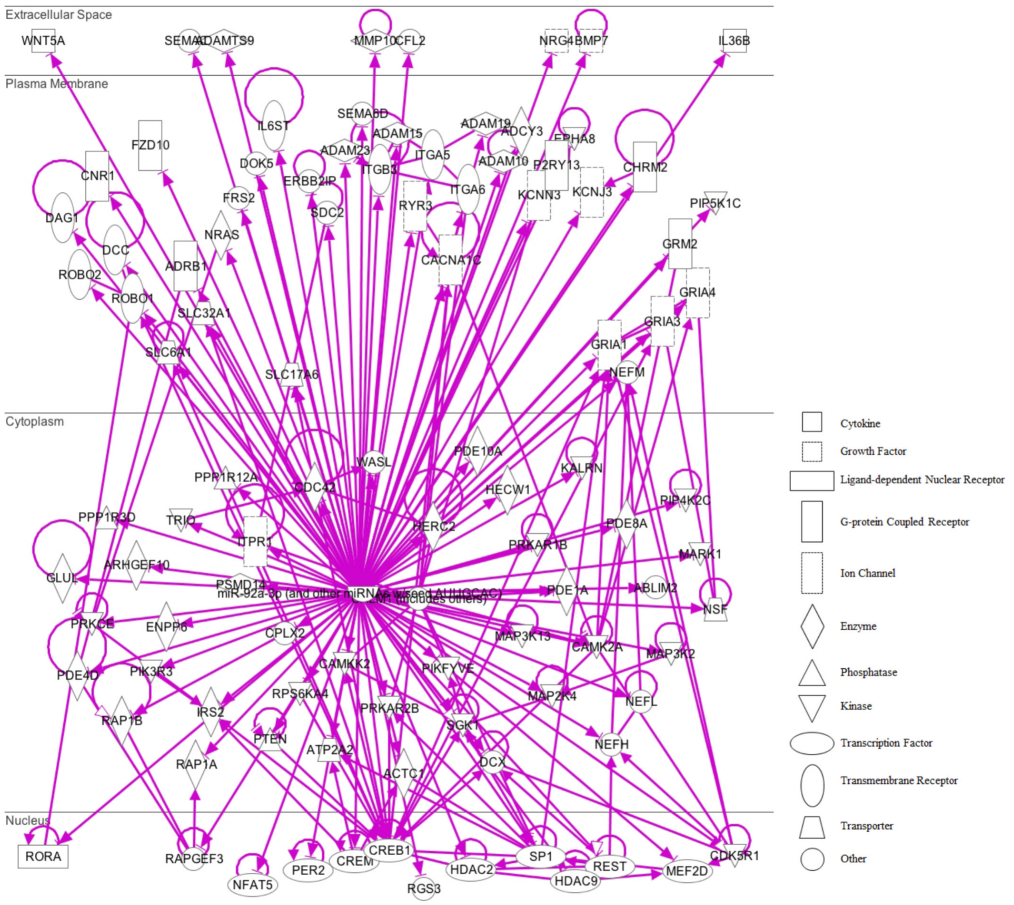

FIGURE 7 | IPA pathway representation of miR-92a targets. 103 predicted and probed targets mRNAs are represented. Gene products are positioned according to subcellular localization. Only direct connections (i.e., direct physical contact between two molecules) among the individual gene products are shown; arrow-lines indicate protein-protein binding interactions.

In silico Studies to Search Targets and Putative Pathways Regulated by miR-485-5p

On the other hand, in the case of miR-485-5p, we found 70 target mRNAs with moderate prediction and 61 with high prediction, from a total of 131 targets (**Supplementary Table S4**). Fourteen gene products were present at the extracellular space and correspond to morphogen peptides, Wnt signals, growth factors, and extracellular proteases, among others (**Figure 9**). Furthermore, a large number of gene targeted products (50 mRNAs) are G-coupled receptors, subunits of channel receptors, transporters, adhesion molecules, enzymes, and scaffold proteins (**Figure 9**). The other group corresponded to 45 targets located in the cytosol and includes enzymes such as kinases and phosphatases, among others. Interestingly, there are many transcription factors, along with HDAC and ligand-dependent nuclear receptors, which are predicted to be miR-485 targets. Analysis of the top-10 canonical pathways influenced by miR-485 detected 9 of the same 10 pathways predicted for miR-92, with the exception of Digestive System Development and Function, but including Cardiovascular System Development and Function (**Figure 10A**). Target analysis for miR-485 revealed a large number of genes associated with canonical pathways related to Axonal Guidance Signaling (i.e., similarly to miR-92a), Huntington's Disease Signaling, Molecular Mechanism of Cancer, Ephrin Receptor signaling, Role of Osteoblasts, Osteoclasts and Chondrocytes in Rheumatoid Arthritis; Role of Macrophages, Fibroblasts and Endothelial Cells in Rheumatoid Arthritis, Role of NFATs in Cardiac Hypertrophy, PLC Signaling, CREB Signaling in Neurons and Role of homeobox protein NANOG in Mammalian Embryonic Stem Cell Pluripotency (**Figure 10B**).

Relationship Between miR-92a-3p and miR-485-5p Target Genes

Further analysis centered on regulatory relationships between miR-92a and miR-485 target genes displayed some nodes with proteins that have a pivotal role in brain plasticity (**Figure 11**).

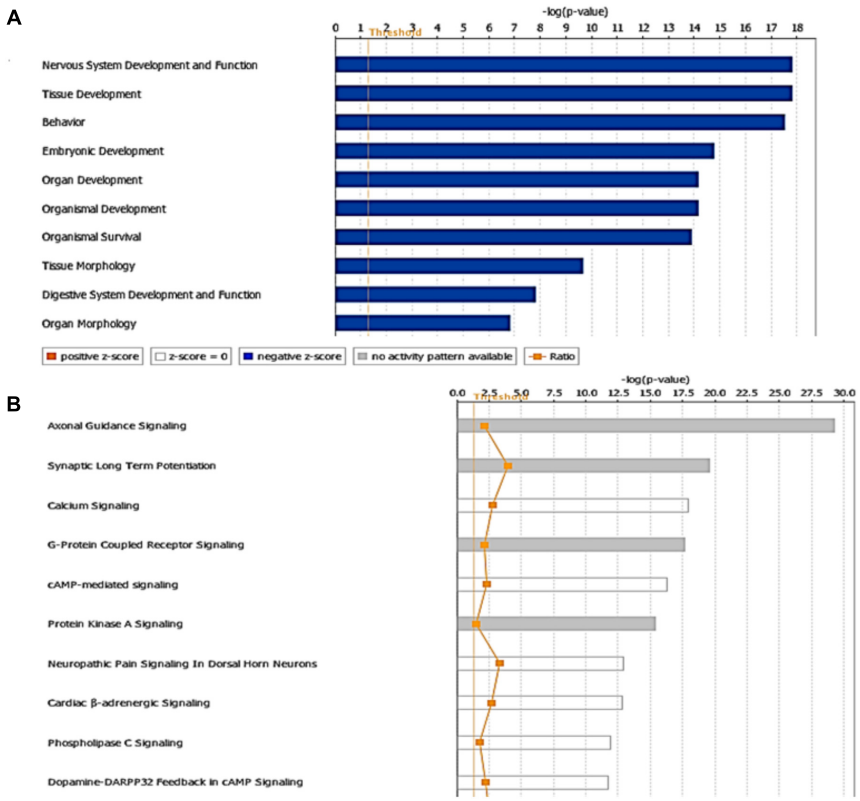

FIGURE 8 | Targets and pathways influenced by miR-92a-3p. Targets were evaluated using Target scan and the pathways associated with genes that are predicted to be targets of miR92a are shown ($P < 0.05$, Fisher's Exact test). **(A)** Top-10 biological functions identified by Ingenuity pathway analysis showing physiological and pathological functions that may be influenced and **(B)** Canonical pathways associated to miR92a ($P < 0.05$, Fisher's Exact test). The ratio was determined as the number of genes in a given pathway divided by the number of genes that make up the pathway. The *P*-value for a given process annotation is calculated by considering the number of genes that participate in a process and the total number of genes that are known to be associated with that process in the selected reference set. Significance of upregulated or downregulated pathways was determined using Fisher's exact test and is presented as the negative logarithm of the *P*-value [–log (*P*-value)]. A multiple corrections test is not available for IPA; therefore, all values are reported as unadjusted *P*-values. The predicted activation state (upregulated or downregulated) of significantly expressed pathways was determined by a *z*-score algorithm that compared the gene expression data set with the expected canonical pathway patterns (http://ingenuity.force.com/ipa). Pathways with positive (orange) and negative (blue) *z*-scores indicate that the pathways are activated and inhibited, respectively. Gray indicates that there is no report. Ratio is calculated as the number of genes that overlap with the corresponding pathway.

These include HDACs (HDAC 2, 4, and 5); CREB1; the TP53; the NCOR1, SNCA, the MAPT and the NR1 subunit of the NMDA receptor (GRIN1). **Figure 11** indicates that these gene products are either connected directly or indirectly to each other. Considering the pivotal role of CREB in hippocampal function (Chen et al., 2001; Carlezon et al., 2005), we decided to determine variations in both its mRNA and protein levels in dorsal hippocampus after 14 days of stress. As shown in **Figure 12A**, CREB mRNAs levels decreased with stress (two-tailed Mann–Whitney analysis, $P < 0.05$); nonetheless this variation was not related to a similar variation in hippocampal protein extract (without nuclei) and nuclear fraction (**Figure 12B**).

DISCUSSION

Stress triggers changes in the activity of several neurocircuits in diverse brain areas, particularly in the hippocampus. Antecedents point out that the intensity, duration and chronicity of exposure to stressors determines how the hippocampus reacts to this challenge (Joels and Baram, 2009). We have previously reported that chronic restraint stress in rat induces anhedonia, depressive- (Bravo et al., 2009; Castaneda et al., 2015; Pacheco et al., 2017) and anxiety-like behaviors (Bravo et al., 2009; Ulloa et al., 2010). Moreover, a recent systematic review and meta-analysis conducted in rodents indicated that different models of chronic stress impair the consolidation of learned memories (Moreira et al., 2016).

One of the most important findings of the present study was that the extent of stress exposure (7 vs. 14 days) triggers a differential response in miRNA levels at dorsal hippocampus and remarkably, we found that some of these miRNAs belong to the miR-379-410 cluster. Moreover, we confirmed by qPCR that miR-92a and miR-485 are induced after 14 days of stress in dorsal hippocampus. Furthermore, chronic administration of CORT during 14 days, used to emulate variations in hormone levels that occur during stress exposure, did not mimic the effect of restraint stress; suggesting that the expression of these

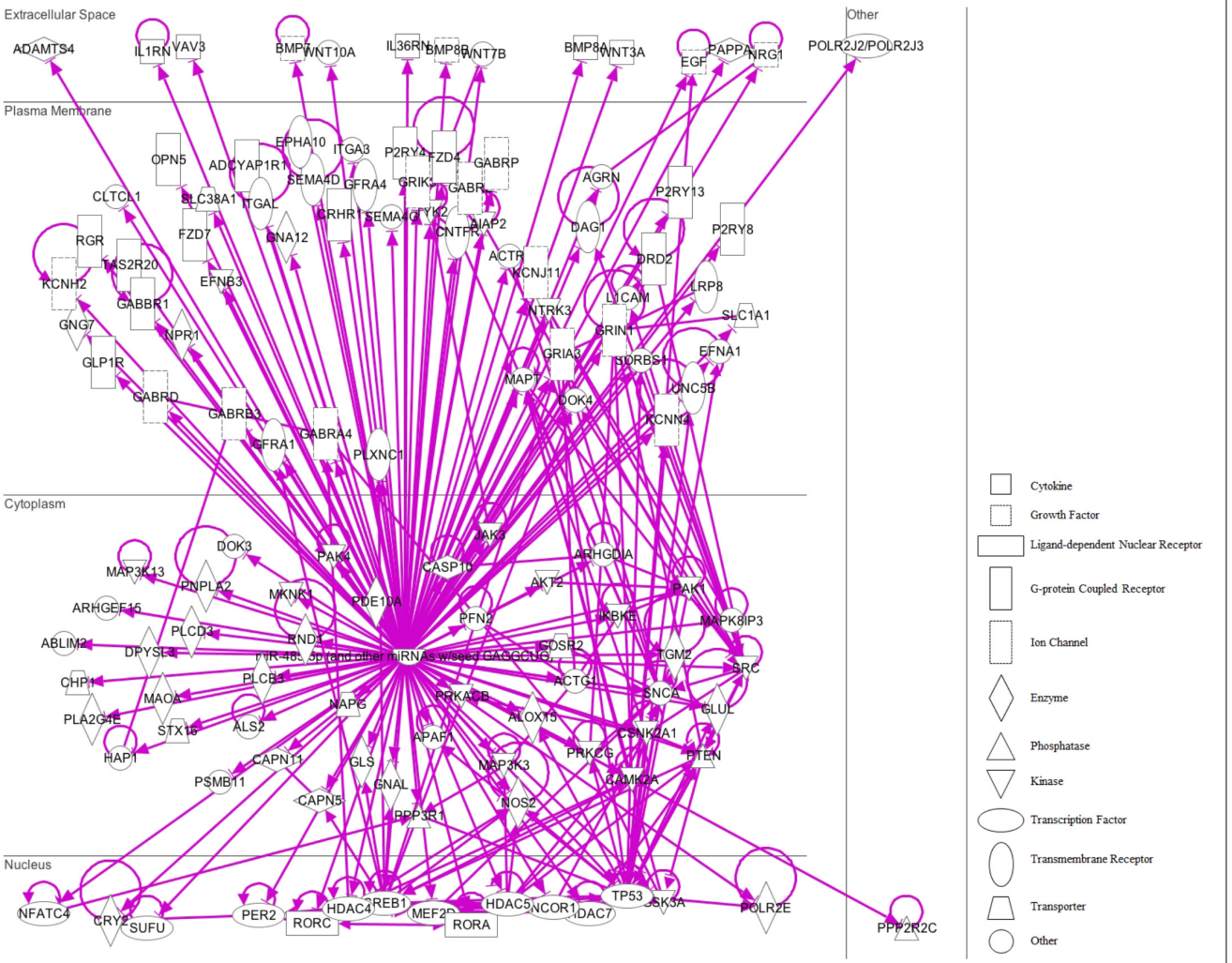

FIGURE 9 | IPA pathway representation of miR-485 targets. 131 predicted targets mRNAs are represented. Gene products are positioned according to subcellular localization. Only direct connections (i.e., direct physical contact between two molecules) among the individual gene products are shown; arrow-lines indicate protein-protein binding interactions.

miRNAs are independent of the effect of this stress hormone. These data indicate that stress triggers changes in the levels of master regulators of mRNAs translation, probably by producing changes in the efficacy of some important transduction signaling pathways in dorsal hippocampus, and hence, determining several neuroplastic changes and functioning of this structure.

The Extent of Repeated Stress Triggers Changes in miRNAs in Dorsal Hippocampus

Evidences recently reviewed indicate that environmental stress exposure may trigger changes in miRNA levels (Hollins and Cairns, 2016). Studies in the prefrontal cortex of adult mice indicated a prominent increase in the levels of different miRNAs after acute stress (2 h) while only minor changes were observed after subchronic restraint (5 days) (Rinaldi et al., 2010). Moreover, these changes were region specific, i.e., with no differences in miRNAs expression in the hippocampus (Rinaldi et al., 2010). In adult male rats, acute immobilization stress triggers an increase in particular miRNA levels, which are reduced after chronic stress in hippocampus and amygdala (Meerson et al., 2010).

The aforementioned antecedents suggest that acute, subchronic, and chronic stress can differentially modify miRNA levels according to specific patterns. With the idea of contributing to this important issue, we chose 7 and 14 days of stress exposure, a particular timing in which we previously observed anhedonic behavior (Castaneda et al., 2015). We observed HPA axis activation (reduction in weight gain, and increase in both fecal output and baseline CORT levels) in both stressed groups, with no sign of adaptation to the homotypic stressor exposure. We used the Affymetrix platform for miRNA expression analysis and mainly detected a rise in miRNA levels

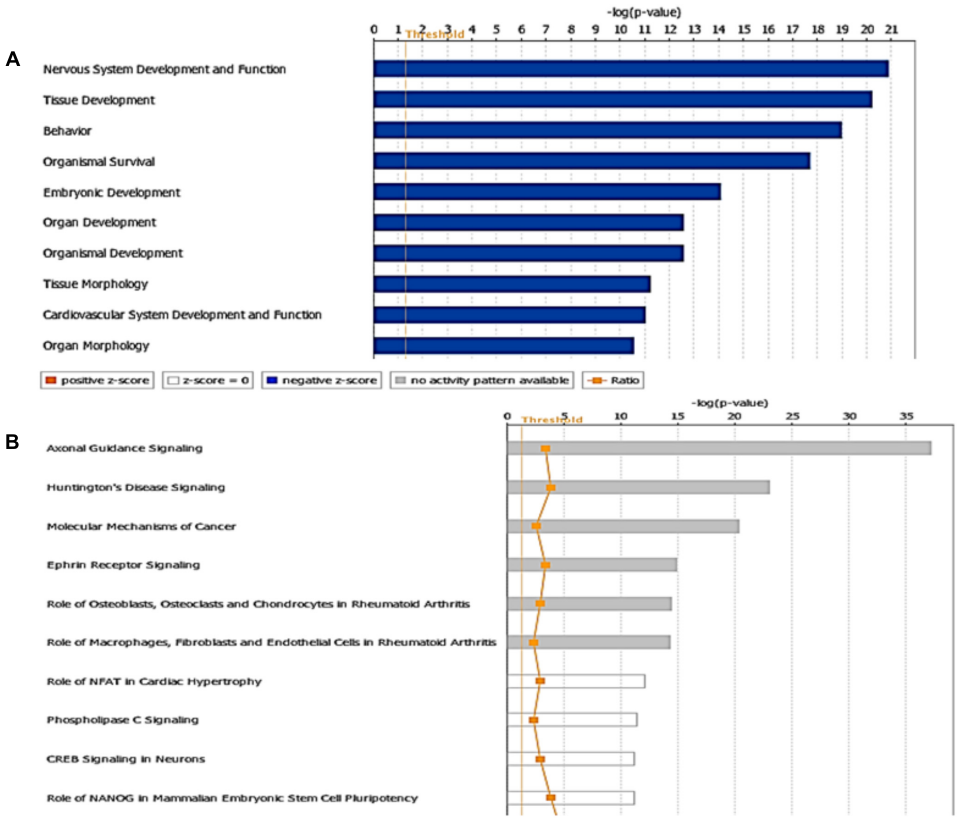

FIGURE 10 | Targets and pathways influenced by miR-485-5p. **(A)** Top-10 biological functions identified by Ingenuity pathway analysis and **(B)** Canonical pathways associated to miR-485a ($P < 0.05$, Fisher's Exact test). The ratio is calculated as the number of genes in a given pathway divided by the number of genes that make up the pathway. The *P*-value for a given process annotation is calculated by considering the number of focus genes that participate in that process and the total number of genes that are known to be associated with that process in the selected reference set. The predicted activation state (upregulated or downregulated) of significantly expressed pathways was determined by a *z*-score algorithm that compared the gene expression data set with the expected canonical pathway patterns (http://ingenuity.force.com/ipa). Pathways with positive and negative *z*-scores indicate that the pathways are activated and inhibited, respectively. Orange color indicates activation of the pathway, blue indicates suppression of the pathway and gray indicates a mixed response. Ratio is calculated as the number of genes that overlap with the corresponding pathway.

and also in some miRNA precursors; variations that may be linked to a stress-induced gene expression profile. It is also important to note that the heatmap miRNAs analysis revealed that miRNA profiling of animals stressed during 7 days was different from that of controls; in contrast, the profile of rats stressed during 14 days was more similar to controls and animals stressed during 7 days. Thus, it is probable that during the first week of stress, more miRNA genes respond to this challenge, and that some compensatory mechanism is triggered to produce a new profile with a lower number of miRNAs that change after 14 days of stress. To sum up, miRNA profiling in dorsal hippocampus depends on the extent of stress exposure and future prospects will consider determining transcriptional, and post-transcriptional mechanisms associated to the stress-induced regulation of miRNA expression.

We were able to confirm by RT-qPCR only two of the three miRNAs that showed the highest increase after 14 days of stress according to chip analysis (miR-92a and miR-485). The discrepancy between the array and qPCR data may depend on a wide repertoire of factors, such as the inherent drawbacks of both techniques and the different normalization and dynamic range of each technique, among others (Morey et al., 2006; Koshiol et al., 2010).

Considering that the chronic stress paradigm is accompanied by a rise in CORT levels, we decided to examine the direct effect of daily administration (14 days) of this hormone on miR-92a and miR-485 levels. Under chronic CORT administration, we have previously observed a depressive-like behavior (high time in immobility in the Forced-swim test) (Ulloa et al., 2010). Additionally, other studies using chronic administration of CORT indicated a reduction in sucrose preference, decreased reward behavior and impaired spatial working-memory (Sterner and Kalynchuk, 2010). In the present study, chronic CORT administration produced a reduction in adrenal gland weight and body weight gain, but did not vary miR-92a and miR-485 levels in dorsal hippocampus. Considering that we do not know how chronic CORT exposure may influence miRNA profiles, we can only conclude that the levels of miR-92a and miR-485 levels are independent of this hormone. Taken altogether, it is plausible that even

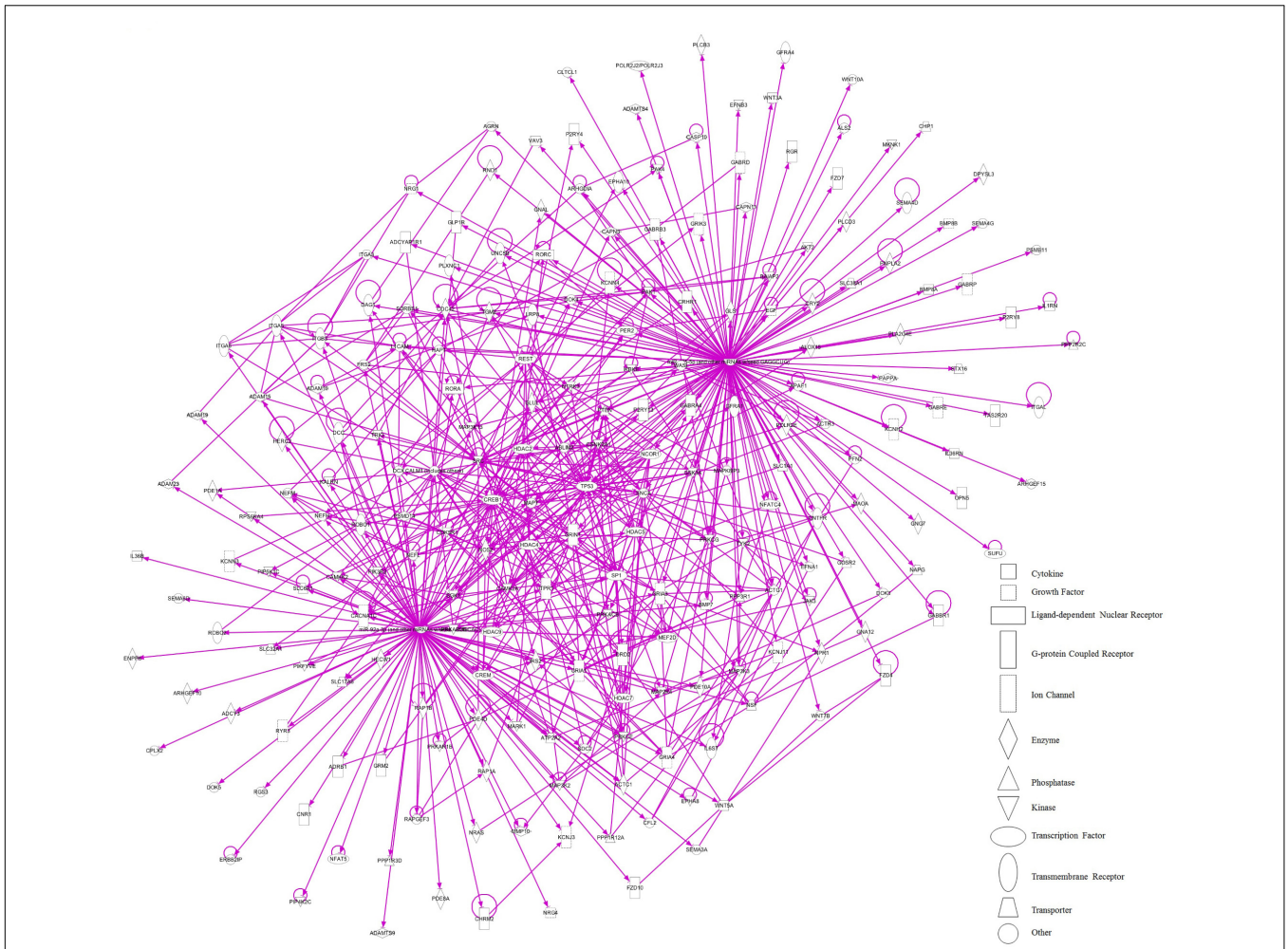

FIGURE 11 | Proposed network regulated by variation of miR-92a and miR-485 induced by chronic stress in dorsal hippocampus. The molecular crosstalk (represented as solid lines for direct relationship) is shown as part of the stress-induced up-regulation of miR-92a and miR-485. Protein as part of a node can be observed such as HDAC 2, 4, and 5; CREB1; the tumor protein 53 (TP53); the nuclear receptor co-repressor 1 (NCOR1), synuclein alpha (SNCA), the microtubule associated protein Tau (MAPT) and the NR1 subunit of NMDA receptor (GRIN1).

though the expression of miR-92a and miR-485 is stress-dependent, but CORT independent, they may regulate either the basal or stress-induced variation in the expression of several genes.

The Predicted Targets for miR-92a and miR-485 Are mRNAs Involved in Neuronal Function

The miR-92a-3p is preferentially expressed in glutamatergic neurons (He et al., 2012), and belongs to a family of highly conserved miRNAs with an identical seed region found in diverse paralog clusters: miR-17-92, miR-106a-363, and miR-106b-25 (Tan et al., 2014). A rise in several members of the miR-17-92a cluster (miR-92a, miR-20a) has been detected in brain samples of patients with Huntington's disease (Marti et al., 2010). Interestingly, after stroke, intravenous administration of exosomes containing members of the miR-17-92 cluster promotes neurite branching, as well as a rise in dendritic spine density in the infarcted brain area of rats (Xin et al., 2017); nonetheless, it is not clear whether a particular miRNA of this cluster is responsible for this effect. On the other hand, deletion of the miR-17-92 cluster in neural progenitors reduces neurogenesis in DG of hippocampus; which was linked to a rise in SGK1 (Li et al., 2016). The GO analysis of targeted mRNAs showed that many of these mRNAs are related to cell proliferation and differentiation (Jin et al., 2016). Additionally, deletion of this cluster promoted depressive-like behaviors, suggesting that members of the cluster may produce antidepressant-like effects (Jin et al., 2016); nonetheless, it is difficult to elucidate which member of this cluster is responsible for the observed effect.

We observed that miR-92a expression is enhanced after 14 days of stress in dorsal hippocampus; a variation that was not accompanied by similar changes in other members of the miR-17-92a cluster (see **Supplementary Tables S1** and **S2**). Nonetheless, we cannot discard the possibility that the

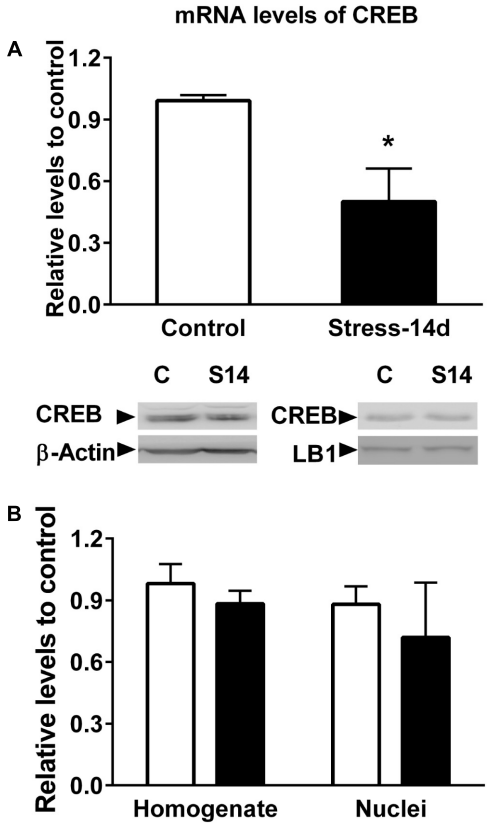

FIGURE 12 | Evaluation of CREB mRNA and protein levels in dorsal hippocampus. **(A)** Comparison of CREB mRNA levels in control and chronically stressed animals. RT-qPCR experiments were conducted to determine CREB mRNA levels and data were analyzed by $2^{-\Delta\Delta Ct}$ using β-actin as normalizer. Bar graph represents mean ± SEM of Control ($n = 6$) and stressed animals ($n = 6$). Differences between both groups were evaluated with two-tailed Mann–Whitney test. $^{*}P < 0.05$. **(B)** Levels of CREB protein levels in homogenate and nuclear fraction obtained from dorsal hippocampus. β-actin and Lamin B1(LB1) were used as loading controls for homogenate and nuclear fractions, respectively. Graphs represent mean ± SEM of each group. Control ($n = 6$) and stressed animals ($n = 4$).

different miRNAs from the cluster may have different half-lives (Ruegger and Grosshans, 2012). In cultured rat hippocampal neurons, pharmacological blockage of neuronal excitability triggers a decrease in miR-92a levels, favoring the rise in levels of its target, the subunit GluA1 of AMPA receptor (Letellier et al., 2014). We have recently reported that chronic stress does not change GluA1 levels in dorsal hippocampus (Pacheco et al., 2017), probably ruling out the contribution of miR-92a in the regulation of GluA1 levels. Additionally, contextual fear conditioning in mice triggers a transient rise in miR-92 levels in the hippocampus and reduces various mRNA targets, such as the neuronal K^+/Cl^- co-transporter 2 (KCC2); CPEB3, a translational regulator in neurons; and the transcription factor MEF2D (Vetere et al., 2014). Additionally, reduction of endogenous miR-92 levels in CA1 neurons prevents variation in these proteins, restricts contextual fear conditioning, and prevents the rise in spine density triggered by memory formation (Vetere et al., 2014). Under this view, it seems that enhanced miR-92a expression may act as compensatory mechanism by limiting the reduction of spine density induced by stress in CA1 (Castaneda et al., 2015; Garcia-Rojo et al., 2017). Additionally, the IPA pathway analysis that we conducted identified canonical pathways associated with miR-92a, such as synaptic LTP, which is a process affected in chronically stressed animals (Pavlides et al., 2002; Alfarez et al., 2003).

We have also shown that some miRNAs residing in the miR379-410 cluster and other stem-loop precursors were mainly up-regulated under stress, suggesting that the expression of this cluster is stress-sensitive. Notably, we detected that stress triggers a rise in the levels of other members of the cluster at 7 days (miR-485, miR-770, miR-758, miR-543, miR-433, miR-154, miR-377, miR-666) and 14 days (miR-485, miR-412, miR-410, miR-127, miR-323, miR-44, miR-411) of stress, and that a few of them were expressed at both stress periods (such as stem-loops miR-300 and miR329). Interestingly, the miR-379-410 cluster, exclusively expressed from the maternal allele, is implicated in diverse neurodevelopmental processes and is a central regulator of neuronal function (Winter, 2015). The expression of this cluster is regulated by neuronal depolarization in a MEF2- and BDNF-dependent manner (Fiore et al., 2009) and at least three of its members (miR-134, miR-329, and miR-381) are crucial for dendritic spine formation induced by neuronal activity (Fiore et al., 2009). Interestingly, we have found that miR-485 levels increase during both of the stress periods evaluated in this study. On the other hand, the increase in neuronal activity of cultured neurons promotes a destabilization of mRNAs that have a common motif in the 3′UTR complementary to the seed domain of several miRNAs, including miR-485 (Cohen et al., 2014). Furthermore, miR-485 decreases TAU mRNA levels in hippocampal neurons, blocks nerve growth factor-induced neurite outgrowth in PC12 cells and reduces the levels of SV2A, a glycoprotein present in synaptic vesicles; suggesting that this miRNA may diminish neurotransmitter release (Cohen et al., 2011). Moreover, overexpression of miR-485 in cultured hippocampal neurons reduces the density of dendritic spines, along with the clustering of PSD-95 and the exposure of AMPA receptor containing GLUA2 subunits at the synaptic plasma membrane (Cohen et al., 2011); however, the mechanisms by which miR-485 produces this effect is unknown. We have recently reported that chronic stress does not produce changes in GLUA2 levels in homogenates obtained from dorsal hippocampus (Pacheco et al., 2017), suggesting that under stress conditions, miR-485 probably targets other mRNAs.

In order to gain insight about probable mRNA targets, we used gene networks based on the IPA tool and found that miR-485 is related to Huntington's disease signaling. Recent evidence suggests a strong relationship between MDD and neurodegenerative diseases, including Huntington's disease, as well as natural processes of aging [reviewed in Reus et al. (2016)]. On the other hand, our *in silico* study identified the top-10 biological functions influenced by miR-92a, nine of

which were shared with miR-485 (Nervous System Development and Function, Tissue Development, Behavior, Embryonic Development, Organ Development, Organismal Development, Organismal Survival, Tissue Morphology, Digestive System Development and Function, and Organ Morphology). The only biological function distinctive of miR-92a was that related to Digestive System Development and Function. This global analysis points out that chronic stress may modify processes related to brain wiring that are fully active during development, but that it probably plays a key role in the adult brain. Interestingly, both miR-92a and miR-485 influence similar canonical pathways, such as axonal guidance signaling, which is relevant during development of the nervous system. This pathway involves the presentation of guidance signals, and both the reception and processing of these signals. The main extracellular signals that influence axonal growth cone dynamics include guidance signal families: NETRINS, SLITS, SEMAPHORINS (SEMA) and EPHRINS (EPH); and their corresponding neuronal receptors; i.e., DCC/UNC5, ROBO, NEUROPILIN/PLEXIN, and EPHS (Dickson, 2002). Some predicted targets of miR-92a actions include ROBO (1 and 2), SEMA3A and SEMA6D, DCC, and EPHA8. Although there is not much information about the role of axonal guidance signaling in MDD or stress-related disorders, some evidence indicates that alterations in these proteins are related to neurological disorders (Dickson, 2002). It is also important to highlight that different guidance molecules seem to have key roles in several aspects of synapse formation (Shen and Cowan, 2010) and dendritic spine stability (Koleske, 2013), a critical phenomenon in several animal models of depression (Castaneda et al., 2015; Pacheco et al., 2017). Interestingly, augmented EPHA4-EPHEXIN1 signaling in the prefrontal cortex and hippocampus has been related to depressive-like behavior observed after repetitive social defeat stress (Zhang et al., 2017), unveiling that pathways that canonically play a pivotal role during development may also be relevant in mature brain, perhaps favoring the development of some mood disorders.

The Combined Rise in miR-92a and miR-485 Levels May Influence Gene Expression, Leading to Altered Neural Plasticity

Our *in silico* study also suggests that the combined effect of miR-92a and miR-485 on their targets may produce alterations in proteins related to neuronal functioning and we will now discuss three aspects especially related to the effect of stress on neuroplasticity. The first one is related to the possible influence of miRNAs on the levels of transcriptional factors. One of them is TB53, which is induced under chronic stress in the hippocampus (Sanchez-Hidalgo et al., 2016) and positively controls neuronal apoptosis (Jordan et al., 1997). On the other hand, the transcriptional factor CREB1—also included in this analysis—has a crucial role in the regulation of gene expression during the development of the nervous system and its expression is reduced in stressed animals (Marsden, 2013). In contrast, reports have shown that hippocampal CREB overexpression exerts antidepressant-like effects (Chen et al., 2001). In the present study, we detected a reduction in CREB mRNA levels in dorsal hippocampus that may be indicative of miRNAs action; nonetheless, we did not observe variations in CREB protein levels. However, there are many possibilities that can explain this discrepancy. For instance, we do not know whether chronic stress triggers changes in the half-life of the protein. On the other hand, since we only evaluated changes in dorsal hippocampus, we do not know whether variations in the levels of CREB protein could be related to a particular neuronal hippocampal stratum. Another possibility is that CREB is not controlled by these miRNAs. Prediction analysis indicated that both miR-92a and miR-485 might also influence gene expression by directly or indirectly targeting HDACs (2, 4, and 5). Some studies have indicated that HDAC2 negatively regulates memory formation, synaptic plasticity (Guan et al., 2009) and density of dendritic spines in hippocampal neurons (MacQueen et al., 2003); i.e., changes also observed under chronic stress (Castaneda et al., 2015; Pacheco et al., 2017). With respect to HDAC4, although it has no catalytic activity, it is able to repress the expression of genes that encode constituents of synapses; thus affecting synaptic architecture and strength (Sando et al., 2012). Additionally, *in vivo* suppression of HDAC4 in hippocampus has been reported to eliminate stress-induced altered behavior (Sailaja et al., 2012), suggesting that this protein has an important role in stress-related behavior (White and Wood, 2014). Considering the global effect of these HDAC in neuron physiology, it is plausible that the rise in both miR-92a and miR-485 may limit the negative effect of HDACs in hippocampal functioning.

The second aspect that is important to discuss concerns the stress-induced dendritic arbor retraction described in dorsal hippocampal neurons (Pinto et al., 2015) that may be related to changes in microtubule-associated proteins. Our analysis also detected the microtubule-associated protein TAU as part of an interaction node generated by miR-92a and miR-485. TAU interacts with tubulin and promotes microtubule stabilization (Avila, 2006); however, TAU knockout-mice do not show stress-induced altered behaviors and atrophy of hippocampal dendrites (Lopes et al., 2016). Considering these evidences, it is plausible that the expression of miR-92a and miR-485 may modulate the negative effect induced by stress.

The third aspect important to highlight is the description of the constitutive subunit of NMDA receptor (GRIN1) as a node of miR-92a and miR-485 interaction. In agreement, we have reported that chronic stress triggers a rise in the levels of GRIN1 mRNA, along with a reduction in protein levels in whole extract of dorsal hippocampus (Pacheco et al., 2017). Although we do not know the physiological consequence of this reduction, some studies have indicated that this subunit is not a restrictive factor in the number of NMDA receptors that are delivered from the endoplasmic reticulum to the synapse (Stephenson et al., 2008). These evidences suggest that stress-induced variation in miR-92a and miR-485 miRNA levels may regulate expression of important genes related to hippocampal physiology.

CONCLUSION

Our study provides evidence that chronic stress triggers changes in the expression of miRNAs in dorsal hippocampus, in a way that is sensitive to the chronicity of the stress exposure. Further studies must be carried out not only to define a timeline of the spectrum of responses associated to repeated stress exposures—in which a transition of miRNA expression profile is produced—but also to determine whether these changes also involve a transition from homeostatic adaptation to a stress-induced condition characterized by poor adaptation. Understanding this transition will be relevant to gain insight about how stress regulates brain plasticity and pathology, especially in brain structures related to memory consolidation and cognitive functions, such as the hippocampus.

The other important finding is that miR-379-410 cluster expression is sensitive to stress, and the mechanisms by which some cluster members change their levels remains to be elucidated. Moreover, we also found that the stress-induced rise in miR-92a and miR-485 levels do not depend on CORT. Furthermore, we found that the pathways that seem to be mainly influenced by miR-92a and miR-485 are related to axonal guidance signaling and cAMP signaling. Additionally, the combined effect of miR-92a and miR-485 may influence transcription factors, along with histone-modifying enzymes, among others. Nonetheless, future studies must be focused to precise the hippocampus subfields and neuronal fate where these changes in miRNAs are occurring and whether they are limited to somatic or dendritic compartments. Similarly, the physiological relevance of the variations in these particular miRNAs should be addressed through interventional approaches, which undoubtedly may unveil whether or not these miRNAs influence dorsal hippocampus functioning. Altogether, these future scenarios will make it feasible to decipher whether the rise in miR-92a and miR-485 in dorsal hippocampus corresponds to a compensatory or maladaptive stress response.

AUTHOR CONTRIBUTIONS

MML, MGP, and JLF designed the experiments. MML, MGP, AP, GGR, and EV performed the experiments. MML, XX, TM, and FA analyzed and interpreted the data. FA, MTB, and JLF wrote the paper. RG, JAC, PR, and EA revised critically the manuscript. All authors edited drafts and approved the final version.

FUNDING

This study was supported by the following grants: FONDECYT 1120528 (JLF), Fondo Central de Investigación, Universidad de Chile ENL025/16 (JLF), ES090079 (JAC). Research in RG and EV laboratories is funded by Instituto Milenio iBio – Iniciativa Científica Milenio MINECON.

ACKNOWLEDGMENTS

The authors wish to thank Dr. Ana María Avalos for proofreading the article.

SUPPLEMENTARY MATERIAL

The Supplementary Material for this article can be found online at: https://www.frontiersin.org/articles/10.3389/fnmol.2018.00251/full#supplementary-material

REFERENCES

Aksoy-Aksel, A., Zampa, F., and Schratt, G. (2014). MicroRNAs and synaptic plasticity–a mutual relationship. *Philos. Trans. R. Soc. Lond. B Biol. Sci.* 369:20130515. doi: 10.1098/rstb.2013.0515

Alfarez, D. N., Joels, M., and Krugers, H. J. (2003). Chronic unpredictable stress impairs long-term potentiation in rat hippocampal CA1 area and dentate gyrus in vitro. *Eur. J. Neurosci.* 17, 1928–1934. doi: 10.1046/j.1460-9568.2003.02622.x

Avila, J. (2006). Tau phosphorylation and aggregation in Alzheimer's disease pathology. *FEBS Lett.* 580, 2922–2927. doi: 10.1016/j.febslet.2006.02.067

Bravo, J. A., Diaz-Veliz, G., Mora, S., Ulloa, J. L., Berthoud, V. M., Morales, P., et al. (2009). Desipramine prevents stress-induced changes in depressive-like behavior and hippocampal markers of neuroprotection. *Behav. Pharmacol.* 20, 273–285. doi: 10.1097/FBP.0b013e32832c70d9

Carlezon, W. A. Jr., Duman, R. S., and Nestler, E. J. (2005). The many faces of CREB. *Trends Neurosci.* 28, 436–445. doi: 10.1016/j.tins.2005.06.005

Castaneda, P., Munoz, M., Garcia-Rojo, G., Ulloa, J. L., Bravo, J. A., Marquez, R., et al. (2015). Association of N-cadherin levels and downstream effectors of Rho GTPases with dendritic spine loss induced by chronic stress in rat hippocampal neurons. *J. Neurosci. Res.* 93, 1476–1491. doi: 10.1002/jnr.23602

Chen, A. C., Shirayama, Y., Shin, K. H., Neve, R. L., and Duman, R. S. (2001). Expression of the cAMP response element binding protein (CREB) in hippocampus produces an antidepressant effect. *Biol. Psychiatry* 49, 753–762. doi: 10.1016/S0006-3223(00)01114-8

Chrousos, G. P., and Harris, A. G. (1998). Hypothalamic-pituitary-adrenal axis suppression and inhaled corticosteroid therapy. 2. *Neuroimmunomodulation* 5, 288–308. doi: 10.1159/000026349

Cohen, J. E., Lee, P. R., Chen, S., Li, W., and Fields, R. D. (2011). MicroRNA regulation of homeostatic synaptic plasticity. *Proc. Natl. Acad. Sci. U.S.A.* 108, 11650–11655. doi: 10.1073/pnas.1017576108

Cohen, J. E., Lee, P. R., and Fields, R. D. (2014). Systematic identification of 3′-UTR regulatory elements in activity-dependent mRNA stability in hippocampal neurons. *Philos. Trans. R. Soc. Lond. B Biol. Sci.* 369:20130509. doi: 10.1098/rstb.2013.0509

Conrad, C. D., Galea, L. A., Kuroda, Y., and Mcewen, B. S. (1996). Chronic stress impairs rat spatial memory on the Y maze, and this effect is blocked by tianeptine pretreatment. *Behav. Neurosci.* 110, 1321–1334. doi: 10.1037/0735-7044.110.6.1321

Dickson, B. J. (2002). Molecular mechanisms of axon guidance. *Science* 298, 1959–1964. doi: 10.1126/science.1072165

Fanselow, M. S., and Dong, H. W. (2010). Are the dorsal and ventral hippocampus functionally distinct structures? *Neuron* 65, 7–19. doi: 10.1016/j.neuron.2009.11.031

Fernandez-Guasti, A., Fiedler, J. L., Herrera, L., and Handa, R. J. (2012). Sex, stress, and mood disorders: at the intersection of adrenal and gonadal hormones. *Horm. Metab. Res.* 44, 607–618. doi: 10.1055/s-0032-1312592

Fiore, R., Khudayberdiev, S., Christensen, M., Siegel, G., Flavell, S. W., Kim, T. K., et al. (2009). Mef2-mediated transcription of the miR379-410 cluster regulates activity-dependent dendritogenesis by fine-tuning Pumilio2 protein levels. *EMBO J.* 28, 697–710. doi: 10.1038/emboj.2009.10

Garcia-Rojo, G., Fresno, C., Vilches, N., Diaz-Veliz, G., Mora, S., Aguayo, F., et al. (2017). The ROCK inhibitor fasudil prevents chronic restraint stress-induced depressive-like behaviors and dendritic spine loss in rat hippocampus. *Int. J. Neuropsychopharmacol.* 20, 336–345. doi: 10.1093/ijnp/pyw108

Guan, J. S., Haggarty, S. J., Giacometti, E., Dannenberg, J. H., Joseph, N., Gao, J., et al. (2009). HDAC2 negatively regulates memory formation and synaptic plasticity. *Nature* 459, 55–60. doi: 10.1038/nature07925

He, M., Liu, Y., Wang, X., Zhang, M. Q., Hannon, G. J., and Huang, Z. J. (2012). Cell-type-based analysis of microRNA profiles in the mouse brain. *Neuron* 73, 35–48. doi: 10.1016/j.neuron.2011.11.010

Hollins, S. L., and Cairns, M. J. (2016). MicroRNA: small RNA mediators of the brains genomic response to environmental stress. *Prog. Neurobiol.* 143, 61–81. doi: 10.1016/j.pneurobio.2016.06.005

Jin, J., Kim, S. N., Liu, X., Zhang, H., Zhang, C., Seo, J. S., et al. (2016). miR-17-92 cluster regulates adult hippocampal neurogenesis, anxiety, and depression. *Cell Rep.* 16, 1653–1663. doi: 10.1016/j.celrep.2016.06.101

Joels, M., and Baram, T. Z. (2009). The neuro-symphony of stress. *Nat. Rev. Neurosci.* 10, 459–466. doi: 10.1038/nrn2632

Jordan, J., Galindo, M. F., Prehn, J. H., Weichselbaum, R. R., Beckett, M., Ghadge, G. D., et al. (1997). p53 expression induces apoptosis in hippocampal pyramidal neuron cultures. *J. Neurosci.* 17, 1397–1405. doi: 10.1523/JNEUROSCI.17-04-01397.1997

Kadmiel, M., Janoshazi, A., Xu, X., and Cidlowski, J. A. (2016). Glucocorticoid action in human corneal epithelial cells establishes roles for corticosteroids in wound healing and barrier function of the eye. *Exp. Eye Res.* 152, 10–33. doi: 10.1016/j.exer.2016.08.020

Kim, E. J., Pellman, B., and Kim, J. J. (2015). Stress effects on the hippocampus: a critical review. *Learn. Mem.* 22, 411–416. doi: 10.1101/lm.037291.114

Koleske, A. J. (2013). Molecular mechanisms of dendrite stability. *Nat. Rev. Neurosci.* 14, 536–550. doi: 10.1038/nrn3486

Koshiol, J., Wang, E., Zhao, Y., Marincola, F., and Landi, M. T. (2010). Strengths and limitations of laboratory procedures for microRNA detection. *Cancer Epidemiol. Biomarkers Prev.* 19, 907–911. doi: 10.1158/1055-9965.EPI-10-0071

Letellier, M., Elramah, S., Mondin, M., Soula, A., Penn, A., Choquet, D., et al. (2014). miR-92a regulates expression of synaptic GluA1-containing AMPA receptors during homeostatic scaling. *Nat. Neurosci.* 17, 1040–1042. doi: 10.1038/nn.3762

Li, Y., Li, S., Yan, J., Wang, D., Yin, R., Zhao, L., et al. (2016). miR-182 (microRNA-182) suppression in the hippocampus evokes antidepressant-like effects in rats. *Prog. Neuropsychopharmacol. Biol. Psychiatry* 65, 96–103. doi: 10.1016/j.pnpbp.2015.09.004

Lopes, S., Vaz-Silva, J., Pinto, V., Dalla, C., Kokras, N., Bedenk, B., et al. (2016). Tau protein is essential for stress-induced brain pathology. *Proc. Natl. Acad. Sci. U.S.A.* 113, E3755–E3763. doi: 10.1073/pnas.1600953113

MacQueen, G. M., Campbell, S., Mcewen, B. S., Macdonald, K., Amano, S., Joffe, R. T., et al. (2003). Course of illness, hippocampal function, and hippocampal volume in major depression. *Proc. Natl. Acad. Sci. U.S.A.* 100, 1387–1392. doi: 10.1073/pnas.0337481100

Malykhin, N. V., and Coupland, N. J. (2015). Hippocampal neuroplasticity in major depressive disorder. *Neuroscience* 309, 200–213. doi: 10.1016/j.neuroscience.2015.04.047

Marsden, W. N. (2013). Synaptic plasticity in depression: molecular, cellular and functional correlates. *Prog. Neuropsychopharmacol. Biol. Psychiatry* 43, 168–184. doi: 10.1016/j.pnpbp.2012.12.012

Marti, E., Pantano, L., Banez-Coronel, M., Llorens, F., Minones-Moyano, E., Porta, S., et al. (2010). A myriad of miRNA variants in control and Huntington's disease brain regions detected by massively parallel sequencing. *Nucleic Acids Res.* 38, 7219–7235. doi: 10.1093/nar/gkq575

McEwen, B. S., and Gianaros, P. J. (2010). Central role of the brain in stress and adaptation: links to socioeconomic status, health, and disease. *Ann. N. Y. Acad. Sci.* 1186, 190–222. doi: 10.1111/j.1749-6632.2009.05331.x

Meerson, A., Cacheaux, L., Goosens, K. A., Sapolsky, R. M., Soreq, H., and Kaufer, D. (2010). Changes in brain MicroRNAs contribute to cholinergic stress reactions. *J. Mol. Neurosci.* 40, 47–55. doi: 10.1007/s12031-009-9252-1

Miller, R. M., Marriott, D., Trotter, J., Hammond, T., Lyman, D., Call, T., et al. (2018). Running exercise mitigates the negative consequences of chronic stress on dorsal hippocampal long-term potentiation in male mice. *Neurobiol. Learn. Mem.* 149, 28–38. doi: 10.1016/j.nlm.2018.01.008

Moreira, P. S., Almeida, P. R., Leite-Almeida, H., Sousa, N., and Costa, P. (2016). Impact of chronic stress protocols in learning and memory in rodents: systematic review and meta-analysis. *PLoS One* 11:e0163245. doi: 10.1371/journal.pone.0163245

Morey, J. S., Ryan, J. C., and Van Dolah, F. M. (2006). Microarray validation: factors influencing correlation between oligonucleotide microarrays and real-time PCR. *Biol. Proced. Online* 8, 175–193. doi: 10.1251/bpo126

Nakade, Y., Fukuda, H., Iwa, M., Tsukamoto, K., Yanagi, H., Yamamura, T., et al. (2007). Restraint stress stimulates colonic motility via central corticotropin-releasing factor and peripheral 5-HT3 receptors in conscious rats. *Am. J. Physiol. Gastrointest. Liver Physiol.* 292, G1037–G1044. doi: 10.1152/ajpgi.00419.2006

Pacheco, A., Aguayo, F. I., Aliaga, E., Munoz, M., Garcia-Rojo, G., Olave, F. A., et al. (2017). Chronic stress triggers expression of immediate early genes and differentially affects the expression of AMPA and NMDA subunits in dorsal and ventral hippocampus of rats. *Front. Mol. Neurosci.* 10:244. doi: 10.3389/fnmol.2017.00244

Pavlides, C., Nivon, L. G., and Mcewen, B. S. (2002). Effects of chronic stress on hippocampal long-term potentiation. *Hippocampus* 12, 245–257. doi: 10.1002/hipo.1116

Paxinos, G. (1982). *The Rat Brain in Stereotaxic Coordinates*. Sydney: Academic Press.

Pinto, V., Costa, J. C., Morgado, P., Mota, C., Miranda, A., Bravo, F. V., et al. (2015). Differential impact of chronic stress along the hippocampal dorsal-ventral axis. *Brain Struct. Funct.* 220, 1205–1212. doi: 10.1007/s00429-014-0713-0

Pittenger, C., and Duman, R. S. (2008). Stress, depression, and neuroplasticity: a convergence of mechanisms. *Neuropsychopharmacology* 33, 88–109. doi: 10.1038/sj.npp.1301574

Reus, G. Z., Titus, S. E., Abelaira, H. M., Freitas, S. M., Tuon, T., Quevedo, J., et al. (2016). Neurochemical correlation between major depressive disorder and neurodegenerative diseases. *Life Sci.* 158, 121–129. doi: 10.1016/j.lfs.2016.06.027

Rinaldi, A., Vincenti, S., De Vito, F., Bozzoni, I., Oliverio, A., Presutti, C., et al. (2010). Stress induces region specific alterations in microRNAs expression in mice. *Behav. Brain Res.* 208, 265–269. doi: 10.1016/j.bbr.2009.11.012

Ruegger, S., and Grosshans, H. (2012). MicroRNA turnover: when, how, and why. *Trends Biochem. Sci.* 37, 436–446. doi: 10.1016/j.tibs.2012.07.002

Sailaja, B. S., Cohen-Carmon, D., Zimmerman, G., Soreq, H., and Meshorer, E. (2012). Stress-induced epigenetic transcriptional memory of acetylcholinesterase by HDAC4. *Proc. Natl. Acad. Sci. U.S.A.* 109, E3687–E3695. doi: 10.1073/pnas.1209990110

Sanchez-Hidalgo, A. C., Munoz, M. F., Herrera, A. J., Espinosa-Oliva, A. M., Stowell, R., Ayala, A., et al. (2016). Chronic stress alters the expression levels of longevity-related genes in the rat hippocampus. *Neurochem. Int.* 97, 181–192. doi: 10.1016/j.neuint.2016.04.009

Sando, R. III, Gounko, N., Pieraut, S., Liao, L., Yates, J. III, and Maximov, A. (2012). HDAC4 governs a transcriptional program essential for synaptic plasticity and memory. *Cell* 151, 821–834. doi: 10.1016/j.cell.2012.09.037

Shen, K., and Cowan, C. W. (2010). Guidance molecules in synapse formation and plasticity. *Cold Spring Harb. Perspect. Biol.* 2:a001842. doi: 10.1101/cshperspect.a001842

Siegel, G., Obernosterer, G., Fiore, R., Oehmen, M., Bicker, S., Christensen, M., et al. (2009). A functional screen implicates microRNA-138-dependent regulation of the depalmitoylation enzyme APT1 in dendritic spine morphogenesis. *Nat. Cell Biol.* 11, 705–716. doi: 10.1038/ncb1876

Smith, M. A., Makino, S., Kvetnansky, R., and Post, R. M. (1995). Stress and glucocorticoids affect the expression of brain-derived neurotrophic factor and neurotrophin-3 mRNAs in the hippocampus. *J. Neurosci.* 15, 1768–1777. doi: 10.1523/JNEUROSCI.15-03-01768.1995

Stephenson, F. A., Cousins, S. L., and Kenny, A. V. (2008). Assembly and forward trafficking of NMDA receptors (Review). *Mol. Membr. Biol.* 25, 311–320. doi: 10.1080/09687680801971367

Sterner, E. Y., and Kalynchuk, L. E. (2010). Behavioral and neurobiological consequences of prolonged glucocorticoid exposure in rats: relevance to depression. *Prog. Neuropsychopharmacol. Biol. Psychiatry* 34, 777–790. doi: 10.1016/j.pnpbp.2010.03.005

Tan, W., Li, Y., Lim, S. G., and Tan, T. M. (2014). miR-106b-25/miR-17-92 clusters: polycistrons with oncogenic roles in hepatocellular carcinoma. *World J. Gastroenterol.* 20, 5962–5972. doi: 10.3748/wjg.v20.i20.5962

Ulloa, J. L., Castaneda, P., Berrios, C., Diaz-Veliz, G., Mora, S., Bravo, J. A., et al. (2010). Comparison of the antidepressant sertraline on differential depression-like behaviors elicited by restraint stress and repeated corticosterone administration. *Pharmacol. Biochem. Behav.* 97, 213–221. doi: 10.1016/j.pbb.2010.08.001

Vetere, G., Barbato, C., Pezzola, S., Frisone, P., Aceti, M., Ciotti, M., et al. (2014). Selective inhibition of miR-92 in hippocampal neurons alters contextual fear memory. *Hippocampus* 24, 1458–1465. doi: 10.1002/hipo.22326

White, A. O., and Wood, M. A. (2014). Does stress remove the HDAC brakes for the formation and persistence of long-term memory? *Neurobiol. Learn. Mem.* 112, 61–67. doi: 10.1016/j.nlm.2013.10.007

Winter, J. (2015). MicroRNAs of the miR379-410 cluster: new players in embryonic neurogenesis and regulators of neuronal function. *Neurogenesis* 2:e1004970. doi: 10.1080/23262133.2015.1004970

Xin, H., Katakowski, M., Wang, F., Qian, J. Y., Liu, X. S., Ali, M. M., et al. (2017). MicroRNA cluster miR-17-92 cluster in exosomes enhance neuroplasticity and functional recovery after stroke in rats. *Stroke* 48, 747–753. doi: 10.1161/STROKEAHA.116.015204

Zhang, J. C., Yao, W., Qu, Y., Nakamura, M., Dong, C., Yang, C., et al. (2017). Increased EphA4-ephexin1 signaling in the medial prefrontal cortex plays a role in depression-like phenotype. *Sci. Rep.* 7, 1–14. doi: 10.1038/s41598-017-07325-2

Zhou, M., Wang, M., Wang, X., Liu, K., Wan, Y., Li, M., et al. (2017). Abnormal expression of MicroRNAs induced by chronic unpredictable mild stress in rat hippocampal tissues. *Mol. Neurobiol.* 55, 917–935. doi: 10.1007/s12035-016-0365-6

Conflict of Interest Statement: The authors declare that the research was conducted in the absence of any commercial or financial relationships that could be construed as a potential conflict of interest.

frontiers in Cellular Neuroscience

ORIGINAL RESEARCH
published: 11 January 2018
doi: 10.3389/fncel.2017.00434

Systematic Analysis of mRNA and miRNA Expression of 3D-Cultured Neural Stem Cells (NSCs) in Spaceflight

Yi Cui[1†], Jin Han[2†], Zhifeng Xiao[2], Yiduo Qi[2], Yannan Zhao[2], Bing Chen[2], Yongxiang Fang[3], Sumei Liu[2], Xianming Wu[2] and Jianwu Dai[2*]*

[1] Reproductive and Genetic Center of National Research Institute for Family Planning, Beijing, China, [2] Key Laboratory of Molecular Developmental Biology, Institute of Genetics and Developmental Biology, Chinese Academy of Sciences, Beijing, China, [3] State Key Laboratory of Veterinary Etiological Biology, Key Laboratory of Veterinary Public Health of Ministry of Agriculture, Lanzhou Veterinary Research Institute, Chinese Academy of Agricultural Sciences, Lanzhou, China

Recently, with the development of the space program there are growing concerns about the influence of spaceflight on tissue engineering. The purpose of this study was thus to determine the variations of neural stem cells (NSCs) during spaceflight. RNA-Sequencing (RNA-Seq) based transcriptomic profiling of NSCs identified many differentially expressed mRNAs and miRNAs between space and earth groups. Subsequently, those genes with differential expression were subjected to bioinformatic evaluation using gene ontology (GO), Kyoto Encyclopedia of Genes and Genomes pathway (KEGG) and miRNA-mRNA network analyses. The results showed that NSCs maintain greater stemness ability during spaceflight although the growth rate of NSCs was slowed down. Furthermore, the results indicated that NSCs tended to differentiate into neuron in outer space conditions. Detailed genomic analyses of NSCs during spaceflight will help us to elucidate the molecular mechanisms behind their differentiation and proliferation when they are in outer space.

Keywords: spaceflight, RNA-seq, 3D culture, NSCs, stemness, differentiation

OPEN ACCESS

Edited by:
Reinhard Schliebs, Paul Flechsig Institute of Brain Research, Leipzig University, Germany

Reviewed by:
Jens Christian Schwamborn, University of Luxembourg, Luxembourg
Seiji Hitoshi, Shiga University of Medical Science, Japan

***Correspondence:**
Jianwu Dai
jwdai@genetics.ac.cn
Jin Han
jin_han@genetics.ac.cn

[†] These authors have contributed equally to this work.

Received: *10 October 2017*
Accepted: *26 December 2017*
Published: *11 January 2018*

Citation:
Cui Y, Han J, Xiao Z, Qi Y, Zhao Y, Chen B, Fang Y, Liu S, Wu X and Dai J (2018) Systematic Analysis of mRNA and miRNA Expression of 3D-Cultured Neural Stem Cells (NSCs) in Spaceflight. Front. Cell. Neurosci. 11:434. doi: 10.3389/fncel.2017.00434

INTRODUCTION

Numerous studies have demonstrated that spaceflight can affect many systems of the human body, such as the skeleton system, nervous system, and cardiovascular system (Riley et al., 1990; Baisch et al., 2000; Campbell and Charles, 2015). It is well known that the physical microenvironment and mechanical stress induce various changes in cellular metabolism, cellular morphology, cell signaling pathway, and cell secretion, among others. Numerous recent studies have specifically focused on the effect of outer space on tissue regeneration by various mechanisms. The environment in outer space induces a cascade of reactions associated with changes to the cytoskeleton, cell cycle, cell structure and function (Wang et al., 2003; Pani et al., 2016). For the successful exploration of space, it is extremely important to explore the mechanism behind such alterations in physical, chemical and biological processes.

Neural stem cells (NSCs) are important seed cells in tissue engineering, which have been regarded as an effective therapy for many neurological diseases. Nerve regeneration through stem-cell-based therapy is a promising treatment for Parkinson's disease, Alzheimer's disease, and other nerve disorders (Marsh and Blurton-Jones, 2017). However, there are still many problems

associated with the clinical application of NSCs, just as the directional differentiation of NSCs was difficult. The vast majority of grafted NSCs differentiate into astrocyte cells, with only a few differentiating into neurons *in vivo* (Zhang et al., 2016). Previous studies suggested that simulated microgravity and spaceflight may influence the proliferation and differentiation status of various kinds of stem cells (Meyers et al., 2004; Zayzafoon et al., 2004; Yuge et al., 2006; Wang et al., 2007; Chen et al., 2011; Zhang et al., 2013; Blaber et al., 2015). In this study we attempted to determine the effect of spaceflight on the growth and differentiation status of NSCs. NSCs were cultured in proliferation medium and differentiation medium separately for 12 days during space flight of in the shuttle Space Transportation SJ-10 and compared with those grown under similar conditions on Earth (**Figure 1**).

It has been demonstrated that a three-dimensional (3D) culture system can recreate a 3D environment that is closer to physiological conditions in terms of cell growth and function (Griffith and Swartz, 2006; Asthana and Kisaalita, 2013). 3D cell culture have been widely used in mechanistic studies of stem cell, disease modeling and pre-clinical drug screening (Brito et al., 2012; Liedmann et al., 2012; Knight and Przyborski, 2015). In this study we used a 3D culture system to evaluate the effect of spaceflight on NSCs. For differentiation analysis, we seeded cells on a 3D collagen sponge scaffold and cultured them in differentiation medium. In proliferation medium the NSCs were amplified by 3D spheroid culture. RNA-Seq analysis was also performed in combination with immunostaining, the results of which indicated that the NSCs retained their stemness during spaceflight, although their proliferative capacity was inhibited. Moreover, the differentiation of NSCs was promoted in the space group. The results also indicated that NSCs readily differentiate into neurons in space.

MATERIALS AND METHODS

Spaceflight Cell Culture Equipment

The spaceflight cell culture experiment was performed in fully automated bioreactors which designed by Shanghai institute of technical physics of the Chinese academy of sciences (China). The automatic cell culture device containing three layers, the culture chamber in the upper and the middle layer, was used to culture NSCs, in which the culture medium could be exchanged automatically. Images of the NSCs cultured in the proliferation medium were recorded by an automatic image acquisition system and transmitted back to the data center on the earth. NSCs cultured in the same device on the earth, were set as a control group. At the end of the 12-day spaceflight, the cells were washed and conserved in RNAlater stabilization reagent or paraformaldehyde by an automatic medium exchange device.

Cell Culture

The NSCs were isolated from rat telencephalon tissues in accordance with a previously described procedure, with slight modifications (Han et al., 2008). All animal experimental procedures were performed in accordance with the Chinese Ministry of Public Health (CMPH) Guide for the Care and Use of Laboratory Animals which was approved by the IACUC Bioethics Committee (IACUC, Institutional Animal Care and Use Committee-Bioethics Committee) of the Institute of Genetics and Developmental Biology, Chinese Academy of Sciences. For proliferation analysis, the cells were suspended at a density of 1×10^6 per chamber in a growth medium consisting of Dulbecco's modified Eagles medium (DMEM) plus Ham's F-12 supplemented with 1% (v/v) antibiotic-antimycotic mixed stock solution, 2% (v/v) B-27 Supplement, 20 ng/mL EGF and 20 ng/mL bFGF. For differentiation analysis, the cells were seeded on a collagen sponge scaffold (3×10^5 cells per collagen scaffold) and then cultured in the differentiation medium [DMEM plus Ham's F-12 supplemented with 1% (v/v) antibiotic-antimycotic mixed stock solution and 1% (v/v) N-2 supplement] (**Figure 1**). At the end of the cell culture, cells were fixed in RNAlater stabilization reagent or paraformaldehyde.

Collagen Sponge Scaffold Preparation

The collagen sponge was prepared as described previously (Chen et al., 2007). Bovine collagen of spongy bone was selected as the raw material. The size of the collagen sponge used to culture NSCs was approximately 5 mm in diameter and 1mm in thickness. The 3D microstructure of the collagen sponge scaffolds

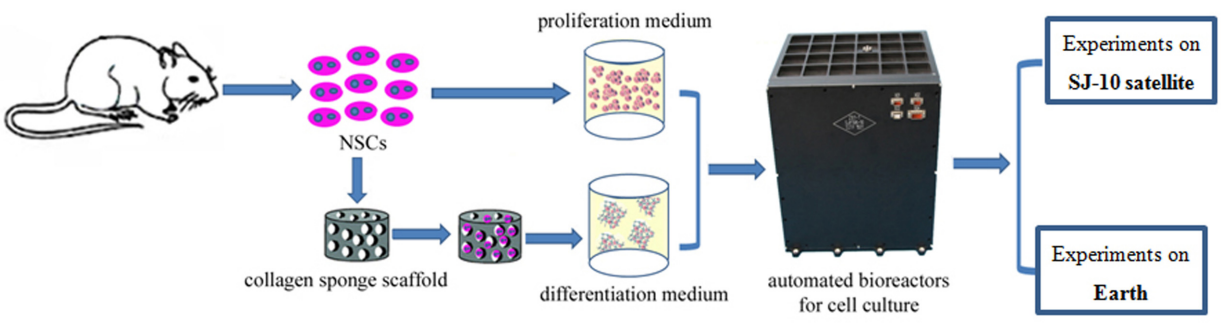

FIGURE 1 | Flow diagram of illustrating the workflow of cell culture conditions of NSCs in the space and ground group.

was observed by a scanning electron microscope (SEM, S-3000N; Hitachi, Tokyo, Japan).

FDA/PI Staining of the NSCs

The combined use of the fluorescein diacetate (FDA) and propidium iodide (PI) is one of the most common fluorescence-based methods to assess the viability of cells. The principle of such staining is that PI can only cross membranes of non-viable cells whereas FDA is metabolized by viable cells, which leads to fluorescein fluorescence. Cells were incubated with this staining solution for 4–5 min at room temperature in the dark, and then the staining solution was removed and phosphate buffered solution (PBS) was added. The staining solution contained 100 μg/ml FDA (5 mg/mL in acetone; Sigma Chemical, St. Louis, MO, United States) and 60 μg/ml PI (2 mg/mL in PBS; Calbiochem,). Samples were analyzed using the Zeiss 200 inverted fluorescent microscope (Carl Zeiss, Jena, Germany).

RNA Extraction

The extraction of total RNA was performed using Trizol reagent (Sigma Chemical, St. Louis, MO, United States), in accordance with the manufacturer's instructions. Briefly, RNA was extracted from the NSCs of the two groups which consisted of polls of three biological replicates. Isolated RNA was purified using the RNeasy Plant Mini Kit (Qiagen Sciences, Valencia, CA, United States). The concentration and integrity of RNA were assessed using agarose gel and the ND-1000 NanoDrop spectrophotometer 2000 (NanoDrop Technologies, Wilmington, DE, United States). A total of 1 μg of RNA from each of two biological replicates was pooled for RNA-Seq library preparation.

RNA-Seq cDNA Library Preparation and Sequencing

Genome-wide transcriptional profiling of NSCs samples from the space and ground groups was performed by RNA-Seq. A total of 12 samples were sequenced for each treatment (groups of proliferating or differentiating NSCs cultured in space or on the earth; three biological replicates per group). The RNA library construction and RNA-Seq were performed using Illumina Genome analyzer IIx Hiseq X. Transcriptome libraries for the Illumina X Ten platform were prepared from the total RNA using Illumina's TruSeq Stranded mRNA LT Sample Prep Kit (Illumina, San Diego, CA, United States), in accordance with the manufacturer's protocol. Sequencing took place on an Illumina X Ten sequencer with 150-bp paired-end reads.

Real-Time PCR Analysis

To validate the RNA-Seq results, we performed qRT-PCR on 16 selected DEGs. Nine of the selected DEGs were stemness-related genes and the rest of seven DEGs were differentiation-related genes. The cDNA samples were generated using the HiScript II Q RT SuperMix for qPCR System (Vazyme, R223-01), in accordance with the manufacturer's instructions. The standard conditions used for real-time PCR were as follows: 95°C for 10 min, followed by 40 cycles of 15 s of denaturation at 95°C and 30 s of annealing/elongation at 55°C. The SYBR® Green signal was measured in each step and each sample was normalized to ACTB as an internal control. Sequences for these primers are listed in **Table 1**. Mean fold gene expression was calculated with the $2^{-\Delta\Delta C_T}$ method (Livak and Schmittgen, 2001). Q-PCR amplification was performed using an ABI 9700 thermocycler (Applied Biosystems Inc., Foster City, CA, United States).

RNA-Seq Data Analysis

The raw sequencing reads were processed through many steps of quality filtering. First, their quality was estimated using the NGS QC Toolkit. Second, low-quality bases and the reads containing ploy-N regions were removed to obtain clean reads. Then the clean reads were mapped to a reference rat genome using TopHat[1] to identify known and novel splice junctions and to generate read alignments for each sample (Kim et al., 2013). The Fragments Per Kilobase of transcript per million mapped reads (FPKM) value of each gene was calculated and normalized using Cufflinks (Trapnell et al., 2012). The read counts of genes in the two groups were obtained using htseq-count (Anders et al., 2015). DEGs were identified using the DESeq functional estimator SizeFactors and nbinomTest (Anders and Huber, 2012). Multiple-test-corrected p-value < 0.05 and absolute fold change > 2 were set as the thresholds for screening significantly differentially expressed genes.

Gene Ontology and KEGG Enrichment Analysis

Differentially expressed genes were extracted and transferred to Entrez IDs, and then these IDs were imported into the R package clusterProfiler to perform Gene Ontology (GO) enrichment analysis (Yu et al., 2012). GO terms with a multiple-test-corrected p-value of <0.05 were defined as being enriched. Non-redundant GO enriched terms were selected and plotted using in-house scripts. KEGG enrichment analysis was performed using clusterProfiler, also with the default parameters.

Regulatory Network Construction

The String database and the BioGrid database were used to extract well-curated interaction genes of before screened DEG genes (Szklarczyk et al., 2015; Chatr-Aryamontri et al., 2017). Then, the expression data of all genes were extracted and imported into Cytoscape (Shannon et al., 2003). The coexpression network was constructed using the ExpressionCorrelation plugin and displayed in Cytoscape. Then, a prefuse force network algorithm was used to generate coregulatory clusters and an attribute circle layout was used to place nodes of each subcluster. Differentially expressed miRNAs were screened using DESeq2 with the thresholds of multiple -hypothesis-corrected p-value < 0.05 and absolute fold

[1]http://tophat.cbcb.umd.edu/

TABLE 1 | The primers of real-time PCR.

No.	Gene symbol	Forward primer	Reverse primer	Product length (bp)	Ta (°C)
1	**Ki67**	TGTGACTGAAGAGCCCATAC	TCTGTGCCGAAGACTCCTTAAA	125	60
2	**Cdkn2b**	TTTGTGGTTGGTTGGTTAGTT	AGTGGTAGCTGGACTTGAG	100	60
3	**Cdkn2a**	GCTCTCCTGCTCTCCTATG	AGAGTGTCTAGGAAGCCC	101	60
4	**Cdk1**	GTCTATGATCCAGCCAAACG	GGACTTCCAGAGGGTTACA	104	60
5	**Cdk12**	GTCTCTGTGGTAGTCCTTGTC	TCTTAGGCGTCTCCTGTATTG	101	60
6	**Pten**	GTGGTGACATCAAAGTAGAGT	GGTCCTGGTATGAAGAACG	100	60
7	**Hdac2**	ACCAAAGGAGCCAAATCAG	GCGAAGGTTTCTTATCCCAG	102	60
8	**Wnt5a**	TTGGTTTGCCACTACTACTGT	GACCCTTGCTTTCTTCCCATAA	111	60
9	**Id3**	CTTAAACTTTGCTCTCCAACC	CAATGGCTAGGCTACGTTC	100	60
10	**Neurog2**	CCAGGGACTGTATCTAGAGC	TCTGTGAAGTGGAGTGCG	111	60
11	**Ezh2**	ATCAGTGTGCTGGAGTCAA	AGAGGAACTGGAAGTCTCAT	117	60
12	**Ncam1**	GTCTGCATCGCTGAGAACAA	ATGGCTGTCTGATTCTCTACAT	101	60
13	Sox2	TACAGCATGTCCTACTCGCA	GAGTGGGAGGAAGAGGTAAC	116	60
14	Notch1	AGGCTTCAGTGGCCCTAA	TTTGTACCCAGCGACATCAT	100	60
15	Pax6	GTCCATCTTTGCTTGGGAAAT	GGTTGCGAAGAACTCTGTTTA	104	60
16	Actb	CCACCATGTACCCAGGCATT	CGGACTCATCGTACTCCTGC	189	60

change > 2. The target genes of these miRNAs were predicted using miRanda (matching score higher than 150 and binding energy less than −30 kcal/mol), and further filtered using expression correlation. The miRNA-target gene regulation network was also constructed using Cytoscape with the prefuse force directed layout algorithm.

Immunofluorescence Staining Analysis

The differentiation status of the NSCs was also assessed by immunofluorescence staining, in accordance with a slightly modified version of procedures in previously published papers (Cui et al., 2016). For immunofluorescence staining analysis, cells were incubated with the primary antibodies Tuj1 (1:500,05-549, Upstate), Map-2 (1:400; M1406, Sigma), and GFAP (1:200; MAB360, Millipore) overnight at 4°C. The secondary antibodies were anti-mouse IgG FITC antibody (1:200; 31547, Invitrogen) and anti-rabbit IgG FITC antibody (1:1000; 31635, Invitrogen) diluted in blocking buffer. Nuclei are counter-stained with Hochest 33342 (1:500; Sigma). The fluorescent images of 3D-cultured NSCs were visualized on a Leica TCS SP5 scanning laser confocal fluorescence microscope (Leica Microsystems). The number of immunostained cells was counted in each of three random fields per well and the fluorescence images were selected randomly. Quantification of the immunofluorescence signal was performed using Image-Pro Plus software (Media Cybernetics, Bethesda, MD, United States).

Statistical Analysis

All values are expressed as mean ± SD (n = 3) and differences were considered significant when $p < 0.05$. The Shapiro–Wilk test was performed to check the normality of all the variables. Data were analyzed statistically by one-way analysis of variance (ANOVA) and the Student's t-test, using SPSS 17.0 software (SPSS GmbH, Munich, Germany).

Accession Number

The cDNA and miRNA sequencing data from space-flighting NSCs have been submitted to the NCBI Sequence Read Archive[2] under accession number SRP126507.

RESULTS

The Stemness and Proliferative Ability of NSCs during Spaceflight

When the satellite returned to earth, we performed FDA/PI staining to determine the cell viability of NSCs. The FDA/PI staining results showed that neurospheres possessed excellent cell viability when they were cultured in proliferation medium (**Figure 2A**). The proliferative process of NSCs could be recorded by an automatic imaging device during spaceflight. The images transmitted from the satellite indicated a decrease in neurosphere volume of the NSCs during spaceflight (**Figure 2B**).

We attempted to determine whether the proliferation status of NSCs was affected during spaceflight and whether NSCs maintain their stemness under such conditions. A heatmap of hierarchical clustering was created for selected DEGs related to stemness or proliferation using the FPKM values between the space and ground groups (**Figure 2C**). The data presented here show that the expression of cell proliferation marker Ki67 was downregulated during spaceflight. Also, the expression of cyclin-dependent kinases Cdk1 is down-regulated, on the contrary, the expression of negative cell cycle regulator Cdkn2a and Cdkn2b were up-regulated during spaceflight as shown in **Figure 2C**. Some cell cycle regulators play an important role in influencing proliferation, the decreased cell proliferation may be a result of cell cycle arrest. As a key process in cell proliferation, the alteration of the length of the cell cycle is associated with

[2]https://trace.ncbi.nlm.nih.gov/Traces/sra/sra.cgi?

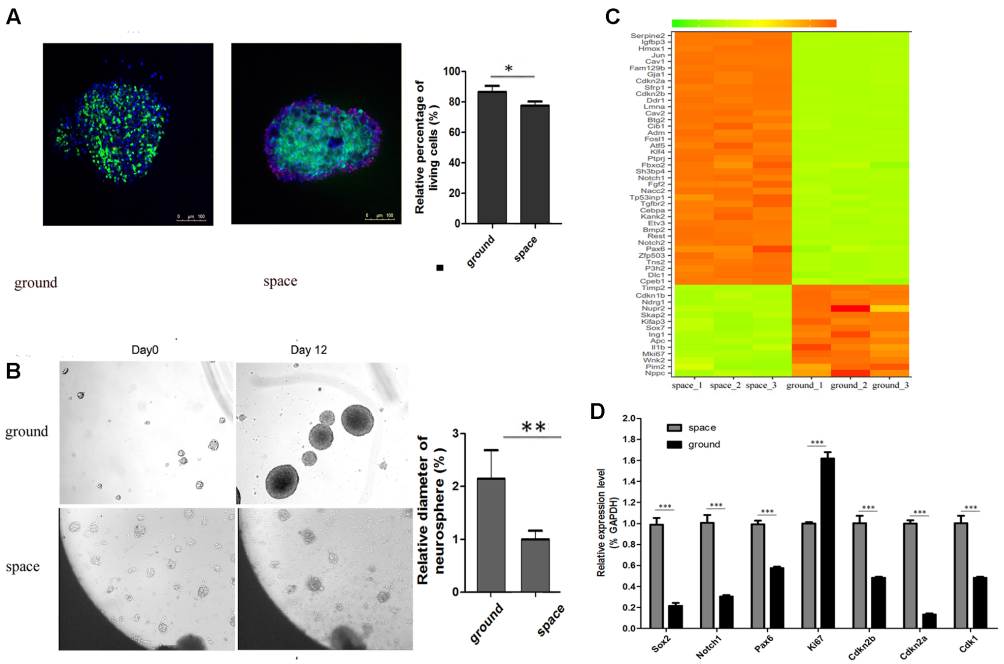

FIGURE 2 | Neurosphere formation of NSCs during spaceflight. **(A)** Representative cell images of the FDA/PI staining of neuroshpheres. **(B)** Representative images of the neurosphere formation process of NSCs during spaceflight. The ground group was set as a control. **(C)** Hierarchical clustering analysis of expression profiles of proliferation-related genes in the proliferating NSCs. Red color indicates a higher *z*-score, while green indicates a lower one. **(D)** The expression levels of stemness and proliferation-related gene were quantified by real-time PCR. ACTB was used as an internal control. Data are presented as mean ± SD of three different experiments. $*p < 0.05$; $**p < 0.01$, $***p < 0.001$ vs. the ground group.

a switch between proliferation and differentiation. Moreover, the transcription factor Pax6 is essential for NSC proliferation, multipotency, and neurogenesis. Increased expression of Pax6 positively promote NSC self-renewal and neurogenesis (Osumi et al., 2008; Sansom et al., 2009; Curto et al., 2014; Gan et al., 2014). The Notch1 signaling pathway has also been demonstrated to control NSC fate (Kiparissides et al., 2011; Zhou et al., 2014; Stergiopoulos and Politis, 2016). The heatmap results indicated that the expression of several key stemness-related genes was upregulated in the Space group. Apart from these cell-cycle and transcription-factor-related genes, the expression of many well-known stemness-related genes such as Rest and Klf4 was also upregulated in the space group (Johnson et al., 2008; Yang et al., 2012; Cui et al., 2014; Zhang et al., 2015).

Furthermore, the validity of RAN-Seq data was confirmed by consistent findings of gene expression changes in the qPCR data analysis (**Figure 2D**). Consistent with the RNA-Seq results, the qPCR results indicated that the expression of the six selected genes was upregulated in the space group. Since the transcription factor Sox2 plays a key role in the maintenance of NSC properties, including proliferation/ survival, self-renewal and neurogenesis (Pevny and Nicolis, 2010; Andreu-Agullo et al., 2011; Thiel, 2013), we also determined the expression of Sox2 by qPCR analysis. Although the RNA-Seq data indicated that there was no notable difference in Sox2 expression between the space and ground groups, the qPCR results demonstrated that the expression of Sox2 was upregulated in the space group.

The Differentiation of NSCs Was Promoted during Spaceflight

Before spaceflight, a single cell suspension of NSCs were seeded on each of the collagen sponge scaffolds, after which the scaffolds were put in the differentiation medium. As shown in a representative SEM image, the seeded NSCs attached well to the scaffold via cytoplasmic extensions and lamellipodia (**Figure 3A**, middle). The SEM results indicated that collagen sponge scaffolds have good biocompatibility with NSCs. Moreover, the FDA/PI staining results showed that 3D-cultured NSCs possessed excellent cell viability when they returned from outer space (**Figure 3A**, right). To further assess the effects of being in space on the neural differentiation of 3D-cultured NSCs, the expression levels of an early neuron marker (Tuj1, neuron -specific tubulin III), an astrocyte marker (Gfap) and a mature neuron marker (Map2) were assayed by immunofluorescence staining. We found that the expression of Map2 increased whereas the expression of Gfap decreased in the space group of NSCs. Meanwhile, no significant alterations in the expression of Tuj1 were identified between the space and ground groups (**Figure 3B**). Our findings suggested that, during spaceflight, NSCs tended to differentiate into neurons, but their differentiation into astrocytes was inhibited.

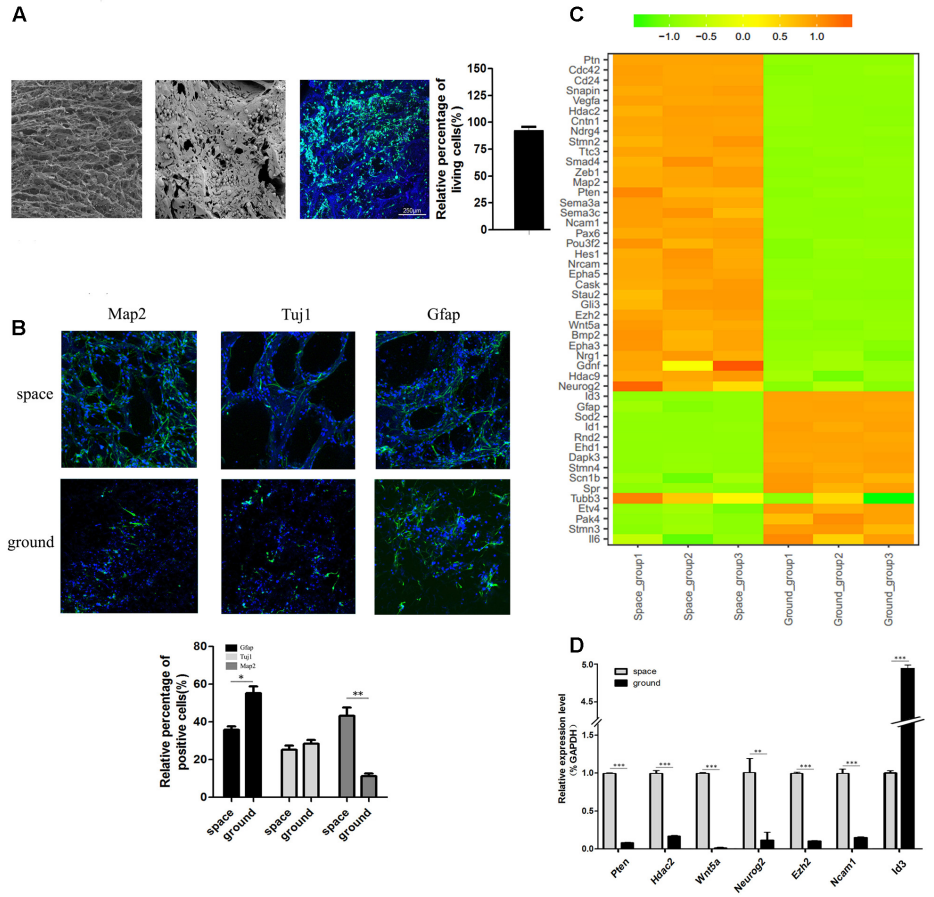

FIGURE 3 | The differentiation status of 3D-cultured NSCs during spaceflight. **(A)** SEM analysis of the collagen sponge scaffold materials (left) and NSCs cultured on them (middle). Representative cell images of the FDA/PI staining of NSCs cultured on these materials (right). **(B)** The expression of the neural markers Tuj1 and Map2 and the astrocyte marker GFAP were detected by immunofluorescence staining. The graph shows the quantitative of positive staining. Data are presented as mean ± SD. $*p < 0.05$, $**p < 0.01$ vs. the ground group. **(C)** Hierarchical clustering analysis of expression profiles of neuron differentiation-related genes in differentiating NSCs. Red indicates a higher *z*-score, while green indicates a lower one. **(D)** The expression level of differentiation-related genes was quantified by real-time PCR. ACTB was used as an internal control. Data are presented as mean ± SD of three different experiments.

Hierarchical clustering of major differentiation-related genes between the space and ground groups was generated (**Figure 3C**). In accordance with the immunofluorescence staining results, the heatmap results indicated that the expression of neuron markers Map2 and Tuj1 was elevated and the expression of the astrocyte marker Gfap was down regulated. In addition, many epigenetic regulators including Hdac2, Hdac9, and Ezh2 were also up-regulated in the space group. It has been reported that Id3 promotes the differentiation of NSCs into astrocytes upon central nervous system (CNS) injury (Bohrer et al., 2015). The expression of Id3 was downregulated in the space group, which supports the finding that the differentiation of NSCs toward astrocytes was suppressed. Moreover, the expression of Pten, Hdac2, Wnt5a, Neurog2, and Ezh2 genes was elevated in the space group which was previously reported to promote the neural differentiation of NSCs (Lange et al., 2006; Sun et al., 2011; Sher et al., 2012; Barton and Fendrik, 2013; Bengoa-Vergniory and Kypta, 2015; Chen et al., 2015). To confirm the RNA-Seq results, we randomly selected seven genes involved in neural differentiation to validate their altered expression using qPCR. The qPCR results proved the validity of the findings obtained by RNA-Seq (**Figure 3D**).

Differential Gene Expression Profiles of NSCs Combined with GO and KEGG Analyses of DEGs between Space and Ground Group

To determine the differential expression profile in NSCs between the space and ground groups, 12 cDNA libraries were constructed for four groups, namely, the proliferating and differentiating NSCs cultured in space or on the earth. Sequencing on the Illumina X Ten platform provided 48036974 and 48395940 paired-end reads for the space and ground group libraries in the differentiation of NSCs, while 46081266 and 46759526 paired-end reads were obtained in the proliferating NSCs, respectively. After filtering, and removing the low-quality reads, the clean reads were pooled together and then mapped to the reference

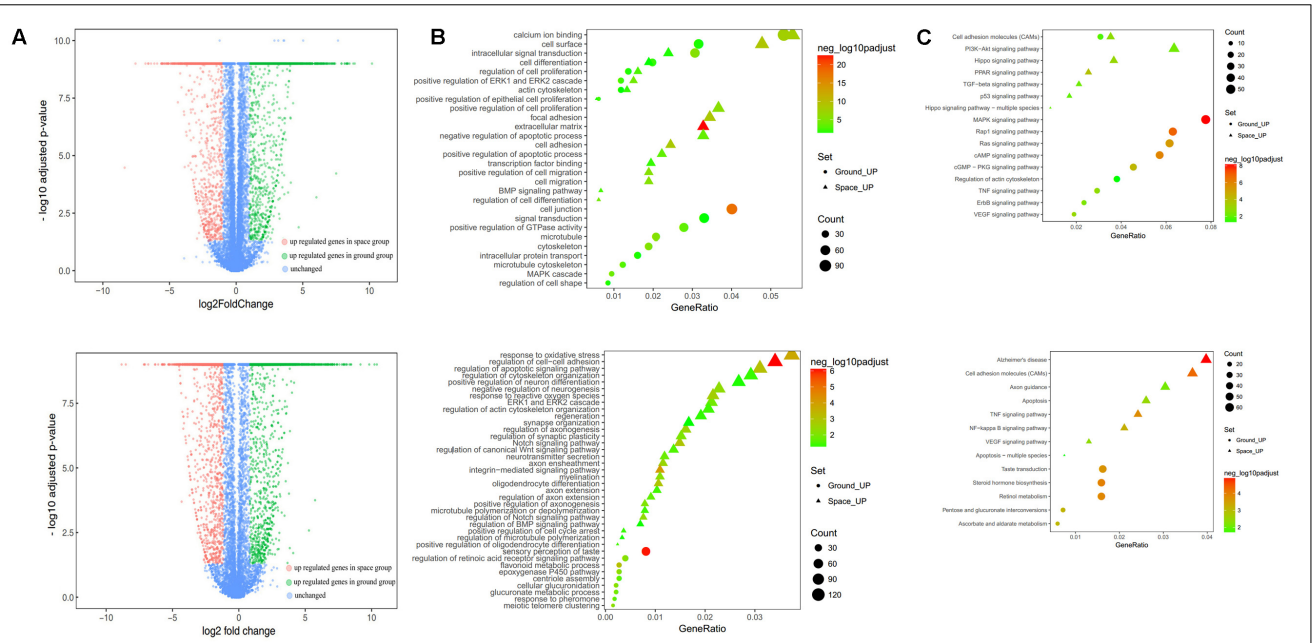

FIGURE 4 | RNA-seq analysis of differential gene expression in the proliferation (top) or differentiating (bottom) group of NSCs between the space and ground groups. **(A)** Volcano plot of genes differentially expressed between the space and ground groups. Significantly up- and downregulated genes are shown as red and green dots, respectively. The blue dots represent genes with no significant difference between the space and ground groups. **(B)** Gene Ontology (GO) biological process analysis for the genes differentially expressed between the space and ground groups. **(C)** KEGG pathway enrichment analysis for the genes differentially expressed between the space and ground groups. Each row shows one significantly enriched (adjusted p-value < 0.05) GO terms. The size of dots indicates the number of up- or downregulated differentially expressed genes between the space and ground groups for the given GO terms. Colors of the dots represent the significance of enrichment, with the significance level increasing from green to red.

genome. On average, 89.46, 87.69, 89.00, and 85.46% of the read pairs in the four groups uniquely mapped to the rat reference genome from the Ensembl database, release 82. We investigated the expression levels of genes between the space and ground groups by comparing these libraries using FPKM analysis, with a false discovery rate (FDR)-adjusted p-value < 0.05 and $|\log_2 \text{ratio}| \geq 1$. In total, 22268 Rattus norvegicus genes were used for the subsequent analyses. Compared with the ground control group, the DEGs with an adjusted p-value < 0.05 and fold change > 2 as determined by DESeq in the space group were screened out. As shown in the volcano plot, 3279 differentially expressed genes were screened in the differentiating NSCs (**Figure 4A**, up), while 1589 DEGs were identified in the prolifeating NSCs between the space and ground groups (**Figure 4A**, down).

The functional classification of DEGs was further examined to better explore the expression patterns and regulatory mechanisms of genes during spaceflight. For a more in-depth analysis using bioinformatics, GO analysis was performed using the DAVID functional annotation tool[3] according to the enrichment scores (**Figure 4B**). Genes matching well-characterized proteins or proteins with putative functions were grouped and summarized using GO. In the proliferating NSCs, GO enrichment analysis showed that the DEGs were particularly associated with cell proliferation, cytoskeleton, cell migration, and cell adhesion, among others. Meanwhile, in the differentiating NSCs, the DEGs were particularly associated with cell adhension, apoptosis, and oxidative stress, among others. The results also showed that the majority of DEGs identified in the differentiating NSCs are involved in the Notch signaling pathway, Wnt signaling pathway, neurotransmitter secretion, and axon extension, among others.

Additionally, these DEGs were assigned to various KEGG pathways (**Figure 4C**). For the pathway enrichment analysis, we mapped those differentially expressed unigenes to terms in the KEGG database and searched for KEGG terms that were significantly enriched compared with the transcriptome background. During the clustering processes, in the differentiating NSCs, the pathways with particular associations were cell adhension, the TNF signaling pathway, and the NF-kappa B signaling pathway. Meanwhile, in the proliferating NSCs, the enriched pathways were the MAPK signaling pathway, the Rap1 signaling pathway, and the cAMP signaling pathway. Our analysis also revealed that apoptosis, cytoskeleton and cell adhesion were affected by spaceflight.

Taken together, these results indicated that many biological processes and signaling pathways are affected by factors prevailing in the environment of outer space. These GO terms and KEGG classifications serve as indications of biological processes of NSCs that differ significantly between outer space

[3]http://david.abcc.ncifcrf.gov/

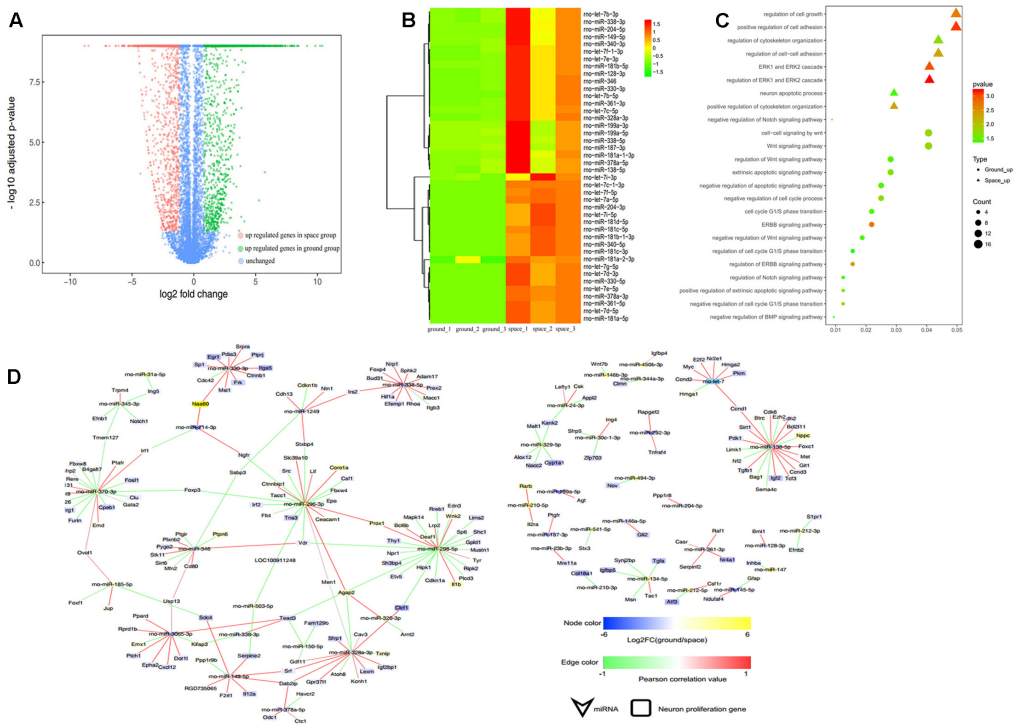

FIGURE 5 | Small RNA sequencing (smRNA-seq) analysis differentially expressed between the Space and Earth groups in the proliferating NSCs. **(A)** Volcano plot of genes differentially expressed between the space and ground groups. Significantly up- and down-regulated genes are shown as red and green dots, respectively. The blue dots represent genes with no significant difference in expression between the space and ground groups. **(B)** Hierarchical clustering analysis of the expression profiles of those proliferation-related miRNAs. Red color indicates a higher *z*-score, while green indicates a lower one. **(C)** The target genes of the differentially expressed miRNAs were subjected to GO analysis in the proliferating NSCs. Each row shows one significantly enriched (adjusted *p*-value < 0.05) Gene Ontology (GO) terms. The size of dots indicates the number of up- or down-regulated genes differentially expressed between the space and ground groups for the given GO terms. Colors of dots represent the significance of enrichment, with the significance level increasing from green to red. **(D)** The miRNA-gene network of these self-renewal-related miRNAs differentially expressed during spaceflight. Node size correlates with "Indegree" computed by Cytoscape. Edges presented as solid lines, dashed lines and dotted lines represent high to low conservation of binding sites. The color of edges is heat-mapped with the fold change value of miRNAs.

and earth, which could offer clues for further studies to determine their functions in space.

Differential miRNA Expression Analysis and Integrated Analysis of miRNAs and Their Target Genes by GO Analysis between Space and Ground Group

Compared with their levels in the ground group, the levels of 93 miRNAs were decreased and those of 90 miRNAs were increased in the proliferating NSCs in the space group; meanwhile, 51 miRNAs were decreased and 91 miRNAs were increased in the differentiating NSCs in the space group (**Figures 5A, 6A**). A substantial number of these miRNAs that were differentially expressed were identified to be involved in cell proliferation, migration, and differentiation, among others. The heatmap results indicated that those miRNAs that were previously reported to be correlated with inhibition of the proliferation of NSCs were upregulated in the space group of NSCs, such as let-7, miR-128, miR-378, miR-138, miR-338, and miR-330 (Godlewski et al., 2008; Zhao et al., 2010; Barca-Mayo and Lu, 2012; Cimadamore et al., 2013; Huang et al., 2015; Choi et al., 2016) (**Figure 5B**). Meanwhile, several differentiation-related miRNAs, such as miR-125, miR-124, miR-134, miR-17, and miR-21, were also up-regulated during spaceflight in the space group of NSCs (**Figure 6B**) (Cui et al., 2012; Xu et al., 2012; Gioia et al., 2014; Jiang et al., 2016; Mao et al., 2016).

To determine the putative functions and target genes of these differentially expressed miRNAs identified in the space group, the functional enrichment of these predicted target genes was analyzed. The miRNAs and their target genes displayed the opposite expression patterns. This suggested that most miRNAs function as crucial regulators by modulating the expression of their target genes associated with the cell cycle, cell growth, metabolic processes, and Wnt signaling in the proliferating NSCs (**Figure 5C**). As shown in **Figure 6C**, in the differentiating NSCs, targeted genes were particularly associated with the cell cycle, cell adhension, Notch signaling and Wnt signaling.

Using the miRNA-target gene pairs predicted by TargetScan, the regulatory networks between differentially expressed miRNAs and their target genes that participate in the proliferation or differentiation of NSCs were constructed (**Figures 5D**, **6D**).

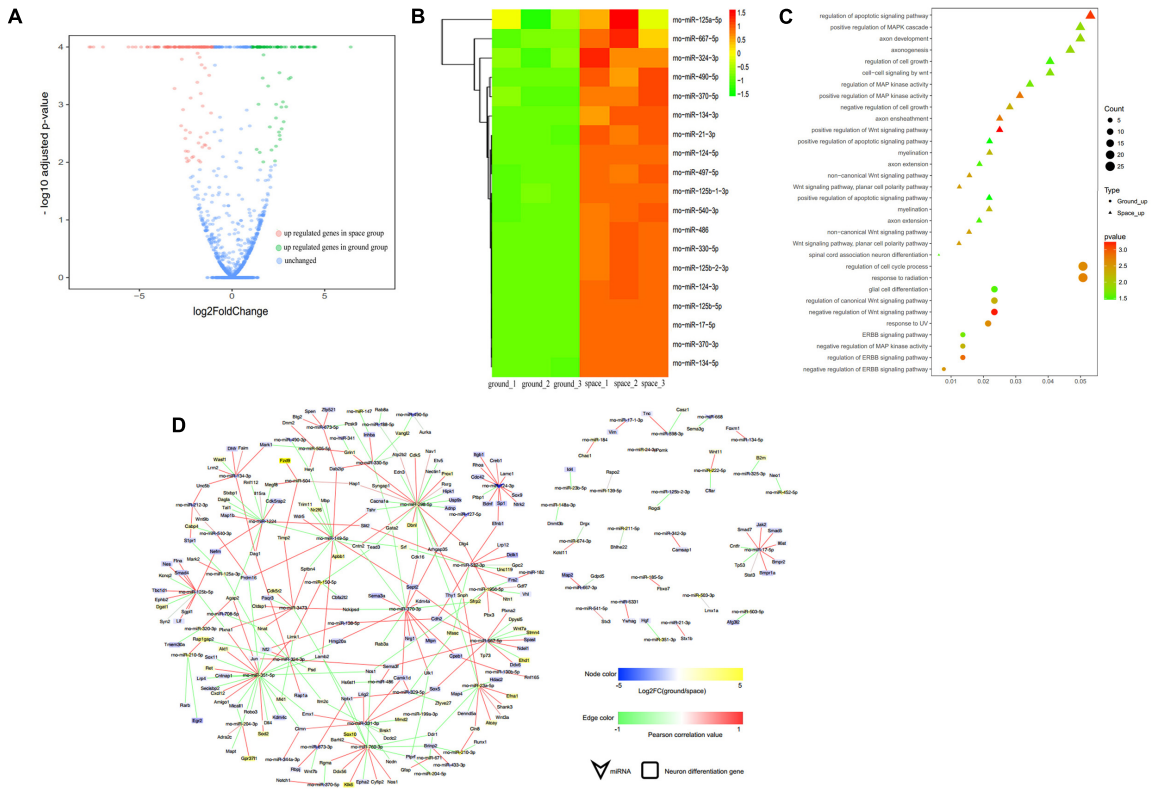

FIGURE 6 | smRNA-seq analysis of miRNAs differentially expressed between the space and ground groups in the differentiating NSCs. **(A)** Volcano plot of genes differentially expressed genes between the space and ground groups. Significantly up- and downregulated genes are shown as red and green dots, respectively. The blue dots represent genes with no significant difference between the space and ground groups. **(B)** Hierarchical clustering analysis of the expression profiles of the neuron differentiation-related miRNAs. Red color indicates a higher *z*-score, while green indicates a lower one. **(C)** The target genes of the differentially expressed miRNAs were subjected to GO analysis in the differentiating NSCs. Each row shows one significantly enriched (adjusted *p*-value < 0.05) Gene Ontology (GO) term. The size of dots indicates the number of up- or down-regulated genes with differential expression between the space and ground groups for the given GO terms. Colors of dots represent the significance of enrichment, with the significance level increasing from green to red. **(D)** The miRNA-gene network of the neuron differentiation-related miRNAs differentially expressed during spaceflight. Node size correlates with "Indegree" computed by Cytoscape. Edges presented as solid lines, dashed lines and dotted lines represent high to low conservation of binding sites. The color of edges is heat-mapped with the fold change value of miRNAs.

These figures show that many target genes associated with the proliferation of NSCs were regulated by these miRNAs differentially expressed between the space and ground groups for the proliferating NSCs, such as cyclin D1, Ccnd2, Lin28b, E2F2, Hmga1, and Hmga2. In addition, bioinformatic analyses indicated that neural differentiation-related genes such as Nestin, Smad4, Stat3, and sp1, were regulated by the miRNAs differentially expressed between the space and ground groups for the differentiating NSCs. The miRNA-gene networks support the assertion that neural differentiation was promoted while cell proliferation was inhibited during spaceflight.

Integrated Bioinformatic Analysis Indicated That the Wnt Signaling Pathway Was Mainly Involved in the Differentiation and Proliferation of NSCs during Spaceflight

The data obtained from RNA-Seq indicated that the expression of many key mediators involved in the Wnt signaling pathway changed in the space group of NSCs; meanwhile, many target genes of the differentially expressed miRNAs were also involved in this pathway. To shed light on the role of Wnt signaling during spaceflight, we constructed a complex network of direct regulation among these differentially expressed genes associated with stem cell self-renewal, differentiation, and Wnt signaling to show the distinct regulatory relationships among them (**Figure 7**). This network analysis indicated that Wnt signaling-related genes, such as Wnt5a and Tcf7, were significantly up-regulated. As a key mediator in the non-canonical Wnt pathway, the up-regulation of Wnt5a has been demonstrated to promote neuron differentiation (Lange et al., 2006). Consistently with this, the stemness-related genes Pax6 and Bmi1 were up-regulated in the space group. In contrast, the expression of the oligodendrocyte markers Galanin (Gal) and Olig2 was downregulated (Fu et al., 2002; Gresle et al., 2015).

Furthermore, the miRNA-Wnt signaling-proliferation/neural differentiation network indicated that miRNAs regulated the differentiation or proliferation of NSCs not only by directly regulating their target genes, but also by regulating molecules

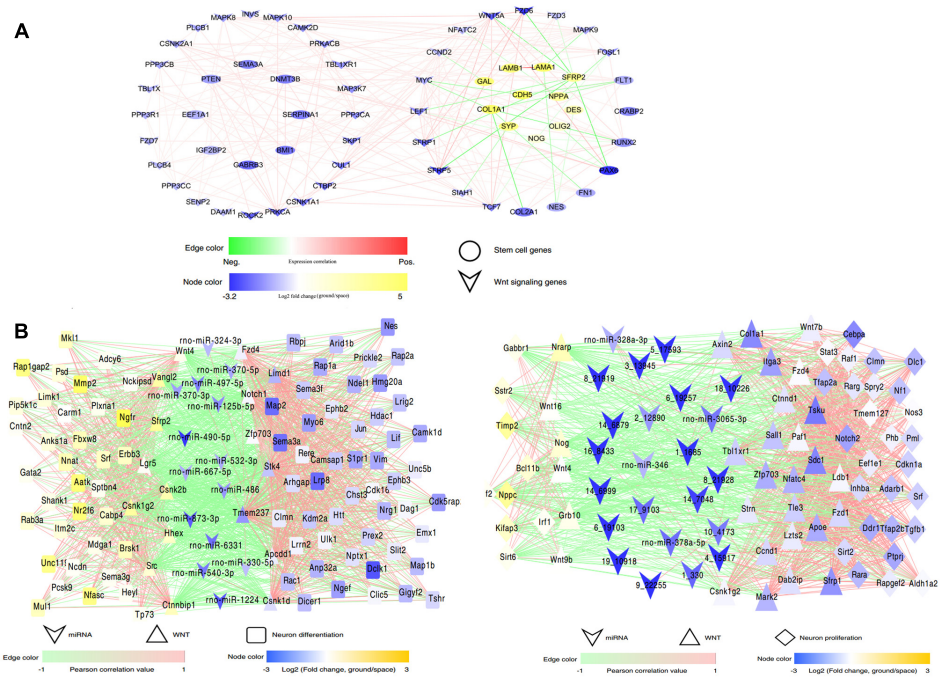

FIGURE 7 | Interaction regulatory network involved in spaceflight. **(A)** The interaction regulatory network between Wnt signaling and neural stem cell development-related genes. **(B)** The interaction regulatory network among miRNAs, Wnt signaling and neural stem cell-related genes in the differentiating (left) or proliferating NSCs (right). MiRNAs and genes are connected by target relationships. The line color represents the strength of the correlation of expression between genes themselves or between gene and miRNAs, with red representing a positive correlation and green representing a negative one. A higher correlation is shown by higher color saturation. Node color represents the fold change of expression (ground vs. space) of related genes or miRNAs.

that constitute the Wnt signaling pathway. For example, in this network, we found that miR-125 directly regulated the neural differentiation-related genes Plxna1, Myo6, and Lif; it may also regulate the Wnt signaling-related gene zfp703 in the differenting NSCs. Taken together, these results indicated that the alteration of the Wnt signaling pathway leads to change of the proliferation or differentiation of NSCs in space, and the exposure to outer space caused alterations of the Wnt signaling pathway in NSCs via different regulatory mechanisms.

DISCUSSION

With the rapid development of space engineering, increasing efforts have been expended on research on stem-cell-based tissue engineering during spaceflight. Recent studies have suggested that NSCs are capable of not only self-proliferating but also differentiating into a variety of terminal cell types, so they might serve as an autologous cell source for regenerative strategies to treat various neurological diseases. For tissue engineering, a 3D cell culture system can generate a 3D structure to permit cellular adhesion, proliferation, and differentiation into a functional tissue construct, which can be regarded as a copy of living tissue (Tian and George, 2011; Kuo et al., 2015; Nandkumar et al., 2015). If 3D cell cultures can be exploited to the full, they hold great potential for regenerating organs by assembling differentiated cells into functional, organ-level tissues. In this study we employed a 3D culture system to evaluate the effect of exposure to outer space environment on neural tissue engineering.

The environment encountered in outer space has a range of challenges for the integrity of living cells and tissue, including microgravity and highly energetic ionizing radiation. In recent years, substantial research in the field of space medicine has focused on the effects of outer space on various stem cells. In the NASA Space Tissue Loss experiment performed on the Space Shuttle Discovery during the NASA STS-131 mission, the results indicated that spaceflight promoted the maintenance of gene expression in embryonic stem cells (Blaber et al., 2015). The behavior of potentially osteogenic murine bone marrow stromal cells (BMSCs) in a 3D culture system was also studied inside the KUBIK aboard the space mission ISS 12S in space. The results indicated that cell proliferation was inhibited in the spaceflight samples, and the microarray results indicated decreased expression of cell-cycle genes in space (Monticone et al., 2010). Previous research also demonstrated that microgravity promotes the proliferation of human neural stem cells (hNSCs), as revealed by using a rotary cell culture system (RCCS). It has been proposed that the RCCS bioreactor would support hNSCs growth by enhancing the function of mitochondria (Chiang et al., 2012). However, to the best of our knowledge, no studies have investigated the molecular mechanisms that occur in NSCs during actual spaceflight, so much has still to be learned about the effects of outer space on NSCs.

Understanding the prevailing molecular mechanism at the genetic level is very useful to evaluate the status of NSCs in outer space. To elucidate the molecular mechanisms behind the effects of exposure to outer space on NSCs, we performed RNA-Seq to study the whole-genome expression profile of mRNAs and miRNAs. High-throughput RNA sequencing approaches have been used extensively to characterize gene expression and determine genetic networks in NSCs. By integrating systematic analysis of miRNA and mRNA expression profiling, possible molecular mechanisms involved in spaceflight could be further explored. Many of the key genes, miRNAs, and signaling pathways involved in the proliferation or differentiation of NSCs during spaceflight have been identified through large-scale analyses of transcriptomes and bioinformatic analysis. Considering that one single miRNA regulates numerous gene targets, miRNAs are now recognized as critical regulators during the differentiation or proliferation process of NSCs. In this study we identified the patterns of mRNAs and miRNAs patterns that were altered during spaceflight and we also performed integrated analysis of miRNA-mRNA profiles. By integrating the transcriptome and miRNAome data, the GO and KEGG analyses indicated that being in space affected the proliferation, cell cycle, differentiation, adhesion, apoptosis, and migration of NSCs. Moreover, the GO analysis of DEGs combined with mRNA–miRNA regulatory network analysis indicated that the variation of Wnt signaling pathways was involved in regulation of the proliferation and differentiation of NSCs during spaceflight.

Wnt signaling is reported to be altered in outer space conditions (Lin et al., 2009; Blaber et al., 2015). Consistent with previous studies, the miRNA-Wnt signaling-proliferation/neural differentiation network constructed in our study shed light on the role of Wnt signaling in NSCs during spaceflight. It shows a robust relationship and interaction between miRNAs and certain genes involved in the Wnt signaling pathway, proliferation and differentiation. The bioinformatic analysis indicated that many differentially expressed miRNAs directly regulate differentiation or proliferation via their target genes, although they may also regulate the differentiation or proliferation of NSCs by influencing the Wnt signaling pathway. Since miRNAs may function as switches and a fine-tuners, they play important roles in the regulatory network. The network indicated that a majority of Wnt signaling components can be regulated by miRNAs, and both miRNAs and Wnt signaling pathway components interact to regulate the differentiation and proliferation processes of NSCs during spaceflight. Mounting evidence has demonstrated that Wnt signaling plays an important role in controlling the proliferation and differentiation of NSCs (Yu et al., 2006; Hirsch et al., 2007; Kalani et al., 2008; Yang et al., 2014). When NSCs were transduced with the Wnt3a-expressing plasmid, the self-renewal ability of neurospheres was elevated and the NSCs tended to differentiation into neurons, on the contrary, the rates of differentiation into glial cells was decreased (Yu et al., 2006). A similar report by Muroyama et al. (2004) reported that the differentiation of NSCs into MAP-2 positive neurons was promoted when cultured in conditioned medium containing Wnt3a protein. Yang et al. (2014) further confirmed that the long-term activation of Wnt signaling can facilitate NSC proliferation and induce a sustained preference for NSCs to differentiate into neurons both *in vitro* and *in vivo*. Furthermore, the Wnt signaling pathway was reported to play a critical role in the development of the nervous system, such as neuroectoderm formation (Mulligan and Cheyette, 2012; Range et al., 2013), neural axon guidance (Lyuksyutova et al., 2003), and neural crest cell migration (Matthews et al., 2008). Thus, understanding the influence of spaceflight on the Wnt signaling pathways is important for successful tissue engineering applications of NSCs in outer space.

This report provides the first evidence that the stemness ability of NSCs was well retained in outer space and their neuron differentiation ability was elevated. Importantly, markers for the stemness of stem cells, such as Sox2, Pax6, and Notch1, were found to be elevated, indicating that NSCs remained in a stem-cell-like state in the proliferation medium during spaceflight, although the proliferation rate did decrease. This was supported by the findings that the expression of mature neuron marker Map2 increased during spaceflight, whereas the astrocyte marker Gfap and the oligodendrocyte markers Gal and Olig2 were all downregulated. Collectively, these results indicated that NSCs tended to differentiate into neurons in outer space.

Our findings suggested that culture in outer space may contribute to tissue engineering by improving the neural differentiation abilities of NSCs *in vitro*, especially when combined with a biomaterial-based 3D culture system. The environment that prevails during spaceflight might have benefits for regenerative medicine purposes during human development and in disease, which should be helpful for NSC-based regenerative medicine. Understanding the mechanisms that occur in NSCs during spaceflight at the genetic level should improve our knowledge of the effects of outer space on living tissue.

AUTHOR CONTRIBUTIONS

YC made substantial contributions to conception and design, acquisition of data, analysis and interpretation of data, and manuscript writing. ZX and BC performed analysis and interpretation of data, and manuscript writing. YQ, YF, and SL made substantial contributions to cell culture. XW contributed to the computational analysis of RNA-Seq data. YZ made a substantial contribution to preparing biomaterial scaffolds. JD and JH made substantial contributions to conception and design, financial support, and analysis and interpretation of data, as well as granting final approval of the version of the manuscript to be published.

FUNDING

This work was supported by "Strategic Priority Research Program of the Chinese Academy of Sciences" (XDA04020000),

Youth Innovation Promotion Association CAS (2015077), National Key R&D Program of China (2016YFC1101500 and 2017YFA0104700), the National Science Foundation of China (81601084), and National Research Institute for Family Planning (2016GJZ06).

ACKNOWLEDGMENTS

We thank Liwen Bianji, Edanz Group China (www.liwenbianji.cn/ac), for editing the English text of a draft of this manuscript.

REFERENCES

Anders, S., and Huber, W. (2012). *Differential Expression of RNA-Seq Data at the Gene Level – the DESeq Package*. Heidelberg: European Molecular Biology Laboratory.

Anders, S., Pyl, P. T., and Huber, W. (2015). HTSeq–a Python framework to work with high-throughput sequencing data. *Bioinformatics.* 31, 166–169. doi: 10.1093/bioinformatics/btu638

Andreu-Agullo, C., Maurin, T., Thompson, C. B., and Lai, E. C. (2011). Ars2 maintains neural stem-cell identity through direct transcriptional activation of Sox2. *Nature* 481, 195–198. doi: 10.1038/nature10712

Asthana, A., and Kisaalita, W. S. (2013). Biophysical microenvironment and 3D culture physiological relevance. *Drug Discov. Today* 18, 533–540. doi: 10.1016/j.drudis.2012.12.005

Baisch, F., Beck, L., Blomqvist, G., Wolfram, G., Drescher, J., Rome, J. L., et al. (2000). Cardiovascular response to lower body negative pressure stimulation before, during, and after space flight. *Eur. J. Clin. Invest.* 30, 1055–1065. doi: 10.1046/j.1365-2362.2000.00750.x

Barca-Mayo, O., and Lu, Q. R. (2012). Fine-tuning oligodendrocyte development by microRNAs. *Front. Neurosci.* 6:13. doi: 10.3389/fnins.2012.00013

Barton, A., and Fendrik, A. J. (2013). Sustained vs. oscillating expressions of Ngn2, Dll1 and Hes1: a model of neural differentiation of embryonic telencephalon. *J. Theor. Biol.* 328, 1–8. doi: 10.1016/j.jtbi.2013.03.004

Bengoa-Vergniory, N., and Kypta, R. M. (2015). Canonical and noncanonical Wnt signaling in neural stem/progenitor cells. *Cell. Mol. Life. Sci.* 72, 4157–4172. doi: 10.1007/s00018-015-2028-6

Blaber, E. A., Finkelstein, H., Dvorochkin, N., Sato, K. Y., Yousuf, R., Burns, B. P., et al. (2015). Microgravity reduces the differentiation and regenerative potential of embryonic stem cells. *Stem Cells Dev.* 24, 2605–2621. doi: 10.1089/scd.2015.0218

Bohrer, C., Pfurr, S., Mammadzada, K., Schildge, S., Plappert, L., Hils, M., et al. (2015). The balance of Id3 and E47 determines neural stem/precursor cell differentiation into astrocytes. *EMBO J.* 34, 2804–2819. doi: 10.15252/embj.201591118

Brito, C., Simao, D., Costa, I., Malpique, R., Pereira, C. I., Fernandes, P., et al. (2012). 3D cultures of human neural progenitor cells: dopaminergic differentiation and genetic modification. [corrected]. *Methods* 56, 452–460. doi: 10.1016/j.ymeth.2012.03.005

Campbell, M. R., and Charles, J. B. (2015). Historical review of lower body negative pressure research in space medicine. *Aerosp. Med. Hum. Perform.* 86, 633–640. doi: 10.3357/AMHP.4246.2015

Chatr-Aryamontri, A., Oughtred, R., Boucher, L., Rust, J., Chang, C., Kolas, N. K., et al. (2017). The BioGRID interaction database: 2017 update. *Nucleic Acids Res.* 45, D369–D379. doi: 10.1093/nar/gkw1102

Chen, B., Lin, H., Wang, J., Zhao, Y., Wang, B., Zhao, W., et al. (2007). Homogeneous osteogenesis and bone regeneration by demineralized bone matrix loading with collagen-targeting bone morphogenetic protein-2. *Biomaterials* 28, 1027–1035. doi: 10.1016/j.biomaterials.2006.10.013

Chen, J., Liu, R., Yang, Y., Li, J., Zhang, X., Wang, Z., et al. (2011). The simulated microgravity enhances the differentiation of mesenchymal stem cells into neurons. *Neurosci. Lett.* 505, 171–175. doi: 10.1016/j.neulet.2011.10.014

Chen, X., Wang, W., Zhang, J., Li, S., Zhao, Y., Tan, L., et al. (2015). Involvement of caspase-3/PTEN signaling pathway in isoflurane-induced decrease of self-renewal capacity of hippocampal neural precursor cells. *Brain Res.* 1625, 275–286. doi: 10.1016/j.brainres.2015.08.047

Chiang, M. C., Lin, H., Cheng, Y. C., Yen, C. H., Huang, R. N., and Lin, K. H. (2012). beta-adrenoceptor pathway enhances mitochondrial function in human neural stem cells via rotary cell culture system. *J. Neurosci. Methods* 207, 130–136. doi: 10.1016/j.jneumeth.2012.04.005

Choi, I., Woo, J. H., Jou, I., and Joe, E. H. (2016). PINK1 deficiency decreases expression levels of mir-326, mir-330, and mir-3099 during brain development and neural stem cell differentiation. *Exp. Neurobiol.* 25, 14–23. doi: 10.5607/en.2016.25.1.14

Cimadamore, F., Amador-Arjona, A., Chen, C., Huang, C. T., and Terskikh, A. V. (2013). SOX2-LIN28/let-7 pathway regulates proliferation and neurogenesis in neural precursors. *Proc. Natl. Acad. Sci. U.S.A.* 110, E3017–E3026. doi: 10.1073/pnas.1220176110

Cui, Y., Han, J., Xiao, Z., Chen, T., Wang, B., Chen, B., et al. (2016). The miR-20-Rest-Wnt signaling axis regulates neural progenitor cell differentiation. *Sci. Rep.* 6:23300. doi: 10.1038/srep23300

Cui, Y., Xiao, Z., Chen, T., Wei, J., Chen, L., Liu, L., et al. (2014). The miR-7 identified from collagen biomaterial-based three-dimensional cultured cells regulates neural stem cell differentiation. *Stem. Cells. Dev.* 23, 393–405. doi: 10.1089/scd.2013.0342

Cui, Y., Xiao, Z., Han, J., Sun, J., Ding, W., Zhao, Y., et al. (2012). MiR-125b orchestrates cell proliferation, differentiation and migration in neural stem/progenitor cells by targeting Nestin. *BMC Neurosci.* 13:116. doi: 10.1186/1471-2202-13-116

Curto, G. G., Nieto-Estevez, V., Hurtado-Chong, A., Valero, J., Gomez, C., Alonso, J. R., et al. (2014). Pax6 is essential for the maintenance and multi-lineage differentiation of neural stem cells, and for neuronal incorporation into the adult olfactory bulb. *Stem. Cells Dev.* 23, 2813–2830. doi: 10.1089/scd.2014.0058

Fu, H., Qi, Y., Tan, M., Cai, J., Takebayashi, H., Nakafuku, M., et al. (2002). Dual origin of spinal oligodendrocyte progenitors and evidence for the cooperative role of Olig2 and Nkx2.2 in the control of oligodendrocyte differentiation. *Development* 129, 681–693.

Gan, Q., Lee, A., Suzuki, R., Yamagami, T., Stokes, A., Nguyen, B. C., et al. (2014). Pax6 mediates ss-catenin signaling for self-renewal and neurogenesis by neocortical radial glial stem cells. *Stem. Cells* 32, 45–58. doi: 10.1002/stem.1561

Gioia, U., Di Carlo, V., Caramanica, P., Toselli, C., Cinquino, A., Marchioni, M., et al. (2014). Mir-23a and mir-125b regulate neural stem/progenitor cell proliferation by targeting Musashi1. *RNA Biol.* 11, 1105–1112. doi: 10.4161/rna.35508

Godlewski, J., Nowicki, M. O., Bronisz, A., Williams, S., Otsuki, A., Nuovo, G., et al. (2008). Targeting of the Bmi-1 oncogene/stem cell renewal factor by microRNA-128 inhibits glioma proliferation and self-renewal. *Cancer Res.* 68, 9125–9130. doi: 10.1158/0008-5472.CAN-08-2629

Gresle, M. M., Butzkueven, H., Perreau, V. M., Jonas, A., Xiao, J., Thiem, S., et al. (2015). Galanin is an autocrine myelin and oligodendrocyte trophic signal induced by leukemia inhibitory factor. *Glia* 63, 1005–1020. doi: 10.1002/glia.22798

Griffith, L. G., and Swartz, M. A. (2006). Capturing complex 3D tissue physiology in vitro. *Nat. Rev. Mol. Cell Biol.* 7, 211–224. doi: 10.1038/nrm1858

Han, J., Wang, B., Xiao, Z., Gao, Y., Zhao, Y., Zhang, J., et al. (2008). Mammalian target of rapamycin (mTOR) is involved in the neuronal differentiation of neural progenitors induced by insulin. *Mol. Cell Neurosci.* 39, 118–124. doi: 10.1016/j.mcn.2008.06.003

Hirsch, C., Campano, L. M., Wohrle, S., and Hecht, A. (2007). Canonical Wnt signaling transiently stimulates proliferation and enhances neurogenesis in neonatal neural progenitor cultures. *Exp.Cell Res.* 313, 572–587. doi: 10.1016/j.yexcr.2006.11.002

Huang, Y., Liu, X., and Wang, Y. (2015). MicroRNA-378 regulates neural stem cell proliferation and differentiation in vitro by modulating Tailless expression. *Biochem. Biophys. Res. Commun.* 466, 214–220. doi: 10.1016/j.bbrc.2015.09.011

Jiang, D., Du, J., Zhang, X., Zhou, W., Zong, L., Dong, C., et al. (2016). miR-124 promotes the neuronal differentiation of mouse inner ear neural stem cells. *Int. J. Mol. Med.* 38, 1367–1376. doi: 10.3892/ijmm.2016.2751

Johnson, R., Teh, C. H., Kunarso, G., Wong, K. Y., Srinivasan, G., Cooper, M. L., et al. (2008). REST regulates distinct transcriptional networks in embryonic and neural stem cells. *PLOS Biol.* 6:e256. doi: 10.1371/journal.pbio.0060256

Kalani, M. Y., Cheshier, S. H., Cord, B. J., Bababeygy, S. R., Vogel, H., Weissman, I. L., et al. (2008). Wnt-mediated self-renewal of neural stem/progenitor cells. *Proc. Natl. Acad. Sci. U.S.A.* 105, 16970–16975. doi: 10.1073/pnas.0808616105

Kim, D., Pertea, G., Trapnell, C., Pimentel, H., Kelley, R., and Salzberg, S. L. (2013). TopHat2: accurate alignment of transcriptomes in the presence of insertions, deletions and gene fusions. *Genome. Biol.* 14:R36. doi: 10.1186/gb-2013-14-4-r36

Kiparissides, A., Koutinas, M., Moss, T., Newman, J., Pistikopoulos, E. N., and Mantalaris, A. (2011). Modelling the Delta1/Notch1 pathway: in search of the mediator(s) of neural stem cell differentiation. *PLOS ONE* 6:e14668. doi: 10.1371/journal.pone.0014668

Knight, E., and Przyborski, S. (2015). Advances in 3D cell culture technologies enabling tissue-like structures to be created *in vitro*. *J. Anat.* 227, 746–756. doi: 10.1111/joa.12257

Kuo, K. C., Lin, R. Z., Tien, H. W., Wu, P. Y., Li, Y. C., Melero-Martin, J. M., et al. (2015). Bioengineering vascularized tissue constructs using an injectable cell-laden enzymatically crosslinked collagen hydrogel derived from dermal extracellular matrix. *Acta Biomater.* 27, 151–166. doi: 10.1016/j.actbio.2015.09.002

Lange, C., Mix, E., Rateitschak, K., and Rolfs, A. (2006). Wnt signal pathways and neural stem cell differentiation. *Neurodegener. Dis.* 3, 76–86. doi: 10.1159/000092097

Liedmann, A., Rolfs, A., and Frech, M. J. (2012). Cultivation of human neural progenitor cells in a 3-dimensional self-assembling peptide hydrogel. *J. Vis. Exp* 59:e3830. doi: 10.3791/3830

Lin, C., Jiang, X., Dai, Z., Guo, X., Weng, T., Wang, J., et al. (2009). Sclerostin mediates bone response to mechanical unloading through antagonizing Wnt/beta-catenin signaling. *J. Bone. Miner. Res.* 24, 1651–1661. doi: 10.1359/jbmr.090411

Livak, K. J., and Schmittgen, T. D. (2001). Analysis of relative gene expression data using real-time quantitative PCR and the $2^{-\Delta\Delta C_T}$ Method. *Methods* 25, 402–408. doi: 10.1006/meth.2001.1262

Lyuksyutova, A. I., Lu, C. C., Milanesio, N., King, L. A., Guo, N., Wang, Y., et al. (2003). Anterior-posterior guidance of commissural axons by Wnt-frizzled signaling. *Science* 302, 1984–1988. doi: 10.1126/science.1089610

Mao, S., Li, X., Wang, J., Ding, X., Zhang, C., and Li, L. (2016). miR-17-92 facilitates neuronal differentiation of transplanted neural stem/precursor cells under neuroinflammatory conditions. *J. Neuroinflammation* 13:208. doi: 10.1186/s12974-016-0685-5

Marsh, S. E., and Blurton-Jones, M. (2017). Neural stem cell therapy for neurodegenerative disorders: the role of neurotrophic support. *Neurochem. Int.* 106, 94–100. doi: 10.1016/j.neuint.2017.02.006

Matthews, H. K., Marchant, L., Carmona-Fontaine, C., Kuriyama, S., Larrain, J., Holt, M. R., et al. (2008). Directional migration of neural crest cells in vivo is regulated by Syndecan-4/Rac1 and non-canonical Wnt signaling/RhoA. *Development* 135, 1771–1780. doi: 10.1242/dev.017350

Meyers, V. E., Zayzafoon, M., Gonda, S. R., Gathings, W. E., and McDonald, J. M. (2004). Modeled microgravity disrupts collagen I/integrin signaling during osteoblastic differentiation of human mesenchymal stem cells. *J. Cell. Biochem.* 93, 697–707. doi: 10.1002/jcb.20229

Monticone, M., Liu, Y., Pujic, N., and Cancedda, R. (2010). Activation of nervous system development genes in bone marrow derived mesenchymal stem cells following spaceflight exposure. *J. Cell. Biochem.* 111, 442–452. doi: 10.1002/jcb.22765

Mulligan, K. A., and Cheyette, B. N. (2012). Wnt signaling in vertebrate neural development and function. *J. Neuroimmune Pharmacol.* 7, 774–787. doi: 10.1007/s11481-012-9404-x

Muroyama, Y., Kondoh, H., and Takada, S. (2004). Wnt proteins promote neuronal differentiation in neural stem cell culture. *Biochem. Biophys. Res. Commun.* 313, 915–921. doi: 10.1016/j.bbrc.2003.12.023

Nandkumar, M. A., Ashna, U., Thomas, L. V., and Nair, P. D. (2015). Pulmonary surfactant expression analysis–role of cell-cell interactions and 3-D tissue-like architecture. *Cell Biol. Int.* 39, 272–282. doi: 10.1002/cbin.10389

Osumi, N., Shinohara, H., Numayama-Tsuruta, K., and Maekawa, M. (2008). Concise review: Pax6 transcription factor contributes to both embryonic and adult neurogenesis as a multifunctional regulator. *Stem. Cells* 26, 1663–1672. doi: 10.1634/stemcells.2007-0884

Pani, G., Verslegers, M., Quintens, R., Samari, N., de Saint-Georges, L., van Oostveldt, P., et al. (2016). Combined exposure to simulated microgravity and acute or chronic radiation reduces neuronal network integrity and survival. *PLOS ONE* 11:e0155260. doi: 10.1371/journal.pone.0155260

Pevny, L. H., and Nicolis, S. K. (2010). Sox2 roles in neural stem cells. *Int. J. Biochem. Cell Biol.* 42, 421–424. doi: 10.1016/j.biocel.2009.08.018

Range, R. C., Angerer, R. C., and Angerer, L. M. (2013). Integration of canonical and noncanonical Wnt signaling pathways patterns the neuroectoderm along the anterior-posterior axis of sea urchin embryos. *PLOS Biol.* 11:e1001467. doi: 10.1371/journal.pbio.1001467

Riley, D. A., Ilyina-Kakueva, E. I., Ellis, S., Bain, J. L., Slocum, G. R., and Sedlak, F. R. (1990). Skeletal muscle fiber, nerve, and blood vessel breakdown in space-flown rats. *FASEB J.* 4, 84–91.

Sansom, S. N., Griffiths, D. S., Faedo, A., Kleinjan, D. J., Ruan, Y., Smith, J., et al. (2009). The level of the transcription factor Pax6 is essential for controlling the balance between neural stem cell self-renewal and neurogenesis. *PLOS Genet.* 5:e1000511. doi: 10.1371/journal.pgen.1000511

Shannon, P., Markiel, A., Ozier, O., Baliga, N. S., Wang, J. T., Ramage, D., et al. (2003). Cytoscape: a software environment for integrated models of biomolecular interaction networks. *Genome. Res.* 13, 2498–2504. doi: 10.1101/gr.1239303

Sher, F., Boddeke, E., Olah, M., and Copray, S. (2012). Dynamic changes in Ezh2 gene occupancy underlie its involvement in neural stem cell self-renewal and differentiation towards oligodendrocytes. *PLOS ONE* 7:e40399. doi: 10.1371/journal.pone.0040399

Stergiopoulos, A., and Politis, P. K. (2016). Nuclear receptor NR5A2 controls neural stem cell fate decisions during development. *Nat. Commun.* 7:12230. doi: 10.1038/ncomms12230

Sun, G., Fu, C., Shen, C., and Shi, Y. (2011). Histone deacetylases in neural stem cells and induced pluripotent stem cells. *J. Biomed. Biotechnol.* 2011:835968. doi: 10.1155/2011/835968

Szklarczyk, D., Franceschini, A., Wyder, S., Forslund, K., Heller, D., Huerta-Cepas, J., et al. (2015). STRING v10: protein-protein interaction networks, integrated over the tree of life. *Nucleic Acids Res.* 43, D447–D452. doi: 10.1093/nar/gku1003

Thiel, G. (2013). How Sox2 maintains neural stem cell identity. *Biochem. J.* 450, e1–e2. doi: 10.1042/BJ20130176

Tian, L., and George, S. C. (2011). Biomaterials to prevascularize engineered tissues. *J. Cardiovasc. Transl. Res.* 4, 685–698. doi: 10.1007/s12265-011-9301-3

Trapnell, C., Roberts, A., Goff, L., Pertea, G., Kim, D., Kelley, D. R., et al. (2012). Differential gene and transcript expression analysis of RNA-seq experiments with TopHat and Cufflinks. *Nat. Protoc.* 7, 562–578. doi: 10.1038/nprot.2012.016

Wang, B., Zhang, S., and Wu, X. Y. (2003). [Effects of microgravity on the gene expression and cellular functions of osteoblasts]. *Space. Med. Med. Eng.* 16, 227–230.

Wang, H. C., Zhang, Z. Y., and Xin, W. G. (2007). Microgravity resulted from 3D dynamic culture induces compounding of bone morrow-derived mesenchymal stem cells with Pluronic F-127 scaffold used for repairing of cartilage defects. *Chin. Tissue Eng. Clin. Recov.* 11, 2609–2613.

Xu, W., Li, P., Qin, K., Wang, X., and Jiang, X. (2012). miR-124 regulates neural stem cells in the treatment of spinal cord injury. *Neurosci. Lett.* 529, 12–17. doi: 10.1016/j.neulet.2012.09.025

Yang, X. T., Bi, Y. Y., Chen, E. T., and Feng, D. F. (2014). Overexpression of Wnt3a facilitates the proliferation and neural differentiation of neural stem cells in vitro and after transplantation into an injured rat retina. *J. Neurosci. Res.* 92, 148–161. doi: 10.1002/jnr.23314

Yang, Y. J., Baltus, A. E., Mathew, R. S., Murphy, E. A., Evrony, G. D., Gonzalez, D. M., et al. (2012). Microcephaly gene links trithorax and REST/NRSF to control neural stem cell proliferation and differentiation. *Cell* 151, 1097–1112. doi: 10.1016/j.cell.2012.10.043

Yu, G., Wang, L. G., Han, Y., and He, Q. Y. (2012). clusterProfiler: an R package for comparing biological themes among gene clusters. *OMICS* 16, 284–287. doi: 10.1089/omi.2011.0118

Yu, J. M., Kim, J. H., Song, G. S., and Jung, J. S. (2006). Increase in proliferation and differentiation of neural progenitor cells isolated from postnatal and adult

mice brain by Wnt-3a and Wnt-5a. *Mol. Cell. Biochem.* 288, 17–28. doi: 10.1007/s11010-005-9113-3

Yuge, L., Kajiume, T., Tahara, H., Kawahara, Y., Umeda, C., Yoshimoto, R., et al. (2006). Microgravity potentiates stem cell proliferation while sustaining the capability of differentiation. *Stem. Cells Dev.* 15, 921–929. doi: 10.1089/scd.2006.15.921

Zayzafoon, M., Gathings, W. E., and McDonald, J. M. (2004). Modeled microgravity inhibits osteogenic differentiation of human mesenchymal stem cells and increases adipogenesis. *Endocrinology* 145, 2421–2432. doi: 10.1210/en.2003-1156

Zhang, L., Han, X., Cheng, X., Tan, X. F., Zhao, H. Y., and Zhang, X. H. (2016). Denervated hippocampus provides a favorable microenvironment for neuronal differentiation of endogenous neural stem cells. *Neural. Regen. Res.* 11, 597–603. doi: 10.4103/1673-5374.180744

Zhang, P., Ha, T., Larouche, M., Swanson, D., and Goldowitz, D. (2015). Kruppel-like factor 4 regulates granule cell Pax6 expression and cell proliferation in early cerebellar development. *PLOS ONE* 10:e0134390. doi: 10.1371/journal.pone.0134390

Zhang, X., Nan, Y., Wang, H., Chen, J., Wang, N., Xie, J., et al. (2013). Model microgravity enhances endothelium differentiation of mesenchymal stem cells. *Naturwissenschaften* 100, 125–133. doi: 10.1007/s00114-012-1002-5

Zhao, C., Sun, G., Li, S., Lang, M. F., Yang, S., Li, W., et al. (2010). MicroRNA let-7b regulates neural stem cell proliferation and differentiation by targeting nuclear receptor TLX signaling. *Proc. Natl. Acad. Sci. U.S.A.* 107, 1876–1881. doi: 10.1073/pnas.0908750107

Zhou, Q. Z., Zhang, G., Long, H. B., Lei, F., Ye, F., Jia, X. F., et al. (2014). Effect of spinal cord extracts after spinal cord injury on proliferation of rat embryonic neural stem cells and Notch signal pathway *in vitro*. *Asian Pac. J. Trop. Med.* 7, 562–567. doi: 10.1016/S1995-7645(14)60094-8

Conflict of Interest Statement: The authors declare that the research was conducted in the absence of any commercial or financial relationships that could be construed as a potential conflict of interest.

Advantages of publishing in Frontiers

OPEN ACCESS
Articles are free to read for greatest visibility and readership

FAST PUBLICATION
Around 90 days from submission to decision

HIGH QUALITY PEER-REVIEW
Rigorous, collaborative, and constructive peer-review

TRANSPARENT PEER-REVIEW
Editors and reviewers acknowledged by name on published articles

Frontiers
Avenue du Tribunal-Fédéral 34
1005 Lausanne | Switzerland

Visit us: www.frontiersin.org
Contact us: info@frontiersin.org | +41 21 510 17 00

REPRODUCIBILITY OF RESEARCH
Support open data and methods to enhance research reproducibility

DIGITAL PUBLISHING
Articles designed for optimal readership across devices

FOLLOW US
@frontiersin

IMPACT METRICS
Advanced article metrics track visibility across digital media

EXTENSIVE PROMOTION
Marketing and promotion of impactful research

LOOP RESEARCH NETWORK
Our network increases your article's readership